PLANT RESPONSES TO THE DARK SCENARIO

EDITED BY: Péter Poór, Attila Ördög, M. Iqbal R. Khan and Chentao Lin

PUBLISHED IN: Frontiers in Plant Science

frontiers Research Topics

ISSN 1664-8714
ISBN 978-2-88971-081-2
DOI 10.3389/978-2-88971-081-2

About Frontiers

Frontiers is more than just an open-access publisher of scholarly articles: it is a pioneering approach to the world of academia, radically improving the way scholarly research is managed. The grand vision of Frontiers is a world where all people have an equal opportunity to seek, share and generate knowledge. Frontiers provides immediate and permanent online open access to all its publications, but this alone is not enough to realize our grand goals.

Frontiers Journal Series

The Frontiers Journal Series is a multi-tier and interdisciplinary set of open-access, online journals, promising a paradigm shift from the current review, selection and dissemination processes in academic publishing. All Frontiers journals are driven by researchers for researchers; therefore, they constitute a service to the scholarly community. At the same time, the Frontiers Journal Series operates on a revolutionary invention, the tiered publishing system, initially addressing specific communities of scholars, and gradually climbing up to broader public understanding, thus serving the interests of the lay society, too.

Dedication to Quality

Each Frontiers article is a landmark of the highest quality, thanks to genuinely collaborative interactions between authors and review editors, who include some of the world's best academicians. Research must be certified by peers before entering a stream of knowledge that may eventually reach the public - and shape society; therefore, Frontiers only applies the most rigorous and unbiased reviews.
Frontiers revolutionizes research publishing by freely delivering the most outstanding research, evaluated with no bias from both the academic and social point of view. By applying the most advanced information technologies, Frontiers is catapulting scholarly publishing into a new generation.

What are Frontiers Research Topics?

Frontiers Research Topics are very popular trademarks of the Frontiers Journals Series: they are collections of at least ten articles, all centered on a particular subject. With their unique mix of varied contributions from Original Research to Review Articles, Frontiers Research Topics unify the most influential researchers, the latest key findings and historical advances in a hot research area! Find out more on how to host your own Frontiers Research Topic or contribute to one as an author by contacting the Frontiers Editorial Office: frontiersin.org/about/contact

PLANT RESPONSES TO THE DARK SCENARIO

Topic Editors:
Péter Poór, University of Szeged, Hungary
Attila Ördög, University of Szeged, Hungary
M. Iqbal R. Khan, Jamia Hamdard University, India
Chentao Lin, University of California, United States

Citation: Poór, P., Ördög, A., Khan, M. I. R., Lin, C., eds. (2021). Plant Responses to the Dark Scenario. Lausanne: Frontiers Media SA. doi: 10.3389/978-2-88971-081-2

Table of Contents

04 ***Editorial: Plant Responses to the Dark Scenario***
Péter Poór, Attila Ördög, Chentao Lin and M. Iqbal R. Khan

06 ***Narrowing Diurnal Temperature Amplitude Alters Carbon Tradeoff and Reduces Growth in C_4 Crop Sorghum***
V. S. John Sunoj, P. V. Vara Prasad, Ignacio A. Ciampitti and Hanafey F. Maswada

22 ***Dark-Induced Hormonal Regulation of Plant Growth and Development***
Deepika, Ankit, Sushma Sagar and Amarjeet Singh

32 ***The Impact of Fruit Etiolation on Quality of Seeds in Tobacco***
Domenica Farci, Patrycja Haniewicz, Emma Cocco, Antonio De Agostini, Pierluigi Cortis, Magdalena Kusaka, Maria C. Loi and Dario Piano

42 ***Radiation and Drought Impact Residual Leaf Conductance in Two Oak Species With Implications for Water Use Models***
Haiyan Qin, Carles Arteaga, Faqrul Islam Chowdhury, Elena Granda, Yinan Yao, Ying Han and Víctor Resco de Dios

55 ***Difference Between Day and Night Temperatures Affects Stem Elongation in Tomato (*Solanum lycopersicum*) Seedlings via Regulation of Gibberellin and Auxin Synthesis***
Kinuka Ohtaka, Akiko Yoshida, Yusuke Kakei, Kosuke Fukui, Mikiko Kojima, Yumiko Takebayashi, Kanako Yano, Shunsuke Imanishi and Hitoshi Sakakibara

67 ***Exogenous Calcium Alleviates Nocturnal Chilling-Induced Feedback Inhibition of Photosynthesis by Improving Sink Demand in Peanut (*Arachis hypogaea*)***
Di Wu, Yifei Liu, Jiayin Pang, Jean Wan Hong Yong, Yinglong Chen, Chunming Bai, Xiaori Han, Xinyue Liu, Zhiyu Sun, Siwei Zhang, Jing Sheng, Tianlai Li, Kadambot H.M. Siddique and Hans Lambers

81 ***Time Lag Between Light and Heat Diurnal Cycles Modulates* CIRCADIAN CLOCK ASSOCIATION 1 *Rhythm and Growth in* Arabidopsis thaliana
Kosaku Masuda, Tatsuya Yamada, Yuya Kagawa and Hirokazu Fukuda

91 ***Plant Defense Responses to Biotic Stress and Its Interplay With Fluctuating Dark/Light Conditions***
Zahra Iqbal, Mohammed Shariq Iqbal, Abeer Hashem, Elsayed Fathi Abd_Allah and Mohammad Israil Ansari

113 ***The Sequential Action of MIDA9/PP2C.D1, PP2C.D2, and PP2C.D5 Is Necessary to Form and Maintain the Hook After Germination in the Dark***
Arnau Rovira, Maria Sentandreu, Akira Nagatani, Pablo Leivar and Elena Monte

125 ***Dark-Induced Barley Leaf Senescence – A Crop System for Studying Senescence and Autophagy Mechanisms***
Ewelina Paluch-Lubawa, Ewelina Stolarska and Ewa Sobieszczuk-Nowicka

frontiers in Plant Science

EDITORIAL
published: 28 May 2021
doi: 10.3389/fpls.2021.688053

Editorial: Plant Responses to the Dark Scenario

Péter Poór[1], Attila Ördög[1], Chentao Lin[2] and M. Iqbal R. Khan[3]**

[1] Department of Plant Biology, University of Szeged, Szeged, Hungary, [2] University of California, Los Angeles, Los Angeles, CA, United States, [3] Department of Botany, Jamia Hamdard University, New Delhi, India

Keywords: circadian, diurnal, germination, senescence, shade avoidance, stress

Editorial on the Research Topic

Plant Responses to the Dark Scenario

INTRODUCTION

Light is one of the most important abiotic factors, which is essential for optimal plant growth and development (Hua, 2013). Thanks to the rhythmic changes in light-dark phases on the Earth, the circadian clock has been evolved in the living organism to synchronize internal regulatory processes (Lu et al., 2017). Although most of the scientific data are coming from the light phase of plant life, the importance of the dark phase is also very significant (Ballaré, 2014). The aim of this Research Topic was to get an insight into new findings/opinions to improve the understanding of plant responses to dark. The topic includes original research and review articles which have been grouped based on four categories.

OPEN ACCESS

Edited and reviewed by:
Nigel G. Halford,
Rothamsted Research,
United Kingdom

****Correspondence:***
Péter Poór
poorpeti@bio.u-szeged.hu
M. Iqbal R. Khan
amu.iqbal@gmail.com

Specialty section:
This article was submitted to Plant Physiology, a section of the journal Frontiers in Plant Science

Received: *30 March 2021*
Accepted: *04 May 2021*
Published: *28 May 2021*

Citation:
Poór P, Ördög A, Lin C and Khan MIR (2021) Editorial: Plant Responses to the Dark Scenario. Front. Plant Sci. 12:688053. doi: 10.3389/fpls.2021.688053

GERMINATION, GROWTH AND DEVELOPMENT IN THE DARK

Generally, a plant's life begins in the dark, when germination is started in the soil. Under this condition, skotomorphogenesis or etiolated growth is characterized by hypocotyl elongation, apical hook formation and appressed cotyledons (Gommers and Monte, 2018).

Rovira et al. identified MISREGULATED IN DARK9 (MIDA9) as a phytochrome interacting factor (PIF)-repressed gene in the dark which is necessary for hook development. MIDA9 encodes the type 2C phosphatase PP2C.D1 which negatively regulates SMALL AUXIN UP RNA (SAUR)-mediated cell elongation. Authors found that PP2C.D1 is required immediately after germination to form the hook. Based on genetic analyses of the PP2C.D family, they described the role of PP2C.D2, PP2C.D5 and PP2C.D1. Besides, they suggested a possible interaction between PP2C.D1 and ethylene in hook formation under darkness.

Other processes of the plant's growth and development in the dark were reviewed by Deepika et al.. The article summarizes dark-mediated changes in plant hormones' regulation of signaling complex CONSTITUTIVE PHOTOMORPHOGENIC/DE-ETIOLATED/FUSCA (COP/DET/FUS) and PIFs that affects plant developmental events such as hook development, elongated hypocotyls, photoperiodic flowering, shortened roots, and plastid development.

DARK-INDUCED SENESCENCE AND RIPENING PHYSIOLOGY

The lack of light caused by shading of the leaves leads to rapid senescence (Liebsch and Keech, 2016). The review of Paluch-Lubawa et al. discussed the effects of dark-induced leaf senescence (DILS) in barley. They focused on the importance of chloroplasts, the role of Rubisco, morphological changes, transcriptomic differences, and autophagy in DILS. They identified two

steps of DILS program: cessation of photosynthesis accompanied by loss of chlorophyll and disintegration of chloroplasts, followed by the terminal phase, marked by the initiation of cell death and autophagy.

Fruit ripening and seed development are highly dependent on light and active photosynthesis. Farci et al. investigated the effects of dark on the growth of capsules of *Nicotiana tabacum* during the whole post-anthesis period. They found that etiolated capsules showed reduced photosynthetic rates but their seeds had an increased mass and volume, an alteration in gibberellins and abscisic acid, and reduced dormancy compared to the uncovered plants showing the effects of dark in fruit physiology.

DARK-INDUCED SENESCENCE AND RIPENING PHYSIOLOGY

The temperature variations between day and night affect plant growth and interact with the time lag to the light cycle. Effects of the time lag on the circadian rhythm and growth were investigated by Masuda et al.. Firstly, the rhythm of the clock gene CIRCADIAN CLOCK ASSOCIATION 1 (CCA1) was measured and shown to be modulated by the time lag with heating every day but not cooling. Seedling growth was also dependent on the time lag of the heating but not on the cooling cycle. These results provide a method to estimate the appropriate combination of light-dark and temperature cycles.

However, seedlings growth is mediated by the regulation of phytohormones depending on the day and night temperatures. Ohtaka et al. found that a positive DIF (Difference in day and night temperature) treatment, higher temperatures promoted stem elongation. This was accompanied by the upregulation of gibberellin and indole-3-acetic acid synthesis genes. Negative DIF inhibited stem elongation, which was accompanied by the downregulation of gibberellin and indole-3-acetic acid synthesis genes. Thus, DIF treatment can be employed as an effective technique in ornamental horticulture.

Effect of diurnal temperature amplitude on photosynthesis/respiration and growth are less-investigated in C4 crops. Sunoj et al. determined the effects of optimal (27°C) and high (35°C) mean temperatures with three different amplitudes (2, 10, and 18°C) in sorghum. Comparing the high mean daytime and night-time temperatures to optimum values, soluble sugars, starch, leaf area and biomass were reduced, while night respiration was increased but photosynthesis did not change. This revealed the importance of understanding the dark phase mechanisms, especially effects of temperature on night respiration.

Understanding the regulation of water homeostasis and stomatal regulation has great importance under global warming. Qin et al. demonstrated how shade and drought impact the residual leaf conductance (g_{res}) in oak species. In addition, the role of nocturnal conductance (g_n) and its relation with g_{res} were also determined. The authors showed that in closely related species the effect of radiation and drought were interactive in the case of g_{res}, which correlated positively with leaf non-structural carbohydrates and negatively with leaf nitrogen content.

Overnight chilling stress causes a serious decrease in yield in many cultivation areas worldwide. Wu et al. examined the effects of exogenous calcium in the alleviation of nocturnal chilling-induced inhibition of photosynthesis in peanut. They found that foliar calcium application enhanced plant growth and alleviated the nocturnal chilling-dependent feedback limitation of photosynthesis by facilitating cyclic electron flow and decreasing the proton gradient across thylakoid membranes.

PLANT DEFENSE RESPONSES IN THE DARK

Plant defense responses against pathogens are mostly well-studied processes but the impact of dark signals are less-investigated. The review of Iqbal et al. discussed the effects of dark/light on plant-pathogen interactions, focusing on the role of reactive oxygen species, phytohormones, and transcription factors.

This Research Topic covers the current knowledge of plant responses to the dark scenario. Contributors gave a deep insight into understanding the effects of dark on growth and development, as well as defense responses of plants. These results can help not only plant scientist but also breeders and promote new perspectives in the research of plant responses under darkness.

AUTHOR CONTRIBUTIONS

PP, AÖ, CL, and MK: writing—review and editing. All authors contributed to the article and approved the submitted version.

REFERENCES

Ballaré, C. L. (2014). Light regulation of plant defense. *Annu. Rev. Plant Biol.* 65, 335–363. doi: 10.1146/annurev-arplant-050213-040145

Gommers, C. M., and Monte, E. (2018). Seedling establishment: a dimmer switch-regulated process between dark and light signaling. *Plant Physiol.* 176, 1061–1074. doi: 10.1104/pp.17.01460

Hua, J. (2013). Modulation of plant immunity by light, circadian rhythm, and temperature. *Curr. Opin. Plant Biol.* 16, 406–413. doi: 10.1016/j.pbi.2013.06.017

Liebsch, D., and Keech, O. (2016). Dark-induced leaf senescence: new insights into a complex light-dependent regulatory pathway. *New Phytol.* 212, 563–570. doi: 10.1111/nph.14217

Lu, H., McClung, C. R., and Zhang, C. (2017). Tick tock: circadian regulation of plant innate immunity. *Annu. Rev. Phytopathol.* 55, 287–311. doi: 10.1146/annurev-phyto-080516-035451

Conflict of Interest: The authors declare that the research was conducted in the absence of any commercial or financial relationships that could be construed as a potential conflict of interest.

frontiers in Plant Science

ORIGINAL RESEARCH
published: 19 August 2020
doi: 10.3389/fpls.2020.01262

Narrowing Diurnal Temperature Amplitude Alters Carbon Tradeoff and Reduces Growth in C_4 Crop Sorghum

V. S. John Sunoj[1,2*], *P. V. Vara Prasad*[1*], *Ignacio A. Ciampitti*[1] *and Hanafey F. Maswada*[1,3]

[1] Department of Agronomy, 2004 Throckmorton Plant Sciences Center, Kansas State University, Manhattan, KS, United States, [2] State Key Laboratory of Conservation and Utilization of Subtropical Agro–bio–resources, College of Forestry, Guangxi University, Nanning, China, [3] Department of Agricultural Botany, Faculty of Agriculture, Tanta University, Tanta, Egypt

OPEN ACCESS

Edited by:
Attila Ördög, University of Szeged, Hungary

Reviewed by:
Graeme Hammer, The University of Queensland, Australia
Marek Zivcak, Slovak University of Agriculture, Slovakia
Toshihiro Obata, University of Nebraska-Lincoln, United States

***Correspondence:**
V. S. John Sunoj
johnsunoj@gmail.com
P. V. Vara Prasad
vara@ksu.edu

Specialty section:
This article was submitted to Plant Abiotic Stress, a section of the journal Frontiers in Plant Science

Received: *09 April 2020*
Accepted: *31 July 2020*
Published: *19 August 2020*

Citation:
Sunoj VSJ, Prasad PVV, Ciampitti IA and Maswada HF (2020) Narrowing Diurnal Temperature Amplitude Alters Carbon Tradeoff and Reduces Growth in C_4 Crop Sorghum. Front. Plant Sci. 11:1262. doi: 10.3389/fpls.2020.01262

Effect of diurnal temperature amplitude on carbon tradeoff (photosynthesis vs. respiration) and growth are not well documented in C_4 crops, especially under changing temperatures of light (daytime) and dark (nighttime) phases in 24 h of a day. Fluctuations in daytime and nighttime temperatures due to climate change narrows diurnal temperature amplitude which can alter circadian rhythms in plant, thus influence the ability of plants to cope with temperature changes and cause contradictory responses in carbon tradeoff, particularly in night respiration during dark phase, and growth. Sorghum [*Sorghum bicolor* (L.) Moench] is a key C_4 cereal crop grown in high temperature challenging agro-climatic regions. Hence, it is important to understand its response to diurnal temperature amplitude. This is the first systematic investigation using controlled environmental facility to monitor the response of sorghum to different diurnal temperature amplitudes with same mean temperature. Two sorghum hybrids (DK 53 and DK 28E) were grown under optimum (27°C) and high (35°C) mean temperatures with three different diurnal temperature amplitudes (2, 10, and 18°C) accomplished by modulating daytime and nighttime temperatures [optimum daytime and nighttime temperatures (ODNT): 28/26, 32/22, and 36/18°C and high daytime and nighttime temperatures (HDNT): 36/34, 40/30, and 44/26°C]. After exposure to different temperature conditions, total soluble sugars, starch, total leaf area and biomass were reduced, while night respiration and specific leaf area were increased with narrowing of diurnal temperature amplitude (18 to 2°C) of HDNT followed by ODNT. However, there was no influence on photosynthesis across different ODNT and HDNT. Contradiction in response of foliar gas exchange and growth suggests higher contribution of night respiration for maintenance rather than growth with narrowing of diurnal temperature amplitude of ODNT and HDNT. Results imply that diurnal temperature amplitude has immense impact on the carbon tradeoff and growth, regardless of hybrid variation. Hence, diurnal temperature amplitude and night respiration should be considered while quantifying response and screening for high

temperature tolerance in sorghum genotypes and comprehensive understanding of dark phase mechanisms which are coupled with stress response can further strengthen screening procedures.

Keywords: high night temperature, diurnal temperature amplitude, sorghum, night respiration, carbohydrates composition, growth

INTRODUCTION

Sorghum (*Sorghum bicolor* (L.) Moench) is an economically important C_4 cereal crop for more than 500 million people around the globe due to its versatile usage as staple food, bioenergy, feed for livestock and industrial products (Maikasuwa and Ala, 2013; Tari et al., 2013; Ciampitti and Prasad, 2020). Sorghum occupies an important role in global food security along with other cereal crops such as wheat, millets, rice and maize (Ciampitti and Prasad, 2020; Maswada et al., 2020). Sorghum is relatively hardy crop as compared to C_3 cereal crops, mainly grown in the semi-arid regions. In C_4 crops, C_4 photosynthetic pathway and related anatomical advantages enable them to tolerate warmer temperatures compared to C_3 crops by maintaining photosynthesis *via*, concentrating CO_2 and promoting the carboxylase activity of ribulose 1,5 bisphosphate carboxylate/oxygenase (Rubisco) and reducing the oxygenation activity (Sage and Kubien, 2007; Wang et al., 2012). However, anticipated more abrupt changes in weather, high daytime and nighttime temperatures can be important limiting factors for the growth, development and productivity of sorghum (Prasad et al., 2006b; Prasad et al., 2008a; Djanaguiraman et al., 2014).

Temperature and light cycles of light (day) and dark (night) phases of 24 h of a day synchronize circadian rhythms which includes subcellular level (gene expression, calcium signaling and activities of enzymes) and cell and tissue level (gas exchange, seed germination, hypocotyl elongation and behavior of leaves, flowers, and stomata) cycles to adjust with existing environmental conditions. Meanwhile, changes in temperature cycle, either increase or decrease in daytime or nighttime temperature, can adversely affect normal rhythmic response of plants (McClung, 2006; Srivastava et al., 2019). Negative impacts of high daytime and nighttime temperatures on different cereal crops has been well documented including in finger millet (Opole et al., 2018), maize (Sunoj et al., 2016; Lizaso et al., 2018), rice (Prasad et al., 2006a; Lin et al., 2020; Wang et al., 2020), and wheat (Prasad et al., 2008b; Prasad et al., 2015; Impa et al., 2018).

Each crop has cardinal or critical temperatures (minimum temperature, optimum temperature, and maximum temperature) with thresholds below (minimum temperature) or above (maximum temperature) in which no growth or development or physiological process occurs. Temperatures below and above optimum negatively impacts physiological process, traits, growth, development, and yield. Any growth temperature is the mean of daytime maximum and nighttime minimum temperatures. The same mean temperature can be obtained by different daily temperature (either daytime maximum and nighttime minimum temperatures or diurnal temperature range or amplitude). Identification of mean temperature threshold of growing season (different phenological stages) and responses of crop or process to different temperatures provides basis for quantifying impacts of climate change and adaptation options (Luo, 2011). For sorghum, the maximum critical threshold mean temperature is considered as 34°C (Hammer et al., 1993; Maiti, 1996), while, the optimum daytime and nighttime temperatures are 32 and 22°C, respectively (mean temperature of 27°C) (Prasad et al., 2006b). On a global scale prediction by inter-governmental panel for climate change (IPCC), pointed out a rise of 1.5 to 2°C in mean temperature by end of the 21st century which is expected to be accompanied with more frequent heat waves and warmer nights (IPCC, 2018). These can negatively affect sorghum productivity, thereby a threat to global food security and economic status of farming community and allied industries.

In sorghum, high daytime and nighttime temperatures are reported to cause abortion of flowers, reduced pollen germination, phospholipid saturation of pollen, seed set, grain number and yield, biomass accumulation, photosynthesis, quantum yield of PS II, activities of antioxidant enzymes and increased reactive oxygen species (ROS), leaf night respiration, and thylakoid membrane damage (Prasad et al., 2006b; Prasad and Djanaguiraman, 2011; Djanaguiraman et al., 2014; Prasad et al., 2015; Singh et al., 2015; Sunoj et al., 2017; Djanaguiraman et al., 2018a; Narayanan et al., 2018). Even though, high daytime and nighttime temperatures negatively affect crops, nighttime temperature is more critical for crops grown on larger spatial or temporal scales. High nighttime temperature is negatively affecting at wide range of growth and developmental stages of crops and influencing responses of morphological, physiological, biochemical, and yield traits (Peng et al., 2004; Prasad et al., 2008a; Prasad et al., 2008b; Mohammed and Tarpley, 2009; Welch et al., 2010; Lobell et al., 2012; Djanaguiraman et al., 2013; Narayanan et al., 2015; Djanaguiraman et al., 2018b; Impa et al., 2018; Opole et al., 2018). Furthermore, due to climate change the rate of increase in daytime and nighttime temperatures can differ leading to lower diurnal amplitude (difference between daytime maximum and nighttime minimum temperatures) (Vose et al., 2005; Wang et al., 2017). Lower diurnal amplitude can negatively influence crop growth (Sunoj et al., 2016).

Abbreviations: ODNT, optimum daytime and nighttime temperature; HDNT, high daytime and nighttime temperature; *Fv*/*Fm*, maximum photochemical efficiency of PSII; PAR, photosynthetic active radiation; TB, total aboveground biomass accumulation; TLA, total leaf area; SLA, Specific leaf area; TSS, total soluble sugars; RS, reducing sugars; NRS, non-reducing sugars.

Studies to understand the effect of different diurnal temperature amplitudes with same mean temperature on C_4 cereal crops are limited as compared to response of crops to either high daytime and nighttime temperatures (Myster and Moe, 1995; Sunoj et al., 2016). There are few studies to understand the effect of diurnal temperature amplitudes has been reported in different C_3 crops such as cucumber (Xiong et al., 2011), orange (Bueno et al., 2012), eggplant, sweet pepper, tomato, melon, and watermelon (Inthichack et al., 2013; Inthichack et al., 2014; Matsuda et al., 2014). These studies revealed that diurnal temperature amplitude influence several morphological traits, foliar mineral composition, gas exchange and carbohydrate composition and metabolism. Hence, it is important to understand such responses in key food grain crops such as sorghum.

Important role of photosynthesis during light phase of a day in plant growth is beyond doubt. Response of light and dark phase gas exchange [day-time photosynthesis (CO_2 assimilation) and night-time respiration (CO_2 release), respectively] revealed that diurnal temperature amplitude induced night respiration during dark phase of a day has important role in carbon tradeoff (photosynthesis verses night respiration) which is one of the important factor determines the magnitude of growth along with other leaf traits and light interception (Hammer and Muchow, 1994; Ravi Kumar et al., 2009; Sunoj et al., 2016; Impa et al, 2018). Our study on C_4 cereal crop maize [hybrid maize (DKC 47-27RIB, DEKALB, USA); Sunoj et al., 2016] systematically demonstrated the impact of different diurnal temperature amplitudes (2, 8, and 10°C) with optimum (30°C) and high (35°C) mean temperatures on vegetative growth. The study proved that, narrowing of diurnal temperature amplitude did not affected photosynthesis, but it increased leaf night respiration and reduced growth. At the same time, intensity of impact of narrowing of diurnal temperature amplitude on plant growth was varied among optimum and high mean temperature conditions.

Though, above study on maize provided a new insights on plant response to diurnal temperature amplitude and night respiration along with photosynthesis, it does not account the possibility of crop to crop variation and maintaining same or showing contrasting pattern of responses among different genotypes of same crop. It is also crucial to understand how sorghum, a relative more tolerant crop to abiotic stresses compared to maize, respond to these changes and current study is relevant as the sorghum grown in such regions which are experiencing and expecting higher temperatures in near future. Furthermore, based on available literatures, there are no reports dealing with response of sorghum to diurnal temperature amplitudes with an emphasis on carbon tradeoff and growth. Hence, this study was conducted to understand change in the pattern of response among different genotypes of same crop. To fill this knowledge gap, we performed current study with specific objective to quantify the impact of diurnal temperature amplitudes on growth, carbohydrate composition and carbon tradeoff in two sorghum hybrids. This research will help us to understand the dark phase processes, night respiration, and carbon utilization under temperature stress conditions. The results can be used to modify and strengthen the screening protocol for high temperature tolerance in sorghum. We hypothesize that dark phase (carbohydrate utilization *via* night respiration) and light phase (carbohydrate synthesis *via* photosynthesis) response are equally important and differentially influenced by diurnal temperature amplitude, thus affecting carbon trade-off and growth of sorghum genotypes.

MATERIALS AND METHODS

Plant Material and Growth Conditions

The research was carried out using controlled environment facility at the Department of Agronomy, Kansas State University, Manhattan, Kansas, USA. Two *Sorghum bicolor* (L.) Moench hybrids (DK 53 and DK 28E; DEKALB, USA) were used for study. The sorghum seedlings were grown in 7 L plastic pots (21 cm height and 22 cm width) filled with growing medium (Metro mix 360 growing medium, Hummert International, Topeka, Kansas, USA). Pots were fertilized before sowing with macronutrients [35 g per pot; Osmocote classic; controlled release plant nutrients (14:14:14 NPK)], micronutrient (4 g per pot; Micro max; Hummert International, Topeka, Kansas, USA) and liquid iron (Iron 5%: Bonide products, Oriskany, New York, USA). Three seeds per pot were sown at a depth of 5 cm. To avoid incidence of sucking pest, 1 g of systemic insecticide Marathon {1% Imidacloprid, 1-[(6-Chloro-3-pyridinyl) methyl]-N-nitro-2-imidazolidin-mine; OHP Inc, Maryland, Pennsylvania, USA} was applied to each pot.

After sowing, pots were maintained inside growth chambers (Conviron Model PGR15; Winnipeg, MB, Canada) with controlled daytime and nighttime temperature conditions (32/22°C; optimum mean temperature 27°C), relative humidity (60% RH), 12 h of photoperiod (0600 to 1800 h) and photosynthetic active radiation (PAR) of 800 m mol m^{-2} s^{-1} at the plant canopy level using cool fluorescent lamps. To replicate the diurnal temperature variations in natural condition, a transition time of 7 h was set from day time maximum to night time minimum and *vice versa*. Air temperature was monitored at 10 min intervals throughout the experiment using HOBO data logger (Onset UTBi-001; TidbiT v2 Temperature logger; Bourne, Massachusetts, USA).

Temperature Conditions

At third leaf stage [vegetative growth stage (GS-1); subdivision: third leaf collar stage (S1); Roozeboom and Prasad, 2016], sorghum seedlings were thinned to one plant per pot and growth chamber temperatures were adjusted to two different mean temperature conditions [optimum mean daytime and nighttime temperature (ODNT); 27°C and high mean daytime and nighttime temperature (HDNT); 35°C] with three different combinations of daytime and nighttime temperatures resulting in diurnal temperature amplitudes of 2, 10, and 18°C in different growth chambers (Sunoj et al., 2016). Three chambers were programmed with ODNT and other three chambers with HDNT. The diurnal temperature amplitudes (2, 10, and 18°C) with the ODNT was established by adjusting the daytime and

nighttime temperatures (°C ± SD; standard deviation) to 28°C (± 0.3)/26°C (± 0.4), 32°C (± 0.5)/22°C (± 0.6), and 36°C (± 0.4)/18°C (± 0.6). Similarly, for achieving the different temperature amplitude with same HDNT, the dayime and nighttime temperatures were adjusted to 36°C (± 0.5)/34°C (± 0.3), 40°C (± 0.5)/30°C (± 0.5), and 44°C (± 0.4)/26°C (± 0.6) (**Figure 1**). Another independent experiment was repeated with similar growth conditions, genotypes and temperature conditions. A common set of growth, physiological and biochemical traits were recorded from both the experiments after exposing the seedlings to different temperature conditions for 40 days [reproductive growth stage (GS-2); subdivision: booting stage (S5); Roozeboom and Prasad, 2016].

Foliar Gas Exchange and Photochemical Efficiency of PS II

Photosynthesis and night respiration were recorded from fully expanded mature leaves of sorghum seedlings using portable photosynthesis system (LI-6400 XT; LI-COR, Lincoln, NE, USA). On the final day (40^{th} day) of exposure to different temperature conditions, a minimum of six photosynthesis and night respiration measurements were recorded between 10:00 to 10:15 h and 22:00 to 22:15 h (growth chamber time settings), respectively. In order to maintain equal duration of exposure to day and night temperatures and light and dark phase, growth chamber programs were systematically adjusted to delay by 40 min between chamber to chamber from the actual time, which helped to over-come the time lag between chambers while measuring photosynthesis and leaf night respiration. This adjustment allowed us to capture the leaf photosynthesis and night respiration measurements exactly after 4 h exposure to light (PAR; 800 µmol m^{-2} s^{-1}; 0600 h to 1000 h) and dark (PAR; 0 µmol m^{-2} s^{-1}; 1800 to 2200 h) across all different temperature conditions. The CO_2 concentration was set to 400 µmol mol^{-1} in the leaf chamber of the portable photosynthesis system and block temperature was adjusted to respective day (while measuring photosynthesis) and night (while measuring night respiration) temperature according to the growth chamber setting. The flow rate for photosynthesis measurement was 500 µmol s^{-1} and was adjusted to 100 µmol s^{-1} for measuring night respiration to minimize fluctuations (using the Li-6400/Li-6400XT; Portable Photosynthesis System; Version 6; LI-COR, Lincoln, Nebraska, USA; Sunoj et al., 2016). While measuring night respiration, sufficient care was taken to avoid exposure to PAR from any external sources and prior to recording night respiration, it was further confirmed by measuring the light with light sensor reader and six sensor quantum bar (field scout and light scout; Spectrum technologies, Inc., Aurora, Illinois, USA).

Maximum photochemical efficiency of PSII (*Fv*/*Fm*) of sorghum leaves was measured between 1000 and 1015 h after 30 min of dark adaptation using chlorophyll fluorometer (OS30p+; OptiSciences, Hudson, New Hampshire, USA) with light pulse intensity of 3000 µmol m^{-2} s^{-1} and pulse duration of 3 s (Sunoj et al., 2016).

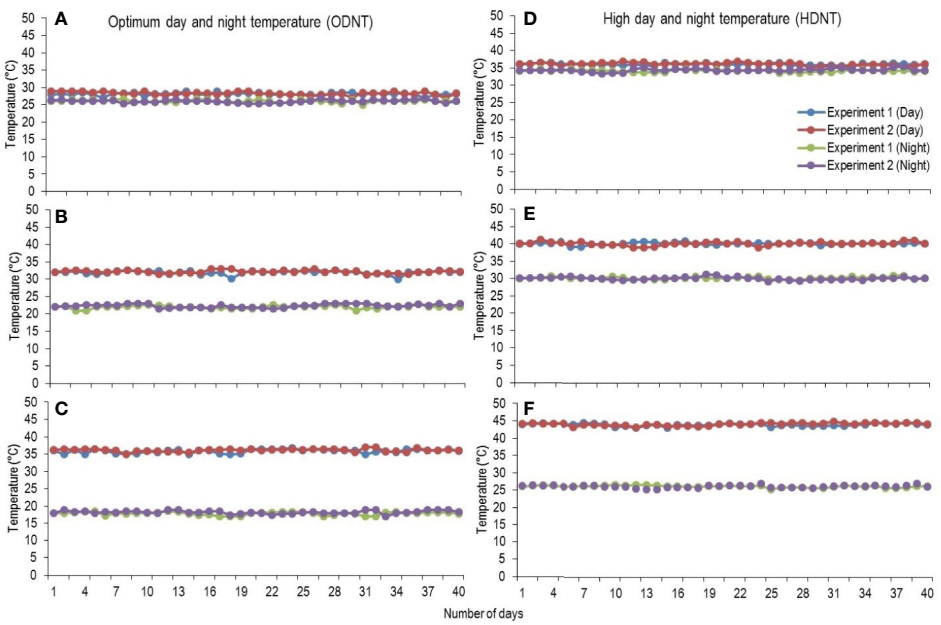

FIGURE 1 | Maximum daytime (from 10:00 h to 14:00 h) and minimum nighttime temperature (from 22:00 h to 02:00 h) of two mean temperatures (27 and 35°C) with three diurnal temperature amplitudes (2 10, and 18°C) exposure lasting 40 days in controlled environment chambers. Mean optimum temperature [optimum mean daytime and nighttime temperature (ODNT)] 27°C: **(A)** Day/night temperature 28/26°C (diurnal temperature amplitude 2°C), **(B)** 32/22°C (diurnal temperature amplitude 10°C) and **(C)** 36/18°C (diurnal temperature amplitude 18°C). Mean high temperature [high mean day/night temperature (HDNT)] 35°C: **(D)** Day/night temperature 36/34°C (diurnal temperature amplitude 2°C), **(E)** 40/30°C (diurnal temperature amplitude 10°C) and **(F)** 44/26°C (diurnal temperature amplitude 18°C).

Carbohydrate Composition

At the end of temperature exposure, contents of total soluble sugars (TSS), reducing sugars (RS), non-reducing sugars (NRS), and starch were determined from the middle portion of fully opened mature leaves (without midrib). Tissue samples were collected from same leaves immediately after recording photosynthesis and immersed in liquid nitrogen and stored at -80°C until further analysis. Each sample was ground into powder using liquid nitrogen, homogenized thoroughly with ethanol (70%) and incubated at 70°C in a water bath for 30 min and filtered. The filtrate was used for the estimation of TSS [Phenol sulfuric acid method (Dubois et al., 1956)] and RS [Nelson Somogyi method (Somogyi, 1952)]. The NRS were estimated from the difference between TSS and RS (Malhotra and Sarkar, 1979). After filtration, the filter paper with the solid residue was kept in hot air oven at 50°C for drying and the dried residue was carefully collected and used for the estimation of starch by following anthrone method by Hedge and Hofreiter (1962).

Total Above Ground Biomass Accumulation, Total Leaf Area, and Specific Leaf Area

Leaves were detached from the shoot and packed in zip lock bags to avoid drying and total leaf area (TLA) was measured using leaf area meter (LI 3100 area meter, LI-COR, Lincoln, Nebraska, USA). The total above ground biomass (TB) accumulation was calculated by cutting the plants from base and drying at 60°C in hot air oven until constant weight was obtained. The leaves that were detached to measure leaf area also included to calculate total biomass. Specific leaf area (SLA) was estimated by as ratio of total leaf area to the leaf dry weight (leaf area/leaf dry weight).

Experimental Design and Statistical Analysis

Two independent controlled environmental chamber experiments were conducted with four biological replications per genotype per temperature conditions. The experimental design was randomized complete block (RCBD) for both experiments. Analysis of variance (ANOVA) was performed for all the measured traits using generalized linear model (GLM) in SPSS (SPSS Inc. Ver.16, USA) using temperatures, hybrids and their interactions as factors. The means were compared using Tukey's honestly significant difference (HSD) range test. Correlations and regressions among different traits were performed using Sigma Plot (Systat Inc. Ver. 12.5, USA).

RESULTS

Across two indepentend experiments, there were significant (P<0.05) effect of temperature and hybrids when exposed to optimum (27°C; ODNT) and high (35°C; HDNT) daytime and nighttime temperatures with three diurnal temperature amplitudes (2, 10, and 18°C) on several physiological, biochemical and growth traits (**Tables 1** and **2**). Interaction effect of hybrids and temperature conditions was significant (P<0.05) on nine out of 10 measured traits (**Tables 1** and **2**). When exposed to different temperature conditions, both hybrids and measured traits were followed the same pattern in both experiments, which confirming the consistency and repeatability in results and response of hybrids. To demonstrate this, data from two independent experiments are independently presented here.

Effects on Growth

In spite of differences among hybrids and diurnal temperature amplitudes, growth of seedlings indicated by total aboveground biomass accumulation (TB) and total leaf area (TLA) were significantly (P<0.01) higher and specific leaf area (SLA) was significantly (P<0.05) lower under ODNT compared to HDNT (**Table 1**). At the same time, TB and TLA of both hybrids were reduced and SLA was increased with narrowing diurnal temperature amplitude (18 to 2°C) regardless of two mean temperatures (ODNT and HDNT) (**Table 1** and **Figure 2**). Seedlings exposed to ODNT with highest diurnal temperature amplitude (18°C) recorded higher TB and TLA; and lowest SLA, while lowest TB and TLA and higher SLA was observed under HDNT with narrow diurnal temperature amplitude (2°C) across different day and night conditions (**Table 1** and **Figure 2**).

Among the hybrids, DK 28E attained higher TB, TLA, and SLA across all the diurnal temperature amplitudes irrespective of both different mean temperatures, expect an opposite trend in TB and TLA at narrow diurnal temperature amplitude of 2°C (**Figure 2**). On an average of two experiments, as compared to narrow diurnal temperature amplitude (2°C) with ODNT and HDNT, highest percentage increase of 189% in TB was in DK 28E and 58% in TLA was in DK 53 under highest diurnal temperature amplitude (18°C) with ODNT, while highest percentage reduction of 19% in SLA was observed in DK 53 (**Table 3**).

Effects on Carbon Tradeoff and Photochemical Efficiency of PSII

There was a contradiction observed in carbon tradeoff (photosynthesis *vs.* night respiration) in both hybrids exposed to different temperature conditions. Photosynthesis was not significantly varied across different diurnal temperature amplitudes with different mean temperatures and among hybrids, while there was a distinct variation found in night respiration (**Tables 1** and **3** and **Figure 3**). The night respiration was significantly (P<0.01) higher across different diurnal temperature amplitudes with HDNT compared to diurnal temperature amplitudes with ODNT (**Table 1**). Night respiration was 37% and 48% less in DK 53 and 36% and 47% in DK 28E under 18°C diurnal temperature amplitudes with ODNT and HDNT, respectively, as compared to 2°C (**Table 3**). Regardless of different mean temperatures, magnitude of night respiration was increased with narrowing diurnal temperature amplitude, and among hybrids, DK 53 showed slightly higher increase than DK 28 (**Figure 3**). Meanwhile,

TABLE 1 | Effect of two mean temperatures [27°C (optimum mean daytime and nighttime temperature; ODNT) and 35°C (high mean daytime and nighttime temperature; HDNT)] with three diurnal temperature amplitudes (2, 10, and 18°C) on growth and carbon tradeoff in sorghum hybrids (DK 53 and DK 28E).

Temperature conditions (T)		Total biomass (g plant^{-1})	Total leaf area (dm^2 plant^{-1})	Specific leaf area(cm^2 g^{-1}DW)	Photosynthesis (μmol m^{-2} s^{-1})	Photochemical efficiency of PSII (*Fv*/*Fm*)	Night respiration (μmol m^{-2} s^{-1})
Experiment I							
Day/Night temperature	Temperature amplitude						
Optimum (ODNT; 27°C)							
28/26°C	2°C	116.6 ± 11.5^{c}	89.21 ± 2.62^{c}	187.6 ± 7.21^{a}	24.31 ± 1.09^{a}	0.795 ± 0.005^{a}	0.499 ± 0.001^{c}
32/22°C	10°C	228.6 ± 10.5^{b}	110.3 ± 3.65^{b}	176.4 ± 8.44^{b}	23.22 ± 1.30^{a}	0.790 ± 0.005^{ab}	0.426 ± 0.002^{e}
36/18°C	18°C	281.1 ± 11.0^{a}	128.8 ± 5.21^{a}	166.5 ± 6.35^{c}	23.91 ± 1.55^{a}	0.780 ± 0.005^{cd}	0.347 ± 0.001^{f}
Mean		208.8 ± 10.5	109.4 ± 3.6	176.8 ± 7.4	23.81 ± 1.5	0.788 ± 0.005	0.424 ± 0.001
High (HDNT; 35°C)							
36/34°C	2°C	79.57 ± 10.6^{d}	75.83 ± 2.02^{d}	217.9 ± 5.23^{a}	22.79 ± 1.60^{a}	0.770 ± 0.005^{e}	0.802 ± 0.002^{a}
40/30°C	10°C	110.5 ± 11.4^{c}	80.68 ± 2.74^{d}	195.2 ± 7.82^{b}	22.77 ± 1.35^{a}	0.775 ± 0.003^{de}	0.575 ± 0.002^{b}
44/26°C	18°C	127.8 ± 9.95^{c}	105.7 ± 4.06^{b}	183.7 ± 8.56^{bc}	22.44 ± 1.32^{a}	0.785 ± 0.003^{bc}	0.476 ± 0.002^{d}
Mean		106.0 ± 10.2**	87.41 ± 2.4**	198.9 ± 7.2*	22.67 ± 1.2^{NS}	0.777 ± 0.003*	0.617 ± 0.002**
Hybrids (H)							
	DK 53	136.4 ± 11.1	90.35 ± 2.98	187.4 ± 7.80	22.78 ± 1.28	0.787 ± 0.004	0.542 ± 0.001
	DK 28E	178.4 ± 10.5**	106.5 ± 3.78**	188.3 ± 6.51^{NS}	23.70 ± 1.46^{NS}	0.778 ± 0.003 ^{NS}	0.500 ± 0.002*
Probability values							
	T	<0.01	<0.01	<0.01	0.183	<0.05	<0.01
	H	<0.01	<0.01	0.738	0.059	<0.652	<0.01
	T x H	<0.01	<0.01	<0.05	0.089	<0.05	<0.01
Experiment II							
Optimum (ODNT; 27°C)							
28/26°C	2°C	109.8 ± 11.0^{de}	82.05 ± 2.16^{e}	197.5 ± 10.2^{a}	23.60 ± 1.35^{a}	0.795 ± 0.004^{a}	0.521 ± 0.002^{c}
32/22°C	10°C	206.5 ± 10.95^{b}	118.2 ± 4.32^{b}	179.2 ± 9.41^{b}	22.75 ± 1.55^{a}	0.780 ± 0.003^{b}	0.425 ± 0.002^{d}
36/18°C	18°C	249.7 ± 11.55^{a}	132.0 ± 4.94^{a}	165.3 ± 6.33^{bc}	23.30 ± 1.51^{a}	0.795 ± 0.003^{a}	0.305 ± 0.003^{f}
Mean		188.7 ± 10.2	110.7 ± 3.2	180.7 ± 8.1	23.22 ± 1.23	0.790 ± 0.003	0.417 ± 0.002
High (HDNT; 35°C)							
36/34°C	2°C	88.31 ± 8.55^{e}	73.36 ± 2.12^{f}	213.3 ± 11.4^{a}	23.00 ± 1.90^{a}	0.780 ± 0.003^{b}	0.895 ± 0.002^{a}
40/30°C	10°C	122.1 ± 9.80^{cd}	90.66 ± 2.84^{d}	199.6 ± 10.5^{b}	23.80 ± 1.55^{a}	0.774 ± 0.003^{b}	0.535 ± 0.001^{b}
44/26°C	18°C	138.4 ± 12.2^{c}	105.4 ± 3.82^{c}	182.9 ± 6.93^{c}	22.91 ± 1.60^{a}	0.775 ± 0.007^{b}	0.420 ± 0.002^{e}
Mean		116.2 ± 11.2**	89.79 ± 3.2**	198.6 ± 7.4*	23.24 ± 1.50^{NS}	0.776 ± 0.005*	0.617 ± 0.002**
Hybrids (H)							
	DK 53	130.1 ± 11.2	91.56 ± 2.94	186.9 ± 6.9	23.15 ± 1.58	0.783 ± 0.003	0.537 ± 0.002
	DK 28E	174.8 ± 10.2**	109.0 ± 3.79**	192.3 ± 8.2 ^{NS}	23.30 ± 1.57^{NS}	0.783 ± 0.004^{NS}	0.497 ± 0.002*
Probability values							
	T	<0.01	<0.01	<0.01	0.840	<0.05	<0.01
	H	<0.01	<0.01	<0.068	0.777	0.796	<0.05
	T x H	<0.01	<0.01	<0.05	0.576	<0.05	<0.01

*Values in each column are mean of both sorghum hybrids (DK 53and DK 28E) with ± standard error under different day and night temperatures of ODNT and HDNT. Values followed by different letters indicates significant difference according to Tukey's HSD (P<0.01; the test was conducted independently for each experiments). The mean values of ODNT and HDNT (irrespective of hybrids and three diurnal temperature amplitudes) and two sorghum hybrids (DK 53and DK 28E; irrespective of three diurnal temperature amplitudes of ODNT and CDNT) were compared using student's t-test and * and ** corresponding to significance at P < 0.05 and P < 0.01, respectively. NS indicate non-significant.*

photochemical efficiency of PSII (*Fv*/*Fm*) of both hybrids under different diurnal temperature amplitudes of HDNT and ODNT was not uniform in both experiments (**Tables 1** and **3**). HDNT slightly reduced *Fv*/*Fm* compared with ODNT (**Table 1**). Though there was a significant difference (P<0.05) among temperature conditions and its interaction with hybrids, values of *Fv*/*Fm* ranged between 0.77 to 0.81 across hybrids, temperature conditions, and experiments (**Figure 3**).

Effects on Carbohydrate Composition of Sorghum Hybrids

In both experiments, content of total soluble sugars (TSS), reducing sugars (RS), non-reducing sugars (NRS) and starch of both hybrids were significantly (P<0.01) altered after the exposure to different temperature conditions (**Table 2**). TSS, NRS, RS, and starch were reduced with narrowing diurnal temperature amplitudes (18 to 2°C), except RS under HDNT which showed an opposite trend (**Figure 4**). Regardless of the diurnal temperature amplitudes, across both experiments, carbohydrate composition was decreased under HDNT compared with ODNT (**Table 2**).

On an average, among hybrids, percentage increase in majority of carbohydrate components were high in DK 28E than DK 53 under diurnal temperature amplitude of 18°C with ODNT (195% in TSS, 397% in NRS, and 33% in starch) and HDNT (78% in TSS, 195% in NRS, and 49% in starch) as compare to 2°C diurnal amplitude (**Table 4**). At the same time, an opposite trend in hybrid response was observed in RS (**Figure 4**).

TABLE 2 | Effect of two mean temperatures [27°C (optimum mean daytime and nighttime temperature; ODNT) and 35°C (high mean daytime and nighttime temperature; HDNT)] with three diurnal temperature amplitudes (2, 10, and 18°C) on carbohydrate composition in sorghum hybrids (DK 53 and DK 28E).

Temperature conditions (T)		Total soluble sugars (mg g^{-1} DW)	Reducing sugars (mg g^{-1} DW)	Non-reducing sugars (mg g^{-1} DW)	Starch (mg g^{-1} DW)
Experiment I					
Day/Night temperature	Temperature amplitude				
Optimum (ODNT; 27°C)					
28/26°C	2°C	5.05 ± 0.06^{c}	2.30 ± 0.08^{b}	2.75 ± 0.09^{e}	144.5 ± 7.37^{bc}
32/22°C	10°C	6.25 ± 0.05^{b}	2.15 ± 0.06^{bc}	4.10 ± 0.05^{c}	169.5 ± 6.55^{a}
36/18°C	18°C	14.1 ± 0.05^{a}	4.55 ± 0.07^{a}	9.55 ± 0.07^{a}	181.0 ± 5.10^{a}
Mean		8.47 ± 0.05	3.00 ± 0.07	5.47 ± 0.08	165.0 ± 6.21
High (HDNT; 35°C)					
36/34°C	2°C	3.70 ± 0.08^{d}	2.00 ± 0.07^{c}	1.70 ± 0.06^{f}	116.0 ± 5.20^{d}
40/30°C	10°C	4.70 ± 0.07^{c}	1.60 ± 0.07^{d}	3.10 ± 0.05^{d}	135.5 ± 5.15^{c}
44/26°C	18°C	6.00 ± 0.08^{b}	1.35 ± 0.06^{e}	4.65 ± 0.07^{b}	155.0 ± 6.40^{b}
Mean		4.80 ± 0.08**	1.65 ± 0.06*	3.15 ± 0.06*	135.5 ± 5.5*
Hybrids (H)					
	DK 53	6.13 ± 0.13	2.13 ± 0.08	4.00 ± 0.07	137.3 ± 6.01
	DK 28E	7.13 ± 0.16*	2.52 ± 0.06*	4.62 ± 0.06*	163.2 ± 5.92**
Probability values					
	T	<0.01	<0.01	<0.01	<0.01
	H	<0.05	<0.05	<0.05	<0.01
	T x H	<0.01	<0.01	<0.01	<0.05
Experiment II					
Optimum DNT (27°C)					
28/26°C	2°C	5.00 ± 0.04^{c}	3.25 ± 0.04^{c}	1.75 ± 0.06^{d}	141.0 ± 4.10^{c}
32/22°C	10°C	6.60 ± 0.05^{b}	3.75 ± 0.07^{b}	2.85 ± 0.08^{c}	169.5 ± 6.55^{b}
36/18°C	18°C	11.95 ± 0.30^{a}	5.05 ± 0.07^{a}	6.90 ± 0.07^{a}	193.5 ± 8.10^{a}
Mean		7.85 ± 0.04	4.02 ± 005	3.83 ± 0.06	168.0 ± 6.5
High (HDNT; 35°C)					
36/34°C	2°C	3.85 ± 0.07^{d}	2.20 ± 0.04^{d}	1.65 ± 0.07^{d}	112.0 ± 4.70^{d}
40/30°C	10°C	4.75 ± 0.07^{c}	1.75 ± 0.04^{e}	3.00 ± 0.05^{c}	137.5 ± 6.20^{c}
44/26°C	18°C	6.65 ± 0.07^{b}	1.50 ± 0.04^{f}	5.15 ± 0.08^{b}	161.0 ± 4.45^{b}
Mean		5.08 ± 0.07**	1.82 ± 0.047**	3.27 ± 0.06^{NS}	136.8 ± 0.05**
Hybrids (H)					
	DK 53	6.13 ± 0.08	2.87 ± 0.05	3.27 ± 0.06	146.0 ± 5.88
	DK 28E	6.80 ± 0.12*	2.97 ± 0.05*	3.83 ± 0.07*	158.8 ± 5.48*
Probability values					
	T	<0.01	<.01	<0.01	<0.01
	H	<0.05	<0.05	<0.05	<0.05
	T x H	<0.01	<0.01	<0.01	<0.01

*Values in each column are mean of both sorghum hybrids (DK 53 and DK 28E) with ± standard error under different day and night temperatures of ODNT and HDNT. Values followed by different letters indicates significant difference according to Tukey's HSD (P<0.01; the test was conducted independently for each experiments). The mean values of ODNT and HDNT (irrespective of hybrids and three diurnal temperature amplitudes) and two sorghum hybrids (DK 53and DK 28E; irrespective of three diurnal temperature amplitudes of ODNT and CDNT) were compared using student's t-test and * and ** corresponding to significance at P < 0.05 and P < 0.01, respectively. NS indicate non-significant.*

Relationship of Night Respiration With Growth Traits and Carbohydrates

Total biomass was positively correlated with starch (n=72; $P<0.01$; $R^2 = 0.77$) and TSS (n=72; $P<0.01$; $R^2 = 0.73$) while negatively with night respiration (n=72; $P<0.01$; $R^2 = 0.52$) (**Figure 5**). Night respiration showed significant negative relationships with TSS (n=72; $P<0.01$; $R^2 = 0.49$), RS (n=72; $P<0.01$; $R^2 = 0.23$), NRS (n=72; $P<0.01$; $R^2 = 0.48$) and starch (n=72; $P<0.01$; $R^2 = 0.73$) (**Figures 6A–D**). TLA was positively correlated with starch (n=72; $P<0.01$; $R^2 = 0.90$), TSS (n=72; $P<0.01$; $R^2 = 0.65$) and TB (n=72; $P<0.01$; $R^2 = 0.78$) and negatively with SLA (n=72; $P<0.01$; $R^2 = 0.44$) (**Figures 7A–D**). Meanwhile, a weak relationship was observed between night respiration and *Fv*/*Fm* as well as with photosynthesis (data not shown). Night respiration showed negative correlation with TLA (n=72; $P<0.01$; $R^2 = 0.64$) and positive correlation with SLA (n=72; $P<0.01$; $R^2 = 0.62$) (**Supplementary Figure S1**). SLA was negatively correlated with starch (n=72; $P<0.01$; $R^2 = 0.41$), TSS (n=72; $P<0.01$; $R^2 = 0.40$) and TB (n=72; $P<0.01$; $R^2 = 0.33$) (**Supplementary Figure S2**).

DISCUSSION

Our current study shows that narrowing of diurnal temperature amplitude (18 to 2°C) caused reduction in total leaf area and above ground total biomass along with an increase in night respiration and SLA and changes in carbohydrate composition [total soluble sugars, reducing sugars, non-reducing sugars and starch] in selected sorghum hybrids (**Figures 2–4**). However, photosynthesis was not affected with changes in diurnal temperature amplitude ranges (2, 10, and 18°C) tested in this study indicating altered carbon tradeoff (**Figure 3**). Overall

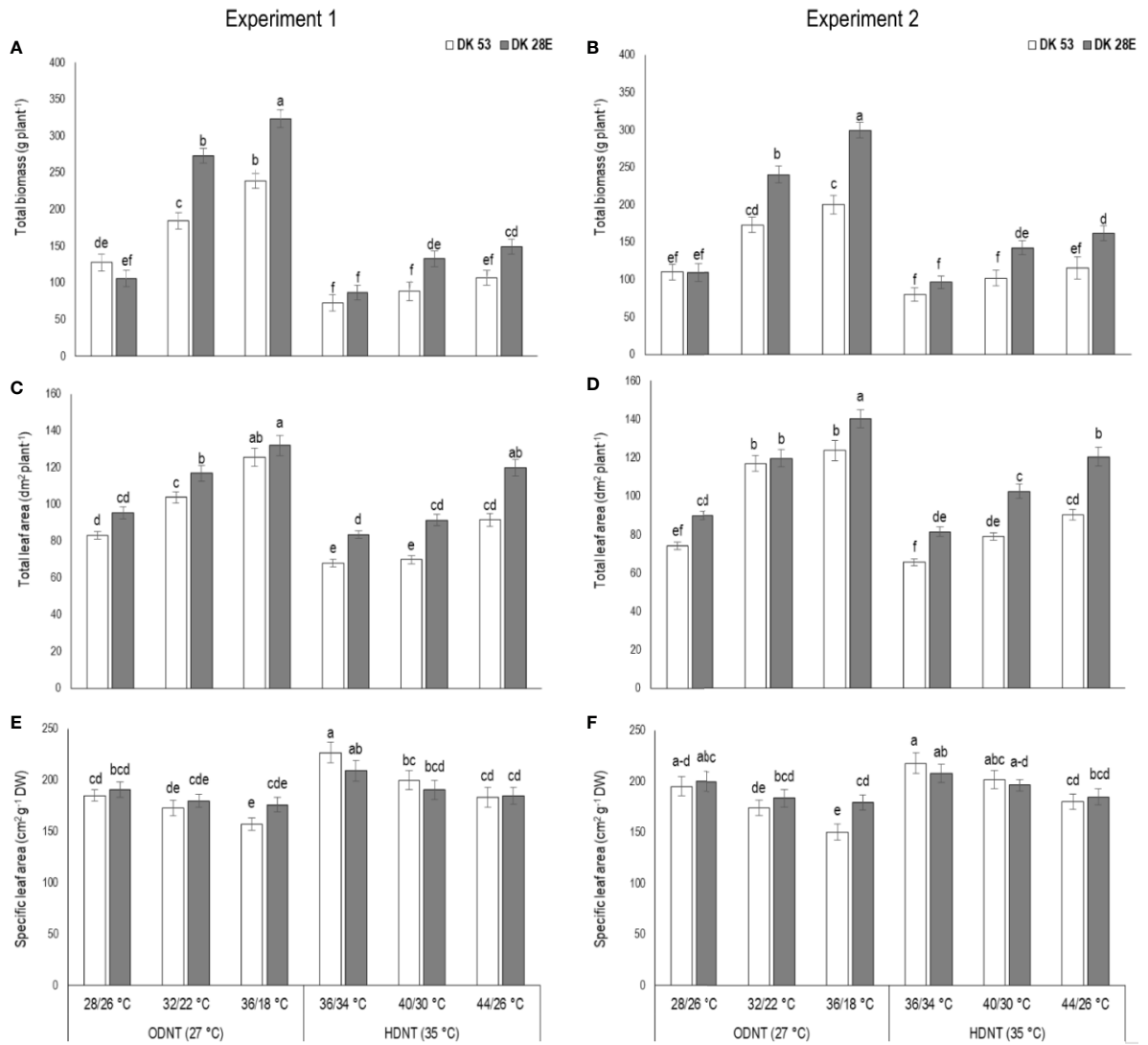

FIGURE 2 | Effect of two mean temperatures (27 and 35°C) [27°C (optimum mean daytime and nighttime temperature; ODNT) and 35°C(high mean daytime and nighttime temperature; HDNT)] with three diurnal temperature amplitudes (2, 10, and 18°C) on **(A, B)** total biomass (TB), **(C, D)** total leaf area (TLA) and **(E, F)** specific leaf area (SLA) of two sorghum hybrids [DK 53 (white bar) and DK 28E (gray bar)]. Different letters in bar indicates significant difference according to Tukey's HSD ($P<0.01$; the test was conducted independently for each experiments). Each bar is mean value with standard error. Dry weight (DW).

response of physiological, biochemical and growth traits of sorghum hybrids were similar to those observed on maize (Sunoj et al., 2016). Growth traits of sorghum hybrids were severely reduced under HDNT (35°C) followed by ODNT (27°C) with narrow diurnal temperature amplitude of 2°C having lower daytime and higher nighttime temperatures as compared to diurnal temperature amplitudes of 10 and 18°C, except SLA. Simultaneously, opposite trend in growth traits was observed in wider diurnal temperature amplitude of 18°C, where temperature at daytime was high and nighttime was low (**Figure 2**). The impact of above contrasting daytime and nighttime temperatures of extremes of diurnal temperature amplitudes (2 and 18°C) on growth of sorghum hybrids specifies importance of diurnal temperature amplitude for sustaining optimum plant growth.

Light and dark phases in 24 h of a day are crucial for plant growth due active photosynthesis (CO_2 assimilation) in daytime and respiration (CO_2 release) in nighttime which are two components of foliar gas exchange correspondingly contributing and significant for carbon tradeoff and are inevitable for overall growth, development and yield (O'Leary and Plaxton, 2016; Sunoj et al., 2016). Despite similar rates of photosynthesis, there were significant differences in night respiration and total above ground biomass accumulation in both sorghum hybrids across all the deployed temperature conditions (ODNT and HDNT) in current study (**Figures 2** and **3**). This trend raises questions about the utilization of assimilated CO_2 in the form of photosynthates and its end products (sucrose and starch) for growth and the influence of respiration. These differential responses in photosynthesis and

TABLE 3 | Percentage change in growth and carbon tradeoff in two sorghum hybrids (DK 53 and DK 28E) under diurnal temperature amplitudes of 10°C and 18°C compared to narrow diurnal temperature ampltude of 2°C with two mean temperatures [27°C (optimum mean daytime and nighttime temperature; ODNT) and 35°C (high mean daytime and nighttime temperature; HDNT)].

Temperature conditions/Hybrids		Total biomass	Total leaf area	Specific leaf area	Photosynthesis	Photochemical efficiency of PSII (*Fv*/*Fm*)	Night respiration
DK 53							
Day/Night temperature	Temperature amplitude				Percentage (%) change		
Optimum (ODNT; 27°C)							
32/22°C	10°C	50	40	-9	-4.3	-1.9	-15
36/18°C	18°C	85	58	-19	-0.5	-1.3	-37
High (HDNT; 35°C)							
40/30°C	10°C	25	12	-7	7.8	0.5	-30
44/26°C	18°C	45	36	-9	4.3	0.6	-48
DK 28E							
Optimum (ODNT; 27°C)					Percentage (%) change		
32/22°C	10°C	138	28	-10	-3.8	-0.6	-18
36/18°C	18°C	189	47	-18	-2.4	-0.6	-36
High (HDNT; 35°C)							
40/30°C	10°C	50	18	-7	-3.8	-0.6	-39
44/26°C	18°C	70	46	-11	-5.7	0.6	-47

Values in each column are mean of percentage change of two experiments.

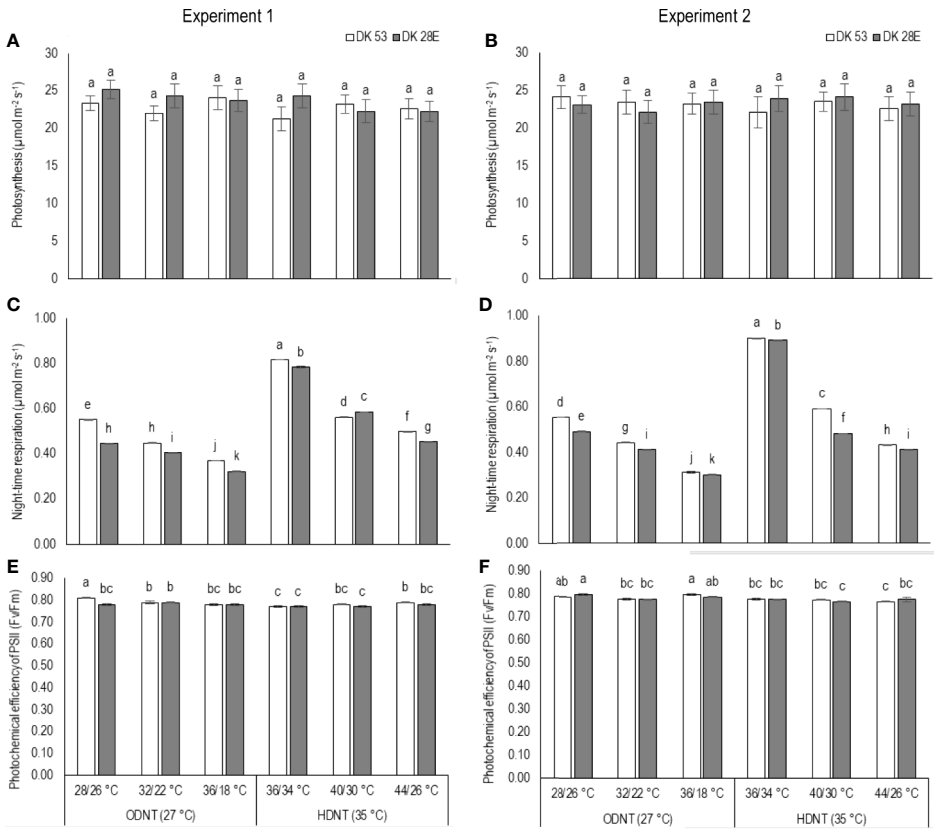

FIGURE 3 | Effect of two mean temperatures (27 and 35°C) [27°C (optimum mean daytime and nighttime temperature; ODNT) and 35°C (high mean daytime and nighttime temperature; HDNT)] with three diurnal temperature amplitudes (2, 10, and 18°C) on **(A, B)** photosynthesis (P_N), **(C, D)** photochemical efficiency of PSII (*Fv*/*Fm*) and **(E, F)** night respiration of two sorghum hybrids [DK 53 (white bar) and DK 28E (gray bar)]. Different letters in bar indicates significant difference according to Tukey's HSD ($P<0.01$; the test was conducted independently for each experiments). Each bar is mean value with standard error. Dry weight (DW).

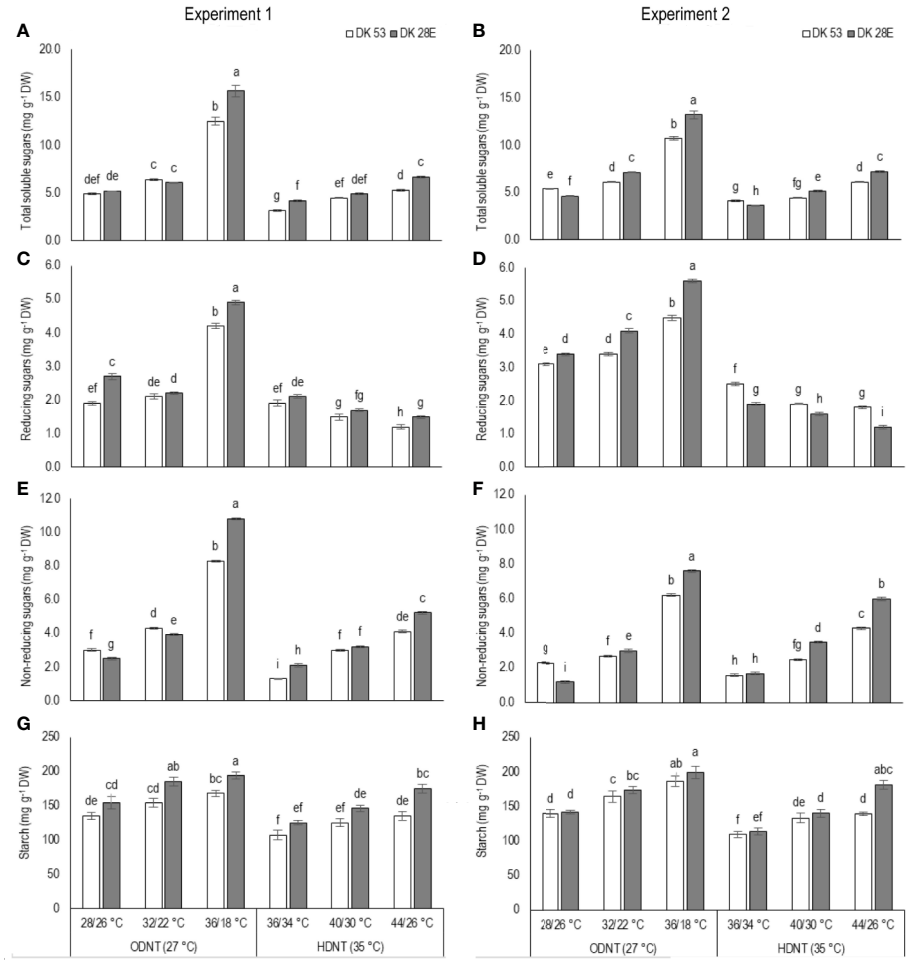

FIGURE 4 | Effect of two mean temperatures (27 and 35°C) [27°C (optimum mean daytime and nighttime temperature; ODNT) and 35°C (high mean daytime and nighttime temperature; HDNT)] with three diurnal temperature amplitudes (2, 10, and 18°C) on **(A, B)** total soluble sugars (TSS), **(C, D)** reducing sugars (RS), **(E, F)** non-reducing sugars (NRS) and **(G, H)** starch of two sorghum hybrids [DK 53 (white bar) and DK 28E (gray bar)]. Different letters in bar indicates significant difference according to Tukey's HSD ($P<0.01$; the test was conducted independently for each experiments). Each bar is mean value with standard error. Dry weight (DW).

above ground biomass accumulation point towards changes in night respiration and carbohydrate composition in response to temperature. However, there was also a strong relationship between total leaf area and biomass accumulation (**Figure 7**). Such an effect may arise from differential effects of temperature treatments on leaf area expansion (Tardieu et al., 1999), as consequent differences in leaf area will affect extent of light interception and hence, plant growth. This confounding effect of plant size needs to be considered when considering treatment effects on growth and biomass.

Correspondingly, Prasad et al., 2008 reported the same kind of response in photosynthetic performance of sorghum hybrid (DK 28E), in which, high day and night temperatures was set to 40/30°C (diurnal temperature amplitude of 10°C with mean temperature of 35°C and one of the day/night temperature condition used in the current study) and such response can be attributed to the ability of C_4 crops to undergo thermal acclimation (Dwyer et al., 2007; Sage and Kubien, 2007; Wang et al., 2012). This was further supported by the stable photosynthesis in C_4 crop maize under high temperature conditions (Sunoj et al., 2016; Rotundo et al., 2019). Additionally, previous studies on diverse C3 and C4 crops also demonstrated zero impact of high temperature on the subsequent day photosynthesis (potato: Lafta and Lorenzen, 1995; tomato: Huckstadt et al., 2013), while it has impact on night respiration, carbohydrate composition and growth (rice: Peraudeau et al., 2015; maize: Sunoj et al., 2016). Contrastingly, in C3 crop quinoa, photosynthesis and night respiration was increased under high temperature condition (Eustis et al., 2020).

Furthermore, decrease in photochemical efficiency of photosystem II (PSII) (Fv/Fm) is considered as indicator of photoinhibition or photodamage of PSII in plants under diverse

TABLE 4 | Percentage change in carbohydrate composition in two sorghum hybrids (DK 53 and DK 28E) under diurnal temperature amplitutes of 10 and 18°C compared to narrow diurnal temperature ampltude of 2°C with two mean temperatures [27°C (optimum mean daytime and nighttime temperature; ODNT) and 35°C (high mean daytime and nighttime temperature; HDNT)].

Temperature conditions/ Hybrids		Total soluble sugars	Reducing sugars	Non-reducing sugars	Starch
DK 53					
Day/Night temperature	Temperature amplitude		Percentage (%) change		
Optimum (ODNT; 27°C)					
32/22°C	10°C	21	10	32	16
36/18°C	18°C	125	74	174	29
High (HDNT; 35°C)					
40/30°C	10°C	22	-23	90	19
44/26°C	18°C	56	-32	190	27
DK 28E					
Optimum (ODNT; 27°C)			Percentage (%) change		
32/22°C	10°C	35	3	86	21
36/18°C	18°C	195	72	397	33
High (HDNT; 35°C)					
40/30°C	10°C	28	-18	76	20
44/26°C	18°C	78	-33	195	49

Values in each column are mean of percentage change of two experiments.

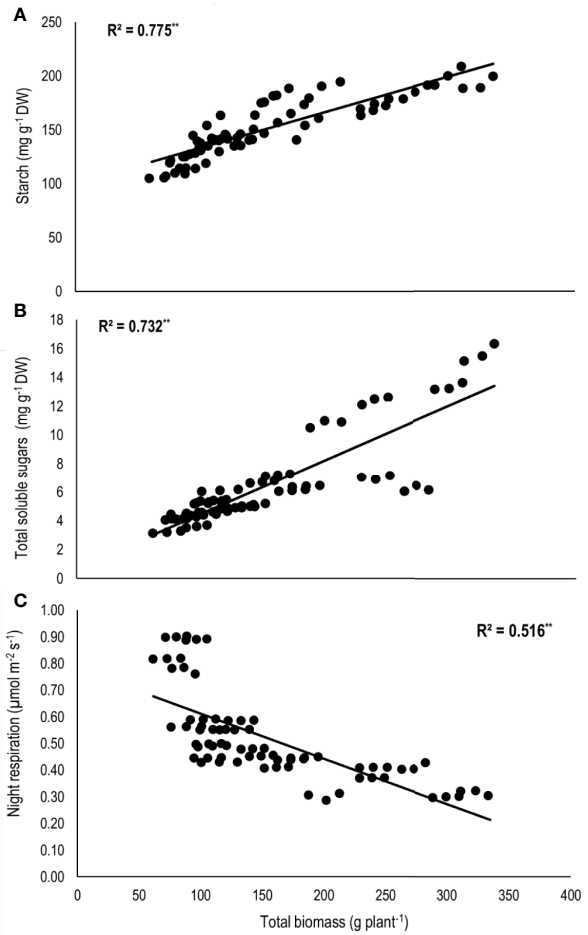

FIGURE 5 | Relationship of total biomass (TB) with **(A)** starch, **(B)** total soluble sugars (TSS), and **(C)** night respiration of two sorghum hybrids (DK 53 and DK 28E) exposed to two mean temperatures (27 and 35°C) [27°C (optimum mean daytime and nighttime temperature; ODNT) and 35°C (high mean daytime and nighttime temperature; HDNT)] with three diurnal temperature amplitudes (2, 10, and 18°C). Coefficient of determination (R^2) followed by ** significant at $P < 0.01$. Dry weight (DW).

abiotic stresses (Huang et al., 2016; Sunoj et al., 2016), varied across different temperature conditions (**Figure 3**). Besides, initial and reversible photoinhibition of PSII protects PSI from photoinhibition by limiting supply of electrons from PSII, which allow to keep the oxidative status of PSI under stress conditions. Hence, *F*v/*F*m values indicates health of leaves as well as total functionality of photosystems (PSII and PSI) (Joliot and Johnson, 2011; Takagi et al., 2017; Kadota et al., 2019). However, all the *F*v/*F*m values in both sorghum hybrids and temperature conditions in current study were equal or higher than 0.77 and this was only a slight change from the standard value (0.78) of F_v/F_m representing uninterrupted functioning of PSII (Huang et al., 2016; Huang et al., 2018). The above minor reduction implies that photosystems (PSII and PSI) and linear electron flow (LEF) were slightly affected with narrow diurnal temperature amplitudes, even under HDNT. Nevertheless, the impact of variation in temperatures was not sufficient to tamper the light dependent reaction and thereby light independent (dark) reaction of photosynthesis in sorghum hybrids. It was one of the reasons resulted for and reflected from stable photosynthesis.

In plants, other than energy cost for ion uptake in roots and transport inside root and shoot, respiration [light phase (daytime) and dark phase (nighttime) respiration] has two main functions, which are maintenance and growth (Johnson, 1990; Atkin et al., 2000). Respiration is the controlled oxidation of energy-rich photosynthates or its end-products (sucrose and starch) synthesised from photosynthesis by the collective reactions of glycolysis, the tricarboxylic acid cycle and mitochondrial electron transport chain which produce CO_2, adenosine 5-triphosphate (ATP), and low-molecular-weight molecules required for the biosynthesis of proteins and lipids and various metabolites essential for growth and plants to acclimation to stress (Atkin et al., 2000; O'Leary and Plaxton, 2016). Approximately, 30 to 70% of photosynthetically generated carbohydrates serve as major substrate as compared to the seldom used fatty acids that are utilized for respiration; and rate of respiration varies with plant species and status of growth conditions (optimum or sub or supra optimum) (Mohammed and Tarpley, 2011).

Respiration, especially at dark phase (night respiration), plays a significant role in recovery from injuries or damages caused due to the oxidative stress under optimum and diverse abiotic stress (moderate to severe injuries) conditions, in addition to contribution towards overall growth (Sunoj et al., 2016; Impa et al., 2018). However, depending on the extent of injuries or damage due to any type of stress, more resources are channelled for repair or maintenance respiration rather than contributing to growth, therefore, growth processes of the plants are negatively

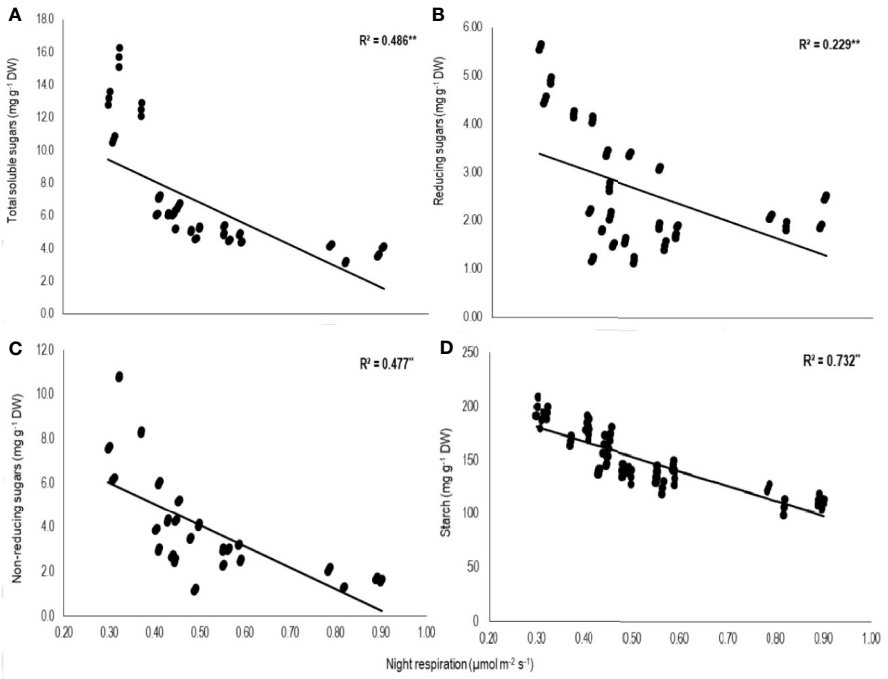

FIGURE 6 | Relationship of night respiration with **(A)** total soluble sugars (TSS), **(B)** reducing sugars (RSS), **(C)** non-reducing sugars (NRS), and **(D)** starch of two sorghum hybrids (DK 53 and DK 28E) exposed to two mean temperatures (27 and 35°C) [27°C (optimum mean daytime and nighttime temperature; ODNT) and 35°C (high mean daytime and nighttime temperature; HDNT)] with three diurnal temperature amplitudes (2, 10, and 18°C). Coefficient of determination (R^2) followed by ** significant at $P < 0.01$. respectively. Dry weight (DW).

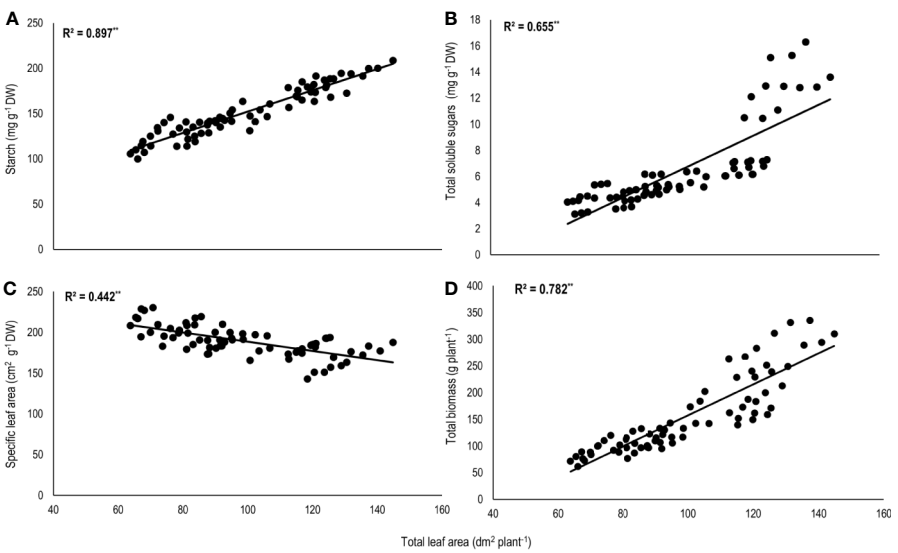

FIGURE 7 | Relationship of total leaf area (TLA) with **(A)** starch, **(B)** total soluble sugars (TSS), **(C)** specific leaf area (SLA), and **(D)** total biomass (TB) of two sorghum hybrids (DK 53 and DK 28E) exposed to two mean temperatures (27 and 35°C) [27°C (optimum mean daytime and nighttime temperature; ODNT) and 35°C (high mean daytime and nighttime temperature; HDNT)] with three diurnal temperature amplitudes (2, 10, and 18°C). Coefficient of determination (R^2) followed by ** significant at $P < 0.01$. Dry weight (DW).

affected (Loka and Oosterhuis, 2010; Mohammed and Tarpley, 2011; Sunoj et al., 2016).

In current study, higher night respiration and reduction in assimilated total soluble sugars (reducing and non-reducing sugars), starch and biomass accumulation in both sorghum hybrids under narrowing diurnal temperature amplitude of ODNT and HDNT (**Figures 2–4**) imply higher level of carbohydrate utilization for the maintenance rather than growth. This was further evident from the negative correlations of night respiration with carbohydrate composition (**Figure 6**) and total biomass and positive correlation among total biomass and carbohydrate composition (**Figure 5**). Carbohydrate composition consist of glucose, fructose, and maltose which are reducing sugars, sucrose is major transported non-reducing sugar in plants and starch is a polysaccharide stored in carbon sinks of plants and synthesized from sucrose (Loka and Oosterhuis, 2010; Halford et al., 2011). Meanwhile, highest night respiration under HDNT with 2°C diurnal temperature amplitude (**Figure 3**) specifies that balance between two functions (maintenance and growth) of night respiration differs with the type and intensity of stress (Djanaguiraman et al., 2013; Sperling et al., 2015; Sunoj et al., 2016; Impa et al., 2018). High daytime and nighttime temperature reported to increase the night respiration and reduce ATP, carbohydrate composition and growth in diverse crops as well (cotton: Loka and Oosterhuis, 2010; soybean: Djanaguiraman et al., 2013; maize: Sunoj et al., 2016). In contrast, non-significant relatioship between night respiration and growth was also reported (tomato, soybean and lettuce: Frantz et al., 2004; rice: Peraudeau et al., 2015). At the same time, dark phase in plants are equally important as light phase not only due to contribution of night respiration but also because of its effect on synchronization of circadian clock to manage the redox state of photosystems, response of hormones and induction or control of different mechanisms which are collectively responsible for sustainable growth under optimum and tolerance under stress conditions (McClung, 2006; Sunoj et al., 2016; Srivastava et al., 2019).

Studies in sorghum have also shown a strong influence of temperature on leaf initiation, appearance, and expansion rates, all of which are important for development of plant leaf area and hence, light interception (LI) and biomass accumulation (Hammer and Muchow, 1994; Ravi Kumar et al., 2012). In the current experiment, overall, there was positive correlation of total leaf area with total biomass and carbohydrates (**Figure 7**). This indicates the contribution of plant size *via* leaf area to differences in biomass accumulation in addition to night respiration and utilization of carbohydrates (**Figures 3–6**), rather than from photosynthesis, which was stable across different temperature conditions (**Figure 3**). Progressive increases in total leaf area and biomass with increasing diurnal temperature amplitudes under both ODNT and HDNT further indicates the important role of leaf area in effecting biomass accumulation (**Figure 2**).

Some research has shown that leaf area expansion under different temperature conditions is independent of carbohydrate availability (Tardieu et al., 1999; Volkenburgh, 1999), so that SLA is a consequence of the temperature-driven potential leaf area expansion and available assimilates. SLA increases (i.e. more leaf area per unit dry weight) when environmental conditions have greater negative effect on assimilate availability than on leaf expansion rate (Tardieu et al., 1999). The negative correlation of SLA with total leaf area (**Figure 7**) indicates reduced availability of assimilates for plants that had been restricted in leaf area. The smaller plants found in narrow diurnal temperature amplitudes under both ODNT and HDNT (**Figure 2**) also had higher night respiration, which is consistent with their increased SLA and the overall positive association of SLA with night respiration (**Supplementary Figure S1**). Hence, it is likely that a combination of temperature effects on leaf expansion and night time respiration are generating the consequences observed on biomass accumulation. The importance of leaf area expansion on growth under diverse temperature conditions might also explain findings in studies in other crops where a nonsignificant relationship between night respiration and growth was reported (Frantz et al., 2004; Peraudeau et al., 2015).

Although the contribution of night respiration for growth may be confounded by effects on leaf expansion, understanding the crop and genotypic response of night respiration to the variation in day and night temperatures remains important. This is due to the fact that overall contribution of respiration is approximately 50% of the total annual CO_2 input from the terrestrial ecosystem to atmosphere by taking part in plant growth and development (Gifford, 2003; O'Leary and Plaxton, 2016). Furthermore, our results indicate that effects of temperature on night respiration have a significant impact on biomass accumulation. This implies the importance of maintaining an optimum diurnal temperature amplitude that does not cause extreme maximum or minimum temperature is critical for attaining maximum growth and biomass.

CONCLUSIONS

The results from the current study clearly demonstrated the importance of diurnal temperature amplitude on growth of sorghum. Relative to optimum mean daytime and nighttime temperature (27°C), high mean daytime and nighttime temperature (35°C) had negative impacts on physiology and growth of sorghum. Carbon tradeoff in sorghum was significantly altered under different diurnal temperatures amplitude with optimum or high mean temperatures. This was evident from stable CO_2 assimilation (light phase photosynthesis), altered utilization (dark phase night respiration) and changes in total leaf area, specific leaf area and biomass accumulation and their relationships. Narrowing of diurnal temperature amplitude resulted increase in night respiration by utilizing the carbohydrate for maintenance rather than growth. These reveals the importance of understanding the dark phase mechanisms along with better understating the above ground biomass, leaf area components, and related light interception under different temperature conditions. Both hybrids monitored in current study to understand inter

genotypic differences showed same pattern of response to diurnal temperature amplitudes. However, research with larger number of genotypes are needed to further confirm and understand genotypic response to different diurnal amplitude for the same mean temperature. Results from current study ascertain that impacts of diurnal temperature amplitude on leaf area, biomass accumulation and night respiration should be incorporated while quantifying the impact of temperature on growth and yield of crops. In addition, methods should consider appropriate temperature conditions and temperature amplitude while screening for temperature tolerant/sensitive genotypes. Furthermore, greater importance should be given to breed for genotypes/hybrids to maintain productivity and yield in areas facing or expecting high night temperatures and changing temperature amplitude. However, it is strongly recommended that separate studies should be conducted for different crops irrespective of their photosynthetic pathway (C_3 or C_4) under field conditions to achieve conclusions that are more realistic conditions without restrictions of root growth and natural light conditions. Finally, further research to understand optimum respiration under different temperature conditions will be important to identify crops or genotypes within crops that will be more suitable under changing climatic conditions.

DATA AVAILABILITY STATEMENT

The raw data supporting the conclusions of this article will be made available by the authors, without undue reservation.

AUTHOR CONTRIBUTIONS

VS, IC, and PP designed the research. VS and HM conducted the experiment, collected and analyzed the data and contributed to statistical analysis. VS and HM drafted the manuscript. PP and IC suggested critical comments and corrections while preparing manuscript. All authors contributed to the article and approved the submitted version.

FUNDING

Financial support from Center for Sorghum Improvement at Kansas State University (KSU) and United States Agency for International Development (USAID) through Sustainable Agricultural and Natural Resource Management (SANREM) Collaborative Research Support Program for conducting the research. Preparation and publication of the manuscript was supported through Feed the Future Innovation Lab for Collaborative Research on Sustainable Intensification (Grant no. AID-OAA-L-14-00006).

ACKNOWLEDGMENTS

We thank Department of Agronomy at Kansas State University (KSU) for providing the research facilities. Contribution no 20-255-J from Kansas Agricultural Experiment Station.

SUPPLEMENTARY MATERIAL

The Supplementary Material for this article can be found online at: https://www.frontiersin.org/articles/10.3389/fpls.2020.01262/full#supplementary-material

SUPPLEMENTARY FIGURE S1 | Relationship of night respiration with **(A)** total leaf area (TLA) and **(B)** specific leaf area (SLA) of two sorghum hybrids (DK 53 and DK 28E) exposed to two mean temperatures (27 and 35°C) (27°C [optimum mean daytime and nighttime temperature; ODNT] and 35°C (high mean daytime and nighttime temperature; HDNT]) with three diurnal temperature amplitudes (2, 10, and 18°C). Coefficient of determination (R^2) followed by ** corresponding to significance at $P<0.01$. Dry weight (DW).

SUPPLEMENTARY FIGURE S2 | Relationship of specific leaf area (SLA) with **(A)** starch, **(B)** total soluble sugars (TSS) and **(C)** total biomass (TB) of two sorghum hybrids (DK 53 and DK 28E) exposed to two mean temperatures (27 and 35°C) (27°C [optimum mean daytime and nighttime temperature; ODNT] and 35°C (high mean daytime and nighttime temperature; HDNT]) with three diurnal temperature amplitudes (2, 10, and 18°C). Coefficient of determination (R^2) followed by ** corresponding to significance at $P<0.01$. Dry weight (DW).

REFERENCES

Atkin, O. K., Millar, A. H., Gardestrom, P., and Day, D. A. (2000). "Photosynthesis, carbohydrate metabolism and respiration in leaves of higher plants," in *Photosynthesis: Physiology and Metabolism*. Eds. R. C. Leegood, T. D. Sharkey and S. A. von Caemmerer (Netherlands: Academic Publishers), 153–175.

Bueno, A. C. R., Prudente, D. A., Machado, E. C., and Ribeiro, R. V. (2012). Daily temperature amplitude affects the vegetative growth and carbon metabolism of orange trees in a rootstock-dependent manner. *J. Plant Growth Regul.* 31, 309–319. doi: 10.1007/s00344-011-9240-x

Ciampitti, I. A., and Prasad, P. V. V. (2020). *Sorghum: State of art and future perspective* (New Jersey, USA: John Wiley & Sons).

Djanaguiraman, M., Prasad, P. V. V., and Schapaugh, W. T. (2013). High day or nighttime temperature alters leaf assimilation reproductive success, and phosphatidic acid of pollen grain in soybean [*Glycine max* (L.) Merr.]. *Crop Sci.* 53, 1594–1604. doi: 10.2135/cropsci2012.07.0441

Djanaguiraman, M., Prasad, P. V. V., Murugan, M., Perumal, R., and Reddy, U. K. (2014). Physiological differences among sorghum (*Sorghum bicolor* L., Moench) genotypes under high temperature stress. *Environ. Exp. Bot.* 100, 43–54. doi: 10.1016/j.envexpbot.2013.11.013

Djanaguiraman, M., Perumal, R., Jagadish, S. V. K., Ciampitti, I. A., Welti, R., and Prasad, P. V. V. (2018a). Sensitivity of sorghum pollen and pistil to high-temperature stress. *Plant Cell Environ.* 41, 1065–1082. doi: 10.1111/pce.13089

Djanaguiraman, M., Perumal, R., Ciampitti, I. A., Gupta, S. K., and Prasad, P. V. V. (2018b). Quantifying pearl millet response to high temperature stress: thresholds, sensitive stages, genetic variability and relative sensitivity of pollen and pistil. *Plant Cell Environ.* 41, 993–1007. doi: 10.1111/pce.12931

Dubois, M., Gilles, K. A., Hamilton, J. K., Rebers, P. A., and Smith, F. (1956). Colorimetric method for determination of sugars and related substances. *Anal. Chem.* 28, 350–356. doi: 10.1021/ac60111a017

Dwyer, S. A., Ghannoum, O. A., and Caemmerer, S. V. (2007). High temperature acclimation of C_4 photosynthesis is linked to changes in photosynthetic biochemistry. *Plant Cell Environ.* 30, 53–66. doi: 10.1111/j.1365-3040.2006.01605.x

Eustis, A., Murphy, K. M., and Barrios-Masias, F. H. (2020). Leaf gas exchange performance of ten quinoa genotypes under a simulated heat wave. *Plants* 9:81. doi: 10.3390/plants9010081

Frantz, M. J., Cometti, N. N., and Bugbee, B. (2004). Night temperature has a minimal effect on respiration and growth in rapidly growing plants. *Ann. Bot.* 94, 155–166. doi: 10.1093/aob/mch122

Gifford, R. M. (2003). Plant respiration in productivity models: conceptualization, representation and issues for global terrestrial carbon-cycle research. *Funct. Plant Biol.* 30, 171–186. doi: 10.1071/FP02083

Halford, N. G., Curtis, T. Y., Muttucumaru, N., Postles, J., and Mottram, D. S. (2011). Sugars in crop plants. *Ann. Appl. Biol.* 158, 1–25. doi: 10.1111/j.1744-7348.2010.00443.x

Hammer, G. L., and Muchow, R. C. (1994). Assessing climatic risk to sorghum production in water-limited subtropical environments. I. Development and testing of a simulation model. *Field Crops Res.* 36, 221–234. doi: 10.1016/0378-4290(94)90114-7

Hammer, G. L., Carberry, P. S., and Muchow, R. C. (1993).). Modeling genotypic and environmental control of leaf area dynamics in grain sorghum. I. Whole plant level. *Field Crops Res.* 33, 293–310. doi: 10.1016/0378-4290(93)90087-4

Hedge, J. E., and Hofreiter, B. T. (1962). "Estimation of carbohydrate," in *Methods in Carbohydrate Chemistry*. Eds. R. L. Whistler and J. N. Be Miller (New York, USA: Academic Press), 17–22.

Huang, W., Yang, Y., Hu, H., Cao, K. F., and Zhang, S. (2016). Sustained diurnal stimulation of cyclic electron flow in two tropical tree species *Erythrophleum guineense* and *Khaya ivorensis*. *Front. Plant Sci.* 7, 1068. doi: 10.3389/fpls.2016.01068. Article 1068.

Huang, W., Quan, X., Zhang, S. B., and Liu, T. (2018). In vivo regulation of proton motive force during photosynthetic induction. *Environ. Exp. Bot.* 148, 109–116. doi: 10.1016/j.envexpbot.2018.01.001

Huckstadt, A. B., Suthaparan, A., Mortensen, L. M., and Gislerod, H. R. (2013). The effect of low night and high day temperatures on photosynthesis in tomato. *Am. J. Plant Sci.* 4, 2323–2331. doi: 10.4236/ajps.2013.412288

Impa, M. S., Sunoj, V. S. J., Krassovskaya, I., Raju, B. R., Obata, T., and Jagadish, S. V. K. (2018). Carbon balance and source-sink metabolic changes in winter wheat exposed to high night-time temperature. *Plant Cell Environ.* 42, 1233–1246. doi: 10.1111/pce.13488

Inthichack, P., Nishimura, Y., and Fukumoto, Y. (2013). Diurnal temperature alternations on plant growth and mineral absorption in eggplant, sweet pepper, and tomato. *Hortic. Environ. Biotechnol.* 54, 37–43. doi: 10.1007/s13580-013-0106-y

Inthichack, P., Nishimura, Y., and Fukumoto, Y. (2014). Effect of diurnal amplitude on plant growth and mineral composition in cucumber, melon and water melon. *Pak. J. Biol. Sci.* 17, 1030–1036. doi: 10.3923/pjbs.2014.1030.1036

IPCC (2018). *Summary for Policymakers" in Global warming of 1.5°C. An IPCC Special Report on the impacts of global warming of 1.5°C above pre-industrial levels and related global greenhouse gas emission pathways, in the context of strengthening the global response to the threat of climate change, sustainable development, and efforts to eradicate poverty*. Eds. V. Masson-Delmotte, P. Zhai, H. O. Pörtner, D. Roberts, J. Skea, P. R. Shukla, A. Pirani, W. Moufouma-Okia, C. Péan, R. Pidcock, S. Connors, J. B. R. Matthews, Y. Chen, X. Zhou, M. Gomis II, E. Lonnoy, T. Maycock, M. Tignor and T. Waterfield (Geneva, Switzerland: World Meteorological Organization).

Johnson, I. R. (1990). Plant respiration in relation to growth, maintenance, ion uptake and nitrogen assimilation. *Plant Cell Environ.* 13, 319–328. doi: 10.1111/j.1365-3040.1990.tb02135.x

Joliot, P., and Johnson, G. (2011). Regulation of cyclic and linear electron flow in higher plants. *Proc. Natl. Acad. Sci. U.S.A.* 108, 13317–13322. doi: 10.1073/pnas.1110189108

Kadota, K., Furutani, R., Makino, A., Suzuki, Y., Wada, S., and Miyake, C. (2019). Oxidation of P700 induces alternative electron flow in photosystem I in wheat leaves. *Plants* 8, 152. doi: 10.3390/plants8060152

Lafta, A. M., and Lorenzen, J. H. (1995). Effect of high temperature on plant growth and carbohydrate metabolism in potato. *Plant Physiol.* 109, 637–643. doi: 10.1104/pp.109.2.637

Lin, G., Yang, Y., Chen, X., Yu, X., Wu, Y., and Xiong, F. (2020). Effects of high temperature during two growth stages on caryopsis development and physicochemical properties of starch in rice. *Int. J. Biol. Macromol.* 14, 301–310. doi: 10.1016/j.ijbiomac.2019.12.190

Lizaso, J. I., Ruiz-Ramosa, M., Rodrigueza, L., Gabaldon-Lealb, C., Oliveirac, J. A., Loriteb, I. J., et al. (2018). Impact of high temperatures in maize: phenology and yield components. *Field Crops Res.* 216, 129–140. doi: 10.1016/j.fcr.2017.11.013

Lobell, D. B., Sibley, A., and Ortiz Monasterio, J. I. (2012). Extreme heat effects on wheat senescence in India. *Nat. Clim. Change* 2, 186–189. doi: 10.1038/nclimate1356

Loka, D. A., and Oosterhuis, D. M. (2010). Effect of high night temperatures on cotton respiration: ATP levels and carbohydrate content. *Environ. Exp. Bot.* 68, 258–263. doi: 10.1016/j.envexpbot.2010.01.006

Luo, Q. (2011). Temperature thresholds and crop production: a review. *Climatic Change* 109, 583–598. doi: 10.1007/s10584-011-0028-6

Maikasuwa, M. A., and Ala, A. L. (2013). Trend analysis of area and productivity of sorghum in Sokoto state, Nigeria 1993–2012. *Eur. Sci. J.* 9, 69–75. doi: 10.19044/esj.2013.v9n16p%25p

Maiti, R. K. (1996). Sorghum Science. Lebanon, NH, USA: Science Publishers.

Malhotra, S. S., and Sarkar, S. K. (1979). Effects of sulphur dioxide on sugar and free amino acid content of pine seedlings. *Physiol. Plant* 47, 223–228.

Maswada, F. H., Sunoj, V. S. J., and Prasad, P. V. V. (2020). A comparative study on the effect of seed pre-sowing treatments with microwave radiation and salicylic acid in alleviating the drought-induced damage in wheat. *J. Plant Growth Regul*. doi: 10.1007/s00344-020-10079-3

Matsuda, R., Ozawa, N., and Fujiwara, K. (2014). Leaf photosynthesis plant growth, and carbohydrate accumulation of tomato under different photoperiods and diurnal temperature differences. *Sci. Hortic.* 170, 150–158. doi: 10.1016/j.scienta.2014.03.014

McClung, C. R. (2006). Historical perspective essay: Plant circadian rhythm. *Plant Cell* 8, 792–803. doi: 10.1105/tpc.106.040980

Mohammed, A. K., and Tarpley, L. (2009). Impact of high nighttime temperature on respiration membrane stability, antioxidant capacity, and yield of rice plants. *Crop Sci.* 49, 313–322. doi: 10.2135/cropsci2008.03.0161

Mohammed, A. K., and Tarpley, L. (2011). ""Effects of high night temperature on crop physiology and productivity," in *Plant growth regulators provide a management option, global warming impacts – case studies on the economy, human health, and on urban and natural environments*. Ed. S. Casalegno, (IntechOpen). doi: 10.5772/24537

Myster, J., and Moe, R. (1995). Effect of diurnal temperature alternations on plant morphology in some greenhouse crops - A mini review. *Sci. Hortic.* 62, 205–215. doi: 10.1016/0304-4238(95)00783-P

Narayanan, S., Prasad, P. V. V., Fritz, A. K., Boyle, D. L., and Gill, B. S. (2015). Impact of high night-time and high daytime temperature stress on winter wheat. *J. Agron. Crop Sci.* 201, 206–218. doi: 10.1111/jac.12101

Narayanan, S., Prasad, P. V. V., and Welti, R. (2018). Alterations in wheat pollen lipidome during high day and night temperature stress. *Plant Cell Environ.* 41, 1749–1761.

Opole, R. A., Prasad, P. V. V., Djanaguiraman, M., Vimala, K., Kirkham, M. B., and Upadhyaya, H. D. (2018). Thresholds, sensitive stages and genetic variability of finger millet to high temperature stress. *J. Agron. Crop Sci.* 204, 477–492. doi: 10.1111/jac.12279

O'Leary, B. M., and Plaxton, W. C. (2016). *"Plant Respiration"* (New Jersey, USA: John Willy & Sons).

Peng, S., Huang, J., Sheehy, J. E., Laza, R. C., Visperas, R. M., Zhong, X., et al. (2004). Rice yields decline with higher night temperature from global warming. *Proc. Natl. Acad. Sci.* 101, 9971–9975. doi: 10.1073/pnas.0403720101

Peraudeau, S., Lafarge, T., Roques, S., Quinones, C. O., Clement-Vidal, A., Ouwerkerk, P. B. F., et al. (2015). Effect of carbohydrates and night temperature on night respiration in rice. *J. Exp. Bot.* 66, 3931–3944. doi: 10.1093/jxb/erv193

Prasad, P. V. V., and Djanaguiraman, M. (2011). High night temperature decreases leaf photosynthesis and pollen function in grain sorghum. *Funct. Plant Biol.* 38, 993–1003. doi: 10.1071/FP11035

Prasad, P. V. V., Boote, K. J., Allen, L. H.Jr, Sheehy, J. E., and Thomas, J. M. G. (2006a). Species, ecotypes and cultivar differences in spikelet fertility and harvest index of rice in response to high temperature stress. *Field Crops Res.* 95, 398–411. doi: 10.1016/j.fcr.2005.04.008

Prasad, P. V. V., Boote, K. J., and Allen, L. H.Jr (2006b). Adverse high temperature effects on pollen viability, seed-set, seed yield and harvest index of grain-sorghum [*Sorghum bicolor* (L.) Moench] are more severe at elevated carbon dioxide due to high tissue temperature. *Agric. Forest. Meteorol.* 139, 237–251. doi: 10.1016/j.agrformet.2006.07.003

Prasad, P. V. V., Pisipati, S., Mutava, R. N., and Tuinstra, M. R. (2008a). Sensitivity of grain sorghum to high temperature stress during reproductive development. *Crop Sci.* 48, 1911–1917. doi: 10.2135/cropsci2008.01.0036

Prasad, P. V. V., Pisipati, S. R., Ristic, Z., Bukovnik, U., and Fritz, A. K. (2008b). Impact of nighttime temperature on physiology and growth of spring wheat. *Crop Sci.* 48, 2372–2380. doi: 10.2135/cropsci2007.12.0717

Prasad, P. V. V., Djanaguiraman, M., Perumal, R., and Ciampitti, I. A. (2015). Impact of high temperature stress on floret fertility and individual grain weight of grain sorghum: Sensitive stages and thresholds for temperature and duration. *Front. Plant Sci.* 6, 820. doi: 10.3389/fpls.2015.00820

Ravi Kumar, S., Hammer, G. L., Broad, I., Harland, P., and McLean, G. (2009). Modelling environmental effects on phenology and canopy development of diverse sorghum genotypes. *Field Crops Res.* 111, 157–165. doi: 10.1016/j.fcr.2008.11.010

Roozeboom, K. L., and Prasad, P. V. V. (2016). "Sorghum Growth and Development," in *Sorghum: State of art and future perspective*. Eds. I. A. Ciampitti and P. V. V. Prasad (New Jersey, USA: John Willy & Sons), 1–18.

Rotundo, J. L., Tang, T., and Messina, C. D. (2019). Response of maize photosynthesis to high temperature: Implications for modeling the impact of global warming. *Plant Physiol. Biochem.* 141, 202–205. doi: 10.1016/j.plaphy.2019.05.035

Sage, R. F., and Kubien, D. S. (2007). The temperature response of C_3 and C_4 photosynthesis. *Plant Cell Environ.* 30, 1086–1106. doi: 10.1111/j.1365-3040.2007.01682.x

Singh, V., Nguyen, C. T., van Oosterom, E. J., Chapman, S. C., Jordan, D. R., and Hammer, G. L. (2015). Sorghum genotypes differ in high temperature responses for seed set. *Field Crops Res.* 171, 32–40. doi: 10.1016/j.fcr.2014.11.003

Somogyi, M. (1952). Estimation of sugars by colorimetric method. *J. Biol. Chem.* 200, 245.

Sperling, O., Earles, J. M., Secchi, F., Godfrey, J., and Zwieniecki, M. A. (2015). Frost induces respiration and accelerates carbon depletion in trees. *PloS One* 10 (12), e0144124. doi: 10.1371/journal.pone.0144124

Srivastava, D., Shamim, M., Kumar, M., Mishra, A., Maurya, R., Sharma, D., et al. (2019). Role of circadian rhythm in plant system: An update from development to stress response. *Environ. Exp. Bot.* 162, 256–271. doi: 10.1016/j.envexpbot.2019.02.025

Sunoj, V. S. J., Shroyer, K. J., Jagadish, S. V. K., and Prasad, P. V. V. (2016). Diurnal temperature amplitude alters physiological and growth response of maize (*Zea mays* L.) during the vegetative stage. *Environ. Exp. Bot.* 130, 113–121. doi: 10.1016/j.envexpbot.2016.04.007

Sunoj, V. S. J., Impa, M. S., Chiluwal, A., Perumal, R., Prasad, P. V. V., and Jagadish, S. V. K. (2017). Resilience of pollen and post flowering response in diverse sorghum genotypes exposed to heat stress under field conditions. *Crop Sci.* 57, 1–12. doi: 10.2135/cropsci2016.08.0706

Takagi, D., Ishizaki, K., Hanawa, H., Mabuchi, T., Shimakawa, G., Yamamotod, H., et al. (2017). Diversity of strategies for escaping reactive oxygen species production within photosystem I among land plants: P700 oxidation system is prerequisite for alleviating photoinhibition in photosystem I. *Physiol. Plant* 161, 56–74. doi: 10.1111/ppl.12562

Tardieu, F., Granier, C., and Muller, B. (1999). Research review: modelling leaf expansion in a fluctuating environment: are changes in specific leaf area a consequence of changes in expansion rate? *New Phytol.* 143, 33–43. doi: 10.1046/j.1469-8137.1999.00433.x

Tari, I., Laskay, G., Takacs, Z., and Poor, P. (2013). Response of sorghum to abiotic stresses: A review. *J. Agron. Crop Sci.* 199, 264–274. doi: 10.1111/jac.12017

Volkenburgh, E. V. (1999). Leaf expansion-An integrating plant behavior. *Plant Cell Environ.* 22, 1463–1473. doi: 10.1046/j.1365-3040.1999.00514.x

Vose, R. S., Easterling, D. R., and Gleason, B. (2005). Maximum and minimum temperature trends for the globe: an update through 2004. *Geophys. Res.* 32, 23822. doi: 10.1029/2005GL024379

Wang, C., Guo, L., Li, Y., and Wang, Z. (2012). Systematic comparison of C_3 and C_4 plants based on metabolic network analysis. *BMC Syst. Biol.* 6 (2), S9. doi: 10.1186/1752-0509-6-S2-S9

Wang, K., Li, Y., Wang, Y., and Yang, X. (2017). On the asymmetry of urban daily air temperature cycle. *J. Geophys. Res. Atmos.* 122, 5625–5635. doi: 10.1002/2017JD026589

Wang, Y., Zhang, Y., Shi, Q., Chen, H., Xiang, J., Hu, G., et al. (2020). Decrement of sugar consumption in rice young panicle under high temperature aggravates spikelet number reduction. *Rice Sci.* 27, 44–55. doi: 10.1016/j.rsci.2019.12.005

Welch, J. R., Vincent, J. R., Auffhammer, M., Moya, P. F., Dobermann, A., and Dawe, D. (2010). Rice yields in tropical/subtropical Asia exhibit large but opposing sensitivities to minimum and maximum temperatures. *Proc. Natl. Acad. Sci.* 33, 14562–14567. doi: 10.1073/pnas.1001222107

Xiong, J., Patil, G. G., Moe, R., and Torre, S. (2011). Effects of diurnal temperature alternations and light quality on growth, morphogenesis and carbohydrate content of *Cucumis sativus* L. *Sci. Hortic.* 128, 54–60. doi: 10.1016/j.scienta.2010.12.013

Conflict of Interest: The authors declare that the research was conducted in the absence of any commercial or financial relationships that could be construed as a potential conflict of interest.

frontiers in Plant Science

MINI REVIEW
published: 07 October 2020
doi: 10.3389/fpls.2020.581666

Dark-Induced Hormonal Regulation of Plant Growth and Development

*Deepika, Ankit, Sushma Sagar and Amarjeet Singh**

National Institute of Plant Genome Research, New Delhi, India

The sessile nature of plants has made them extremely sensitive and flexible toward the constant flux of the surrounding environment, particularly light and dark. The light is perceived as a signal by specific receptors which further transduce the information through the signaling intermediates and effector proteins to modulate gene expression. Signal transduction induces changes in hormone levels that alters developmental, physiological and morphological processes. Importance of light for plants growth is well recognized, but a holistic understanding of key molecular and physiological changes governing plants development under dark is awaited. Here, we describe how darkness acts as a signal causing alteration in hormone levels and subsequent modulation of the gene regulatory network throughout plant life. The emphasis of this review is on dark mediated changes in plant hormones, regulation of signaling complex COP/DET/FUS and the transcription factors PIFs which affects developmental events such as apical hook development, elongated hypocotyls, photoperiodic flowering, shortened roots, and plastid development. Furthermore, the role of darkness in shade avoidance and senescence is discussed.

Keywords: dark, signaling, hormone, growth, development

OPEN ACCESS

Edited by:
M. Iqbal R. Khan,
Jamia Hamdard University, India

Reviewed by:
Sushma Mishra,
Dayalbagh Educational Institute, India
Jigang Li,
China Agricultural University, China

***Correspondence:**
Amarjeet Singh
amarjeet.singh@nipgr.ac.in

Specialty section:
This article was submitted to Plant Physiology, a section of the journal Frontiers in Plant Science

Received: *09 July 2020*
Accepted: *16 September 2020*
Published: *07 October 2020*

Citation:
Deepika, Ankit, Sagar S and Singh A (2020) Dark-Induced Hormonal Regulation of Plant Growth and Development. Front. Plant Sci. 11:581666. doi: 10.3389/fpls.2020.581666

INTRODUCTION

Light and dark, both act as environmental cues that regulate plant growth and development from seedling emergence till senescence. Plant development begins in the soil where darkness acts as a signal for etiolation which is characterized by elongated hypocotyl and shortened roots, apical hook of closed cotyledons covering shoot apical meristem and impaired chloroplast development (Arsovski et al., 2012; Mazzella et al., 2014; Gommers and Monte, 2018). This mode of plant growth is known as skotomorphogenesis. It is an evolutionary advanced program in angiosperms to safely get seedling through the soil to light (Seluzicki et al., 2017). Nonetheless, exposure of seeds to continuous light during early development causes seedling de-etiolation (photomorphogenesis) characterized by attenuated hypocotyl growth, root growth acceleration, apical hook straightening and chloroplast maturation.

Being photoautotrophs, plants have evolved with the diverse set of photoreceptors. *Arabidopsis* photoreceptors have been classified as phytochromes (phyA-E, red/far-red light), cryptochromes (cry1-2), phototropins (phot1-2) and zeitlupe family members (*ZTL*, blue/UV-A light and *UVR8*; UV-B light) (Galvao and Fankhauser, 2015; Mishra and Khurana, 2017; Podolec and Ulm, 2018). Light-mediated activation of different photoreceptors and subsequent release of the dark-mediated photomorphogenic repression leads to light-dependent plant development. Some of the major mechanisms that play important role in photomorphogenic

development are phosphorylation of phytochrome interacting factors (PIFs), ubiquitin-mediated proteolysis (UMP), and modulation of CONSTITUTIVE PHOTOMORPHOGENIC/DE-ETIOLATED/FUSCA (COP/DET/FUS) complex activity, organization and subcellular localization of positive regulators of light signaling like ELONGATED HYPOCTYL 5 (HY5), LONG AFTER FAR-RED LIGHT1 (LAF) and LONG HYPOCOTYL AFTER FAR-RED LIGHT1 (HFR1) (Huang et al., 2014; Pham et al., 2018). Dark germinated seedlings become sensitive to fluctuations of the day/night cycles when they are first exposed to light. Therefore, growth and development of seedling comes under the control of circadian clock components. Ample amount of information is available about how plants sense and respond to the complex light spectra, but the information is missing about their behavior under darkness, and light and dark signal interaction. Since, light simply reverses the dark-mediated development by activation of the photoreceptors, it has been speculated that the inactive photoreceptors might act as dark receptors and mediate the dark-triggered signal transduction (Seluzicki et al., 2017; Gommers and Monte, 2018; Armarego-marriott and Sandoval-ibañez, 2020). Nonetheless, exact mechanism of dark sensing and perception is still unknown, and the idea of darkness perception by the inactive light receptors is a matter of debate. Though, regulation of seedling establishment by the light and dark signaling in *Arabidopsis* was recently reviewed (Gommers and Monte, 2018), enough literature is not available for light and dark signal integration and consequent phenotypic alterations.

In this review, an update about how plants make sense of darkness and use it as a signal during different phases of skotomorphogenic development e.g., apical hook formation, hypocotyl elongation, shortened roots, photoperiodic flowering, and plastid development is provided. Moreover, how endogenous clock integrates plant growth and development with photoperiods, and the effect of darkness on the plant responses such as, shade avoidance and dark-mediated senescence is discussed.

DARKNESS AS A SIGNAL

As mentioned earlier, it is presumed that darkness might be perceived by the inactive light receptors that could activate the COP/DET/FUS complex proteins and the PIFs. The proteins of COP/DET/FUS complex are encoded by a group of pleiotropic genes. These proteins are assembled in three different functional complexes, i.e., SUPPRESSOR OF PHYA105 (COPI-SPA), COP10-DET1-DDB1 (CDD), and COP9 signalosome complex (CSN), all of them are connected by a scaffold protein CULLIN4 (CUL4) (Chen et al., 2010; Pokhilko et al., 2011; Dong et al., 2014; Huang et al., 2016). In darkness, COPI-SPA and CDD complex act together to degrade positive regulators of photomorphogenesis like HY5, LAF and HFR1 via UMP. However, these complexes also prevent degradation of PIFs (PIF3 and 4) by inhibiting a brassinosteroid (BR) signaling component BRASSINOSTEROID-INSENSITIVE 2 (BIN2) (Dong et al., 2014; Huang et al., 2016; Wang and Guo, 2018; **Figure 1**). The function of CSN complex is to derubylate and thus positively regulates the activity of CUL4 which is present on both COP1-SPA and CDD complexes (Chen et al., 2010; Dong et al., 2014). Additionally, DET1 interacts with PIFs under darkness to stabilize them (Dong et al., 2014; Pham et al., 2018). PIFs in turn activate a diverse set of hormone biosynthetic and signaling genes that promote etiolation and repression of photomorphogenic response (Leivar et al., 2008; Paik et al., 2017). In *Arabidopsis*, PIF1, 3, 4, and 5 are involved in skotomorphogenesis, as indicated by normal light-grown seedling like growth of quadruple mutant *pif1pif3pif4pif5* (*pifq)* under complete darkness (Dong et al., 2014; Pfeiffer et al., 2014).

In the forthcoming sections, how darkness regulates development of specific skotomorphogenic structures such as, apical hook, elongated hypocotyls, and shortened roots is discussed.

HORMONAL REGULATION OF PLANT DEVELOPMENT IN DARK

Apical Hook Development

Within 24 h of seed germination, after hypocotyl elongation, darkness induces the development of an apical hook (Mazzella et al., 2014) with curvature formation by modulating several hormonal pathways (de Wit et al., 2016). An asymmetrical distribution of auxin (auxin concentration increases at concave side and inhibit cell expansion) causes differential cell expansion and division at both the sides of the hypocotyl. This leads to faster growth at the outer side compared to inner side, which culminates in the hook formation (Béziat and Kleine-Vehn, 2018; Gommers and Monte, 2018; Wang and Guo, 2018). Asymmetric distribution of auxin is facilitated by the influx and efflux carriers on the cell membrane. In *Arabidopsis*, influx carriers AUXIN1 (AUX1) and LIKE AUXIN (LAX3) localize at the epidermal cells and vascular cylinder of the hook. These carriers facilitate the polar and basipetal flow of auxin from shoot apical meristem and cotyledons to hypocotyl. Efflux carrier PIN1 facilitates the outward flow of auxin through vascular cylinder and inner epidermis. PIN3 facilitates the auxin flow from vascular tissues to outer cortex and epidermis, whereas PIN4 and 7 support the auxin flow from vascular tissue to cortex and epidermis. In addition, ABCB transporter 1 and 19 which are localized at inner epidermal cells of the hook, steer the auxin transport to the convex side (Vandenbussche et al., 2010; Wu et al., 2010; Žádníkova et al., 2010, 2016; Farquharson, 2017; Wang and Guo, 2018). The maintenance of differential auxin gradient involves the co-ordination of auxin synthesis, transport and signaling. YUCs and TAR2 are the flavin monooxygenases and tryptophan aminotransferase related enzymes, which, respectively, catalyze two initial steps in the auxin biosynthesis pathway. These genes are differentially expressed in the apical hook region and their mutants (*yuc1/2/4/6, tar2*) display impaired hook phenotype due to developmental defects (Stepanova et al., 2008, 2011; Vandenbussche et al., 2010; Abbas et al., 2013; Cao et al., 2019). The auxin signaling mutants like *iaa3*, *iaa12* and *iaa13* lack apical hook, suggesting the involvement of auxin signaling in apical

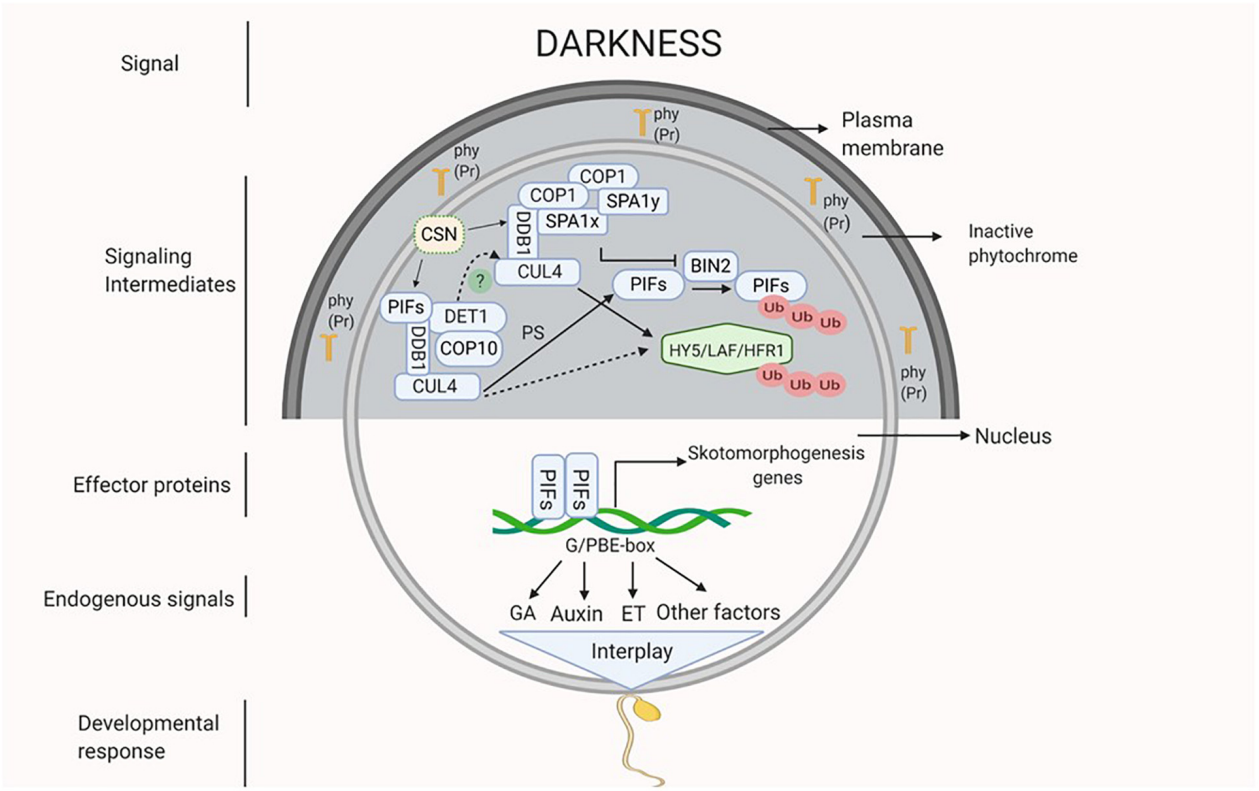

FIGURE 1 | Darkness acts as a signal which might be perceived by inactive phytochromes (Pr form of phy) that activates the signaling intermediates COP1-SPA complex (CUL4-DDB1-COP1-SPA) and CDD complex (CUL4-DDB1-COP10-DET1) which interact with each other (dotted line). Active COP1-SPA complex lead to degradation of HY5 and inactivates BIN2 which causes degradation of PIFs by UMP and active CDD stabilizes PIFs. Active PIFs induces the expression of phytohormones (ET, GA and auxin) biosynthesis and signaling genes and of other skotomorphogenesis signals. Hormonal interplay along with many other factors integrate to generate skotomorphogenic developmental response.

hook formation. Moreover, AUX/IAAs regulate auxin signaling effector proteins; auxin response factors (ARFs) (Žádníkova et al., 2010, 2016; Abbas et al., 2013).

The apical hook development is tightly regulated by signals from cell wall and root-hypocotyl interaction. The cell wall status affects apical hook bending by transcriptional regulation of *PIN*s and *AUX1* through ARF2 (Aryal et al., 2020; Sampathkumar and Eng, 2020). Recently, it was shown that auxin gradient formed at the root tip by PIN2 is required for root growth in response to gravity (Zhu and Gallem, 2019). The root auxin gradient gradually extends toward hypocotyl and might trigger the hypocotyl bending resulting in hook formation. A balanced concentration of hormones ABA and GA has been shown to be essential for a close interaction between root and hypocotyl (Baral et al., 2020).

PIFs have been involved in different aspects of gradient formation such as, auxin synthesis and polar auxin transport (PAT). In *Arabidopsis*, PIF4 and PIF5 induce the expression of *YUCCA* genes (Pfeiffer et al., 2014) and PIN localization regulatory kinase *WAG2* (Willige et al., 2012; Mazzella et al., 2014). Darkness induced phytohormones such as, GA and ethylene (ET) affect PAT indirectly by modulating the expression of *WAG2* (Willige et al., 2012) and *ETHYLENE INSENSITIVE 3/EIN3-LIKE1* (*EIN3/EIL1*) (Wabnik et al., 2016; Wang and Guo, 2018). PIFs and EIN3/EIL1 co-regulate the curvature formation by directly binding to *HOOKLESS 1* (*HLS1*) promoter. *HLS1*, which codes for a putative N-acetyltransferase and transcriptionally regulated by EIN3/EIL1 is a key regulator of apical hook development (Wang and Guo, 2018). Markedly, PIFs enhance the expression of *HLS1* by binding to its promoter at a site different from that of EIN3/EIL1. In addition, PIFs work in tandem with EIN3/EIL1 to integrate hormonal signals such as, GA, JA, and physical factors including, light and mechanical pressure (Zhang et al., 2018). Besides acting along with PIFs, EIN3 also induces the expression *PIF3* (Zhong et al., 2012). Also, divergent roles of ET in the light- and dark- mediated seedling growth are recently shown (Yu and Huang, 2017; Harkey et al., 2018, 2019; Gu et al., 2019).

In response to darkness, GA accumulates and binds to its receptor gibberellin insensitive dwarf 1 (GID1) and targets DELLAs (GAI, RGA), the negative regulators of GA signaling for UMP degradation (de Lucas et al., 2008). GA is essential for skotomorphogenesis as GA mutant *ga1* seedlings and GA biosynthesis inhibitor Paclobutrazol (PAC) treated seedlings show light-grown phenotype and are unable to form hook even when grown in the complete darkness (Achard et al.,

2007; Feng et al., 2008; Arana et al., 2011; Zhang et al., 2018). Antagonistic to auxin, GA promotes cell expansion and division on the convex side of hypocotyl (Alabadí et al., 2008; Arana et al., 2011).

In darkness, ET synthesis is enhanced by the transcriptional activation of *ACS8* by PIF5 in GA dependent manner (Arana et al., 2011). In addition to darkness, physical factors such as, soil depth and compactness, mechanical pressure generated by hypocotyl against soil induce ET production (Zhong et al., 2014; de Wit et al., 2016). ET positively regulates skotomorphogenesis as dark-grown seedlings when treated with exogenous ET, produces exaggerated hooks (Mazzella et al., 2014). Similar to auxin and GA, ET also regulates cell division but at the apical basal parts of the hook. In addition, ET maintains auxin gradient by regulating its synthesis, transport and signaling (An et al., 2012; Chang et al., 2013; Wang et al., 2014; Wabnik et al., 2016; Zhang et al., 2018). JA and SA both are negative regulators of apical hook formation, and both of them act by disrupting ET signaling. JA activated MYC2 promotes the degradation of EIN3/EIL1. Also, MYC2 and NON-EXPRESSOR OF PR GENES1 (NPR1, SA signaling mediator) individually interact with EIN3 and inhibits its binding to the promoter of *HLS1* (Zhang et al., 2018; Bertoni, 2020; Huang et al., 2020).

Hypocotyl Elongation

Another remarkable phenotype observed under darkness is an elongated hypocotyl. Darkness leads to this phenotype by modulating the levels of phytohormones such as, auxin, BR, ET, and GA (Reed et al., 2018). Irreversible increase in the plant organ size is primarily caused by cell expansion. Expansion of a cell is characterized by the vacuole enlargement and selective cell wall loosening, which releases the wall pressure and allows the water to flow inside (Cosgrove, 2016a,b). Consistently, the up-regulation of several auxin responsive cell wall loosening related genes such as, *EXPANSIN*s (*EXPA4,11*), *EXPANSIN- LIKE* (*EXLA3*) and *XYLOGLUCAN ENDOTRANSGLUCOSYLASE/HYDROLASE* (*XTH18,19*) was found in dark-grown seedlings (Cosgrove, 2005; Orden et al., 2010; Majda, 2018). Auxin acidifies the wall matrix by stimulating the activity of epidermal cell H^+-ATPases and K^+ channels, thereby, generating the turgor pressure (Ivakov et al., 2017; Majda, 2018; Duman et al., 2020). Therefore, cell wall remodeling by auxin and cell wall generated signals promotes hypocotyl elongation. PIFs maintain auxin gradient and induce the expression of wall loosening enzymes (Rougemont et al., 2012; Leivar and Monte, 2014). PIF4 remains functional under darkness by binding directly to BR stabilized protein BZR1 (Wang et al., 2012). Active PIF4-BZR1 module positively regulates the synthesis of GA by targeting DELLAs. Thus, darkness acts through the functional PIF4-BZR1 by regulating the level of phytohormones. ABA has been found to be a negative regulator of hypocotyl elongation in the dark-grown seedlings. ABA induces the expression of DELLAs (*GAI* and *RGA*) and inhibits the expression of auxin biosynthetic genes and membrane H^+-ATPases (Hayashi et al., 2014; Lorrai et al., 2018).

Shortened Roots

Like shoots, roots also sense light, consequently, root morphology is altered after light perception (Lee et al., 2017). Dark-germinated seedlings have short and thin primary roots with reduced lateral roots, whereas, the phenotype is reversed after light exposure (Dyachok et al., 2011). So, how the dark signaling represses root growth, and the light perceived at axial end of the plant alters root morphology is a curious question?

When light grown seedlings were decapitated or treated with PAT inhibitors, they showed inhibition of lateral root development (Salisbury et al., 2007), like the etiolated seedlings. This indicated that auxin synthesized in cotyledons in response to light acts as a positive regulator of lateral root emergence. Also, light facilitates auxin transport from apical part of shoot to root (Lee et al., 2016, 2017). In darkness, COP1 inhibits *PIN1* gene expression in shoot. PIN1 is essential for shoot to root PAT therefore, repression of its expression leads to the root growth suppression. But, when shoot is exposed to light, COP1 moves out from the nucleus, relieving the suppression of *PIN1* gene expression (Sassi et al., 2012; Gangappa and Botto, 2016). The HY5 deficient mutant also exhibits defects in lateral root elongation and growth, suggesting the involvement of HY5 in maintaining shoot to root continuum (Sibout et al., 2006). Light activates photoreceptors which interact with COP1, leading to its inactivation. Light-dependent inactivation of COP1 inhibits COP1 mediated degradation of HY5 thereby, promoting HY5 activity. Interestingly, light stabilized HY5 targets COP1 for degradation, thereby, shoot to root PAT is resumed that leads to altered root morphology (Mazzella et al., 2014). Moreover, HY5 translocation from shoot to root promotes root growth (Zhang et al., 2017). The dark-induced hormonal regulation of skotomorphogenic development is summarized in **Figure 2**.

Photoperiodic Flowering

Plants sense diurnal variations which affect flowering and accordingly are classified as short- day, long-day and day neutral plants. Importance of darkness in short-day plants is evident from the fact that disruption of dark period with light significantly affects flowering (Andrés and Coupland, 2012; Johansson and Staiger, 2015; Cao et al., 2016). Under long-day condition, light inhibits the expression of flowering genes; *HEADING DATE 3A* (*HD3A*) and *RICE FT-LIKE1* (*RFT1*) in rice by activating an inhibitor HEADING DATE 1 (HD1), whereas, under short-days, HD1 induces the expression of *HD3A* and *RFT1* (Ishikawa et al., 2005). Interruption of long duration of darkness with short exposure of light induces PHOTOPERIOD1 (PPD1) mediated activation of FT1, which after moving from leaves into shoot apical meristem promotes accelerated flowering in wheat (Pearce et al., 2017). Moreover, a night break (NB) causes transcriptional up-regulation of *PPD1* in wheat, levels of which increases with multiple NB and length of darkness. Thus, a period of darkness plays an important role in regulating photoperiodic flowering in plants.

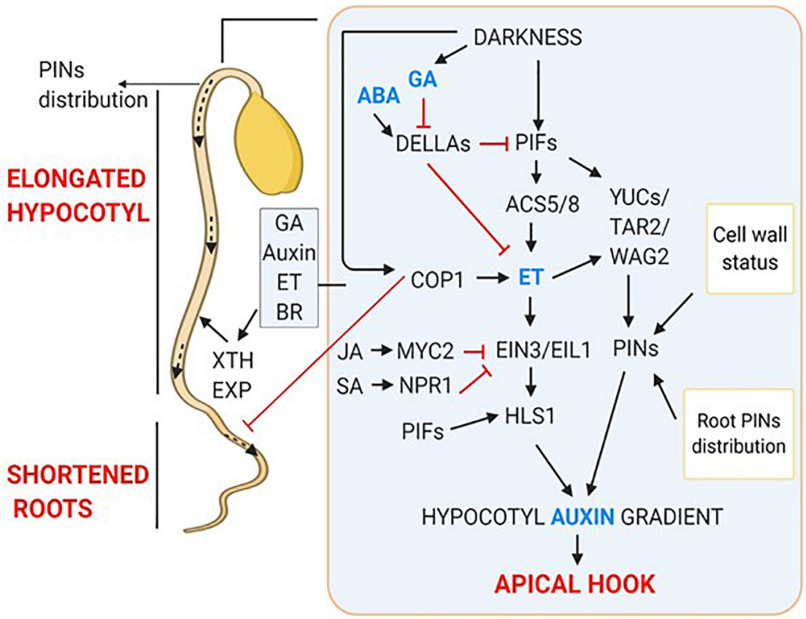

FIGURE 2 | Hormonal regulation of skotomorphogenic organs; apical hook, elongated hypocotyls and shortened roots. Dark-induced signaling results in increased gradient of GA, ET and Auxin which together interplay to form apical hook. Outside inset showing hormonal regulation of hypocotyl elongation and short roots.

Light- and Dark-Dependent Plastid Development

Development of plastids could be understood by the studies on the dark-grown seedlings. Plastids could be of various types like, proplastids, eoplasts, etioplasts, chloroplasts and chromoplasts based on their morphological characters, function and tissue location (Liebers et al., 2017). In the cotyledon of the dark-grown seedlings, eoplasts develop into etioplast and at this stage, the development of a prolamellar body (PLB) occurs (Bastien et al., 2016). A PLB is made up of regular arrangements of NADPH, the chlorophyll precursor protochlorophyllide (Pchlide), protochlorophyllide-oxido-reductase (POR), and the thylakoid membrane lipids monogalactosyldiacylglycerol (MGDG) and digalactosyldiacylglycerol (DGDG). In light, various nuclear genes which code for chloroplast biogenesis related proteins are expressed. This results in thylakoid membrane development and POR induced chlorophyll biosynthesis. The proplastids in the shoot apical meristem are directly converted to chloroplast during primary leaf development (Liebers et al., 2017).

Molecular Aspects of Plastid Development

TFs involved in early developmental process regulate the expression of plastid development related genes. PIF1 and PIF3 accumulate in dark-grown seedlings and repress the chlorophyll biosynthesis genes, whereas, in response to red light PIFs undergo active phy (Pfr) mediated degradation (Gommers and Monte, 2018; Hernández-Verdeja et al., 2020). Similarly, in light, EIN3 is directly targeted and degraded by crys and phys (Gommers and Monte, 2018).

In an early response to light the expression of *HY5*, which regulates the downstream components of chloroplast development, is induced. In dark COP1 mediates the degradation of HY5 and stabilization of PIF and EIN3. Under blue light, cryptochrome represses the expression of *COP1* leading to enhanced HY5 activity, which is required for chloroplast development (Hernández-Verdeja et al., 2020). PIFs and HY5 act as negative and positive regulators, respectively, of chlorophyll and carotenoid synthesis. Therefore, PIFs and HY5 compete for the same binding site (G-box) on the promoter of common target genes, and eventually they regulate chloroplast development antagonistically (Toledo-Ortiz et al., 2014). In addition, HY5-PIF module controls the photosynthetic gene transcription by regulating *PHYTOENE SYNTHASE* (*PSY*) gene, which catalyzes a rate limiting step in carotenoid biosynthesis pathway (Toledo-Ortiz et al., 2014). Thus, the PIF-HY5 regulatory mechanism is crucial for the proplastid development. Golden2-Like (GLK) nuclear TFs which work independently of phytochromes and PIFs are also the key regulators of plastid biogenesis (Liu et al., 2020). GLKs strongly activate the chlorophyll biosynthesis enzymes and light-harvesting chlorophyll binding proteins including, GlutRNA reductase (HEMA1), magnesium chelatase (CHLH), pchlide oxidoreductase (POR-B) and chlidea oxygenase (CAO).

Two RNA polymerases; nuclear encoded RNA polymerase (NEP) and plastid encoded RNA polymerases (PEP) are involved in the proplastid biogenesis (Hernández-Verdeja et al., 2020). In dark, plastid gene transcription is driven by NEP whereas, upon light exposure, transition of NEP to PEP occurs leading to PEP driven transcription. In light, the main transcriptional activity is taken-up by PEP, thus, the transcription of PEP associated genes

increases. PRIN2, a plastid localized redox regulated protein is required for PEP activity. In dark, PRIN2 forms a homo-dimer via di-sulfide bonds, however, upon exposure to light it get reduced to PRIN2 monomers, and contributes to PEP activity (Díaz et al., 2018). PEP mediated increase in transcription and light induced communication between developing chloroplast and nucleus through antero-retrograde signaling results in completion of chloroplast biogenesis (Pogson et al., 2015).

Hormonal Regulation of Plastid Development

Some phytohormones control the chlorophyll biosynthesis, thereby, regulate the chloroplast biogenesis. For example, in the dark-grown *Arabidopsis* seedlings cytokinin treatment induces the formation of prothylakoids whereas, these thylakoid membranes developed after about 6 h of light treatment in cytokinin untreated seedlings (Cortleven and Schmülling, 2015). The chlorophyll biosynthesis begins with the conversion of glutamate to 5-aminolevulinic acid (ALA), followed by the production of chlorophyll precursor, Pchlide. POR catalyzes the conversion of Pchlide into chlorophyllide which after esterification forms chlorophyll. Cytokinin promotes ALA synthesis and enhances POR activity to support the chloroplast biogenesis (Liu et al., 2017). GA regulated DELLA proteins are involved in the induction of *PORA* and *PORB* genes (Cheminant et al., 2011). Involvement of ET signaling has also been found in plastid development. In the double mutant of ET signaling; *ein3eil1* expression of Pchlide/chlorophyll synthesis genes *HEMA1*, *GUN4,* and *GUN5* was increased under darkness. PIF3 has been known to inhibit the expression of these genes (Stephenson et al., 2009; Shin et al., 2009), consistently, their expression was higher in *pif3* mutant. Moreover, *ein3eil1mutant* but not *pif3* had reduced expression of *PORA* and *PORB* genes. Thus, EIN3/EIL1 negatively regulate Pchlide/chlorophll biosynthesis through PIF3, but stimulate *PORA* and *PORB* independently of PIF3 (Zhong et al., 2014). These observations clearly suggest the crucial role of phytohormones in plastid development.

Shade Avoidance: An Intermediate Response Between Light and Dark

Due to their sessile nature, plants face shade arising from the neighboring vegetation canopies. In the shade, plants compete for their resources particularly red/far-red (R:FR) photon flux ratio. In response to shade, plants channelize their energy toward hypocotyl and stem elongation, enhanced apical dominance and early flowering, all of them collectively termed as shade avoidance syndrome (SAS) (de Wit et al., 2016). Along with photoreceptors, phytohormones like ET, GA, Auxin, and BR are implicated in shade-induced plant responses (Das et al., 2016; Yang and Li, 2017).

In the past decade, shade related research was carried out mainly in *Arabidopsis*, and indicated a crucial role of auxin in the shade avoidance response (Sessa et al., 2018). In the *Arabidopsis* seedlings, auxin accumulates in response to shade resulting in hypocotyl cells elongation (Ma and Li, 2019). A low R:FR ratio (as in case of shade) has been found to promote petiole elongation in *Arabidopsis* (Roig-Villanova and Martínez-García, 2016). Phytochrome B (phyB) is the key shade avoidance response regulating photoreceptor, whereas, phyD and phyE function redundantly in promoting shade-induced elongation (Franklin et al., 2003). In contrast, phyA represses the elongation response induced by low R/FR light (Martínez-García et al., 2014). phyB becomes active in the presence of light having high R:FR ratio. Upon activation, it translocates into the nucleus and interacts with PIFs. This interaction causes phosphorylation and subsequent inactivation of PIFs leading to their degradation via UMP (de Wit et al., 2016). Hence, PIF-dependent transcriptional activation of auxin homeostasis and cell wall remodeling related genes is inhibited (Courbier and Pierik, 2019). While, under light of low R:FR, phyB remains inactive, thus allowing PIFs to accumulate and induce the transcription of *YUCCA* genes (Müller-Moulé et al., 2016), resulting in enhanced auxin concentration in the cell. PIF4, 5, and 7 directly regulate several auxin biosynthesis and signaling genes in response to shade (Hornitschek et al., 2012; Li et al., 2012). A HomeoBox2 (ATHB2) TF acts as a positive regulator and Long Hypocotyl in Far-red 1/Slender In Canopy Shade 1 (HFR1/SICS1) (an atypical bHLH protein), acts as a negative regulator of PIFs controlled shade avoidance response (Sessa et al., 2018). Cryptochromes (cry1 and cry2) are involved in low blue light (LBL)-induced shade avoidance response. CRY1 and CRY2 physically interact with PIFs and regulates their activity for LBL induced hypocotyl growth (Ma et al., 2016; Sessa et al., 2018).

Phytohormones in Shade Avoidance Response

Upon low R: FR exposure, bioactive GA levels increases and the accumulated GA inhibits the DELLAs. The DELLA proteins directly interact with PIFs and this interaction prevents PIFs binding to DNA, thereby, negatively regulating the expression of cell elongation related genes (Li et al., 2016). Moreover, GA is implicated in shade-induced flowering, as silencing *GA20ox2* expression results in delayed flowering in *Arabidopsis* under far-red light conditions (Yang and Li, 2017). In addition, ET is proposed to be a positive regulator of shade-induced petiole elongation, and is involved in organ specific shade avoidance response (Yang and Li, 2017). ABA biosynthesis mutants, *nced3-2* and *aba2-1* show increased branching under low R:FR suggesting that ABA suppresses branching under shade (Yang and Li, 2017). NPR1 also plays a crucial role in petiole elongation in shade (Nozue et al., 2018). Interestingly, elevated auxin and BR production in response to PIFs activation under low R:FR light costs both SA and JA based defenses (Martínez et al., 2018).

Day-Night Transitions

The rhythmic behavior of the biological processes is maintained by an endogenous oscillator/pacemaker called the circadian clock. This clock, under natural conditions maintains a period of 24 h, regulated by transitions from day to night (light/dark) and vice versa. As the clock is tightly coupled with diurnal cycles, it modulates many gene regulatory networks (GRNs) based on

time of the day. When an organism is subjected to constant light or dark for a longer time, the rhythms dampen out and require transition from the existing environment. Since, plant life begins under complete darkness, the seedling growth during this period is clock independent, till it experiences light/dark (photoperiod) cycles (Salome et al., 2008). The fact that *Arabidopsis* seedling growth becomes photoperiod sensitive after de-etiolation was established by growing plants in continuous light and dark, separately. Until 12 h, similar hypocotyl length was observed in both conditions, and only prolonged exposure of darkness (> 12 h) resulted in elongated hypocotyls, suggesting the process to be short-day specific (Niwa et al., 2009; Seluzicki et al., 2017). Then, how clock is integrated with photoperiod after de-etiolation, was disclosed by the growth pattern of WT and clock mutants (*CCA1*-ox and *elf3*) seedlings in short-day conditions. WT seedlings elongated normally after prolonged darkness, but in both the clock mutants seedling elongation started at the beginning of the dark period and continued till it prolonged, indicating an inhibitory effect of clock genes during initial hours of darkness (Fankhauser et al., 2007). Interestingly, temporal transcriptional induction of *PIF1, 3, 4,* and *5* was also observed during late-night hours coinciding with the seedling etiolation (Leivar et al., 2012). PIFs are degraded during the day through PHY mediated photobodies, and are kept in check during early-night by clock evening complex (EC) genes (Huang et al., 2016). Another clock complex gene, *TIMING OF CAB EXPRESSER 1* (*TOC1*) represses PIFs level during early- and mid-night (Soy et al., 2016; Paik et al., 2017). Therefore, clock exerts its effect by controlling the temporal expression of *PIF* genes under darkness.

Dark-Induced Senescence

Senescence is an age triggered developmental process characterized by an ordered and programmable degradation. The degradation involves the mobilization of building blocks at various levels of organization e.g., cell, tissue, organ and the organism, culminating in plant death (Lim et al., 2007). Its initiation, progression and completion are tightly linked to various external and internal cues (Kim et al., 2016; Law et al., 2018). Darkness is one of the external cues that positively regulate leaf senescence, and the process is called dark-induced senescence (DIS). DIS is physiologically quite different from an age-triggered leaf senescence (Kiddle et al., 2011). Interestingly, darkness only promotes senescence of individual plant organs, and inhibits senescence at the whole plant level (Keech et al., 2010; Sakuraba et al., 2014; Law et al., 2018), suggesting the involvement of other factors for death of the whole plant.

PIFs involvement in DIS became evident when PIF single and quadruple (*pifq*) mutants exhibited delayed leaf senescence, and their overexpressing plants showed the opposite phenotype (Song et al., 2014). Moreover, *PIF3, 4* and *5* were significantly up-regulated in both age triggered senescence and DIS. Evidences indicate that PIFs mediate transcriptional activation of many SENESCENCE ASSOCIATED GENES (SAGs), i.e., *STAY GREEN 1* (*SGR1*) and *NON-YELLOW COLORING1* (*NYC1*) and other senescence promoting TFs such as *WRKY22* and *NAC* (Zhang et al., 2015). Additionally, PIF4/5 have been shown to transcriptionally enhance the expression of *ABSCISIC ACID 5* (*ABI5*) and *ENHANCED EM LEVELS* (*EEL*) (Qi et al., 2020). *ABI5, EEL,* and PIFs act together in a coherent feed forward loop to increase the expression of *ORESARA1* (*ORE1*), a master regulator of senescence. Subsequently, PIFs, ORE1, ABI5, and EIN3 interplay to activate SAGs which finally lead to breakdown of chlorophyll, degradation of photosynthetic machinery culminating in leaf senescence (Sakuraba et al., 2014; Qiu et al., 2015; Liebsch and Keech, 2016).

CONCLUSION AND FUTURE DIRECTIONS

Dark and light independently activate diverse signaling pathways which alter the levels of plant growth regulators consequently leading to a specific response. Efforts made in the past two decades in the area of skotobiology have advanced our understanding of how plant behaves and make sense of the dark period. The role of multifunctional dark signaling intermediates COP/DET/FUS and transcription factor PIF has been explored in diverse areas. We have provided the latest information about darkness acting as a signal during various plant growth processes such as, skotomorphogenesis, day-night transitions, shade avoidance, and senescence. Differential accumulation of several phytohormones, their regulatory effects on diverse molecular components and, in turn, the interplay of molecular players that determines the pattern of growth and development in dark has been elaborated. However, a complete understanding of the dark and light signaling integration needs exploration of the inter-organ communication mechanisms, necessary for establishment/transfer of hormonal gradients. Also, the hormonal interplay and regulatory mechanism underlying the integration of other subterranean environmental cues such as, soil compactness, temperature, biotic and abiotic factors with dark signaling, is still enigmatic and requires in-depth exploration in future.

AUTHOR CONTRIBUTIONS

AS conceptualized and designed the study. Deepika, Ankit, and SS compiled the data. Deepika, Ankit, and AS wrote the manuscript. All authors read and approved the final version of the manuscript.

ACKNOWLEDGMENTS

We acknowledge DBT (Department of Biotechnology) – e-Library Consortium (DeLCON) for providing access to e-resources and financial support from National Institute of Plant Genome Research (NIPGR) core research grant. Deepika and SS are thankful to council of scientific and industrial research (CSIR), India for research fellowships.

REFERENCES

Abbas, M., Alabadí, D., and Blázquez, M. A. (2013). Differential growth at the apical hook: all roads lead to auxin. *Front. Plant Sci.* 4:441. doi: 10.3389/fpls.2013.00441

Achard, P., Liao, L., Jiang, C., Desnos, T., Bartlett, J., Fu, X., et al. (2007). DELLAs contribute to plant photomorphogenesis. *Plant Physiol.* 143, 1163–1172. doi: 10.1104/pp.106.092254

Alabadí, D., Gallego-Bartolomé, J., Orlando, L., García-Cárcel, L., Rubio, V., Martínez, C., et al. (2008). Gibberellins modulate light signaling pathways to prevent Arabidopsis seedling de-etiolation in darkness. *Plant J.* 53, 324–335. doi: 10.1111/j.1365-313X.2007.03346.x

An, F., Zhang, X., Zhu, Z., Ji, Y., He, W., Jiang, Z., et al. (2012). Coordinated regulation of apical hook development by gibberellins and ethylene in etiolated Arabidopsis seedlings. *Cell Res.* 22, 915–927. doi: 10.1038/cr.2012.29

Andrés, F., and Coupland, G. (2012). The genetic basis of flowering responses to seasonalcues. *Nat. Publ. Gr.* 13, 627–639. doi: 10.1038/nrg3291

Arana, V., Vandenbussche, F., Petra, Z., Gallego-bartolome, J., Guardiola, V., Van Der Straeten, D., et al. (2011). Hierarchy of hormone action controlling apical hook development in Arabidopsis. *Plant J.* 67, 622–634. doi: 10.1111/j.1365-313X.2011.04621.x

Armarego-marriott, T., and Sandoval-ibañez, O. (2020). Beyond the darkness: recent lessons from etiolation and de-etiolation studies. *JXB* 71, 1215–1225. doi: 10.1093/jxb/erz496

Arsovski, A. A., Galstyan, A., Guseman, J. M., and Nemhauser, J. L. (2012). Photomorphogenesis. *Arabidopsis Book* 10:e01475. doi: 10.1199/tab.0147

Aryal, B., Jonsson, K., Baral, A., Sancho-andres, G., Kierzkowska, A. R., Kierzkowski, D., et al. (2020). Interplay between cell Wall and Auxin mediates the control of differential cell elongation during apical hook development. *Curr. Biol* 30, 1733–1739.e3. doi: 10.1016/j.cub.2020.02.055

Baral, A., Morris, E., Aryal, B., Jonsson, K., Verger, S., Xu, T., et al. (2020). External mechanical cues reveal core molecular pathway behind tissue bending in plants. *bioRxiv* [Preprint]. doi: 10.1101/2020.03.05.978296

Bastien, O., Botella, C., Chevalier, F., Block, M. A., Jouhet, J., Breton, C., et al. (2016). New insights on thylakoid biogenesis in plant cells. *Int. Rev. Cell Mol. Biol.* 323, 1–30. doi: 10.1016/bs.ircmb.2015.12.001

Bertoni, G. (2020). Ethylene versus salicylic acid in apical hook formation. *Plant Cell* 32:531. doi: 10.1105/tpc.20.00031

Béziat, C., and Kleine-Vehn, J. (2018). The road to auxin-dependent growth repression and promotion in apical hooks. *Curr. Biol.* 28, R519–R525. doi: 10.1016/j.cub.2018.01.069

Cao, K., Cui, L., Ye, L., Zhou, X., Bao, E., Zhao, H., et al. (2016). Effects of red light and night break treatments on growth and flowering of tomato plants. *Front. Plant Sci.* 7:527. doi: 10.3389/fpls.2016.00527

Cao, M., Chen, R., Li, P., Yu, Y., Zheng, R., and Ge, D. (2019). Differential growth of the apical hook. *Nature* 568, 240–243. doi: 10.1038/s41586-019-1069-7

Chang, K. N., Zhong, S., Weirauch, M. T., Hon, G., Pelizzola, M., Li, H., et al. (2013). Temporal transcriptional response to ethylene gas drives growth hormone cross-regulation in Arabidopsis. *eLIFE* 2, e00675. doi: 10.7554/eLife.00675

Cheminant, S., Wild, M., Bouvier, F., Pelletier, S., Renou, J. P., Erhardt, M., et al. (2011). DELLAs regulate chlorophyll and carotenoid biosynthesis to prevent photooxidative damage during seedling deetiolation in Arabidopsis. *Plant Cell* 23, 1849–1860. doi: 10.1105/tpc.111.085233

Chen, H., Huang, X., Gusmaroli, G., Terzaghi, W., Lau, O. S., Yanagawa, Y., et al. (2010). Arabidopsis CULLIN4-Damaged DNA Binding Protein 1 Interacts with CONSTITUTIVELY PHOTOMORPHOGENIC1-SUPPRESSOR OF PHYA Complexes to Regulate Photomorphogenesis and Flowering Time. *Plant Cell* 22, 108–123. doi: 10.1105/tpc.109.065490

Cortleven, A., and Schmülling, T. (2015). Regulation of chloroplast development and function by cytokinin. *J. Exp. Bot.* 66, 4999–5013. doi: 10.1093/jxb/erv132

Cosgrove, D. J. (2005). Growth of the plant cell wall. *Nat. Rev. Mol. Cell Biol.* 6, 850–861. doi: 10.1038/nrm1746

Cosgrove, D. J. (2016a). Catalysts of plant cell wall loosening. *F1000Res.* 5:119. doi: 10.12688/f1000research.7180.1

Cosgrove, D. J. (2016b). Plant cell wall extensibility: connecting plant cell growth with cell wall structure, mechanics, and the action of wall modifying enzymes. *JXB* 67, 463–476. doi: 10.1093/jxb/erv511

Courbier, S., and Pierik, R. (2019). Canopy light quality modulates stress responses in plants. *iScience* 22, 441–452. doi: 10.1016/j.isci.2019.11.035

Das, D., St. Onge, K. R., Voesenek, L. A. C. J., Pierik, R., and Sasidharan, R. (2016). Ethylene- and shade-induced hypocotyl elongation share transcriptome patterns and functional regulators. *Plant Physiol.* 172, 718–733. doi: 10.1104/pp.16.00725

de Lucas, M., Davière, J. M., Rodríguez-Falcón, M., Pontin, M., Iglesias-Pedraz, J. M., Lorrain, S., et al. (2008). A molecular framework for light and gibberellin control of cell elongation. *Nature* 451, 480–484. doi: 10.1038/nature06520

de Wit, M., Galvão, V. C., and Fankhauser, C. (2016). Light-mediated hormonal regulation of plant growth and development. *Annu. Rev. Plant Biol.* 67, 513–537. doi: 10.1146/annurev-arplant-043015-112252

Díaz, M. G., Hernández-Verdeja, T., Kremnev, D., Crawford, T., Dubreuil, C., and Strand, Å. (2018). Redox regulation of PEP activity during seedling establishment in *Arabidopsis thaliana*. *Nat. Commun.* 9:50. doi: 10.1038/s41467-017-02468-2

Dong, J., Tang, D., Gao, Z., Yu, R., Li, K., He, H., et al. (2014). Arabidopsis DE-ETIOLATED1 represses photomorphogenesis by positively regulating phytochrome-interacting factors in the dark. *Plant Cell* 26, 3630–3645. doi: 10.1105/tpc.114.130666

Duman, Z., Eliyahu, A., Abu-abied, M., and Sadot, E. (2020). The contribution of cell wall remodeling and signaling to lateral organs formation. *Isr. J. Plant Sci.* 67, 110–127. doi: 10.1163/22238980-20191115

Dyachok, J., Zhu, L., Liao, F., He, J., Huq, E., and Blancaflor, E. B. (2011). SCAR mediates light-induced root elongation in arabidopsis through photoreceptors and proteasomes. *Plant Cell* 23, 3610–3626. doi: 10.1105/tpc.111.088823

Fankhauser, C., Nozue, K., Covington, M. F., Duek, P. D., Harmer, S. L., and Maloof, J. N. (2007). Rhythmic growth explained by coincidence between internal and external cues. *Nature* 448, 358–361. doi: 10.1038/nature05946

Farquharson, K. (2017). Division of labor during apical hook formation. *Plant Cell* 29, 917–918. doi: 10.1105/tpc.17.00357

Feng, S., Martinez, C., Gusmaroli, G., Wang, Y., Zhou, J., Wang, F., et al. (2008). Coordinated regulation of *Arabidopsis thaliana* development by light and gibberellins. *Nature* 451, 475–479. doi: 10.1038/nature06448

Franklin, K. A., Praekelt, U., Stoddart, W. M., Billingham, O. E., Halliday, K. J., and Whitelam, G. C. (2003). Phytochromes B, D, and E act redundantly to control multiple physiological responses in arabidopsis. *Plant Physiol.* 131, 1340–1346. doi: 10.1104/pp.102.015487

Galvao, V. C., and Fankhauser, C. (2015). Sensing the light environment in plants: photoreceptors and early signaling steps. *Curr. Opin. Neurobiol.* 34, 46–53. doi: 10.1016/j.conb.2015.01.013

Gangappa, S. N., and Botto, J. F. (2016). The multifaceted roles of HY5 in plant growth and development. *Mol. Plant* 9, 1353–1365. doi: 10.1016/j.molp.2016.07.002

Gommers, C. M. M., and Monte, E. (2018). Seedling establishment: a dimmer switch-regulated process between dark and light signaling. *Plant Physiol.* 176, 1061–1074. doi: 10.1104/pp.17.01460

Gu, S. Y., Wang, L. C., Cheuh, C. M., and Lo, W. S. (2019). CHITINASE like1 regulates root development of dark-grown seedlings by modulating ethylene biosynthesis in *Arabidopsis thaliana*. *Front. Plant Sci.* 10:600. doi: 10.3389/fpls.2019.00600

Harkey, A. F., Watkins, J. M., Olex, A. L., DiNapoli, K. T., Lewis, D. R., Fetrow, J. S., et al. (2018). Identification of transcriptional and receptor networks that control root responses to ethylene. *Plant Physiol.* 176, 2095–2118. doi: 10.1104/pp.17.00907

Harkey, A. F., Yoon, G. M., Seo, D. H., DeLong, A., and Muday, G. K. (2019). Light modulates ethylene synthesis, signaling, and downstream transcriptional networks to control plant development. *Front. Plant Sci.* 10:1094. doi: 10.3389/fpls.2019.01094

Hayashi, Y., Takahashi, K., Inoue, S. I., and Kinoshita, T. (2014). Abscisic acid suppresses hypocotyl elongation by dephosphorylating plasma membrane H+-ATPase in *Arabidopsis thaliana*. *Plant Cell Physiol.* 55, 845–853. doi: 10.1093/pcp/pcu028

Hernández-Verdeja, T., Vuorijoki, L., and Strand, Å. (2020). Emerging from the darkness: interplay between light and plastid signaling during chloroplast biogenesis. *Physiol. Plant.* 169, 397–406. doi: 10.1111/ppl.13100

Hornitschek, P., Kohnen, M. V., Lorrain, S., Rougemont, J., Ljung, K., López-Vidriero, I., et al. (2012). Phytochrome interacting factors 4 and 5 control

seedling growth in changing light conditions by directly controlling auxin signaling. *Plant J.* 71, 699–711. doi: 10.1111/j.1365-313X.2012.05033.x

Huang, H., Alvarez, S., Bindbeutel, R., Shen, Z., Naldrett, M. J., Evans, B. S., et al. (2016). Identification of evening complex associated proteins in arabidopsis by affinity purification and mass spectrometry. *Mol. Cell. Proteomics* 15, 201–217. doi: 10.6019/PXD002606

Huang, P., Dong, Z., Guo, P., Zhang, X., Qiu, Y., Li, B., et al. (2020). Salicylic acid suppresses apical hook formation via NPR1-mediated repression of EIN3 and EIL1 in Arabidopsis. *Plant Cell* 32, 612–629. doi: 10.1105/tpc.19.00658

Huang, X., Ouyang, X., and Deng, X. W. (2014). Beyond repression of photomorphogenesis: role switching of COP / DET / FUS in light signaling. *Curr. Biol.* 21, 96–103. doi: 10.1016/j.pbi.2014.07.003

Ishikawa, R., Tamaki, S., Yokoi, S., Inagaki, N., Shinomura, T., Takano, M., et al. (2005). Suppression of the floral activator Hd3a is the principal cause of the night break effect in rice. *Plant Cell* 17, 3326–3336. doi: 10.1105/tpc.105.037028.1

Ivakov, A., Flis, A., Apelt, F., Scherer, U., Stitt, M., Kragler, F., et al. (2017). Cellulose synthesis and cell expansion are regulated by different mechanisms in growing Arabidopsis hypocotyls. *Plant Cell* 29, 1305–1315. doi: 10.1105/tpc.16.00782

Johansson, M., and Staiger, D. (2015). Time to flower: interplay between photoperiod and the circadian clock. *JXB* 66, 719–730. doi: 10.1093/jxb/eru441

Keech, O., Pesquet, E., Gutierrez, L., Ahad, A., Bellini, C., Smith, S. M., et al. (2010). Leaf senescence is accompanied by an early disruption of the microtubule network in arabidopsis. *Plant Physiol.* 154, 1710–1720. doi: 10.1104/pp.110.163402

Kiddle, S., Kim, Y., Penfold, C. A., Jenkins, D., Zhang, C., Morris, K., et al. (2011). High-resolution temporal profiling of transcripts during arabidopsis leaf senescence reveals a distinct chronology of processes and regulation. *Plant Physiol.* 23, 873–894. doi: 10.1105/tpc.111.083345

Kim, J., Woo, H. R., and Nam, H. G. (2016). Toward systems understanding of leaf senescence: an integrated multi-omics perspective on leaf senescence research. *Mol. Plant* 9, 813–825. doi: 10.1016/j.molp.2016.04.017

Law, S. R., Chrobok, D., Juvany, M., Delhomme, N., Lindén, P., Brouwer, B., et al. (2018). Darkened leaves use different metabolic strategies for senescence and survival. *Plant Physiol.* 177, 132–150. doi: 10.1104/pp.18.00062

Lee, H., Park, Y., Ha, J., Baldwin, I. T., and Park, C. (2017). Multiple Routes of Light Signaling during Root Photomorphogenesis. *Trends Plant Sci.* 22, 803–812. doi: 10.1016/j.tplants.2017.06.009

Lee, H.-J., Ha, J.-H., Kim, S.-G., Choi, H.-K., Kim, Z. H., Han, Y.-J., et al. (2016). Stem-piped light activates phytochrome B to trigger light responses in *Arabidopsis thaliana* roots. *Sci. Signal.* 9:ra106. doi: 10.1126/scisignal.aaf6530

Leivar, P., and Monte, E. (2014). PIFs: systems integrators in plant development. *Plant Cell* 26, 56–78. doi: 10.1105/tpc.113.120857

Leivar, P., Monte, E., Oka, Y., Liu, T., Carle, C., Castillon, A., et al. (2008). Article multiple phytochrome-interacting bHLH transcription factors repress premature seedling photomorphogenesis in darkness. *Curr. Biol.* 18, 1815–1823. doi: 10.1016/j.cub.2008.10.058

Leivar, P., National, S., and Sentandreu, M. (2012). Phytochrome-imposed oscillations in PIF3 protein abundance regulate hypocotyl growth under diurnal light/dark conditions in Arabidopsis. *Plant J.* 71, 390–401. doi: 10.1111/j.1365-313X.2012.04992.x

Li, K., Yu, R., Fan, L. M., Wei, N., Chen, H., and Deng, X. W. (2016). DELLA-mediated PIF degradation contributes to coordination of light and gibberellin signalling in Arabidopsis. *Nat. Commun.* 7:11868. doi: 10.1038/ncomms11868

Li, L., Ljung, K., Breton, G., Schmitz, R. J., Pruneda-Paz, J., Cowing-Zitron, C., et al. (2012). Linking photoreceptor excitation to changes in plant architecture. *Genes Dev.* 26, 785–790. doi: 10.1101/gad.187849.112

Liebers, M., Grübler, B., Chevalier, F., Lerbs-Mache, S., Merendino, L., Blanvillain, R., et al. (2017). Regulatory shifts in plastid transcription play a key role in morphological conversions of plastids during plant development. *Front. Plant Sci.* 8:23. doi: 10.3389/fpls.2017.00023

Liebsch, D., and Keech, O. (2016). Dark-induced leaf senescence: new insights into a complex light-dependent regulatory pathway. *New Phytol.* 212, 563–570. doi: 10.1111/nph.14217

Lim, P. O., Kim, H. J., and Nam, H. G. (2007). Leaf Senescence. *Annu. Rev. Plant Biol.* 58, 115–136. doi: 10.1146/annurev.arplant.57.032905.105316

Liu, L., Lin, N., Liu, X., Yang, S., Wang, W., and Wan, X. (2020). From chloroplast biogenesis to chlorophyll accumulation: the interplay of light and hormones on gene expression in *Camellia sinensis* cv. Shuchazao Leaves. *Front. Plant Sci.* 11, 256. doi: 10.3389/fpls.2020.00256

Liu, X., Li, Y., and Zhong, S. (2017). Interplay between light and plant hormones in the control of Arabidopsis seedling chlorophyll biosynthesis. *Front. Plant Sci.* 8:1433. doi: 10.3389/fpls.2017.01433

Lorrai, R., Boccaccini, A., Ruta, V., Possenti, M., Costantino, P., and Vittorioso, P. (2018). Abscisic acid inhibits hypocotyl elongation acting on gibberellins. DELLA proteins and auxin. *AoB Plants* 10:ply061. doi: 10.1093/aobpla/ply061

Ma, D., Li, X., Guo, Y., Chu, J., Fang, S., Yan, C., et al. (2016). Cryptochrome 1 interacts with PIF4 to regulate high temperature-mediated hypocotyl elongation in response to blue light. *Proc. Natl. Acad. Sci. U.S.A.* 113, 224–229. doi: 10.1073/pnas.1511437113

Ma, L., and Li, G. (2019). Auxin-dependent cell elongation during the shade avoidance response. *Front. Plant Sci.* 10:914. doi: 10.3389/fpls.2019.00914

Majda, M. (2018). The role of auxin in cell wall expansion. *Int. J. Mol. Sci.* 19:951. doi: 10.3390/ijms19040951

Martínez, C., Espinosa-Ruíz, A., Lucas, M., Bernardo-García, S., Franco-Zorrilla, J. M., and Prat, S. (2018). PIF 4-induced BR synthesis is critical to diurnal and thermomorphogenic growth. *EMBO J.* 37:e99552. doi: 10.15252/embj.201899552

Martínez-García, J. F., Gallemí, M., Molina-Contreras, M. J., Llorente, B., Bevilaqua, M. R. R., and Quail, P. H. (2014). The shade avoidance syndrome in Arabidopsis: the antagonistic role of phytochrome A and B differentiates vegetation proximity and canopy shade. *PLoS One* 9:e109275. doi: 10.1371/journal.pone.0109275

Mazzella, M. A., Casal, J. J., Jorge, P., and Fox, A. R. (2014). Hormonal networks involved in apical hook development in darkness and their response to light. *Front. Plant Sci.* 5:52. doi: 10.3389/fpls.2014.00052

Mishra, S., and Khurana, J. P. (2017). Emerging roles and new paradigms in signaling mechanisms of plant cryptochromes. *CRC Crit. Rev. Plant Sci.* 36, 89–115. doi: 10.1080/07352689.2017.1348725

Müller-Moulé, P., Nozue, K., Pytlak, M. L., Palmer, C. M., Covington, M. F., Wallace, A. D., et al. (2016). YUCCA auxin biosynthetic genes are required for Arabidopsis shade avoidance. *PeerJ* 2016:e2574. doi: 10.7717/peerj.2574

Niwa, Y., Yamashino, T., and Mizuno, T. (2009). The circadian clock regulates the photoperiodic response of hypocotyl elongation through a coincidence mechanism in *Arabidopsis thaliana*. *Plant Cell Physiol.* 1, 838–854. doi: 10.1093/pcp/pcp028

Nozue, K., Devisetty, U. K., Lekkala, S., Mueller-Moulé, P., Bak, A., Casteel, C. L., et al. (2018). Network analysis reveals a role for salicylic acid pathway components in shade avoidance. *Plant Physiol.* 178, 1720–1732. doi: 10.1104/pp.18.00920

Orden, V., Wolf, S., Vissenberg, K., Delacourt, J., Assoumou, Y., and Pelletier, S. (2010). A role for pectin de-methylesterification in a developmentally regulated growth acceleration in dark- grown Arabidopsis hypocotyls. *New Phytol.* 188, 726–739. doi: 10.1111/j.1469-8137.2010.03409.x

Paik, I., Kathare, P. K., Kim, J., and Huq, E. (2017). Expanding roles of PIFs in signal integration from multiple processes. *Mol. Plant* 10, 1035–1046. doi: 10.1016/j.molp.2017.07.002

Pearce, S., Shaw, L. M., Lin, H., Cotter, J. D., Li, C., and Dubcovsky, J. (2017). Night-break experiments shed light on the photoperiod1-mediated flowering. *Plant Physiol.* 174, 1139–1150. doi: 10.1104/pp.17.00361

Pfeiffer, A., Shi, H., Tepperman, J. M., Zhang, Y., and Quail, P. H. (2014). Combinatorial complexity in a transcriptionally centered signaling hub in Arabidopsis. *Mol. Plant* 7, 1598–1618. doi: 10.1093/mp/ssu087

Pham, V. N., Kathare, P. K., and Huq, E. (2018). Phytochromes and phytochrome interacting factors. *Plant Physiol.* 176, 1025–1038. doi: 10.1104/pp.17.01384

Podolec, R., and Ulm, R. (2018). Photoreceptor-mediated regulation of the COP1 / SPA E3 ubiquitin ligase. *Curr. Opin. Plant Biol.* 45, 18–25. doi: 10.1016/j.pbi.2018.04.018

Pogson, B. J., Ganguly, D., and Albrecht-Borth, V. (2015). Insights into chloroplast biogenesis and development. *Biochim. Biophys. Acta Bioenerg.* 1847, 1017–1024. doi: 10.1016/j.bbabio.2015.02.003

Pokhilko, A., Ramos, J. A., Holtan, H., Maszle, D. R., Khanna, R., and Millar, A. J. (2011). Ubiquitin ligase switch in plant photomorphogenesis: a hypothesis. *J. Theor. Biol.* 270, 31–41. doi: 10.1016/j.jtbi.2010.11.021

Qi, L., Liu, S., Li, C., Fu, J., Jing, Y., Cheng, J., et al. (2020). PHYTOCHROME-INTERACTING FACTORS Interact with the ABA Receptors PYL8 and PYL9 to

Orchestrate ABA Signaling in Darkness. *Mol. Plant* 13, 414–430. doi: 10.1016/j.molp.2020.02.001

Qiu, K., Li, Z., Yang, Z., Chen, J., Wu, S., Zhu, X., et al. (2015). EIN3 and ORE1 accelerate degreening during ethylene-mediated leaf senescence by directly activating chlorophyll catabolic genes in Arabidopsis. *PLoS Genet.* 11:e1005399. doi: 10.1371/journal.pgen.1005399

Reed, J. W., Wu, M., Reeves, P. H., Hodgens, C., Yadav, V., Hayes, S., et al. (2018). Three auxin response factors promote hypocotyl elongation. *Plant Physiol.* 178, 864–875. doi: 10.1104/pp.18.00718

Roig-Villanova, I., and Martínez-García, J. F. (2016). Plant responses to vegetation proximity: a whole life avoiding shade. *Front. Plant Sci.* 7:236. doi: 10.3389/fpls.2016.00236

Rougemont, J., Ljung, K., Lo, I., Solano, R., Trevisan, M., Pradervand, S., et al. (2012). Phytochrome interacting factors 4 and 5 control seedling growth in changing light conditions by directly controlling auxin signaling. *Plant J.* 1, 699–711. doi: 10.1111/j.1365-313X.2012.05033.x

Sakuraba, Y., Jeong, J., Kang, M., Kim, J., Paek, N., and Choi, G. (2014). PIF4 and PIF5 induce leaf senescence in Arabidopsis. *Nat. Commun.* 5:4636. doi: 10.1038/ncomms5636

Salisbury, F. J., Hall, A., Grierson, C. S., Halliday, K. J., Buildings, K., Road, M., et al. (2007). Phytochrome coordinates Arabidopsis shoot and root development. *Plant J.* 50, 429–438. doi: 10.1111/j.1365-313X.2007.03059.x

Salome, P. A., Xie, Q., and McClung, C. R. (2008). Circadian timekeeping during early Arabidopsis development. *Plant Physiol.* 147, 1110–1125. doi: 10.1104/pp.108.117622

Sampathkumar, A., and Eng, R. C. (2020). Plant biology: bending of plant organs. *Curr. Biol.* 30, R402–R405. doi: 10.1016/j.cub.2020.03.010

Sassi, M., Lu, Y., Zhang, Y., Wang, J., Dhonukshe, P., Blilou, I., et al. (2012). COP1 mediates the coordination of root and shoot growth by light through modulation of PIN1- and PIN2-dependent auxin transport in Arabidopsis. *Development* 3412, 3402–3412. doi: 10.1242/dev.078212

Seluzicki, A., Burko, Y., and Chory, J. (2017). Dancing in the dark: darkness as a signal in plants. *Plant Cell Environ.* 40, 2487–2501. doi: 10.1111/pce.12900

Sessa, G., Carabelli, M., Possenti, M., Morelli, G., and Ruberti, I. (2018). Multiple pathways in the control of the shade avoidance response. *Plants* 7:102. doi: 10.3390/plants7040102

Shin, J., Kim, K., Kang, H., Zulfugarov, I. S., Bae, G., Lee, C. H., et al. (2009). Phytochromes promote seedling light responses by inhibiting four negatively-acting phytochrome-interacting factors. *Proc. Natl. Acad. Sci. U.S.A.* 106, 7660–7665. doi: 10.1073/pnas.0812219106

Sibout, R., Sukumar, P., Hettiarachchi, C., Holm, M., Muday, G. K., and Hardtke, C. S. (2006). Opposite root growth phenotypes of hy5 versus hy5 hyh mutants correlate with increased constitutive auxin signaling. *PLoS Genet.* 2:e202. doi: 10.1371/journal.pgen.0020202

Song, Y., Yang, C., Gao, S., Zhang, W., Li, L., and Kuai, B. (2014). Age-triggered and dark-induced leaf senescence require the bHLH transcription factors PIF3, 4, and 5. *Mol. Plant* 7, 1776–1787. doi: 10.1093/mp/ssu109

Soy, J., Leivar, P., González-schain, N., Martín, G., Diaz, C., and Sentandreu, M. (2016). Molecular convergence of clock and photosensory pathways through PIF3 – TOC1 interaction and co-occupancy of target promoters. *Proc. Natl. Acad. Sci. U.S.A.* 113, 4870–4875. doi: 10.1073/pnas.1603745113

Stepanova, A. N., Robertson-Hoyt, J., Yun, J., Benavente, L. M., Xie, D. Y., Doležal, K., et al. (2008). TAA1-mediated auxin biosynthesis is essential for hormone crosstalk and plant development. *Cell* 133, 177–191. doi: 10.1016/j.cell.2008.01.047

Stepanova, A. N., Yun, J., Robles, L. M., Novak, O., He, W., Guo, H., et al. (2011). The Arabidopsis YUCCA1 flavin monooxygenase functions in the indole-3-pyruvic acid branch of auxin biosynthesis. *Plant Cell* 23, 3961–3973. doi: 10.1105/tpc.111.088047

Stephenson, P. G., Fankhauser, C., and Terry, M. J. (2009). PIF3 is a repressor of chloroplast development. *Proc. Natl. Acad. Sci. U.S.A.* 106, 7654–7659. doi: 10.1073/pnas.0811684106

Toledo-Ortiz, G., Johansson, H., Lee, K. P., Bou-Torrent, J., Stewart, K., Steel, G., et al. (2014). The HY5-PIF regulatory module coordinates light and temperature control of photosynthetic gene transcription. *PLoS Genet.* 10:e1004416. doi: 10.1371/journal.pgen.1004416

Vandenbussche, F., Petrášek, J., Žádníková, P., Hoyerová, K., Pešek, B., Raz, V., et al. (2010). The auxin influx carriers AUX1 and LAX3 are involved in auxin-ethylene interactions during apical hook development in *Arabidopsis thaliana* seedlings. *Development* 137, 597–606. doi: 10.1242/dev.040790

Wabnik, K., Abuzeineh, A., Gallemi, M., Van Der Straeten, D., Zádníková, P., Smith, R. S., et al. (2016). A model of differential growth-guided apical hook formation in plants. *Plant Cell* 28, 2464–2477. doi: 10.1105/tpc.15.00569

Wang, S., Zhang, S., Sun, C., Xu, Y., Chen, Y., Yu, C., et al. (2014). Auxin response factor (OsARF12), a novel regulator for phosphate homeostasis in rice (Oryza sativa). *New Phytol.* 201, 91–103. doi: 10.1111/nph.12499

Wang, Y., and Guo, H. (2018). Tansley insight on hormonal regulation of the dynamic apical hook development. *New Phytol.* 222, 1230–1234. doi: 10.1111/nph.15626

Wang, Z., Bai, M., and Oh, E. (2012). Brassinosteroid signaling network and regulation of photomorphogenesis. *Annu. Rev. Genet.* 46, 701–724. doi: 10.1146/annurev-genet-102209-163450

Willige, B. C., Ogiso-tanaka, E., Zourelidou, M., and Schwechheimer, C. (2012). WAG2 represses apical hook opening downstream from gibberellin and PHYTOCHROME INTERACTING FACTOR 5. *Development* 139, 4020–4028. doi: 10.1242/dev.081240

Wu, G., Cameron, J. N., Ljung, K., and Spalding, E. P. (2010). A role for ABCB19-mediated polar auxin transport in seedling photomorphogenesis mediated by cryptochrome 1 and phytochrome B. *Plant J.* 62, 179–191. doi: 10.1111/j.1365-313X.2010.04137.x

Yang, C., and Li, L. (2017). Hormonal regulation in shade avoidance. *Front. Plant Sci.* 8:1527. doi: 10.3389/fpls.2017.01527

Yu, Y., and Huang, R. (2017). Integration of ethylene and light signaling affects hypocotyl growth in Arabidopsis. *Front. Plant Sci.* 8:57. doi: 10.3389/fpls.2017.00057

Žádníkova, P., Petrášek, J., Marhavý, P., Raz, V., Vandenbussche, F., Ding, Z., et al. (2010). Role of PIN-mediated auxin efflux in apical hook development of *Arabidopsis thaliana*. *Development* 137, 607–617. doi: 10.1242/dev.041277

Žádníkova, P., Wabnik, K., Abuzeineh, A., Gallemi, M., Van Der Straeten, D., Smith, R. S., et al. (2016). A model of differential growth-guided apical hook formation in plants. *Plant Cell* 28, 2464–2477. doi: 10.1105/tpc.15.00569

Zhang, X., Ji, Y., Xue, C., Ma, H., Xi, Y., Huang, P., et al. (2018). Integrated regulation of apical hook development by transcriptional coupling of EIN3 / EIL1 and PIFs in Arabidopsis. *Plant Cell* 30, 1971–1988. doi: 10.1105/tpc.18.00018

Zhang, Y., Li, C., Zhang, J., Wang, J., Yang, J., Lv, Y., et al. (2017). Dissection of HY5/HYH expression in Arabidopsis reveals a root-autonomous HY5-mediated photomorphogenic pathway. *PLoS One* 12:e0180449. doi: 10.1371/journal.pone.0180449

Zhang, Y., Liu, Z., Chen, Y., He, J., and Bi, Y. (2015). Plant Science PHYTOCHROME-INTERACTING FACTOR 5 (PIF5) positively regulates dark-induced senescence and chlorophyll degradation in Arabidopsis. *Plant Sci.* 237, 57–68. doi: 10.1016/j.plantsci.2015.05.010

Zhong, S., Shi, H., Xue, C., Wang, L., Xi, Y., Li, J., et al. (2012). A molecular framework of light-controlled phytohormone action in arabidopsis. *Curr. Biol.* 22, 1530–1535. doi: 10.1016/j.cub.2012.06.039

Zhong, S., Shi, H., Xue, C., Wei, N., Guo, H., and Deng, X. W. (2014). Ethylene-orchestrated circuitry coordinates a seedling's response to soil cover and etiolated growth. *Proc. Natl. Acad. Sci. U.S.A.* 111, 3913–3920. doi: 10.1073/pnas.1402491111

Zhu, Q., and Gallem, M. (2019). Root gravity response module guides differential growth determining both root bending and apical hook formation in Arabidopsis. *Development* 146:dev175919. doi: 10.1242/dev.175919

Conflict of Interest: The authors declare that the research was conducted in the absence of any commercial or financial relationships that could be construed as a potential conflict of interest.

frontiers in Plant Science

ORIGINAL RESEARCH
published: 08 October 2020
doi: 10.3389/fpls.2020.563971

The Impact of Fruit Etiolation on Quality of Seeds in Tobacco

Domenica Farci[1†], Patrycja Haniewicz[1†], Emma Cocco[2], Antonio De Agostini[3], Pierluigi Cortis[3], Magdalena Kusaka[1], Maria C. Loi[2] and Dario Piano[1,2*]*

[1]Department of Plant Physiology, Warsaw University of Life Sciences—SGGW, Warsaw, Poland, [2]Laboratory of Plant Physiology and Photobiology, Department of Life and Environmental Sciences, University of Cagliari, Cagliari, Italy, [3]Department of Life and Environmental Sciences, University of Cagliari, Cagliari, Italy

Seed's maturity and integrity are essential requirements for germination, and they rely on nutrients availability and a correct phytohormones' balance. These aspects are prerequisites for prompt germination at the end of the dormancy period and strictly depend on chloroplast metabolism and photosynthesis. In the present work, capsules of *Nicotiana tabacum* were grown in dark during the whole post-anthesis period. Among others, photosynthetic rates, dormancy, and phytohormones levels in seeds were found to be significantly different with respect to controls. In particular, etiolated capsules had expectedly reduced photosynthetic rates and, when compared to controls, their seeds had an increased mass and volume, an alteration in hormones level, and a consequently reduced dormancy. The present findings show how, during fruit development, the presence of light and the related fruit's photosynthetic activity play an indirect but essential role for reaching seeds maturity and dormancy. Results highlight how unripe fruits are versatile organs that, depending on the environmental conditions, may facultatively behave as sink or source/sink with associated variation in seed's reserves and phytohormone levels.

Keywords: dormancy, germination, *Nicotiana tabacum*, phytohormones, photosynthesis, post-anthesis, ripening, photomorphogenesis

OPEN ACCESS

Edited by:
Péter Poór,
University of Szeged, Hungary

Reviewed by:
Branka Salopek Sondi,
Rudjer Boskovic Institute, Croatia
Kai Shu,
Northwestern Polytechnical University, China
Helene S. Robert,
Central European Institute of Technology (CEITEC), Czechia

***Correspondence:**
Dario Piano
dario.piano@unica.it
Domenica Farci
domenica_farci@sggw.edu.pl

†These authors share first authorship

Specialty section:
This article was submitted to Plant Physiology, a section of the journal Frontiers in Plant Science

Received: *20 May 2020*
Accepted: *14 September 2020*
Published: *08 October 2020*

Citation:
Farci D, Haniewicz P, Cocco E, De Agostini A, Cortis P, Kusaka M, Loi MC and Piano D (2020) The Impact of Fruit Etiolation on Quality of Seeds in Tobacco. Front. Plant Sci. 11:563971. doi: 10.3389/fpls.2020.563971

INTRODUCTION

Fruits and seeds are the key players in plant reproduction and species dynamics (Hamilton and May, 1977; Springthorpe and Penfield, 2015). Their properties and functions are intimately related and follow the same fate (Hamilton and May, 1977; Aharoni and O'Connell, 2002; Springthorpe and Penfield, 2015). Immediately after anthesis, flower pollination and fruit formation take place, resulting in seeds (pre-) maturation while the fruit ripens (Sumner and Mollon, 2000).

Fruit ripening and seed development are processes strictly depending on the photosynthates trafficking (Kourmpetli and Drea, 2014). In this respect, fruits are unique organs that are both centers of photosynthates accumulation, behaving as sinks and sources of photosynthates due to their photosynthetic parenchyma (Lytovchenko et al., 2011). This bivalent behavior starts from the early stages of fruit formation, lasts immediately until ripening (Yamaki, 2010), and appears to be important for seeds development (Lytovchenko et al., 2011). Accordingly, the photosynthates accumulation is shared between leaves and developing-unripe fruits, resulting in a characteristic species-specific profile of their relative contribution (Hidaka et al., 2019).

In fruits, the ratio between their own contribution and the one from leaves strictly depends on their photosynthetic capabilities. Considering that fruits are also sink organs with the ability to increase the concentration of photosynthates and solutes by their own, leaves are a subordinated source for photosynthates production according to the Münch scheme (Christy and Ferrier, 1973). On one hand, by allocation mechanisms, the photosynthates from leaves are promptly translocated to the fruits to an extent that is defined by the fruit itself, the species, and the environmental conditions (Hidaka et al., 2019). On the other hand, if the photosynthates production from fruits and the related coordination role are obvious, it is not obvious their precise contribution with respect to leaves (Baïram et al., 2019). Accordingly, for a given species, the leaves contribution is primarily expected to depend on the fruits' photosynthetic capabilities, hence on the extent and efficiency of the fruit photosynthetic parenchyma, as well as the final mass to be reached. Related to this, it must be also noticed that while fruit growth takes place, the surface of fruits increases proportionally but the number of stomata remains the same (Hiratsuka et al., 2015), suggesting that the leaves contribution increases while the ripening is approached. In fact, the resulting reduction of stomata's density brings to a decreased efficiency in gas exchanges and related photosynthetic rates (Hiratsuka et al., 2015). This causes an increased difference in solutes concentration between sink and sources; hence, it brings to an increased flow of photosynthates from leaves to fruits (Christy and Ferrier, 1973). Under this complex phenomenology, it is evident that a fine reciprocal regulation is needed to harmonize the photosynthetic activities of these two districts and their related productions (Baïram et al., 2019). This role of coordination is pivotally modulated by phytohormones that tune an efficient photosynthate trafficking and allocation (Robert, 2019). In this study, immediately after pollination, flowers were shielded from light to induce etiolation. The etiolated capsules presented expectedly reduced photosynthetic rates and significative differences when compared to controls, especially with respect to seeds properties. Under etiolated conditions, the contribution of photosynthates from external sources is dominant, and the differences in seeds and fruits allow to infer about the contribution of each source in normal light conditions, eventually providing evidence for the essential role of balancing and regulation played by the fruit during development. Here, the etiolation of tobacco capsules, which were subjected to targeted light starvation, provides evidence about the primary role played by the photosynthetic activity in green-unripe fruits. This role appears strongly mediated by phytohormones that act by driving fruit development and demonstrates how photomorphogenesis is essential in fruits for reaching the seed's maturity and dormancy.

Abbreviations: ABA, Abscisic acid; cZ, Cis-Zeatin; cZR, Cis-Zeatin-9-riboside; D2-GA_1, Giberellin-d2; D2-JA, Jasmonic-2,4,4-d3-(acetyl-2,2-d2) acid; D4-SA, Salicylate-d4; D5-IAA, Indole-2,4,5,6,7-d5-3-acetic acid; D6-ABA, Abscisic acid-d6; DPA, Day post-anthesis; GA_1, Gibberellins; IAA, Indole-3-acetic acid; IAA-Asp, Indole-3-acetylaspartic acid; JA, Jasmonate; JA-ILE, Jasmonoyl isoleucine; OPDA, 12-oxo-phytodienoic acid; PSII, Photosystem II; SA, Salicylate.

MATERIALS AND METHODS

Growth and Cultivation of Tobacco Plants

Seeds of *Nicotiana tabacum* (cv. *Petit havana*) were imbibed in tap water by incubating them for 24 h at 4°C under dark conditions. After imbibition, seeds were sowed, and plants were grown for 15–20 weeks under a constant temperature of 25°C, 50% relative humidity, a light regime of 12 h/day, and a light intensity of 150–200 μmol photons/(s·m^2).

Induction of Etiolation

At their early developmental stage, the etiolation of capsules was induced as follows. At the 2nd day post-anthesis (DPA), when pollination has already taken place and the ovary started to swell, the senescent corolla was removed, and the green ovary was covered till the insertion of the peduncle on the inflorescence axis by a triple-layered pocket made of black-crepe paper. This paper shielded the ovary from light but allowed the gas exchange between the ovary and the environment. The protective coverage was maintained in place for 2–3 weeks, allowing the period of swelling and seeds' maturation to take place under dark conditions.

Similar experiments were extended to the whole leafage; the whole plant was covered with a single pocket of black-crepe paper, leaving only the inflorescence uncovered, but flowers were abscised after 2–5 DPA.

Control plants, which were plants not subjected to etiolation in any of their parts, provided capsules and seeds for controls data ("external controls"). Uncovered capsules from test plants (plants subjected to etiolation in some of their parts) were also used as "internal controls." In this case, neither capsules nor seeds did show significant differences with respect to "external controls" (see following paragraphs).

Experiments were performed on a pool of three test plants and three control plants.

Photosynthetic Measurements

The photosynthetic activity on etiolated and control capsules was recorded by using a Mini PPM 100 fluorimeter (EARS, The Netherlands). This handy fluorimeter is provided with a holed spacer (~0.5 cm diameter) that allows measurements on a very small photosynthetic surface. In these conditions, the measurement on a flat surface (e.g., leaf) or a slightly bent surface (e.g., capsules) does not affect the efficiency of the measurement and makes the instrument ideal for this specific need. After 15 min of dark adaptation, a pulse width modulation (PWM) of 7.2 kHz at 455 nm was provided. Each saturating pulse carried about 2,500–3,000 μmol photosynthetically active radiation (PAR) in an ambient, where the resulting intensity was of about 5–15 μmol PAR. The fluorescence was recorded with an infrared optical bandpass filter in the range of 700–780 nm. The maximum fluorescence (F_m), the fluorescence in ambient light (F_0), and the photosynthetic yield (Y) were used as a discriminant of the photosynthetic activity (De Agostini et al., 2020) between etiolated capsules and controls, with the latter represented by leaves and non-etiolated capsules. All the measurements were performed

in three repetitions, each in a different leaf or capsule from three different plants, finally providing a dataset of nine measurements shown here as mean ± SD for each studied condition. The means between control and test samples were compared and weighted according to the *t*-test. No differences were observed between "internal" and "external" control experiments (see section Induction of Etiolation). However, the data shown for these experiments are referred to the internal controls.

Germination Tests

Germination tests were performed on 30 and 90 DPA seeds in three repetitions of 50 seeds each for etiolated and control capsules from three different individuals. After imbibition, seeds were sowed by equally spreading them on a 20-cm diameter pot filled with opportunely-wetted soil as described in section Growth and Cultivation of Tobacco Plants. After sowing, germination was monitored daily for the following 30 days, and it was recorded and expressed by three basic indexes: the total number of germinated seeds (n_t) expressed in % (N_t); the partial number of germinated seeds (n_p) from the last check, also expressed in % (N_p); and the % of mortality (M) estimated at the end of the experiment. The indexes' percentages were referred to the total number of seeds sowed. The three parameters were defined as: $N_t = (n_t/50) \times 100$; $N_p = [(n_t - n_{t-1})/50] \times 100$; and $M = 1 - (N_t)$, where n_t is the number of germinated seeds at a given time, n_{t-1} is the number of germinated seeds at the last but one measurement, and 50 is the number of sowed seeds. To better appreciate the trend, the collected data were adapted to a logistic curve using the software mycurvefit,[1] and the obtained equation was graphically represented using the software PLOT 2.[2] In the plot, each daily value is given as mean ± SD of three independent germination experiments performed in the same conditions for seeds collected from etiolated and control capsules. We considered as germinated each seed having both the primary root and the cotyledons protruded. These two main criteria were assessed as follows: after sowing, the white primary root emitted by germinated seeds could be easily identified in the dark background provided by the soil; and a few days after, the cotyledon leaves could be also observed, confirming the "root-count." No differences were observed between "internal" and "external" control experiments (see section Induction of Etiolation), thus the data shown here are referred to the latter unless otherwise specified.

Seeds and Capsules Biometrics

Experiments were performed on a pool of three plants, with three independent measurements for each plant providing a dataset of nine values for each parameter: capsule weight, total seeds weight per capsules, averaged seed weight, empty capsule weight (capsule without seeds), seeds length, and seeds width. This design was followed for the etiolated and control capsules. No differences were observed between "internal" and "external" control experiments (see section Induction of Etiolation), and thus, the data shown here are referred to the latter unless otherwise specified. Concerning the weight and dimensions of the seeds, measurements were performed on a sample of 50 seeds under the schemes described in the previous paragraphs (three samples from the same plant and the whole repeated for three different plants). The weight of seeds and capsules was measured using an analytical balance (readability ± 0.01%) at 20°C and 70% relative humidity. The averaged values obtained for each parameter are given as mean ± SD. For a given parameter, the means between control and test samples were compared and weighted according to the *t*-test. The dimensions of seeds were measured using imageJ (Schneider et al., 2012).

Analysis of Seed's Phytohormones and Their Metabolites by Mass Spectrometry

For quantitative measurement of phytohormones, 45 days old seeds from etiolated and control capsules were collected. Prior analyses, the seeds were kept in dark at 20°C. The analysis was performed as previously reported (Mahalingam, 2019), with some minor modifications. Briefly, for each sample, 200 mg of seeds were quickly washed with double distilled water and dried down in a 2 ml Eppendorf tube. Phytohormones were extracted using cold methanol, while deuterium-labeled internal standards (a mixture of D5-IAA, D6-ABA, D4-SA, D2-JA at 1.25 µM each, and D2-GA1 at 2.5 µM – Sigma Aldrich, St. Louis) were solubilized in acetonitrile (50, 50, v/v) and used as marker. After shaking for 25 min, the sample was centrifuged at 16,000 *g* for 10 min. The obtained supernatant was stored into a new tube, and the pellet was subjected to a second extraction. These two supernatants were pooled and dried down using a speed-vac. Pellets were re-dissolved in 200 µl of 15% methanol. The liquid chromatography (LC) separation was performed with a ZORBAX Eclipse Plus C18 column (2.1 × 100 mm, Agilent) at 0.45 ml/min flow rate. The mobile phases A (0.1% formic acid) and B (0.1% formic acid/90% acetonitrile) were mixed according to the following gradient: 5% B for 1 min, to 60% B in 4 min, to 100% B in 2 min, hold at 100% B for 3 min, to 5% B in 0.5 min. Phytohormones levels were quantified using a Shimadzu LC system interfaced with a Sciex QTRAP 6500+ mass spectrometer equipped with a TurboIonSpray (TIS) electrospray ion source. The sample acquisition and data analysis were controlled by the Analyst software (version 1.6.3). Tuning and calibration of the QTRAP 6500+ mass spectrometer were performed according to the manufacturer's recommendations. Phytohormones were detected using multiple reaction monitoring (MRM) transitions that were optimized using the standards. The instrument was set-up to acquire in positive and negative ion switching. For phytohormones' quantification, an external standard curve was prepared using a series of standards with different concentrations of unlabeled phytohormones and fixed concentrations of the deuterium-labeled standards. Eventually, the data normalization was based on the internal standards: D5-IAA, D2-JA, D4-SA, D6-ABA, and D2-GA_1 to account for both experimental variation and hormone extraction/ionization

[1]https://mycurvefit.com/
[2]https://apps.micw.org/apps/plot2/index.php

efficiency. The amounts of the detected phytohormones were expressed in ng/g. Measurements were performed in three repetitions from different plants. The averaged values are given as mean ± SD. The means between control and test samples were compared and weighted according to *t*-test.

Statistics

Whole measurements were performed in nine independent repetitions (three samples from the same plant and the whole repeated for three different plants) for each condition (etiolated and control). Mass spectrometry (MS) analysis and germination tests were performed in three repetitions each one on seeds from a different plant. All the values resulting from each dataset are given as mean ± SD. Statistical tests were performed using GraphPad[3] with *t*-test analysis. Statistical significance of differences was estimated by the *p* relative to each test and control pool for a given parameter.

RESULTS

Etiolated Capsules Complete Their Maturation and Their Fate Depends on Leaves

To assess their own photosynthetic contribution, tobacco capsules were covered at the 2nd DPA by applying a pocket consisting of a triple layer of black-crepe paper (**Figure 1**). This setup prevented the passage of light and allowed to test fruit maturation under dark conditions. In these conditions, fruit development and maturity took place in 15–20 DPA without any major difference compared to controls. The only exception was that dark-grown capsules underwent etiolation (**Figure 2**).

Etiolated Capsules Carry Photosynthesis With Low Rates

Dark-developed capsules appeared etiolated (**Figure 2**) in their carpel region. On the contrary, sepals maintained the typical photosynthetic parenchyma even if they were also kept in the dark, suggesting different regulation mechanisms with respect to photomorphogenesis/skotomorphogenesis (**Figure 2**). Given the light-green color of the etiolated capsules, we investigated whether they may perform photosynthesis and to which extent. Basic photosynthetic parameters measured on etiolated capsules were compared with control capsules and leaves from the same plants (**Table 1**). In particular, the estimated maximum efficiency of PSII [$Y = (F_m - F_0)/F_m = 1 - (F_0/F_m)$] was used as a reference for the photosynthetic rate, assuming an ideal situation, where the whole PSII reaction centers in the sample are fully open. These values were found to be low in dark-developed capsules ($Y = 48.40 \pm 0.34\%$), while control capsules showed rates ($Y = 67 \pm 0.53\%$) roughly comparable to leaves ($Y = 71.60 \pm 0.61\%$). Lower Y values of control capsules with respect to leaves values must be interpreted considering the morpho-structural adaptation of leaves to maximize light capture and photosynthetic efficiency.

[3]https://www.graphpad.com/quickcalcs/ttest1.cfm

FIGURE 1 | Tobacco capsules were covered to induce etiolation. At the 2nd DPA, a pocket consisting of a triple layer of black-crepe paper was applied. This setup allowed the development and maturation of the fruits in the absence of light.

FIGURE 2 | Morphological differences between dark-developed and light-developed capsules (controls). Both capsules grew normally with the only difference ascribable to the color; the control capsules (grown under normal light) were green, while the test capsules (grown in the dark) underwent etiolation.

TABLE 1 | Measures of the main photosynthetic parameters on dark-grown capsules and controls (leaves and light-developed capsules).

	Etiolated capsules (dark-developed)	Control capsules (light-developed)	Leaves (internal control)
F_0^*	150.33 ± 2.78	357.11 ± 7.15	462.89 ± 11.24
F_m^*	291.22 ± 5.91	1084.67 ± 8.82	1637.78 ± 26.34
F_0/F_m^*	0.52 ± 0.01	0.33 ± 0.01	0.28 ± 0.01
Y (%)*	48.4 ± 0.34	67 ± 0.53	71.6 ± 0.61

*The fluorescence in ambient light (F_0) and the maximum fluorescence (F_m) are the fluorescence level of dark-adapted sample when all the photosystem II reaction centers are open or closed, respectively; Y is the photosynthetic yield; and F_0/F_m an indication of fluorescence not related to photochemistry. For each condition, data were expressed as mean ± SD on nine independent measurements from three different individuals. The p indicate statistical significance for a given measurement between etiolated and control capsules. *Indicates a value of $p < 0.0001$ between etiolated and control capsules for a given parameter.*

Consistently, the F_0/F_m ratio, which is an indication of fluorescence not related to photochemistry, was observed to be comparable for leaves and control capsules, with values of 0.28 ± 0.01 and 0.33 ± 0.01, respectively, while the dark-developed capsules presented almost two times higher values (~0.52 ± 0.01). These values for the etiolated capsules suggested a low efficient photosynthetic apparatus and confirmed a dominant etiolated profile (**Table 1**; $p < 0.0001$). Analysis of leaves and not-etiolated capsules from control plants (external controls, see section Induction of Etiolation) and test plants (internal controls, see section Induction of Etiolation) were comparable (data not shown).

Seeds of Etiolated Capsules Are Heavier and Bigger Respect to Controls

Except for the etiolation, the two types of capsules did not show any difference in development and shape (**Figure 2**). Accordingly, we investigated whether the etiolation could affect the fitness and the quality of seeds. For both samples, dried capsules, seeds, and empty capsules (obtained after careful removal of the whole seeds) were weighed finding that the full dark-developed capsules were ~24% heavier (**Supplementary Table 1**; **Figure 3**). This difference was mainly attributed to the seeds since empty-etiolated capsules were only exceeding the weight of the controls by ~2.05% (**Supplementary Table 1**; **Figure 3**), while the seeds total mass was ~50% higher in seeds from etiolated capsules (**Supplementary Table 1**; **Figure 3**). Next, we attempted to investigate whether the difference in seeds' mass was due either to their number, density, or both. Dimensionally, seeds from etiolated capsules were ~26.70 and ~33.16% bigger in length and width, respectively, and the two types of seeds had an almost constant ratio of ~1.3 for each dimension (length 996/786 = 1.27; width 720/541 = 1.33; **Supplementary Table 1**). Interestingly, these values suggested that, if the seed shape is approximated to the one of an ellipsoid, and the 1.3 ratio is assumed to be valid also for the third dimension (thickness), then the volume of seeds from etiolated capsules can be estimated as ~2.2 times bigger than the one of controls. On the other hand, the weight of the seeds was found to be increased ~41% (~0.41 times) with respect to controls (**Supplementary Table 1**; **Figure 3**). Accordingly, dimensions and morphology between the two types of seeds differed significantly finding them increased with respect to the volume and decreased with respect to the density. Finally, a difference in pigmentation between the two types of seeds sometimes appeared as an evident feature, but not always obvious (**Figure 4**).

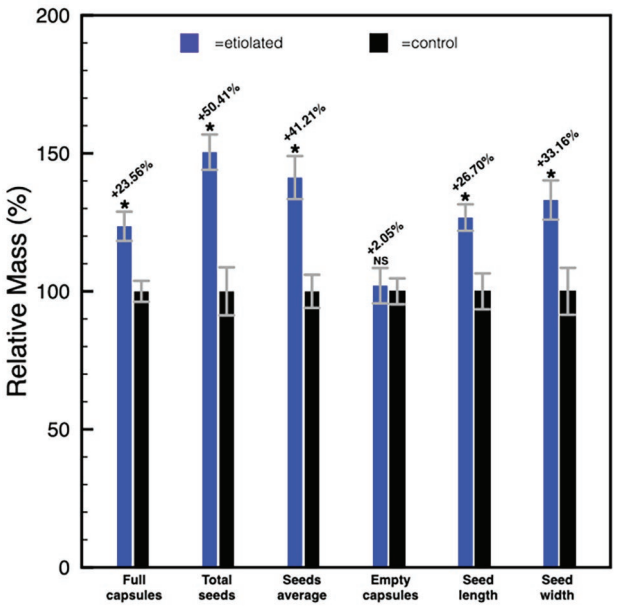

FIGURE 3 | Histogram representing the differences between etiolated and control capsules. Full capsules, seeds, and empty capsules were measured and the differences were expressed as a relative mass with respect to controls. Values are expressed as mean ± SD on nine capsules and on their related total seeds content from three different plants. Mean ± SD of seeds' mass and dimensions were calculated from nine replicas of 50 seeds collected from nine different capsules of three different plants. *p* indicate statistical significance between a given parameter in test plants and controls. NS, not significant; *indicates values of $p < 0.0001$.

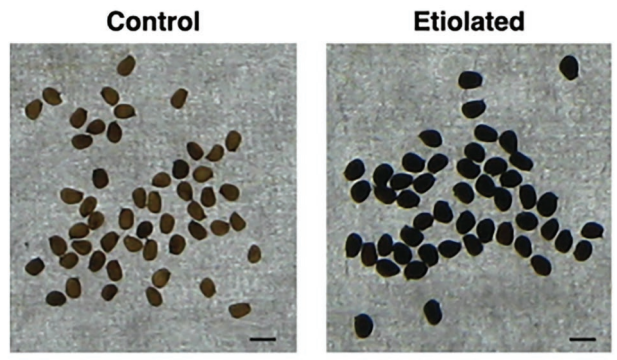

FIGURE 4 | Dimension and morphology of seeds from controls and etiolated capsules. Seeds from etiolated capsules were found to be evidently bigger when compared to controls. Moreover, differences in pigmentation sometimes appeared as an evident feature. The scale bar at the bottom-right indicates 1 mm.

Seeds of Etiolated Capsules Have a Reduced Dormancy

Given the considerable differences in weight between seeds from etiolated and control capsules, we investigated any physiological difference between the two pools. We started this part of the study considering the known decay of seeds dormancy within time in *N. tabacum* L. (Leubner-Metzger, 2005; Finch-Savage and Leubner-Metzger, 2006), and the declined germinability after 6 months of storage without any priming treatment (Min, 2001). Accordingly, germination tests were performed on 30 and 90 DPA seeds. Experiments performed on 30 DPA seeds evidenced a typical primary dormancy of the controls (**Figure 5**) with a percentage of germinability of ~16% (**Figure 5**), while, unexpectedly, seeds from etiolated capsules did not show any reluctance to germinate with final rates of ~80% (**Figure 5**).

These differences were much less pronounced on 90 DPA seeds (**Figure 6**), and the difference in the level of dormancy appeared slightly inverted respect to the previous comparison between the 30 DPA seeds. Considering the germination capabilities of the 30 DPA seeds from etiolated capsules, the same seeds type at 90 DPA showed a further reduced physiological dormancy, in agreement with previous evidence (Leubner-Metzger, 2005; Finch-Savage and Leubner-Metzger, 2006). This observation was also evidenced by their prompter ability to emit the embryonic root with respect to controls (data not shown). In particular, for 90 DPA seeds, the time needed for 50% of seeds to germinate (G_{50}) is reached by seeds from etiolated capsules at less than half a day before the one from controls (**Figure 6**). Finally, 90 DPA seeds from etiolated capsules were also found to be less vital, carrying a reluctance to germinate, due to mortality and/or dormancy, equal to ~8%,

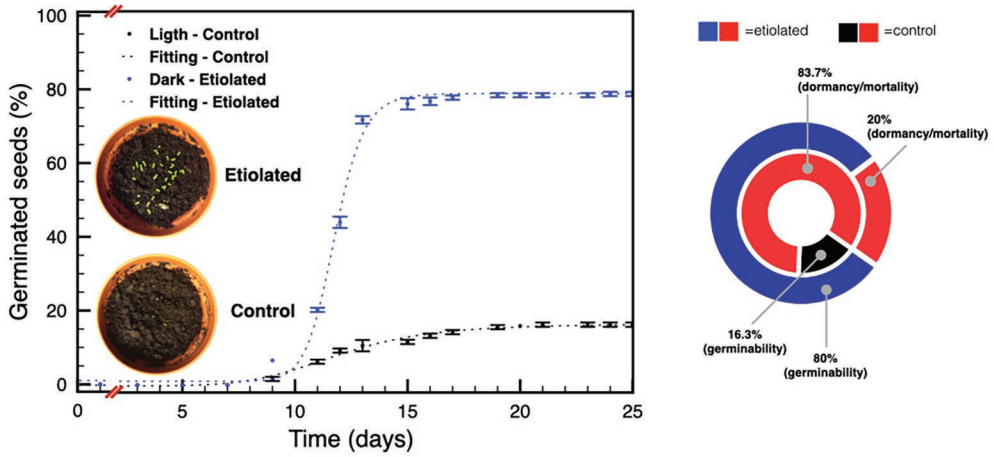

FIGURE 5 | Germination tests on seeds 30 DPA. The plot shows the germination speed of both groups of seeds; the diagram summarizes the plot results and indicates the dormancy/mortality extent in both groups. Data were expressed as mean ± SD of three replicates.

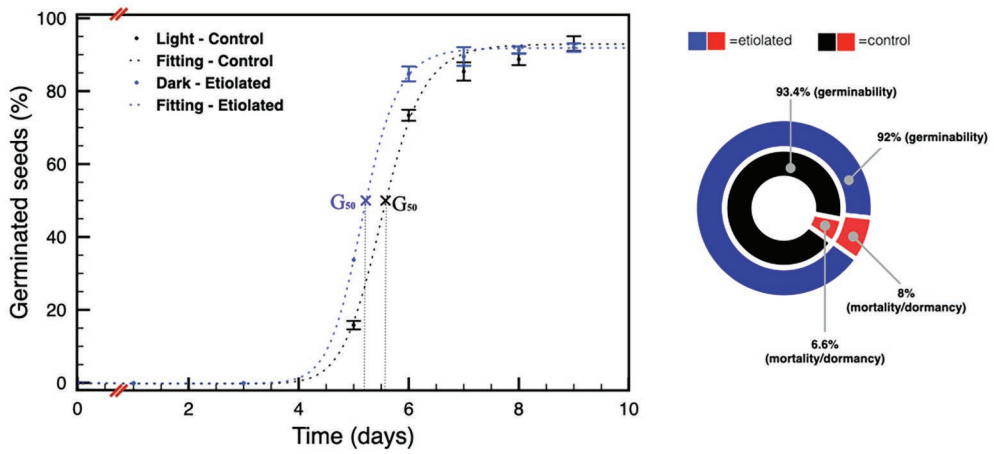

FIGURE 6 | Germination tests on seeds 90 DPA. The plot shows the germination speed of both groups of seeds; the diagram summarizes the plot results and indicates the dormancy/mortality extent in both groups. Data were expressed as mean ± SD of three replicates.

TABLE 2 | Phytohormones levels for 45 day post-anthesis (DPA) seed from etiolated capsules (dark) and control capsules (light).

Phytohormone	Light (ng/g)	Dark (ng/g)	Δ% respect to controls
SA**	54.937 ± 2.021	83.681 ± 6.853	+52.31
IAA-Asp***	28.066 ± 4.789	97.313 ± 1.553	+246.67
ABA***	26.062 ± 1.259	41.752 ± 1.878	+60.21
IAA**	12.336 ± 1.437	29.526 ± 2.890	+139.3
GA_1ǂ	6.542 ± 0.192	<0.8	-
OPDA**	4.803 ± 0.393	9.437 ± 0.809	+96.56
JA-ILE**	1.069 ± 0.025	1.514 ± 0.091	+40.65
JA***	1.037 ± 0.048	1.484 ± 0.021	+41.83
cZR***	0.201 ± 0.009	0.521 ± 0.049	+157.5
cZ*	0.013 ± 0.005	0.028 ± 0.004	+150

Values are mean ± SD of three replicates. The p indicate statistical significance between the levels of a given hormone in seeds from etiolated capsules with respect to controls.
**Indicates values of $p < 0.05$, for each phytohormone.*
***Indicates values of $p < 0.005$, for each phytohormone.*
****Indicates values of $p < 0.0005$, for each phytohormone.*
ǂThe LOD of GA_1 is 0.8 nM.

which is a higher value when compared to the ~7% of the 90 DPA seeds from controls (**Supplementary Table 1**; **Figure 6**).

Seeds From Etiolated Capsules Carry Altered Levels of Hormones and Their Metabolites

Finally, we analyzed the concentration of the phytohormones and their metabolites in 45 DPA seeds collected from both etiolated and control capsules. Except for gibberellins (GA_1), which were found to be less concentrated with respect to controls, the whole phytohormones were increased in seeds from etiolated capsules (**Table 2**). In particular, auxins (*IAA* and *IAA-Asp*) and cytokinins (cZ and *cZR*) were found to be present with concentrations 2 and 3.5 times higher, respectively, when compared to controls. This tendency was also observed for the inhibitory hormone abscisic acid (ABA), even if less pronounced (1.6 times). As already mentioned, the level of gibberellins was found to be exceptionally low in seeds from etiolated capsules, especially when considering the already low levels normally found in controls (seeds under dormancy).

Among other differences, seeds from etiolated capsules carried levels of auxins (IAA-Asp) much higher (more than double amounts) than ABA. On the contrary, these two phytohormones (IAA-Asp and ABA) had almost equivalent values in seeds from control capsules. Taking into account the reduced levels of gibberellins, these differences explained the absence of dormancy in seeds from etiolated capsules, and hence, suggested that the auxins levels might be primarily involved in the anomalous properties of seeds.

Similarly, also other phytohormones and their metabolites such as OPDA, JA, JA-ILE, and SA were found with higher levels on seeds from etiolated capsules when compared to controls (**Table 2**).

DISCUSSION

The autotrophic metabolism characterizes the whole first stage of fruit differentiation and ripening, and persists until the advanced stages of veraison (White, 2002; Carrari and Fernie, 2006; Prasanna et al., 2007). In most of the fruits, the end of this long process becomes evident by the change from green to the typical colors of a given species (White, 2002; Prasanna et al., 2007). As a metabolic implication of these events, fruits turn their metabolism from autotrophic to heterotrophic indicating that the phenological stage of veraison is reached (Perkins-Veazie, 1995; Trainotti et al., 1999; Aharoni and O'Connell, 2002; Blanco-Portales et al., 2002; Benìtez-Burraco et al., 2003; Collu et al., 2017). From this moment, a final hormone-mediated stage of senescence takes place, and fruits are subjected to an intense recycle of substances by mobilizing them to the rest of the plant while accumulating antimicrobial components and pigments to which a primary function of antioxidants is associated (Sun et al., 2018; Piano et al., 2019).

The advanced stages of ripening have been deeply studied, and their control mechanisms are mediated by phytohormones (Kumar et al., 2014; Robert, 2019). In particular, fruit ripening is regulated by ethylene, while seeds dormancy, which is essential for the embryonic differentiation, is regulated by a fine balance between ABA and gibberellins, or/and auxins (Kucera et al., 2005; Weiss and Ori, 2007; Sreenivasulu, 2017; Figueiredo and Köhler, 2018). Contrary to the ripening and its heterotrophic aspects, the first stages of fruit development and its autotrophic phase are less described. This is particularly true with respect to the metabolic contribution of fruit photosynthesis to both, seed development and fruit growth. To understand the extent of the own photosynthetic contribution in fruits, we have studied the growth of *N. tabacum* capsules in absence of light by inducing etiolation in fruits. Under these growth conditions, we have looked at the main observable differences in photosynthetic parameters, the mass of carpels, the mass of seeds, dimensions of seeds, germinability and mortality of seeds, and phytohormones levels. Dark-developed tobacco capsules underwent to etiolation with the typical exception of the receptacle region, which maintained the characteristic green color indicating the persistency of the photosynthetic parenchyma (**Figures 1, 2**). This aspect suggests the presence of different regulation mechanisms standing behind these two anatomical parts of the fruit when the fruit itself is subjected to a prolonged dark period. In association with the reduction of the photosynthetic parenchyma, it was observed a significant increase in the weight of seeds from etiolated capsules (**Supplementary Table 1**; **Figure 3**). These striking differences can be interpreted as evidence for increased sink properties of the etiolated fruits in a condition, where fruits are not able to perform their own photosynthesis (**Supplementary Table 1**; **Figure 3**). Hence, under normal light conditions, photosynthates originate not only from elsewhere sources in the plant (leaves) but also from the fruit itself. These observations are consistent with the Münch scheme according to which the mass of photosynthates (*P*) moves through the phloem as a result of the difference in solute concentration between the sink, fruits, and the source, leaves (Christy and Ferrier, 1973). In the case of etiolated capsules, the absence of photosynthates production causes an increased difference in concentration with respect to the sources. This is evidently correlated with the difference in seeds mass; accordingly,

we propose that the ratio between seeds mass from controls and etiolated capsules (m_c/m_e) can be reasonably assumed as an approximation of the ratio between the differences in photosynthates concentrations for the same conditions ($\Delta[P]_c/\Delta[P]_e$). This assumption can be described by the following formula $\Delta[P]_c/\Delta[P]_e = m_c/m_e$. In this respect, it is possible to estimate the contribution of the capsule in photosynthates production under normal light conditions. In fact, the $\Delta[P]_c$ can be expressed as the difference between the solute concentration in the source (C), which is strictly depending on the photosynthetic rate on leaves and assumed to be constant in both conditions, and the solute concentration in the sink, which can be considered composed of two components: a basal one (B) and a photosynthetic one (A), so that $\Delta[P]_c = C - B - A$. Similarly, for the etiolated conditions, it is valid that $\Delta[P]_e = C - B$, where A, in this case, is missing due to the absence of the photosynthetic activity in etiolated capsules. Accordingly, the equation becomes $\Delta[P]_c/\Delta[P]_e = m_c/m_e = C - B - A/C - B$. From this equation can be obtained the photosynthetic contribution as $A = (C - B)[1 - (m_c/m_e)] = \Delta[P]_e [1 - (m_c/m_e)]$. This equation gives an indicative value of the fruit contribution in presence of light, and it uses the etiolated condition ($\Delta[P]_e$) as a reference. Certainly, this value is characteristic of specific experimental conditions (e.g., light conditions) and species studied, thus it should be found empirically for each case. In our study, if we consider the seeds mass shown in **Supplementary Table 1**, the component $[1 - (m_c/m_e)]$ assumes a value of $[1 - (61.5/92.5)] = 0.3351$. It means that, here, due to the photosynthetic contribution of the capsule (A), the value $\Delta[P]_c$ will decrease of 33% in etiolated capsules. It is worth to stress that we assume a constant basal contribution (B) that is not affected by light itself, but it is only related with the basal metabolism and is equivalent to the metabolic rate in absence of light (where only respiration takes place and CO_2 is emitted). This is an important detail which Reich et al. have elegantly shown to be only depending on the nitrogen availability (Reich et al., 2006).

Seeds from dark-developed capsules have not only a difference in mass but also in their tendency to germinate; in fact, they show an almost absent dormancy, as observable by their peculiarity to germinate immediately after the senescence of the fruit (**Figure 5**). The effect of environmental factors, in particular temperature, light, and age, on seed germinability/dormancy is well documented (Bhatt et al., 2016). These effects are also known to be reflected endogenously as changes in phytohormones levels, especially ABA and GA, that finally result in different timing of seed germinability/dormancy (Chen et al., 2020). These properties are in line with what is observed in the present work, where light affects seeds maturity/maturation with a hormone-mediated mechanism.

The characteristically reduced dormancy of seeds from etiolated capsules was associated with a counterintuitive presence of GA_1 levels much lower when compared to ABA levels, which, on the contrary, are significantly increased when compared to controls (**Table 2**). These differences suggest that a common but opposite regulation system acts on genes related to the biosynthesis of both these phytohormones affecting their levels. Along the same line, "dark-developed" seeds carried also a significantly increased level of auxins when compared to controls (**Table 2**). The ratio between total auxins level, with particular reference to the most common IAA and *IAA-Asp*, and the ABA, is ~3 times higher in seeds from etiolated capsules with respect to a value of ~1.5 times in controls. This striking difference allows us to attribute to auxins the anomalous germination properties of dark-developed seeds. In this respect, it is important to mention that *IAA*, the free and active form, is in equilibrium with IAA-Asp, which is, especially in the seed, functioning as a reservoir that can be promptly released as soon as the levels of free IAA decrease. This steady-state equilibrium, based on the conjugated form as a reservoir (Ljung et al., 2002; Seidel et al., 2006), would guaranty a constant conversion to IAA keeping efficiently high its levels. Such a scheme would be consistent with the typical IAA properties of attracting nutrients (Ferguson and Beveridge, 2009), a fact that would also explain the results shown in **Figure 3** and **Supplementary Table 1**.

Similarly, also the main cytokinins, in particular *cZ* and *cZR*, increased their levels in dark-developed seeds. This effect could be considered in the frame of the increased sink properties of dark-developed seeds to which the phloem would bring not only nutrients but also cytokinins (Jameson and Song, 2016). Accordingly, being the level of phytohormones the main difference between the two types of seeds, these differences are expected to influence the embryos differently explaining the observed germination profiles (**Figures 5, 6**).

Fruits are centers of photosynthates accumulation, and this sink-organ property is essential for allowing their optimal development. However, young fruits have photosynthetic parenchyma that let them perform photosynthesis; thus, they behave as source organs, allowing proper development of the seed (Lytovchenko et al., 2011). In the present study, the dual role of tobacco fruits as sink-and-source organs evidently emerged by showing how the flower, first, and the fruit, after, behaves as a hormone-mediated self-regulating center able to balance its metabolic rate by a variable supply of external photosynthates sources. In fact, the induced etiolation of fruits is associated with the increased mass of seeds and ovaries, suggesting the presence of two sources of photosynthates: (i) the fruit itself, which is not working under etiolation, and (ii) the leaves, which compensate the absence of photosynthesis in etiolated fruits. Under etiolation, fruits cannot behave as a source organs, and their missing contribution is compensated by the other centers, mainly leaves. In line with the Münch theory (Christy and Ferrier, 1973), this implies a delayed retro-regulation due to the long distance between sources and sink and a stronger inertial effect driven by the bigger difference of solutes concentration between leaves and flowers. On the contrary, under normal light conditions, the fruit behaves as source organ and drives the photosynthates accumulation, getting a fast response and contributing significantly to the production and storage (Ruan et al., 1997; Patrick and Offler, 2001; Lalonde et al., 2003). Interestingly, considering the storage of photosynthates with respect to

the observed decreased density of seeds, this feature can be explained with the tendency to store starch and glucans with different branching properties, as frequently observed under stress conditions (MacNeill et al., 2017).

Moreover, the contribution of sepals, shown to not etiolate even when the whole flower is covered, should be also taken into account. The absence of etiolation in sepals suggests a regulation mechanism rather linked with leaves than with the capsule, ultimately implying that the mechanism described above for leaves is most likely valid also for this part of the flower. Furthermore, in tobacco plants, sepals are reported to remain green in all the flower developmental stages, to have the level of chlorophyll similar to those of leaves, and timing of senescence different than in petals (Müller et al., 2010). This last observation might also be valid for the etiolation mechanism, ultimately keeping green the sepals even in the absence of light. However, the fine contribution of sepals, which is difficult to study due to their reduced dimensions, remains to be elucidated, especially in terms of photosynthetic rates.

The dynamics and regulation mechanisms related to the development of fruits and seeds are essential not only for understanding the extent of the sink/source behavior in fruits with respect to other source organs but also for future applications aimed at implementing seeds quality and stability as well as fruits production. The present study evidenced the relevancy of the heterotrophic phase of fruits in contributing to reach the final stage of their ripening and maturity.

DATA AVAILABILITY STATEMENT

All datasets presented in this study are included in the article/**Supplementary Material**.

AUTHOR CONTRIBUTIONS

DP conceived the study, participated in its design and coordination, performed the experimental measurements, processed the experimental data, interpreted the data, and drafted and revised the manuscript. DF participated in the design and coordination of the study, performed the experimental measurements, interpreted the data, and drafted and revised the manuscript. PH contributed to interpreting the data and helped in drafting the manuscript. AA and PC contributed to interpreting the results, and helped in drafting the manuscript. EC and MK helped in analyzing seeds morphology and dimensions and in revising the manuscript. ML participated in the design and coordination of the study and helped in drafting the manuscript. All authors contributed to the article and approved the submitted version.

SUPPLEMENTARY MATERIAL

The Supplementary Material for this article can be found online at: https://www.frontiersin.org/articles/10.3389/fpls.2020.563971/full#supplementary-material

REFERENCES

Aharoni, A., and O'Connell, A. P. (2002). Gene expression analysis of strawberry achene and receptacle maturation using DNA microarrays. *J. Exp. Bot.* 53, 2073–2087. doi: 10.1093/jxb/erf026

Baïram, E., leMorvan, C., Delaire, M., and Buck-Sorlin, G. (2019). Fruit and leaf response to different source-sink ratios in apple, at the scale of the fruit-bearing branch. *Front. Plant Sci.* 10:1039. doi: 10.3389/fpls.2019.01039

Benìtez-Burraco, A., Blanco-Portales, R., Redondo-Nevado, J., Bellido, M. L., Moyano, E., Caballero, J. L., et al. (2003). Cloning and characterization of two ripening-related strawberry (*Fragaria x ananassa* cv. *Chandler*) pectate lyase genes. *J. Exp. Bot.* 383, 633–645. doi: 10.1093/jxb/erg065

Bhatt, A., Gairola, S., and El-Keblawy, A. A. (2016). Seed colour affects light and temperature requirements during germination in two Lotus species (*Fabaceae*) of the Arabian subtropical deserts. *Rev. Biol. Trop.* 64, 483–492. doi: 10.15517/rbt.v64i2.18575

Blanco-Portales, R., Medina-Escobar, N., López-Ráez, J. A., González-Reyes, J. A., Villalba, J. M., Moyano, E., et al. (2002). Cloning, expression and immunolocalization pattern of a cinnamyl alcohol dehydrogenase gene from strawberry (*Fragaria* × *ananassa* cv. *Chandler*). *J. Exp. Bot.* 53, 1723–1734. doi: 10.1093/jxb/erf029

Carrari, F., and Fernie, A. R. (2006). Metabolic regulation underlying tomato fruit development. *J. Exp. Bot.* 57, 1883–1897. doi: 10.1093/jxb/erj020

Chen, F., Zhou, W., Yin, H., Luo, X., Chen, W., Liu, X., et al. (2020). Shading of the mother plant during seed development promotes subsequent seed germination in soybean. *J. Exp. Bot.* 71, 2072–2084. doi: 10.1093/jxb/erz553

Christy, A. L., and Ferrier, J. M. (1973). A mathematical treatment of Munch's pressure flow hypothesis of phloem translocation. *Plant Physiol.* 52, 531–538. doi: 10.1104/pp.52.6.531

Collu, G., Farci, D., Esposito, F., Pintus, F., Kirkpatrick, J., and Piano, D. (2017). New insights into the operative network of FaEO, an enone oxidoreductase from *Fragaria* × *ananassa* Duch. *Plant Mol. Biol.* 94, 125–136. doi: 10.1007/s11103-017-0597-5

De Agostini, A., Caltagirone, C., Caredda, A., Cicatelli, A., Cogoni, A., Farci, D., et al. (2020). Heavy metal tolerance of orchid populations growing on abandoned mine tailings: a case study in Sardinia island (Italy). *Ecotoxicol. Environ. Saf.* 189:110018. doi: 10.1016/j.ecoenv.2019.110018

Ferguson, B. J., and Beveridge, C. A. (2009). Roles for auxin, cytokinin, and strigolactone in regulating shoot branching. *Plant Physiol.* 149, 1929–1944. doi: 10.1104/pp.109.135475

Figueiredo, D. D., and Köhler, C. (2018). Auxin: a molecular trigger of seed development. *Genes Dev.* 32, 479–490. doi: 10.1101/gad.312546.118

Finch-Savage, W. E., and Leubner-Metzger, G. (2006). Seed dormancy and the control of germination. *New Phytol.* 171, 501–523. doi: 10.1111/j.1469-8137.2006.01787.x

Hamilton, W. D., and May, R. M. (1977). Dispersal in stable habitats. *Nature* 269, 578–581. doi: 10.1038/269578a0

Hidaka, K., Miyoshi, Y., Ishii, S., Suzui, N., Yin, Y. G., Kurita, K., et al. (2019). Dynamic analysis of photosynthate translocation into strawberry fruits using non-invasive 11C-labeling supported with conventional destructive measurements using 13C-labeling. *Front. Plant Sci.* 9:1946. doi: 10.3389/fpls.2018.01946

Hiratsuka, S., Suzuki, M., Nishimura, H., and Nada, K. (2015). Fruit photosynthesis in Satsuma mandarin. *Plant Sci.* 241, 65–69. doi: 10.1016/j.plantsci.2015.09.026

Jameson, P. E., and Song, J. (2016). Cytokinin: a key driver of seed yield. *J. Exp. Bot.* 67, 593–606. doi: 10.1093/jxb/erv461

Kourmpetli, S., and Drea, S. (2014). The fruit, the whole fruit, and everything about the fruit. *J. Exp. Bot.* 65, 4491–4503. doi: 10.1093/jxb/eru144

Kucera, B., Cohn, M., and Leubner-Metzger, G. (2005). Plant hormone interactions during seed dormancy release and germination. *Seed Sci. Res.* 15, 281–307. doi: 10.1079/SSR2005218

Kumar, R., Khurana, A., and Sharma, A. K. (2014). Role of plant hormones and their interplay in development and ripening of fleshy fruits. *J. Exp. Bot.* 65, 4561–4575. doi: 10.1093/jxb/eru277

Lalonde, S., Tegeder, M., Throne-Holst, M., Frommer, W. B., and Patrick, J. W. (2003). Phloem loading and unloading of sugars and amino acids. *Plant Cell Environ.* 26, 37–56. doi: 10.1046/j.1365-3040.2003.00847.x

Leubner-Metzger, G. (2005). β-1,3-glucanase gene expression in low-hydrated seeds as a mechanism for dormancy release during tobacco after-ripening. *Plant J.* 41, 133–145. doi: 10.1111/j.1365-313X.2004.02284.x

Ljung, K., Hul, A. K., Kowalczyk, M., Marchant, A., Celenza, J., Cohen, J. D., et al. (2002). Biosynthesis, conjugation, catabolism and homeostasis of indole-3-acetic acid in *Arabidopsis thaliana*. *Plant Mol. Biol.* 50, 309–332. doi: 10.1023/a:1016024017872

Lytovchenko, A., Eickmeier, I., Pons, C., Osorio, S., Szecowka, M., Lehmberg, K., et al. (2011). Tomato fruit photosynthesis is seemingly unimportant in primary metabolism and ripening but plays a considerable role in seed development. *Plant Physiol.* 157, 1650–1663. doi: 10.1104/pp.111.186874

MacNeill, G. J., Mehrpouyan, S., Minow, M. A. A., Patterson, J. A., Tetlow, I. J., and Emes, M. J. (2017). Starch as a source, starch as a sink: the bifunctional role of starch in carbon allocation. *J. Exp. Bot.* 68, 4433–4453. doi: 10.1093/jxb/erx291

Mahalingam, R. (2019). Analysis of the barley malt rootlet proteome. *Int. J. Mol. Sci.* 21:179. doi: 10.3390/ijms21010179

Min, T. G. (2001). Effect of storage temperature and humidity on germinability and longevity of primed tobacco seeds. *Korean J. Crop Sci.* 46, 321–324.

Müller, G. L., Drincovich, M. F., Andreo, C. S., and Lara, M. V. (2010). Role of photosynthesis and analysis of key enzymes involved in primary metabolism throughout the lifespan of the tobacco flower. *J. Exp. Bot.* 61, 3675–3688. doi: 10.1093/jxb/erq187

Patrick, J. W., and Offler, C. E. (2001). Compartmentation of transport and transfer events in developing seeds. *J. Exp. Bot.* 52, 551–564. doi: 10.1093/jexbot/52.356.551

Perkins-Veazie, P. (1995). Growth and ripening of strawberry fruit. *Hortic. Rev.* 17, 267–297. doi: 10.1002/9780470650585.ch8

Piano, D., Cocco, E., Guadalupi, G., Kalaji, H. M., Kirkpatrick, J., and Farci, D. (2019). Characterization under quasi-native conditions of the capsanthin/capsorubin synthase from *Capsicum annuum* L. *Plant Physiol. Biochem.* 143, 165–175. doi: 10.1016/j.plaphy.2019.09.007

Prasanna, V., Prabha, T. N., and Tharanathan, R. N. (2007). Fruit ripening phenomena—an overview. *Crit. Rev. Food Sci. Nutr.* 47, 1–19. doi: 10.1080/10408390600976841

Reich, P. B., Tjoelker, M. G., Machado, J. L., and Oleksyn, J. (2006). Universal scaling of respiratory metabolism, size and nitrogen in plants. *Nature* 439, 457–461. doi: 10.1038/nature04282

Robert, H. S. (2019). Molecular communication for coordinated seed and fruit development: what can we learn from auxin and sugars? *Int. J. Mol. Sci.* 20:936. doi: 10.3390/ijms20040936

Ruan, Y. L., Patrick, J. W., and Brady, C. J. (1997). Protoplast hexose carrier activity is a determinate of genotypic difference in hexose storage in tomato fruit. *Plant Cell Environ.* 20, 341–349. doi: 10.1046/j.1365-3040.1997.d01-73.x

Schneider, C. A., Rasband, W. S., and Eliceiri, K. W. (2012). NIH image to ImageJ: 25 years of image analysis. *Nat. Methods* 9, 671–675. doi: 10.1038/nmeth.2089

Seidel, C., Walz, A., Park, S., Cohen, J. D., and Ludwig-Müller, J. (2006). Indole-3-acetic acid protein conjugates: novel players in auxin homeostasis. *Plant Biol.* 8, 340–345. doi: 10.1055/s-2006-923802

Springthorpe, V., and Penfield, S. (2015). Flowering time and seed dormancy control use external coincidence to generate life history strategy. *Elife* 4:e05557. doi: 10.7554/eLife.05557

Sreenivasulu, N. (2017). Systems biology of seeds: deciphering the molecular mechanisms of seed storage, dormancy and onset of germination. *Plant Cell Rep.* 36, 633–635. doi: 10.1007/s00299-017-2135-y

Sumner, P., and Mollon, J. D. (2000). Chromaticity as a signal of ripeness in fruits taken by primates. *J. Exp. Biol.* 203, 1987–2000.

Sun, T., Yuan, H., Cao, H., Yazdani, M., Tadmor, Y., and Li, L. (2018). Carotenoid metabolism in plants: the role of plastids. *Mol. Plant* 11, 58–74. doi: 10.1016/j.molp.2017.09.010

Trainotti, L., Spolaore, S., Pavanello, A., Baldan, B., and Casadoro, G. (1999). A novel E-type endo-β-1,4-glucanase with a putative cellulose-binding domain is highly expressed in ripening strawberry fruits. *Plant Mol. Biol.* 40, 323–332. doi: 10.1023/a:1006299821980

Weiss, D., and Ori, N. (2007). Mechanisms of cross talk between gibberellin and other hormones. *Plant Physiol.* 144, 1240–1246. doi: 10.1104/pp.107.100370

White, P. J. (2002). Recent advances in fruit development and ripening: an overview. *J. Exp. Bot.* 53, 1995–2000. doi: 10.1093/jxb/erf105

Yamaki, S. (2010). Metabolism and accumulation of sugars translocated to fruit and their regulation. *J. Jpn. Soc. Hortic. Sci.* 79, 1–15. doi: 10.2503/jjshs1.79.1

Conflict of Interest: The authors declare that the research was conducted in the absence of any commercial or financial relationships that could be construed as a potential conflict of interest.

frontiers in Plant Science

ORIGINAL RESEARCH
published: 27 November 2020
doi: 10.3389/fpls.2020.603581

Radiation and Drought Impact Residual Leaf Conductance in Two Oak Species With Implications for Water Use Models

*Haiyan Qin[1], Carles Arteaga[2], Faqrul Islam Chowdhury[3], Elena Granda[4], Yinan Yao[1], Ying Han[1] and Víctor Resco de Dios[1,2,5]**

[1] School of Life Sciences and Engineering, Southwest University of Science and Technology, Mianyang, China, [2] Department of Crop and Forest Sciences, University of Lleida, Lleida, Spain, [3] Institute of Forestry and Environmental Sciences, University of Chittagong, Chattogram, Bangladesh, [4] Department of Life Sciences, University of Alcalá, Alcalá de Henares, Spain, [5] Joint Research Unit CTFC-AGROTECNIO, Universitat de Lleida, Lleida, Spain

OPEN ACCESS

Edited by:
Attila Ördög, University of Szeged, Hungary

Reviewed by:
Ismael Aranda, National Institute for Agricultural and Food Research and Technology (INIA), Spain
J.D. Lewis, Fordham University, United States
Yasutomo Hoshika, Institute for Sustainable Plant Protection, Italian National Research Council, Italy

***Correspondence:**
Víctor Resco de Dios
v.rescodedios@gmail.com

Specialty section:
This article was submitted to Plant Abiotic Stress, a section of the journal Frontiers in Plant Science

Received: *11 September 2020*
Accepted: *10 November 2020*
Published: *27 November 2020*

Citation:
Qin H, Arteaga C, Chowdhury FI, Granda E, Yao Y, Han Y and Resco de Dios V (2020) Radiation and Drought Impact Residual Leaf Conductance in Two Oak Species With Implications for Water Use Models. Front. Plant Sci. 11:603581. doi: 10.3389/fpls.2020.603581

Stomatal closure is one of the earliest responses to water stress but residual water losses may continue through the cuticle and incomplete stomatal closure. Residual conductance (g_{res}) plays a large role in determining time to mortality but we currently do not understand how do drought and shade interact to alter g_{res} because the underlying drivers are largely unknown. Furthermore, g_{res} may play an important role in models of water use, but the exact form in which g_{res} should be incorporated into modeling schemes is currently being discussed. Here we report the results of a study where two different oak species were experimentally subjected to highly contrasting levels of drought (resulting in 0, 50 and 80% losses of hydraulic conductivity) and radiation (photosynthetic photon flux density at 1,500 μmol m^{-2} s^{-1} or 35–45 μmol m^{-2} s^{-1}). We observed that the effects of radiation and drought were interactive and species-specific and g_{res} correlated positively with concentrations of leaf non-structural carbohydrates and negatively with leaf nitrogen. We observed that different forms of measuring g_{res}, based on either nocturnal conductance under high atmospheric water demand or on the water mass loss of detached leaves, exerted only a small influence on a model of stomatal conductance and also on a coupled leaf gas exchange model. Our results indicate that, while understanding the drivers of g_{res} and the effects of different stressors may be important to better understand mortality, small differences in g_{res} across treatments and measurements exert only a minor impact on stomatal models in two closely related species.

Keywords: cuticular conductance, stomatal conductance, night conductance, dark respiration, drought, shade

INTRODUCTION

Plant transpiration through stomatal pores and leaf cuticles dominates global evapotranspiration (Hetherington and Woodward, 2003). As water stress intensifies under global warming, there is an increasing interest toward understanding ecological variation in residual leaf conductance (g_{res}). After stomatal closure, water loss continues until mortality due to a mixture of cuticular water loss

and incomplete stomatal closure (residual conductance; Blackman et al., 2016; Martin-Stpaul et al., 2017).

Studies addressing ecological and physiological variation in the drivers of residual conductance are currently rare (Heredia-Guerrero et al., 2018). According to a recent review on this topic (Duursma et al., 2019), only 10 studies have addressed the effect of drought on g_{res} and, from those, only 4 had been performed on trees. Consequently, multi-factorial studies addressing ecological variation in residual conductance are much needed to understand its variation. For instance, while shade and drought are both known to decrease residual conductance (Boyer et al., 1997; Shepherd and Wynne Griffiths, 2006), it is currently unknown whether the effect of both stressors would be additive or interactive. However, the effects of residual conductance on mortality have been documented to be dramatic: time to mortality nearly doubles if g_{res} declines from 4 to 2 mmol m^{-2} s^{-1} (Duursma et al., 2019).

Understanding the physiological and ecological drivers of g_{res} has been the topic of some discussion (Riederer and Müller, 2007; Fernández et al., 2017). Some studies report that variations in the degree of sclerophylly (as indicated by leaf mass area) would increase g_{res} because leaves that are more scleromorphic will show thicker cuticles, but other work has demonstrated that changes in wax composition may compensate for such effect (Bueno et al., 2020). Another alternative, explored to a lesser degree, is that further reductions in g_{res} may be inhibited by changing carbohydrate allocation priorities (Zhang et al., 2020). In other words, as non-structural carbohydrate reserve pools deplete, cuticle production to prevent cuticular water losses may be limited by NSC availability.

Understanding variation in residual conductance is also necessary for models of water use (Leuning, 1995; Barnard and Bauerle, 2013; De Kauwe et al., 2015), where residual conductance acts as the intercept of commonly used stomatal models (g_{int}). The most common stomatal models being used in land surface models are Ball-Berry model types, which have the general form:

$$g_s = g_{int} + m A/C_a f(D) \quad (1)$$

Where g_s is stomatal conductance, A, C_a, and D represent photosynthesis, ambient CO_2 concentration and vapor pressure deficit, respectively, and m is the slope parameter. When g_{int} is estimated through regression fitting, it may either be equal to 0, which creates problems because then the ratio of intercellular to ambient CO_2 (C_i/C_a) does not vary with light (Collatz et al., 1991; Leuning, 1995; Duursma et al., 2019), or it may be negative, which is nonsensical.

There are at least two possible definitions of g_{int}: (1) g_0, which represents the lowest conductance reached as photosynthesis tends to 0 because light declines (Leuning, 1995; Barnard and Bauerle, 2013); (2) g_{min}, which refers to the residual conductance after (complete or not) stomatal closure under strong water stress (Duursma et al., 2019). We note that some studies use g_{min} and g_{res} interchangeably but, for clarity, we will differentiate them here as previously defined.

The problem then becomes how to measure g_0 and g_{min}. g_0 could simply be measured as daytime conductance (g_d) under low light in non-droughted plants and, similarly, g_{min} could similarly be measured from g_d in droughted plants (for as long as photosynthesis tends to zero, in both cases; Barnard and Bauerle, 2013; Duarte et al., 2016). Additionally, residual conductance has most often been measured by monitoring the water mass loss in detached leaves (g_{MLD}; Kerstiens, 1996; Schuster et al., 2017). g_0 and g_{min} could thus be measured with this method by comparing g_{MLD} in plants that have grown under strong light limitation or under strong water limitation, respectively. The problem with this approach, however, is that some acclimation responses (particularly in response to low radiation) could alter leaf morphology and it is unclear whether g_0 measured through g_{MLD} after low light acclimation would be representative of that in plants without acclimation to low radiation.

An alternative would be to use nocturnal conductance (g_n; Lombardozzi et al., 2017) in non-droughted and droughted plants. An advantage would be that photosynthesis would always be zero in this case. Duursma et al. (2019), however, proposed that g_n should not be used given the evidence of active regulation of stomatal conductance overnight (Resco De Dios et al., 2019), and that the drivers of nocturnal conductance could differ from those driving daytime conductance (Ogle et al., 2012). Amongst other processes, g_n varies through time due to circadian regulation (Resco De Dios et al., 2015). However, g_n often retains some sensitivity to D such that maximum stomatal closure and, potentially, residual conductance, may be achieved at lower D than during the daytime (Barbour and Buckley, 2007). One could thus hypothesize that measurements of g_n under high D may be indicative of g_{res}.

Regardless of how g_0 and g_{min} are estimated, Duursma et al. (2019) proposed to replace Eq. 1 by:

$$g_s = \max\left[\max\left(g_0, g_{min}\right), m A/C_a f(D)\right] \quad (2)$$

That is, according to Eq. 2, residual conductance would not be added to the right-hand term of Eq. 1. Instead, one would use measured residual conductance (the maximum between g_0 and g_{min}) as an actual minimum (De Kauwe et al., 2015). However, this formulation has not yet been tested against data and, therefore, we do not yet know whether it enhances the predictive power of stomatal models.

Here we evaluate the effects of shade and water stress on g_{res} across two different oak species, the deciduous *Quercus faginea* and the sclerophyll *Q. ilex*. These two species are common in the calcareous soils from Spain and the Western Mediterranean Basin and we expected conductance to be significantly lower in *Q. ilex*, a species with a more conservative water use. More specifically, we sought to test: (1) how do drought and shade interact to affect g_{res}? and (2) what are some of the possible mechanisms underlying variation in g_{res} across drought and shade treatments? Because g_{MLD} is probably the most accepted method to measure residual conductance, here we focused on g_{MLD}. In particular, we addressed whether g_{MLD} would be driven by water stress (as indicated by water potential), NSC, LMA, or nitrogen concentration (N_{mass}, an indicator of photosynthetic

capacity), and whether g_{res} could limit respiration. We also sought to understand: (3) whether we obtain different values of g_{res} depending upon whether it is measured from g_{MLD}, g_n, and g_d; and (4) how do we incorporate residual conductance into Ball-Berry type stomatal models and what are the consequences of variation in g_{res} across treatments and types of measurements for coupled leaf gas exchange models?

MATERIALS AND METHODS

Experimental Design and Growing Conditions

The experiment was performed at the experimental fields from the University of Lleida (Spain; 41.62 N, 0.59 E). We built a rain-out shelter covered by clear polyethylene plastic, which is commonly used in greenhouse building. Half of the structure received solar radiation (sun treatment), with a maximum photosynthetically active radiation (PAR) of 1,500 μmol m^{-2} s^{-1}. The other half was covered by a dense shading cloth (shade treatment) with a maximum PAR of 35–45 μmol m^{-2} s^{-1}, which was near the light compensation point in this species (*data not shown*). The structure had openings on both sides to increase ventilation. Temperature inside the rain out shelter was 3°C higher than outside, but differences between the sun and shade treatment were negligible. Full details on the infrastructure have been provided elsewhere (Resco De Dios et al., 2020).

For this study we sourced 2 year-old seedlings from local nurseries (n = 120). The ecotypes for both species were original from the mountain range of the Iberian System. Plants were grown in 11 L cubic pots (20 cm × 20 cm × 27.5 cm). The substrate used was Humin Substrat Neuhaus N6 [Klasman-Deilmann GmbH, Geeste, Germany], a commercial potting mix. Pots were regularly fertilized with a slow release NPK MgO fertilizer (17-09-11-2, Osmocote Universal, KB, Ecully, France) and daily watered to field capacity until treatment implementation. The position of the pots was randomly shifted every other week.

The plants grew for 4 months into the rainout shelter before experiment inception in July 2017. That is, they developed new leaves under the assigned experimental light conditions. Although we cannot discard legacy effects from the previous growing season in the nursery (Aranda et al., 2001), all plants were treated equally.

We performed a full factorial experiment with the plants experiencing two light treatments crossed with three water stress treatments. Half of the plants grew under the sun treatment and the other half under the shade treatment, as previously described. We implemented three different water stress treatments using three different levels of percent loss of hydraulic conductivity (PLC): (i) P_0, where plants were irrigated at field capacity; (ii) P_{50}, where plants experienced 50% losses in hydraulic conductivity and which represents an important stress; and (iii) P_{80}, where the plant experienced 80% losses in hydraulic conductivity, which represents a major stress and potentially mortality (Resco et al., 2009).

We kept plants at field capacity until treatment implementation. We then stopped watering and allowed plants to dehydrate and we measured midday stem water potential (Ψ_{md}) every other day in a subset of plants (n = 5). The levels of PLC were controlled from the relation between midday shoot water potential (Ψ_{md}) and PLC values reported previously in vulnerability curves from *Quercus faginea Lam.* (Esteso-Martínez et al., 2006) and *Quercus ilex L.* (Peguero-Pina et al., 2014). Shoot Ψ_{md} was regularly measured during treatment implementation with a pressure bomb (PMS 1000, PMS Instruments, Albany, Oregon) after clipping the sample and allowing for equilibration in the dark for ∼30 min. Once plants reached the target PLC, we kept soil moisture constant at that level for 2 weeks. This was achieved by weighing a subset of pots (n = 5 per each treatment) and adding back the water that had evaporated every day. We also measured native embolism to test the actual levels of PLC that we achieved in every treatment, as previously published (Resco De Dios et al., 2020). It is important to note that we did not always reach the target PLC levels (see **Supplementary Table 1**), but treatment implementation was successful in that we created a gradient in water availability with our treatments. Full details have been provided by Resco De Dios et al. (2020).

Gas Exchange Measurements

Leaf gas exchange was measured with a portable photosynthesis system (LI-6400XT, Li-Cor Inc., Lincoln, NE, United States). We measured 3–5 plants in each treatment at two different periods during the night: between 23:00 h and 01:00 h and between 03:00 h and 05:00 h, and also during the day (10:00–13:00 h). We did not observe significant differences between the stomatal conductance measured over night at the different times (p = 0.79) and measurements were pooled together in subsequent analyses. To understand if measurement errors arising from low flux rates affected our measurements, we also conducted measurements with an empty chamber for 4–5 h, following previously published protocols (Resco De Dios et al., 2013). Results were always one or more orders of magnitude lower or negative. Given these results, we concluded that leaf observations were reliable and that a general correction was not required.

Block temperature was set at 25°C during the night and at 30°C during the day, CO_2 at 400 ppm and relative humidity at ∼30%. This meant that D during nighttime measurements was at ∼2.2 kPa, which was substantially higher than that naturally occurring during the night (Resco De Dios et al., 2020). We chose this design to induce nocturnal stomatal closure and test whether g_n indicates g_{res}.

During the daytime, we performed measurements at two different levels of PAR: 1,500 μmol m^{-2} s^{-1} and 40 μmol m^{-2} s^{-1}. We first measured under growth PAR (1,500 μmol m^{-2} s^{-1} for plants in the sun treatment and 40 μmol m^{-2} s^{-1} for plants in the shadow treatment) and then at the other PAR level (40 μmol m^{-2} s^{-1} for plants in the sun treatment and 1,500 μmol m^{-2} s^{-1} for plants in the shadow treatment). The leaves were exposed for 10–20 min under the different light intensities until acclimation to the new light level. We only used data measured under growth PAR for analyses, and the rest was reserved for model validation. We note that a sudden exposure to 1,500 μmol

m^{-2} s^{-1} for a plant growing in the shade would represent a sunfleck, and this could affect the performance of steady-state stomatal models (Way and Pearcy, 2012). When the leaf did not cover the chamber completely, it was scanned and we corrected measurements for leaf area.

In order to parameterize the photosynthesis component of the coupled leaf gas exchange model, we also measured the response of photosynthesis (A) to different internal CO_2 concentrations (C_i) following the protocols from Long and Bernacchi (2003). Briefly, we started measurements with an ambient CO_2 concentration (C_a) of 400 ppm and, after 5 min of acclimation, we sequentially changed C_a to 300, 250, 200, 150, 100, 50, 0, 400, 500, 650, 800, 1000, 1250, and 1500 ppm. These measurements were performed at saturating light (1,500 μmol m^{-2} s^{-1}), setting block temperature at 30°C and with RH as high as we could achieve, which was ∼50%.

Measurements of g_{MLD}

g_{MLD} was measured as the mass loss of detached leaves following Phillips et al. (2010) in five leaves per treatment, weighting the leaves every 5 min during 2 h after collection. We wrapped the petiole with paraffilm so that only water lost through the leaf was measured. We performed the measurements in the laboratory, briefly after collection, where we monitored the temperature and relative humidity. Residual conductance was then calculated as:

$$g_{\mathrm{MLD}} = E_{\mathrm{MLD}} P D^{-1} \quad (3)$$

where E_{MLD} is mass loss per projected leaf area (mol m^{-2} s^{-1}), P is atmospheric pressure (kPa) and D is the vapor pressure deficit (kPa). g_0 was defined as g_{MLD} when the leaf originated from the shade treatment at P_0 (P_0_shade) and g_{min} was defined as g_{MLD} at P_{80} in the sun treatment (P_{80}_sun).

Analyses of Non-structural Carbohydrates and Elemental Composition

To better understand the physiological mechanisms explaining variations in g_{res} with treatments, we analyzed the concentrations of non-structural carbohydrates, changes in leaf mass per area (LMA) and nitrogen concentrations (N_{mass}). We collected all the leaves in five plants for each treatment. Immediately after collection, we scanned the leaves to measure the total area and they were then microwaved for 30 s and 700W to stop further metabolic processes. We then oven dried the samples (48 h in 105°C) and recorded the dry mass. Leaf area and dry weight was used to estimate LMA.

We followed previously developed protocols for extracting the percentage for sugar and starch (Palacio et al., 2007). This method consists of grinding the dried leaves with a mill (IKA A10, IKA-Werke, Staufen, Denmark) and making two extractions: one for extracting soluble sugars (sugars from now on) and a second extraction for starch. The first step of the sugar extraction consisted of adding 10 ml of ethanol (80% v/v) to 50 mg of sample, which we then left for 30 min at 60°C in water bath, and then we centrifuged (NEYA 8, REMI ELEKTROTECHNIK LTD., Vasai, India) the sample for 10 min at 3200 rpm. In the second step we added 50 μl of the supernatant, 450 μl of ethanol (80%), 500 μl of phenol (28%), and 2500 μl of sulfuric acid (96%), we shook the mix and let it stand for 30 min. In the third step we read the absorbance at 490 nm with spectrophotometer (Spectrophotometer UV-1600PC, VWR, Radnor, PA, United States) after removing the supernatant and drying the sample at 70°C during 16 h.

In the starch extraction, we added 4 ml of sodium acetate (pH 4.5) to the dry sample and left it for 60 min in a water bath (60°C). Once the sample cooled down, we added 1 ml of Amyloglucosidase (0.5% w/v) and we incubated the mix in the stove for 16 h at 50°C. We then added sample 50 μl of supernatant, 450 μl of sodium acetate (pH 4.5), 500 μl of phenol (28%), and 2,500 μl of sulfuric acid (96%). We then mixed it and let sit for 30 min, and then we measured the absorbance at 490 nm with the spectrophotometer.

We analyzed nitrogen concentration in an elemental analyzer (Carlo Erba 1110 Elemental Analyzer) at the University of Wyoming following previously published procedures (Hoffman et al., 2019).

Statistical Analyses

We examined statistical differences across treatments in g_{MLD}, g_n, and g_d using an ANOVA (followed by Tukey's HSD test) with species, light and water treatments as explanatory variables. Measurements of g_{MLD}, were conducted on different individuals within a treatment. Consequently, we examined whether values were comparable within a given treatment by examining variation in the mean ± 95% CI in g_{MLD}, g_n, and g_d.

To examine potential drivers of variation in g_{res}, we additionally performed correlation analyses between conductance and NSC, LMA, gas exchange parameters and Ψ_{md}.

All data was analyzed with R 3.6.3 (R Core Team, 2020) using base packages and, additionally, "corrplot" for plotting the correlation table (Wei and Simko, 2017).

Modeling

In order to examine the effects of the different forms of measuring residual conductance over stomatal predictions and coupled photosynthetic responses, we performed two exercises. First, we examined the effects on stomatal predictions on different implementations of Eqs 1, 2. Second, we examined the effects of the different measured values of g_{res} on a photosynthesis-stomatal conductance coupled model.

For the first exercise, we compared the performance of different versions of the Ball-Berry (BB) model (Ball et al., 1987). First, we examined the version proposed by Duursma et al. (2019, BBD):

$$g_{\mathrm{s}} = \max\left[\max\left(g_0, g_{\min}\right), m\ \mathrm{A}\ \mathrm{RH}/C_{\mathrm{a}}\right] \quad (4)$$

and we used three different forms of the left hand term [max (g_0, g_{min})]. That is, we compared model performance when the left hand term used g_0 and g_{min} estimated from g_{MLD} (BBD_{MLD}), g_n (BBD_n), and g_d (BBD_d). In all cases, g_0 was defined as conductance (g_{MLD}, g_n, or g_d, depending on the case) in the

shade treatment without water stress (P_0_shade) and g_{min} as conductance in the sun under strong water stress (P_{80}_sun).

We compared these results with the original version of the Ball-Berry model (BB):

$$g_s = g_{int} + m\,A\,RH/C_a \quad (5)$$

where g_{int} and m were both estimated through least squares fitting.

Finally, we used an intermediate option where we used Eq. 5 but where g_{int} was replaced by actual g_{MLD} measurements (BB_meas_g_{MLD}), instead of being estimated through least squares. We also tried with g_n, in addition to g_{MLD}, but differences were negligible, as will be discussed later in more detail.

Model calibration was performed with data collected under growth PAR (1,500 μmol m^{-2} s^{-1} for sun treatment and 40 μmol m^{-2} s^{-1} for the shade treatment). Model validation was performed with data collected under different PAR levels. That is, with PAR at 40 μmol m^{-2} s^{-1} for the sun treatment and at 1,500 μmol m^{-2} s^{-1} for the shade treatment. Model comparison was performed calculating the Akaike Information Criterion (AIC) and a model was considered more plausible when the AIC was smaller by a difference of 2 or more units (Burnham and Anderson, 2002). We also examined the variation in the slope, intercept and R^2 of the observed *vs* predicted relationship.

For the second exercise, we simulated the effects of the different values of g_{MLD}, g_n and g_d on predictions of C_i with varying PAR and on the effect temperature on leaf evaporation. We used the A/C_i curves to parameterize a coupled photosynthesis model (Duursma, 2015) and we conducted the simulation following previously published protocols (Duursma et al., 2019). We note that differences in mesophyll conductance across species and treatments could affect estimates of photosynthetic parameters (Flexas et al., 2012).

RESULTS

Effects of Shade and Drought on g_{MLD} and g_n

We observed that g_{MLD} varied significantly with species and light and also with light and water (**Table 1** and **Figure 1**). The interactions between species and light resulted in g_{MLD} significantly declining from 6.9 in the sun to 3.4 mmol m^{-2} s^{-1} shadow in *Q. faginea*. However, g_{MLD} in *Q. ilex* did not differ across light levels (5.6 in the sun and 4.4 mmol m^{-2} s^{-1} in the shade). The interaction between light and water was such that g_{MLD} declined with drought in the sun treatment (from 7.4 at P_0 to 5.5 mmol m^{-2} s^{-1} at P_{80}), but g_{MLD} increased with drought in the shade from 3.1 at P_{50} to 5.0 mmol m^{-2} s^{-1} at P_{80}).

Variation in g_n followed a pattern of variation similar to that of g_{MLD} in that it also varied significantly with species and light treatments (**Table 1** and **Figure 2**). g_n was not different between species at the shade treatment (4.5 and 5.6 mmol m^{-2} s^{-1} in *Q. faginea* and *Q. ilex*, respectively), but there was a significant increase in g_n in *Q. faginea* (7.8 mmol m^{-2} s^{-1}) in the sun treatment. Instead, g_n in *Q. ilex* at the sun treatment was similar to that in the shade (4.0 mmol m^{-2} s^{-1}; **Figure 1B**). Differences across water treatments were not significant.

TABLE 1 | ANOVA Table on the effects of species, light treatment, water treatment on residual conductance measured from the mass loss of detached leaves (g_{MLD}), from nocturnal conductance (g_n), and also from daytime conductance (g_d).

Factor	Df	*F*	*P*-value
***g*MLD**			
Species	1	0.12	0.73
Light	1	23.4	<0.0001
Water	2	1.35	0.27
Species × Light	1	5.41	0.02
Species × Water	2	0.75	0.48
Light × Water	2	4.04	0.02
Species × Light × Water	2	0.35	0.71
gn			
Species	1	0.89	0.35
Light	1	1.27	0.26
Water	2	2.14	0.12
Species × Light	1	4.98	0.03
Species × Water	2	2.53	0.09
Light × Water	2	0.14	0.87
Species × Light × Water	2	0.20	0.82
gd			
Species	1	5.84	0.02
Light	1	51.21	<0.001
Water	2	138.66	<0.001
Species × Light	1	16.99	<0.001
Species × Water	2	1.08	0.34
Light × Water	2	91.74	<0.001
Species × Light × Water	2	21.24	<0.001

Effects of Shade and Drought on g_d

Of particular relevance for this study is to examine g_d when A_{net} approaches zero (**Figure 3B**), so that one can test the potential use of g_d as an indicator of residual conductance. There are different definitions in the literature as to what is meant by photosynthesis approaching zero (Leuning, 1995; Barnard and Bauerle, 2013). Here we used g_d when A_{net} was at, or below, 1 μmol m^{-2} s^{-1}. In *Q. faginea*, this occurred under the shade treatments at all water stress levels, where g_d varied between 14.6 and 29.5 mmol m^{-2} s^{-1} (**Figure 3**).

In *Q. ilex*, A_{net} was always below 1 μmol m^{-2} s^{-1} in the shadow treatments at all water stress levels. However, there was significant variation in g_d as it varied from 58 mmol m^{-2} s^{-1} in P_0 to 14 and 4 mmol m^{-2} s^{-1} in P_{50} and P_{80}, respectively. Within the sun treatments, A_{net} was always below 1 under water stress (at P_{50} and P_{80}) where g_d varied between 4 and 1 mmol m^{-2} s^{-1}, respectively. g_d under water stress (P_{50} and P_{80}) was not different between shadow and sun treatments (**Figures 3A,B**).

Differences Between g_{MLD}, g_n, and g_d

Within a given treatment, g_n was indistinguishable from g_{MLD}: 95% CI error bars always overlapped (**Figure 3C**). In *Q. faginea*,

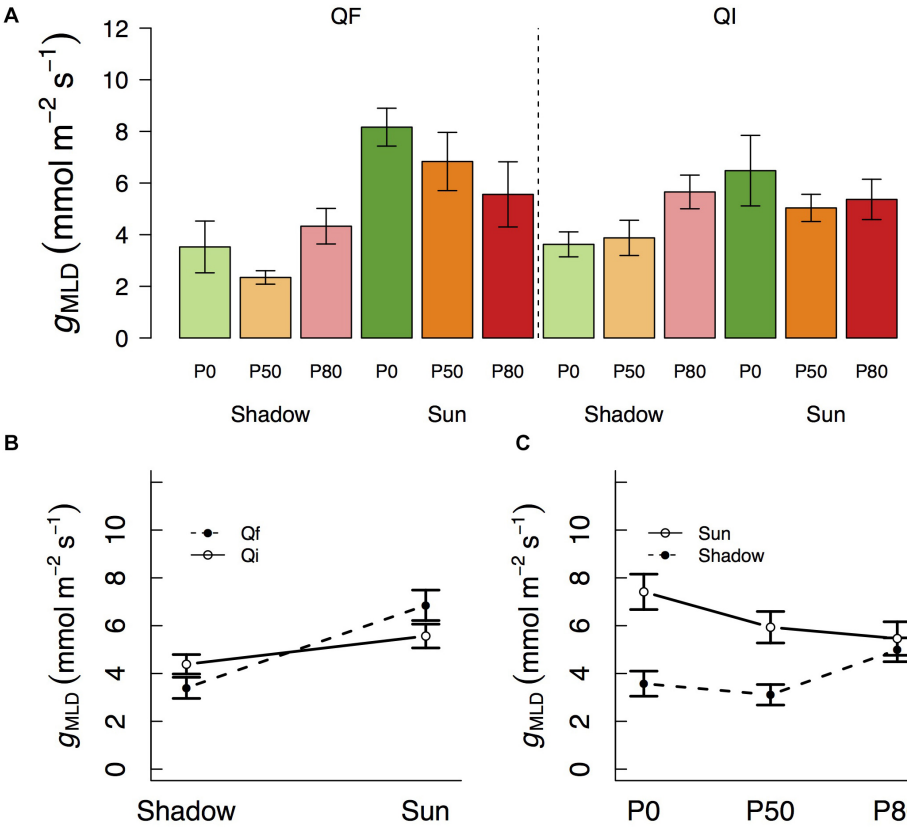

FIGURE 1 | (A) Variation in residual conductance measured from the mass loss of detached leaves (g_{MLD}) across different light treatments (shadow vs sun) and water treatments (P_0, P_{50}, and P_{80}). Significant interactions across treatments are plotted in **(B,C)**. Bars indicate mean values per treatment and error bars indicate SE.

values of g_{MLD} were usually below those of g_n, but the absolute difference was less than 4 mmol m^{-2} s^{-1}. In *Q. ilex*, the difference between g_n and g_{MLD} was less than 1 mmol m^{-2} s^{-1}.

In contrast, g_d was consistently and significantly above both, g_{MLD} and g_n in *Q. faginea*. It should be noted that, for this comparison, we only used g_d when A_{net} was below 1 μmol m^{-2} s^{-1}. That is, we did not seek to compare values of g_d with g_{MLD} and g_n if A_{net} was above 1 μmol m^{-2} s^{-1} because, in that case, photosynthesis does not tend to zero. The average difference of g_d with g_{MLD} was 17.7 mmol m^{-2} s^{-1} and the average difference of g_d with g_n was 10 mmol m^{-2} s^{-1}. The only case in which g_d was not different from g_{MLD} and g_n was in the sun treatments in *Q. ilex*.

Correlates Explaining Variation in g_{MLD}

Overall, the relationships between the different indicators of g_{MLD} and other physiological parameters were species-specific (**Figure 4A**). The only exceptions were N_{mass} and NSC concentrations which had a negative and a positive correlation, respectively, with g_{MLD} in both species (**Figure 4**). In turn, N_{mass} correlated negatively with NSC concentrations and LMA in both species. NSC also correlated with LMA in both species, albeit positively. In *Q. faginea*, g_{MLD} and g_n also correlated positively with LMA and g_{MLD} also correlated positively. In *Q. ilex*, g_n showed a negative correlation with respiration (R) and a positive correlation with Ψ_{md} and with A_{net}. NSC concentrations were negatively affected by the shade treatment (**Supplementary Figure 1A**).

Modeling g_d: Comparing Different Formulations of the BB Model

We first compared the performance of the model proposed by Duursma et al. (2019) when g_0 and g_{min} had been defined on the basis of g_{MLD} (BBD_{MLD}), of g_n (BBD_n), and of g_d (BBD_d). In all cases, the original g_0 and g_{min} were defined as the level conductance (g_{MLD}, g_n, or g_d, depending on case) in the P_0_shade treatment (low light) and in the P_{80}_sun treatment, respectively, (high water stress).

Model performance was superior when the model was based on g_{MLD} (BBD_{MLD}), but differences with the model based on g_n were minor (ΔAIC = 0.3 for *Q. faginea* and 2.3 for *Q. ilex*). However, the model based on g_d showed consistently a larger AIC, indicating smaller plausibility (**Table 2**).

We compared the performance of these three models against the original Ball- Berry (BB) and we observed that BBD_{MLD} and BBD_n performed better only in *Q. faginea*, where the difference in AIC was bigger than 4. For *Q. ilex*, however, the AIC was similar across models although the intercept of the observed

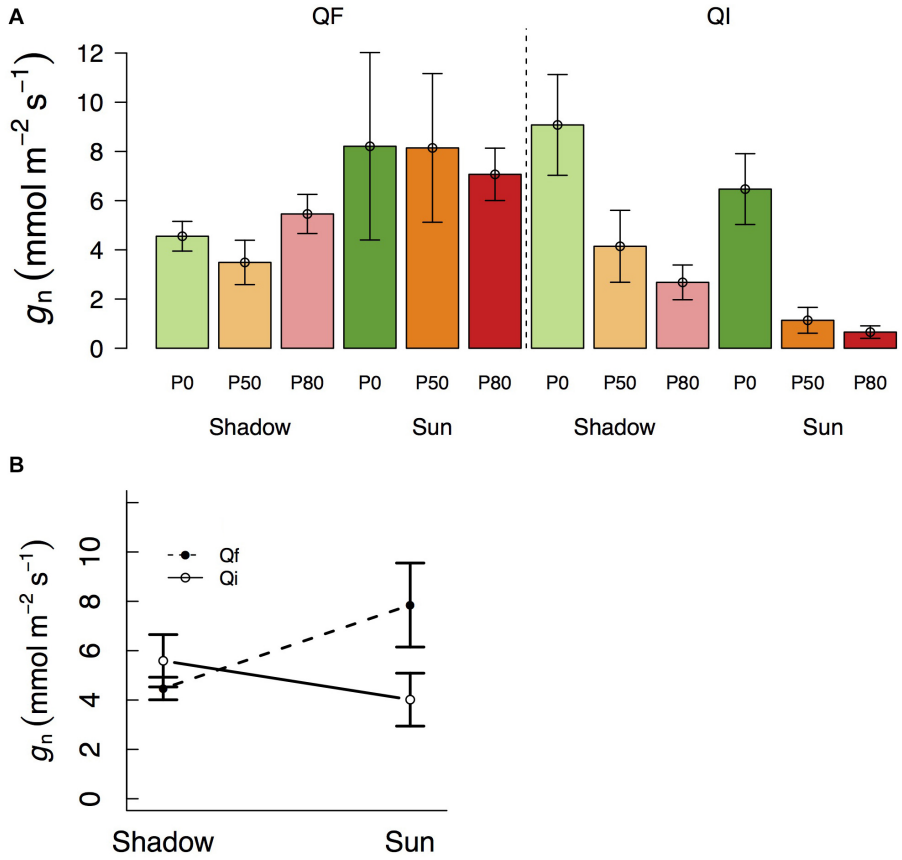

FIGURE 2 | (A) Variation in residual conductance measured from nocturnal conductance under high *D* (g_n) across different light treatments (shadow vs sun) and water treatments (P_0, P_{50}, and P_{80}). Significant interactions across treatments are plotted in **(B)**. Bars indicate mean values per treatment and error bars indicate SE.

vs predicted relationship was significantly different from 0 only in the BB model.

Finally, we compared the performance of the Ball-Berry model but where, instead of fitting g_{int} through least squares, we use actual g_{MLD} measurements (BB_meas_g_{MLD}), which we defined originally as g_{MLD} under water stress (P_{80}_sun). We observed that this was the best model in *Q. ilex* as it had the smallest AIC although the difference was not significant with BBD_{MLD} (ΔAIC = 1.64). In *Q. faginea*, BB_meas_g_{MLD} peformed worst than BBD_{MLD} (Δ AIC = 2.6).

Differences between BB_meas_g_{MLD} were significant with the BB model (AIC = 2 for both species) and it was also more plausible than the BBD_d model in *Q. faginea* (AIC > 2). Differences between BB_meas_g_{int} and the other models were not significant. We tried fitting BB_meas_g_{int} with different values of g_{int} (e.g., using values under shade, or from g_n), but differences were not significant (*data not shown*).

Modeling g_d: Coupled Leaf Gas Exchange Model

Depending on how g_{res} was measured, we found significant differences of simulated gas exchange. In particular, when g_d was used we always observed higher values of C_i at any PAR level and also higher leaf transpiration rates (E_l) as temperatures increased because g_d was often larger than g_{MLD} and g_n (**Figure 5**).

Generally speaking, there was little difference in simulated C_i and E_l regardless of whether g_{MLD} or g_n were used, and whether they were defined from g_0 or from g_{min}. The only exception was that, in *Q. ilex*, there were some differences in predicted C_i (particularly at low PAR levels) and in predicted leaf transpiration (particularly at peak E_l) when g_{res} was defined from g_n: using g_n from the P_0_shade (g_0) treatment led to higher predicted C_i and E_l than using g_n from the P_{80}_sun treatment (g_{min}). It should be noticed that g_n from the P_0_shade treatment was one order of magnitude larger than g_n from the P_{80}_sun treatment (9.1 vs 0.6 mmol m^{-2} s^{-1}, respectively).

DISCUSSION

We observed that residual conductance varied significantly across light and water treatments in an interactive (non-additive) fashion and the responses differed across species. There were no significant differences as to whether residual conductance was measured from g_{MLD} or from g_n, but the values were significantly higher when using g_d. g_{MLD} was positively correlated with NSC concentrations, suggesting that further

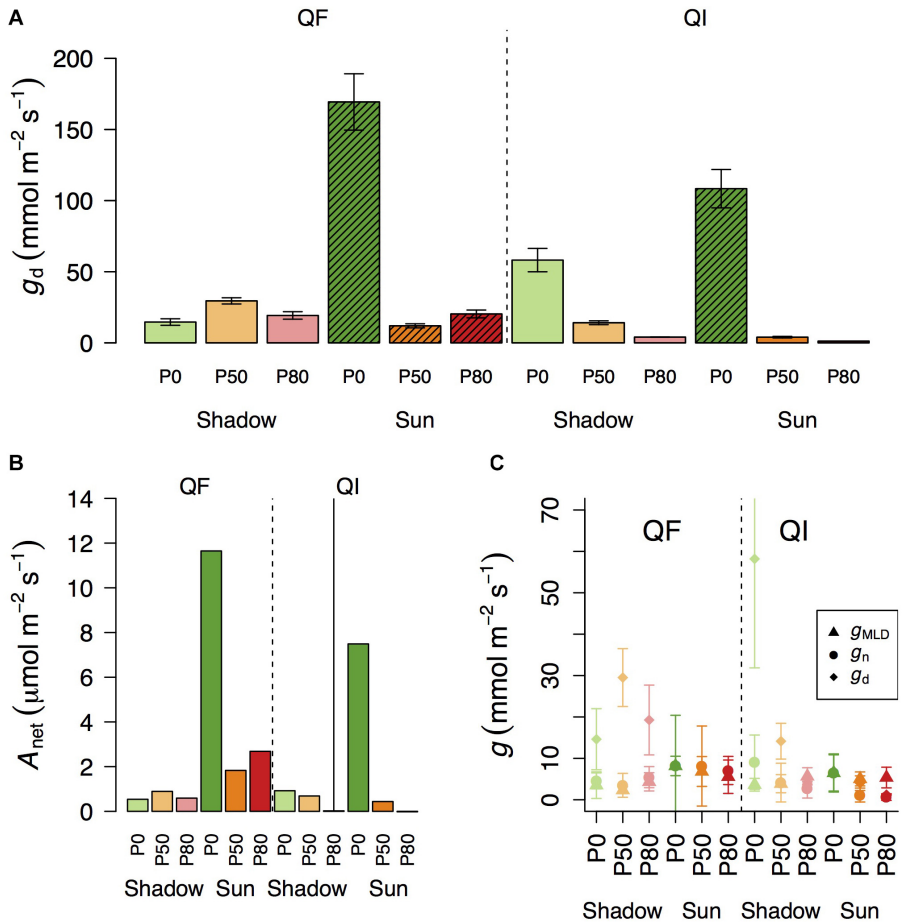

FIGURE 3 | Variation in daytime leaf conductance (**A**, g_d) and net assimilation (**B**, A_{net}) across different light treatments (shadow vs sun) and water treatments (P_0, P_{50}, and P_{80}). Bars indicate mean values per treatment and error bars indicate SE. Hatched bars in **(A)** indicate that A_{net} in that treatment is significantly higher than 1. **(C)** Differences in residual conductance as measured by from the mass loss of detached leaves (g_{MLD}), from nocturnal conductance under high D (g_n), or from g_d when A_{net} was smaller than 1 [note that some values of g_d are missing in **(C)** if A_{net} for that treatment was higher than 1]. Error bars indicate 95% CI.

reductions in g_{MLD} under drought may be limited by low NSC availability. From a modeling perspective, the small measured differences between g_{MLD} and g_n generally did not impact model performance. Although residual conductance differed significantly under experimental treatment, such differences in residual conductance showed only a moderate impact on model performance. That is, model performance did not critically depend upon whether residual conductance was measured under strong shade or under strong water stress. There was also little difference in model fit when either g_{MLD} or g_n were used as an absolute minimum in Eq. 4 (BBD_{MLD} or BBD_n), or when they were used as the intercept of the BB equation (BB_meas_g_{MLD}).

Shade and Drought Interact as Drivers of g_{MLD} Although Responses Are Species-Specific

We observed that g_{MLD} declined under increasing drought in the sun treatment. In the shade treatment, however, g_{MLD} remained low and constant, regardless of the water treatment. This result indicates that drought only affects g_{MLD} under high light because, under shade, light limitations lower g_{MLD} to a minimum that is not affected by water stress. It is worth noting that, at least for some species, full acclimation after changes in the light growth environment may require more than one growing season (Aranda et al., 2001). In other words, the strong limitation imposed by the low light over g_{MLD} may increase even more in subsequent years.

Previous studies had identified how g_{MLD} often decreases under exposure to water stress and light, as a result of changes in wax composition, when each effect is examined in isolation (Shepherd and Wynne Griffiths, 2006). However, our experiment may be the first to examine g_{MLD} responses in a multifactorial experiment. Interestingly, light and water effects were not additive. That is, we did not observe a lower g_{MLD} under low light and high water stress, as would be expected from an additive effect of both factors.

The response to shade was, however, species-specific. g_{MLD} increased in the sun treatment only in the deciduous

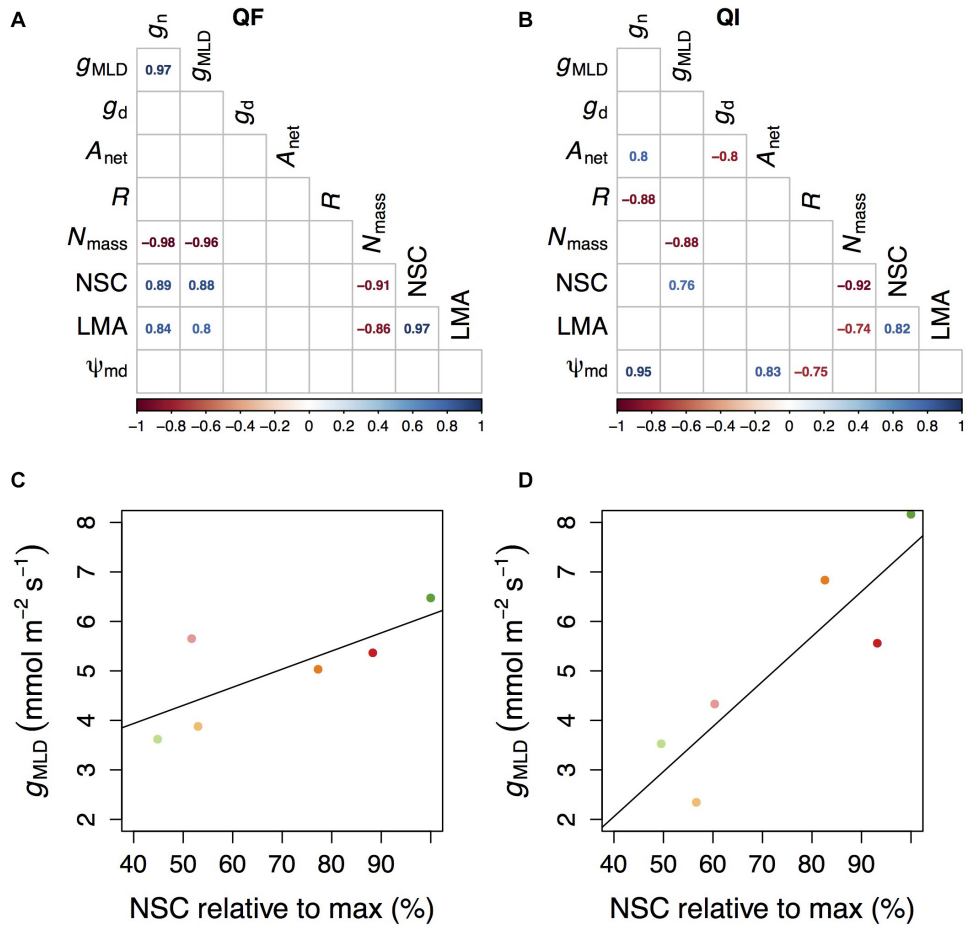

FIGURE 4 | Correlation table between the measured parameters in *Q. faginea* (Qf, **A**) and *Q. ilex* (Qi, **B**). Relationship between conductance measured as mass loss of detached leaves under and non-structural concentrations (NSC) in Qf **(C)** and Qi **(D)**. NSC are provided relative to the maximum values measured in our experiment. Values in **(C,D)** indicate mean per treatment, and each treatment is indicated by a different color following the same convention as in **Figures 1–3**.

TABLE 2 | Model comparison. We compared for *Q. faginea* (QF) and *Q. ilex* (QI) different models based on the Akaike Information Criterion (AIC), the change in AIC relative to the lowest (ΔAIC) and the R^2, slope and intercept of the observed vs predicted relationship. For the slope and intercept we show the mean value (and SE).

	g_{int} (mmol m^{-2} s^{-1})	AIC	Δ AIC	R^2	Slope		Intercept	
QF								
BBD_{MLD}	5.5	−106.88	0	0.88	1.04	(0.09)	0.001	(0.005)
BBD_n	7.1	−106.6	0.28	0.87	1.06	(0.09)	0.0006	(0.005)
BBD_d	20.3	−102.32	4.56	0.84	*1.23*	*(0.13)*	*−0.013*	*(0.007)*
BB[1]	8.9	−102.3	4.58	0.85	1.02	(0.09)	−0.01	(0.006)
BB_meas_g_{MLD}	5.5	−104.3	2.58	0.86	0.99	(0.09)	0.002	(0.005)
QI								
BBD_{MLD}	5.3	−98.52	1.64	0.97	**1.2**	**(0.05)**	−0.0001	(0.003)
BBD_n	9.1	−96.22	3.94	0.97	**1.2**	**(0.05)**	−0.002	(0.008)
BBD_d	58.2	−69.92	30.24	0.85	**1.6**	**(0.17)**	**−0.067**	**(0.01)**
BB[1]	16.8	−98.14	2.02	0.98	**1.3**	**(0.05)**	**−0.018**	**(0.004)**
BB_meas_g_{MLD}	5.3	−100.16	0	0.98	**1.2**	**(0.04)**	−0.001	(0.003)

The models compared include the Ball-Berry model (Eq. 5, BB), the BB model where the intercept is measured, rather than estimated (BB_meas_g_{MLD}) and the modification of the Ball-Berry model proposed by Duursma (Eq. 4, BBD) using g_{MLD} (BBD_{MLD}), g_n (BBD_n), or g_d (BBD_d) as g_0 and g_{min}. We also provide the values of the intercept, g_{int} (the maximum between g_0 and g_{min} in the first three models), that were used in each case. Values in bold (or italics) in slope and intercept indicate values significantly (or marginally) different from 1 and 0, respectively.

[1]*Note that g_{int} in this case is estimated through least squares, rather than measured as in the other models.*

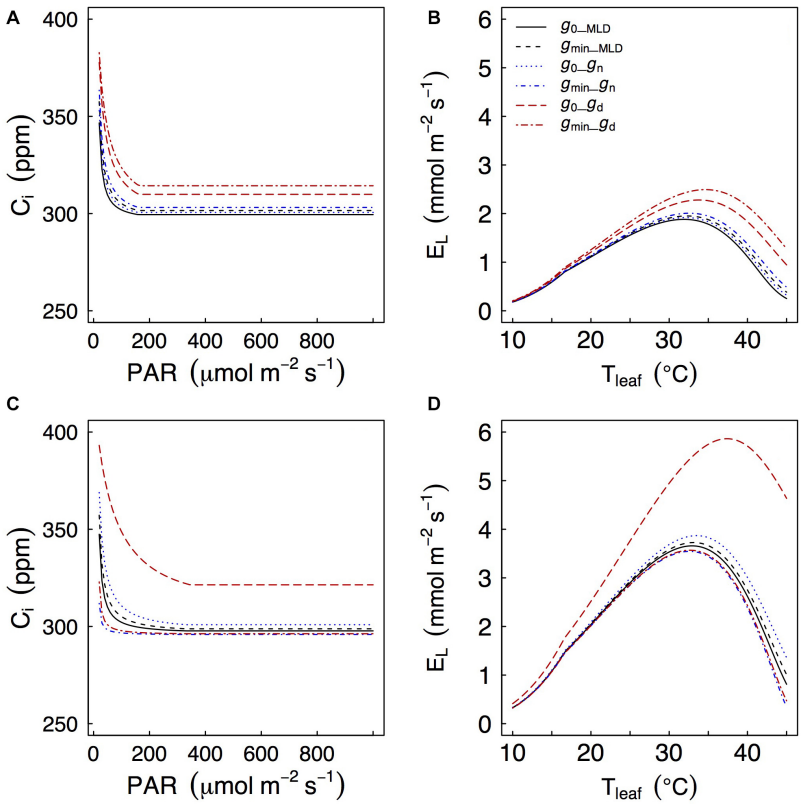

FIGURE 5 | Effects of different values of g_{res} on a coupled photosynthesis model as in Duursma et al. (2019). Models are for *Q. faginea* **(A,B)** and *Q. ilex* **(C,D)**. g_0 and g_{min} represent g_{res} under low light (P_0_shadow treatment) and water stress (P_{80}_sun treatment), respectively. Subscripts $_{MLD}$, $_n$, and $_d$ indicate that g_0 or g_{min} (depending on case) were estimated from mass loss of detached leaves, from nocturnal conductance, or from daytime conductance.

Q. faginea, whereas the increase in *Q. ilex* g_{MLD} under sun was not significant.

g_{MLD} Correlated With Low NSC Concentrations

We can speculate that the reason why g_{MLD} was not lower under the high water stress and shade treatment (relative to other shade treatments under less water stress) is related to carbohydrate limitations. We observed a significant and positive correlation between NSC and g_{MLD} across species. A synthesis of variation in NSC across species reports that a minimum NSC of 46% is always conserved (Martínez-Vilalta et al., 2016). In our results we also observed a minimum NSC that was close to the 46% of the maximum NSC that we measured (**Figures 4C,D**).

A possible explanation on why g_{MLD} did not decrease further under the joint drought and shade stress is related to a lack of NSC to feed the building of additional wax and/or epidermal layers. That is, once plants have reached the minimum NSC threshold of 46% relative to maximum, they will seek to preserve their NSC for other functions, such as osmoregulation, at the expense of building thicker cuticles or additional wax layers. We note that osmoregulation under shade may be impaired in oaks (Aranda et al., 2005; Rodriguez-Calcerrada et al., 2010).

At any rate, this is the first study, to our knowledge to raise this possibility. This result should thus be interpreted with caution. We acknowledge that the correlation between g_{MLD} and NSC may have been affected by jointly considering plants under different light and water regimes. Subsequent work would thus be needed to confirm this hypothesis.

Residual Conductance in Relation to Respiration, LMA and N_{mass}

Despite stomatal closure, g_{res} did not limit CO_2 diffusion out of the leaf. In fact, there was a negative correlation between nocturnal conductance and respiration in one of our (*Q. ilex*) species, indicating higher CO_2 efflux at lower g_n and, consequently, that reduced g_n levels were far from limiting respiration. This contradicts earlier studies that cytotoxic CO_2 build-up could occur under nocturnal stomatal closure (Fricke, 2019) but it aligns along with the results of modeling, indicating that only under conductances that are orders of magnitude lower to those reported here could a cytotoxic CO_2 build-up occur (Resco De Dios et al., 2019).

g_{MLD} increased in the sun in *Q. faginea*. LMA also increased with light (*data not shown*) and it was significantly correlated with g_n and with g_{MLD} in *Q. faginea*. LMA is an indicator of the degree of sclerophylly, which could serve to decrease residual conductance by increasing cuticle thickness. However, LMA also increased with light in the sclerophyll *Q. ilex*, where LMA did not correlate with g_n or g_{MLD}. This result matches with previous

studies in *Quercus* indicating that any effects of LMA in g_n and g_{MLD} may be modified by changes in the cuticle composition (Bueno et al., 2020). We note that this argument is speculative and based only on circumstantial evidence.

N_{mass} showed a negative correlation with g_{MLD} in both species, and with g_n in *Q. faginea*. This result indicates that species with a higher photosynthetic investment will decrease the investment in residual conductance. This points toward a potential mechanism underlying the trade-off between investment for C uptake (higher N_{mass}) and preventing catastrophic water losses (reduced g_{MLD}). Further studies will be necessary to test the generality of this hypothesis.

Residual Conductance May Be Measured via g_{MLD} or via g_n Under High D

Measurements of nocturnal conductance under the relatively high D from this experiment were statistically indistinguishable from independent measurements of residual conductance indicating that the latter was driving the former. It had been previously argued that measurements of g_n would not be valid indicators of residual conductance, because g_n is actively regulated (Duursma et al., 2019). Our results suggest that this argument from Duursma et al. (2019) may only be valid when g_n is measured under low D.

Previous studies document that stomata often reach complete closure (or as complete as it can be) under lower D in the night, than in the day (Barbour and Buckley, 2007). This phenomenon would explain why g_n was much lower than g_d although D was comparable, and it is likely explained by the capacity of stomata to sense and open in response to light.

We also show how modeling results were not affected by either using g_{MLD} or g_n. This result, however, needs to be interpreted with caution. We only focused on BB-type stomatal models and other results may be obtained in different model types. For instance, as Duursma et al. (2019) noted, changing minimum conductance from 2 to 4 mmol m^{-2} s^{-1} halved the time to reach mortality in a hydraulics model because it doubled the water losses (Duursma et al., 2019). Although differences were statistically not significant between g_{MLD} and g_n, we still observed differences in mean residual conductance of 4 mmol m^{-2} s^{-1} across measurements, indicating that measurement errors and other sources of uncertainty may play a large for other model types, such as mortality models.

Modeling g_s

We acknowledge our dataset was limited to thoroughly test the best form of the BB model: we sampled under highly contrasting light and water conditions, but only once in time. We would thus need data over more time periods for a more thorough evaluation. However, our dataset allows for the development of some hypotheses, which may be expanded in subsequent studies.

We observed that there were only little differences between Eq. 5, where the original BB function was used but including measured g_{MLD} (BB_meas_g_{MLD}), instead of the version proposed by Duursma et al. (2019; Eq. 4). Duursma et al. (2019) note that residual conductance acts as an actual minimum in the function they propose. However, if the goal is to use residual conductance as an actual stomatal minimum, one could consider the following equation instead:

$$g_s = \max\left(\min\left(g_0, g_{min}\right), m\,A\,RH/Ca\right) \quad (6)$$

where the minimum between g_0 and g_{min} is chosen [not the maximum, as proposed by Duursma et al. (2019)].

At any rate, we did not observe major differences in model performance between the BBD model or Eq. 5. This result indicates that it is unlikely that losses in model performance will derive from the adoption of the alternative model formulations, as proposed by previous studies (De Kauwe et al., 2015; Duursma et al., 2019).

Our results also indicate that g_{MLD} and g_n can both be interchangeably, and that the choice between g_0 and g_{min} exerts negligible consequences for model fitting. Earlier studies indicate a major effect of g_{res} (De Kauwe et al., 2015; Duursma et al., 2019). This is because those studies used a wide range of g_{res} values (10–40 mmol m^{-2} s^{-1}, depending on the case), much higher that the variability we reported here when using g_{MLD} and g_n across treatments (**Table 2**). Synthesis studies similarly indicate limited variation in g_{res} within a family (Duursma et al., 2019). After discarding g_d as a reliable indicator of g_{res}, our results indicate a minor effect of different methods and approaches used for measuring g_{res} and for modeling water use, at least in our two closely related species.

DATA AVAILABILITY STATEMENT

The raw data supporting the conclusions of this article will be made available by the authors, without undue reservation.

AUTHOR CONTRIBUTIONS

VR designed the experiment. CA performed research with the help of FC. VR analyzed the data and wrote the manuscript with important feedback from all co-authors. All authors contributed to the article and approved the submitted version.

FUNDING

We acknowledge funding from the Natural Science Foundation in China (31850410483), the talent proposals from Sichuan Province (2020JDRC0065), the Southwest University of Science and Technology talents fund (18ZX7131), and the Spanish MICINN (AGL2015-69151-R). EG is supported by MCIU/AEI/FEDER, UE [Postdoctoral Contract (IJCI-2017-32511)].

ACKNOWLEDGMENTS

We acknowledge technical assistance from P. Sopeña, M.J. Pau, B. Lavaquiol, A. Cunill, and J. Hedo. We remain grateful to

earlier comments from E. Gil-Pelegrín, J.J. Peguero-Pina, D. Sancho-Knapik, D.G. Williams, and D.T. Tissue.

SUPPLEMENTARY MATERIAL

The Supplementary Material for this article can be found online at: https://www.frontiersin.org/articles/10.3389/fpls.2020.603581/full#supplementary-material

Supplementary Figure 1A | Variation in leaf non-structural carbohydrate concentrations measured across different light treatments (shadow vs sun) and water treatments (P_0, P_{50}, and P_{80}) in *Quercus faginea* (QF) and *Q. ilex* (QI). Bars indicate mean values per treatment and error bars indicate SE.

Supplementary Table 1A | Target midday water potential (Ψ_{md}) to reach the desired PLC according to Esteso-Martínez et al. (2006) for Q. *faginea* and to Peguero-Pina et al. (2014) for *Q. ilex*, and actual values. Mean (and SE) actual values are presented. The letters in "Actual PLC" indicate the results of *post hoc* analyses (Tukey HSD). This is a reproduction (with permission from the publisher) of **Table 1** originally published in Resco De Dios et al. (2020).

REFERENCES

Aranda, I., Bergasa, L. F., Gil, L., and Pardos, J. A. (2001). Effects of relative irradiance on the leaf structure of *Fagus sylvatica* L. seedlings planted in the understory of a *Pinus sylvestris* L. stand after thinning. *Ann. For. Sci.* 58, 673–680. doi: 10.1051/forest:2001154

Aranda, I., Castro, L., Pardos, M., Gil, L., and Pardos, J. A. (2005). Effects of the interaction between drought and shade on water relations, gas exchange and morphological traits in cork oak (*Quercus suber* L.) seedlings. *For. Ecol. Manag.* 210, 117–129. doi: 10.1016/j.foreco.2005.02.012

Ball, T. J., Woodrow, I. E., and Berry, J. A. (1987). "A model predicting stomatal conductance and its contribution to the control of photosynthesis under different environmental conditions," in *Progress in Photosynthesis Research*, ed. J. Biggins (Dordrecht: Martinus Nijhoff), 221–224. doi: 10.1007/978-94-017-0519-6_48

Barbour, M. M., and Buckley, T. N. (2007). The stomatal response to evaporative demand persists at night in *Ricinus communis* plants with high nocturnal conductance. *Plant Cell Environ.* 30, 711–721. doi: 10.1111/j.1365-3040.2007.01658.x

Barnard, D. M., and Bauerle, W. L. (2013). The implications of minimum stomatal conductance on modeling water flux in forest canopies. *J. Geophys. Res. Biogeosci.* 118, 1322–1333. doi: 10.1002/jgrg.20112

Blackman, C. J., Pfautsch, S., Choat, B., Delzon, S., Gleason, S. M., and Duursma, R. A. (2016). Toward an index of desiccation time to tree mortality under drought. *Plant Cell Environ.* 39, 2342–2345. doi: 10.1111/pce.12758

Boyer, J. S., Wong, S. C., and Farquhar, C. D. (1997). CO_2 and water vapor exchange across leaf cuticle (epidermis) at various water potentials. *Plant Physiol.* 114, 185–191. doi: 10.1104/pp.114.1.185

Bueno, A., Sancho-Knapik, D., Gil-Pelegrin, E., Leide, J., Peguero-Pina, J. J., Burghardt, M., et al. (2020). Cuticular wax coverage and its transpiration barrier properties in *Quercus coccifera* L. leaves: does the environment matter?. *Tree Physiol.* 40, 827–840. doi: 10.1093/treephys/tpz110

Burnham, K. P., and Anderson, D. R. (2002). *Model Selection and Multi/Model Inference: A Practical Information-Theoretic Approach*. New York, NY: Springer-Verlag.

Collatz, G. J., Ball, J. T., Grivet, C., and Berry, J. A. (1991). Physiological and environmental regulation of stomatal conductance, photosynthesis and transpiration: a model that includes a laminar boundary layer. *Agric. For. Meteorol.* 54, 107–136. doi: 10.1016/0168-1923(91)90002-8

De Kauwe, M. G., Kala, J., Lin, Y. S., Pitman, A. J., Medlyn, B. E., Duursma, R. A., et al. (2015). A test of an optimal stomatal conductance scheme within the CABLE Land Surface Model. *Geosci. Model. Dev.* 8, 431–452. doi: 10.5194/gmd-8-431-2015

Duarte, A. G., Katata, G., Hoshika, Y., Hossain, M., Kreuzwieser, J., Arneth, A., et al. (2016). Immediate and potential long-term effects of consecutive heat waves on the photosynthetic performance and water balance in Douglas-fir. *J. Plant Physiol.* 205, 57–66. doi: 10.1016/j.jplph.2016.08.012

Duursma, R. A. (2015). Plantecophys - an R package for analysing and modelling leaf gas exchange data. *PLoS One* 10:e0143346. doi: 10.1371/journal.pone.0143346

Duursma, R. A., Blackman, C. J., Lopez, R., Martin-Stpaul, N. K., Cochard, H., and Medlyn, B. E. (2019). On the minimum leaf conductance: its role in models of plant water use, and ecological and environmental controls. *New Phytol.* 221, 693–705. doi: 10.1111/nph.15395

Esteso-Martínez, J., Camarero, J. J., and Gil-Pelegrín, E. (2006). Competitive effects of herbs on *Quercus faginea* seedlings inferred from vulnerability curves and spatial-pattern analyses in a Mediterranean stand (Iberian System, northeast Spain). *Écoscience* 13, 378–387. doi: 10.2980/i1195-6860-13-3-378.1

Fernández, V., Bahamonde, H. A., Javier Peguero-Pina, J., Gil-Pelegrín, E., Sancho-Knapik, D., Gil, L., et al. (2017). Physico-chemical properties of plant cuticles and their functional and ecological significance. *J. Exp. Bot.* 68, 5293–5306. doi: 10.1093/jxb/erx302

Flexas, J., Barbour, M. M., Brendel, O., Cabrera, H. M., Carriqui, M., Diaz-Espejo, A., et al. (2012). Mesophyll diffusion conductance to CO_2: an unappreciated central player in photosynthesis. *Plant Sci.* 193–194, 70–84. doi: 10.1016/j.plantsci.2012.05.009

Fricke, W. (2019). Night-time transpiration - favouring growth? *Trends Plant Sci.* 24, 311–317. doi: 10.1016/j.tplants.2019.01.007

Heredia-Guerrero, J. A., Guzman-Puyol, S., Benitez, J. J., Athanassiou, A., Heredia, A., and Dominguez, E. (2018). Plant cuticle under global change: biophysical implications. *Glob. Chan. Biol.* 24, 2749–2751. doi: 10.1111/gcb.14276

Hetherington, A. M., and Woodward, F. I. (2003). The role of stomata in sensing and driving environmental change. *Nature* 424, 901–908. doi: 10.1038/nature01843

Hoffman, A. S., Albeke, S. E., Mcmurray, J. A., Evans, R. D., and Williams, D. G. (2019). Nitrogen deposition sources and patterns in the greater yellowstone ecosystem determined from ion exchange resin collectors, lichens, and isotopes. *Sci. Total Environ.* 683, 709–718. doi: 10.1016/j.scitotenv.2019.05.323

Kerstiens, G. (1996). Cuticular water permeability and its physiological significance. *J. Exp. Bot.* 47, 1813–1832. doi: 10.1093/jxb/47.12.1813

Leuning, R. (1995). A critical appraisal of a combined stomatal-photosynthesis model for C3 plants. *Plant Cell Environ.* 18, 339–355. doi: 10.1111/j.1365-3040.1995.tb00370.x

Lombardozzi, D. L., Zeppel, M. J. B., Fisher, R. A., and Tawfik, A. (2017). Representing nighttime and minimum conductance in CLM4.5: global hydrology and carbon sensitivity analysis using observational constraints. *Geosci. Model. Dev.* 10, 321–331. doi: 10.5194/gmd-10-321-2017

Long, S. P., and Bernacchi, C. J. (2003). Gas exchange measurements, what can they tell us about the underlying limitations to photosynthesis? Procedures and sources of error. *J. Exp. Bot.* 54, 2393–2401. doi: 10.1093/jxb/erg262

Martínez-Vilalta, J., Sala, A., Asensio, D., Galiano, L., Hoch, G., Palacio, S., et al. (2016). Dynamics of non-structural carbohydrates in terrestrial plants: a global synthesis. *Ecol. Monogr.* 86, 495–516. doi: 10.1002/ecm.1231

Martin-Stpaul, N., Delzon, S., and Cochard, H. (2017). Plant resistance to drought depends on timely stomatal closure. *Ecol. Lett.* 20, 1437–1447. doi: 10.1111/ele.12851

Ogle, K., Lucas, R. W., Bentley, L. P., Cable, J. M., Barron-Gafford, G. A., Griffith, A., et al. (2012). Differential daytime and night-time stomatal behavior in plants from North American deserts. *New Phytol.* 194, 464–476. doi: 10.1111/j.1469-8137.2012.04068.x

Palacio, S., Maestro, M., and Montserrat-Marti, G. (2007). Relationship between shoot-rooting and root-sprouting abilities and the carbohydrate and nitrogen reserves of Mediterranean dwarf shrubs. *Ann. Botany* 100, 865–874. doi: 10.1093/aob/mcm185

Peguero-Pina, J. J., Sancho-Knapik, D., Barron, E., Camarero, J. J., Vilagrosa, A., and Gil-Pelegrin, E. (2014). Morphological and physiological divergences within *Quercus ilex* support the existence of different ecotypes depending on climatic dryness. *Ann. Bot.* 114, 301–313. doi: 10.1093/aob/mcu108

Phillips, N. G., Lewis, J. D., Logan, B. A., and Tissue, D. T. (2010). Inter- and intra-specific variation in nocturnal water transport in *Eucalyptus*. *Tree Physiol.* 30, 586–596. doi: 10.1093/treephys/tpq009

R Core Team (2020). *R: A Language and Environment for Statistical Computing*. Vienna: R Foundation for Statistical Computing.

Resco, V., Ewers, B. E., Sun, W., Huxman, T. E., Weltzin, J. F., and Williams, D. G. (2009). Drought-induced hydraulic limitations constrain leaf gas exchange recovery after precipitation pulses in the C3 woody legume, *Prosopis velutina*. *New Phytol.* 181, 672–682. doi: 10.1111/j.1469-8137.2008.02687.x

Resco De Dios, V., Arteaga, C., Peguero-Pina, J. J., Sancho-Knapik, D., Qin, H., Zveushe, O. K., et al. (2020). Hydraulic and photosynthetic limitations prevail over root non-structural carbohydrate reserves as drivers of resprouting in two Mediterranean oaks. *Plant Cell Environ.* 43, 1944–1957. doi: 10.1111/pce.13781

Resco De Dios, V., Chowdhury, F. I., Granda, E., Yao, Y., and Tissue, D. T. (2019). Assessing the potential functions of nocturnal stomatal conductance in C3 and C4 plants. *New Phytol.* 223, 1696–1706. doi: 10.1111/nph.15881

Resco De Dios, V., Diaz-Sierra, R., Goulden, M. L., Barton, C. V., Boer, M. M., Gessler, A., et al. (2013). Woody clockworks: circadian regulation of night-time water use in *Eucalyptus globulus*. *New Phytol.* 200, 743–752. doi: 10.1111/nph.12382

Resco De Dios, V., Roy, J., Ferrio, J. P., Alday, J. G., Landais, D., Milcu, A., et al. (2015). Processes driving nocturnal transpiration and implications for estimating land evapotranspiration. *Sci. Rep.* 5:10975.

Riederer, M., and Müller, C. (2007). *Biology of the Plant Cuticle*. Hoboken, NJ: Blackwell Publishing.

Rodriguez-Calcerrada, J., Pardos, J. A., and Aranda, I. (2010). Contrasting responses facing peak drought in seedlings of two co-occurring oak species. *Forestry* 83, 369–378. doi: 10.1093/forestry/cpq019

Schuster, A. C., Burghardt, M., and Riederer, M. (2017). The ecophysiology of leaf cuticular transpiration: are cuticular water permeabilities adapted to ecological conditions? *J. Exp. Bot.* 68, 5271–5279. doi: 10.1093/jxb/erx321

Shepherd, T., and Wynne Griffiths, D. (2006). The effects of stress on plant cuticular waxes. *New Phytol.* 171, 469–499.

Way, D. A., and Pearcy, R. W. (2012). Sunflecks in trees and forests: from photosynthetic physiology to global change biology. *Tree Physiol.* 32, 1066–1081.

Wei, T., and Simko, V. (2017). *R Package "Corrplot": Visualization of a Correlation Matrix (Version 0.84)*. Available online at: https://github.com/taiyun/corrplot (accessed September 1, 2020).

Zhang, P., Wen, Y., Wang, L., Zhang, H., Wang, G. G., and Wu, T. (2020). Leaf structural carbohydrate decreased for *Pinus thunbergii* along coast-inland gradients. *Forests* 11:449.

Conflict of Interest: The authors declare that the research was conducted in the absence of any commercial or financial relationships that could be construed as a potential conflict of interest.

frontiers in Plant Science

ORIGINAL RESEARCH
published: 08 December 2020
doi: 10.3389/fpls.2020.577235

Difference Between Day and Night Temperatures Affects Stem Elongation in Tomato (*Solanum lycopersicum*) Seedlings via Regulation of Gibberellin and Auxin Synthesis

*Kinuka Ohtaka[1,2,3], Akiko Yoshida[1,4], Yusuke Kakei[5], Kosuke Fukui[1,6], Mikiko Kojima[1], Yumiko Takebayashi[1], Kanako Yano[5], Shunsuke Imanishi[5] and Hitoshi Sakakibara[1,2]**

[1] RIKEN Center for Sustainable Resource Science, Yokohama, Japan, [2] Graduate School of Bioagricultural Sciences, Nagoya University, Nagoya, Japan, [3] Department of Chemical and Biological Sciences, Faculty of Science, Japan Women's University, Tokyo, Japan, [4] Department of International Environmental and Agricultural Science, Tokyo University of Agriculture and Technology, Tokyo, Japan, [5] NARO, Institute of Vegetable and Floriculture Science, Tsu, Japan, [6] Department of Biochemistry, Okayama University of Science, Okayama, Japan

OPEN ACCESS

Edited by:
M. Iqbal R. Khan,
Jamia Hamdard University, India

Reviewed by:
Dr. Aditi Gupta,
Centre for Research in Agricultural Genomics (CRAG), Spain
Cris Argueso,
Colorado State University, United States

***Correspondence:**
Hitoshi Sakakibara
sakaki@agr.nagoya-u.ac.jp

Specialty section:
This article was submitted to Plant Physiology, a section of the journal Frontiers in Plant Science

Received: *29 June 2020*
Accepted: *16 November 2020*
Published: *08 December 2020*

Citation:
Ohtaka K, Yoshida A, Kakei Y, Fukui K, Kojima M, Takebayashi Y, Yano K, Imanishi S and Sakakibara H (2020) Difference Between Day and Night Temperatures Affects Stem Elongation in Tomato (Solanum lycopersicum) Seedlings via Regulation of Gibberellin and Auxin Synthesis. Front. Plant Sci. 11:577235. doi: 10.3389/fpls.2020.577235

Temperature is a critical environmental factor governing plant growth and development. The difference between day temperature (DT) and night temperature (NT), abbreviated as DIF, influences plant architecture. Subjecting plants to artificial DIF treatments is an effective strategy in ornamental horticulture. For example, negative DIF (when DT – NT < 0) generally inhibits stem elongation, resulting in dwarf plants. However, the mechanisms underlying stem growth regulation by DIF remains to be completely elucidated. In this study, we aimed to analyze the growth, transcriptome, and phytohormone profiles of tomato (*Solanum lycopersicum*) seedlings grown under different DIF treatments. Under positive DIF (when DT – NT > 0), in contrast to the control temperature (25°C/20°C, DT/NT), high temperature (30°C/25°C) increased stem length and thickness, as well as the number of xylem vessels. Conversely, compared with the positive high temperature DIF treatment (30°C/25°C), under negative DIF treatment (25°C/30°C) stem elongation was inhibited, but stem thickness and the number of xylem vessels were not affected. The negative DIF treatment decreased the expression of gibberellin (GA)-, auxin-, and cell wall-related genes in the epicotyl, as well as the concentrations of GAs and indole-3-acetic acid (IAA). The expression of these genes and concentrations of these hormones increased under high temperature compared to those under the control temperature positive DIF. Our results suggest that stem length in tomato seedlings is controlled by changes in GA and IAA biosynthesis in response to varying day and night temperatures.

Keywords: auxin, DIF, gibberellin, *Solanum lycopersicum*, stem elongation, tomato

Abbreviations: CT, control temperature; DT, day temperature; +DIF, positive DIF; -DIF, negative DIF; HT, high temperature; NT, night temperature.

INTRODUCTION

Plants modulate their growth according to their environmental conditions. In particular, temperature is a critical factor affecting plant growth. Each plant species has a suitable temperature range. Within this range, higher temperatures generally promote shoot growth, including leaf expansion and stem elongation and thickening. However, temperatures above the optimal range suppress growth. In addition to the absolute temperature, the difference in temperature between day and night can affect growth. Normally, night temperatures are lower than daytime temperatures, and plants modulate their growth pattern and metabolism in response to this temperature change. Altering the temperature difference between day and night is one method through which plant growth is controlled in ornamental horticulture. The difference between day temperature (DT) and night temperature (NT), abbreviated as DIF, is defined as DT– NT. Positive DIF occurs when DT is higher than NT, zero DIF occurs when DT is the same as NT, and negative DIF occurs when DT is lower than NT. Negative DIF can be used to control plant height as an alternative to agricultural chemicals (Shimizu, 2007). While the effects were plant species-dependent, it has been reported that negative DIF inhibits stem elongation compared to positive DIF in various plants, including *Lilium longiflorum*, *Dendranthema grandiflora*, *Cucumis sativus* (Shimizu, 2007), and *Solanum lycopersicum* (Went, 1944; de Koning, 1988).

Previous studies have suggested that phytohormones are involved in regulating plant growth in response to temperature. Gibberellin (GA) is known to play a key role in stem elongation (Davière and Achard, 2013; Binenbaum et al., 2018; Ferrero et al., 2019). Indole-3-acetic acid (IAA), an auxin, also plays an important role in cell elongation in the hypocotyl, the epicotyl, and other organs (Leyser, 2018; Zhao, 2018). In *Arabidopsis thaliana,* higher temperatures promote hypocotyl elongation mediated by phytochrome-interacting factor 4 (PIF4)-dependent auxin biosynthesis (Franklin et al., 2011; Nomoto et al., 2012; Sun et al., 2012). It has been demonstrated that PIF4 function is regulated by GA via DELLA proteins, which are key negative regulators of GA signaling (Koini et al., 2009; Stavang et al., 2009).

Studies have found that stem elongation under different DIF treatments is accompanied by a change in GA content in *Campanula isophylla* and *Pisum sativum* (Jensen et al., 1996; Grindal et al., 1998; Stavang et al., 2005). In *P. sativum*, inhibition of stem elongation under negative DIF was weaker in GA-related mutants than that in the wild type (Grindal et al., 1998). In *A. thaliana*, non-bioactive GA_{29} content was lower under a negative DIF treatment than that under a positive DIF treatment, while IAA concentration was higher under a positive DIF treatment than that under a negative DIF treatment (Thingnaes et al., 2003). In *Raphaus sativus* L., differences in stem elongation under DIF treatments followed a similar pattern to changes in IAA content (Hayata et al., 2001). These studies suggest the involvement of these hormones in the effect of DIF on stem elongation. However, these hormones and the expression of their genes have not been investigated in detail. Further, temperature not only affects stem elongation but also stem thickness; however, the effect of DIF on vascular development has not been properly characterized to date.

In this study, we aimed to elucidate the mechanisms underlying stem growth regulation by DIF. To this end, we examined the effects of different DIF treatments on tomato (*S. lycopersicum*), which is one of the most important vegetable crops. Our analyses of growth, transcriptomes, and hormones strongly suggest that negative DIF-dependent inhibition of stem elongation is mediated by the repression of GA and IAA synthesis accompanied by the regulation of cell wall-related genes. We also report that negative DIF treatment has a minimal effect on stem thickening in tomato seedling.

RESULTS

Higher Temperatures Under Positive DIF Promote Stem Elongation and Thickening in Tomato Seedlings

To examine the effect of temperature under positive DIF on plant growth, tomato seedlings (Managua RZ) were grown under control (25°C/20°C, CT) and high temperatures (30°C/25°C, HT) (**Supplementary Figures 1A,B**). The stem, hypocotyl, and epicotyl lengths and diameters were significantly greater under HT than those under CT (**Figures 1A–C**). Histological analysis of hypocotyl cross sections showed that the number of xylem vessels (diameter $>$ 50 μm) were significantly greater under HT than that under CT (**Figures 1D,E**), indicating that higher temperatures under positive DIF promote stem elongation, stem thickening, and vascular development in tomato seedlings.

Negative DIF Inhibits Stem Elongation, but Maintains Promotion of Stem Thickening

To examine the effect of negative DIF on tomato seedling growth, tomato seedlings were grown under HT (30°C/25°C, positive DIF) or with night and day temperatures reversed (25°C/30°C, negative DIF) (**Supplementary Figures 1B,C**). Under the negative DIF treatment, temperature-dependent stem elongation was inhibited both in the hypocotyl and epicotyl (**Figures 2A,B**). The difference in hypocotyl and epicotyl elongation between DIF treatments could be detected from 3 d after the onset of the treatments, and it became significant at 5 d (**Supplementary Figures 2A–C**). Conversely, hypocotyl and epicotyl thickness were similar under both DIF treatments (**Figure 2C** and **Supplementary Figures 2D,E**). The number of xylem vessels (diameter $>$ 50 μm) was also similar (**Figures 2D,E**), indicating that the negative DIF treatment inhibited stem elongation without any negative effect on stem thickening. The size of cotyledons and true leaves was also similar under both treatments (**Supplementary Figure 2F**).

To determine whether these responses were cultivar-specific, we tested the effect of the same DIF treatments on four other tomato cultivars. Similar to Managua RZ, the negative DIF treatment decreased stem length in all four tomato cultivars,

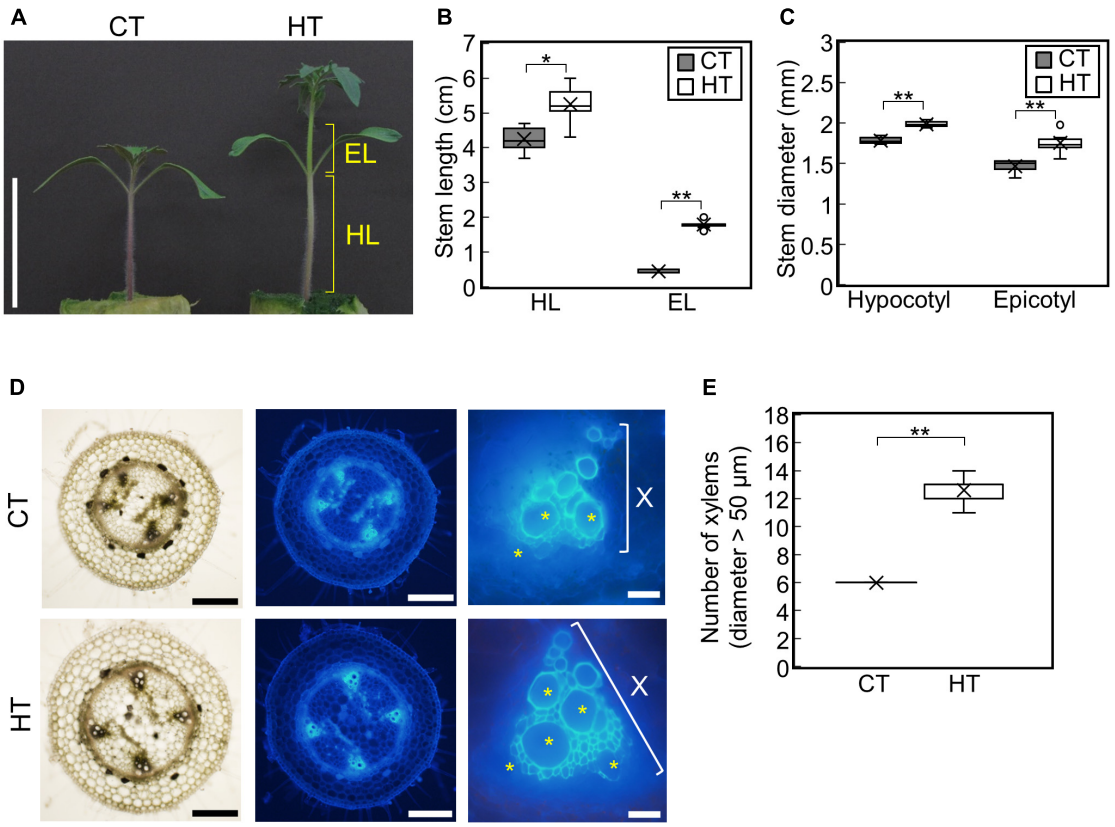

FIGURE 1 | Effect of temperature on growth of tomato seedlings. Young tomato seedlings were grown for 7 days under 25°C/20°C (control temperature) and 30°C/25°C (high temperature). **(A)**, Growth of seedlings. Tomato seedlings were photographed at 7 days. Scale bar = 5 cm. **(B)**, Hypocotyl and epicotyl length. **(C)**, Hypocotyl and epicotyl diameter. Data are shown as boxplots (n = 7). **(D)**, Cross sections of hypocotyls. Asterisks indicate xylems (diameter > 50 μm). Scale bars = 500 μm (left and middle panels) and 50 μm (right panels). **(E)**, Number of xylems (diameter > 50 μm) in the cross section. Data are shown as boxplots (n = 5). Cross marks in boxplot indicate the mean values. *P < 0.01; **P < 0.001 (Student's t test). CT, control temperature; HT, high temperature; HL, hypocotyl length; EL, epicotyl length; X, xylem area.

but it did not affect stem thickness (**Supplementary Figure 3**). This suggests that the growth responses observed are a common feature among tomato seedlings.

Negative DIF Affects Gene Expression

To examine the mechanisms underlying stem growth regulation under the DIF treatments, we analyzed epicotyl transcriptomes in seedlings grown under positive or negative DIF for 7 d (**Supplementary Figures 1B,C**) and explored differentially expressed genes (DEGs). Microarray analysis revealed more than 5000 DEGs, with some upregulated and downregulated by negative DIF treatment (**Figure 3A**). We performed gene ontology (GO) analysis using the top 300 upregulated and downregulated genes (P < 0.05) (**Supplementary Tables 1, 2**). Enriched GO terms in biological process were found in cell wall macromolecule catabolic/metabolic process and (programmed) cell death (**Figure 3B**). Since stem elongation is related to cell wall modification, we focused on cell wall-related genes for further analyses. In addition, hormone-related genes could be involved in temperature-dependent regulation of epicotyl elongation; consequently, GA and IAA-related genes were also included in further analyses. In total, seven DEGs associated with the cell wall, GA, and IAA, as well as a *PIF4* homolog possibly related to temperature-dependent hypocotyl elongation, were chosen for further analyses (**Figure 3C**).

GA and IAA Biosynthesis Genes Were Downregulated in Stems Under the Negative DIF Treatment

Among the identified DEGs, a key gene of *de novo* GA biosynthesis, namely *GA20-oxidase* (*SlGA20ox1*: Solyc03g006880), was downregulated (**Figure 3C**). Using reverse transcriptase real-time PCR, we confirmed that the expression of *SlGA20ox1* was significantly downregulated in both hypocotyls and epicotyls under the negative DIF treatment (**Figure 4A**). The following genes involved in IAA biosynthesis were also among the downregulated DEGs: *YUCCA (YUC)*, which encodes a flavin monooxygenase-like enzyme; *TRYPTOPHAN AMINOTRANSFERASE OF ARABIDOPSIS (TAA)*; and IAA responsive factor *SMALL AUXIN UP RNA (SAUR)* (**Figure 3C**). Our reverse transcriptase real-time PCR

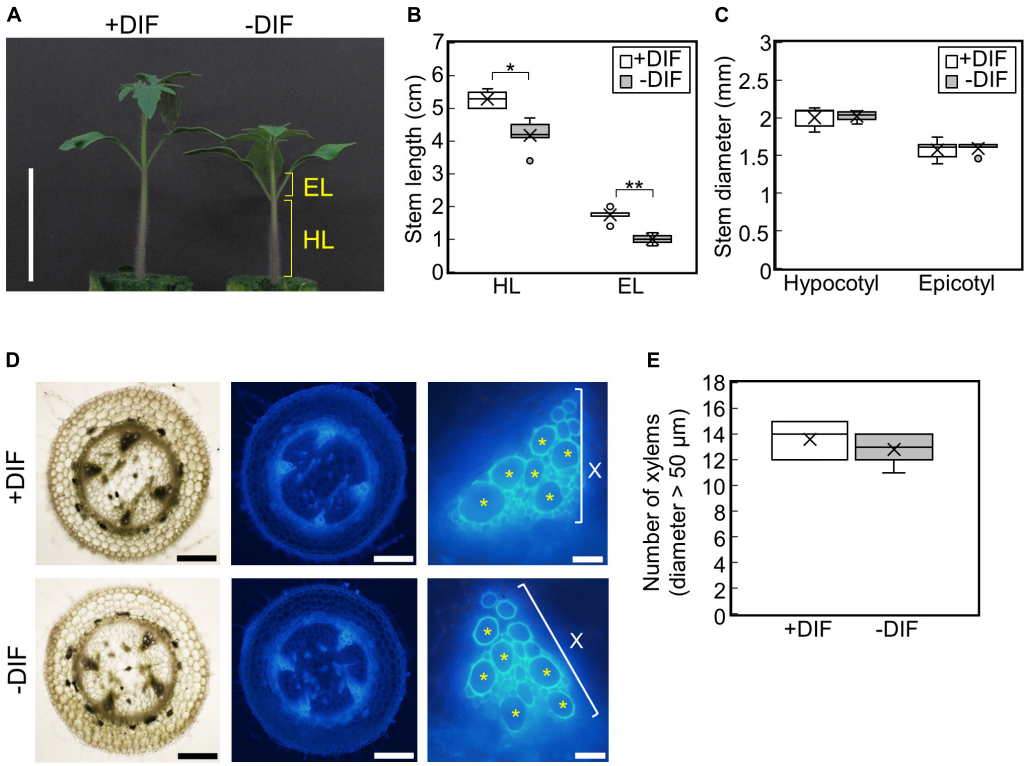

FIGURE 2 | Effect of DIF treatment on growth of tomato seedlings. Young tomato seedlings were grown for 7 days under 30°C/25°C (positive DIF) and 25°C/30°C (negative DIF). **(A)**, Growth of seedlings. Seedlings of tomato were photographed at 7 days. Scale bar = 5 cm. **(B)**, Hypocotyl and epicotyl length. **(C)**, Hypocotyl and epicotyl diameter. Data are shown as boxplots ($n = 5$). **(D)**, Cross sections of hypocotyls. Asterisks indicate xylems (diameter > 50 μm). Scale bars = 500 μm (left and middle panels) and 50 μm (right panels). **(E)**, Number of xylems (diameter > 50 μm) in the cross section. Data are shown as boxplots ($n = 5$). Cross marks in boxplot indicate the mean values. $^*P < 0.01$; $^{**}P < 0.001$ (Student's *t* test). +DIF, positive DIF; -DIF, negative DIF; HL, hypocotyl length; EL, epicotyl length; X, xylem area.

analysis confirmed that *SlTAA1* (Solyc05g031600) and *SlYUC* (Solyc08g068160) were downregulated in tomato epicotyl tissues under the negative DIF treatment (**Figures 4B,C**). *SlSAUR47* (Solyc04g053000) was significantly downregulated in both hypocotyl and epicotyl tissues under the negative DIF treatment (**Figure 4D**).

Cell Wall Modification Genes Were Downregulated in Stems Under the Negative DIF Treatment

In our transcriptome analysis, *expansins* (*SlEXP2*; Solyc06g049050 and *SlEXP1*; Solyc06g051800) and *Xyloglucan endotransglucosylase/hydrolase* (*SlXTH2*; Solyc07g009380) were downregulated (**Figure 3C**). Our reverse transcriptase real-time PCR analysis revealed that *SlEXP2* and *SlXTH2* were significantly downregulated in both hypocotyls and epicotyls under the negative DIF treatment (**Figures 4E,G**). *SlEXP1* was also downregulated in epicotyls under the negative DIF treatment (**Figure 4F**). These results are in line with the negative DIF treatment-driven repression of stem elongation.

We further examined the expression of *PIF4*, but the expression of *SlPIF4* (Solyc07g043580), a homolog of *A. thaliana PIF4*, was not affected by DIF treatment (**Figure 4H**).

Higher Temperatures Under Positive DIF Upregulate Genes for GA and IAA Biosynthesis, as Well as Cell Wall Modification in Epicotyls

We next examined the expression of the DEGs under the CT (25°C/20°C) and HT (30°C/25°C) positive DIF treatments (**Supplementary Figures 1A,B**) using reverse transcriptase real-time PCR. *SlGA20ox1*, *SlYUC*, *SlEXP2*, and *SlXTH2* were upregulated in epicotyls under the HT treatment (**Figures 5A,C,E,G**). *SlSAUR47* and *SlEXP1* were also upregulated in both hypocotyls and epicotyls under the HT treatment (**Figures 5D,F**). These results are consistent with the positive DIF treatment-driven promotion of stem elongation. In addition, *SlPIF4* was upregulated in epicotyls under the HT treatment (**Figure 5H**).

Phytohormone Concentrations Are Consistent With Stem Elongation and Gene Expression Patterns in Response to DIF Treatments

We further investigated the effect of growth temperature on phytohormone concentrations in hypocotyls and epicotyls

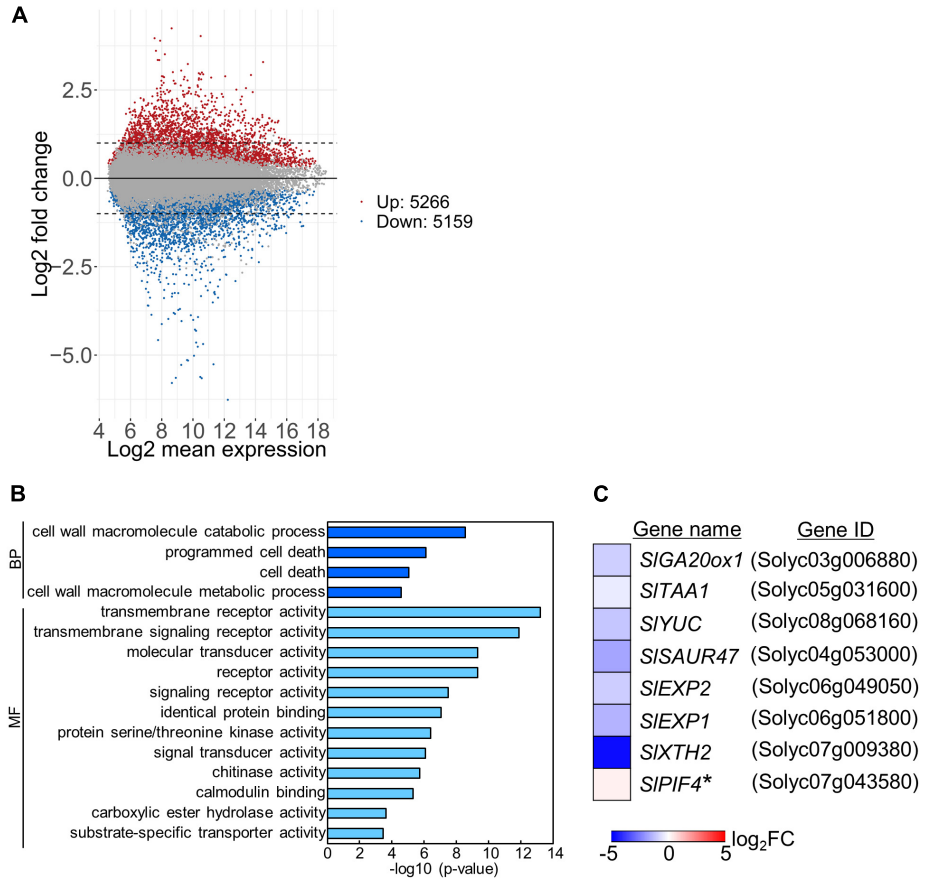

FIGURE 3 | Transcriptome analysis of tomato under positive and negative DIF treatments. Total RNA was extracted from epicotyls of tomato seedlings grown for 7 days under positive DIF and negative DIF and subjected to microarray analysis with three biological replicates. **(A)**, MA plots of microarray data in the positive DIF and negative DIF treatments. Red and blue dots represent genes upregulated (Up: 5266 genes) and downregulated (Down: 5159), respectively, under negative DIF in comparison with positive DIF. Gray dots represent genes that did not significantly differ between DIF treatments. **(B)**, GO terms enriched among the DEGs (top 300 upregulated and top 300 downregulated genes; $P < 0.05$) identified. **(C)**, List of 8 genes associated with stem elongation. The relative expression level of each gene under negative DIF compared with that under positive DIF is shown on the heatmap, which represents the $\log_2$ fold-change (FC). The color scale is shown at the bottom. +DIF, positive DIF; -DIF, negative DIF; BP, Biological Process; MF, Molecular Function.

(**Figure 6**). Under positive and negative DIF treatments, GA_1 and GA_4, bioactive forms, could only be quantified in epicotyls under the positive DIF treatment, whereas they were below the quantification limit in all other tissues (**Figures 6A,B**). Another bioactive form, GA_7, was also below the quantification limit (**Figure 6C**). The concentrations of the precursors, including GA_9, GA_{19}, GA_{20}, GA_{24}, and GA_{44}, were lower in hypocotyls or epicotyls, while that of GA_{53} was higher, under the negative DIF treatment compared with those under the positive DIF treatment (**Figures 6D,F–J**).

When we analyzed hormone species under the CT and HT positive DIF treatments (**Figure 7**), GA_1 and GA_4 were only detected in epicotyls under the HT treatment (**Figures 7A,B**). Concentrations of the inactive precursors GA_{15}, GA_{24}, and GA_{44} in epicotyls were higher under the HT treatment than those under the CT treatment (**Figures 7E,H,I**). Conversely, concentrations of GA_{53} were lower under the HT treatment those under the CT treatment (**Figure 7J**). These patterns were opposite to the changes that occurred following negative DIF treatment (**Figure 6**).

IAA concentrations in negative DIF-treated hypocotyls and epicotyls were slightly but significantly lower than those in positive DIF-treated tissues (**Figure 6K**). In contrast, the concentrations of IAA in hypocotyls and epicotyls were higher under HT than those under CT (**Figure 7K**). These results were consistent with the expression pattern of IAA biosynthesis and signaling genes (**Figures 4**, **5**).

We also quantified the concentration of cytokinins (CKs) because the involvement of this hormone in vascular development is well-documented (Kieber and Schaller, 2014). Several N^6-(Δ^2-isopentenyl) adenine (iP)-type and *trans*-zeatin-type (tZ-type) species had higher concentrations in negative DIF-treated epicotyls than positive DIF-treated epicotyls (**Supplementary Figure 4**). Conversely, an opposite effect was found under the CT and HT treatments (**Supplementary Figure 5**).

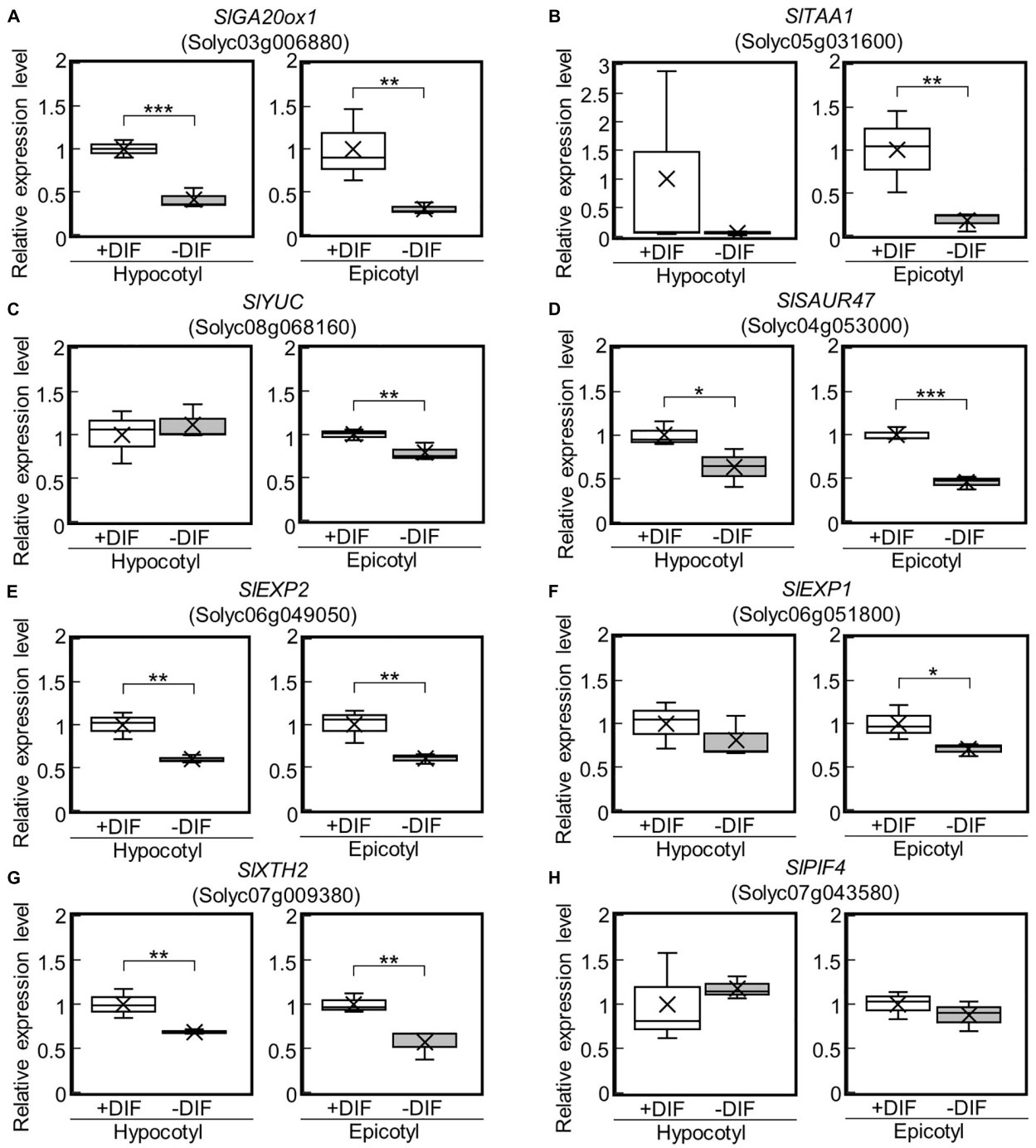

FIGURE 4 | Expression of GA-, IAA-, and cell wall-related genes in epicotyls and hypocotyls under negative and positive DIF treatments. The expression of *SlGA20ox1* **(A)**, IAA-related genes (*SlTAA1*, *SlYUC*, *SlSAUR47*) **(B–D)**, cell wall-related genes (*SlEXP2*, *SlEXP1*, *SlXTH2*) **(E–G)**, and *SlPIF4* **(H)** in epicotyls and hypocotyls grown under positive and negative DIF treatments were analyzed using reverse transcriptase real-time PCR. Data are shown as boxplots ($n = 3$). Cross marks in boxplot indicate the mean values. $^{*}P < 0.1$; $^{**}P < 0.05$; $^{***}P < 0.01$ (Student's *t* test). +DIF, positive DIF; -DIF, negative DIF.

DISCUSSION

In this study, we demonstrated that DT and NT affect stem growth in tomato seedlings, and that this is possibly mediated by the regulation of GA-, IAA-, and cell wall-related genes. Under the positive DIF treatment, higher temperatures promoted stem elongation, and this was accompanied by the upregulation of GA and IAA synthesis genes, resulting in higher concentrations of their active forms. Conversely, negative DIF inhibited stem elongation, which was accompanied by the downregulation of

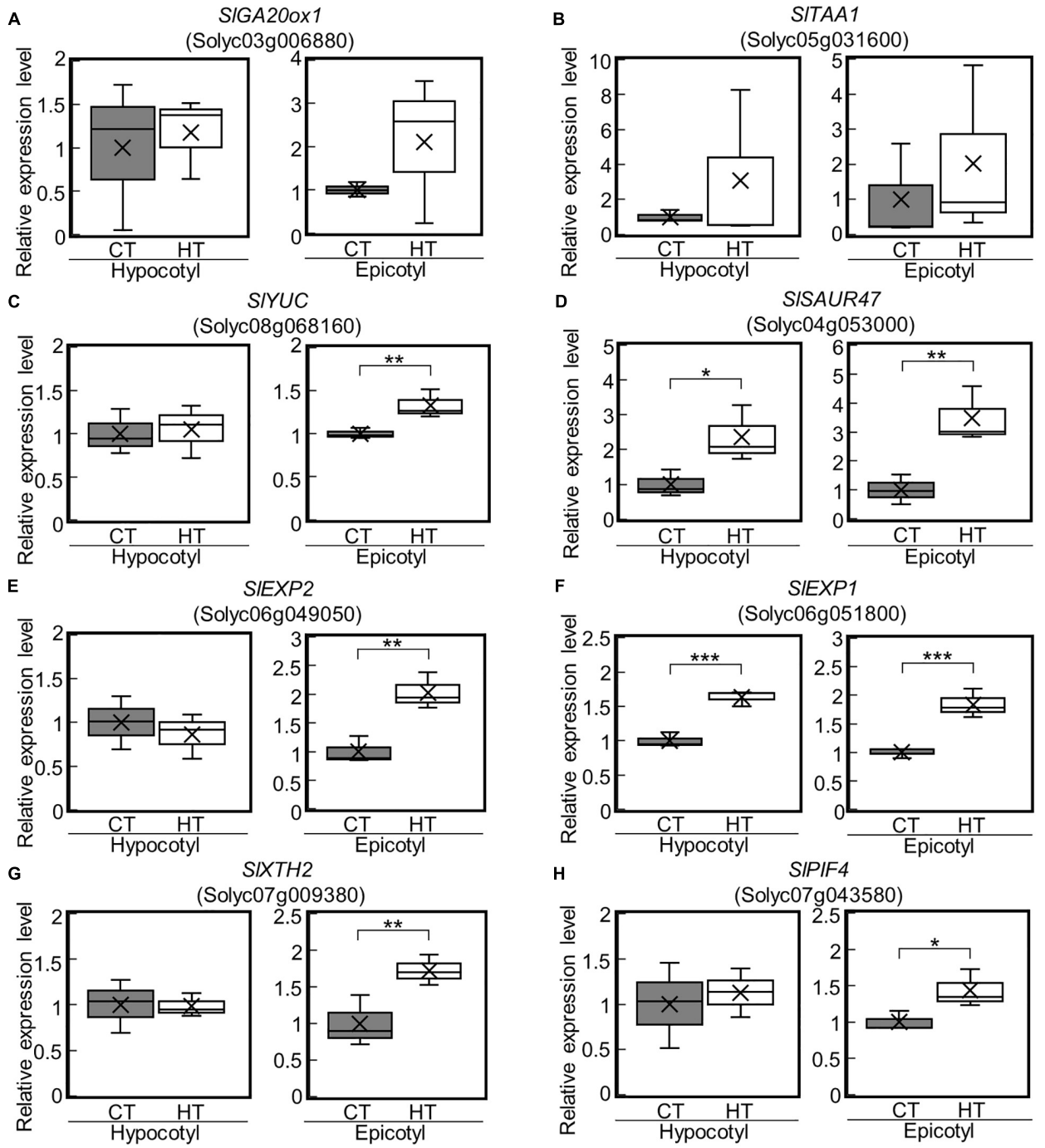

FIGURE 5 | Expression of GA-, IAA-, and cell wall-related genes in epicotyls and hypocotyls under two different temperatures. The expression of *SlGA20ox1* **(A)**, IAA-related genes (*SlTAA1*, *SlYUC*, *SlSAUR47*) **(B–D)**, cell wall-related genes (*SlEXP2*, *SlEXP1*, *SlXTH2*) **(E–G)**, and *SlPIF4* **(H)** in epicotyls and hypocotyls grown under control and high temperatures were analyzed by reverse transcriptase real-time PCR. Data are shown as boxplots ($n = 3$). Cross marks in boxplot indicate the mean values. $^{*}P < 0.1$; $^{**}P < 0.05$; $^{***}P < 0.01$ (Student's *t* test). CT, control temperature; HT, high temperature.

GA and IAA synthesis genes and decrease in GA and IAA concentrations. Although numerous studies have investigated plant growth regulation in response to temperature, our study provides information about possible mechanisms regulating stem growth under DIF treatments.

Under the negative DIF treatment, the concentrations of GA_1, GA_4, and some GA precursors were lower, whereas those of GA_{53} were higher, compared with those under positive DIF treatment. Furthermore, the expression of *SlGA20ox1* was downregulated under the negative DIF treatment. In contrast,

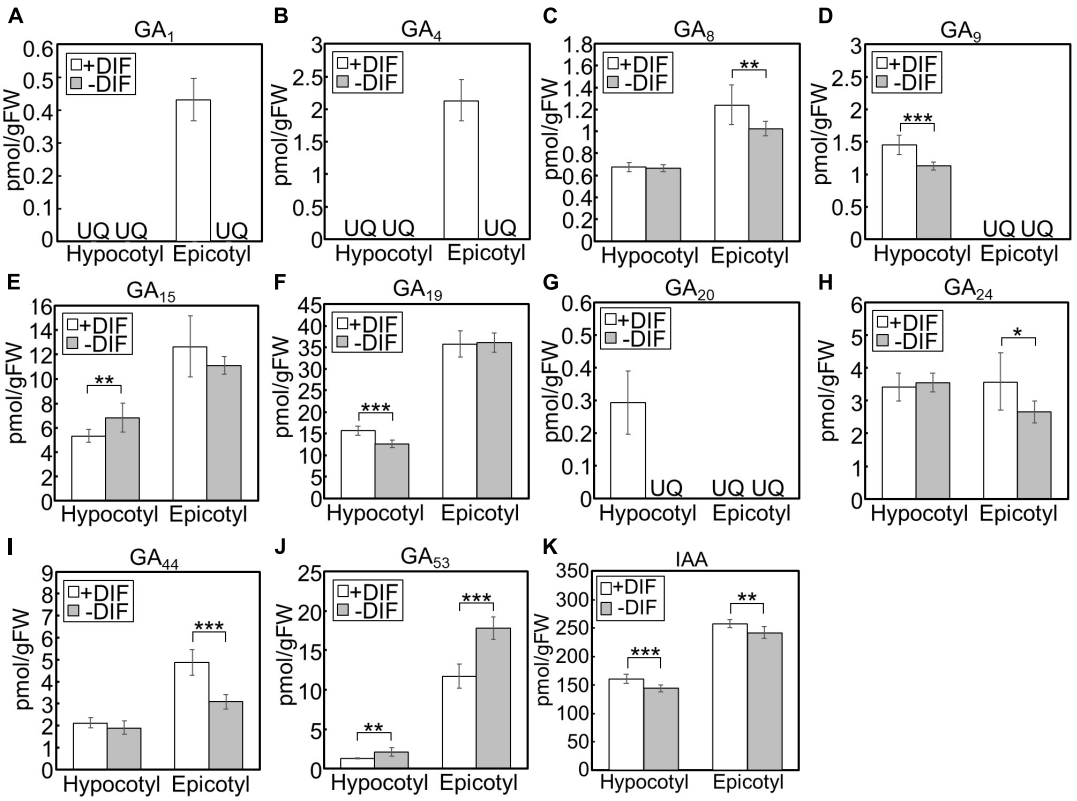

FIGURE 6 | GA and IAA concentration in hypocotyls and epicotyls under negative and positive DIF treatments. Hypocotyls and epicotyls of tomato seedlings grown for 7 days under positive and negative DIF treatments were harvested and subjected to hormone analysis. The concentrations of GAs **(A–J)** and IAA **(K)** were quantified using liquid chromatography-tandem mass spectrometry. Data are represented as mean ± SD (n = 4 or 5). *$P < 0.1$; **$P < 0.05$; ***$P < 0.01$ (Student's t test). GA_7 and GA_{12} were below the quantification limit. +DIF, positive DIF; -DIF, negative DIF; FW, fresh weight; UQ, under quantification limit.

under the positive DIF treatment (i.e., higher temperatures), upregulation of *SlGA20ox1* was observed and this treatment had the opposite effect on the profile of GA_1, GA_4 and the precursors, compared to that of the negative DIF treatment. Since *GA20ox* catalyzes the following multi-step reactions: $GA_{12}/GA_{53} \rightarrow GA_{15}/GA_{44} \rightarrow GA_{24}/GA_{19} \rightarrow GA_9/GA_{20}$, these results were consistent with the downregulation or upregulation of *SlGA20ox1* expression. In addition, as GA_8 is the inactivated form of GA_1, lower GA_8 concentrations in negative DIF-treated epicotyls supported weakened GA activity. *GA20ox* plays a key role in the GA biosynthesis pathway and affects bioactive GA content (Yamaguchi, 2008). In *A. thaliana*, the over-expression of *GA20ox* enhances hypocotyl elongation (Huang et al., 1998; Coles et al., 1999; Ferrero et al., 2019), and the expression of *GA20ox* (*GA20ox1*) is upregulated by high temperatures in hypocotyls (Stavang et al., 2009). Thus, it is suggested that *SlGA20ox1* plays a key role in regulating stem elongation in tomato seedlings in response to different DIF conditions.

IAA is involved in thermomorphogenesis, such as stem elongation, in response to higher temperatures (Quint et al., 2016). In *A. thaliana* hypocotyls, high temperatures induce the expression of *YUC*, *TAA* and *SAUR,* which facilitates stem elongation (Stavang et al., 2009; Franklin et al., 2011). In our analysis, these homologs were downregulated under the negative DIF treatment and upregulated under the high temperature positive DIF treatment, suggesting that these IAA-related genes also play a role in regulating stem elongation in tomato in response to temperature conditions.

Expression patterns of the cell wall-related genes *SlEXP1*, *SlEXP2*, and *SlXTH2* were correlated with GA- and IAA-biosynthesis genes. EXPs are cell wall loosening proteins, which cause cell wall expansion (Marowa et al., 2016). Previous studies have shown that *EXPs* are involved in stem elongation of *Oryza sativa* (Cho and Kende, 1997a,b; Lee and Kende, 2001, 2002; Choi et al., 2003; Zou et al., 2015) and respond to GA (Cho and Kende, 1997b; Lee and Kende, 2001, 2002). *EXP1* has been found to be regulated by temperature in *Agrostis scabra* and *Agrostis stolonifera* (Xu et al., 2007). XTH catalyzes Xyloglucan endohydrolysis and endotransglycosylation, which is involved in the modification of cell wall structures (Rose et al., 2002). It has also been reported that *EXPs* and *XTHs* are regulated by IAA (Goda et al., 2004; Majda and Robert, 2018; Lehman and Sanguinet, 2019). The response of cell wall-related genes to temperature might be mediated by GA and/or IAA action in tomato seedlings.

Previous studies investigating the molecular mechanisms behind temperature acclimation in *A. thaliana* identified PIF4 as a key regulator (Proveniers and van Zanten, 2013;

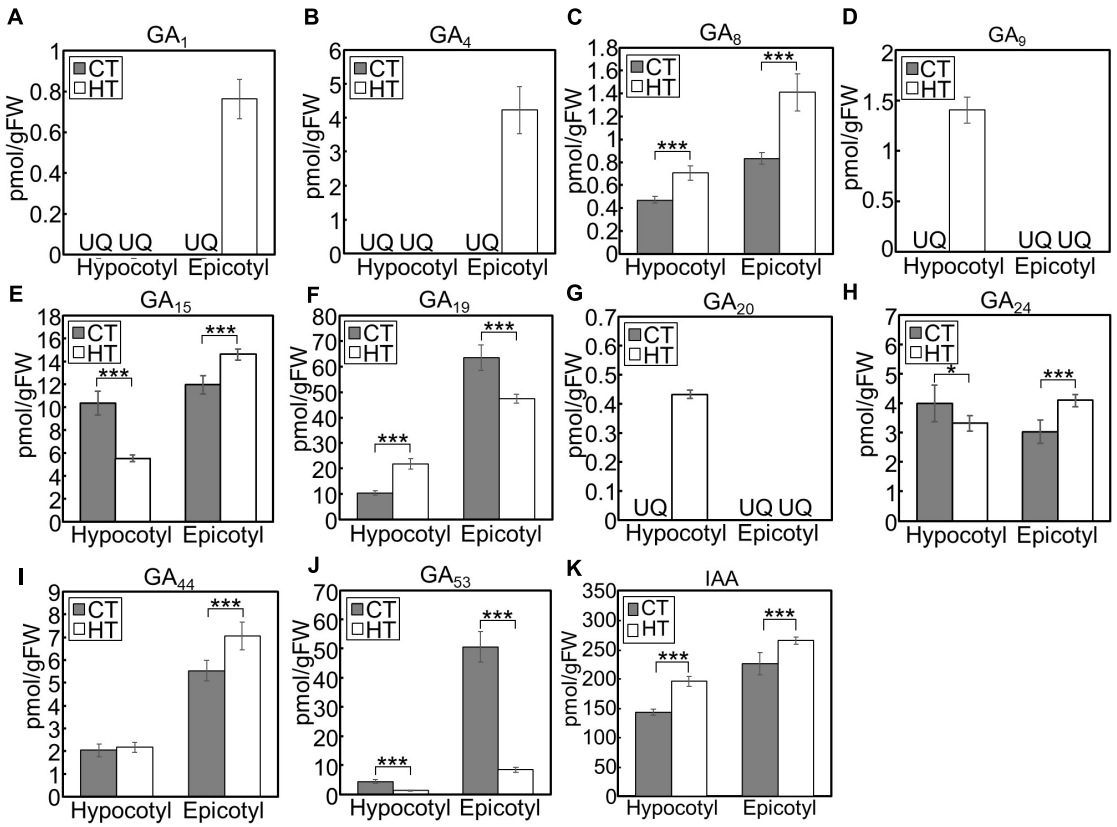

FIGURE 7 | GA and IAA concentration in hypocotyls and epicotyls under two different temperatures. Hypocotyls and epicotyls of tomato seedlings grown for 7 days under control and high temperatures were harvested and subjected to hormone analysis. The concentrations of GAs **(A–J)** and IAA **(K)** were quantified using liquid chromatography-tandem mass spectrometry. Data are represented as mean ± SD (n = 4 or 5). $^{*}P < 0.1$; $^{***}P < 0.01$ (Student's t test). GA_7 and GA_{12} were below the quantification limit. CT, control temperature; HT, high temperature; FW, fresh weight; UQ, under quantification limit.

de Wit et al., 2014; Quint et al., 2016). Expression of *PIF4* was upregulated by high temperatures and was found to control GA and IAA biosynthesis and signaling (Koini et al., 2009; Stavang et al., 2009; Franklin et al., 2011; Sun et al., 2012). In our experiment, *SlPIF4* was upregulated in epicotyls under the high temperature positive DIF treatment, suggesting that similar regulatory systems are employed in tomato seedlings. Conversely, *SlPIF4* expression was not affected by the negative DIF treatment. The role of PIF4 in the regulation of stem elongation under negative DIF remains to be clarified. Future studies should focus on constructing a loss-of-function mutant to help understand its role.

Stem thickness and vessel development did not differ significantly between the negative and positive DIF treatments. Limited studies have reported the effect of temperature on stem thickness and vessel development. Among the phytohormones, CKs play an important role in vascular development (Kieber and Schaller, 2014). In a cytokinin biosynthesis mutant of *A. thaliana*, stem thickness and the number of xylems were significantly decreased (Matsumoto-Kitano et al., 2008). Another recent study suggests that CK is involved in the variation in xylem development in Dutch and Japanese tomato cultivars (Qi et al., 2020). However, in our experimental conditions, the concentration of endogenous cytokinin was increased in the negative DIF and decreased in the positive DIF treatments, suggesting that CK plays a minor role in the regulation of xylem development under these DIF treatments. Further analysis is needed to elucidate the mechanisms underlying temperature-dependent regulation of stem thickness and xylem development.

It is believed that the quality of seedlings greatly affects the final agricultural yield. Our results show that short-term negative DIF treatment can control plant height without affecting stem thickness. This might be an effective technique for growing tomatoes in nurseries. Since stem thickening is accompanied by vascular development, it may give a positive effect on mineral transport, the partition of assimilates, and fruit growth. Findings in this study would shed light on mechanisms of possible new agricultural practices.

MATERIALS AND METHODS

Plant Materials and Growth Conditions

The tomato (*S. lycopersicum*) cultivar used in this study was Managua RZ (RIJK ZWAAN, Netherlands), except for the

growth comparison of tomato cultivars under DIF treatments (**Supplementary Figure 3**). In the comparison experiment, we used CF Momotaro-York and Daiki B Baria (Takii Seed, Kyoto, Japan), and Rinka and Reiyo (Sakata Seed, Kanagawa, Japan).

Tomato seeds were imbibed in water in a petri dish at 28°C in the dark for 2 d. After imbibition, germinated seeds were transferred to a wet rockwool block (Nippon Rockwool Corporation, Japan) and were grown at 23°C/23°C (DT/NT, 16 h photoperiod) under 130 to 140 μmol photons m^{-2} s^{-1} of fluorescent illumination for 5–6 d. Next, the young seedlings, whose cotyledons were fully opened, were further grown on the rockwool block with liquid culture medium under the following two temperature-condition pairs: 25°C/20°C and 30°C/25°C, or 30°C/25°C and 25°C/30°C (DT/NT, 16 h photoperiod) under 300 μmol photons m^{-2} s^{-1} of light for 7 d (**Supplementary Figure S1**). The liquid culture medium contained nutrients at the following concentrations: 5 mM KNO_3, 1 mM $NH_4H_2PO_4$, 0.5 mM $MgSO_4$, 5.5 mM $Ca(NO_3)_2$, 27 μM Fe-EDTA, 25 μM KCl, 10 μM H_3BO_3, 1 μM $MnSO_4$, 1 μM $ZnSO_4$, 0.25 μM $CuSO_4$, and 0.04 μM Na_2MoO_4.

Fluorescent Observation of Xylem

The middle section of the tomato seedling hypocotyls was harvested and fixed in a 4% paraformaldehyde phosphate buffer solution (Nacalai Tesque, Kyoto, Japan). The fixed hypocotyls were thinly sliced (∼0.5 mm) with a razor blade, and cross sections were observed with fluorescence microscopy (Mirror unit with U-FUW, Olympus BX53, Olympus, Japan). The diameter of vessels was measured using the ImageJ software (Abramoff et al., 2004).

GA, IAA, and CK Quantification

Phytohormones were extracted and semi-purified as previously described (Kojima et al., 2009; Kojima and Sakakibara, 2012). CKs were quantified using an ultra-performance liquid chromatography (UPLC)-electrospray interface (ESI) tandem quadrupole mass spectrometer (qMS/MS) (AQUITY UPLC™ System/Xevo-TQS; Waters, Milford, MA, United States) as described previously (Kojima et al., 2009) with an ODS column (AQUITY UPLC HSS T3, 1.8mm, 2.1 x 100 mm; Waters). IAA and GAs were quantified using an ultra-high performance liquid chromatography (UHPLC)-ESI quadrupole-orbitrap mass spectrometer (UHPLC/Q-Exactive™; Thermo Fisher Scientific, United States) as described previously (Kojima and Sakakibara, 2012; Shinozaki et al., 2015) with an ODS column (AQUITY UPLC HSS T3, 1.8mm, 2.1 x 100 mm; Waters).

RNA Extraction

Hypocotyls and epicotyls were frozen in liquid nitrogen and ground to a fine powder with a mortar and pestle. Total RNA was extracted using an RNeasy Mini kit with an RNase-Free DNase Set (Cat. No. 74104/79254, Qiagen, Hilden, Germany). The RNA in samples was quantified using a NanoDrop-1000 spectrophotometer and the quality was monitored using an Agilent 2100 Bioanalyzer (Agilent Technologies, Santa Clara, CA, United States).

Microarray and Data Analysis

Total RNA was extracted from epicotyls of young seedlings grown for 7 d under 30°C/25°C (positive DIF) and 25°C/30°C (negative DIF) (DT/NT, 16 h photoperiod) as described in the preceding subsection. Three biological replicates were used for microarray analysis. Target labeling was performed according to the manual of the Low Input Quick Amp Labeling Kit, One-Color (Agilent Technologies). We used a tomato custom-designed microarray (platform ID "GPL21511"). Hybridization was performed according to the manufacturer's instructions. We scanned the microarray images using an Agilent DNA Microarray Scanner G2565CA (Agilent Technologies). Scanned images were converted to signal data using Feature Extraction software (Agilent Technologies). Value definition in the data matrix was Log2. GO enrichment analysis among DEGs (top 300 upregulated and top 300 downregulated genes; $P < 0.05$) was performed using the GO Analysis Toolkit and Database for Agricultural Community (AgriGO, http://systemsbiology.cau.edu.cn/agriGOv2/) (Tian et al., 2017).

Reverse Transcriptase Real-time PCR

First-strand cDNA was synthesized using SuperScript™ III First-Strand Synthesis SuperMix (Invitrogen, Waltham, MA, United States). Real-time PCR was performed using a StepOnePlus Real Time PCR system (Applied Biosystems, Waltham, MA, United States) and a KAPA SYBR FAST qPCR Master Mix (2×) Kit (Kapa Biosystems, London, United Kingdom) under the following conditions: 95°C for 3 min; followed by 40 cycles of 95°C for 3 s and 60°C for 20 s. Gene expression was calculated using the ΔΔCT method and normalized to that of the ubiquitin homolog as the housekeeping gene (Solyc01g056940). The following primers were used: for the housekeeping gene (Solyc01g056940), forward primer 5′-CG TGGTGGTGCTAAGAAGAG-3′, reverse primer 5′-ACGAAG CCTCTGAACCTTTC-3′; for *SlGA20ox1* (Solyc03g006880), forward primer 5′-TGGCGTTCCATCAGTCCAAA-3′, reverse primer 5′-TTCGAGGGTTGTTGGAGTCC-3′; for *SlTAA1* (Solyc05g031600), forward primer 5′-TGAAGCACACCCTGC ATTTG-3′, reverse primer 5′-ACTTCCAAATCTTCTTCCACT CCTT-3′; for *SlYUC* (Solyc08g068160), forward primer 5′-GC CCTCGTGGCTAAAGGAA-3′, reverse primer 5′-CCACTGCA TAAAGTCCACACTCTC-3′; for *SlSAUR47* (Solyc04g053000), forward primer 5′-GAAGAACAGTTTGGCTTCGATTAC-3′, reverse primer 5′-CGGTATGTGAGATCAACAAACA-3′; for *SlEXP2* (Solyc06g049050), forward primer 5′-TTCGAAGGGTG CCCTGTAT-3′, reverse primer 5′-TGAATATCACCAGCAC CTCCA-3′; for *SlEXP1* (Solyc06g051800), forward primer 5′-CGCTGGCATTGTTCCTGT-3′, reverse primer 5′-CTGC ACCTGCTACATTCGTG-3′; for *SlXTH2* (Solyc07g009380), forward primer 5′-TATGCACAAGGCAAGGGAGA-3′, reverse primer 5′-TGTATTGTCTTATTGGTGTCCCATC-3′; for *SlPIF4* (Solyc07g043580), forward primer 5′-ATCAAGCAGCTGCAAT GTGC-3′, reverse primer 5′-CTGCTGAGTTTGCTGTGCTG-3′.

DATA AVAILABILITY STATEMENT

Microarray data have been deposited in the National Center for Biotechnology Information Gene Expression Omnibus (NCBI GEO) database under accession number GSE131496.

AUTHOR CONTRIBUTIONS

KO, AY, SI, and HS designed research. KO, AY, YK, KF, MK, YT, and KY performed research. KO and YK analyzed the data. KO and HS wrote the manuscript. All authors contributed to the article and approved the submitted version.

FUNDING

This research was supported by the Cross-ministerial Strategic Innovation Promotion Program (SIP) and partially by JSPS KAKENHI Grant Number JP19H05462.

ACKNOWLEDGMENTS

We thank Momo Okumura, Mayumi Tanigawa, and Mizuki Yamada for their advice on tomato cultivation. Microarray analysis was assisted by the National Agriculture and Food Research Organization (NARO).

SUPPLEMENTARY MATERIAL

The Supplementary Material for this article can be found online at: https://www.frontiersin.org/articles/10.3389/fpls.2020.577235/full#supplementary-material

Supplementary Figure 1 | Schematic representation of growth conditions in the study. **(A)** Control temperature treatment, 25°C/20°C (DT/NT). **(B)** High temperature/positive DIF treatment, 30°C/25°C (DT/NT). **(C)** Negative DIF treatment, 25°C/30°C (DT/NT). Young tomato seedlings were grown for 7 days under each condition. White bars show the light period, black bars show the dark period, and red arrowheads show the sampling time for the experiments. Further details are explained in the Materials and Methods.

Supplementary Figure 2 | Growth of tomato plants under negative and positive DIF treatments. Young tomato seedlings were grown for 7 days under positive and negative DIF treatments. **(A)** Growth of seedlings. Seedlings of tomato were photographed at 0, 1, 3, 5, and 7 days. Scale bars = 5 cm. **(B,C)** Hypocotyl and epicotyl length, respectively. **(D,E)** Hypocotyl and epicotyl diameters, respectively. **(F)** Cotyledons and true leaves photographed at 7 days after onset of DIF treatments. Scale bars = 5 cm. Data are represented as mean ± SD (n = 3 or 4). $^{*}P < 0.05$; $^{**}P < 0.01$ (Student's t test). +DIF, positive DIF; -DIF, negative DIF.

Supplementary Figure 3 | Growth comparison of five tomato cultivars under DIF treatments. Seedlings of five tomato cultivars, Daiki B baria (DaikiB), Rinka, CF momotaro-york (CFMY), Managua RZ (MA), and Reiyo (RYO) were grown for 7 days under positive and negative DIF. **(A)** Growth of seedlings. Seedlings of tomato were photographed at 7 days. Scale bars = 5 cm. **(B,C)** Hypocotyl and epicotyl length, respectively. **(D,E)** Hypocotyl and epicotyl diameter, respectively. Data are shown as boxplots (n = 3). Cross marks in boxplot indicate the mean values. $^{*}P < 0.05$; $^{**}P < 0.01$ (Student's t test). +DIF, positive DIF; -DIF, negative DIF.

Supplementary Figure 4 | Concentration of CKs in hypocotyls and epicotyls under positive and negative DIF treatments. Hypocotyls and epicotyls of tomato seedlings grown for 7 days under positive and negative DIF treatments were harvested and subjected to hormone analysis. The concentration of CKs were quantified using liquid chromatography-tandem mass spectrometry. Data are represented as mean ± SD (n = 3 to 5). tZ, *trans*-zeatin; tZR, tZ riboside; tZRPs, tZR 5′-phosphates; tZ7G, tZ-*7N*-glucoside; tZ9G, tZ-*9N*-glucoside; tZOG, tZ-*O*-glucoside; tZROG, tZR-*O*-glucoside; iP, N^6-(Δ^2-isopentenyl)adenine; iPR, iP riboside; iPRPs, iPR 5′-phosphates; iP7G, iP-*7N*-glucoside; iP9G, iP-*9N*-glucoside. $^{*}P < 0.1$; $^{**}P < 0.05$; $^{***}P < 0.01$ (Student's t test). tZRPOG, tZRP-*O*-glucoside was below the quantification limit. +DIF, positive DIF; -DIF, negative DIF; FW, fresh weight; UQ, under quantification limit.

Supplementary Figure 5 | Concentration of CKs in hypocotyls and epicotyls under two different temperatures. Hypocotyls and epicotyls of tomato seedlings grown for 7 days under control and high temperatures were harvested and subjected to hormone analysis. The concentration of CKs were quantified using liquid chromatography-tandem mass spectrometry. Data are represented as mean ± SD (n = 3 to 5). tZ, *trans*-zeatin; tZR, tZ riboside; tZRPs, tZR 5′-phosphates; tZ7G, tZ-*7N*-glucoside; tZ9G, tZ-*9N*-glucoside; tZOG, tZ-*O*-glucoside; tZROG, tZR-*O*-glucoside; iP, N^6-(Δ^2-isopentenyl)adenine; iPR, iP riboside; iPRPs, iPR 5′-phosphates; iP7G, iP-*7N*-glucoside; iP9G, iP-*9N*-glucoside. $^{*}P < 0.1$; $^{**}P < 0.05$; $^{***}P < 0.01$ (Student's t test). tZRPOG, tZRP-*O*-glucoside was below the quantification limit. CT, control temperature; HT, high temperature; FW, fresh weight; UQ, under quantification limit.

REFERENCES

Abramoff, M. D., Magalhaes, P. J., and Ram, S. J. (2004). Image processing with ImageJ. *Biophoton. Int.* 11, 36–42.

Binenbaum, J., Weinstain, R., and Shani, E. (2018). Gibberellin localization and transport in plants. *Trends Plant Sci.* 23, 410–421. doi: 10.1016/j.tplants.2018.02.005

Cho, H. T., and Kende, H. (1997a). Expansins and internodal growth of deepwater rice. *Plant Physiol.* 113, 1145–1151. doi: 10.1104/pp.113.4.1145

Cho, H. T., and Kende, H. (1997b). Expression of expansin genes is correlated with growth in deepwater rice. *Plant Cell* 9, 1661–1671. doi: 10.1105/tpc.9.9.1661

Choi, D., Lee, Y., Cho, H. T., and Kende, H. (2003). Regulation of expansin gene expression affects growth and development in transgenic rice plants. *Plant Cell* 15, 1386–1398. doi: 10.1105/tpc.011965

Coles, J. P., Phillips, A. L., Croker, S. J., Garcia-Lepe, R., Lewis, M. J., and Hedden, P. (1999). Modification of gibberellin production and plant development in *Arabidopsis* by sense and antisense expression of gibberellin 20-oxidase genes. *Plant J.* 17, 547–556. doi: 10.1046/j.1365-313X.1999.00410.x

Davière, J. M., and Achard, P. (2013). Gibberellin signaling in plants. *Development* 140, 1147–1151. doi: 10.1242/dev.087650

de Koning, A. N. M. (1988). The effect of different day/night temperature regimes on growth, development and yield of glasshouse tomatoes. *J. Hortic. Sci.* 63, 465–471. doi: 10.1080/14620316.1988.11515880

de Wit, M., Lorrain, S., and Fankhauser, C. (2014). Auxin-mediated plant architectural changes in response to shade and high temperature. *Physiol. Plant.* 151, 13–24. doi: 10.1111/ppl.12099

Ferrero, L. V., Viola, I. L., Ariel, F. D., and Gonzalez, D. H. (2019). Class I TCP transcription factors target the gibberellin biosynthesis gene *GA20ox1* and the growth-promoting genes *HBI1* and *PRE6* during thermomorphogenic growth in *Arabidopsis*. *Plant Cell Physiol.* 60, 1633–1645. doi: 10.1093/pcp/pcz137

Franklin, K. A., Lee, S. H., Patel, D., Kumar, S. V., Spartz, A. K., Gu, C., et al. (2011). Phytochrome-interacting factor 4 (PIF4) regulates auxin biosynthesis at high temperature. *Proc. Natl. Acad. Sci. U.S.A.* 108, 20231–20235. doi: 10.1073/pnas.1110682108

Goda, H., Sawa, S., Asami, T., Fujioka, S., Shimada, Y., and Yoshida, S. (2004). Comprehensive comparison of auxin-regulated and brassinosteroid-regulated

genes in Arabidopsis. *Plant Physiol.* 134, 1555–1573. doi: 10.1104/pp.103.034736

Grindal, G., Ernstsen, A., Reid, J. B., Junttila, O., Lindgård, B., and Moe, R. (1998). Endogenous gibberellin A1 levels control thermoperiodic stem elongation in *Pisum sativum*. *Physiol. Plant.* 102, 523–531. doi: 10.1034/j.1399-3054.1998.1020406.x

Hayata, Y., Kotani, K., and Li, X. X. (2001). Effects of day and night temperatures on hypocotyl elongation and endogenous levels of indole-3-acetic and abscisic acids in radish (*Raphaus sativus* L.). *Engei Gakkai Zasshi* 70, 443–447. doi: 10.2503/jjshs.70.443

Huang, S., Raman, A. S., Ream, J. E., Fujiwara, H., Cerny, R. E., and Brown, S. M. (1998). Overexpression of 20-oxidase confers a gibberellin-overproduction phenotype in Arabidopsis. *Plant Physiol.* 118, 773–781. doi: 10.1104/pp.118.3.773

Jensen, E., Eilertsen, S., Ernsten, A., Juntilla, O., and Moe, R. (1996). Thermoperiodic control of stem elongation and endogenous gibberellins in *Campanula isophylla*. *J. Plant Growth Regul.* 15, 167–171. doi: 10.1007/BF00190580

Kieber, J. J., and Schaller, G. E. (2014). Cytokinins. *Arabidopsis Book* 12:e0168. doi: 10.1199/tab.0168

Koini, M. A., Alvey, L., Allen, T., Tilley, C. A., Harberd, N. P., Whitelam, G. C., et al. (2009). High temperature-mediated adaptations in plant architecture require the bHLH transcription factor PIF4. *Curr. Biol.* 19, 408–413. doi: 10.1016/j.cub.2009.01.046

Kojima, M., Kamada-Nobusada, T., Komatsu, H., Takei, K., Kuroha, T., Mizutani, M., et al. (2009). Highly sensitive and high-throughput analysis of plant hormones using MS-probe modification and liquid chromatography-tandem mass spectrometry: an application for hormone profiling in *Oryza sativa*. *Plant Cell Physiol.* 50, 1201–1214. doi: 10.1093/pcp/pcp057

Kojima, M., and Sakakibara, H. (2012). Highly sensitive high-throughput profiling of six phytohormones using MS-probe modification and liquid chromatography-tandem mass spectrometry. *Methods Mol. Biol.* 918, 151–164. doi: 10.1007/978-1-61779-995-2_11

Lee, Y., and Kende, H. (2001). Expression of β-expansins is correlated with internodal elongation in deepwater rice. *Plant Physiol.* 127, 645–654. doi: 10.1104/pp.010345

Lee, Y., and Kende, H. (2002). Expression of α-expansin and expansin-like genes in deepwater rice. *Plant Physiol.* 130, 1396–1405. doi: 10.1104/pp.008888

Lehman, T. A., and Sanguinet, K. A. (2019). Auxin and cell wall crosstalk as revealed by the *Arabidopsis thaliana* cellulose synthase mutant radially swollen 1. *Plant Cell Physiol.* 60, 1487–1503. doi: 10.1093/pcp/pcz055

Leyser, O. (2018). Auxin signaling. *Plant Physiol.* 176, 465–479. doi: 10.1104/pp.17.00765

Majda, M., and Robert, S. (2018). The role of auxin in cell wall expansion. *Int. J. Mol. Sci.* 19:951. doi: 10.3390/ijms19040951

Marowa, P., Ding, A., and Kong, Y. (2016). Expansins: roles in plant growth and potential applications in crop improvement. *Plant Cell Rep.* 35, 949–965. doi: 10.1007/s00299-016-1948-4

Matsumoto-Kitano, M., Kusumoto, T., Tarkowski, P., Kinoshita-Tsujimura, K., Václavíková, K., Miyawaki, K., et al. (2008). Cytokinins are central regulators of cambial activity. *Proc. Natl. Acad. Sci. U.S.A.* 105, 20027–20031. doi: 10.1073/pnas.0805619105

Nomoto, Y., Kubozono, S., Miyachi, M., Yamashino, T., Nakamichi, N., and Mizuno, T. (2012). A circadian clock- and PIF4-mediated double coincidence mechanism is implicated in the thermosensitive photoperiodic control of plant architectures in *Arabidopsis thaliana*. *Plant Cell Physiol.* 53, 1965–1973. doi: 10.1093/pcp/pcs141

Proveniers, M. C., and van Zanten, M. (2013). High temperature acclimation through PIF4 signaling. *Trends Plant Sci.* 18, 59–64. doi: 10.1016/j.tplants.2012.09.002

Qi, X., Takahashi, H., Kawasaki, Y., Ohta, Y., Isozaki, M., Kojima, M., et al. (2020). Differences in xylem development between Dutch and Japanese tomato (*Solanum lycopersicum*) correlate with cytokinin levels in hypocotyls. *Ann. Bot.* 126, 315–322. doi: 10.1093/aob/mcaa094

Quint, M., Delker, C., Franklin, K. A., Wigge, P. A., Halliday, K. J., and Van Zanten, M. (2016). Molecular and genetic control of plant thermomorphogenesis. *Nat. Plants* 2:15190. doi: 10.1038/NPLANTS.2015.19

Rose, J. K. C., Braam, J., Fry, S. C., and Nishitani, K. (2002). The XTH family of enzymes involved in xyloglucan endotransglucosylation and endohydrolysis: current perspectives and a new unifying nomenclature. *Plant Cell Physiol.* 43, 1421–1435. doi: 10.1093/pcp/pcf171

Shimizu, H. (2007). Effect of day and night temperature alternations on plant morphogenesis. *Environ. Control Biol.* 45, 259–265. doi: 10.2525/ecb.45.259

Shinozaki, Y., Hao, S., Kojima, M., Sakakibara, H., Ozeki-Iida, Y., Zheng, Y., et al. (2015). Ethylene suppresses tomato (*Solanum lycopersicum*) fruit set through modification of gibberellin metabolism. *Plant J.* 83, 237–251. doi: 10.1111/tpj.12882

Stavang, J. A., Gallego-Bartolomé, J., Gómez, M. D., Yoshida, S., Asami, T., Olsen, J. E., et al. (2009). Hormonal regulation of temperature-induced growth in Arabidopsis. *Plant J.* 60, 589–601. doi: 10.1111/j.1365-313X.2009.03983.x

Stavang, J. A., Lindgård, B., Erntsen, A., Lid, S. E., Moe, R., and Olsen, J. E. (2005). Thermoperiodic stem elongation involves transcriptional regulation of gibberellin deactivation in pea. *Plant Physiol.* 138, 2344–2353. doi: 10.1104/pp.105.063149

Sun, J., Qi, L., Li, Y., Chu, J., and Li, C. (2012). PIF4-mediated activation of *YUCCA8* expression integrates temperature into the auxin pathway in regulating *Arabidopsis* hypocotyl growth. *PLoS Genet.* 8:e1002594. doi: 10.1371/journal.pgen.1002594

Thingnaes, E., Torre, S., Ernstsen, A., and Moe, R. (2003). Day and night temperature responses in *Arabidopsis*: effects on gibberellin and auxin content, cell size, morphology and flowering time. *Ann. Bot.* 92, 601–612. doi: 10.1093/aob/mcg176

Tian, T., Liu, Y., Yan, H., You, Q., Yi, X., Du, Z., et al. (2017). agriGO v2.0: a GO analysis toolkit for the agricultural community, 2017 update. *Nucleic Acids Res.* 45, W122–W129. doi: 10.1093/nar/gkx382

Went, F. W. (1944). Plant growth under controlled conditions. II. Thermoperiodicity in growth and fruiting of tomato. *Am. J. Bot.* 31, 135–150. doi: 10.2307/2437636

Xu, J., Tian, J., Belanger, F. C., and Huang, B. (2007). Identification and characterization of an expansin gene *AsEXP1* associated with heat tolerance in C3 *Agrostis* grass species. *J. Exp. Bot.* 58, 3789–3796. doi: 10.1093/jxb/erm229

Yamaguchi, S. (2008). Gibberellin metabolism and its regulation. *Annu. Rev. Plant Biol.* 59, 225–251. doi: 10.1146/annurev.arplant.59.032607.092804

Zhao, Y. (2018). Essential roles of local auxin biosynthesis in plant development and in adaptation to environmental changes. *Annu. Rev. Plant Biol.* 29, 417–435. doi: 10.1146/annurev-arplant-042817-040226

Zou, H., Wenwen, Y., Zang, G., Kang, Z., Zhang, Z., Huang, J., et al. (2015). *OsEXPB2*, a β-expansin gene, is involved in rice root system architecture. *Mol. Breed.* 35:41. doi: 10.1007/s11032-015-0203-y

Conflict of Interest: The authors declare that the research was conducted in the absence of any commercial or financial relationships that could be construed as a potential conflict of interest.

frontiers in Plant Science

ORIGINAL RESEARCH
published: 21 December 2020
doi: 10.3389/fpls.2020.607029

Exogenous Calcium Alleviates Nocturnal Chilling-Induced Feedback Inhibition of Photosynthesis by Improving Sink Demand in Peanut (*Arachis hypogaea*)

Di Wu[1], Yifei Liu[1,2,3], Jiayin Pang[2,4], Jean Wan Hong Yong[3,5], Yinglong Chen[2,4], Chunming Bai[2,6], Xiaori Han[1], Xinyue Liu[1], Zhiyu Sun[1], Siwei Zhang[1], Jing Sheng[7], Tianlai Li[1], Kadambot H.M. Siddique[2,4] and Hans Lambers[2,3,8]*

[1]College of Land and Environment, National Key Engineering Laboratory for Efficient Utilization of Soil and Fertilizer Resources, Northeast China Plant Nutrition and Fertilization Scientific Observation and Research Center for Ministry of Agriculture and Rural Affairs, Key Laboratory of Protected Horticulture of Education Ministry and Liaoning Province, Shenyang Agricultural University, Shenyang, China, [2]The UWA Institute of Agriculture, The University of Western Australia, Perth, WA, Australia, [3]School of Biological Sciences, The University of Western Australia, Perth, WA, Australia, [4]School of Agriculture and Environment, The University of Western Australia, Perth, WA, Australia, [5]Department of Biosystems and Technology, Swedish University of Agricultural Sciences, Alnarp, Sweden, [6]Liaoning Academy of Agricultural Sciences, Shenyang, China, [7]Jiangsu Academy of Agricultural Sciences, Nanjing, China, [8]College of Resources and Environmental Sciences, Key Laboratory of Plant-Soil Interactions, Ministry of Education, National Academy of Agriculture Green Development, China Agricultural University, Beijing, China

OPEN ACCESS

Edited by:
Péter Poór, University of Szeged, Hungary

Reviewed by:
Eugeniusz Małkowski, University of Silesia of Katowice, Poland
Muhammad Ahsan Farooq, Zhejiang University, China

***Correspondence:**
Yifei Liu
yifeiliu6@hotmail.com

Specialty section:
This article was submitted to Plant Physiology, a section of the journal Frontiers in Plant Science

Received: *16 September 2020*
Accepted: *17 November 2020*
Published: *21 December 2020*

Citation:
Wu D, Liu Y, Pang J, Yong JWH, Chen Y, Bai C, Han X, Liu X, Sun Z, Zhang S, Sheng J, Li T, Siddique KHM and Lambers H (2020) Exogenous Calcium Alleviates Nocturnal Chilling-Induced Feedback Inhibition of Photosynthesis by Improving Sink Demand in Peanut (Arachis hypogaea). Front. Plant Sci. 11:607029. doi: 10.3389/fpls.2020.607029

Arachis hypogaea (peanut) is a globally important oilseed crop with high nutritional value. However, upon exposure to overnight chilling stress, it shows poor growth and seedling necrosis in many cultivation areas worldwide. Calcium (Ca^{2+}) enhances chilling resistance in various plant species. We undertook a pot experiment to investigate the effects of exogenous Ca^{2+} and a calmodulin (CaM) inhibitor on growth and photosynthetic characteristics of peanut exposed to low night temperature (LNT) stress following warm sunny days. The LNT stress reduced growth, leaf extension, biomass accumulation, gas exchange rates, and photosynthetic electron transport rates. Following LNT stress, we observed larger starch grains and a concomitant increase in nonstructural carbohydrates and hydrogen peroxide (H_2O_2) concentrations. The LNT stress further induced photoinhibition and caused structural damage to the chloroplast grana. Exogenous Ca^{2+} enhanced plant growth following LNT stress, possibly by allowing continued export of carbohydrates from leaves. Foliar Ca^{2+} likely alleviated the nocturnal chilling-dependent feedback limitation on photosynthesis in the daytime by increasing sink demand. The foliar Ca^{2+} pretreatment protected the photosystems from photoinhibition by facilitating cyclic electron flow (CEF) and decreasing the proton gradient (ΔpH) across thylakoid membranes during LNT stress. Foliar application of a CaM inhibitor increased the negative impact of LNT stress on photosynthetic processes, confirming that Ca^{2+}–CaM played an important role in alleviating photosynthetic inhibition due to the overnight chilling-dependent feedback.

Keywords: low night temperature, growth, calcium, photosynthesis, peanut

INTRODUCTION

Arachis hypogaea, peanut or groundnut, is a grain legume crop with high nutritional value that is primarily grown in tropical and subtropical regions (annual production ∼46 million tons). It originates from tropical South America and provides a vital global source of vegetable oil and protein (Prasad et al., 2003; Bertioli et al., 2016; Lambers et al., 2020). Temperature is critical for peanut growth. Low, but non-freezing (0–12°C) temperature stress, particularly overnight chilling, is a major factor limiting peanut growth, which restricts its production areas (Bagnall et al., 1988; Wan, 2003; Liu et al., 2013; Song et al., 2020). Low-temperature extremes impose variable stresses on plant growth, and the chilling/low-temperature episodes in both the dark and the light may range from several hours to days (Allen and Ort, 2001).

Photosynthesis, a pivotal growth process, is sensitive to low-temperature stress. Preceding warmer ambient temperature and/or following high light exposure further intensifies the chilling-induced negative effects on photosynthetic processes (Powles et al., 1983; Liu et al., 2013; Zhang et al., 2014; Liu, 2020; Song et al., 2020). In peanut cultivation regions, especially those in northern China, severe low-temperature stress often occurs at night, followed by warm sunny days with high light intensity. The effects of nocturnal chilling stress (0–12°C) on the photosynthetic machinery have been assessed in several species with a tropical/subtropical origin, including coffee (*Coffea arabica*; Guo and Cao, 2004; Bauer et al., 2006), tomato (*Solanum lycopersicum*; Liu et al., 2012), soybean (*Glycine max*; Van Heerden et al., 2004), avocado (*Persea Americana*; Whiley, 1999), and mango (*Mangifera indica*; Nir et al., 1997; Allen et al., 2000). Little attention has been given to the physiological responses to peanut overnight chilling stress (Liu et al., 2013; Song et al., 2020). In regions prone to nocturnal chilling, the peanut is at risk of variable foliar curling and necrosis (Bagnall et al., 1988; Wan, 2003; Liu et al., 2013). With global climate change associated with the increasing frequency of extreme weather events, such as low night temperature (LNT), nocturnal/overnight chilling stress, and frost attacks in recent years, peanut production in temperate climate zones is facing new challenges (Cramer et al., 2018; Maxwell et al., 2019).

"Chemical priming" or the pretreatment of plants with selected chemical compounds can stimulate plant physiological mechanisms to cope with biotic or abiotic stresses (Beckers and Conrath, 2007; Savvides et al., 2016). Several approaches have been tested to examine its efficacy in ameliorating the adverse effects of chilling stress on crops. Exogenous foliar calcium (Ca^{2+}) application can alleviate leaf damage and growth inhibition during chilling stress. Pretreatment of exogenous Ca^{2+} improved acclimation to chilling stress in low-temperature sensitive plant species, such as peanut (Liu et al., 2013; Song et al., 2020), wheat (*Triticum aestivum*; You et al., 2002), Chinese crab apple (*Malus hupehensis*; Li et al., 2017b), and tomato (Liu et al., 2012; Zhang et al., 2014), although the mechanism remains unclear (Liu, 2020). Ca^{2+}, as an essential plant mineral nutrient, plays an important role in maintaining the stability of cell walls and membranes (Ali et al., 2003; Song et al., 2020). Ca^{2+} ions also serve as a ubiquitous second messenger in plant signal-transduction networks (Anil and Rao, 2001). Under abiotic stress, plants can initiate a series of physiological and biochemical processes by increasing the concentration of free Ca^{2+} in the cytosol and combining Ca^{2+} with calmodulin (CaM), thus playing an important role in the transmission, response, and acclimation of plants to multiple stresses (Kader and Lindberg, 2010). Ca^{2+} ions participate in a wide variety of environmental stresses, such as drought (La Verde et al., 2018), salt (Knight et al., 1997), low-temperature (Knight et al., 1996), oxidative stress (Price et al., 1994), and hypoxia (Subbaiah et al., 1994). Furthermore, Ca^{2+} is involved in regulating carbohydrate metabolism in the cytosol (Brauer et al., 1990), as well as increasing the translocation of photosynthetic carbohydrates to sinks (Joham, 1957; Navazio et al., 2020; Song et al., 2020).

Studies have demonstrated that foliar application of Ca^{2+} maintains leaf gas exchange and plant growth in peanut (Liu et al., 2013; Song et al., 2020), tomato (Zhang et al., 2014), and cucumber (*Cucumis sativus*; Zhang et al., 2012) exposed to LNT stress. Exogenous Ca^{2+} application sustains photosynthetic capacity by maintaining stomatal conductance (Chen et al., 2001), key enzyme activities in the Calvin-Benson-Bassham (CBB) cycle (You et al., 2002; Navazio et al., 2020), continued thylakoid electron transfer (Ai et al., 2006), and sustaining antioxidant capacity (Liu et al., 2015). Other studies have indicated that Ca^{2+} reduces the concentration of reactive oxygen species (ROS; Bhattacharjee, 2009; Liu et al., 2015), enhances cyclic electron flow (CEF; Zhang et al., 2014), and increases the xanthophyll cycle (Yang et al., 2013) during temperature stress. Applying Ca^{2+} improves cold resistance in tomato by increasing the concentration of soluble sugars, slowing down freezing, and enhancing the concentration of protoplasm in cells (Jiang et al., 2002; Liu et al., 2012).

In our previous study, foliar application of Ca^{2+} significantly enhanced peanut growth and photosynthesis under LNT stress

Abbreviations: CK, Control; C_i, Intercellular CO_2 concentration; CEF, Cyclic electron flow; DAT, Days after temperature treatment; ETR(I), Relative electron transport rate in Photosystem I; ETR(II), Relative electron transport rate in Photosystem II; F, Fluorescence yield measured briefly before application of a saturation pulse; Fo, Minimal fluorescence yield of the dark-adapted sample with all PSII centers open; Fo', Minimal fluorescence yield of the illuminated sample with all PSII centers open; Fm, Maximal fluorescence yield of the dark-adapted sample with all PSII centers closed; Fm′, Maximal fluorescence yield of the illuminated sample with all PSII centers closed; Fv/Fm, Maximal photochemistry efficiency in Photosystem II; FH2, Fenghua 2; g_s, Stomatal conductance; LNT, Low night temperature stress; TFP, Trifluoperazine; PAR, Photosynthetically active radiation measured in μmol quanta·m^{-2}·s^{-1}; Pred, P700 reduction coefficient under light; NPQ, Non-photochemical quenching; Fv'/Fm′, Light-adapted maximum quantum yield of PSII; OEC, Oxygen-evolving complex; PQ, Plastoquinone; Pm, Maximal P700 signal; Pm′, Real-time P700 signal under light; Pn, Net photosynthetic rate; PSI, Photosystem I; PSII, Photosystem II; qP, Photochemical quenching coefficient; ROS, Reactive oxygen species; Tr, Transpiration rate; Y(II), ΦPSII – Actual quantum yield in PSII under light; Y(NO), Non-regulatory quantum yield in PSII under light; Y(NPQ), Regulatory quantum yield in PSII under light; Y(I), ΦPSI – Actual quantum yield in PSI under light; Y(ND), Quantum yield of PSI non-photochemical energy dissipation due to the donor-side limitation; Y(NA), Quantum yield of PSI non-photochemical energy dissipation due to the acceptor-side limitation; Y(CEF)/Y(II), Ratio of the quantum yield of CEF to Y(II).

and during its recovery under normal temperature (Liu et al., 2013; Song et al., 2020); however, the underlying physiological mechanism how exogenous Ca^{2+} alleviating inhibition of photosynthesis by nocturnal chilling in peanut remains poorly understood. Therefore, the present study examined the effects of exogenous Ca^{2+} and a CaM inhibitor, trifluoperazine (TFP) on photosynthetic reactions and growth in peanut exposed to long-term (days) and short-term (hours) LNT stress.

MATERIALS AND METHODS

Plant Material and Experimental Design

The widely planted high-yielding peanut cultivar in China, Fenghua No. 2, was used in this study. Uniform peanut seeds were pre-germinated in a Petri dish for 36 h at 27°C and then planted in 32-cavity trays (one seed per cavity) for 7 days. Seedlings with average sizes were then transplanted into 150 pots (200 mm height, 260 mm diameter, 1 seedling per pot) filled with 4 kg of a standard horticultural substrate (Changchun Xihe Agro-technology Co. Ltd., Jilin, China). The pots were moved into an artificial climate chamber (Conviron, Winnipeg, Canada) with a day temperature of 25°C, night temperature of 20°C, and relative humidity (RH) of 60 ± 5%. All seedlings received a 12 h (from 6:00 to18:00) photoperiod at a photosynthetic photon flux density (PPFD) of 1,000 μmol quanta·m^{-2}·s^{-1} and CO_2 concentration of 400 ± 5 μmol·mol^{-1}. After 5 days of acclimation, 100 pots with uniform seedlings were selected and divided into four groups (25 pots per group) for the four treatments [LNT, LNT + Ca, LNT + TFP, and the control (CK); **Table 1**].

The optimum concentration of exogenous Ca^{2+} (15 mM $CaCl_2$) and CaM inhibitor (5 mM TFP) and the application technique were established in our previous experiments (Liu et al., 2013; Song et al., 2020). The seedling leaves were sprayed until dripping with ultrapure water. For the LNT + Ca and LNT + TFP treatments, 15 mM Ca^{2+} or 5 mM TFP, respectively, was evenly applied twice a day (at 8:00 and 16:00) on 3 days [0, 5, and 10 days of LNT treatment (DoL)]. In our previous experiments, we found that long-term LNT stress reduced leaf photosynthetic gas exchange significantly during the seedling stage. In our system, a duration of ≥1 DoL was defined as long-term LNT stress and <1 DoL was short-term LNT stress. This study assessed the effects of exogenous Ca^{2+} and a CaM inhibitor (TFP) on both long-term and short-term LNT stresses.

TABLE 1 | Details of the four treatments used in the study.

Treatment	Day temperature	Night temperature	Foliar spray application (2 × daily) at 0, 5, and 10 days of LNT treatment
Control (CK)	25°C	20°C	Ultrapure water
LNT		8°C	Ultrapure water
LNT + Ca		8°C	15 mM Ca^{2+}
LNT + TFP		8°C	5 mM TFP

Plant Sampling and Measurements

Three seedlings per treatment at 1, 6, and 11 DoL were selected for measurements of biomass, plant height, leaf area, leaf relative chlorophyll concentration, leaf gas exchange, and leaf hydrogen peroxide (H_2O_2) concentration. Chlorophyll was estimated on the third-youngest fully expanded leaf of the main stem with a chlorophyll meter (SPAD-502 Plus, Japan). Leaf gas exchange was measured on the same leaf using an open system (GFS-3000, Heinz Walz GmbH, Effeltrich, Germany) at 1, 6, and 11 DoL. During gas exchange measurements, the leaf cuvette temperature was set to 25°C and 60% RH. The CO_2 concentration was maintained at 400 μmol·mol^{-1}. An LED array provided a PPFD of 1,000 μmol quanta·m^{-2}·s^{-1}. The third-youngest fully expanded leaf was kept in the chamber, ensuring that the thermocouple touched it on the lower side. Leaf gas exchange parameters included net photosynthetic rate (Pn), stomatal conductance (g_s), atmospheric CO_2 concentration (C_a), transpiration rate (Tr), intercellular CO_2 concentration (C_i), water-use efficiency ($WUE = Pn / Tr$), and leaf stomatal limitation ($Ls = 1 - C_i / C_a$). Leaf area was measured using an LI-3000C (LI-COR Biosciences, Lincoln NE, United States). After oven-drying at 105°C for 30 min and then 70°C to a constant weight, dry weights of leaves and whole plants were recorded. Leaf mass per unit leaf area (LMA) was calculated as $LMA = \text{leaf dry weight} / \text{leaf area}$.

Hydrogen peroxide concentration was measured on the third-youngest fully expanded leaf of the main stem, as described by Li et al. (2017a). Briefly, finely ground leaves (60 mg fresh weight) were placed in a 2 ml microcentrifuge tube before adding 2 ml of 5% (w/v) TCA, and centrifuged 10,000 *g* for 10 min at 4°C. The supernatant (1 ml) was added to 0.1 ml of 20% (v/v) $TiCl_4$ and 0.2 ml of concentrated ammonia. The mixture was centrifuged at 5,000 *g* for 10 min at 4°C. The pellet was dissolved in 3 ml of 1 M H_2SO_4 and the absorbance recorded at 410 nm.

At 6:00 AM on 1, 6, and 11 DoL, the third-youngest fully expanded leaves from six seedlings per treatment (pooled as three biological replicates per treatment) were ground to a powder after oven-drying at 105°C for 30 min and 70°C to constant weight for carbohydrate analysis. Soluble sugars were extracted from approximately 100 mg of the above leaf powder with 80% (v/v) ethanol at 85°C and quantified using the microtiter method (Hendrix, 1993). Pellets containing starch were oven-dried overnight at 60°C. Starch in the pellet was first gelatinized by adding 1 ml of 0.2 M KOH and incubated in a boiling water bath for 30 min (Rufty and Huber, 1983). After cooling, 0.2 ml of 1 M acetic acid was added, and the solution incubated with 2 ml acetate buffer (pH 4.6) containing amyloglucosidase (6 units, Roche, Basel, Switzerland) at 55°C for 1 h. The reaction was terminated in a boiling water bath, and the resulting supernatant analyzed for glucose (Song et al., 2020).

Chloroplast ultrastructure and chlorophyll fluorescence parameters were measured at 11 h of LNT treatment (HoL). Chloroplast ultrastructure was determined using methods previously reported (Strand et al., 1999). The third youngest fully expanded leaves were sliced and observed under a microscope at Centre for Microscopy, Characterization, and Analysis at

Shenyang Agricultural University. The samples were fixed in 4% (v/v) glutaraldehyde, fixed after 2% (w/v) osmic acid, washed in 20 mM phosphate buffer, dehydrated by gradient ethanol, soaked in Epon812 resin, embedded, and polymerized. The resin was sliced (90 nm thickness) with a LEICA EM UC7 ultrathin slicer (Leica Microsystems, Wetzlar, Germany) and stained using uranyl acetate and lead citrate. The slices were observed and photographed by transmission electron microscopy (TEM; LSM 510; Carl-Zeiss AG, Oberkochen, Germany).

Chlorophyll fluorescence images were determined at 11 HoL with an imaging-pulse-amplitude-modulated (PAM) chlorophyll fluorometer (Heinz Walz, GmbH, Effeltrich, Germany) as described elsewhere (Li et al., 2014). Plants were fully dark-adjusted for >30 min at 11 HoL to measure the maximal photochemical efficiency of photosystem II $\left[\mathrm{Fv}/\mathrm{Fm}=(\mathrm{Fm}-\mathrm{Fo})/\mathrm{Fm}\right]$ and the coefficient of non-photochemical quenching $(\mathrm{NPQ}=\mathrm{Fm}/\mathrm{Fm}'-1)$. Fluorescence images of leaves were obtained accordingly.

Measurements of rapid light curves (RLCs) of chlorophyll fluorescence parameters were determined at 11 HoL with Dual-PAM-100 measuring systems (Heinz Walz, GmbH, Effeltrich, Germany). The software Dual PAM v1.19 was used to control Dual-PAM-100 measuring systems to calculate the chlorophyll fluorescence and absorption changes simultaneously. Measurements were conducted using the software's standard procedures and appropriate modifications based on our previous research (Shi et al., 2019; Song et al., 2020). The RLCs were determined after fully dark adjustment at 11 HoL (>30 min) at light intensities of 24, 32, 50, 108, 186, 286, 515, 773, 1,192, 1,469, and 1,823 μmol quanta·m^{-2}·s^{-1}. The exposure for each light intensity was 30 s and the saturation pulse was 1,000 μmol quanta·m^{-2}·s^{-1} for 300 ms. All measurements were conducted at 25°C. The PSII parameters were measured using a Dual-PAM 100 device based on the saturation pulse method. The chlorophyll fluorescence parameters were calculated as: the actual quantum yield of PSII in the actinic light [AL; $\mathrm{Y(II)}=(\mathrm{Fm'}-\mathrm{F})/\mathrm{Fm}]$, the quantum yield of non-regulatory energy dissipation $\left[\mathrm{Y(NO)}=\mathrm{F}/\mathrm{Fm}\right]$, the regulatory quantum yield in PSII $\left[\mathrm{Y(NPQ)}=1-\mathrm{Y(II)}-\mathrm{Y(NO)}\right]$, and the relative electron transfer rate of PSII $\left[\mathrm{ETR(II)}=\mathrm{PAR}\times\mathrm{Y(II)}\times0.84\times0.5\right]$. The PSI parameters were measured using a Dual-PAM 100 device based on the P700 signal (absorption differences between 830 and 875 nm). The P700 parameters were calculated as: the actual quantum yield of PSI $\left[\mathrm{Y(I)}=1-\mathrm{Y(NA)}-\mathrm{Y(ND)}\right]$, the quantum yield of non-photochemical energy dissipation due to donor-side limitation $\left[\mathrm{Y(ND)}=1-\mathrm{P700red}\right]$, the quantum yield of non-photochemical energy dissipation due to acceptor side limitation $\left[\mathrm{Y(NA)}=(\mathrm{Pm}-\mathrm{Pm}')/\mathrm{Pm}\right]$, and the electron transfer rate of PSI $\left[\mathrm{ETR(I)}=\mathrm{PAR}\times\mathrm{Y(I)}\times0.84\times0.5\right]$ (Schreiber and Klughammer, 2008). The CEF value $\left[\mathrm{CEF}=\mathrm{ETR(I)}-\mathrm{ETR(II)}\right]$ and the ratio of the quantum yield of CEF to Y(II) $\left[\mathrm{Y(CEF)}/\mathrm{Y(II)}=(\mathrm{Y(I)}-\mathrm{Y(II)})/\mathrm{Y(II)}\right]$ were used to determine cyclic electron transfer (Yang et al., 2018).

A functionally intact photosynthetic apparatus was characterized by the slow decay of P515 signal after dark adaptation (high membrane integrity) and fast decay after illumination (high ATP-synthase activity; Schreiber and Klughammer, 2008; Zhang et al., 2014; Yang et al., 2018). In this study, the dual-beam 550–515 nm difference signal (electrochromic shift) was monitored simultaneously at 11 HoL using the P515/535 module of the Dual-PAM-100 (Heinz Walz, GmbH, Effeltrich, Germany). Balancing and calibrating of the P515 signal using the automated routine of the software Dual-PAM v1.19 occurred before each measurement (Schreiber and Klughammer, 2008; Suzuki et al., 2011). After 1 h of dark adjustment, P515 changes induced by saturating single turnover flashes were recorded to evaluate the integrity of the thylakoid membrane. After 10 min of pre-illumination at 630 μmol quanta·m^{-2}·s^{-1} and 4 min of dark adjustment, P515 changes induced by saturating single turnover flashes were recorded to evaluate ATP-synthase activity. Slow dark–light–dark induction transients of the 550–515 nm signals reflect changes in both membrane potential (electrochromic pigment absorbance shift) and zeaxanthin concentration. These transients were measured after 11 h of full dark adjustment. AL (630 μmol quanta m^{-2} s^{-1}) was turned on after 30 s and off at 330 s. Based on analyzing light-off responses of the P515 signal, the membrane potential ($\Delta\psi$) and proton gradient (ΔpH) components of the proton-motive force (pmf) were also assessed accordingly.

Statistical Analyses

Statistical analyses were carried out using one-way ANOVA in SPSS 19.0 (Chicago, IL, United States). One-hundred uniform seedlings were included in this study and allocated to four groups (i.e., 25 seedlings per group). Three of the 25 seedlings per group were used for non-destructive measurements of leaf gas exchange, chlorophyll fluorescence, and P700 parameters. The remaining seedlings per treatment were selected for destructive sampling for seedling growth, TEM observations, and measurements of leaf area, biomass, and H_2O_2 and carbohydrate concentrations. The results are presented as mean values and SEs of three biological replicates. *Post hoc* LSD tests at $p \leq 0.05$ were performed to determine differences among treatments. Significant differences are indicated as $^{*}p \leq 0.05$ among treatments. All graphs were plotted using Origin 8.0 and Excel 2016 software.

RESULTS

Long-Term LNT Stress

Plant Growth

At 6 and 11 DoL, LNT decreased plant height, total plant dry weight, leaf dry weight, leaf area, LMA, and relative chlorophyll concentration in peanut, while the opposite was true for LNT + Ca. LNT + TFP further decreased these parameters at 6 and 11 DoL (**Figures 1A–F**). The LNT treatment had higher leaf H_2O_2 concentration than CK at 6 and 11 DoL; in contrast, LNT + Ca reduced it dramatically, and LNT + TFP increased it further (**Figure 1G**).

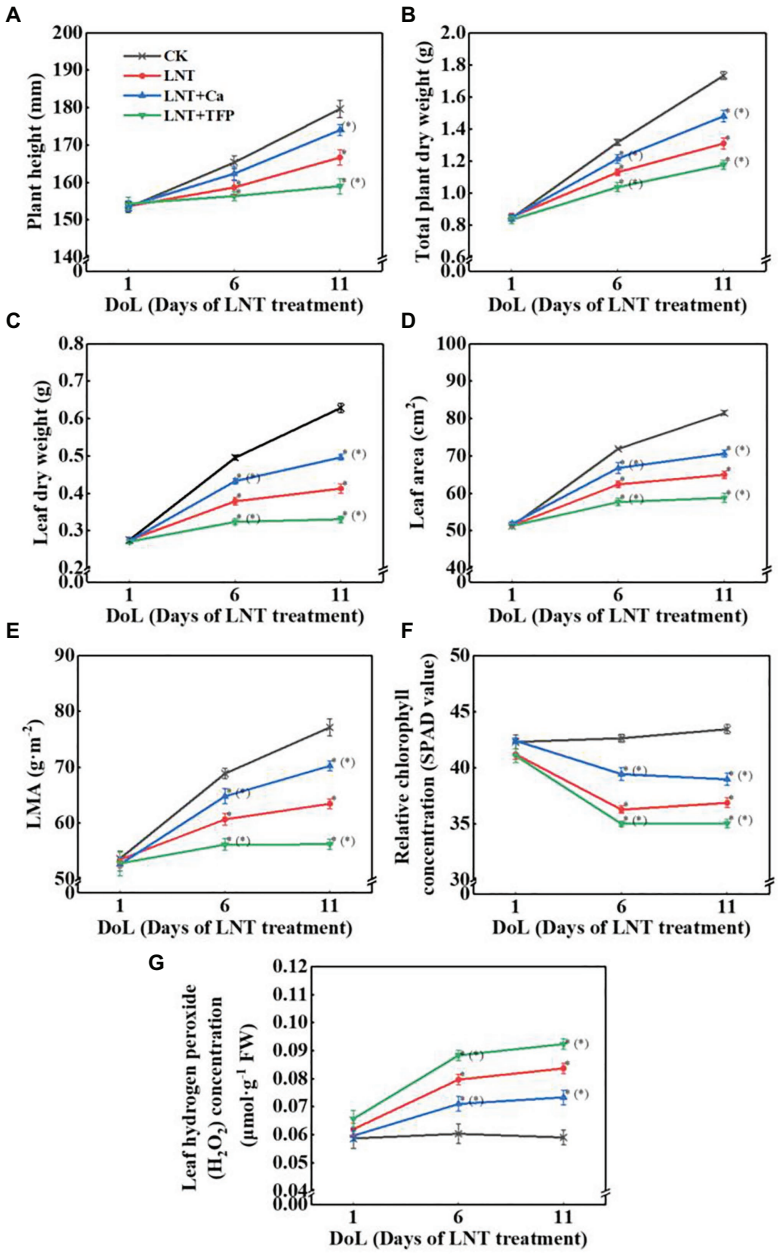

FIGURE 1 | Effect of exogenous calcium (Ca^{2+}) and a calmodulin inhibitor (TFP) on **(A)** plant height, **(B)** total plant dry weight (per plant including all organs), **(C)** leaf dry weight, **(D)** leaf area, **(E)** leaf mass per unit leaf area (LMA), **(F)** relative chlorophyll concentration (SPAD value), and **(G)** hydrogen peroxide (H_2O_2) concentration in peanut leaves under long-term low night temperature (LNT) stress [1, 6, and 11 days of LNT treatment (DoL)]. Values are means of three biological replicates ± SE ($n = 3$). *indicate significant differences among treatments at $p \leq 0.05$. Significant differences between the three treatments under LNT stress are shown in parentheses.

Concentrations of Soluble Sugars, Starch, and Total Nonstructural Carbohydrates

Low night temperature enhanced soluble sugar concentrations at 6 and 11 DoL, particularly and starch and total nonstructural carbohydrates at 1, 6, and 11 DoL. The reverse was true for LNT + Ca, relative to LNT. LNT + TFP increased the concentrations of soluble sugars, starch, and total nonstructural carbohydrates at 6 and 11 DoL (**Figures 2A–C**).

Leaf Gas Exchange

Low night temperature decreased Pn, g_s, Tr, WUE, and Ls and dramatically increased C_i at 1, 6, and 11 DoL. Compared with LNT, LNT + Ca increased dramatically Pn at 1, 6, and 11 DoL, increased g_s, Tr, and Ls at 6 and 11 DoL, and markedly decreased C_i at 6 and 11 DoL. Conversely, LNT + TFP dramatically decreased Pn, g_s, Tr, and Ls at 6 and 11 DoL, decreased WUE at 11 DoL, and increased C_i at 6 and 11 DoL (**Figures 3A–E**).

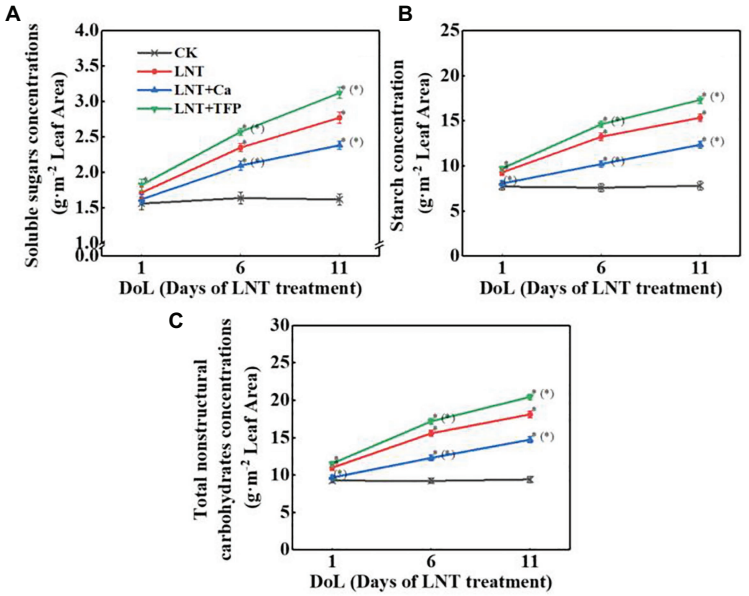

FIGURE 2 | Effect of exogenous Ca^{2+} and a calmodulin inhibitor (TFP) on the concentrations of **(A)** soluble sugars, **(B)** starch, and **(C)** total nonstructural carbohydrates in peanut leaves under long-term LNT stress (1, 6, and 11 DoL). Values are means of three biological replicates ± SE (n = 3). *indicates significant differences among treatments at $p \leq 0.05$. Significant differences between the three treatments under LNT stress are shown in parentheses.

Short-Term LNT Stress

Chloroplast Ultrastructure

Short-term LNT stress (11 HoL) damaged the chloroplast grana; LNT + Ca alleviated the damage, while LNT + TFP exacerbated the damage. Short-term LNT stress increased the size of starch grains and reduced the number of plastoglobules; LNT + Ca alleviated this effect, while LNT + TFP exacerbated it (**Figures 4A–D**).

Fv/Fm and NPQ

The leaves in LNT treatment had lower Fv/Fm than CK, while LNT + Ca had similar values to CK (**Figure 5A**). The leaves in the LNT treatment had significantly higher NPQ than CK; LNT + Ca had lower NPQ and LNT + TFP had higher NPQ than LNT (**Figure 5B**).

Photosystems Activities

The effective quantum yield of PSII photochemistry [Y(II)] decreased gradually with increasing light intensity in all treatments. The LNT treatment had significantly lower Y(II) than CK. LNT + Ca increased Y(II), while LNT + TFP reduced it further, relative to LNT (**Figure 6A**). The quantum yield of regulated energy dissipation in PSII [Y(NPQ)] increased rapidly with increasing light intensity in all treatments. The LNT treatment had significantly higher Y(NPQ) than CK before the light intensity reached 773 μmol quanta m^{-2} s^{-1}. LNT + Ca decreased Y(NPQ), while LNT + TFP increased it further, relative to LNT (**Figure 6B**). In contrast, the quantum yield of non-regulated energy dissipation in PSII [Y(NO)] increased gradually with increasing light intensity. The LNT treatment had higher Y(NO) than CK. LNT + Ca decreased Y(NO), while LNT + TFP increased it, relative to LNT (**Figure 6C**).

The effective quantum yield of PSI photochemistry [Y(I)] followed the same trend as Y(II) (**Figure 6D**). The quantum yield of PSI non-photochemical energy dissipation due to the donor-side limitation [Y(ND)] increased gradually with increasing light intensity in all treatments. The LNT treatment had significantly higher Y(ND) than CK. LNT + Ca decreased Y(ND) while LNT + TFP increased it further, relative to LNT (**Figure 6E**). The quantum yield of PSI non-photochemical energy due to the acceptor-side limitation [Y(NA)] increased rapidly when initially exposed to light, before quickly declining and stabilizing in all treatments. The LNT treatment had significantly lower Y(NA) than CK. LNT + Ca enhanced Y(NA), while LNT + TFP decreased it further, relative to LNT (**Figure 6F**).

Photosynthetic Electron Transport

The electron transfer rate of PSII [ETR(II)] and PSI [ETR(I)] in leaves rapidly rose with increasing light intensity. The LNT treatment had significantly lower ETR(II) and ETR(I) than CK. LNT + Ca increased both ETR(II) and ETR(I), while LNT + TFP reduced them (**Figures 7A,B**). The CEF around PSI (CEF) increased with increasing light intensity in all treatments. The LNT treatment significantly increased CEF, relative to CK, and LNT + Ca stimulated it more than LNT, while LNT + TFP inhibited it from 186 μmol quanta m^{-2} s^{-1} onwards (**Figure 7C**). All LNT treatments had higher ratios of the quantum yield of CEF to Y(II) [Y(CEF)/Y(II)] than CK beyond 186 μmol quanta m^{-2} s^{-1} (**Figure 7D**).

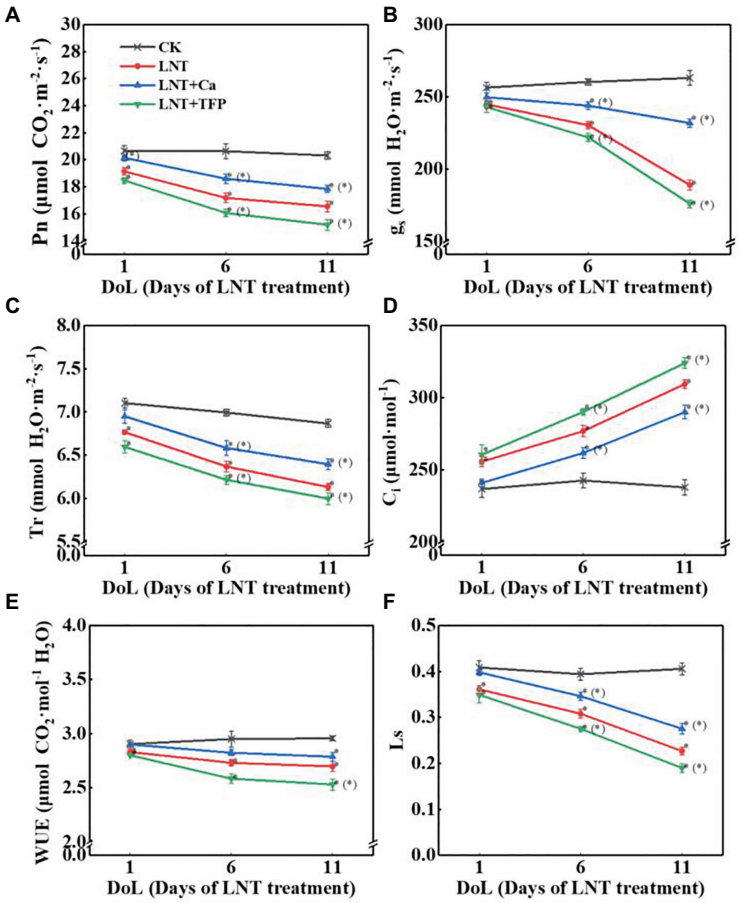

FIGURE 3 | Effect of exogenous Ca^{2+} and a calmodulin inhibitor (TFP) on peanut gas exchange characteristics **(A)** net photosynthetic rate (Pn), **(B)** stomatal conductance (g_s), **(C)** transpiration rate (Tr), **(D)** intercellular CO_2 concentration (C_i), **(E)** water-use efficiency (WUE), and **(F)** leaf stomatal limitation (Ls) in peanut leaves under long-term LNT stress (1, 6, and 11 DoL). Values are means of three biological replicates ± SE (n = 3). *indicates significant differences among treatments at $p \leq 0.05$. Significant differences between the three treatments under LNT stress are shown in parentheses.

Proton-Motive Force, Thylakoid Membrane Integrity, and ATP-Synthase Activity

The faster decay of the P515 signal after adjustment to darkness and the slower decay after irradiation to AL in the LNT treatments indicated that the thylakoid membrane integrity was impaired and inhibited ATP-synthase activity, relative to CK (**Figures 8A,B**). It also indicated that the rate of proton transfer from the lumen to the stroma *via* ATP-synthase was largely inhibited at 11 HoL. LNT + Ca pretreatment increased thylakoid membrane integrity and ATP-synthase activity while LNT + TFP decreased it.

The $\Delta\psi$ and ΔpH components of the proton-motive force (pmf) can be estimated by analyzing light-off responses of the P515 signal (**Figure 8C**). The difference between the signal of steady-state and the "dark baseline" reflects substantial Δψ. The "undershoot" below the "dark baseline" is considered a measure for the steady-state ΔpH. The LNT treatments had significantly lower Δψ than CK; LNT + Ca increased it further, and LNT + TFP slightly decreased it (**Figure 8D**). In contrast, the LNT treatments had significantly higher ΔpH than CK; LNT + Ca decreased it slightly, and LNT + TFP increased it slightly (**Figure 8D**). The relative extent of zeaxanthin formation can be judged from the increase in the "dark baseline" apparent after light-off (**Figure 8E**). The "dark baseline" of the LNT, LNT + Ca, and LNT + TFP treatments decreased significantly more than CK, indicating a decline in zeaxanthin concentration. Compared with LNT, LNT + Ca increased zeaxanthin concentration, while LNT + TFP decreased it.

DISCUSSION

LNT Stress-Induced Feedback Inhibition of Photosynthesis Was Mainly Due to Limited Growth/Sink Demand

Nocturnal chilling stress significantly inhibited growth and leaf expansion (**Figures 1A–E**), which is consistent with earlier findings in tomato (Zhang et al., 2014; Lu et al., 2020) and melon (*Cucumis melo*; Hao et al., 2016). Other studies have demonstrated that peanut exhibited poor growth (associated

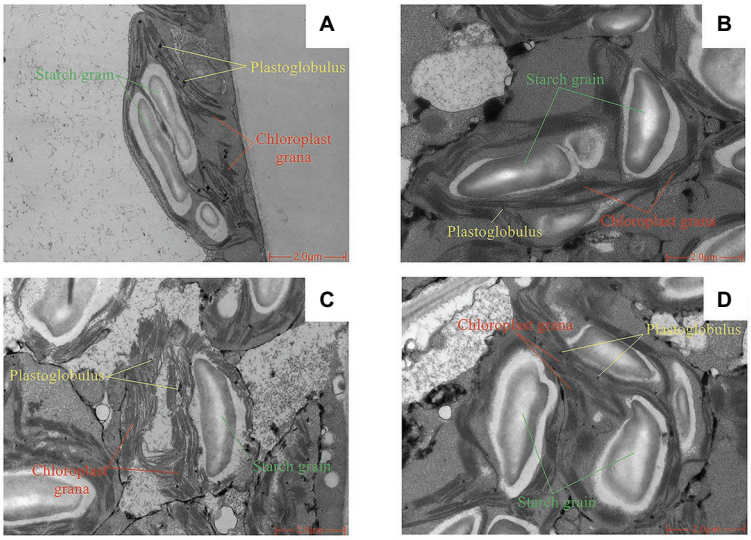

FIGURE 4 | Effect of exogenous Ca^{2+} and a calmodulin inhibitor (TFP) on chloroplast ultrastructure of peanut leaves under short-term LNT stress (11 HoL). **(A)** CK; **(B)** LNT; **(C)** LNT + Ca, and **(D)** LNT + TFP.

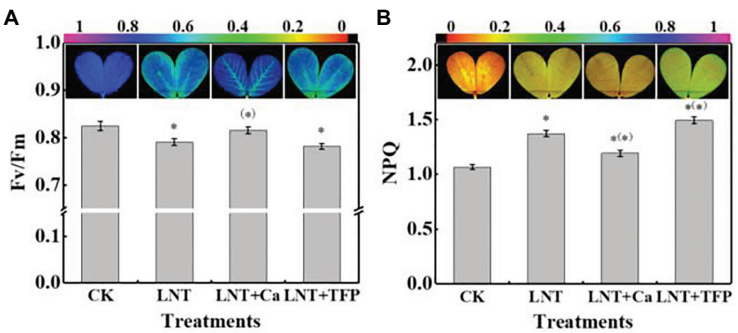

FIGURE 5 | Effect of exogenous Ca^{2+} and a calmodulin inhibitor (TFP) on chlorophyll fluorescence parameters and images **(A)** maximum photochemical efficiency of PSII (Fv/Fm) and **(B)** non-photochemical quenching (NPQ) coefficient in peanut leaves under short-term LNT stress (11 HoL). Values are means of three biological replicates ± SE (n = 3). *indicates significant differences among treatment at $p \leq 0.05$. Significant differences between the three treatments under LNT stress are shown in parentheses.

with foliar necrosis and curling) when grown below 15°C (Wan, 2003; Liu et al., 2013). LNT stress generally reduces leaf area, stem diameter, and shoot and root dry matter accumulation (Solanke and Sharma, 2008; Dias et al., 2011; Hajihashemi et al., 2018). Leaf expansion rates change with the environmental temperature. Specifically, chilling stress reduces leaf expansion rates and leaf area in sorghum (*Sorghum bicolor*), maize, and sunflower (*Helianthus annuus*; Tardieu et al., 1999). LNT stress can also reduce leaf growth, the concentration of photosynthetic pigments and shoot and root dry matter accumulation in tomato (Latef and He, 2011), melon (Hao et al., 2016), and peanut (Song et al., 2020).

We demonstrated that even a short-term (11 HoL) overnight chilling stress significantly increased soluble sugar, starch, and total nonstructural carbohydrate concentrations in leaves (**Figures 2A–C**). Our TEM results confirmed that the short-term (11 HoL) LNT stress severely damaged the chloroplast grana and expansion of starch grains in leaves, relative to CK (**Figures 4A,B**). The accumulation of major photoassimilates (soluble sugars and starch) in leaves is critical for balancing photosynthate production and sugar consumption for tissue growth and development. A coordinated mutual relationship exists among plant growth/sink utilization and photosynthesis, rather than a simple one-way dependence of growth on photosynthesis (Adams et al., 2013; Lambers and Oliveira, 2019). Carbohydrate synthesis occurs in photosynthesizing leaves (sources) to provide substrates for plant growth (e.g., leaf expansion, stem, and root development) and maintain non-photosynthetic plant tissues (sinks; Cohu et al., 2014; Lambers and Oliveira, 2019). Our findings suggest that nocturnal chilling stress directly inhibits peanut growth and nonstructural carbohydrate translocation from source to sink, resulting in a

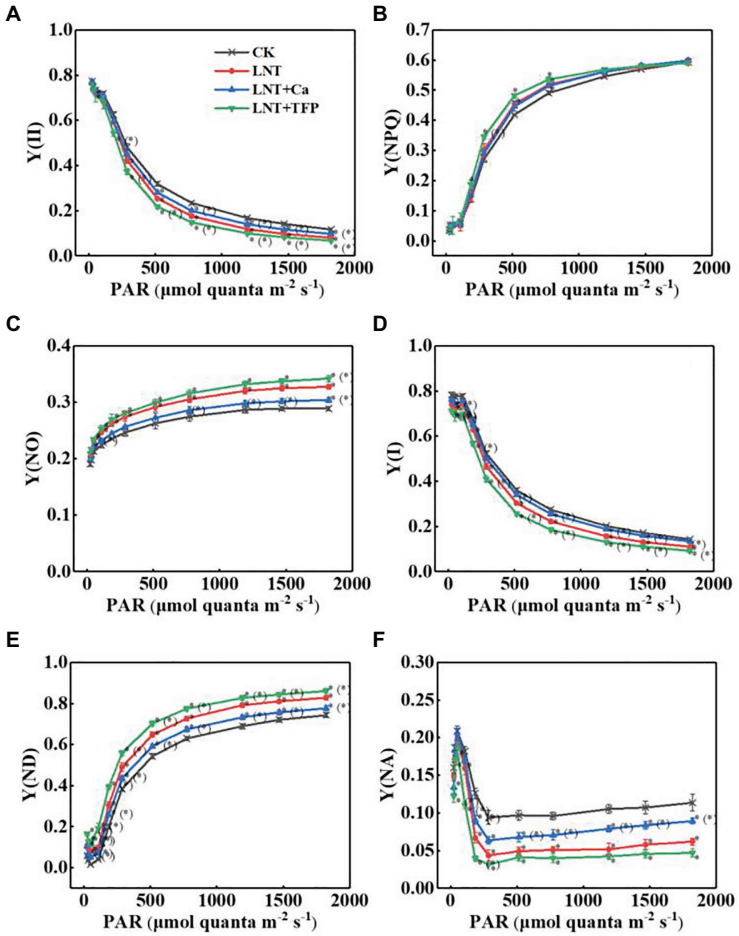

FIGURE 6 | Effect of exogenous Ca^{2+} and a calmodulin inhibitor (TFP) on the rapid light curves (RLCs) of photosystems parameters **(A)** Y(II), **(B)** Y(NPQ), **(C)** Y(NO), **(D)** Y(I), **(E)** Y(ND), and **(F)** Y(NA) in peanut leaves under short-term LNT stress (11 HoL). Values are means of three biological replicates ± SE (n = 3). *indicates significant differences among treatments at $p \leq 0.05$. Significant differences between the three treatments under LNT stress are shown in parentheses.

significant accumulation of nonstructural carbohydrates in photosynthetically active leaves (**Figures 2, 4**), which are consistent with studies on maize (Adams et al., 2013) and peanut (Song et al., 2020).

This study showed that the negative impact of LNT stress on peanut photosynthesis was due to reduced export of nonstructural carbohydrates, as we only exposed plants to nocturnal chilling stress (**Figures 1–4**). The imbalance between source and sink/growth can further exert feedback downregulation or inhibition of leaf photosynthesis *via* nonstructural carbohydrate accumulation in photosynthesizing leaves (Foyer, 1988; Koch, 1996; Paul and Foyer, 2001; Paul and Pellny, 2003). In particular, we demonstrated that significant accumulation of nonstructural carbohydrates in leaves, even in short-term (11 HoL) LNT-stressed plants impaired photosynthetic machinery, including photosystems activities, thylakoid electron transport, carbon fixation, chloroplast morphology, and photoinhibition (**Figures 3–8**). Our results suggest that in the early stage of short-term LNT stress (without light), the significant accumulation of nonstructural carbohydrates damaged thylakoid membranes (**Figures 4–6**). Consequently, thylakoid membrane disintegration might be related to over-reduction and damage of the photosynthetic electron transport chain after short-term or long-term LNT stress followed by warm sunny days (with light; **Figures 5–8**; Song et al., 2020). Our findings are consistent with other studies, which reported that insufficient sink activity and growth inhibition can lead to significant accumulation of nonstructural carbohydrates in leaves and severe photoinhibition (Urban and Alphonsout, 2007; Adams et al., 2013). Indeed, there is evidence that long-term chilling/cold stress can inhibit the activities of photosynthetic reaction centers, thus restricting the electron transport chain and carbon fixation (Kasuga et al., 2004; Baker, 2008; Lu et al., 2020; Song et al., 2020). Our results further demonstrated that even a short-term LNT stress could also result in the decreases of the thylakoid membranes integrity and ATPase activity (**Figure 7**) and the increase of Y(NO), which is the non-regulated energy loss in PSII – a high value of Y(NO) reflecting the inability of the plant to protect itself against damage by excess excitation (**Figure 6**). It is plausible that the PSII super-complex

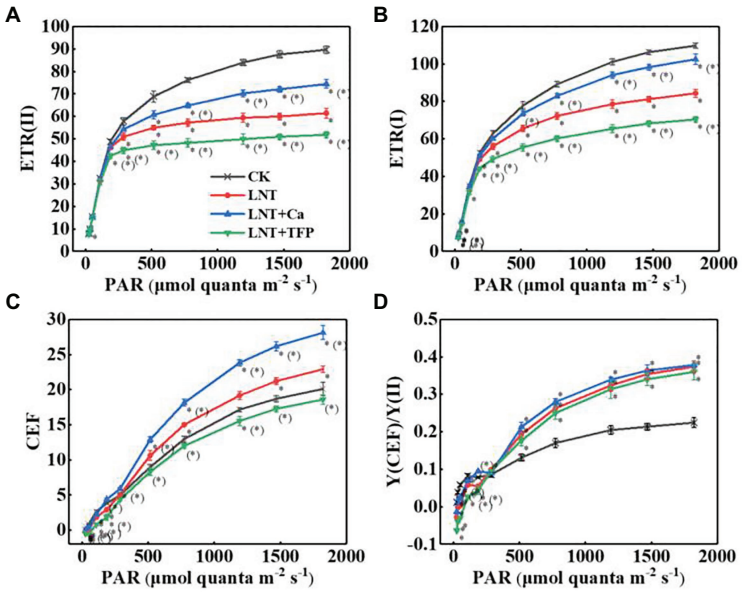

FIGURE 7 | Effect of exogenous Ca^{2+} and a calmodulin inhibitor (TFP) on the RLCs of photosynthetic electron transport **(A)** ETR(II), **(B)** ETR(I), **(C)** CEF, and **(D)** Y(CEF)/Y(II) in peanut leaves under short-term LNT stress (11 HoL). Values are means of three biological replicates ± SE (n = 3). *indicates significant differences among treatment at $p \leq 0.05$. Significant differences between the three treatments under LNT stress are shown in parentheses.

was photo-damaged after the short-term (11 HoL) LNT stress (**Figures 5, 6**). The impact of the short-term LNT (11 HoL) stress on the light-dependent reactions was mainly reflected by slower electron transfer of thylakoids (**Figure 7**), reduced ATP and NADPH formation, and inhibition of carbon assimilation (**Figures 3, 8**), leading to significant H_2O_2 accumulation (**Figure 1G**) and impaired photosynthetic apparatus (**Figures 5, 6**). We also found that short-term LNT (11 HoL) stress stimulated the operation of cyclic photosynthetic electron transport around PSI, consistent with findings in Scots pine (*Pinus sylvestris*; Ivanov et al., 2001), maize (Savitch et al., 2011; Zhang et al., 2014), and tomato (Lu et al., 2020) exposed to long-term chilling stress.

Chemical Priming by Exogenous Ca^{2+} Restored Nocturnal Chilling-Dependent Feedback Inhibition of Photosynthesis Was Mainly Due to Improved Growth/Sink Demand

Exogenous Ca^{2+} reduced the accumulation of nonstructural carbohydrates and H_2O_2 in leaves (sources) when undergoing overnight chilling stress (**Figures 1, 2, 4**). There are pieces of evidence that exogenous Ca^{2+} can serve to maintain photosynthetic processes by improving chilling stress resilience (Brauer et al., 1990) in tomato (Zhang et al., 2014; Liu et al., 2015), wheat (You et al., 2002), Chinese crab apple (Li et al., 2017b), and peanut (Liu et al., 2013; Song et al., 2020). In particular, Ca^{2+} is a critical essential element for peanut – a calciphilous legume crop – and directly connected to plant growth processes and responses to phytohormones (Wan, 2003; White and Broadley, 2003; Thor, 2019); and Ca^{2+} is involved in regulating a series of cellular activities, including plant cell division and elongation, cytoplasmic flow, and photomorphogenesis (Kader and Lindberg, 2010). The key function of Ca^{2+} is to serve as an intracellular messenger involved in many physiological processes and signaling pathways, ranging from plant tissue development (Michard et al., 2011; Monshausen et al., 2011; Ortiz-Ramírez et al., 2017; Zhang et al., 2017) to environmental stress responses (Knight et al., 1996, 1997). Ca^{2+} is involved in the regulation of carbohydrate metabolism, which can directly contribute to the regulation of sucrose synthesis, such as the inhibition of cytosolic Fru1,6-bisPase, activation of sucrose-phosphate synthase, and turnover of inorganic pyrophosphate (Brauer et al., 1990; Eckardt, 2001; Lu et al., 2013). In particular, Ca^{2+} is an important component of several signal-transduction pathways including sugar-signaling and auxin-signaling (Ohto and Nakamura, 1995; Gounaris, 2001). Moreover, Ca^{2+} regulation has been implicated in phloem function (Eckardt, 2001). Our results demonstrated that exogenous Ca^{2+} indirectly relieved a further decline in g_s and Tr under LNT stress (**Figure 3**), consistent with previous studies in *Arabidopsis* (Dong et al., 2013), cotton (*Gossypium hirsutum*; Joham, 1957), tomato (Liu et al., 2015), and spinach (*Spinacea oleracea*; Brauer et al., 1990), where Ca^{2+} improved the synthesis, phloem loading, and export of photosynthetic carbohydrates (Joham, 1957; Eckardt, 2001; Lu et al., 2013).

Based on our analyses, leaf morphology (**Figures 1A–E**), analytical chemical profiling (**Figures 1F, 2**), ultrastructural observations by TEM (**Figure 4**), gas exchange (**Figure 3**), and photosynthetic apparatus activity assessment (**Figures 5–8**) demonstrated that the restored LNT-linked damage to the

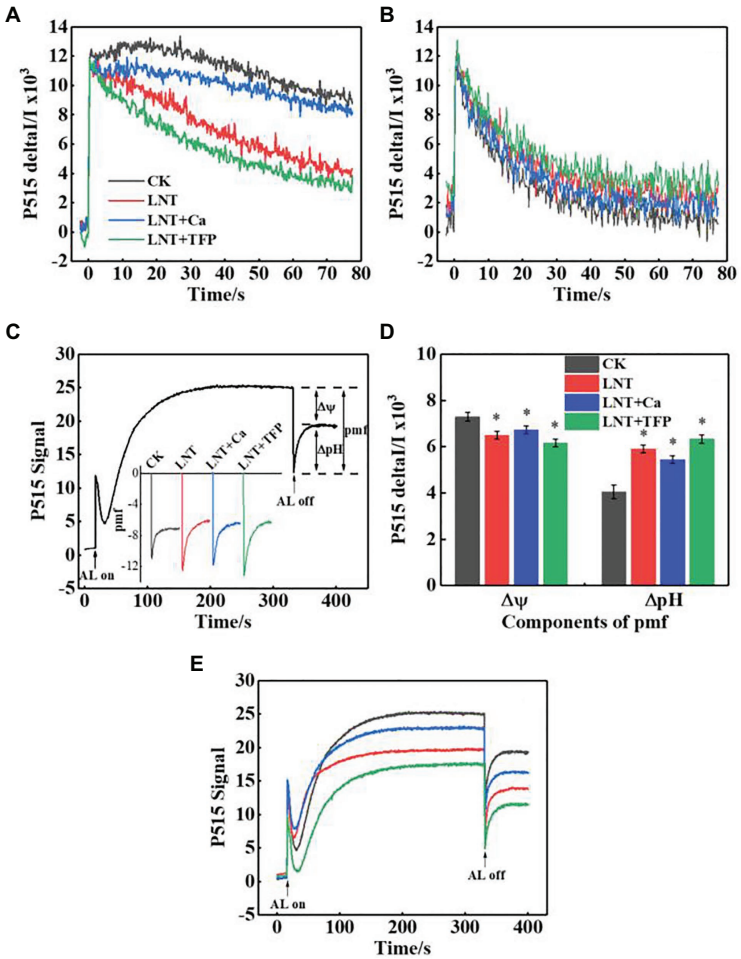

FIGURE 8 | Effect of exogenous Ca^{2+} and a calmodulin inhibitor (TFP) on slow P515 induction transients of peanut leaves under short-term LNT stress (11 HoL). **(A)** Rapid kinetics of P515 induced by saturating single turnover flashes after dark acclimation for 1 h; **(B)** fast kinetics of P515 induced by saturating single turnover flashes after pre-illumination for 10 min at 1,000 μmol photons·m^{-2}·s^{-1} followed by 4 min darkness; **(C)** complete recording of light-on and light-off responses and enlarged display of light-off response to light quality with the indication of the estimated proton gradient (ΔpH) and membrane potential (Δψ) components of proton-motive force (pmf). Slow "dark–light–dark" induction transients of the 515 nm signal were measured. Actinic light (AL; 630 µmol·photons m^{-2} s^{-1}) was turned on after 30 s and off after 330 s; **(D)** ΔpH and Δψ components of the pmf estimated from the curves of slow P515 kinetics; **(E)** changes in the P515 signal of slow dark–light–dark induction transients indicate the relative zeaxanthin concentration. Values are means of three biological replicates ± SE (n = 3). *indicates significant differences among treatments at $p \leq 0.05$. Significant differences between the three treatments under LNT stress are shown in parentheses.

photosynthetic machinery by exogenous Ca^{2+} might be a consequence, rather than a cause, of enhanced growth (sink demand) and stimulated export of nonstructural carbohydrates in photosynthesizing leaves. The accumulation of nonstructural carbohydrates in leaves generally impairs chloroplast structure, thylakoid membranes, and the photosynthetic electron transport chain (Foyer, 1988; Pammenter et al., 1993; Paul and Foyer, 2001; Song et al., 2020). We observed similar LNT-linked damage to peanut chloroplast structure and thylakoid membranes (**Figures 3–8**). Interestingly, exogenous Ca^{2+} relieved LNT impairment to chloroplast structure, thylakoid membranes, and photosystems activities; Ca^{2+} can bind to extrinsic luminal protein PsbO and sustain the oxygen-evolving complex (OEC; Heredia and Rivas, 2003; Sasi et al., 2018). The high concentration of Ca^{2+} in the lumen of the thylakoid membrane would stabilize the OEC against photodamage during environmental stress (Takahashi and Murata, 2008). In the present study, exogenous Ca^{2+} priming reduced Y(NO) undergoing short-term LNT stress, whereas short-term LNT and LNT + TFP resulted in an increase of Y(NO) indirectly (**Figure 6C**). It is known that Ca^{2+} application affects the expression of LHC stress-related protein 3, which is crucial for the energy-dependent component of NPQ (Terashima et al., 2012). In addition, exogenous Ca^{2+} can enhance the activities of several key enzymes in the Calvin-Benson-Bassham cycle, improving CEF and the PSII reaction center activity (Terashima et al., 2012; Hochmal et al., 2015). Our data suggested that Ca^{2+} priming helped to reduce damage to the PSI acceptor-side of the short-term LNT-stressed leaves by inducing a rapid increase in the CEF rate, thereby protecting the PSI reaction center (**Figures 6E, 7C,D**). More research is

needed to ascertain the molecular changes associated with short and long-term LNT stress and the associated CEF pathway (i.e., the PGR5/PGRL1- or NDH-dependent CEF pathway) during Ca^{2+} priming.

We found that exogenous application of a CaM inhibitor (TFP) caused further downregulation of leaf physiology and additional growth inhibition (**Figures 1**–**3**). The LNT + TFP treatment caused a significant increase of soluble sugar, starch, and total nonstructural carbohydrate concentrations, relative to LNT (**Figure 2**). TFP enters plant cells through the cell membrane and prevents the formation of a Ca^{2+}–CaM complex, which is essential for the functional CaM-linked signaling pathways during abiotic stress (Hepler, 2005; Liu et al., 2013). The Ca^{2+}–CaM complex may play an important role in facilitating Ca^{2+} signal transduction to alleviate nocturnal chilling-dependent feedback inhibition of photosynthesis under short-term and long-term LNT stress. More research is needed to unravel the specific molecular mechanism(s) underpinning the Ca^{2+}–CaM complex formation and signaling events during LNT stress.

Taken together, we show that exogenous Ca^{2+} alleviated nocturnal chilling-dependent feedback inhibition of photosynthesis. The impairment of the photosynthetic apparatus was prevented by improving sink demand through the continued export of nonstructural carbohydrates during exogenous Ca^{2+} priming.

CONCLUSION

Both short-term (11 HoL) and long-term (1, 6, and 11 DoL) LNT stress inhibited peanut growth, leaf nonstructural carbohydrates export, and photosynthetic processes. Even a short-term LNT stress altered photosystems activities, thylakoid electron transport, and chloroplast morphology by causing significant accumulation of nonstructural carbohydrates in leaves. Our findings demonstrate that exogenous Ca^{2+} alleviated LNT-dependent feedback inhibition of photosynthesis by improving sink demand and facilitating nonstructural carbohydrate export from chloroplasts. In addition, Ca^{2+} priming reduced damage to the foliar photosynthetic electron transport chain by stimulating CEF and reducing the ΔpH. The poorer growth performance of TFP-pretreated seedlings than LNT-stressed seedlings confirmed the role of Ca^{2+} in alleviating LNT stress. These observations confirm the involvement of CaM in this Ca^{2+} priming restorative effect against LNT stress.

DATA AVAILABILITY STATEMENT

The original contributions presented in the study are included in the article/**Supplementary Material**, further inquiries can be directed to the corresponding author.

AUTHOR CONTRIBUTIONS

YL, TL, and XH designed the experiment. DW, CB, and SZ conducted the experiment and collected data for preliminary analysis. YL, JP, XL, ZS, and JS further analyzed the data and prepared the manuscript. HL, JP, JY, YC, and KS revised the manuscript. All authors contributed to the article and approved the submitted version.

FUNDING

This research was funded by the Natural Science Foundation of China (Project No. 31772391 and 31301842) and National Peanut Research System (Project No. CARS-13- Nutrient Management).

ACKNOWLEDGMENTS

This study was carried out with support from the National Key Research and Development Plan (Project No. 2018YFD0201206), Sheng Jing Talents Project (Project No. RC170338), and China Scholarship Council Project.

SUPPLEMENTARY MATERIAL

The Supplementary Material for this article can be found online at: https://www.frontiersin.org/articles/10.3389/fpls.2020.607029/full#supplementary-material

REFERENCES

Adams, W. W., Muller, O., Cohu, C. M., and Demmig-Adams, B. (2013). May photoinhibition be a consequence, rather than a cause, of limited plant productivity? *Photosynth. Res.* 117, 31–34. doi: 10.1007/s11120-013-9849-7

Ai, X. Z., Wang, X. F., Cui, Z. F., and Wang, Z. L. (2006). Effect of calcium on photosynthesis of cucumber under low light intensity and sub-optimal temperature. *Sci. China Chem.* 39, 1865–1871.

Ali, G. S., Reddy, V. S., Lindgren, P. B., Jakobek, J. L., and Reddy, A. S. N. (2003). Differential expression of genes encoding calmodulin-binding proteins in response to bacterial pathogens and inducers of defence responses. *Plant Mol. Biol.* 51, 803–815. doi: 10.1023/A:1023001403794

Allen, D. J., and Ort, D. R. (2001). Impacts of chilling temperatures on photosynthesis in warm-climate plants. *Trends Plant Sci.* 6, 36–42. doi: 10.1016/S1360-1385(00)01808-2

Allen, D. J., Ratner, K., Giller, Y. E., Gussakovsky, E. E., Shahak, Y., and Ort, D. R. (2000). An overnight chill induces a delayed inhibition of photosynthesis at midday in mango (*Mangifera indica L.*). *J. Exp. Bot.* 51, 1893–1902. doi: 10.1093/jexbot/51.352.1893

Anil, V. S., and Rao, K. S. (2001). Calcium-mediated signal transduction in plants: a perspective on the role of Ca^{2+} and CDPKs during early plant development. *J. Plant Physiol.* 158, 1237–1256. doi: 10.1078/0176-1617-00550

Bagnall, D. J., King, R. W., and Farquhar, G. D. (1988). Temperature-dependent feedback inhibition of photosynthesis in peanut. *Planta* 175, 348–354. doi: 10.1007/BF00396340

Baker, N. R. (2008). Chlorophyll fluorescence: a probe of photosynthesis in vivo. *Annu. Rev. Plant Biol.* 59, 89–113. doi: 10.1146/annurev.arplant.59.032607.092759

Bauer, H., Wierer, R., Hatheway, W. H., and Larcher, W. (2006). Photosynthesis of *Coffea arabica* after chilling. *Physiol. Plant.* 64, 449–454. doi: 10.1111/j.1399-3054.1985.tb08521.x

Beckers, G. J. M., and Conrath, U. (2007). Priming for stress resistance: from the lab to the field. *Curr. Opin. Plant Biol.* 10, 425–431. doi: 10.1016/j.pbi.2007.06.002

Bertioli, D. J., Cannon, S. B., Froenicke, L., Huang, G., Farmer, A. D., Cannon, E. K. S., et al. (2016). The genome sequences of *Arachis duranensis* and *Arachis ipaensis*, the diploid ancestors of cultivated peanut. *Nat. Genet.* 48, 438–446. doi: 10.1038/ng.3517

Bhattacharjee, S. (2009). Involvement of calcium and calmodulin in oxidative and temperature stress of *Amaranthus lividus* L. during early germination. *J. Environ. Biol.* 30, 557–562.

Brauer, M., Sanders, D., and Stitt, M. (1990). Regulation of photosynthetic sucrose synthesis: a role for calcium? *Planta* 182, 236–243. doi: 10.1007/BF00197117

Chen, X. M., Zheng, G. S., and Zhang, S. W. (2001). Effect of Ca^{2+} on photosynthetic characteristics of a tree peony in the protective field. *Acta Hortic. Sin.* 28, 572–574.

Cohu, C. M., Muller, O., Adams, W. W., and Demmig-Adams, B. (2014). Leaf anatomical and photosynthetic acclimation to cool temperature and high light in two winter versus two summer annuals. *Physiol. Plant.* 152, 164–173. doi: 10.1111/ppl.12154

Cramer, W., Guiot, J., Fader, M., Garrabou, J., Gattuso, J. -P., Iglesias, A., et al. (2018). Climate change and interconnected risks to sustainable development in the Mediterranean. *Nat. Clim. Chang.* 8, 972–980. doi: 10.1038/s41558-018-0299-2

Dias, P. M. B., Brunel-Muguet, S., Dürr, C., Huguet, T., Demilly, D., and Wagner, M. H. (2011). QTL analysis of seed germination and pre-emergence growth at extreme temperatures in *Medicago truncatula*. *Theor. Appl. Genet.* 122, 429–444. doi: 10.1007/s00122-010-1458-7

Dong, H. S., Myoung-Goo, C., Hyun, K. L., Misuk, C., Sang-Bong, C., Giltsu, C., et al. (2013). Calcium dependent sucrose uptake links sugar signaling to anthocyanin biosynthesis in *Arabidopsis*. *Biochem. Biophys. Res. Commun.* 430, 634–639. doi: 10.1016/j.bbrc.2012.11.100

Eckardt, N. A. (2001). A calcium-regulated gatekeeper in phloem sieve tubes. *Plant Cell* 13, 989–992. doi: 10.1105/tpc.13.5.989

Foyer, C. H. (1988). Feedback inhibition of photosynthesis through source-sink regulation in leaves. *Plant Physiol. Biochem.* 26, 483–492.

Gounaris, Y. (2001). A qualitative model for the mechanism of sugar accumulation in cold-stressed plant tissues. *Theory Biosci.* 120, 149–165. doi: 10.1007/s12064-001-0014-z

Guo, Y. H., and Cao, K. F. (2004). Effect of the night chilling on photosynthesis of two coffee species grown under different irradiances. *J. Hortic. Sci. Biotechnol.* 79, 713–716. doi: 10.1080/14620316.2004.11511831

Hajihashemi, S., Noedoost, F., Geuns, J. M. C., Djalovic, I., and Siddique, K. H. M. (2018). Effect of cold stress on photosynthetic traits, carbohydrates, morphology, and anatomy in nine cultivars of *Stevia rebaudiana*. *Front. Plant Sci.* 9:1430. doi: 10.3389/fpls.2018.01430

Hao, J. H., Gu, F., Zhu, J., Lu, S., Liu, Y., Li, Y., et al. (2016). Low night temperature affects the phloem ultrastructure of lateral branches and raffinose family oligosaccharide (RFO) accumulation in RFO-transporting plant melon (*Cucumis melo* L.) during fruit expansion. *PLoS One* 11:e0160909. doi: 10.1371/journal.pone.0160909

Hendrix, D. L. (1993). Rapid extraction and analysis of nonstructural carbohydrates in plant tissues. *Crop Sci.* 33, 1306–1311. doi: 10.2135/cropsci1993.0011183X003300060037x

Hepler, P. K. (2005). Calcium: a central regulator of plant growth and development. *Plant Cell* 17, 2142–2155. doi: 10.1105/tpc.105.032508

Heredia, P., and Rivas, J. D. L. (2003). Calcium-dependent conformational change and thermal stability of the isolated *PsbO* protein detected by FTIR spectroscopy. *Biochemist* 42, 11831–11838. doi: 10.1021/bi034582j

Hochmal, A. K., Schulze, S., Trompelt, K., and Hippler, M. (2015). Calcium-dependent regulation of photosynthesis. *Biochim. Biophys. Acta* 1847, 993–1003. doi: 10.1016/j.bbabio.2015.02.010

Ivanov, A. G., Sane, P. V., Zeinalov, Y., Malmberg, G., Gardeström, P., Huner, N. P. A., et al. (2001). Photosynthetic electron transport adjustments in overwintering scots pine (*Pinus sylvestris* L.). *Planta* 213, 575–585. doi: 10.1007/s004250100522

Jiang, F. Y., Li, Y., and Weng, B. Q. (2002). Review on the physiology of chilling stress and chilling resistance of plants. *Fujian Agric. Sci. Tech.* 17, 190–195. doi: 10.19303/j.issn.1008-0384.2002.03.016

Joham, H. E. (1957). Carbohydrate distribution as affected by a calcium deficiency in cotton. *Plant Physiol.* 32, 113–117. doi: 10.1104/pp.32.2.113

Kader, M. A., and Lindberg, S. (2010). Cytosolic calcium and pH signaling in plants under salinity stress. *Plant Signal. Behav.* 5, 233–238. doi: 10.4161/psb.5.3.10740

Kasuga, M., Miura, S., Shinozaki, K., and Yamaguchi-Shinozaki, K. (2004). A combination of the *Arabidopsis DREB1A* gene and stress-inducible *rd29A* promoter improved drought—and low—temperature stress tolerance in tobacco by gene transfer. *Plant Cell Physiol.* 45, 346–350. doi: 10.1093/pcp/pch037

Knight, H., Trewavas, A. J., and Knight, M. R. (1996). Cold calcium signaling in *Arabidopsis* involves two cellular pools and a change in calcium signature after acclimation. *Plant Cell* 8, 489–503. doi: 10.1105/tpc.8.3.489

Knight, H., Trewavas, A. J., and Knight, M. R. (1997). Calcium signalling in *Arabidopsis thaliana* responding to drought and salinity. *Plant J.* 12, 1067–1078. doi: 10.1046/j.1365-313X.1997.12051067.x

Koch, K. E. (1996). Carbohydrate-modulated gene expression in plants. *Annu. Rev. Plant Physiol. Plant Mol. Biol.* 47, 509–540. doi: 10.1146/annurev.arplant.47.1.509

Lambers, H., Costa, P. D. B., Oliveira, R. S., and Silveira, F. A. O. (2020). Towards more sustainable cropping systems: lessons from native *Cerrado* species. *Theor. Exp. Plant Physiol.* 32, 175–195. doi: 10.1007/s40626-020-00180-z

Lambers, H., and Oliveira, R. S. (2019). *Plant physiological ecology*. *3rd Edn*. Switzerland, AG: Springer Nature Press.

Latef, A. A. H. A., and He, C. (2011). *Arbuscular mycorrhizal* influence on growth, photosynthetic pigments, osmotic adjustment and oxidative stress in tomato plants subjected to low-temperature stress. *Acta Physiol. Plant.* 33, 1217–1225. doi: 10.1007/s11738-010-0650-3

La Verde, V., Dominici, P., and Astegno, A. (2018). Towards understanding plant calcium signaling through calmodulin-like proteins: a biochemical and structural perspective. *Int. J. Mol. Sci.* 19:1331. doi: 10.3390/ijms19051331

Li, H., Liu, S. S., Yi, C. Y., Wang, F., Zhou, J., Xia, X. J., et al. (2014). Hydrogen peroxide mediates abscisic acid-induced *HSP70* accumulation and heat tolerance in grafted cucumber plants. *Plant Cell Environ.* 37, 2768–2780. doi: 10.1111/pce.12360

Li, L. J., Lu, X. C., Ma, H. Y., and Lyu, D. G. (2017a). Jasmonic acid regulates the ascorbate—glutathione cycle in *Malus baccata* Borkh. Roots under low root-zone temperature. *Acta Physiol. Plant.* 39:174. doi: 10.1007/s11738-017-2469-7

Li, L. J., Su, H., Ma, H. Y., and Lyu, D. G. (2017b). Differential proteomic analysis reveals the effect of calcium on *Malus baccata* Borkh. Leaves under temperature stress. *Int. J. Mol. Sci.* 18:1755. doi: 10.3390/ijms18081755

Liu, Y. F. (2020). Calcium chemical priming might play a significant role in relieving overnight chilling-dependent inhibition of photosynthesis in crops: a review. *Basic Clin. Pharmacol. Toxicol.* 126, 109–110.

Liu, Y. F., Han, X. R., Zhan, X. M., Yang, J. F., Wang, Y. Z., Song, Q. B., et al. (2013). Regulation of calcium on peanut photosynthesis under low night temperature stress. *J. Integr. Agric.* 12, 2172–2178. doi: 10.1016/S2095-3119(13)60411-6

Liu, Y. F., Qi, M. F., and Li, T. L. (2012). Photosynthesis, photoinhibition, and antioxidant system in tomato leaves stressed by low night temperature and their subsequent recovery. *Plant Sci.* 196, 8–17. doi: 10.1016/j.plantsci.2012.07.005

Liu, Y. F., Zhang, G. X., Qi, M. F., and Li, T. L. (2015). Effects of calcium on photosynthesis, antioxidant system, and chloroplast ultrastructure in tomato leaves under low night temperature stress. *J. Plant Growth Regul.* 34, 263–273. doi: 10.1007/s00344-014-9462-9

Lu, Y. Q., Liu, H. P., Wang, Y., Zhang, X. Z., and Han, Z. H. (2013). Synergistic roles of leaf boron and calcium during the growing season in affecting sugar and starch accumulation in ripening apple fruit. *Acta Physiol. Plant.* 35, 2483–2492. doi: 10.1007/s11738-013-1283-0

Lu, J. Z., Wang, Z. Q., Yang, X. L., Wang, F., Qi, M. F., Li, T. L., et al. (2020). Cyclic electron flow protects photosystem I donor side under low night temperature in tomato. *Environ. Exp. Bot.* 177:104151. doi: 10.1016/j.envexpbot.2020.104151

Maxwell, S. L., Butt, N., Maron, M., McAlpine, C. A., Chapman, S., Ullmann, A., et al. (2019). Conservation implications of ecological responses to extreme weather and climate events. *Divers. Distrib.* 25, 613–625. doi: 10.1111/ddi.12878

Michard, E., Lima, P. T., Borges, F., Silva, A. C., Portes, M. T., Carvalho, J. E., et al. (2011). Glutamate receptor-like genes form Ca^{2+} channels in pollen tubes and are regulated by pistil D-serine. *Science* 332, 434–437. doi: 10.1126/science.1201101

Monshausen, G. B., Miller, N. D., Murphy, A. S., and Gilroy, S. (2011). Dynamics of auxin-dependent Ca^{2+} and pH signaling in root growth revealed by integrating high-resolution imaging with automated computer vision-based analysis. *Plant J.* 65, 309–318. doi: 10.1111/j.1365-313X.2010.04423.x

Navazio, L., Formentin, E., Cendron, L., and Szabo, I. (2020). Chloroplast calcium signalling in the spotlight. *Front. Plant Sci.* 11:186. doi: 10.3389/fpls.2020.00186

Nir, G., Ratner, K., Gussakovsky, E. E., and Shahak, Y. (1997). Photoinhibition of photosynthesis in mango leaves: effect of chilly nights. *Acta Hortic.* 455, 228–235. doi: 10.17660/actahortic.1997.455.30

Ohto, M., and Nakamura, K. (1995). Sugar-induced increase of calcium-dependent protein kinases associated with the plasma membrane in leaf tissues of tobacco. *Plant Physiol.* 109, 973–981. doi: 10.1104/pp.109.3.973

Ortiz-Ramírez, C., Michard, E., Simon, A. A., Damineli, D. S. C., Hernández-Coronado, M., Becker, J. D., et al. (2017). Glutamate receptor-like channels are essential for chemotaxis and reproduction in mosses. *Nature* 549, 91–95. doi: 10.1038/nature23478

Pammenter, N. W., Loreto, F., and Sharkey, T. D. (1993). End product feedback effects on photosynthetic electron transport. *Photosynth. Res.* 35, 5–14. doi: 10.1007/BF02185407

Paul, M. J., and Foyer, C. H. (2001). Sink regulation of photosynthesis. *J. Exp. Bot.* 52, 1383–1400. doi: 10.1093/jexbot/52.360.1383

Paul, M. J., and Pellny, T. K. (2003). Carbon metabolite feedback regulation of leaf photosynthesis and development. *J. Exp. Bot.* 54, 539–547. doi: 10.1093/jxb/erg052

Powles, S. B., Berry, J. A., and BjÖRkman, O. (1983). Interaction between light and chilling temperature on the inhibition of photosynthesis in chilling-sensitive plants. *Plant Cell Environ.* 6, 117–123. doi: 10.1111/j.1365-3040.1983.tb01884.x

Prasad, P. V. V., Boote, K. J., Allen, L. H. Jr., and Thomas, J. M. G. (2003). Super-optimal temperatures are detrimental to peanut (*Arachis hypogaea* L.) reproductive processes and yield at both ambient and elevated carbon dioxide. *Glob. Chang. Biol.* 9, 1775–1787. doi: 10.1046/j.1365-2486.2003.00708.x

Price, A. H., Taylor, A., Ripley, S. J., Griffiths, A., Trewavas, A. J., and Knight, M. R. (1994). Oxidative signals in tobacco increase cytosolic calcium. *Plant Cell* 6, 1301–1310. doi: 10.1105/tpc.6.9.1301

Rufty, T. W., and Huber, S. C. (1983). Changes in the starch formation and activities of sucrose phosphate synthase and cytoplasmic fructose-1,6-bisphosphatase in response to source-sink alterations. *Plant Physiol.* 72, 474–480. doi: 10.1104/pp.72.2.474

Sasi, S., Venkatesh, J., Daneshi, R. F., and Gururani, M. A. (2018). Photosystem II extrinsic proteins and their putative role in abiotic stress tolerance in higher plants. *Plan. Theory* 7:100. doi: 10.3390/plants7040100

Savitch, L. V., Ivanov, A. G., Gudynaite-Savitch, L., Huner, N. P., and Simmonds, J. (2011). Cold stress effects on PSI photochemistry in *Zea mays*: differential increase of FQR-dependent cyclic electron flow and functional implications. *Plant Cell Physiol.* 52, 1042–1054. doi: 10.1093/pcp/pcr056

Savvides, A., Ali, S., Tester, M., and Fotopoulos, V. (2016). Chemical priming of plants against multiple abiotic stresses: mission possible? *Trends Plant Sci.* 21, 329–340. doi: 10.1016/j.tplants.2015.11.003

Schreiber, U., and Klughammer, C. (2008). New accessory for the dual-PAM-100: the P515/535 module and examples of its application. *PAM Appl. Notes* 1, 1–10.

Shi, Q., Pang, J., Yong, J. W. H., Bai, C., Pereira, C. G., Song, Q., et al. (2019). Phosphorus-fertilisation has differential effects on leaf growth and photosynthetic capacity of *Arachis hypogaea* L. *Plant Soil* 447, 99–116. doi: 10.1007/s11104-019-04041-w

Solanke, A. U., and Sharma, A. K. (2008). Signal transduction during cold stress in plants. *Physiol. Mol. Biol. Plants* 14, 69–79. doi: 10.1007/s12298-008-0006-2

Song, Q. B., Liu, Y. F., Pang, J. Y., Yong, J. W., Chen, Y. L., Bai, C. M., et al. (2020). Supplementary calcium restores peanut (*Arachis hypogaea*) growth and photosynthetic capacity under low nocturnal temperature. *Front. Plant Sci.* 10:1637. doi: 10.3389/fpls.2019.01637

Strand, A., Hurry, V., Henkes, S., Huner, N., Gustafsson, P., Gardestrom, P., et al. (1999). Acclimation of *Arabidopsis* leaves developing at low temperatures. Increasing cytoplasmic volume accompanies increased activities of enzymes in the Calvin cycle and in the sucrose-biosynthesis pathway. *Plant Physiol.* 119, 1387–1398. doi: 10.1104/pp.119.4.1387

Subbaiah, C. C., Bush, D. S., and Sachs, M. M. (1994). Elevation of cytosolic calcium precedes anoxic gene expression in maize suspension-cultured cells. *Plant Cell* 6, 1747–1762. doi: 10.1105/tpc.6.12.1747

Suzuki, K., Ohmori, Y., and Ratel, E. (2011). High root temperature blocks both linear and cyclic electron transport in the dark during chilling of the leaves of rice seedlings. *Plant Cell Physiol.* 52, 1697–1707. doi: 10.1093/pcp/pcr104

Takahashi, S., and Murata, N. (2008). How do environmental stresses accelerate photoinhibition? *Trends Plant Sci.* 13, 178–182. doi: 10.1016/j.tplants.2008.01.005

Tardieu, F., Granier, C., and Muller, B. (1999). Modelling leaf expansion in a fluctuating environment: are changes in specific leaf area a consequence of changes in expansion rate? *New Phytol.* 143, 33–34. doi: 10.1046/j.1469-8137.1999.00433.x

Terashima, M., Petroutsos, D., Hüdig, M., Tolstygina, I., Trompelt, K., Gäbelein, P., et al. (2012). Calcium-dependent regulation of cyclic photosynthetic electron transfer by a CAS, ANR1, and PGRL1 complex. *PNAS* 109, 17717–17722. doi: 10.1073/pnas.1207118109

Thor, K. (2019). Calcium-nutrient and messenger. *Front. Plant Sci.* 10:440. doi: 10.3389/fpls.2019.00440

Urban, L., and Alphonsout, L. (2007). Girdling decreases photosynthetic electron fluxes and induces sustained photoprotection in mango leaves. *Tree Physiol.* 27, 345–352. doi: 10.1093/treephys/27.3.345

Van Heerden, P. D. R., Strasser, R. J., and Krüger, G. H. J. (2004). Reduction of dark chilling stress in N_2-fixing soybean by nitrate as indicated by chlorophyll *a* fluorescence kinetics. *Physiol. Plant.* 121, 239–249. doi: 10.1111/j.0031-9317.2004.0312.x

Wan, S. B. (2003). *Peanut cultivation in China*. Shanghai: Shanghai Science and Technology Press.

Whiley, A. W. (1999). Cool orchard temperatures or growing trees in containers can inhibit leaf gas exchange of avocado and mango. *J. Amer. Soc. Hort. Sci.* 124, 46–51. doi: 10.21273/JASHS.124.1.46

White, P. J., and Broadley, M. R. (2003). Calcium in plants. *Ann. Bot.* 92, 487–511. doi: 10.1093/aob/mcg164

Yang, S., Wang, F., Guo, F., Meng, J. J., Li, X. G., Dong, S. T., et al. (2013). Exogenous calcium alleviates photoinhibition of PSII by improving the xanthophyll cycle in peanut (*Arachis hypogaea*) leaves during heat stress under high irradiance. *PLoS One* 8:e71214. doi: 10.1371/journal.pone.0071214

Yang, X., Xu, H., Shao, L., Li, T., Wang, Y., and Wang, R. (2018). The response of photosynthetic capacity of tomato leaves to different LED light wavelength. *Environ. Exp. Bot.* 150, 161–171. doi: 10.1016/j.envexpbot.2018.03.013

You, J. H., Lu, J. M., and Yang, W. J. (2002). Effects of Ca^{2+} on photosynthesis and related physiological indexes of wheat seedlings under low-temperature stress. *Acta Agron. Sin.* 28, 693–696.

Zhang, Y., Cruickshanks, N., Yuan, F., Wang, B., Pahuski, M., Wulfkuhle, J., et al. (2017). Targetable T-type calcium channels drive glioblastoma. *Cancer Res.* 77, 3479–3490. doi: 10.1158/0008-5472.CAN-16-2347

Zhang, G. X., Liu, Y. F., Ni, Y., Meng, Z. J., Lu, T., and Li, T. L. (2014). Exogenous calcium alleviates low night temperature stress on the photosynthetic apparatus of tomato leaves. *PLoS One* 9:e97322. doi: 10.1371/journal.pone.0097322

Zhang, Z. S., Yang, C., Gao, H. Y., Wang, W. W., Sun, X. J., Meng, X. L., et al. (2012). Effects of cucumber leaf's PSII activity and electron transfer on its PSI activity in the recovery process after chilling-induced photoinhibition. *Chin. J. Appl. Ecol.* 23, 1049–1054.

Conflict of Interest: The authors declare that the research was conducted in the absence of any commercial or financial relationships that could be construed as a potential conflict of interest.

frontiers in Plant Science

ORIGINAL RESEARCH
published: 11 February 2021
doi: 10.3389/fpls.2020.614360

Time Lag Between Light and Heat Diurnal Cycles Modulates *CIRCADIAN CLOCK ASSOCIATION 1* Rhythm and Growth in *Arabidopsis thaliana*

*Kosaku Masuda[1,2], Tatsuya Yamada[1], Yuya Kagawa[1] and Hirokazu Fukuda[1]**

[1] Graduate School of Engineering, Osaka Prefecture University, Osaka, Japan, [2] Japan Society for the Promotion of Science, Tokyo, Japan

Plant growth responses to cues such as light, temperature, and humidity enable the entrainment of the circadian rhythms with diurnal cycles. For example, the temperature variations between day and night affect plant growth and accompany the time lag to light cycle. Despite its importance, there has been no systematic investigation into time lags, and the mechanisms behind the entrainment of the circadian rhythms with multiple cycles remain unknown. Here, we investigated systemically the effects of the time lag on the circadian rhythm and growth in *Arabidopsis thaliana*. To investigate the entrainment status of the circadian clock, the rhythm of the clock gene *CIRCADIAN CLOCK ASSOCIATION 1* (*CCA1*) was measured with a luciferase reporter assay. As a result, the rhythm was significantly modulated by the time lag with +10°C heating for 4 h every day but not −10°C cooling. A model based on coupled cellular oscillators successfully described these rhythm modulations. In addition, seedling growth depended on the time lag of the heating cycle but not that of the cooling cycle. Based on the relationship between the *CCA1* rhythms and growth, we established an estimation method for the effects of the time lag. Our results found that plant growth relates to the *CCA1* rhythm and provides a method by which to estimate the appropriate combination of light–dark and temperature cycles.

Keywords: circadian clock, dark cycle, entrainment, phase response curve, singularity response, synchronization

OPEN ACCESS

Edited by:
Péter Poór,
University of Szeged, Hungary

Reviewed by:
Xiaodong Xu,
Henan University, China
Antony Dodd,
John Innes Centre, United Kingdom

***Correspondence:**
Hirokazu Fukuda
fukuda@me.osakafu-u.ac.jp

Specialty section:
This article was submitted to Plant Physiology, a section of the journal Frontiers in Plant Science

Received: *05 October 2020*
Accepted: *24 December 2020*
Published: *11 February 2021*

Citation:
Masuda K, Yamada T, Kagawa Y and Fukuda H (2021) Time Lag Between Light and Heat Diurnal Cycles Modulates CIRCADIAN CLOCK ASSOCIATION 1 Rhythm and Growth in Arabidopsis thaliana. Front. Plant Sci. 11:614360. doi: 10.3389/fpls.2020.614360

INTRODUCTION

Organisms on earth have been found to have circadian clocks that are adapted to 24 h periods for environmental cycles. This includes plants, whose circadian clocks have important roles in various physiological processes, such as photosynthesis and flowering (Dodd et al., 2014; Creux and Harmer, 2019). The plant circadian clock responds to environmental changes and is entrained by the diurnal light–dark cycle (Webb et al., 2019). Entrainment to the light–dark cycle provides some advantages to plants, namely, circadian resonance, in which plants grow larger in an environment with periods that are similar to the intrinsic period of the circadian clock (Dodd et al., 2005; Higashi et al., 2015; Resco de Dios et al., 2016).

In nature and horticultural practices, the light–dark cycle is usually accompanied by a temperature cycle, which is associated with a day temperature that is higher than the night temperature. The temperature cycle is another strong entrainment cue (zeitgeber) for the plant circadian clock. In horticultural studies, the phase differences between light and temperature cycles have been found to have crucial effects on plant growth. Most plants exhibit optimal growth with the in-phase regime, in which the day temperature is higher than the night temperature (which we have termed +DIF) (Xiong et al., 2011, Xiao et al., 2018). The antiphase regime, that is, when the night temperature is higher than the day temperature (which we have termed −DIF), suppresses the elongation growth of the stems and the leaves of various plant species (Thingnaes et al., 2003; Xiong et al., 2011). Therefore, +DIF conditions are preferable for plant growth. However, time lags between light and temperature cycles can frequently occur due to unsettled weather. Furthermore, in horticultural facilities, the time lag is also artificially generated by supplemental lighting at night or cooling during the day (Anpo et al., 2018; Kozai et al., 2019). The spatial unevenness under lighting or air conditioning and the thermal conductivity of air and soil/water might also generate a spatial time lag in DIF. As such time lags might affect plant production yields, the elucidation of their effects is required to improve horticultural practices. However, there has been no systematic investigation into the time lag of temperature cycles and the entrainment behavior of circadian rhythms under dual-zeitgeber cycles.

Variations in the circadian rhythm due to environmental stimuli have been addressed using the phase response curve (PRC) (Johnson et al., 2003). The PRC describes the extent of phase shift as a function of the phase with a stimulus. This provides significant information for entrainment, for example, the entrainment range and stable locking phase for environmental cycles (Johnson et al., 2003; Granada et al., 2009). In previous studies, PRCs for darkness and temperature stimuli have been reported (Michael et al., 2003; Fukuda et al., 2008; Thines and Harmon, 2010). If the application duration of the stimulus is sufficiently short (e.g., heating for 4 h), the effect of the stimulus will be relatively weak on the circadian rhythm (Masuda et al., 2021). Consequently, the rhythm can be modulated to various forms by using weak stimuli. This modulation can be estimated numerically using a phase oscillator model (Fukuda et al., 2013). In contrast, if the duration of the applied stimulus is long, the effects are too strong to modulate the circadian rhythm into various forms. Therefore, to elucidate the rhythm modulation using dual zeitgebers, it is appropriate that the duration of the temperature stimuli be short.

In this study, the promoter activity rhythms of *CIRCADIAN CLOCK ASSOCIATED1* (*CCA1*) were measured to investigate the effects of time lags on the circadian rhythm. *CCA1* is one of the core clock genes of the plant circadian clock and is closely related to stress responses (Lai et al., 2012). In addition, the PRC of the *CCA1* rhythms for various stimuli have been measured in previous studies (Fukuda et al., 2008; Ohara et al., 2015; Masuda et al., 2017, 2021). We analyzed the *CCA1* rhythm in *Arabidopsis thaliana* under long-day conditions (L/D = 16/8 h) with periodic temperature stimuli (±10°C for 4 h). To elucidate the modulation of the *CCA1* rhythms using this time lag, we simulated numerically the rhythm using a phase oscillator model. In addition, we also measured the fresh weight of the seedlings and their leaf area to evaluate the effects of time lag on seedling growth.

MATERIALS AND METHODS

Measurement of *CCA1* Rhythms

To investigate the *CCA1* rhythms in each individual, we utilized transgenic *A. thaliana CCA1*::*LUC*, which carries luciferase reporters driven by the promoters of the clock gene *CCA1* (Nakamichi et al., 2004). Plants were grown on gellan gum-solidified Murashige–Skoog medium (MS Plant Salt Mixture, Wako Chemical Co.) at the standard concentration with 2% (w/v) sucrose in 40-mm-diameter dishes (one individual per dish) under L/D = 12/12 h and 100 μmol m^{-2} s^{-1} fluorescent white light at 22 ± 0.5°C for 7 days. The plants were treated with 500 μl of 1 mM luciferin (D-Luciferin Firefly, potassium salt, BIOSYNTH AG, in water) 24 h before the start of bioluminescence monitoring. Bioluminescence measurements were carried out using an automatic luminescence measuring system known as *Kondotron* with 20 plants under light-emitting diode (LED) illumination with a red LED (60 μmol m^{-2} s^{-1} light conditions, λ_p = 660 nm) and blue LED (15 μmol m^{-2} s^{-1} under light conditions, λ_p = 470 nm) at 22 ± 0.5°C for 7 days (Kondo et al., 1993; Fukuda et al., 2008). The photoperiod was set to L/D = 16/8 h, and the first dark period was started 16 h after the beginning of the measurements as an in-phase initial condition. Periodic temperature stimuli (+10 or −10°C from 22°C for 4 h within a 24 h period) were applied with four time lags (Δt = 2, 8, 14, and 20 h after turning on the light, referred to as "light on"), as shown in **Figure 1A**. In addition, as an antiphase initial condition, the first dark period was started 4 h after the measurements began, where the *CCA1* rhythm started with an inversed phase to the light–dark cycle. As controls, experiments were also performed using L/D = 16/8 h conditions under both in-phase and antiphase initial conditions at 22°C without temperature cycles. The heating and the control of the in-phase initial conditions were carried out once. The cooling and the control of the antiphase initial conditions were repeated two times. After measuring the bioluminescence, we measured plant size using both fresh weight of the areal part and projected leaf area (PLA) (**Figure 1B**), to evaluate the effects on productivity for commercial agriculture (Kozai et al., 2019).

Oscillation Analysis

Bioluminescence of the *CCA1* rhythm was initially normalized as follows:

$$\bar{l}_i = \frac{1}{2w+1} \sum_{k=-w}^{w} l_{i+k}, \quad (1)$$

$$L_i = (l_i - \bar{l}_i)/\bar{l}_i \quad (2)$$

where l_i is the ith time point of bioluminescence and $\bar{l}_i$ is the moving averaged bioluminescence (**Figure 1C**).

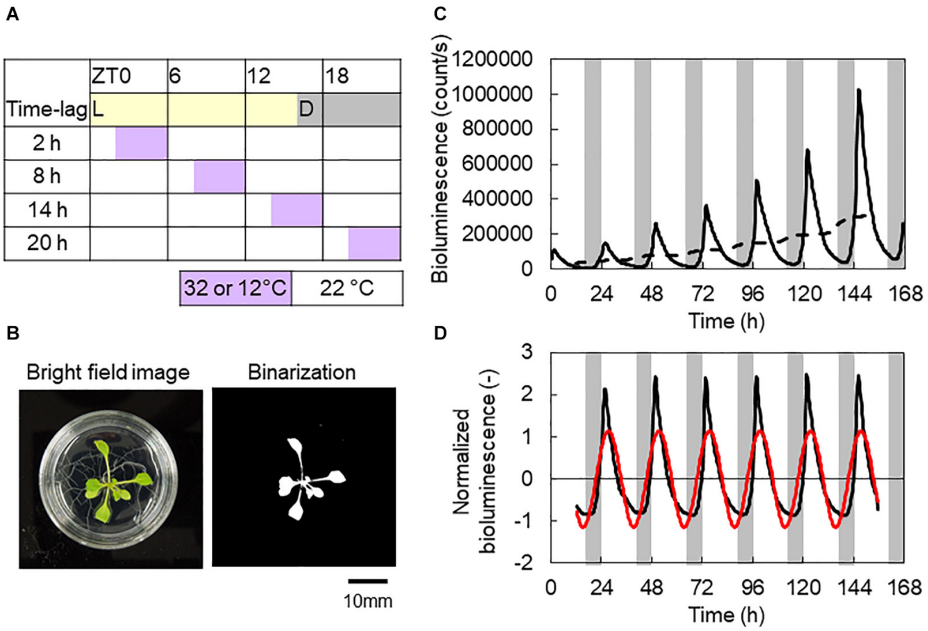

FIGURE 1 | Experimental conditions and representative analysis data. **(A)** Time table of L/D = 16/8 h and 4 h ± 10°C conditions. **(B)** Bright-field and binarization images of an *Arabidopsis thaliana* seedling. Projected leaf area (PLA) measured by banalization of the areal part. **(C)** Bioluminescence of a *CCA1::LUC* seedling. Solid and broken lines are raw data and its moving average, respectively. **(D)** Normalized bioluminescence (black line) and the first Fourier series (red line). Data were from control conditions with in-phase initial conditions **(B–D)**.

w is the half window size of the moving average. The measurement intervals were 20 min, so w was set to 36 for the 24 h window averaging. L_i is the normalized bioluminescence (**Figure 1D**).

Then, to determine the amplitude and phase of the *CCA1* rhythm, we obtained the first Fourier series, $A\cos\theta(t)$, of L_i (red cosine curve in **Figure 1D**). The first Fourier component was obtained with the following equations:

$$a_1 = \frac{2}{h-2w}\sum_{i=1+w}^{h-w} L_i \cos\left(2\pi\frac{i\Delta s}{T}\right),$$

$$b_1 = \frac{2}{h-2w}\sum_{i=1+w}^{h-w} L_i \sin\left(2\pi\frac{i\Delta s}{T}\right), \quad (3)$$

where T = 24 h and the measurement interval Δs = 1/3 h. h is the number of the time course data. Using a_1 and b_1, the amplitude A and phase $\theta(t)$ were determined as follows:

$$A = \sqrt{a_1^2 + b_1^2}, \quad (4)$$

$$\theta(t) = 2\pi\frac{t}{T} - \theta_1, \quad (5)$$

$$\theta_1 = \tan^{-1}\frac{b_1}{a_1}. \quad (6)$$

where θ_1 indicates the phase delay in the *CCA1* rhythm in response to the light–dark cycles, that is, the locking phase, which appeared at light-on [$\theta(0) = -\theta_1$]. We used the Tukey–Kramer test for multiple comparisons for A at a significance level of 0.05. We also used the Watson–Williams test with Bonferroni correction for multiple comparisons for θ_1 at a significance level of 0.05 (Watson and Williams, 1956). The mean of locking phase $\bar{\theta}_1$ (which is termed the circular mean) is defined as $\arg\{\frac{1}{N}\sum_{j=1}^{N} e^{i\theta_{1,j}}\}$, where $\theta_{1,j}$ is the locking phase (rad) of the jth individual.

Numerical Simulation of Circadian Rhythm Modulations

Since the plant circadian clock has an enormous number of cellular oscillators, the individual-level circadian rhythms represent synchronization among the oscillators (Fukuda et al., 2013). In addition, for the dual-zeitgeber cycles, each oscillator is modulated through the multiple phase responses. Therefore, the population dynamics of the cellular oscillators and their synchronization states are described as follows:

$$\frac{d\phi_j}{dt} = \omega_j + p_D(t)Z_D(\phi_j) + p_T(t)Z_T(\phi_j) + \frac{K}{N}\sum_{k=1}^{N}\sin(\phi_k - \phi_j), \quad (7)$$

$$R(t)\,e^{i\Phi(t)} = \frac{1}{N}\sum_{j=1}^{N} e^{i\phi_j(t)}, \quad (8)$$

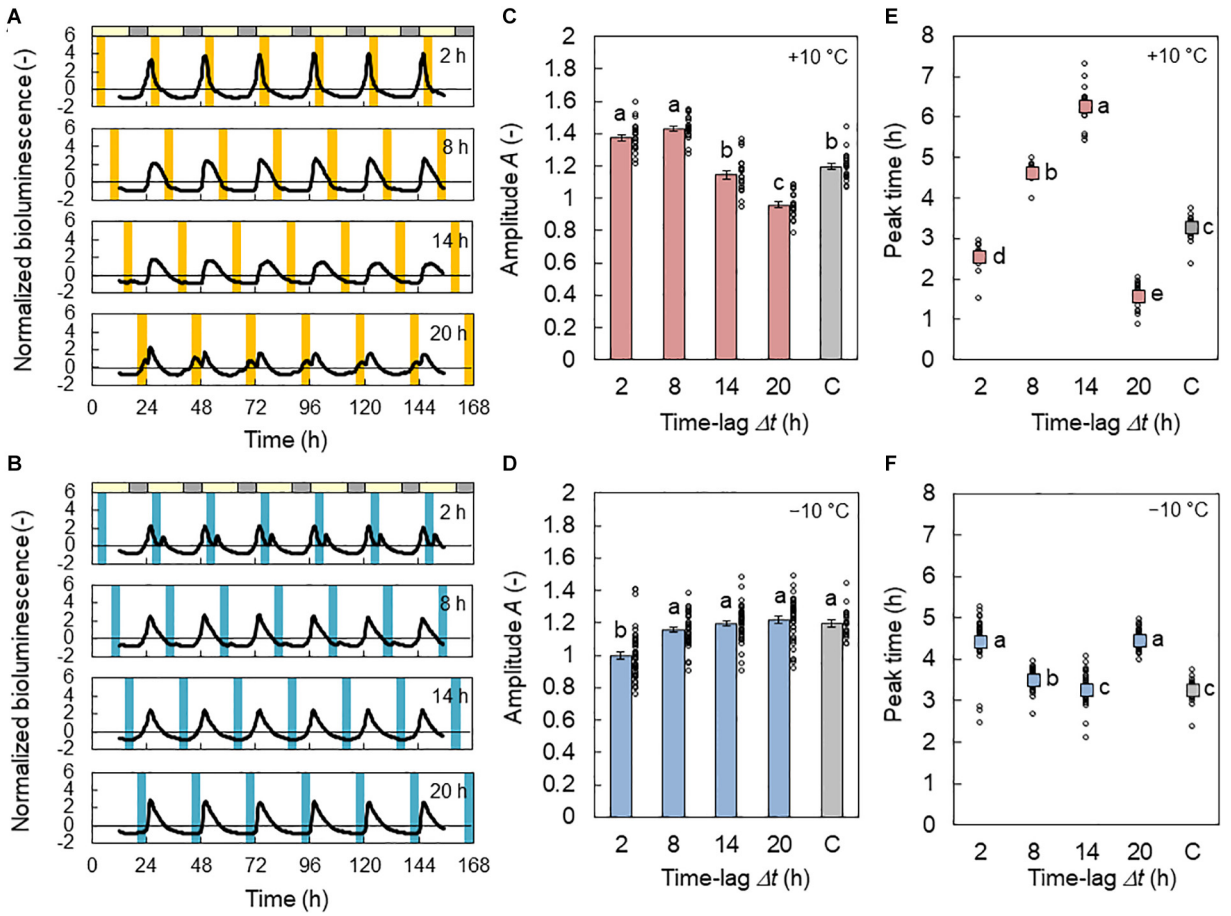

FIGURE 2 | Effect of time lag on the *CCA1* rhythm in conditions of L/D = 16/8 h and 4 h ± 10°C cycles for the in-phase initial conditions. **(A,B)** Normalized bioluminescence of *CCA1*::*LUC* in +10°C **(A)** and −10°C **(B)** conditions. **(C,D)** Amplitude *A* of the bioluminescence oscillation in +10°C **(C)** and −10°C **(D)** conditions (mean ± SEM, n = 20 individuals in +10°C, 40 in −10°C, and 20 in the control condition). The control condition is labeled C. The circles indicate the individual data points. Different letters indicate significant differences for each panel (Tukey–Kramer test, $p < 0.05$). **(E,F)** Peak time in +10°C **(E)** and −10°C **(F)** conditions (circular mean, n = 20 individuals in +10°C, 40 in −10°C, and 20 in the control condition). The circles indicate the individual data. Different letters indicate significant differences for each panel (Watson–Williams test with Bonferroni correction, $p < 0.05$).

where ϕ_j and ω_j are the phase and natural frequency of the jth oscillator, respectively. K represents the coupling strength, and N is the number of oscillators. ω_j takes a normal distribution with a standard deviation σ_ω and a mean value ω_0. $p_D(t)$ and $p_T(t)$ indicate the presence of stimulus for 8 h dark and 4 h +10°C or 4 h −10°C stimuli, respectively [$p(t)$ = 1 for stimulus on and $p(t)$ = 0 for stimulus off]. They are described as follows:

$$p_D(t) = \begin{cases} 1, & 16 + 24m \le t < 24 + 24m \\ 0, & other \end{cases} \quad (9)$$

$$p_T(t) = \begin{cases} 1, & \Delta t + 24m \le t < \Delta t + 4 + 24m \\ 0, & other \end{cases} \quad (10)$$

where m is an integer. $Z_D(\phi)$ and $Z_T(\phi)$ are the phase sensitivity functions for dark and temperature stimuli, respectively (Masuda et al., 2021). They are described using the same formula, as follows: $Z(\phi) = a\sin(\phi - \alpha)$. We used the previously obtained values of a and α for 8 h darkness and 4 h ± 10°C stimuli (Masuda et al., 2021). In addition, the collective rhythm X of the oscillators is denoted as $X(t) = \frac{1}{N}\sum_{j=1}^{N}\cos(\phi_j(t)) = R(t)\cos(\Phi(t))$, where $R(t)$ and $\Phi(t)$ correspond to the amplitude and phase of the individual-level rhythms, respectively. In this study, parameters were set as N = 1,000, K = 0.01, $\omega_0 = 2\pi/23\ h^{-1}$ rad, and $\sigma_\omega = 0.2\omega_0$.

RESULTS

Modulations of the *CCA1* Rhythms by the Temperature Cycles

In **Figure 2A**, the normalized bioluminescence of *CCA1*::*LUC* under L/D = 16/8 h with 4 h +10°C cycles is shown. At Δt = 8 h (+10°C in days), the rhythm was amplified (**Figure 2C**) from the basic amplitude, which was 1.20 when the temperature cycle was absent. In contrast, at Δt = 20 h (+10°C in late

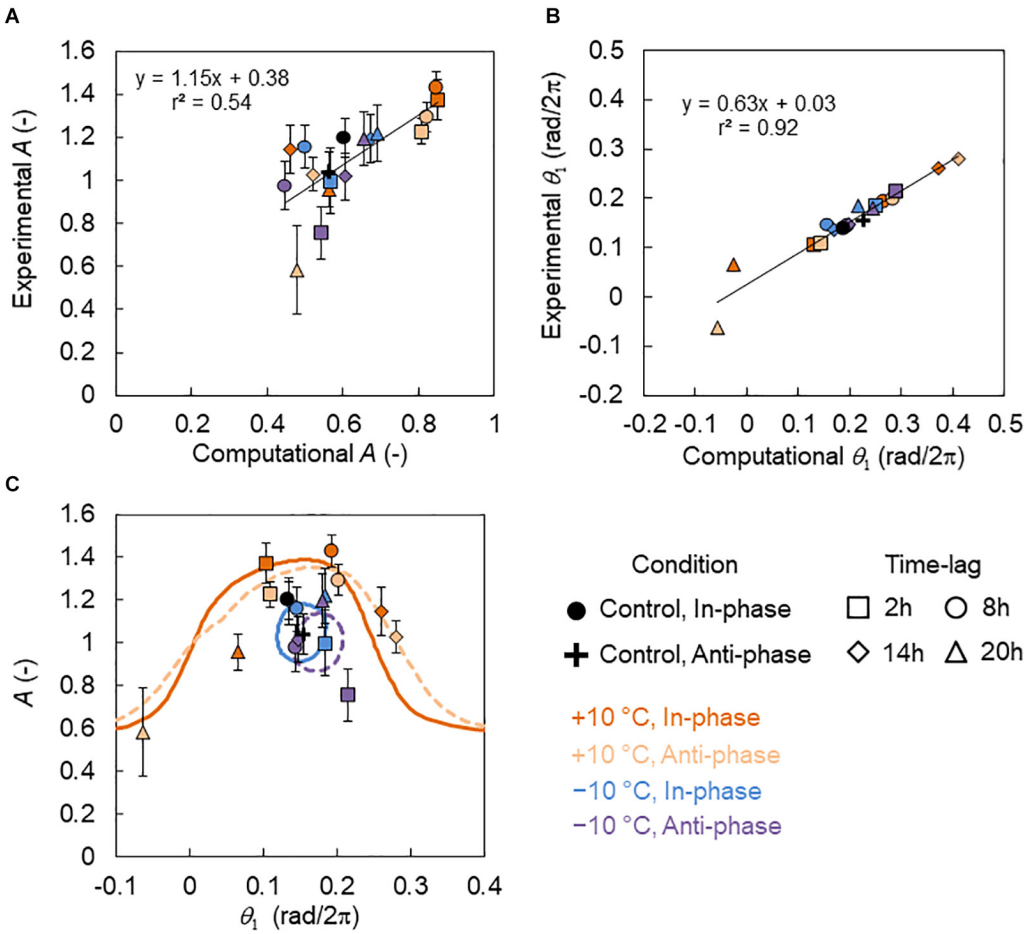

FIGURE 3 | Relationship between the amplitude and locking phase of the *CCA1* rhythms in the experiments and simulations. **(A)** Correlation between amplitudes A in the experiment and simulation (mean ± SD in experiment). **(B)** Correlation between the locking phase θ_1 in the experiment and the simulation (circular mean in experiment). The black lines indicate regression lines. **(C)** Relationship between A (mean ± SD) and θ_1 (circular mean). The symbols indicate the experimental data points. The colored lines indicate the relationship between A and θ_1 in the simulation. The solid lines indicate the in-phase conditions and the broken lines indicate the antiphase conditions. The simulation values of A and θ_1 were calibrated using the regression lines in **(A)** and **(B)** as $A_{calibrated} = 1.15A + 0.38$ and $\theta_{1,calibrated} = 0.63\theta_1 + 0.03$.

night), the *CCA1* rhythm was disturbed, and its amplitude was reduced. **Figure 2B** shows the *CCA1* rhythm under the cooling conditions (L/D = 16/8 h with 4 h −10°C cycles). Only at Δt = 2 h (−10°C in early days) was the *CCA1* rhythm disturbed and reduced (**Figure 2D**). When the amount of amplitude change is compared (the maximum value minus minimum value), the effect of the −10°C condition was 53% smaller than that of the +10°C condition.

The peak times for the *CCA1* rhythms are shown in **Figures 2E,F**. For the +10°C condition, at Δt = 2, 8, and 14 h, the peak appeared 2.5, 4.6, and 6.2 h after light on, respectively. Thus, the increment of Δt increased the phase delay of the *CCA1* rhythm. In contrast, at Δt = 20 h, the peak appeared after 1.6 h; that is, the phase delay substantially decreased. For the −10°C condition, at Δt = 2, 8, and 14 h, the peak appeared at 4.4, 3.5, and 3.3 h after light on, respectively. Thus, the increment of Δt provides a slight phase advance for the *CCA1* rhythm. However, at Δt = 20 h, the peak appeared at 4.4 h; that is, the phase delay was increased. The amount of phase change between the maximum and minimum values of the peak times at −10°C was also 75% smaller than that at +10°C. Under the antiphase initial conditions, the changes in A and peak time were similar to those under the in-phase initial conditions (**Supplementary Figure S1**), but a small effect of initial conditions was observed due to a transient in the first LD cycle.

Numerical Simulation of the Amplitude and Phase Modulations

We performed the numerical simulation using a phase oscillator model with PRCs (Eq. 7). **Figure 3A** shows the relationship between experimental and computational amplitudes A, and there was a high correlation (correlation coefficient r = 0.74, $p < 0.01$). However, experimental A was dispersed in the low-amplitude state ($A < 0.6$), indicating that amplitude estimation was difficult. **Figure 3B**, however, shows the relationship between

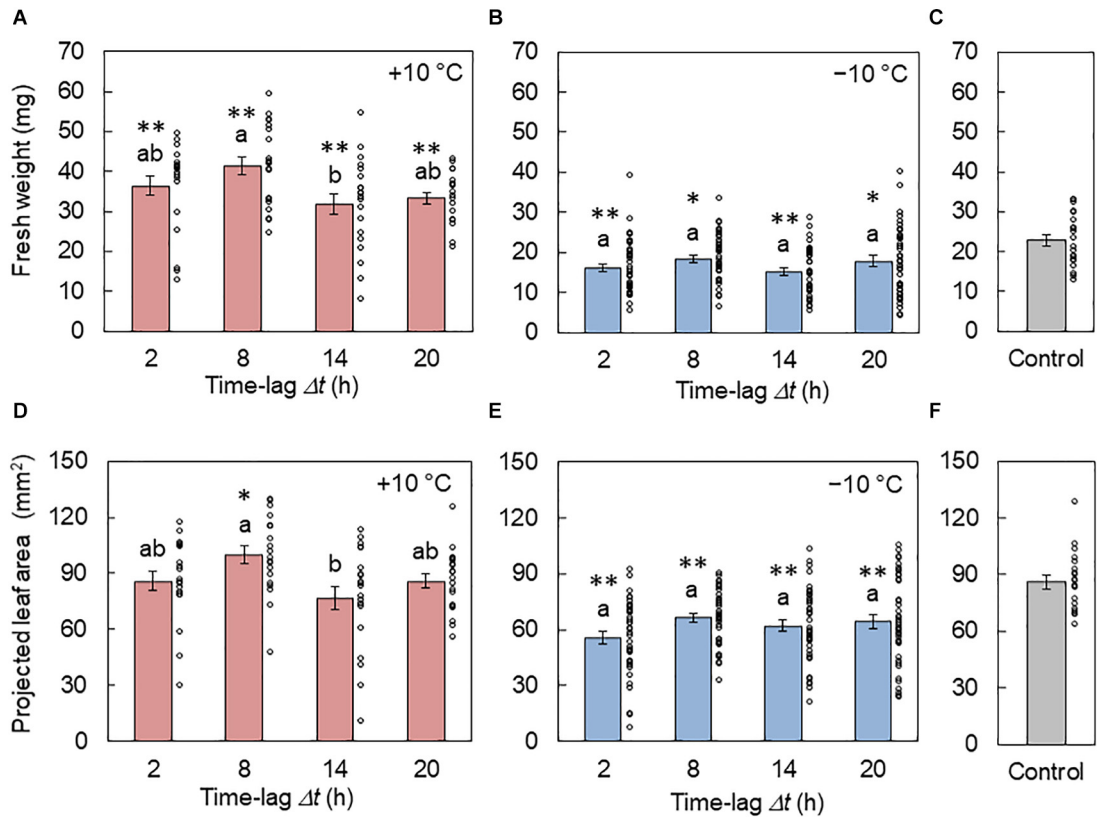

FIGURE 4 | Effect of the time lag on plant growth in conditions of L/D = 16/8 h and 4 h ± 10°C cycles. **(A–C)** Fresh weights of the areal part from the +10°C **(A)**, −10°C **(B)**, and control **(C)** conditions (mean ± SEM, n = 20 individuals in **(A)** and **(C)** and 40 in **(B)**). **(D–F)** Projected leaf areas from the +10°C **(D)**, −10°C **(E)**, and control **(F)** conditions (mean ± SEM, n = 20 individuals in **(D)** and **(F)** and 40 in **(E)**. The circles indicate the individual data points. Two conditions that do not have the same letter indicate significant differences for each panel (Tukey–Kramer test, $p < 0.05$). Asterisks indicate significant differences with the control condition (Welch's t-test, $^{*}p < 0.05$, $^{**}p < 0.01$).

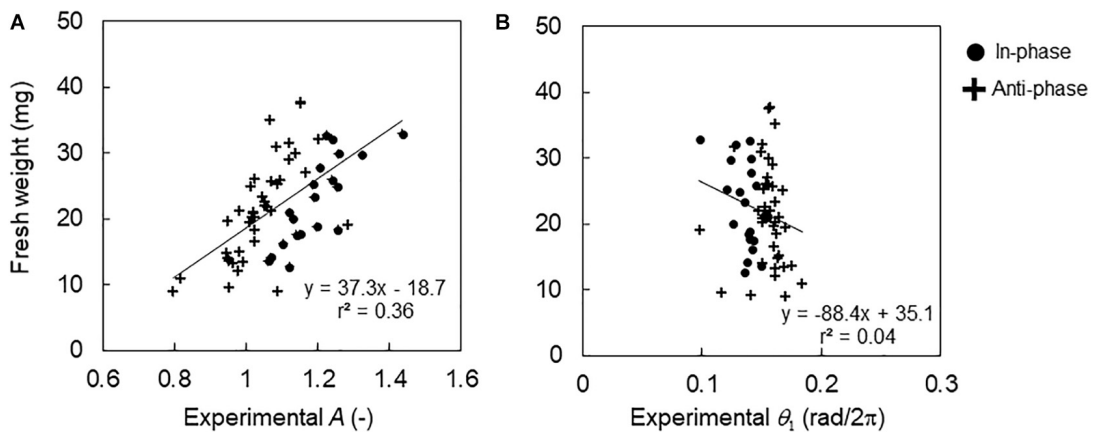

FIGURE 5 | Relationship between fresh weight and *CCA1* rhythms in the control conditions. **(A)** Relationship between fresh weight and amplitude A in individuals. **(B)** Relationship between fresh weight and locking phase θ_1 in the individuals. The black lines indicate regression lines.

the experimental and computational locking phase θ_1, and there was a very high correlation ($r = 0.96$, $p < 0.01$).

The relationship between A and θ_1 in the experiment and simulation is shown in **Figure 3C**, where the simulation values of A and θ_1 were calibrated using the regression lines in **Figures 3A,B**. Under the +10°C condition, the value of A showed a peak around $\theta_1 = 0.15$ rad/2π, while under the −10°C conditions, A varied on a small loop. This indicates

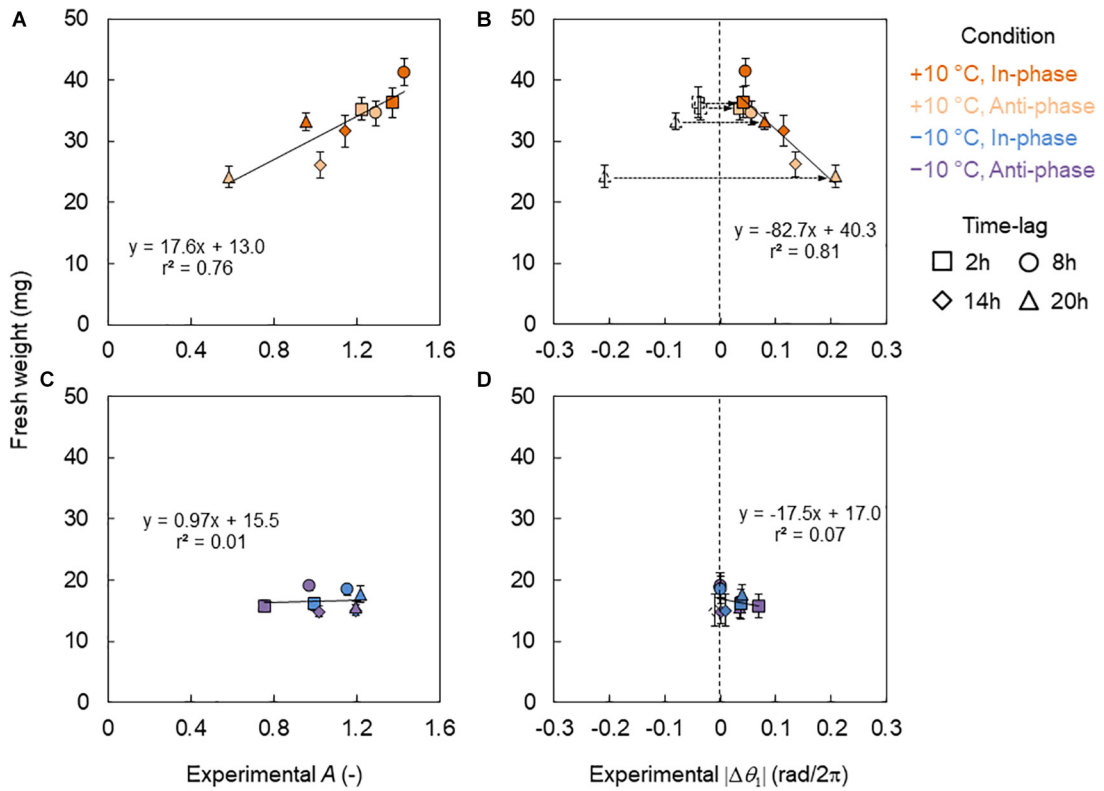

FIGURE 6 | Relationship between fresh weights and *CCA1* rhythms in the conditions of L/D = 16/8 h and 4 h ± 10°C cycles. **(A,B)** Relationship between fresh weight and amplitude *A* **(A)** and difference of the locking phase $|\Delta\theta_1|$ **(B)** in +10°C. **(C,D)** Relationship between fresh weight and *A* **(C)** and $|\Delta\theta_1|$ **(D)** in the −10°C. The blank symbols indicate data with negative values. Dotted arrows indicate the transform from negative to positive values. The colored symbols indicate data with positive values and the absolute value of the negatives in **(B,D)**. The solid lines indicate regression lines. **(B,D)** The regression lines are for the colored symbols.

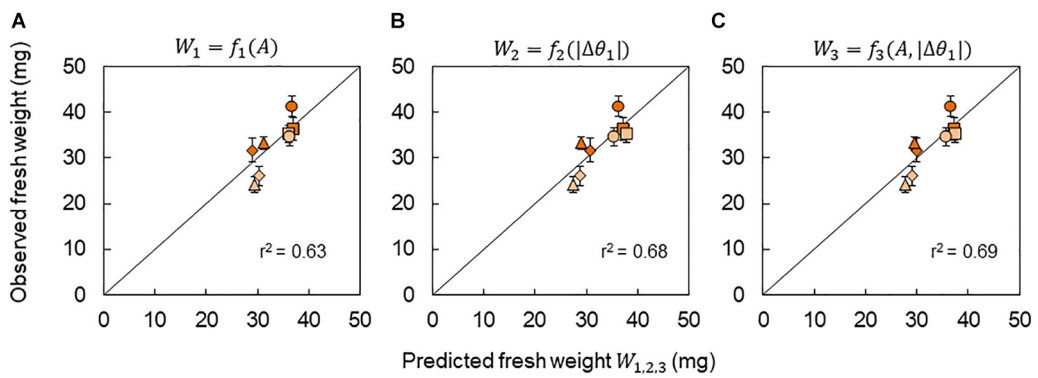

FIGURE 7 | Prediction of fresh weight based on the *CCA1* rhythms. Correlation between observed fresh weight and predicted fresh weight using models $W_1 = f_1(A)$ **(A)**, $W_2 = f_2(|\Delta\theta_1|)$ **(B)**, and $W_3 = f_3(A, |\Delta\theta_1|)$ **(C)**. The value of r^2 indicates the coefficient of determination for the line with a slope of 1. Symbols indicate the same conditions as shown in **Figure 6**.

that the modification range at −10°C was smaller than that at +10°C.

Effect of Time Lag on Growth

In **Figures 4A,B**, the fresh weights of the areal part of plants from the +10 and −10°C conditions are shown, respectively. The weight was larger at Δt = 8 h and smaller at Δt = 14 h under the +10°C condition. In contrast, there was no significant difference between the time lags under the −10°C condition. **Figures 4D,E** show the PLA under the +10 and −10°C conditions, respectively. Similar results were observed between the fresh weight and PLA. By the comparison of the control conditions, it was found that the +10°C cycle tended to enhance growth while the −10°C cycle suppressed growth.

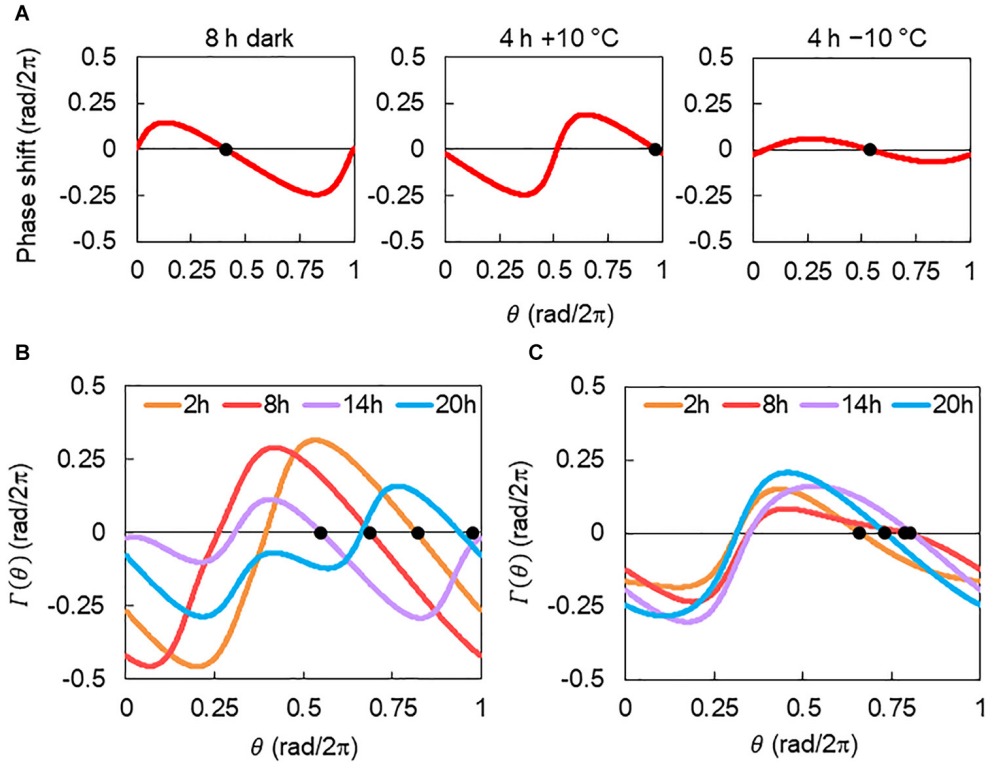

FIGURE 8 | Description of combined phase response curve (PRC). **(A)** PRCs for 8 h dark and 4 h ± 10°C stimuli. PRCs were reconstructed with a = 0.20 and α = 0.13 for 8 h darkness, a = 0.39 and α = 0.58 for 4 h +10°C, and a = 0.10 and α = 0.13 for 4 h −10°C stimuli (Masuda et al., 2021). Black dots indicate the stable points. **(B)** The combined PRC Γ(θ) of 8 h dark and 4 h +10°C condition. **(C)** Γ(θ) of 8 h dark and 4 h −10°C condition. Each curve corresponds to Γ(θ) for Δt = 2, 8, 14, or 20 h. Black dots indicate the stable point of each Γ(θ).

Figure 5 shows the relationship between the fresh weight and the *CCA1* rhythm under the control conditions. The fresh weight increased with the increasing amplitude of A with a correlation (r = 0.60, $p < 0.01$). In contrast, the locking phase θ_1 showed almost the same value; the mean values of phase $\bar{\theta}_1$ were 0.14 and 0.16 rad/2π (peak time 3.3 and 3.7 h) for the in-phase and antiphase initial conditions, respectively. Therefore, the fresh weight showed no correlation for θ_1 ($r = -0.20$, $p > 0.05$).

In **Figures 6A,B**, the relationship between fresh weight and the *CCA1* rhythm in the +10°C conditions is shown. The fresh weight showed a linear relationship for the amplitude of A (**Figure 6A**) but a mirrored linear relationship for the locking phase θ_1 (**Figure 6B**). Thus, we introduced the absolute value of phase difference $|\Delta\theta_1|$ defined as $|\Delta\theta_1| = |\theta_1 - \bar{\theta}_{1,C}|$, which indicates the amount of phase shift forced by a +10°C cycle (**Figure 6B**). $\bar{\theta}_{1,C}$ is the average of θ_1 under the control conditions. Notably, the fresh weight showed very high correlations with both A and $|\Delta\theta_1|$. However, under the −10°C condition, the fresh weight showed no correlations with either A or $|\Delta\theta_1|$ (**Figures 6C,D**).

Due to the strong correlation between the growth and the *CCA1* rhythm (A and $|\Delta\theta_1|$) under the +10°C condition, a growth prediction based on the *CCA1* rhythm could be demonstrated. In this study, three kinds of prediction model for fresh weight were considered: $W_1 = f_1(A)$, $W_2 = f_2(|\Delta\theta_1|)$, and $W_3 = f_3(A, |\Delta\theta_1|)$, where $W_{1,2,3}$ means the predicted fresh weight in each model. First, the functions $f_1(A)$ and $f_2(|\Delta\theta_1|)$ were obtained experimentally as linear functions from the relationships in **Figures 6A,B**, respectively. The function $f_3(A, |\Delta\theta_1|)$ was also obtained by a linear optimal combination of A and $|\Delta\theta_1|$, that is, $f_3(A, |\Delta\theta_1|) = aA + b|\Delta\theta_1| + c$, using the least square method. We then calculated the A and $|\Delta\theta_1|$ for each Δt in the phase oscillator model (Eq. 7) and the regression lines in **Figures 3A,B** as a calibration. Finally, $A(\Delta t)$ and $|\Delta\theta_1(\Delta t)|$ were obtained and substituted into $W_1 = f_1[A(\Delta t)]$, $W_2 = f_2[|\Delta\theta_1(\Delta t)|]$, or $W_3 = f_3[A(\Delta t), |\Delta\theta_1(\Delta t)|]$, and then we obtained the predicted fresh weight for each Δt. The accuracy rates of the models were high ($r > 0.79$) as shown in **Figure 7**. However, it should be noted that our prediction model cannot be used for the −10°C condition, as there was no correlation between growth and the *CCA1* rhythm.

DISCUSSION

In this study, we investigated the modulation of the *CCA1* rhythms and seedling growth using temperature cycles (4 h ± 10°C) with time lags Δt. The amplitude A and locking phase θ_1 varied, depending on Δt. Under the −10°C condition, there was a decrease in the modulation of A and θ_1 by 53 and 75%,

respectively, compared with those under the +10°C condition (**Figure 2**). In addition, the growth depended on Δt only under the +10°C condition, and not under −10°C (**Figure 4**). Notably, under the +10°C condition, growth showed a high correlation with the *CCA1* rhythms (**Figure 6**).

In our model, light and temperature stimuli affected the *CCA1* rhythms via their PRCs. Consequently, their multiple effects can be estimated based on the combined PRC $\Gamma(\theta)$. **Figure 8A** shows the description of $\Gamma(\theta)$. PRCs for 8 h dark, 4 h +10°C, and 4 h −10°C were obtained in our pervious study (Masuda et al., 2021). Here, we introduced the combined PRC $\Gamma(\theta)$, described as $\Gamma(\theta) = G_D(\theta + \theta_D) + G_T(\theta + \Delta\psi)$, where $G_D(\theta)$ and $G_T(\theta)$ are the PRCs for the 8 h dark and temperature (4 h +10°C or 4 h −10°C) stimuli, respectively. θ_D is a constant that denotes the start time of the dark in relation to the timing of light on, that is, $\theta_D = 2\pi^* \frac{16}{24}$ (rad) in this study. $\Delta\psi$ is the phase delay of the temperature stimuli from light on; $\Delta\psi = 0$ rad indicates the temperature stimulus applied at the light-on time. $\Delta\psi$ was transferred to time lag Δt as $\Delta t = \Delta\psi/2\pi \times 24$ (h) in this study. By considering the $\Gamma(\theta)$, the differences in rhythm modulations between +10°C and −10°C were determined and shown in **Figure 3C**. They were explained as follows: the shape of $\Gamma(\theta)$ changes drastically depending on Δt in +10°C (**Figure 8B**), but it was almost unchanged at −10°C (**Figure 8C**). Therefore, in the −10°C condition, the *CCA1* rhythm was determined to be almost independent of the time lag. In addition, the complex shape of $\Gamma(\theta)$, such as $\Delta t = 14$ and 20 h under +10°C, disturbs the synchrony of cellular oscillators and then suppresses substantially the amplitude of the collective rhythm (around evening in **Supplementary Figure S2A**).

During plant growth, Δt also resulted in a significant effect at the +10°C but not −10°C condition (**Figure 4**). In addition, the growth showed a correlation with the *CCA1* rhythms at +10°C, but no correlation at −10°C (**Figure 6**). As a possible explanation, the variable range for the −10°C was very narrow (on a small loop in **Figure 3C**), so the growth might not be affected by the rhythm modulations. Moreover, using Δt, the degree of DIF was regulated continuously from +DIF to −DIF. Such continuous regulation of DIF provides continuous modulation of the *CCA1* rhythm (**Figure 3C**). Based on our results, the effects of DIF regulation on growth were predictable (**Figure 7**). This prediction method in conjunction with specific growing conditions and/or crop species might be important for practical application in horticulture (Kläring and Schmidt, 2017; Liu et al., 2019). However, as a limitation of this, other situations such as the 12/12 h temperature cycles were not addressed in this study, and further studies are required to determine the growth regulation of DIF.

In this study, we demonstrated growth prediction using the *CCA1* rhythm with a phase oscillator model. The synchronization of the cellular oscillators plays an important role in the modification of circadian rhythms. Although it is difficult to measure such population dynamics directly, our model was utilized for the basic estimation of the optimal time lag. However, although the present study showed a correlation between growth and the *CCA1* rhythms, it did not clarify a causal mechanism between them. The measurement of other clock genes is required to fully elucidate the role of the circadian clock. Moreover, the entrainment of the plant circadian clock also involves complex interactions for endogenous factors (e.g., sugar metabolism and hormone signaling) as well as environmental stimulus (Webb et al., 2019). Further modeling with signaling details and other environmental stimuli is thus required in the future.

DATA AVAILABILITY STATEMENT

The raw data supporting the conclusions of this article will be made available by the authors, without undue reservation.

AUTHOR CONTRIBUTIONS

KM, TY, and HF designed the research. KM, TY, and YK performed the experiments. KM and TY analyzed the data. KM and HF wrote the manuscript. All authors discussed the results and implications and commented on the manuscript.

FUNDING

This study was partially supported by Grants-in-Aid for Scientific Research (No. 18J20079 to KM; Nos. 20H00423, 20H05424, and 20H05540 to HF) provided by the Ministry of Education, Science, Sports, and Culture.

ACKNOWLEDGMENTS

We are grateful to Prof. Takao Kondo for providing the bioluminescence monitoring device and Prof. Norihito Nakamichi for supplying the *CCA1*::*LUC* plants. We would like to thank Editage (www.editage.com) for English language editing.

SUPPLEMENTARY MATERIAL

The Supplementary Material for this article can be found online at: https://www.frontiersin.org/articles/10.3389/fpls.2020.614360/full#supplementary-material

REFERENCES

Anpo, M., Fukuda, H., and Wada, T. (2018). *Plant Factory Using Artificial Light: Adapting to Environmental Disruption and Clues to Agricultural Innovation*. San Diego, CA: Elsevier.

Creux, N., and Harmer, S. (2019). Circadian rhythms in plants. *Cold Spring Harb. Perspect. Biol.* 11:a034611. doi: 10.1101/cshperspect.a034611

Dodd, A. N., Kusakina, J., Hall, A., Gould, P. D., and Hanaoka, M. (2014). The circadian regulation of photosynthesis. *Photosynth. Res.* 119, 181–190. doi: 10.1007/s11120-013-9811-8

Dodd, A. N., Salathia, N., Hall, A., Kevei, E., Toth, R., Nagy, F., et al. (2005). Plant circadian clocks increase photosynthesis, growth, survival, and competitive advantage. *Science* 309, 630–633. doi: 10.1126/science.1115581

Fukuda, H., Murase, H., and Tokuda, I. (2013). Controlling circadian rhythms by dark-pulse perturbations in *Arabidopsis thaliana*. *Sci. Rep.* 3:1533. doi: 10.1038/srep01533

Fukuda, H., Uchida, Y., and Nakamichi, N. (2008). Effect of a dark pulse under continuous red light on the *Arabidopsis thaliana* circadian rhythm. *Environ. Control Biol.* 46, 123–128. doi: 10.2525/ecb.46.123

Granada, A., Hennig, R. M., Ronacher, B., Kramer, A., and Herzel, H. (2009). Phase response curves elucidating the dynamics of coupled oscillators. *Methods Enzymol.* 454, 1–27. doi: 10.1016/S0076-6879(08)03801-9

Higashi, T., Nishikawa, S., Okamura, N., and Fukuda, H. (2015). Evaluation of growth under non-24 h period lighting conditions in *Lactuca sativa* L. *Environ. Control Biol.* 53, 7–12. doi: 10.2525/ecb.53.7

Johnson, C. H., Elliott, J. A., and Foster, R. (2003). Entrainment of circadian programs. *Chronobiol. Int.* 20, 741–774. doi: 10.1081/CBI-120024211

Kläring, H. P., and Schmidt, A. (2017). Diurnal temperature variations significantly affect cucumber fruit growth. *HortScience* 52, 60–64. doi: 10.21273/HORTSCI11215-16

Kondo, T., Strayer, C. A., Kulkarni, R. D., Taylor, W., Ishiura, M., Golden, S. S., et al. (1993). Circadian rhythms in prokaryotes: luciferase as a reporter of circadian gene expression in cyanobacteria. *Proc. Natl. Acad. Sci. U.S.A.* 90, 5672–5676. doi: 10.1073/pnas.90.12.5672

Kozai, T., Niu, G., and Takagaki, M. (2019). *Plant Factory: an Indoor Vertical Farming System for Efficient Quality Food Production*. San Diego, CA: Elsevier Science & Technology.

Lai, A. G., Doherty, C. J., Mueller-Roeber, B., Kay, S. A., Schippers, J. H., and Dijkwel, P. P. (2012). CIRCADIAN CLOCK-ASSOCIATED 1 regulates ROS homeostasis and oxidative stress responses. *Proc. Natl. Acad. Sci. U.S.A.* 109, 17129–17134. doi: 10.1073/pnas.1209148109

Liu, Y., Ren, X., and Jeong, B. R. (2019). Manipulating the difference between the day and night temperatures can enhance the quality of *Astragalus membranaceus* and *Codonopsis lanceolate* plug seedlings. *Agronomy* 9:654. doi: 10.3390/agronomy9100654

Masuda, K., Kitaoka, R., Ukai, K., Tokuda, I. T., and Fukuda, H. (2017). Multicellularity enriches the entrainment of *Arabidopsis circadian* clock. *Sci. Adv.* 3:e1700808. doi: 10.1126/sciadv.1700808

Masuda, K., Tokuda, I. T., Nakamichi, N., and Fukuda, H. (2021). The singularity response reveals entrainment properties of the plant circadian clock. *Nat. Commun.* 12:864. doi: 10.1038/s41467-021-21167-7

Michael, T. P., Salome, P. A., and McClung, C. R. (2003). Two *Arabidopsis circadian* oscillators can be distinguished by differential temperature sensitivity. *Proc. Natl. Acad. Sci. U.S.A.* 100, 6878–6883. doi: 10.1073/pnas.1131995100

Nakamichi, N., Ito, S., Oyama, T., Yamashino, T., Kondo, T., and Mizuno, T. (2004). Characterization of plant circadian rhythms by employing *Arabidopsis* cultured cells with bioluminescence reporters. *Plant Cell Physiol.* 45, 57–67. doi: 10.1093/pcp/pch003

Ohara, T., Fukuda, H., and Tokuda, I. T. (2015). Phase response of the *Arabidopsis thaliana* circadian clock to light pulses of different wavelengths. *J. Biol. Rhythms* 30, 95–103. doi: 10.1177/0748730415576426

Resco de Dios, V., Loik, M. E., Smith, R., Aspinwall, M. J., and Tissue, D. T. (2016). Genetic variation in circadian regulation of nocturnal stomatal conductance enhances carbon assimilation and growth. *Plant Cell Environ.* 39, 3–11. doi: 10.1111/pce.12598

Thines, B., and Harmon, F. G. (2010). Ambient temperature response establishes ELF3 as a required component of the core *Arabidopsis circadian* clock. *Proc. Natl. Acad. Sci. U. S. A.* 107, 3257–3262. doi: 10.1073/pnas.0911006107

Thingnaes, E., Torre, S., Ernstsen, A., and Moe, R. (2003). Day and night temperature responses in *Arabidopsis:* effects on gibberellin and auxin content, cell size, morphology and flowering time. *Ann. Bot.* 92, 601–612. doi: 10.1093/aob/mcg176

Watson, G. S., and Williams, E. J. (1956). On the construction of significance tests on the circle and the sphere. *Biometrika* 43, 344–352. doi: 10.2307/2332913

Webb, A. A., Seki, M., Satake, A., and Caldana, C. (2019). Continuous dynamic adjustment of the plant circadian oscillator. *Nat. Commun.* 10:550. doi: 10.1038/s41467-019-08398-5

Xiao, F., Yang, Z., Han, W., Li, Y., Qiu, Y., Sun, Q., et al. (2018). Effects of day and night temperature on photosynthesis, antioxidant enzyme activities, and endogenous hormones in tomato leaves during the flowering stage. *J. Hortic. Sci. Biotechnol.* 93, 306–315. doi: 10.1080/14620316.2017.1369171

Xiong, J., Patil, G. G., Moe, R., and Torre, S. (2011). Effects of diurnal temperature alternations and light quality on growth, morphogenesis and carbohydrate content of *Cucumis sativus* L. *Sci. Hortic.* 128, 54–60. doi: 10.1016/j.scienta.2010.12.013

Conflict of Interest: The authors declare that the research was conducted in the absence of any commercial or financial relationships that could be construed as a potential conflict of interest.

frontiers in Plant Science

REVIEW
published: 04 March 2021
doi: 10.3389/fpls.2021.631810

Plant Defense Responses to Biotic Stress and Its Interplay With Fluctuating Dark/Light Conditions

*Zahra Iqbal[1], Mohammed Shariq Iqbal[2], Abeer Hashem[3,4], Elsayed Fathi Abd_Allah[5] and Mohammad Israil Ansari[6]**

[1] Molecular Crop Research Unit, Department of Biochemistry, Chulalongkorn University, Bangkok, Thailand, [2] Amity Institute of Biotechnology, Amity University, Lucknow, India, [3] Botany and Microbiology Department, College of Science, King Saud University, Riyadh, Saudi Arabia, [4] Mycology and Plant Disease Survey Department, Plant Pathology Research Institute, ARC, Giza, Egypt, [5] Plant Production Department, College of Food and Agricultural Sciences, King Saud University, Riyadh, Saudi Arabia, [6] Department of Botany, University of Lucknow, Lucknow, India

Plants are subjected to a plethora of environmental cues that cause extreme losses to crop productivity. Due to fluctuating environmental conditions, plants encounter difficulties in attaining full genetic potential for growth and reproduction. One such environmental condition is the recurrent attack on plants by herbivores and microbial pathogens. To surmount such attacks, plants have developed a complex array of defense mechanisms. The defense mechanism can be either preformed, where toxic secondary metabolites are stored; or can be inducible, where defense is activated upon detection of an attack. Plants sense biotic stress conditions, activate the regulatory or transcriptional machinery, and eventually generate an appropriate response. Plant defense against pathogen attack is well understood, but the interplay and impact of different signals to generate defense responses against biotic stress still remain elusive. The impact of light and dark signals on biotic stress response is one such area to comprehend. Light and dark alterations not only regulate defense mechanisms impacting plant development and biochemistry but also bestow resistance against invading pathogens. The interaction between plant defense and dark/light environment activates a signaling cascade. This signaling cascade acts as a connecting link between perception of biotic stress, dark/light environment, and generation of an appropriate physiological or biochemical response. The present review highlights molecular responses arising from dark/light fluctuations *vis-à-vis* elicitation of defense mechanisms in plants.

Keywords: biotic stress, dark, defense response, light, plant protection, transcription factor

OPEN ACCESS

Edited by:
Péter Poór,
University of Szeged, Hungary

Reviewed by:
Amarjeet Singh,
National Institute of Plant Genome Research (NIPGR), India
Jing Yang,
Yunnan Agricultural University, China

***Correspondence:**
Mohammad Israil Ansari
ansari_mi@lkouniv.ac.in

Specialty section:
This article was submitted to Plant Abiotic Stress, a section of the journal Frontiers in Plant Science

Received: *21 November 2020*
Accepted: *08 February 2021*
Published: *04 March 2021*

Citation:
Iqbal Z, Iqbal MS, Hashem A, Abd_Allah EF and Ansari MI (2021) Plant Defense Responses to Biotic Stress and Its Interplay With Fluctuating Dark/Light Conditions. Front. Plant Sci. 12:631810. doi: 10.3389/fpls.2021.631810

INTRODUCTION

Plants are prone to a number of biotic stress conditions. The suite of molecular and cellular processes is triggered once the plant senses stress (Rejeb et al., 2014; Lamers et al., 2020), which in turn activates a cross-wired mesh of morphological, physiological, and biochemical mechanisms (Nejat and Mantri, 2017; Saijo and Loo, 2020). Plants have developed complex sensory mechanisms to identify biotic invasion and overcome the detriment of growth, yield, and survival

(Rizhsky et al., 2004; Lamers et al., 2020). Consequently, plants have evolved a surfeit of responses to defend themselves against attacks by a broad spectrum of pests and pathogens, including viruses, nematodes, bacteria, fungi, and herbivorous insects (Hammond-Kosack and Jones, 2000). Thus, plants tend to strike a balance between their response and biotic stress to combat the deleterious effect on their survival (Peck and Mittler, 2020). The molecular mechanisms contributing toward plant defense responses had been elucidated to a great depth (Cheng et al., 2012; Wang Z. et al., 2019). But how and why different signaling pathways converge to biotic stress responses still remain obscure. The light signaling pathway is one such area of interest amongst the research community.

Dark and light alterations are fundamental to plant survival. It affects all aspects of plant growth and development. The light signals are perceived by photoreceptors, which are capable of discriminating various wavelengths of light (Franklin et al., 2004). Photoreceptors, namely, phytochromes (sense red and far-red light), phototropins, and cryptochromes (sense blue light and UV light), develop cues from qualitative and quantitative light alterations (Christie, 2007; Yu et al., 2010; Tilbrook et al., 2013). This sensing activates several signal transduction pathways, which in turn regulate plant growth, physiology, morphology, and immunity (Kami et al., 2010; Moreno and Ballaré, 2014; Mawphlang and Kharshiing, 2017; Tripathi et al., 2019). In addition, photosynthetic reactions themselves regulate biochemical machinery in plant tissues (Lu and Yao, 2018). This is evident by the point that a number of genes are transcriptionally induced by the circadian clock in *Arabidopsis thaliana* and other plants (Harmer et al., 2000; Creux and Harmer, 2019). Circadian clock has been reported to meticulously regulate the defense machinery in plants (Sharma and Bhatt, 2015).

There are two developmental fates of seedling upon germination that are primarily dependent upon the presence or absence of light. In the presence of light, seedlings develop a shorter hypocotyl and open green cotyledons. This default pathway of plant development is termed photomorphogenesis (Bae and Choi, 2008; Pham et al., 2018). On the contrary, plants grown in dark conditions undergoes skotomorphogenesis (plant development under dark conditions), allocating the resources toward hypocotyl elongation rather than on cotyledon or root development (Josse and Halliday, 2008). Elongated hypocotyls, closed cotyledons, and an apical hook at the shoot meristem are characteristic to skotomorphogenetic plant development (Pham et al., 2018). Skotomorphogenesis is accomplished by repressing genes implicated in de-etiolation and photomorphogenic development (Josse and Halliday, 2008). Additionally, the effect of dark/light alteration is not only limited to plant growth and development, but it also impacts other responses to the environment such as defense against pests and pathogens (Ballaré, 2014). Extensive research exists to vindicate the effect of dark/light alterations on plant defense responses, extending from biological to ecological scales (Huner et al., 1998; Roberts and Paul, 2006; Kazan and Manners, 2011; Ballare et al., 2012; Kangasjärvi et al., 2012; Hua, 2013; Garcia-Guzman and Heil, 2014; Saijo and Loo, 2020). But the in-depth mechanistic details with regard to the complex regulatory networks are yet to be explored. The basic research in this direction can assist the idea of sustainable agriculture to ensure food security for the ever-growing world population (Sánchez-Muros et al., 2014; González de Molina et al., 2017; Iqbal et al., 2020a; Saiz-Rubio and Rovira-Más, 2020). The present review recapitulates biochemical, physiological, and molecular aspects of biotic stress and plant defense responses operating in light/dark scenarios.

BIOTIC STRESS AND PLANT DEFENSE RESPONSES

A number of pests, parasites, and pathogens are responsible for infecting plants and inciting biotic stress. Fungal parasites can be either necrotrophic (kill host cell by toxin secretion) or biotrophic (feed on living host cell). They are capable of inducing vascular wilts, leaf spots, and cankers in plants (Laluk and Mengiste, 2010; Doughari, 2015; Sobiczewski et al., 2017). Nematodes feed on plant parts and primarily cause soil-borne diseases leading to nutrient deficiency, stunted growth, and wilting (Lambert and Bekal, 2002; Bernard et al., 2017; Osman et al., 2020). Similarly, viruses are also capable of local and systemic damage resulting in chlorosis and stunting (Pallas and García, 2011). On the contrary, mites and insects impair plants by either feeding (piercing and sucking) on them or laying eggs. The insects might also act as carriers of other viruses and bacteria (Schumann and D'Arcy, 2006). Plants have developed an elaborate immune system to combat such stresses (Taiz and Zeiger, 2006; Saijo and Loo, 2020). Plants have a passive first line of defense, which includes physical barriers such as cuticles, wax, and trichomes to avert pathogens and insects. Plants are also capable of producing chemical compounds to defend themselves from infecting pathogens (Taiz and Zeiger, 2006) (discussed in section "Effect of Dark/Light on Plant–Pathogen Interaction and Associated Mechanisms"). Additionally, plants trigger defense against biotic agents by two levels of pathogen recognition (Dangl and McDowell, 2006).

The first level of pathogen recognition encompasses pattern recognition receptors (PRRs), which identify pathogen-associated molecular patterns (PAMPs). Such plant immunity is categorized as PAMP-triggered immunity (PTI) (Monaghan and Zipfel, 2012). Phytophagous pests respond by identification of herbivore-associated elicitors (HAEs), herbivore-associated molecular patterns (HAMPs), or PRR herbivore effectors (Santamaria et al., 2013). The second level of pathogen recognition encircles plant resistance (R) proteins, which identify specific receptors from a pathogen (Avr proteins) (Dangl and McDowell, 2006; Gouveia et al., 2017; Abdul Malik et al., 2020). It is considered an effective mechanism of plant resistance to pests and involves effector-triggered immunity (ETI) (Kaloshian, 2004; Mur et al., 2008; Spoel and Dong, 2012). ETI stimulates hypersensitive responses (HRs) and triggers programmed cell death (PCD) in infected and surrounding cells (Mur et al., 2008). The proteins encoded by a majority of *R* genes have a specific domain with conserved nucleotide-binding site (NBS). The second next important domain is leucine-rich repeat (LRR). Pathogen effectors are recognized directly (physical association) or indirectly (association of an accessory protein) by NB-LRR

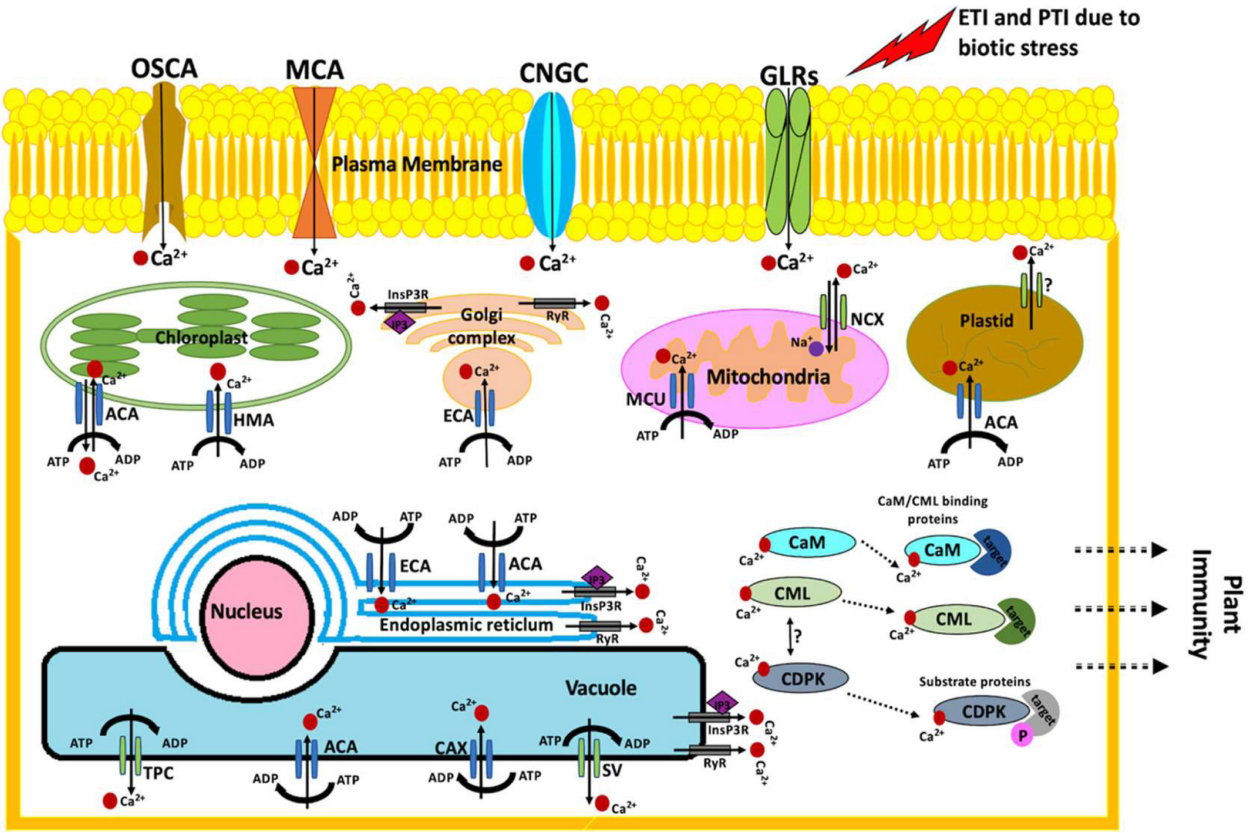

FIGURE 1 | Schematic representation of biotic stress perception and Ca^{2+} signaling for the regulation of plant immune responses. The cytosolic Ca^{2+} levels increase (>200 nM) upon perceiving biotic stress: calcium (Ca^{2+}), Ca^{2+}–dependent protein kinases (CDPKs), calmodulin (CaM), calmodulin-like protein (CML), autoinhibited Ca^{2+}-ATPases (ACAs), ER-type Ca^{2+}-ATPases (ECAs), mitochondrial Ca^{2+} uniporter (MCU), P1-ATPases (e.g., HMA1), Ca^{2+} exchangers (CAX), two-pore channel (TPC), cyclic nucleotide-gated channels (CNGCs), glutamate receptor-like channels (GLRs), stretch-activated Ca^{2+} channels (OSCAs), MID1-complementing activity (MCA), phosphate (P), adenosine triphosphate (ATP), adenosine diphosphate (ADP), 1,4,5-trisphosphate receptor-like channel ($InsP_3R$), 1,4,5-trisphosphate (IP_3), cyclic ADP-ribose (cADPR)-activator ryanodine receptor-like channel (RyR), slow-activating vacuolar channel (SV), and sodium-calcium exchanger (NCX).

receptors (Dodds and Rathjen, 2010). Sometimes, *R* gene-mediated plant response toward invading pathogen provokes a higher degree of defense, termed as systemic acquired resistance (SAR). SAR generates whole-plant systemic resistance against a broad spectrum of pathogens. In SAR, a local encounter results in the stimulation of resistance to the other plant organs through intraplant communication (Fu and Dong, 2013). Generally, both categories of plant immune responses induce the same reaction, but ETI is considered more rigorous to pathogen infection (Tao et al., 2003).

Perturbations in cytosolic calcium (Ca^{2+}) concentrations are the earliest signaling events occurring upon the exposure of plants to biotic stress. Ca^{2+} signals are the center to plant immune signaling pathways (Seybold et al., 2014; Aldon et al., 2018). Rapid and transient perturbations in Ca^{2+} concentrations are crucial to gene reprogramming required to generate an adequate response (Reddy et al., 2011). The plant immune responses differ in their Ca^{2+} signatures. For example, Ca^{2+} transients upon PTI activation returns to basic levels within a few minutes (Lecourieux et al., 2005), while ETI involves a prolonged increase in cytosolic Ca^{2+} levels lasting for several hours (Grant et al., 2000). Lanthanum, a known Ca^{2+} channel blocker, is reported to hinder the immune responses associated with both PTI and ETI (Grant et al., 2000; Boudsocq et al., 2010). Precisely, in response to the biotic invasion, PTI and ETI activate the Ca^{2+} ion channels, resulting in an increase of cytoplasmic Ca^{2+} concentrations (**Figure 1**). In *A. thaliana*, cyclic nucleotide-gated channels (CNGCs), glutamate receptor-like channels (GLRs), stretch-activated Ca^{2+} channels (OSCAs), and the MID1-complementing activity (MCA) families are the four main plasma membrane Ca^{2+}-permeable channels (Dodd et al., 2010; Yuan et al., 2014; Liu et al., 2018). Twenty distinct members of the CNGC family of plasma membrane Ca^{2+}-permeable channels have been identified in *A. thaliana* (Meena and Vadassery, 2015; DeFalco et al., 2016). CNGCs are extensively linked to plant development and biotic stress responses (Meena and Vadassery, 2015; DeFalco et al., 2016; Breeze, 2019). In response to fungal and bacterial pathogens, the Ca^{2+}-permeable channels CNGC2, CNGC4, CNGC11, and CNGC12 are reported to play critical roles in the entry of Ca^{2+} ions inside the plant cell (Yoshioka et al., 2001; Ahn, 2007). The role of CNGC2, CNGC4 (Ma et al., 2012; Chin et al., 2013),

CNGC11, and CNGC12 (Yoshioka et al., 2006; Moeder et al., 2011) has been well established in plant immune responses. Very recently, the function of CNGC19 Ca^{2+} channel was also extended to herbivory-induced Ca^{2+} flux, plant defense responses against pathogen *Spodoptera litura* (Meena et al., 2019), and basal defense signaling to regulate colonization of *Piriformospora indica* on *A. thaliana* roots (Jogawat et al., 2020). The first CNGC from plants was identified nearly two decades ago in barley as a calmodulin (CaM)-binding protein (Schuurink et al., 1998). CNGCs from plants and animals are reported to possess one or more CaM-binding domains at their cytosolic N- and C-termini, but the gating of CNGCs from plants is not well deduced (DeFalco et al., 2016; Fischer et al., 2017; James and Zagotta, 2018). The progress of plant CNGC research has been relatively low due to the difficulties in electrophysiological studies encircling CNGCs. However, the recent technological advances and reliability on reverse genetics using *cngc* mutants have resulted in few successful studies (Gao et al., 2016; Chiasson et al., 2017; Wang et al., 2017; Zhang et al., 2017). CNGC7, CNGC8, and CNGC18 have been specifically reported to act together with CaM2 as a molecular switch that operates in response to cellular Ca^{2+} concentrations (Pan et al., 2019). Additionally, CNGC18 is co-expressed with CPK32, indicating the regulation of its activity by phosphorylation (Zhou et al., 2014). Similarly, GLRs, which are systematically classified into three clades—clade I (GLRs 1.1–1.4), clade II (GLRs 2.1–2.9), and clade III (GLRs 3.1–3.7) (Lacombe et al., 2001)—are linked to plant defense against *Botrytis cinerea* (Sun et al., 2019) and *Hyaloperonospora arabidopsidis* (Manzoor et al., 2013). As such, the role of *AtGLR3.3* and *AtGLR3.6* in aphid-elicited cytosolic Ca^{2+} elevation is also well established (Vincent et al., 2017). *In-vitro* kinase assay confirmed that *AtGLR3.7* is phosphorylated by CDPK3, CDPK16, and CDPK34 at serine-860 site (Wang P.-H. et al., 2019). CDPKs have been extensively associated with plant stress management and development (Singh et al., 2017). The other plasma membrane localized Ca^{2+}-permeable channels, namely, OSCAs (phosphorylation of OSCA1.3 by BIK1) and MCAs (MCA1 and MCA2), are reported to regulate plant stomatal immunity (Thor et al., 2020) and manage hypergravity in *A. thaliana* hypocotyls under dark conditions, respectively (Hattori et al., 2020). Apart from the Ca^{2+} channels localized in the plasma membrane, several other Ca^{2+} channels are known to exist in the endoplasmic reticulum, mitochondria, golgi body, and plant vacuole (Singh et al., 2014; Xu et al., 2015a; Costa et al., 2018; Pandey and Sanyal, 2021). For example, autoinhibited Ca^{2+}-ATPases (ACAs), ER-type Ca^{2+}-ATPases (ECAs), mitochondrial Ca^{2+} uniporter (MCU), P1-ATPases (e.g., HMA1), Ca^{2+} exchangers (CAX), two-pore channel (TPC), 1,4,5-trisphosphate receptor-like channel ($InsP_3R$), 1,4,5-trisphosphate (IP_3), cyclic ADP-ribose (cADPR)-activator ryanodine receptor-like channel (RyR), slow-activating vacuolar channel (SV), and sodium-calcium exchanger (NCX) represents the organellar Ca^{2+} machinery (**Figure 1**). Many of these channels are reported to play pivotal roles in plant immunity (Bose et al., 2011; Pittman, 2011; Spalding and Harper, 2011; Kiep et al., 2015; Costa et al., 2017; Teardo et al., 2017; Yang et al., 2017; Demidchik et al., 2018; Taneja and Upadhyay, 2018; Pandey and Sanyal, 2021).

Once the Ca^{2+} ion enters the cell, it is sensed by an array of Ca^{2+}-binding proteins. The Ca^{2+}-binding proteins work as Ca^{2+} sensors decoding complex Ca^{2+} signatures (Kudla et al., 2018). Ca^{2+} sensors are highly conserved proteins and are classified into (a) CaM and CaM-like proteins (CMLs), (b) calcineurin-B-like proteins (CBLs), and (c) Ca^{2+}-dependent protein kinases (CPKs) and Ca^{2+} and Ca^{2+}/CaM-dependent protein kinase (CCaMK) (Cheng et al., 2002; Luan, 2009; Bender and Snedden, 2013; Ranty et al., 2016). CaM, CMLs, CBLs, and CPKs are comprehensively involved in the cross-talk of various biotic and abiotic stress signals (Ranty et al., 2016; Aldon et al., 2018). Many Ca^{2+} and Ca^{2+} sensor-associated transcription factors (TFs) are implicated in stress signaling in plants (Carrion et al., 1999; Singh and Virdi, 2013; Ranty et al., 2016; Chung et al., 2020; Shen et al., 2020). The largest and best characterized family of Ca^{2+}/CaM-dependent TFs are CAMTAs (Iqbal et al., 2020b). CAMTA3 has been reported enormously as a suppressor of plant biotic defense responses (Benn et al., 2016; Jacob et al., 2018; Kim et al., 2020). It works downstream to MAP kinase (Bjornson et al., 2014) and is directly phosphorylated and degraded by flg22-responsive mitogen-activated protein kinases (MAPKs) (Jiang et al., 2020). Precisely, MPK3 and MPK6 activate CAMTA3 nuclear export and destabilization (Jiang et al., 2020). Similarly, NAC TF, upon interaction with Ca^{2+}/CaM, positively regulates various biotic stress responses in *Solanum lycopersicum* (Wang G. et al., 2016). NAC is also responsive to *Colletotrichum gloeosporioides* and *Ralstonia solanacearum* infection in woodland strawberry (Zhang et al., 2018). WRKY is another Ca^{2+}/CaM-dependent TF (Park et al., 2005; Yan et al., 2018) implicated in pathogen incursion (Park et al., 2005; Bai et al., 2018). *WRKY7*, *WRKY45*, *WRKY43*, *WRKY53*, and *WRKY50* in a Ca^{2+}-driven manner bind to various isoforms of CaM (Park et al., 2005; Popescu et al., 2007). MYB TF is also well characterized as a Ca^{2+}-dependent TF. MYB functions upstream in a vast majority of defense-responsive and abiotic stress-receptive genes (Stracke et al., 2001; Chezem et al., 2017; Li et al., 2019). Similarly taking CMLs into consideration, *AtCML9* works as positive regulator of plant immune response. It was found to be induced by *Pseudomonas syringae* and phytohormones including abscisic acid (ABA) and salicylic acid (SA) (Magnan et al., 2008; Leba et al., 2012). Further, *AtCML9* interacts with WRKY53 and TGA3 TFs, both of which are known to mediate biotic stress responses (Popescu et al., 2007). In concurrence, *AtCML37* and *AtCML42* are associated with defense against herbivorous insects (*Spodoptera littoralis*) (Vadassery et al., 2012; Scholz et al., 2014). Very recently, 17 *AcoCPK* genes from *Ananas comosus* (pineapple) were analyzed for their effect under biotic stress. *AcoCPK1*, *AcoCPK3*, and *AcoCPK6* were shown to render susceptible disease resistance in *A. thaliana* against *Sclerotinia sclerotiorum* (Zhang et al., 2020). Another class of Ca^{2+} sensors, CBLs, are known to specifically interact with a family of plant-specific CBL-interacting protein kinases (CIPKs). CBL interacts with Ca^{2+} and binds with CIPK, resulting in kinase activation. The CBL–CIPK complex actively regulates downstream target proteins by phosphorylation (reviewed by Ma et al., 2020; Tang et al., 2020).

The other initial responses of pathogen attack on plants include the generation of reactive oxygen species (ROS) and activation of mitogen-activated protein kinases (MAPKs) (Muthamilarasan and Prasad, 2013). ROS and MAPKs overlap with other signaling pathways, including light pathways (Goldsmith and Bell-Pedersen, 2013; Foyer, 2018). Furthermore, pest attack on plants activates local or systemic defense responses involving oligogalacturonoids (OGAs), jasmonic acid (JA), and hydrogen peroxide (H_2O_2) signaling pathways (Fürstenberg-Hägg et al., 2013). Plants are also capable of producing volatile compounds that repel attacking pests (discussed in section "Effect of Dark/Light on Plant–Pathogen Interaction and Associated Mechanisms"). These compounds are part of lipoxygenase (LOX) and terpenoid signaling pathways (Pichersky and Gershenzon, 2002; Dudareva et al., 2006). Another pivotal downstream defense mechanism by plants include the generation of defensive proteins and universal stress proteins. These proteins comprise protein inhibitors, lectins, chitinases, α-amylase inhibitors, and polyphenol oxidases (Fürstenberg-Hägg et al., 2013; Lee et al., 2019). Additionally, the role of *pathogenesis-related* (*PR*) genes in plant defense responses has been considerably explored (Ali et al., 2018). *PR* genes translate into proteins that are induced in plants only upon pathological or similar conditions (conditions of non-pathogenic origin) (Jain and Khurana, 2018). They are considered as an important component of plant innate immune response and are implicated in HR and SAR responses (Jain and Khurana, 2018). PR proteins are grouped into 17 families, depending upon their biochemical and molecular properties (van Loon et al., 2006). In *A. thaliana*, five *PR* genes (*PR-1*, *PR-2*, *PR-3*, *PR-4*, and *PR-5*) are routinely explored for their involvement in plant biotic interactions (Hamamouch et al., 2011). *PR-1*, *PR-2*, and *PR-5* are implicated in SA-dependent SAR response, while *PR-3* and *PR-4* are involved in JA-dependent SAR response (Thomma et al., 1998; Hamamouch et al., 2011). An important aspect associated with PR proteins is their simultaneous indulgence in biotic and abiotic stress (Ali et al., 2018). To substantiate this, the 1,000-bp upstream region of all five *PR* genes from *A. thaliana* were analyzed bioinformatically to determine the presence of different motifs associated with a variety of environmental stresses. Intriguingly, all the *PR* genes contained multiple light-responsive motifs (AE-box, GAP-box, GT-1 motif, G-box, GATA-motif, box-4, and chs-CMA2a). The presence of light-responsive motifs in the promoter region of *PR* genes probably implies the binding of light-dependent genes to these conserved sequences (**Figure 2**). This notion itself supports the idea of intense cross-talks between biotic stress responses and light signaling pathways.

Finally, the involvement of phytohormones in regulating plant biotic defense responses cannot be ruled out. ETI and PTI induces specific downstream signaling pathways, in which three phytohormones are crucial, namely, SA, JA, and ethylene (ET). SA regulatory pathways are responsive to biotrophic and hemi-biotrophic pathogenic agents. Similarly, JA and ET pathways are responsive to necrotrophic agents and chewing pests (Bari and Jones, 2009; De Vleesschauwer et al., 2014). SA stimulates the SAR pathway promoting the expression of *PR* genes, which in-turn renders tolerance against a wide range of pathogens (Grant and Lamb, 2006; Fu and Dong, 2013; Ádám et al., 2018). SA, JA, and ET regulatory pathways for plant defense exhibit significant divergence, but they overlap to render defense against pathogenic agents (Glazebrook, 2005; Ku et al., 2018). Additionally, ABA, auxin, brassinosteroids (BRs), cytokinin (CK), gibberellic acid (GA), and peptide hormones also have vital significance in regulating the immune responses of the plants (Bari and Jones, 2009; Ku et al., 2018; Islam et al., 2019; Chen et al., 2020). Amongst all the phytohormones, JA is critical in triggering the plant defense system and cross-talks with other phytohormonal pathways to stimulate the plant immune responses (Yang et al., 2019).

LIGHT AS AN ENVIRONMENTAL CUE

Plants are exposed to variable light intensities that encompass light perception and signaling pathways responsible for growth, development, and immune responses (Hua, 2013; Ballaré, 2014). Nevertheless, plants often confront light intensities that exceed their photosynthetic capacity, inducing light stress (Mishra et al., 2012). Mechanisms encompassing light/dark alteration under stress conditions have been comprehensively studied (Mittler, 2002; Cerdán and Chory, 2003; Jiao et al., 2007; Koussevitzky et al., 2007; Mühlenbock et al., 2008; Alabadí and Blázquez, 2009; Chory, 2010; Kami et al., 2010; Lau and Deng, 2010; Trotta et al., 2014; Kaiserli et al., 2015; Saijo and Loo, 2020). Given the extreme importance of light for survival, immunity, growth, and development, plants have evolved the capability to sense and respond to different spectra of light (visible, infrared, ultraviolet, etc.) through photoreceptors. In *A. thaliana*, five distinctive genes (*PHYA–PHYE*) encode phytochrome protein (Clack et al., 1994; Li et al., 2011). They potentially act as receptors for red and far-red lights (Takano et al., 2009). Similarly, in *A. thaliana*, cryptochromes encoded by *CRY1* and *CRY2* dedicatedly sense blue (∼400 nm) and green (500–600 nm) lights and UV-A (Folta and Maruhnich, 2007; Jiao et al., 2007; Bae and Choi, 2008; Jenkins, 2009).

As previously discussed, plants undergo skotomorphogenesis in the absence of light while photomorphogenesis in the presence of light (see section "Introduction"). Repressor proteins such as constitutive photomorphogenic/de-etiolated1/fusca (COP/DET/FUS) inhibit photomorphogenesis under dark conditions (Hardtke and Deng, 2000; Dong et al., 2014). Mutants with defects in any of these repressor proteins display constitutive photomorphogenic (COP) phenotypes under dark conditions (Lau and Deng, 2012). The repressor proteins are characterized into four categories with overlapping functions and have been studied extensively (Deepika et al., 2020; Pham et al., 2020). The first one is COP1, which is a RING-finger-type ubiquitin E3 ligase (Deng et al., 1992). Under dark conditions, it acts as a repressor of light signaling and accumulates in the nucleus (Xu D. et al., 2014). On the contrary, COP1 is exported out of the nucleus, facilitating photomorphogenesis under light conditions (von Arnim et al., 1997; Hardtke et al., 2000; Seo et al., 2003; Duek et al., 2004; Xu et al., 2016a; Podolec and Ulm, 2018). COP1 acts as a central repressor and facilitates

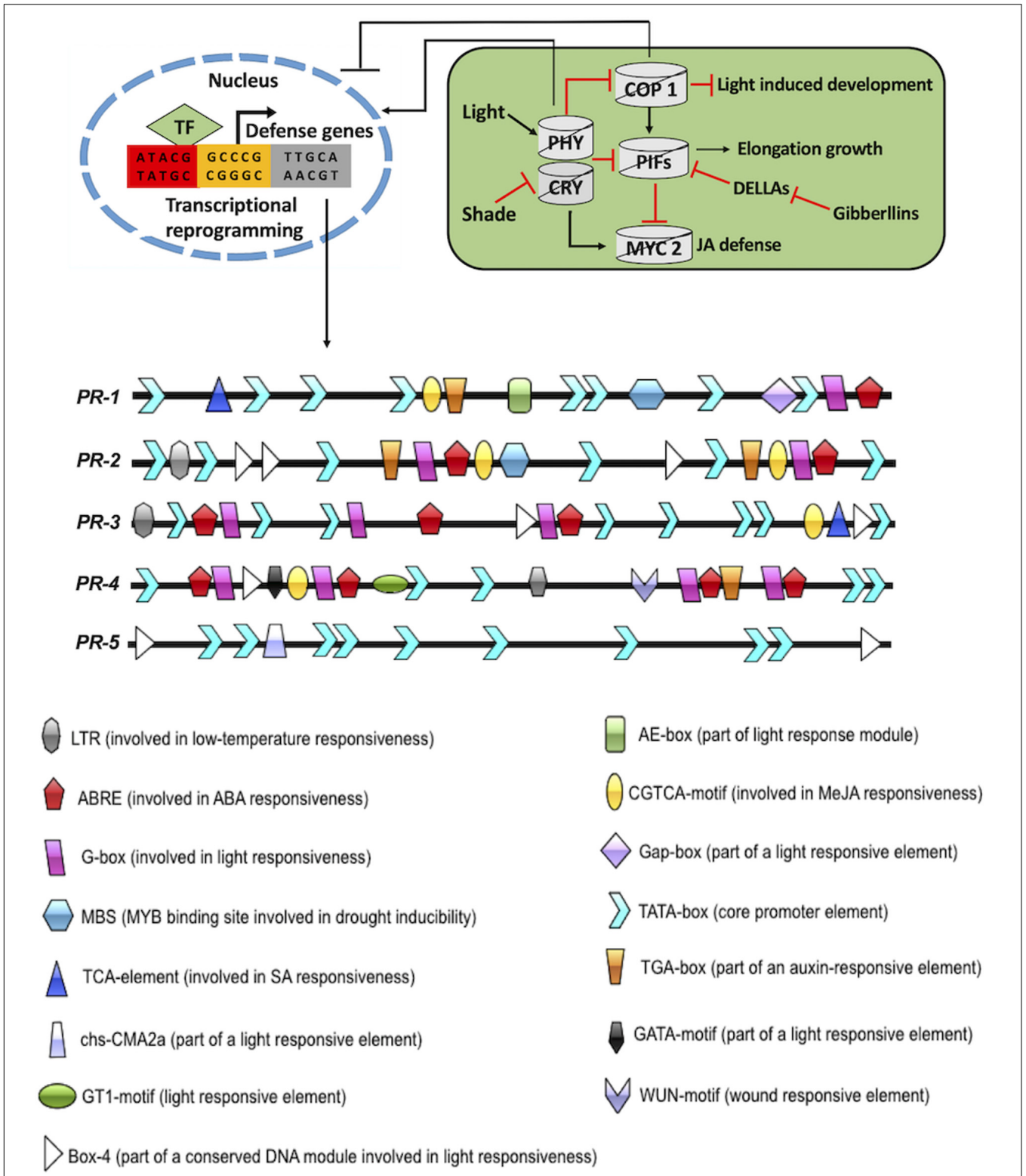

FIGURE 2 | Intersection of plant defense and light signaling. The 1,000-bp upstream sequence of *PR-1*, *PR-2*, *PR-3*, *PR-4*, and *PR-5* were fetched from TAIR10 (https://www.arabidopsis.org/). The motif analysis was done by PLACE database (https://www.dna.affrc.go.jp/PLACE/?action=newplace) and PlantCARE database (http://bioinformatics.psb.ugent.be/webtools/plantcare/html/). The motif structures were drawn using Illustrator for Biological sequences software (http://ibs.biocuckoo.org/).

ubiquitination and degradation of various positive regulators of light, namely, long hypocotyl in far-red 1 (HFR1), long hypocotyl 5 (HY5), and long after far-red light 1 (LAF1) (Hardtke et al., 2000; Osterlund et al., 2000; Jang et al., 2005; Yang et al., 2005). The degradation of positive regulators of light by COP1 is constrained under light by prohibiting COP1 protein from the nucleus. This triggers the initiation event of photomorphogenesis. The function of COP1 has been extensively linked to light signaling (**Figure 2**). However, it is also implicated in the regulation of flowering time, circadian rhythm, and temperature signaling (Ma et al., 2002; Yu et al., 2008; Jeong et al., 2010; Catalá et al., 2011; Menon et al., 2016; Wang W.-X. et al., 2016; Xu et al., 2016b; Hoecker, 2017). COP1 is also known to interact with the suppressor of PHYA 1–4 (SPA 1–4). This interaction results in tetrameric complexes comprising two COP1 and two SPA proteins (COP1/SPA complex) (Zhu et al., 2008). SPA proteins are reported to positively enhance COP1 function (Ordoñez-Herrera et al., 2015). Skotomorphogenesis is accomplished by suppressing the expression of genes involved in photomorphogenic development in the dark (Josse and Halliday, 2008). This is tightly regulated by the COP1–SPA1E3 ligase complex (Osterlund et al., 2000; Josse and Halliday, 2008; Ordoñez-Herrera et al., 2015; Holtkotte et al., 2016; Paik et al., 2019). COP1–SPA1E3 ligase targets HY5 TF for degradation by the proteasome (Osterlund et al., 2000). COP1–SPA complex interacts with CULLIN4 (CUL4) to form CUL4–COP1–SPA complex. CUL4–COP1–SPA complex acts as CULLIN ring E3 ligase (CRL) and degrades positively acting TFs under dark conditions to suppress photomorphogenesis (Chen et al., 2010). Interestingly, CUL4–COP1–SPA complex has a dual function in dark/light-induced photomorphogenesis (Zhu et al., 2015; Paik et al., 2019). CUL4–COP1–SPA complex activates early ubiquitin-mediated degradation of phytochrome interacting factor 1 (PIF1) to trigger light-induced seed germination (Zhu et al., 2015; Paik et al., 2019). The second group of repressor protein is COP9 signalosome (CSN). It is highly conserved and comprises eight subunits (Serino and Deng, 2003). CSN had been reported to be implicated in deneddylation/derubylation of CRLs (Schwechheimer et al., 2001). The third group of repressor protein is de-etiolated1 (DET1), COP10, DNA damage-binding protein 1 (DDB1), and CUL4. DET1 is known to bind histone H2B (Benvenuto et al., 2002). It also regulates PIFs and HFRs to suppress seed germination and photomorphogenesis under dark conditions (Dong et al., 2014; Shi et al., 2015). Finally, the fourth group of repressor protein is PIFs (PIF1–PIF8) that belong to basic helix-loop-helix (bHLH) family of TFs and suppresses photomorphogenesis under dark conditions (Leivar et al., 2008; Shin et al., 2009; Leivar and Quail, 2011; Pham et al., 2018). They bind to the G-box consensus sequence in the 1,000-bp upstream region of light-responsive genes. Under dark conditions, phytochromes physically interact with PIFs to repress light response. The activation of photoreceptors suppresses COP1/SPA E3 ubiquitin ligase complexes and PIFs (Martínez et al., 2018b). This eventually activates HY5 to modulate the expression of light-inducible genes and disrupts PIF function (Chen et al., 2013; Toledo-Ortiz et al., 2014; Gangappa and Kumar, 2017). Upon plant exposure to dark conditions, photoreceptor inactivation enables COP1/SPA- and PIF-mediated disruption of light signaling (Xu X. et al., 2014; Xu et al., 2015b, 2017). This signaling cascade promotes plant growth by involving phyto-hormones (such as BR, auxins, and GA) at the cost of plant immunity (Lozano-Durán and Zipfel, 2015; Martínez et al., 2018b).

Photoreceptors are also responsible to determine the quality of light (R:FR ratios). Upon excitation by R light, phytochromes are transformed into FR light-absorbing state (biologically active "Pfr"). Since red light is absorbed by chlorophyll and carotenoids, its quantity is significantly decreased when penetrating through a dense canopy (Slattery et al., 2017; Walker et al., 2018). Shade-intolerant plants (such as *A. thaliana*) perceive and respond to such conditions by elongating stems and promoting flowering (Fiorucci and Fankhauser, 2017). This is an evolutionary phenomenon developed in plants and is termed shade-avoidance syndrome (SAS). Plants exhibit SAS, which is represented by the elongation of plant parts such as hypocotyls, stems, and petioles (Casal, 2013). Both PHYA and PHYB proteins contribute towards SAS. PHYB restrains SAS under R-enriched light (R:FR $>$ 1), while PHYA restrains SAS under FR-enriched light (R:FR $<$ 1) (Franklin, 2008; Lorrain et al., 2008; Franklin and Quail, 2010; Jaillais and Chory, 2010; Martinez-Garcia et al., 2010; Stamm and Kumar, 2010). This also result in the inactivation of PIF to promote BR and auxin production (Martínez et al., 2018a).

The amalgamation of photochemical and non-photochemical processes (NPQ) dissipates excess excitation energy (EEE) of plants as heat. Photochemical- and NPQ-dissipated EEE maintenance is facilitated by the acidification of the chloroplast lumen, involving PSII-associated proteins (Niyogi, 2000; Müller et al., 2001; Li et al., 2004; Niyogi et al., 2005; Ciszak et al., 2015). EEE eventually results in the formation of ROS, H_2O_2, superoxide (O_2^{-}), and singlet oxygen ($^1O_2$), which overlaps with biotic stress signaling. Light/dark alterations induce plant resistance to pathogen infection and oxidative damage in systemic tissues. This indicates a cross-wired signaling between dark/light conditions and biotic stress (Rossel et al., 2007; Mühlenbock et al., 2008; Szechyńska-Hebda et al., 2010; Zhao et al., 2014). EEE induces SAR and basal response to pathogenic biotrophic bacteria. This response alters ROS and redox signals and thus induces SA, ET, and glutathione (Mühlenbock et al., 2008; Szechyńska-Hebda et al., 2010).

EFFECT OF DARK/LIGHT ON PLANT–PATHOGEN INTERACTION AND ASSOCIATED MECHANISMS

Accumulating evidences indicate that plant response to biotic stress cannot be fully deciphered by studying discrete stress response (Suzuki et al., 2014; Dworak et al., 2016). Such notions support comprehensive study in connection with plant responses to simultaneously appearing stresses. Both qualitative and quantitative changes occur in the intensity of light during dark/light alterations. The majority of invertebrate herbivores with few exceptions (Kreuger and Potter, 2001; VanLaerhoven et al., 2003) are more active at night in comparison with day

because of parasitism or predation constraints during the day (Hassell and Southwood, 1978). The emission of volatiles also affects herbivory with respect to diurnal variation. There are even qualitative and quantitative disparities during day/night in wound-induced volatiles (De Moraes et al., 2001; Gouinguené and Turlings, 2002; Martin et al., 2003). Taking into account the effect of dark/light on pathogen attack upon plants, the number of airborne fungal spores is significantly high at night (dark) in comparison with day (Schmale and Bergstrom, 2004; Gilbert and Reynolds, 2005; Zhang et al., 2005). On the contrary, few fungal spores peak at day (light) time (Gadoury et al., 1998; Su et al., 2000). Along with dark/light alterations, the plant–pathogen interaction is also influenced by an array of factors such as temperature fluctuations, humidity changes, and leaf surface water content resulting from dew conditions at night (Meijer and Leuchtmann, 2000; Koh et al., 2003). The presence of light also reduces germ tube growth and spore germination in plant pathogenic fungi (Mueller and Buck, 2003; Beyer et al., 2004). A number of studies have revealed that pathogen infection is influenced by light/dark conditions before inoculation happens. Tolerance to aphid infestation was also confirmed by high-light pre-exposures in wild-type plants and mutants impaired in protein phosphatase 2A (PP2A) (Rasool et al., 2014). Similarly, inoculation of *Puccinia striiformis* in wheat (*Triticum aestivum*) seedlings was more at low light intensity than dark-grown seedlings (De Vallavieille-Pope et al., 2002). In a few other instances, inoculation irradiances have been found to be inversely proportional to infection (Shafia et al., 2001), indicating a direct impact of dark/light on host tolerance. Recently, nucleotide-binding NLR Rpi-vnt1.1 proteins have been shown to require light for imparting disease resistance against races of the Irish potato famine pathogen *Phytophthora infestans*, which discharge the effector protein AVRvnt1 (Gao et al., 2020). Glycerate 3-kinase (GLYK), which is a nuclear-encoded chloroplast protein, is necessary for the activation of Rpi-vnt1.1. Under light conditions, AVRvnt1 binds to the full-length chloroplast targeted GLYK isoform triggering of Rpi-vnt1.1. However, under the dark scenario, plants generate a shorter truncated GLYK that is devoid of the intact chloroplast transit peptide, thus compromising Rpi-vnt1.1-mediated resistance. The conversion between full-length and short-length GLYK transcripts is governed by light-dependent promoter selection mechanism. In plants that are devoid of Rpi-vnt1.1, the occurrence of AVRvnt1 decreases GLYK accumulation in chloroplasts, hence reducing GLYK contribution to basal immunity. The findings are thus clearly depictive of the fact that the pathogen-driven functional alteration of the chloroplast results in a light-dependent immune response (Gao et al., 2020). Plausibly, plants are more prone to pathogen attack in the dark than during the day. However, it cannot be held true for all pathogens attacking the plant systems.

There occur two mechanisms that contribute to the regulation of plant defense responses during dark/light fluctuations: first, the energetic significance of light-dependent chemical reactions (depends on the capacity of photosynthetic electron transport to produce ATP and reducing power); and second, perception of light (shade and R:FR exposure conditions) and regulation of downstream light-dependent signaling pathways (Roberts and Paul, 2006). The following subsections highlight both the mechanisms with respect to photosynthesis, ROS accumulation, and light signaling.

Photosynthetic Processes and Reactive Oxygen Species Accumulation in Biotic Stress

Photosynthesis captures light energy via electron transport chain (ETC) for assimilation of carbon dioxide as well as repair and growth of plant body. The vital metabolites so produced from photosynthesis are utilized in carbon fixation, fatty acid biosynthesis, assimilation of nitrogen into amino acids, etc. (Nunes-Nesi et al., 2010). These light-driven pathways occurring in chloroplast can impact short term-induced plant defense responses (Delprato et al., 2015). Intriguingly, some part of the biosynthetic pathways of ABA, JA, and SA (plant defense hormones) also occur in the plastids (Bobik and Burch-Smith, 2015). This might impact plant defense in the dark due to the hormonal cross-talk in plant–microbe interaction. Moreover, chloroplast acts as a site for ROS generation upon stress perception. Leaves get acclimatized to light fluctuations during growth and development, as calvin cycle enzymes and light-harvesting complexes are adjusted to efficiently manage the available light. However, photosynthetic electron transport produces more electrons when carbon fixation is halted or light fluctuations occur. This helps in the generation of more electrons for the electron acceptor $NADP^+$. Under such circumstances, free electrons from ETC are transferred to oxygen leading to ROS generation. Additionally, the light-dependent events and pathways occurring in the chloroplast impact short and long-term-induced plant defense responses via photorespiration resulting in the generation of H_2O_2 in the peroxisomes (Lu and Yao, 2018). Under acute light stress conditions, impairment in chlorophyll synthesis and disruption of chloroplast can also lead to the accumulation of ROS. This might surpass the potential of the antioxidant system in the chloroplast (Apel and Hirt, 2004). Nevertheless, ROS has also been very well implicated in plant defense against pathogens (Torres, 2010; Nath et al., 2017; Huang et al., 2019), and any deviation of the redox balance in the chloroplast can impact ROS regulated plant defense (**Figure 3**). For instance, lipid peroxidation occurs when ROS accumulates upon biotic stress perception (De Dios Alché, 2019). The repercussions of the requisite of light/dark fluctuations for chloroplast-derived ROS goes far beyond direct signaling functions of ROS.

As for post pathogen attack, some of the products of lipid peroxidation are reactive electrophiles with a carbonyl group (Vollenweider et al., 2000). These electrophiles are a consequence of ROS impact on membrane lipids or are products arising from lipoxygenase enzyme activity. Many amongst these electrophiles are imperative signaling molecules implicated in the regulation of cell death and defense gene expression (Vollenweider et al., 2000; Alméras et al., 2003; Thoma et al., 2003; Cacas et al., 2005). Hence, light/dark fluctuations impact the production of ROS-derived electrophiles. Such cases are reported in interactions amongst plants and pathogens or their elicitors. Taking into

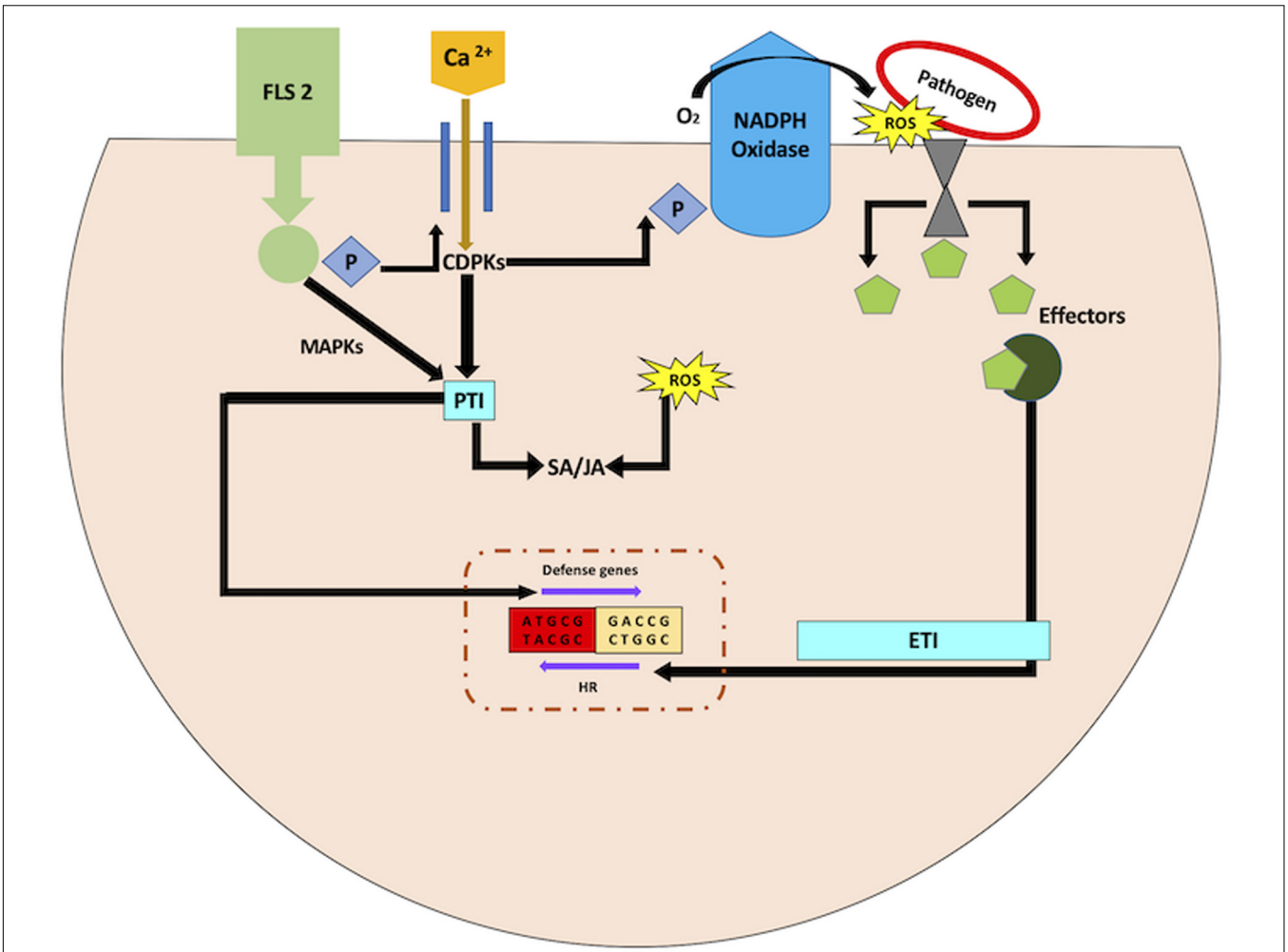

FIGURE 3 | ROS modulation of biotic stress responses. FLS2 receptor kinase triggers the Ca^{2+} flux, followed with mitogen-activated protein kinase (MAPK) and Ca^{2+}–dependent protein kinase (CDPK) cascades. These initial signals contribute to pathogen-associated molecular pattern (PAMP)-triggered immunity (PTI). Effector molecules are synthesized by host-adapted microbes, which suppress PTI. Plant system under such circumstances specifically identifies effector molecules to activate effector-triggered immunity (ETI). This eventually initiates the hypersensitive response (HR).

consideration the response of cryptogein (a known elicitor), cell death was mediated by ROS accumulation in light conditions (Montillet et al., 2005). On the contrary, when plants are subjected to dark conditions, cell death is independent of ROS accumulation and correlates with specific lipoxygenase activity (Montillet et al., 2005).

The primary source of ROS during biotic stress response is not the chloroplast. It is rather NADPH oxidase (respiratory burst oxidase) that is localized in the plasma membrane (Apel and Hirt, 2004; **Figure 3**). This implies that chloroplast-derived ROS in the presence of light may not help with pathogen defense. Nonetheless, this may or may not hold true, since NADPH oxidase does not impede the production of chloroplast-derived ROS. More so, lesion mimic mutants with random necrotic lesions are characterized to comprehend the underlying mechanisms involved in signaling of biotic stress tolerance (Lorrain et al., 2003). These necrotic lesions on the leaves are comparable with those generated in response to HR. Lesion mimic mutants have higher expression of *PR* genes and enhanced resistance against pathogen attack. These mutants highlight the common nexus between biotic stress response and chloroplast ROS based on two observations (Karpinski et al., 2003; Bechtold et al., 2005). First, the formation of lesions in lesion mimic mutants are light-dependent (Brodersen et al., 2002). Second, the functional characterization of these mutants highlights genes implicated in chlorophyll biosynthesis or degradation (Ishikawa et al., 2001; Mach et al., 2001; Pružinská et al., 2003; Wang F. et al., 2016; Lv et al., 2019). Additionally, the change in expression profiles of genes implicated in chlorophyll biosynthesis also leads to light-dependent lesion mimic phenotypes, eventually resulting in enhanced disease tolerance (Molina et al., 1999; Lv et al., 2019). This may be due to the formation of ROS generated by the effect of light on chlorophyll intermediates acting as photosensitizers. The electrons are excited by the absorption of

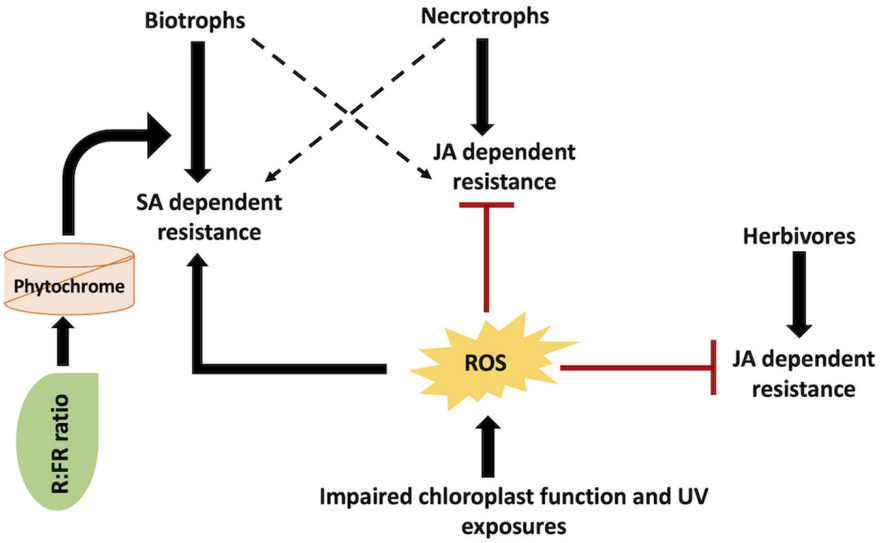

FIGURE 4 | SA/JA mediated cross-talk in light signaling and defense responses against different pathogenic agents: various biotic agents activate different mechanisms. Reactive oxygen species (ROS), salicylic acid (SA), and jasmonic acid (JA).

light energy by photosensitizers. The ROS thus produced acts as signals for pathogen resistance responses. Hence, it is evident that light-derived ROS from either free photosensitive pigments or photosynthetic light-harvesting complexes can influence plant defense signaling.

Plants have decentralized well-defined mechanisms for light-derived ROS in tissues subjected to biotic stress. For instance, the *A. thaliana chlorophyllase 1* (*AtCHL1*) gene is implicated in chlorophyll degradation and removal of photosensitive porphyrin ring intermediates. *AtCHL1* functions to preclude ROS accumulation due to damaged chloroplast (Kariola et al., 2005). This particular gene has been established to be triggered upon necrotrophic infections (Kariola et al., 2005). Plants with impaired *AtCHL1* gene display enhanced tolerance to *Erwinia carotovora* (necrotrophic bacterial pathogen) but reduced tolerance to *Alternaria brassicicola* (a fungal necrotroph) (Kariola et al., 2005). SA-dependent pathway is involved in *E. carotovora* resistance, while JA-dependent pathway is involved in *A. brassicicola* resistance. SA- and JA-mediated plant defense responses are antagonistic in nature (**Figure 4**). As such, *AtCHL1* mediates the equilibrium between SA- and JA-dependent plant–pathogen resistance pathways by adjusting ROS accumulation from chlorophyll metabolites. Similarly, the *A. thaliana ACD2* gene decreases the accumulation of photosensitizers. This results in an increased resistance to *P. syringae* (Mach et al., 2001). It is also noteworthy that several plants generate photosensitizers, which directly play a prominent role in imparting biotic stress tolerance. Phototoxins produce ROS in the presence of white or UV light that directly prevents herbivore or pathogen infection (Downum, 1992; Flors and Nonell, 2006). On the contrary, few fungal pathogens themselves generate photosensitive toxins (namely, cercosporin) leading to plant cell necrosis (Daub and Ehrenshaft, 2000). An entire range of various levels of interaction amongst light, dark, and biotic stress constitutes induced defenses in plants. These levels of interaction include ROS generation, phytochrome signaling, and activation of biotic stress-related genes. Taken together, different biotic agents deploy overlapping signaling pathways with ROS as the key modulator molecule (**Figure 4**). Thus, comprehending the significance and pathways involved in these overlapping responses may be useful in deciphering the overall involvement of light/dark alterations on biotic stress tolerance and resistance mechanisms.

Perception of Light With Respect to Shade and R:FR Exposures; and Regulation of Downstream Light-Dependent Signaling Pathways

The second key mechanism by which light/dark alterations regulate biotic stress responses engages direct light-responsive signaling pathways. The Genoud et al. (1998) has elegantly unraveled this mechanism in *A. thaliana*. The group has identified *psi2* light signaling defective mutant that develops light-dependent random necrotic lesions and has an increased expression of *PR1* gene (Genoud et al., 1998). Further characterization of *psi2* mutant reveals that the biotic stress responses are governed by light at various levels. For example, *PSI2* regulates the responses associated with phytochrome. Moreover, PHYA and PHYB are essential for *PR* gene expression and light-dependent HR lesion formation (Genoud et al., 1998, 2002). Hence, the phytochrome mutants have decreased resistance to *P. syringae*, while the *psi2* mutants have enhanced resistance to *P. syringae*. This is a clear evidence where light signals play a pivotal role in the regulation of induced biotic resistance. However, why and how phytochrome signaling modulate biotic stress responses still remain obscure. On the contrary, the dark conditions or high light stress also operates

molecular pathways that are common with pathogen responses (Mackerness et al., 1999; Rossel et al., 2002; Izaguirre et al., 2003; Kimura et al., 2003; Stratmann, 2003; Zhao et al., 2014). Enormous literature exists on the physiological basis of light dependency in relation to biotic defense, but the in-depth basis of dark/light effect on induced resistance remains elusive. A vital question, therefore, is to ascertain the mechanistic details for such observations. Undoubtedly, light is indispensable for plant growth and development, meaning that there is no unambiguous explanation to connect various observations across distinctive scales of organization. However, there are two modules that can be taken into account: first, resistance, which decreases the rigor of pathogen attack by restricting the activity of pathogen; and second, tolerance, which decreases the adverse effects of pathogen attack on the host plant. The demarcation between resistance and tolerance is critical for comprehension of interaction mechanisms between dark/light and plant defense.

In the field, the shade affects the cumulative radiation balance with plausible influence on biotic environment of the host. The temperature of the surrounding air and organisms is usually lower in shade, influencing a wide range of biological processes including biotic stress. For instance, tree canopies influence the species richness of insectivorous birds that affects herbivory (Strong et al., 2000; Van Bael and Brawn, 2005; Nell et al., 2018). Similarly, canopy shade has varying effects on photosynthetically active radiation (PAR) and UV wavelength (Grant and Heisler, 2001; Heisler et al., 2003; Grant et al., 2005). Additionally, the shade also results in either infestation by many pathogens or protection from the others. Pathogenic infestation is more stern in shade, for example, anthracnose (*C. gloeosporioides*) of *Euonymus fortunei* (Ningen et al., 2005), powdery mildew (*Microsphaera alphitoides*) on oak (*Quercus petraea*) (Kelly, 2002), and coffee rust (*Hemileia vastatrix*) (Soto-Pinto et al., 2002). Nonetheless, very often, plants develop a symbiotic relationship with beneficial microbes to enhance their defense responses and obtain nutrients under deficit conditions. The intense interplay between light signaling and defense mechanisms against beneficial and harmful microorganisms might be imperative for plant growth on high planting densities. Taking into account the beneficial interactions, the best-studied example is the nitrogen-fixing rhizobium bacteria and the leguminous plants (Ferguson et al., 2010). Rhizobium colonizes plant roots to form nodules that fix atmospheric nitrogen into mineral nitrogen for efficient usage by the leguminous plants. In return, the bacteria get carbon sources from the plant, which is essential for their survival (Ferguson et al., 2010). The *Lotus japonicus PhyB* mutant displays a shade-avoidance phenotype (similar to *Arabidopsis* mutant) with lesser number of root nodules in contrast to control plants (Suzuki et al., 2011; Sessa et al., 2018). Experimental validation reveals that the nodulation is decreased in grafted plants with *phyB* shoots and control roots. This is indicative of the fact that the mutations in the shoot tissue decrease nodulation in the roots (Suzuki et al., 2011; Shigeyama et al., 2012). The decreased nodulation in *phyB* mutants can be linked to downregulation of JA-responsive gene expression leading to lower JA levels in roots (Suzuki et al., 2011; Shigeyama et al., 2012). Next, taking into account the impact of R:FR exposures, the plant defense mechanisms against herbivores and pathogens are downregulated under low R:FR conditions (Ballaré, 2014; Ballaré and Austin, 2019; **Figure 5**). This probably implies that the interplay between beneficial interactions and light signaling is species-specific. In yet another example, plants establish a symbiotic relationship with arbuscular mycorrhizal fungi (AMF). These phosphate-acquiring fungi form "arbuscules" to enable phosphate and nitrogen uptake in plants, and in return, they derive carbon sources from plants (Keymer et al., 2017). The exposure of low R:FR ratios to *L. japonicus* roots decreases hyphal development of the AMF *Rhizophagus irregularis*. This is tightly regulated by the downregulation of JA-responsive genes resulting in decreased JA levels in root exudates (Nagata et al., 2015, 2016). At high plant density area, symbiotic relationship with rhizobium and AMF may be under scrutiny during low R:FR light conditions. However, the relationship between plant–microbe beneficial interactions and light signaling is still unclear and requires further investigation to improve plant growth and immunity.

Plants possess a continuous ever-evolving armor of defense mechanisms to prevent the colonization of harmful pathogens (Jones and Dangl, 2006; Nishad et al., 2020). Plants identify the signatures from the impeding pathogens and microbes via PAMPs, HAMPs, ETI, and PTI (Zipfel, 2014; Cui et al., 2015; Peng et al., 2018) (see section "Biotic Stress and Plant Defense Responses"). As already discussed, the antagonistic relationship between JA and SA modulates defense responses against biotrophic and necrotrophic pathogens (Glazebrook, 2005). JA is the central regulatory phytohormone coordinating the defense responses against pathogens and insects (Turner et al., 2002; Santino et al., 2013; Yang et al., 2019). Initial studies indicated that plants exposed to low R:FR or with impaired *PHYB* gene function exhibit reduced resistance to herbivores that is associated with declined sensitivity to JA (McGuire and Agrawal, 2005; Izaguirre et al., 2006; Moreno et al., 2009). Upon herbivory attack, volatile organic compound (VOC) emissions and methyl jasmonate (MeJA)-associated gene expression decreases in *A. thaliana* under low R:FR exposures (Kegge et al., 2013; **Figure 5**). A similar observation has been reported in barley where low R:FR exposure modifies constitutive VOC emissions to regulate the responses associated with plant–plant interactions (Kegge et al., 2015). This is further confirmed in *Solanum* (Cortés et al., 2016). In tomato, a low R:FR ratio affects MeJA-mediated VOC composition. This in turn influences the indirect defense response by enticing the insects (Cortés et al., 2016). Additionally, an intricate regulation of light signaling pathways maintains a balance of the constructive or destructive effects of light on plant growth and immunity. In contrast to the above observations, under low R:FR conditions, *Geranium robertianum* (a shade adapted forest understory plant) does not display downregulation of its JA-related plant defenses (Gommers et al., 2017). It also exhibits a slight increase in resistance against *B. cinerea*. Transcriptome analysis of *G. robertianum* and *Geranium pyrenaicum* (a shade-avoiding plant) reveals a number of genes with an opposite mode of regulation upon encountering shade conditions. Under low R:FR conditions, receptors like kinases FER and THE1 (responsible for shade induced elongation growth) are induced

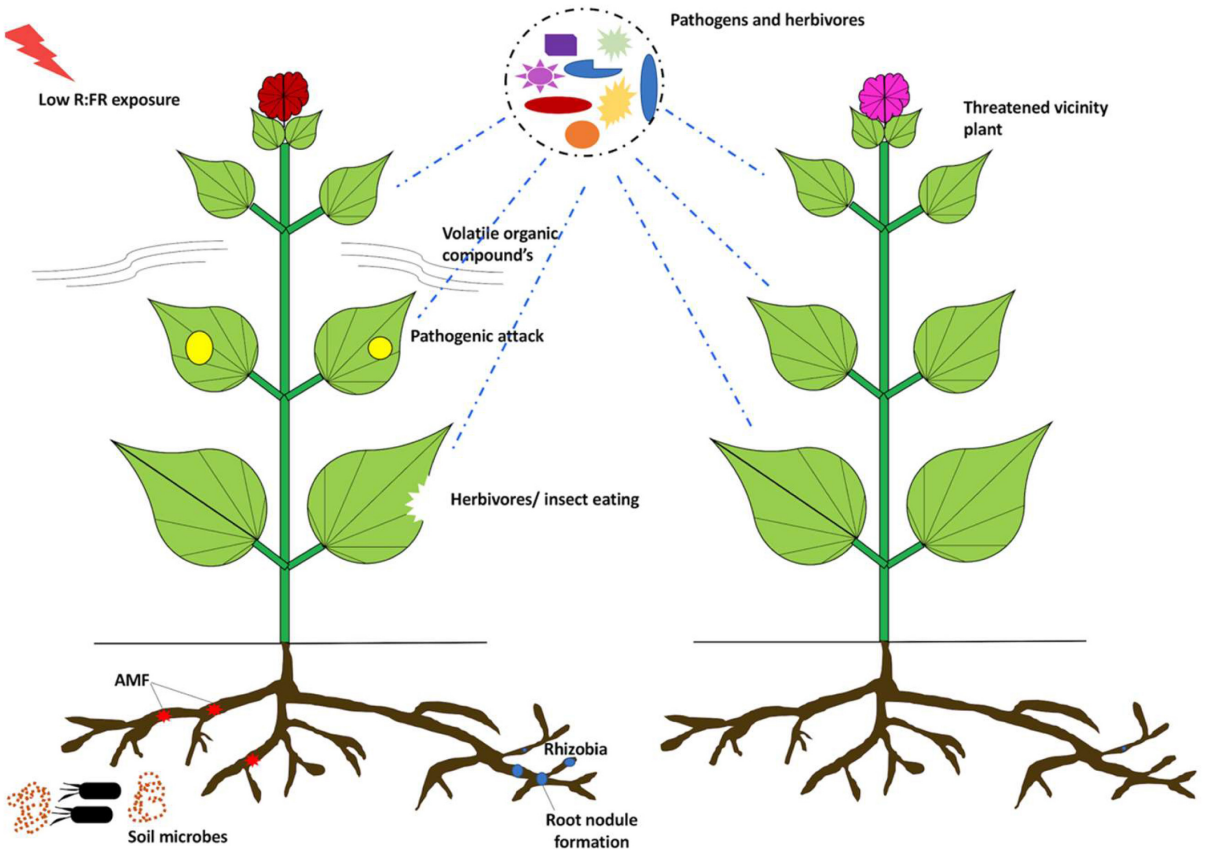

FIGURE 5 | Low R:FR modulation of plant immunity: low R:FR makes the plants more susceptible to pathogens and insects. Low R:FR exposure modulates VOC compositions, exposing plants to herbivory attack. Also, the formation of nodules and arbuscules is impacted by R:FR ratios. Arbuscular mycorrhizal fungi (AMF), volatile organic compounds (VOCs).

in *G. pyrenaicum*. FER and THE1 may be directly involved in regulating plant immunity and growth under shade. Conversely, in *G. robertianum*, exposure to low R:FR ratios leads to suppression of *JAZ* genes, which confer immunity under shade conditions. This establishes a classical example of the plasticity of light signaling in modulating plant growth and defense responses (Hématy et al., 2007; Kessler et al., 2010; Stegmann et al., 2017). Phenotypic and transcriptomic studies unravel a link between SAS- and SA-based defense components in shade-unresponsive *Arabidopsis* mutants (Nozue et al., 2018). JA, SA, and auxin-related signaling pathways are stimulated under low R:FR conditions and contribute strongly toward SAS (Nozue et al., 2018). Prolonged photoperiods positively regulate SA production, SA-related defenses, systemic immunity, and autoimmunity in lesion-mimic mutants (Griebel and Zeier, 2008; Gangappa and Kumar, 2017). Shade-avoidance mechanism under low light conditions restrains defense via a number of mechanisms (Cipollini, 2004). The swing in the distribution of resources to growth under shade may compete with the allocation of resources to plant defense. There might also be an intersection between light signaling and defense signaling. Under shade, stem elongation is regulated by auxin and gibberellins (Vandenbussche and Van Der Straeten, 2004). Auxin is known to interact with defense signaling pathways via a cross-wired mesh involving indole acetic acid (IAA). IAA also decreases JA-regulated generation of defense compounds (Baldwin et al., 1997; Yang et al., 2019). Contrariwise, the expression and concentration of auxins are altered upon wounding and herbivory (Cheong et al., 2002; Schmelz et al., 2003; Machado et al., 2016). Even the stiffening of the cell wall is an antagonistic mechanism between plant defense and shade (Cipollini, 2004), where gibberellin causes cell wall loosening resulting in cell expansion in shade. This can be attributed as an imperative component of plant defense.

Extensive research has been devoted to the mechanistic details as to how phytochromes regulate JA responses in relation to biotic defense responses (Hou et al., 2010; Ballaré, 2014; Leone et al., 2014; Pieterse et al., 2014; Campos et al., 2016). The described mechanism involves the interaction between DELLA proteins (growth repressor) and JAZ proteins (negative defense regulator) (Ballaré, 2014; Pieterse et al., 2014). MYC2 has been very well implicated to activate downstream defense responses (Hou et al., 2010; Verhage et al., 2012; Woldemariam et al., 2013; Liu et al., 2019). The DELLA proteins are degraded to sequester JAZ, resulting in inhibition of MYC2 TF (Hou et al., 2010). JAZ10 protein has been observed to be highly stable in *A. thaliana*

phyB mutant. This could probably be due to the degradation associated with DELLA proteins (Leone et al., 2014). Again, the lower sensitivity of the *jaz10 phyB* double mutant than the *phyB* mutant to *B. cinerea* highlights the importance of JAZ10 in relation to light signaling and biotic stress responses (Cerrudo et al., 2017). Particularly, inactivation of *PHYB* suppresses JA-related plant defense responses exclusive of shade-avoiding morphological changes (Moreno et al., 2009). In contrast, the JAZ absence reinforces JA-related plant defenses without compromising plant growth in *phyB* (Campos et al., 2016). Thus, plant defense activation or suppression is not dependent upon growth promotion or inhibition. This is suggestive of the fact that growth, light signaling, and defense trade-off are effective adaptive responses. Both JA- and SA-dependent defense responses are downregulated under low R:FR conditions. This also overlaps with NPR1 phosphorylation inhibition leading to reduced defense induction (de Wit et al., 2013). Also, for JA-related defense responses, prolonged photoperiods require the involvement of PHYA, cryptochromes, DELLAs, and the JA-regulating TF MYC2 (Cagnola et al., 2018). Conversely, short photoperiods result in PIF4-mediated growth elevation and immunity suppression. This is in concert with the fact that the elevated PIF4 accumulation and activation in the dark are dependent upon COP1/DET1 (Gangappa et al., 2017; Gangappa and Kumar, 2017). The COP1/DET1–PIF4 complex is also essential for autoimmunity suppression at high temperatures in *snc1* and *cpr5* mutants (Gangappa and Kumar, 2017). These studies are indicative of crucial involvement of the COP1/DET1-PIF module in prioritizing growth over plant immunity.

In addition, BR signaling apart from being involved in growth responses also plays a vital role in biotic stress responses (Planas-Riverola et al., 2019). BR signaling is linked with flagellin (a well-known PAMP) recognition upon pathogen attack. This is accomplished by the interaction between the BR receptor kinase BRI1 and its coreceptor BAK1 (Chinchilla et al., 2007). BR inhibits the defense machinery of plants by inducing *Brassinazole-resistant 1* (*BZR1*) gene (Lozano-Durán et al., 2013; Lozano-Durán and Zipfel, 2015). BZR1 is an important component of the BAP/D module, which is very well implicated in plant growth and development (Bouré et al., 2019). Under low R:FR conditions, BR responses may be involved in growth via the BAP/D module that can supersede flagellin-mediated plant defense response. It is also pertinent to mention that low R:FR affects the primary metabolism of plants (Yang et al., 2016; de Wit et al., 2018). Upon infecting plants, pathogens target carbohydrates as the key source of carbon for their survival. The enhanced susceptibility under low R:FR or in the phytochrome mutants may be due to higher accessibility of carbohydrates by the pathogens in plant tissues. Secondary metabolite production and defense-related gene expression (*viz.* MAPK and *PR* genes) are usually correlated with high concentrations of sugar accumulation in plant tissues (Bolouri Moghaddam and Van Den Ende, 2012). Reduced plant defense has been observed for *B. cinerea* under low R:FR conditions (Cargnel et al., 2014). This obstructed plant defense is a result of declined defense-related gene expression and metabolite production (Cargnel et al., 2014). Thus, low R:FR exposure declines defense-related pathways and enriches soluble sugars in plants, eventually inducing lesion formation in infected plant tissue (**Figure 5**). Taken together, plant growth responses to shade conditions are intricately cross-wired with the immune response generated by the plants upon pathogen exposure.

CONCLUSION AND FUTURE PROSPECTS

Exposure of plants to a combination of adverse environmental cues such as biotic stresses and light fluctuations coerces the efforts to meet enormous food demand. Despite the massive usage of pesticides and insecticides in the last few decades, the overall crop losses due to pathogen attack have not been reduced significantly. Monitoring infection time, plant growth, and other important parameters such as light/dark conditions can result in a better understanding of plant defense toward pathogens, particularly when extrapolated to field conditions. The present review provides an elaborate information on how plants perceive and respond to multiple dark/light alterations and biotic stresses. Light and dark conditions together or independently modulate a diverse range of signaling pathways to control pivotal plant growth and defense regulators. The function of multi-faceted dark/light signaling intermediates such as COP, CRY, PHY, and PIF has been extensively covered to highlight the impact of dark and light modulations on plant biotic defense responses. Even though significant efforts have been made to deep dive into the plant–microbe interactions and their association with light signaling, the mechanistic details encircling this complex intersection are obscure. Thus, the basic research to comprehend the mechanisms involved in the integrated circuitry of plant immunity and dark/light interactions, at both biological and ecological scales, will pave the way to overcome the limitations associated with crop losses globally.

AUTHOR CONTRIBUTIONS

MIA conceptualized and designed the study. ZI, MSI, AH, and EFA compiled the data and wrote the manuscript. All authors have read the manuscript and agreed for publication.

FUNDING

King Saud University, Saudi Arabia, research group (No. RG-1435-014).

ACKNOWLEDGMENTS

We acknowledge the past and present members of our laboratory as well as our scientific collaborator in the field of plant stress physiology. We would like to extend our sincere appreciation to the Deanship of Scientific Research at King Saud University for funding this research group (No. RG-1435-014).

REFERENCES

Abdul Malik, N. A., Kumar, I. S., and Nadarajah, K. (2020). Elicitor and receptor molecules: orchestrators of plant defense and immunity. *Intern. J. Mol. Sci.* 21:963. doi: 10.3390/ijms21030963

Ádám, A. L., Nagy, Z. Á, Kátay, G., Mergenthaler, E., and Viczián, O. (2018). Signals of systemic immunity in plants: progress and open questions. *Intern. J. Mol. Sci.* 19:1146. doi: 10.3390/ijms19041146

Ahn, I. P. (2007). Disturbance of the Ca2+/calmodulin-dependent signalling pathway is responsible for the resistance of *Arabidopsis* dnd1 against *Pectobacterium carotovorum* infection. *Mol. Plant Pathol.* 8, 747–759. doi: 10.1111/j.1364-3703.2007.00428.x

Alabadí, D., and Blázquez, M. A. (2009). Molecular interactions between light and hormone signaling to control plant growth. *Plant Mol. Biol.* 69:409. doi: 10.1007/s11103-008-9400-y

Aldon, D., Mbengue, M., Mazars, C., and Galaud, J.-P. (2018). Calcium signalling in plant biotic interactions. *Intern. J. Mol. Sci.* 19:665. doi: 10.3390/ijms19030665

Ali, S., Ganai, B. A., Kamili, A. N., Bhat, A. A., Mir, Z. A., Bhat, J. A., et al. (2018). Pathogenesis-related proteins and peptides as promising tools for engineering plants with multiple stress tolerance. *Microbiol. Res.* 212, 29–37. doi: 10.1016/j.micres.2018.04.008

Alméras, E., Stolz, S., Vollenweider, S., Reymond, P., Mène-Saffrané, L., and Farmer, E. E. (2003). Reactive electrophile species activate defense gene expression in *Arabidopsis*. *Plant J.* 34, 205–216. doi: 10.1046/j.1365-313X.2003.01718.x

Apel, K., and Hirt, H. (2004). Reactive oxygen species: metabolism, oxidative stress, and signal transduction. *Annu. Rev. Plant Biol.* 55, 373–399. doi: 10.1146/annurev.arplant.55.031903.141701

Bae, G., and Choi, G. (2008). Decoding of light signals by plant phytochromes and their interacting proteins. *Annu. Rev. Plant Biol.* 59, 281–311. doi: 10.1146/annurev.arplant.59.032607.092859

Bai, Y., Sunarti, S., Kissoudis, C., Visser, R. G., and Van Der Linden, C. (2018). The role of tomato WRKY genes in plant responses to combined abiotic and biotic stresses. *Front. Plant Sci.* 9:801. doi: 10.3389/fpls.2018.00801

Baldwin, I. T., Zhang, Z.-P., Diab, N., Ohnmeiss, T. E., Mccloud, E. S., Lynds, G. Y., et al. (1997). Quantification, correlations and manipulations of wound-induced changes in jasmonic acid and nicotine in Nicotiana sylvestris. *Planta* 201, 397–404. doi: 10.1007/s004250050082

Ballaré, C. L. (2014). Light regulation of plant defense. *Annu. Rev. Plant Biol.* 65, 335–363. doi: 10.1146/annurev-arplant-050213-040145

Ballaré, C. L., and Austin, A. T. (2019). Recalculating growth and defense strategies under competition: key roles of photoreceptors and jasmonates. *J. Exper. Bot.* 70, 3425–3434. doi: 10.1093/jxb/erz237

Ballare, C. L., Mazza, C. A., Austin, A. T., and Pierik, R. (2012). Canopy light and plant health. *Plant Physiol.* 160, 145–155. doi: 10.1104/pp.112.200733

Bari, R., and Jones, J. D. (2009). Role of plant hormones in plant defence responses. *Plant Mol. Biol.* 69, 473–488. doi: 10.1007/s11103-008-9435-0

Bechtold, U., Karpinski, S., and Mullineaux, P. M. (2005). The influence of the light environment and photosynthesis on oxidative signalling responses in plant-biotrophic pathogen interactions. *Plant Cell Environ.* 28, 1046–1055. doi: 10.1111/j.1365-3040.2005.01340.x

Bender, K. W., and Snedden, W. A. (2013). Calmodulin-related proteins step out from the shadow of their namesake. *Plant Physiol.* 163, 486–495. doi: 10.1104/pp.113.221069

Benn, G., Bjornson, M., Ke, H., De Souza, A., Balmond, E. I., Shaw, J. T., et al. (2016). Plastidial metabolite MEcPP induces a transcriptionally centered stress-response hub via the transcription factor CAMTA3. *Proc. Natl. Acad. Sci. U.S.A.* 113, 8855–8860. doi: 10.1073/pnas.1602582113

Benvenuto, G., Formiggini, F., Laflamme, P., Malakhov, M., and Bowler, C. (2002). The photomorphogenesis regulator DET1 binds the amino-terminal tail of histone H2B in a nucleosome context. *Curr. Biol.* 12, 1529–1534. doi: 10.1016/S0960-9822(02)01105-3

Bernard, G. C., Egnin, M., and Bonsi, C. (2017). "The impact of plant-parasitic nematodes on agriculture and methods of control," in *Nematology-Concepts, Diagnosis and Control*, eds M. M. Shah and M. Mahamood (London: IntechOpen). doi: 10.5772/intechopen.68958

Beyer, M., Röding, S., Ludewig, A., and Verreet, J. A. (2004). Germination and survival of Fusarium graminearum macroconidia as affected by environmental factors. *J. Phytopathol.* 152, 92–97. doi: 10.1111/j.1439-0434.2003.00807.x

Bjornson, M., Benn, G., Song, X., Comai, L., Franz, A. K., Dandekar, A. M., et al. (2014). Distinct roles for mitogen-activated protein kinase signaling and CALMODULIN-BINDING TRANSCRIPTIONAL ACTIVATOR3 in regulating the peak time and amplitude of the plant general stress response. *Plant Physiol.* 166, 988–996. doi: 10.1104/pp.114.245944

Bobik, K., and Burch-Smith, T. M. (2015). Chloroplast signaling within, between and beyond cells. *Front. Plant Sci.* 6:781. doi: 10.3389/fpls.2015.00781

Bolouri Moghaddam, M. R., and Van Den Ende, W. (2012). Sugars and plant innate immunity. *J. Exper. Bot.* 63, 3989–3998. doi: 10.1093/jxb/ers129

Bose, J., Pottosin, I., Shabala, S. S. S., Palmgren, M. G., and Shabala, S. (2011). Calcium efflux systems in stress signaling and adaptation in plants. *Front. Plant Sci.* 2:85. doi: 10.3389/fpls.2011.00085

Boudsocq, M., Willmann, M. R., Mccormack, M., Lee, H., Shan, L., He, P., et al. (2010). Differential innate immune signalling via Ca 2+ sensor protein kinases. *Nature* 464, 418–422. doi: 10.1038/nature08794

Bouré, N., Kumar, S. V., and Arnaud, N. (2019). The BAP module: a multisignal integrator orchestrating growth. *Trends Plant Sci.* 24, 602–610. doi: 10.1016/j.tplants.2019.04.002

Breeze, E. (2019). State of (in) flux: Action of a CNGC Ca2+ channel in defense against herbivory. *Plant Cell* 31, 1423–1424. doi: 10.1105/tpc.19.00372

Brodersen, P., Petersen, M., Pike, H. M., Olszak, B., Skov, S., Ødum, N., et al. (2002). Knockout of *Arabidopsis* accelerated-cell-death11 encoding a sphingosine transfer protein causes activation of programmed cell death and defense. *Genes Dev.* 16, 490–502. doi: 10.1101/gad.218202

Cacas, J.-L., Vailleau, F., Davoine, C., Ennar, N., Agnel, J. P., Tronchet, M., et al. (2005). The combined action of 9 lipoxygenase and galactolipase is sufficient to bring about programmed cell death during tobacco hypersensitive response. *Plant Cell Environ.* 28, 1367–1378. doi: 10.1111/j.1365-3040.2005.01369.x

Cagnola, J. I., Cerdan, P. D., Pacin, M., Andrade, A., Rodriguez, V., Zurbriggen, M. D., et al. (2018). Long-day photoperiod enhances jasmonic acid-related plant defense. *Plant Physiol.* 178, 163–173. doi: 10.1104/pp.18.00443

Campos, M. L., Yoshida, Y., Major, I. T., De Oliveira Ferreira, D., Weraduwage, S. M., Froehlich, J. E., et al. (2016). Rewiring of jasmonate and phytochrome B signalling uncouples plant growth-defense tradeoffs. *Nat. Commun.* 7, 1–10. doi: 10.1038/ncomms12570

Cargnel, M. D., Demkura, P. V., and Ballaré, C. L. (2014). Linking phytochrome to plant immunity: low red: far-red ratios increase *Arabidopsis* susceptibility to B otrytis cinerea by reducing the biosynthesis of indolic glucosinolates and camalexin. *New Phytol.* 204, 342–354. doi: 10.1111/nph.13032

Carrion, A. M., Link, W. A., Ledo, F., Mellström, B., and Naranjo, J. R. (1999). DREAM is a Ca 2+-regulated transcriptional repressor. *Nature* 398, 80–84. doi: 10.1038/18044

Casal, J. J. (2013). Photoreceptor signaling networks in plant responses to shade. *Annu. Rev. Plant Biol.* 64, 403–427. doi: 10.1146/annurev-arplant-050312-120221

Catalá, R., Medina, J., and Salinas, J. (2011). Integration of low temperature and light signaling during cold acclimation response in *Arabidopsis*. *Proc. Natl. Acad. Sci. U.S.A.* 108, 16475–16480. doi: 10.1073/pnas.1107161108

Cerdán, P. D., and Chory, J. (2003). Regulation of flowering time by light quality. *Nature* 423, 881–885. doi: 10.1038/nature01636

Cerrudo, I., Caliri-Ortiz, M. E., Keller, M. M., Degano, M. E., Demkura, P. V., and Ballaré, C. L. (2017). Exploring growth-defence trade-offs in *Arabidopsis*: phytochrome B inactivation requires JAZ10 to suppress plant immunity but not to trigger shade-avoidance responses. *Plant Cell Environ.* 40, 635–644. doi: 10.1111/pce.12877

Chen, D., Xu, G., Tang, W., Jing, Y., Ji, Q., Fei, Z., et al. (2013). Antagonistic basic helix-loop-helix/bZIP transcription factors form transcriptional modules that integrate light and reactive oxygen species signaling in *Arabidopsis*. *Plant Cell* 25, 1657–1673. doi: 10.1105/tpc.112.104869

Chen, H., Huang, X., Gusmaroli, G., Terzaghi, W., Lau, O. S., Yanagawa, Y., et al. (2010). *Arabidopsis* CULLIN4-damaged DNA binding protein 1 interacts with CONSTITUTIVELY PHOTOMORPHOGENIC1-SUPPRESSOR OF PHYA complexes to regulate photomorphogenesis and flowering time. *Plant Cell* 22, 108–123. doi: 10.1105/tpc.109.065490

Chen, Y. L., Fan, K. T., Hung, S. C., and Chen, Y. R. (2020). The role of peptides cleaved from protein precursors in eliciting plant stress reactions. *New Phytol.* 225, 2267–2282. doi: 10.1111/nph.16241

Cheng, S.-H., Willmann, M. R., Chen, H.-C., and Sheen, J. (2002). Calcium signaling through protein kinases. The *Arabidopsis* calcium-dependent protein kinase gene family. *Plant Physiol.* 129, 469–485. doi: 10.1104/pp.005645

Cheng, X., Tian, C., Li, A., and Qiu, J. (2012). Advances on molecular mechanisms of plant-pathogen interactions. *Yi Chuan Hereditas* 34, 134–144. doi: 10.3724/SP.J.1005.2012.00134

Cheong, Y. H., Chang, H.-S., Gupta, R., Wang, X., Zhu, T., and Luan, S. (2002). Transcriptional profiling reveals novel interactions between wounding, pathogen, abiotic stress, and hormonal responses in *Arabidopsis*. *Plant Physiol.* 129, 661–677. doi: 10.1104/pp.002857

Chezem, W. R., Memon, A., Li, F.-S., Weng, J.-K., and Clay, N. K. (2017). SG2-type R2R3-MYB transcription factor MYB15 controls defense-induced lignification and basal immunity in *Arabidopsis*. *Plant Cell* 29, 1907–1926. doi: 10.1105/tpc.16.00954

Chiasson, D. M., Haage, K., Sollweck, K., Brachmann, A., Dietrich, P., and Parniske, M. (2017). A quantitative hypermorphic CNGC allele confers ectopic calcium flux and impairs cellular development. *eLife* 6:e25012. doi: 10.7554/eLife.25012.036

Chin, K., Defalco, T. A., Moeder, W., and Yoshioka, K. (2013). The *Arabidopsis* cyclic nucleotide-gated ion channels AtCNGC2 and AtCNGC4 work in the same signaling pathway to regulate pathogen defense and floral transition. *Plant Physiol.* 163, 611–624. doi: 10.1104/pp.113.225680

Chinchilla, D., Zipfel, C., Robatzek, S., Kemmerling, B., Nürnberger, T., Jones, J. D., et al. (2007). A flagellin-induced complex of the receptor FLS2 and BAK1 initiates plant defence. *Nature* 448, 497–500. doi: 10.1038/nature05999

Chory, J. (2010). Light signal transduction: an infinite spectrum of possibilities. *Plant J.* 61, 982–991. doi: 10.1111/j.1365-313X.2009.04105.x

Christie, J. M. (2007). Phototropin blue-light receptors. *Annu. Rev. Plant Biol.* 58, 21–45. doi: 10.1146/annurev.arplant.58.032806.103951

Chung, J.-S., Koo, S. C., Jin, B. J., Baek, D., Yeom, S.-I., Chun, H. J., et al. (2020). Rice CaM-binding transcription factor (OsCBT) mediates defense signaling via transcriptional reprogramming. *Plant Biotechnol. Rep.* 14, 309–321. doi: 10.1007/s11816-020-00603-y

Cipollini, D. (2004). Stretching the limits of plasticity: can a plant defend against both competitors and herbivores? *Ecology* 85, 28–37. doi: 10.1890/02-0615

Ciszak, K., Kulasek, M., Barczak, A., Grzelak, J., Maćkowski, S., and Karpiński, S. (2015). PsbS is required for systemic acquired acclimation and post-excess-light-stress optimization of chlorophyll fluorescence decay times in *Arabidopsis*. *Plant Signal. Behav.* 10:e982018. doi: 10.4161/15592324.2014.982018

Clack, T., Mathews, S., and Sharrock, R. A. (1994). The phytochrome apoprotein family in*Arabidopsis* is encoded by five genes: the sequences and expression ofPHYD andPHYE. *Plant Mol. Biol.* 25, 413–427. doi: 10.1007/BF00043870

Cortés, L. E., Weldegergis, B. T., Boccalandro, H. E., Dicke, M., and Ballaré, C. L. (2016). Trading direct for indirect defense? Phytochrome B inactivation in tomato attenuates direct anti-herbivore defenses whilst enhancing volatile-mediated attraction of predators. *New Phytol.* 212, 1057–1071. doi: 10.1111/nph.14210

Costa, A., Luoni, L., Marrano, C. A., Hashimoto, K., Köster, P., Giacometti, S., et al. (2017). Ca2+-dependent phosphoregulation of the plasma membrane Ca2+-ATPase ACA8 modulates stimulus-induced calcium signatures. *J. Exper. Bot.* 68, 3215–3230. doi: 10.1093/jxb/erx162

Costa, A., Navazio, L., and Szabo, I. (2018). The contribution of organelles to plant intracellular calcium signalling. *J. Exper. Bot.* 69, 4175–4193. doi: 10.1093/jxb/ery185

Creux, N., and Harmer, S. (2019). Circadian rhythms in plants. *Cold Spring Harb. Perspect. Biol.* 11:a034611. doi: 10.1101/cshperspect.a034611

Cui, H., Tsuda, K., and Parker, J. E. (2015). Effector-triggered immunity: from pathogen perception to robust defense. *Annu. Rev. Plant Biol.* 66, 487–511. doi: 10.1146/annurev-arplant-050213-040012

Dangl, J. L., and McDowell, J. M. (2006). Two modes of pathogen recognition by plants. *Proc. Natl. Acad. Sci. U.S.A.* 103, 8575–8576. doi: 10.1073/pnas.0603183103

Daub, M. E., and Ehrenshaft, M. (2000). The photoactivated *Cercospora toxin* cercosporin: contributions to plant disease and fundamental biology. *Annu. Rev. Phytopathol.* 38, 461–490. doi: 10.1146/annurev.phyto.38.1.461

De Dios Alché, J. (2019). A concise appraisal of lipid oxidation and lipoxidation in higher plants. *Redox Biol.* 23:101136. doi: 10.1016/j.redox.2019.101136

De Moraes, C. M., Mescher, M. C., and Tumlinson, J. H. (2001). Caterpillar-induced nocturnal plant volatiles repel conspecific females. *Nature* 410, 577–580. doi: 10.1038/35069058

De Vallavieille-Pope, C., Huber, L., Leconte, M., and Bethenod, O. (2002). Preinoculation effects of light quantity on infection efficiency of *Puccinia striiformis* and *P. triticina* on wheat seedlings. *Phytopathology* 92, 1308–1314. doi: 10.1094/PHYTO.2002.92.12.1308

De Vleesschauwer, D., Xu, J., and Höfte, M. (2014). Making sense of hormone-mediated defense networking: from rice to *Arabidopsis*. *Front. Plant Sci.* 5:611. doi: 10.3389/fpls.2014.00611

de Wit, M., George, G. M., Ince, Y. Ç, Dankwa-Egli, B., Hersch, M., Zeeman, S. C., et al. (2018). Changes in resource partitioning between and within organs support growth adjustment to neighbor proximity in Brassicaceae seedlings. *Proc. Natl. Acad. Sci. U.S.A.* 115, E9953–E9961. doi: 10.1073/pnas.1806084115

de Wit, M., Spoel, S. H., Sanchez-Perez, G. F., Gommers, C. M., Pieterse, C. M., Voesenek, L. A., et al. (2013). Perception of low red: far-red ratio compromises both salicylic acid-and jasmonic acid-dependent pathogen defences in *Arabidopsis*. *Plant J.* 75, 90–103. doi: 10.1111/tpj.12203

Deepika, A., Sagar, S., and Singh, A. (2020). Dark-induced hormonal regulation of plant growth and development. *Front. Plant Sci.* 11:581666. doi: 10.3389/fpls.2020.581666

DeFalco, T. A., Marshall, C. B., Munro, K., Kang, H.-G., Moeder, W., Ikura, M., et al. (2016). Multiple calmodulin-binding sites positively and negatively regulate *Arabidopsis* CYCLIC NUCLEOTIDE-GATED CHANNEL12. *Plant Cell* 28, 1738–1751. doi: 10.1105/tpc.15.00870

Delprato, M. L., Krapp, A. R., and Carrillo, N. (2015). Green light to plant responses to pathogens: the role of chloroplast light-dependent signaling in biotic stress. *Photochem. Photobiol.* 91, 1004–1011. doi: 10.1111/php.12466

Demidchik, V., Shabala, S., Isayenkov, S., Cuin, T. A., and Pottosin, I. (2018). Calcium transport across plant membranes: mechanisms and functions. *New Phytol.* 220, 49–69. doi: 10.1111/nph.15266

Deng, X.-W., Matsui, M., Wei, N., Wagner, D., Chu, A. M., Feldmann, K. A., et al. (1992). COP1, an *Arabidopsis* regulatory gene, encodes a protein with both a zinc-binding motif and a Gβ homologous domain. *Cell* 71, 791–801. doi: 10.1016/0092-8674(92)90555-Q

Dodd, A. N., Kudla, J., and Sanders, D. (2010). The language of calcium signaling. *Annu. Rev. Plant Biol.* 61, 593–620. doi: 10.1146/annurev-arplant-070109-104628

Dodds, P. N., and Rathjen, J. P. (2010). Plant immunity: towards an integrated view of plant-pathogen interactions. *Nat. Rev. Genet.* 11, 539–548. doi: 10.1038/nrg2812

Dong, J., Tang, D., Gao, Z., Yu, R., Li, K., He, H., et al. (2014). *Arabidopsis* DE-ETIOLATED1 represses photomorphogenesis by positively regulating phytochrome-interacting factors in the dark. *Plant Cell* 26, 3630–3645. doi: 10.1105/tpc.114.130666

Doughari, J. (2015). An overview of plant immunity. *J. Plant Pathol. Microbiol.* 6:104172. doi: 10.4172/2157-7471.1000322

Downum, K. R. (1992). Tansley review no. 43. Light-activated plant defence. *New Phytol.* 122, 401–420. doi: 10.1111/j.1469-8137.1992.tb00068.x

Dudareva, N., Negre, F., Nagegowda, D. A., and Orlova, I. (2006). Plant volatiles: recent advances and future perspectives. *Crit. Rev. Plant Sci.* 25, 417–440. doi: 10.1080/07352680600899973

Duek, P. D., Elmer, M. V., Van Oosten, V. R., and Fankhauser, C. (2004). The degradation of HFR1, a putative bHLH class transcription factor involved in light signaling, is regulated by phosphorylation and requires COP1. *Curr. Biol.* 14, 2296–2301. doi: 10.1016/j.cub.2004.12.026

Dworak, A., Nykiel, M., Walczak, B., Miazek, A., Szworst-Łupina, D., Zagdańska, B., et al. (2016). Maize proteomic responses to separate or overlapping soil drought and two-spotted spider mite stresses. *Planta* 244, 939–960. doi: 10.1007/s00425-016-2559-6

Ferguson, B. J., Indrasumunar, A., Hayashi, S., Lin, M. H., Lin, Y. H., Reid, D. E., et al. (2010). Molecular analysis of legume nodule development and autoregulation. *J. Integr. Plant Biol.* 52, 61–76. doi: 10.1111/j.1744-7909.2010.00899.x

Fiorucci, A.-S., and Fankhauser, C. (2017). Plant strategies for enhancing access to sunlight. *Curr. Biol.* 27, R931–R940. doi: 10.1016/j.cub.2017.05.085

Fischer, C., Defalco, T. A., Karia, P., Snedden, W. A., Moeder, W., Yoshioka, K., et al. (2017). Calmodulin as a Ca2+-sensing subunit of *Arabidopsis* cyclic nucleotide-gated channel complexes. *Plant Cell Physiol.* 58, 1208–1221. doi: 10.1093/pcp/pcx052

Flors, C., and Nonell, S. (2006). Light and singlet oxygen in plant defense against pathogens: phototoxic phenalenone phytoalexins. *Acc. Chem. Res.* 39, 293–300. doi: 10.1021/ar0402863

Folta, K. M., and Maruhnich, S. A. (2007). Green light: a signal to slow down or stop. *J. Exper. Bot.* 58, 3099–3111. doi: 10.1093/jxb/erm130

Foyer, C. H. (2018). Reactive oxygen species, oxidative signaling and the regulation of photosynthesis. *Environ. Exper. Bot.* 154, 134–142. doi: 10.1016/j.envexpbot.2018.05.003

Franklin, K. A. (2008). Shade avoidance. *New Phytol.* 179, 930–944. doi: 10.1111/j.1469-8137.2008.02507.x

Franklin, K. A., Larner, V. S., and Whitelam, G. C. (2004). The signal transducing photoreceptors of plants. *Intern. J. Dev. Biol.* 49, 653–664. doi: 10.1387/ijdb.051989kf

Franklin, K. A., and Quail, P. H. (2010). Phytochrome functions in *Arabidopsis* development. *J. Exper. Bot.* 61, 11–24. doi: 10.1093/jxb/erp304

Fu, Z. Q., and Dong, X. (2013). Systemic acquired resistance: turning local infection into global defense. *Annu. Rev. Plant Biol.* 64, 839–863. doi: 10.1146/annurev-arplant-042811-105606

Fürstenberg-Hägg, J., Zagrobelny, M., and Bak, S. (2013). Plant defense against insect herbivores. *Intern. J. Mol. Sci.* 14, 10242–10297. doi: 10.3390/ijms140510242

Gadoury, D. M., Stensvand, A., and Seem, R. C. (1998). Influence of light, relative humidity, and maturity of populations on discharge of ascospores of *Venturia inaequalis*. *Phytopathology* 88, 902–909. doi: 10.1094/PHYTO.1998.88.9.902

Gangappa, S. N., Berriri, S., and Kumar, S. V. (2017). PIF4 coordinates thermosensory growth and immunity in *Arabidopsis*. *Curr. Biol.* 27, 243–249. doi: 10.1016/j.cub.2016.11.012

Gangappa, S. N., and Kumar, S. V. (2017). DET1 and HY5 control PIF4-mediated thermosensory elongation growth through distinct mechanisms. *Cell Rep.* 18, 344–351. doi: 10.1016/j.celrep.2016.12.046

Gao, C., Xu, H., Huang, J., Sun, B., Zhang, F., Savage, Z., et al. (2020). Pathogen manipulation of chloroplast function triggers a light-dependent immune recognition. *Proc. Natl. Acad. Sci. U.S.A.* 117, 9613–9620. doi: 10.1073/pnas.2002759117

Gao, Q.-F., Gu, L.-L., Wang, H.-Q., Fei, C.-F., Fang, X., Hussain, J., et al. (2016). Cyclic nucleotide-gated channel 18 is an essential Ca2+ channel in pollen tube tips for pollen tube guidance to ovules in *Arabidopsis*. *Proc. Natl. Acad. Sci. U.S.A.* 113, 3096–3101. doi: 10.1073/pnas.1524629113

Garcia-Guzman, G., and Heil, M. (2014). Life histories of hosts and pathogens predict patterns in tropical fungal plant diseases. *New Phytol.* 201, 1106–1120. doi: 10.1111/nph.12562

Genoud, T., Buchala, A. J., Chua, N.-H., and Métraux, J.-P. (2002). Phytochrome signalling modulates the SA-perceptive pathway in *Arabidopsis*. *Plant J.* 31, 87–95. doi: 10.1046/j.1365-313x.2002.01338.x

Genoud, T., Millar, A. J., Nishizawa, N., Kay, S. A., Schäfer, E., Nagatani, A., et al. (1998). An *Arabidopsis* mutant hypersensitive to red and far-red light signals. *Plant Cell* 10, 889–904. doi: 10.1105/tpc.10.6.889

Gilbert, G. S., and Reynolds, D. R. (2005). Nocturnal fungi: *Airborne spores* in the canopy and understory of a tropical rain forest 1. *Biotropica J. Biol. Conserv.* 37, 462–464. doi: 10.1111/j.1744-7429.2005.00061.x

Glazebrook, J. (2005). Contrasting mechanisms of defense against biotrophic and necrotrophic pathogens. *Annu. Rev. Phytopathol.* 43, 205–227. doi: 10.1146/annurev.phyto.43.040204.135923

Goldsmith, C. S., and Bell-Pedersen, D. (2013). Diverse roles for MAPK signaling in circadian clocks. *Adv. Genet.* 84, 1–39. doi: 10.1016/B978-0-12-407703-4.00001-3

Gommers, C. M., Keuskamp, D. H., Buti, S., Van Veen, H., Koevoets, I. T., Reinen, E., et al. (2017). Molecular profiles of contrasting shade response strategies in wild plants: differential control of immunity and shoot elongation. *Plant Cell* 29, 331–344. doi: 10.1105/tpc.16.00790

González de Molina, M., Soto Fernández, D., Infante-Amate, J., Aguilera, E., Vila Traver, J., and Guzmán, G. I. (2017). Decoupling food from land: the evolution of Spanish agriculture from 1960 to 2010. *Sustainability* 9:2348. doi: 10.3390/su9122348

Gouinguené, S. P., and Turlings, T. C. (2002). The effects of abiotic factors on induced volatile emissions in corn plants. *Plant Physiol.* 129, 1296–1307. doi: 10.1104/pp.001941

Gouveia, B. C., Calil, I. P., Machado, J. P. B., Santos, A. A., and Fontes, E. P. (2017). Immune receptors and co-receptors in antiviral innate immunity in plants. *Front. Microbiol.* 7:2139. doi: 10.3389/fmicb.2016.02139

Grant, M., Brown, I., Adams, S., Knight, M., Ainslie, A., and Mansfield, J. (2000). The RPM1 plant disease resistance gene facilitates a rapid and sustained increase in cytosolic calcium that is necessary for the oxidative burst and hypersensitive cell death. *Plant J.* 23, 441–450. doi: 10.1046/j.1365-313x.2000.00804.x

Grant, M., and Lamb, C. (2006). Systemic immunity. *Curr. Opin. Plant Biol.* 9, 414–420. doi: 10.1016/j.pbi.2006.05.013

Grant, R. H., Apostol, K., and Gao, W. (2005). Biologically effective UV-B exposures of an oak-hickory forest understory during leaf-out. *Agric. For. Meteorol.* 132, 28–43. doi: 10.1016/j.agrformet.2005.06.008

Grant, R. H., and Heisler, G. M. (2001). Multi-waveband solar irradiance on tree-shaded vertical and horizontal surfaces: cloud-free and partly cloudy skies. *Photochem. Photobiol.* 73, 24–31. doi: 10.1562/0031-8655(2001)073<0024:MWSIOT>2.0.CO;2

Griebel, T., and Zeier, J. (2008). Light regulation and daytime dependency of inducible plant defenses in *Arabidopsis*: phytochrome signaling controls systemic acquired resistance rather than local defense. *Plant Physiol.* 147, 790–801. doi: 10.1104/pp.108.119503

Hamamouch, N., Li, C., Seo, P. J., Park, C. M., and Davis, E. L. (2011). Expression of *Arabidopsis* pathogenesis-related genes during nematode infection. *Mol. Plant Pathol.* 12, 355–364. doi: 10.1111/j.1364-3703.2010.00675.x

Hammond-Kosack, K., and Jones, J. D. G. (2000). Responses to plant pathogens. *Biochem. Mol. Biol. Plants* 1, 1102–1156.

Hardtke, C. S., and Deng, X.-W. (2000). The cell biology of the COP/DET/FUS proteins. Regulating proteolysis in photomorphogenesis and beyond? *Plant Physiol.* 124, 1548–1557. doi: 10.1104/pp.124.4.1548

Hardtke, C. S., Gohda, K., Osterlund, M. T., Oyama, T., Okada, K., and Deng, X. W. (2000). HY5 stability and activity in *Arabidopsis* is regulated by phosphorylation in its COP1 binding domain. *EMBO J.* 19, 4997–5006. doi: 10.1093/emboj/19.18.4997

Harmer, S. L., Hogenesch, J. B., Straume, M., Chang, H.-S., Han, B., Zhu, T., et al. (2000). Orchestrated transcription of key pathways in *Arabidopsis* by the circadian clock. *Science* 290, 2110–2113. doi: 10.1126/science.290.5499.2110

Hassell, M., and Southwood, T. (1978). Foraging strategies of insects. *Annu. Rev. Ecol. Syst.* 9, 75–98. doi: 10.1146/annurev.es.09.110178.000451

Hattori, T., Otomi, Y., Nakajima, Y., Soga, K., Wakabayashi, K., Iida, H., et al. (2020). MCA1 and MCA2 are involved in the response to hypergravity in *Arabidopsis hypocotyls*. *Plants* 9:590. doi: 10.3390/plants9050590

Heisler, G. M., Grant, R. H., and Gao, W. (2003). Individual-and scattered-tree influences on ultraviolet irradiance. *Agric. For. Meteorol.* 120, 113–126. doi: 10.1016/j.agrformet.2003.08.024

Hématy, K., Sado, P.-E., Van Tuinen, A., Rochange, S., Desnos, T., Balzergue, S., et al. (2007). A receptor-like kinase mediates the response of *Arabidopsis* cells to the inhibition of cellulose synthesis. *Curr. Biol.* 17, 922–931. doi: 10.1016/j.cub.2007.05.018

Hoecker, U. (2017). The activities of the E3 ubiquitin ligase COP1/SPA, a key repressor in light signaling. *Curr. Opin. Plant Biol.* 37, 63–69. doi: 10.1016/j.pbi.2017.03.015

Holtkotte, X., Dieterle, S., Kokkelink, L., Artz, O., Leson, L., Fittinghoff, K., et al. (2016). Mutations in the N-terminal kinase-like domain of the repressor of photomorphogenesis SPA 1 severely impair SPA 1 function but not light responsiveness in *Arabidopsis*. *Plant J.* 88, 205–218. doi: 10.1111/tpj.13241

Hou, X., Lee, L. Y. C., Xia, K., Yan, Y., and Yu, H. (2010). DELLAs modulate jasmonate signaling via competitive binding to JAZs. *Dev. Cell* 19, 884–894. doi: 10.1016/j.devcel.2010.10.024

Hua, J. (2013). Modulation of plant immunity by light, circadian rhythm, and temperature. *Curr. Opin. Plant Biol.* 16, 406–413. doi: 10.1016/j.pbi.2013.06.017

Huang, H., Ullah, F., Zhou, D.-X., Yi, M., and Zhao, Y. (2019). Mechanisms of ROS regulation of plant development and stress responses. *Front. Plant Sci.* 10:800. doi: 10.3389/fpls.2019.00800

Huner, N. P., Oquist, G., and Sarhan, F. (1998). Energy balance and acclimation to light and cold. *Trends Plant Sci.* 3, 224–230. doi: 10.1016/S1360-1385(98)01248-5

Iqbal, Z., Iqbal, M. S., Ahmad, A., Memon, A. G., and Ansari, M. I. (2020a). New prospects on the horizon: genome editing to engineer plants for desirable traits. *Curr. Plant Biol.* 24, 100171. doi: 10.1016/j.cpb.2020.100171

Iqbal, Z., Iqbal, M. S., Singh, S. P., and Buaboocha, T. (2020b). Ca2+/calmodulin complex triggers CAMTA transcriptional machinery under stress in plants: signaling cascade and molecular regulation. *Front. Plant Sci.* 11:598327. doi: 10.3389/fpls.2020.598327

Ishikawa, A., Okamoto, H., Iwasaki, Y., and Asahi, T. (2001). A deficiency of coproporphyrinogen III oxidase causes lesion formation in *Arabidopsis*. *Plant J.* 27, 89–99. doi: 10.1046/j.1365-313x.2001.01058.x

Islam, W., Naveed, H., Zaynab, M., Huang, Z., and Chen, H. Y. (2019). Plant defense against virus diseases; growth hormones in highlights. *Plant Signal. Behav.* 14:1596719. doi: 10.1080/15592324.2019.1596719

Izaguirre, M. M., Mazza, C. A., Biondini, M., Baldwin, I. T., and Ballaré, C. L. (2006). Remote sensing of future competitors: impacts on plant defenses. *Proc. Natl. Acad. Sci. U.S.A.* 103, 7170–7174. doi: 10.1073/pnas.0509805103

Izaguirre, M. M., Scopel, A. L., Baldwin, I. T., and Ballaré, C. L. (2003). Convergent responses to stress. Solar ultraviolet-B radiation and *Manduca sexta* herbivory elicit overlapping transcriptional responses in field-grown plants of Nicotiana longiflora. *Plant Physiol.* 132, 1755–1767. doi: 10.1104/pp.103.024323

Jacob, F., Kracher, B., Mine, A., Seyfferth, C., Blanvillain-Baufumé, S., Parker, J. E., et al. (2018). A dominant-interfering camta3 mutation compromises primary transcriptional outputs mediated by both cell surface and intracellular immune receptors in *Arabidopsis thaliana*. *New Phytol.* 217, 1667–1680. doi: 10.1111/nph.14943

Jaillais, Y., and Chory, J. (2010). Unraveling the paradoxes of plant hormone signaling integration. *Nat. Struct. Mol. Biol.* 17, 642–645. doi: 10.1038/nsmb0610-642

Jain, D., and Khurana, J. P. (2018). "Role of pathogenesis-related (PR) proteins in plant defense mechanism," in *Molecular Aspects of Plant-Pathogen Interaction*, eds A. Singh and I. Singh (Singapore: Springer), 265–281. doi: 10.1007/978-981-10-7371-7_12

James, Z. M., and Zagotta, W. N. (2018). Structural insights into the mechanisms of CNBD channel function. *J. Gen. Physiol.* 150, 225–244. doi: 10.1085/jgp.201711898

Jang, I.-C., Yang, J.-Y., Seo, H. S., and Chua, N.-H. (2005). HFR1 is targeted by COP1 E3 ligase for post-translational proteolysis during phytochrome A signaling. *Genes Dev.* 19, 593–602. doi: 10.1101/gad.1247205

Jenkins, G. I. (2009). Signal transduction in responses to UV-B radiation. *Annu. Rev. Plant Biol.* 60, 407–431. doi: 10.1146/annurev.arplant.59.032607.092953

Jeong, R.-D., Chandra-Shekara, A., Barman, S. R., Navarre, D., Klessig, D. F., Kachroo, A., et al. (2010). Cryptochrome 2 and phototropin 2 regulate resistance protein-mediated viral defense by negatively regulating an E3 ubiquitin ligase. *Proc. Natl. Acad. Sci. U.S.A.* 107, 13538–13543. doi: 10.1073/pnas.1004529107

Jiang, X., Hoehenwarter, W., Scheel, D., and Lee, J. (2020). Phosphorylation of the CAMTA3 transcription factor triggers its destabilization and nuclear export. *Plant Physiol.* 184, 1056–1071. doi: 10.1104/pp.20.00795

Jiao, Y., Lau, O. S., and Deng, X. W. (2007). Light-regulated transcriptional networks in higher plants. *Nat. Rev. Genet.* 8:217. doi: 10.1038/nrg2049

Jogawat, A., Meena, M. K., Kundu, A., Varma, M., and Vadassery, J. (2020). Calcium channel CNGC19 mediates basal defense signaling to regulate colonization by *Piriformospora indica* in *Arabidopsis* roots. *J. Exper. Bot.* 71, 2752–2768. doi: 10.1093/jxb/eraa028

Jones, J. D., and Dangl, J. L. (2006). The plant immune system. *Nature* 444, 323–329. doi: 10.1038/nature05286

Josse, E.-M., and Halliday, K. J. (2008). Skotomorphogenesis: the dark side of light signalling. *Curr. Biol.* 18, R1144–R1146. doi: 10.1016/j.cub.2008.10.034

Kaiserli, E., Paldi, K., O'donnell, L., Batalov, O., Pedmale, U. V., Nusinow, D. A., et al. (2015). Integration of light and photoperiodic signaling in transcriptional nuclear foci. *Dev. Cell* 35, 311–321. doi: 10.1016/j.devcel.2015.10.008

Kaloshian, I. (2004). Gene-for-gene disease resistance: bridging insect pest and pathogen defense. *J. Chem. Ecol.* 30, 2419–2438. doi: 10.1007/s10886-004-7943-1

Kami, C., Lorrain, S., Hornitschek, P., and Fankhauser, C. (2010). Light-regulated plant growth and development. *Curr. Top. Dev. Biol.* 91, 29–66. doi: 10.1016/S0070-2153(10)91002-8

Kangasjärvi, S., Neukermans, J., Li, S., Aro, E.-M., and Noctor, G. (2012). Photosynthesis, photorespiration, and light signalling in defence responses. *J. Exper. Bot.* 63, 1619–1636. doi: 10.1093/jxb/err402

Kariola, T., Brader, G., Li, J., and Palva, E. T. (2005). Chlorophyllase 1, a damage control enzyme, affects the balance between defense pathways in plants. *Plant Cell* 17, 282–294. doi: 10.1105/tpc.104.025817

Karpinski, S., Gabrys, H., Mateo, A., Karpinska, B., and Mullineaux, P. M. (2003). Light perception in plant disease defence signalling. *Curr. Opin. Plant Biol.* 6, 390–396. doi: 10.1016/S1369-5266(03)00061-X

Kazan, K., and Manners, J. M. (2011). The interplay between light and jasmonate signalling during defence and development. *J. Exper. Bot.* 62, 4087–4100. doi: 10.1093/jxb/err142

Kegge, W., Ninkovic, V., Glinwood, R., Welschen, R. A., Voesenek, L. A., and Pierik, R. (2015). Red: far-red light conditions affect the emission of volatile organic compounds from barley (*Hordeum vulgare*), leading to altered biomass allocation in neighbouring plants. *Ann. Bot.* 115, 961–970. doi: 10.1093/aob/mcv036

Kegge, W., Weldegergis, B. T., Soler, R., Eijk, M. V. V., Dicke, M., Voesenek, L. A., et al. (2013). Canopy light cues affect emission of constitutive and methyl jasmonate-induced volatile organic compounds in *Arabidopsis thaliana*. *New Phytol.* 200, 861–874. doi: 10.1111/nph.12407

Kelly, D. L. (2002). The regeneration of *Quercus petraea* (sessile oak) in southwest Ireland: a 25-year experimental study. *For. Ecol. Manag.* 166, 207–226. doi: 10.1016/S0378-1127(01)00670-3

Kessler, S. A., Shimosato-Asano, H., Keinath, N. F., Wuest, S. E., Ingram, G., Panstruga, R., et al. (2010). Conserved molecular components for pollen tube reception and fungal invasion. *Science* 330, 968–971. doi: 10.1126/science.1195211

Keymer, A., Pimprikar, P., Wewer, V., Huber, C., Brands, M., Bucerius, S. L., et al. (2017). Lipid transfer from plants to arbuscular mycorrhiza fungi. *eLife* 6:e29107. doi: 10.7554/eLife.29107.051

Kiep, V., Vadassery, J., Lattke, J., Maaß, J. P., Boland, W., Peiter, E., et al. (2015). Systemic cytosolic Ca2+ elevation is activated upon wounding and herbivory in *Arabidopsis*. *New Phytol.* 207, 996–1004. doi: 10.1111/nph.13493

Kim, Y., Gilmour, S. J., Chao, L., Park, S., and Thomashow, M. F. (2020). *Arabidopsis* CAMTA transcription factors regulate pipecolic acid biosynthesis and priming of immunity genes. *Mol. Plant* 13, 157–168. doi: 10.1016/j.molp.2019.11.001

Kimura, M., Yamamoto, Y. Y., Seki, M., Sakurai, T., Sato, M., Abe, T., et al. (2003). Identification of *Arabidopsis* genes regulated by high light-stress using cDNA microarray. *Photochem. Photobiol.* 77, 226–233. doi: 10.1562/0031-8655(2003)077<0226:IOAGRB>2.0.CO;2

Koh, K., Bell, G., Martin, D., and Walker, N. (2003). Shade and airflow restriction effects on creeping bentgrass golf greens. *Crop Sci.* 43, 2182–2188. doi: 10.2135/cropsci2003.2182

Koussevitzky, S., Nott, A., Mockler, T. C., Hong, F., Sachetto-Martins, G., Surpin, M., et al. (2007). Signals from chloroplasts converge to regulate nuclear gene expression. *Science* 316, 715–719. doi: 10.1126/science.1140516

Kreuger, B., and Potter, D. A. (2001). Diel feeding activity and thermoregulation by Japanese beetles (Coleoptera: Scarabaeidae) within host plant canopies. *Environ. Entomol.* 30, 172–180. doi: 10.1603/0046-225X-30.2.172

Ku, Y.-S., Sintaha, M., Cheung, M.-Y., and Lam, H.-M. (2018). Plant hormone signaling crosstalks between biotic and abiotic stress responses. *Intern. J. Mol. Sci.* 19:3206. doi: 10.3390/ijms19103206

Kudla, J., Becker, D., Grill, E., Hedrich, R., Hippler, M., Kummer, U., et al. (2018). Advances and current challenges in calcium signaling. *New Phytol.* 218, 414–431. doi: 10.1111/nph.14966

Lacombe, B., Becker, D., Hedrich, R., Desalle, R., Hollmann, M., Kwak, J. M., et al. (2001). The identity of plant glutamate receptors. *Science* 292, 1486–1486. doi: 10.1126/science.292.5521.1486b

Laluk, K., and Mengiste, T. (2010). Necrotroph attacks on plants: wanton destruction or covert extortion? *Am. Soc. Plant Biol.* 8:e0136. doi: 10.1199/tab.0136

Lambert, K., and Bekal, S. (2002). Introduction to plant-parasitic nematodes. *Plant Health Instruct.* 10, 1094–1218. doi: 10.1094/PHI-I-2002-1218-01

Lamers, J., Van Der Meer, T., and Testerink, C. (2020). How plants sense and respond to stressful environments. *Plant Physiol.* 182, 1624–1635. doi: 10.1104/pp.19.01464

Lau, O. S., and Deng, X. W. (2010). Plant hormone signaling lightens up: integrators of light and hormones. *Curr. Opin. Plant Biol.* 13, 571–577. doi: 10.1016/j.pbi.2010.07.001

Lau, O. S., and Deng, X. W. (2012). The photomorphogenic repressors COP1 and DET1: 20 years later. *Trends Plant Sci.* 17, 584–593. doi: 10.1016/j.tplants.2012.05.004

Leba, L. J., Cheval, C., Ortiz-Martín, I., Ranty, B., Beuzón, C. R., Galaud, J. P., et al. (2012). CML9, an *Arabidopsis* calmodulin-like protein, contributes to plant innate immunity through a flagellin-dependent signalling pathway. *Plant J.* 71, 976–989. doi: 10.1111/j.1365-313X.2012.05045.x

Lecourieux, D., Lamotte, O., Bourque, S., Wendehenne, D., Mazars, C., Ranjeva, R., et al. (2005). Proteinaceous and oligosaccharidic elicitors induce different calcium signatures in the nucleus of tobacco cells. *Cell Calc.* 38, 527–538. doi: 10.1016/j.ceca.2005.06.036

Lee, S. Y., Chi, Y. H., Koo, S. S., Oh, H. T., Lee, E. S., Park, J. H., et al. (2019). The physiological functions of universal stress proteins and their molecular mechanism to protect plants from environmental stresses. *Front. Plant Sci.* 10:750. doi: 10.3389/fpls.2019.00750

Leivar, P., Monte, E., Oka, Y., Liu, T., Carle, C., Castillon, A., et al. (2008). Multiple phytochrome-interacting bHLH transcription factors repress premature seedling photomorphogenesis in darkness. *Curr. Biol.* 18, 1815–1823. doi: 10.1016/j.cub.2008.10.058

Leivar, P., and Quail, P. H. (2011). PIFs: pivotal components in a cellular signaling hub. *Trends Plant Sci.* 16, 19–28. doi: 10.1016/j.tplants.2010.08.003

Leone, M., Keller, M. M., Cerrudo, I., and Ballaré, C. L. (2014). To grow or defend? Low red: far-red ratios reduce jasmonate sensitivity in *Arabidopsis* seedlings by promoting DELLA degradation and increasing JAZ10 stability. *New Phytol.* 204, 355–367. doi: 10.1111/nph.12971

Li, J., Han, G., Sun, C., and Sui, N. (2019). Research advances of MYB transcription factors in plant stress resistance and breeding. *Plant Signal. Behav.* 14:1613131. doi: 10.1080/15592324.2019.1613131

Li, J., Li, G., Wang, H., and Deng, X. W. (2011). Phytochrome signaling mechanisms. *Arabidopsis Book Am. Soc. Plant Biol.* 9:e0148. doi: 10.1199/tab.0148

Li, X.-P., Gilmore, A. M., Caffarri, S., Bassi, R., Golan, T., Kramer, D., et al. (2004). Regulation of photosynthetic light harvesting involves intrathylakoid lumen pH sensing by the PsbS protein. *J. Biol. Chem.* 279, 22866–22874. doi: 10.1074/jbc.M402461200

Liu, X., Wang, J., and Sun, L. (2018). Structure of the hyperosmolality-gated calcium-permeable channel OSCA1. 2. *Nat. Commun.* 9, 1–9. doi: 10.1038/s41467-018-07564-5

Liu, Y., Du, M., Deng, L., Shen, J., Fang, M., Chen, Q., et al. (2019). MYC2 regulates the termination of jasmonate signaling via an autoregulatory negative feedback loop. *Plant Cell* 31, 106–127. doi: 10.1105/tpc.18.00405

Lorrain, S., Allen, T., Duek, P. D., Whitelam, G. C., and Fankhauser, C. (2008). Phytochrome-mediated inhibition of shade avoidance involves degradation of growth-promoting bHLH transcription factors. *Plant J.* 53, 312–323. doi: 10.1111/j.1365-313X.2007.03341.x

Lorrain, S., Vailleau, F., Balagué, C., and Roby, D. (2003). Lesion mimic mutants: keys for deciphering cell death and defense pathways in plants? *Trends Plant Sci.* 8, 263–271. doi: 10.1016/S1360-1385(03)00108-0

Lozano-Durán, R., Macho, A. P., Boutrot, F., Segonzac, C., Somssich, I. E., and Zipfel, C. (2013). The transcriptional regulator BZR1 mediates trade-off between plant innate immunity and growth. *eLife* 2:e00983. doi: 10.7554/eLife.00983.023

Lozano-Durán, R., and Zipfel, C. (2015). Trade-off between growth and immunity: role of brassinosteroids. *Trends Plant Sci.* 20, 12–19. doi: 10.1016/j.tplants.2014.09.003

Lu, Y., and Yao, J. (2018). Chloroplasts at the crossroad of photosynthesis, pathogen infection and plant defense. *Intern. J. Mol. Sci.* 19:3900. doi: 10.3390/ijms19123900

Luan, S. (2009). The CBL-CIPK network in plant calcium signaling. *Trends Plant Sci.* 14, 37–42. doi: 10.1016/j.tplants.2008.10.005

Lv, R., Li, Z., Li, M., Dogra, V., Lv, S., Liu, R., et al. (2019). Uncoupled expression of nuclear and plastid photosynthesis-associated genes contributes to cell death in a lesion mimic mutant. *Plant Cell* 31, 210–230. doi: 10.1105/tpc.18.00813

Ma, L., Gao, Y., Qu, L., Chen, Z., Li, J., Zhao, H., et al. (2002). Genomic evidence for COP1 as a repressor of light-regulated gene expression and development in *Arabidopsis*. *Plant Cell* 14, 2383–2398. doi: 10.1105/tpc.004416

Ma, X., Li, Q.-H., Yu, Y.-N., Qiao, Y.-M., and Gong, Z.-H. (2020). The CBL-CIPK pathway in plant response to stress signals. *Intern. J. Mol. Sci.* 21:5668. doi: 10.3390/ijms21165668

Ma, Y., Walker, R. K., Zhao, Y., and Berkowitz, G. A. (2012). Linking ligand perception by PEPR pattern recognition receptors to cytosolic Ca2+ elevation and downstream immune signaling in plants. *Proc. Natl. Acad. Sci. U.S.A.* 109, 19852–19857. doi: 10.1073/pnas.1205448109

Mach, J. M., Castillo, A. R., Hoogstraten, R., and Greenberg, J. T. (2001). The *Arabidopsis*-accelerated cell death gene ACD2 encodes red chlorophyll catabolite reductase and suppresses the spread of disease symptoms. *Proc. Natl. Acad. Sci. U.S.A.* 98, 771–776. doi: 10.1073/pnas.98.2.771

Machado, R. A., Robert, C. A., Arce, C. C., Ferrieri, A. P., Xu, S., Jimenez-Aleman, G. H., et al. (2016). Auxin is rapidly induced by herbivore attack and regulates a subset of systemic, jasmonate-dependent defenses. *Plant Physiol.* 172, 521–532. doi: 10.1104/pp.16.00940

Mackerness, A.-H. S., Surplus, S., Blake, P., John, C., Buchanan-Wollaston, V., Jordan, B., et al. (1999). Ultraviolet-B-induced stress and changes in gene expression in *Arabidopsis thaliana*: role of signalling pathways controlled by jasmonic acid, ethylene and reactive oxygen species. *Plant Cell Environ.* 22, 1413–1423. doi: 10.1046/j.1365-3040.1999.00499.x

Magnan, F., Ranty, B., Charpenteau, M., Sotta, B., Galaud, J. P., and Aldon, D. (2008). Mutations in AtCML9, a calmodulin-like protein from *Arabidopsis thaliana*, alter plant responses to abiotic stress and abscisic acid. *Plant J.* 56, 575–589. doi: 10.1111/j.1365-313X.2008.03622.x

Manzoor, H., Kelloniemi, J., Chiltz, A., Wendehenne, D., Pugin, A., Poinssot, B., et al. (2013). Involvement of the glutamate receptor A t GLR 3.3 in plant defense signaling and resistance to H yaloperonospora arabidopsidis. *Plant J.* 76, 466–480. doi: 10.1111/tpj.12311

Martin, D. M., Gershenzon, J., and Bohlmann, J. (2003). Induction of volatile terpene biosynthesis and diurnal emission by methyl jasmonate in foliage of Norway spruce. *Plant Physiol.* 132, 1586–1599. doi: 10.1104/pp.103.021196

Martínez, C., Espinosa-Ruíz, A., De Lucas, M., Bernardo-García, S., Franco-Zorrilla, J. M., and Prat, S. (2018a). PIF 4-induced BR synthesis is critical to diurnal and thermomorphogenic growth. *EMBO J.* 37:e99552. doi: 10.15252/embj.201899552

Martínez, C., Nieto, C., and Prat, S. (2018b). Convergent regulation of PIFs and the E3 ligase COP1/SPA1 mediates thermosensory hypocotyl elongation by plant phytochromes. *Curr. Opin. Plant Biol.* 45, 188–203. doi: 10.1016/j.pbi.2018.09.006

Martinez-Garcia, J. F., Galstyan, A., Salla-Martret, M., Cifuentes-Esquivel, N., Gallemi, M., and Bou-Torrent, J. (2010). Regulatory components of shade avoidance syndrome. *Adv. Bot. Res.* 53, 65–116. doi: 10.1016/S0065-2296(10)53003-9

Mawphlang, O. I., and Kharshiing, E. V. (2017). Photoreceptor mediated plant growth responses: implications for photoreceptor engineering toward improved performance in crops. *Front. Plant Sci.* 8:1181. doi: 10.3389/fpls.2017.01181

McGuire, R., and Agrawal, A. (2005). Trade-offs between the shade-avoidance response and plant resistance to herbivores? Tests with mutant *Cucumis sativus*. *Funct. Ecol.* 19, 1025–1031. doi: 10.1111/j.1365-2435.2005.01047.x

Meena, M. K., Prajapati, R., Krishna, D., Divakaran, K., Pandey, Y., Reichelt, M., et al. (2019). The Ca2+ channel CNGC19 regulates *Arabidopsis* defense against *Spodoptera herbivory*. *Plant Cell* 31, 1539–1562. doi: 10.1105/tpc.19.00057

Meena, M. K., and Vadassery, J. (2015). Channels hold the key: cyclic nucleotide gated channels (CNGC) in plant biotic stress signaling. *J. Endocytob. Cell Res.* 581, 25–30.

Meijer, G., and Leuchtmann, A. (2000). The effects of genetic and environmental factors on disease expression (stroma formation) and plant growth in *Brachypodium sylvaticum* infected by *Epichloë sylvatica*. *Oikos* 91, 446–458. doi: 10.1034/j.1600-0706.2000.910305.x

Menon, C., Sheerin, D. J., and Hiltbrunner, A. (2016). SPA proteins: SPAnning the gap between visible light and gene expression. *Planta* 244, 297–312. doi: 10.1007/s00425-016-2509-3

Mishra, Y., Jänkänpää, H. J., Kiss, A. Z., Funk, C., Schröder, W. P., and Jansson, S. (2012). *Arabidopsis* plants grown in the field and climate chambers significantly differ in leaf morphology and photosystem components. *BMC Plant Biol.* 12:6. doi: 10.1186/1471-2229-12-6

Mittler, R. (2002). Oxidative stress, antioxidants and stress tolerance. *Trends Plant Sci.* 7, 405–410. doi: 10.1016/S1360-1385(02)02312-9

Moeder, W., Urquhart, W., Ung, H., and Yoshioka, K. (2011). The role of cyclic nucleotide-gated ion channels in plant immunity. *Mol. Plant* 4, 442–452. doi: 10.1093/mp/ssr018

Molina, A., Volrath, S., Guyer, D., Maleck, K., Ryals, J., and Ward, E. (1999). Inhibition of protoporphyrinogen oxidase expression in *Arabidopsis* causes a lesion-mimic phenotype that induces systemic acquired resistance. *Plant J.* 17, 667–678. doi: 10.1046/j.1365-313X.1999.00420.x

Monaghan, J., and Zipfel, C. (2012). Plant pattern recognition receptor complexes at the plasma membrane. *Curr. Opin. Plant Biol.* 15, 349–357. doi: 10.1016/j.pbi.2012.05.006

Montillet, J.-L., Chamnongpol, S., Rustérucci, C., Dat, J., Van De Cotte, B., Agnel, J.-P., et al. (2005). Fatty acid hydroperoxides and H2O2 in the execution of hypersensitive cell death in tobacco leaves. *Plant Physiol.* 138, 1516–1526. doi: 10.1104/pp.105.059907

Moreno, J. E., and Ballaré, C. L. (2014). Phytochrome regulation of plant immunity in vegetation canopies. *J. Chem. Ecol.* 40, 848–857. doi: 10.1007/s10886-014-0471-8

Moreno, J. E., Tao, Y., Chory, J., and Ballaré, C. L. (2009). Ecological modulation of plant defense via phytochrome control of jasmonate sensitivity. *Proc. Natl. Acad. Sci. U.S.A.* 106, 4935–4940. doi: 10.1073/pnas.0900701106

Mueller, D., and Buck, J. (2003). Effects of light, temperature, and leaf wetness duration on daylily rust. *Plant Dis.* 87, 442–445. doi: 10.1094/PDIS.2003.87.4.442

Mühlenbock, P., Szechyńska-Hebda, M., Płaszczyca, M., Baudo, M., Mateo, A., Mullineaux, P. M., et al. (2008). Chloroplast signaling and LESION SIMULATING DISEASE1 regulate crosstalk between light acclimation and immunity in *Arabidopsis*. *Plant Cell* 20, 2339–2356. doi: 10.1105/tpc.108.059618

Müller, P., Li, X.-P., and Niyogi, K. K. (2001). Non-photochemical quenching. A response to excess light energy. *Plant Physiol.* 125, 1558–1566. doi: 10.1104/pp.125.4.1558

Mur, L. A., Kenton, P., Lloyd, A. J., Ougham, H., and Prats, E. (2008). The hypersensitive response; the centenary is upon us but how much do we know? *J. Exper. Bot.* 59, 501–520. doi: 10.1093/jxb/erm239

Muthamilarasan, M., and Prasad, M. (2013). Plant innate immunity: an updated insight into defense mechanism. *J. Biosci.* 38, 433–449. doi: 10.1007/s12038-013-9302-2

Nagata, M., Yamamoto, N., Miyamoto, T., Shimomura, A., Arima, S., Hirsch, A. M., et al. (2016). Enhanced hyphal growth of arbuscular mycorrhizae by root exudates derived from high R/FR treated Lotus japonicus. *Plant Signal. Behav.* 11:e1187356. doi: 10.1080/15592324.2016.1187356

Nagata, M., Yamamoto, N., Shigeyama, T., Terasawa, Y., Anai, T., Sakai, T., et al. (2015). Red/far red light controls arbuscular mycorrhizal colonization via jasmonic acid and strigolactone signaling. *Plant Cell Physiol.* 56, 2100–2109. doi: 10.1093/pcp/pcv135

Nath, M., Bhatt, D., Prasad, R., and Tuteja, N. (2017). "Reactive oxygen species (ROS) metabolism and signaling in plant-mycorrhizal association under biotic and abiotic stress conditions," in *Mycorrhiza-Eco-Physiology, Secondary Metabolites, Nanomaterials*, eds A. Varma, R. Prasad, and N. Tuteja (Cham: Springer), 223–232. doi: 10.1007/978-3-319-57849-1_12

Nejat, N., and Mantri, N. (2017). Plant immune system: crosstalk between responses to biotic and abiotic stresses the missing link in understanding plant defence. *Curr. Issues Mol. Biol.* 23, 1–16. doi: 10.21775/cimb.023.001

Nell, C. S., Abdala-Roberts, L., Parra-Tabla, V., and Mooney, K. A. (2018). Tropical tree diversity mediates foraging and predatory effects of insectivorous birds. *Proce. R. Soc. B* 285:20181842. doi: 10.1098/rspb.2018.1842

Ningen, S. S., Cole, J. C., Smith, M. W., Dunn, D. E., and Conway, K. E. (2005). Increased shade intensity and afternoon irrigation decrease anthracnose severity on three *Euonymus fortunei* cultivars. *Hortscience* 40, 111–113. doi: 10.21273/HORTSCI.40.1.111

Nishad, R., Ahmed, T., Rahman, V. J., and Kareem, A. (2020). Modulation of plant defense system in response to microbial interactions. *Front. Microbiol.* 11:1298. doi: 10.3389/fmicb.2020.01298

Niyogi, K. K. (2000). Safety valves for photosynthesis. *Curr. Opin. Plant Biol.* 3, 455–460. doi: 10.1016/S1369-5266(00)00113-8

Niyogi, K. K., Li, X.-P., Rosenberg, V., and Jung, H.-S. (2005). Is PsbS the site of non-photochemical quenching in photosynthesis? *J. Exper. Bot.* 56, 375–382. doi: 10.1093/jxb/eri056

Nozue, K., Devisetty, U. K., Lekkala, S., Mueller-Moulé, P., Bak, A., Casteel, C. L., et al. (2018). Network analysis reveals a role for salicylic acid pathway components in shade avoidance. *Plant Physiol.* 178, 1720–1732. doi: 10.1104/pp.18.00920

Nunes-Nesi, A., Fernie, A. R., and Stitt, M. (2010). Metabolic and signaling aspects underpinning the regulation of plant carbon nitrogen interactions. *Mol. Plant* 3, 973–996. doi: 10.1093/mp/ssq049

Ordoñez-Herrera, N., Fackendahl, P., Yu, X., Schaefer, S., Koncz, C., and Hoecker, U. (2015). A cop1 spa mutant deficient in COP1 and SPA proteins reveals partial co-action of COP1 and SPA during *Arabidopsis* post-embryonic development and photomorphogenesis. *Mol. Plant* 8, 479–481. doi: 10.1016/j.molp.2014.11.026

Osman, H. A., Ameen, H. H., Mohamed, M., and Elkelany, U. S. (2020). Efficacy of integrated microorganisms in controlling root-knot nematode *Meloidogyne javanica* infecting peanut plants under field conditions. *Bull. Natl. Res. Centre* 44, 1–10. doi: 10.1186/s42269-020-00366-0

Osterlund, M. T., Hardtke, C. S., Wei, N., and Deng, X. W. (2000). Targeted destabilization of HY5 during light-regulated development of *Arabidopsis*. *Nature* 405, 462–466. doi: 10.1038/35013076

Paik, I., Chen, F., Pham, V. N., Zhu, L., Kim, J.-I., and Huq, E. (2019). A phyB-PIF1-SPA1 kinase regulatory complex promotes photomorphogenesis in *Arabidopsis*. *Nat. Commun.* 10, 1–17. doi: 10.1038/s41467-019-12110-y

Pallas, V., and García, J. A. (2011). How do plant viruses induce disease? Interactions and interference with host components. *J. Gen. Virol.* 92, 2691–2705. doi: 10.1099/vir.0.034603-0

Pan, Y., Chai, X., Gao, Q., Zhou, L., Zhang, S., Li, L., et al. (2019). Dynamic interactions of plant CNGC subunits and calmodulins drive oscillatory Ca2+ channel activities. *Dev. Cell* 48, 710–725. doi: 10.1016/j.devcel.2018.12.025

Pandey, G. K., and Sanyal, S. K. (2021). "Ca 2+-ATPase and Ca 2+/cation antiporters," in *Functional Dissection of Calcium Homeostasis and Transport Machinery in Plants*, eds G. K. Pandey and S. K. Sanyal (Cham: Springer), 89–104. doi: 10.1007/978-3-030-58502-0_9

Park, C. Y., Lee, J. H., Yoo, J. H., Moon, B. C., Choi, M. S., Kang, Y. H., et al. (2005). WRKY group IId transcription factors interact with calmodulin. *FEBS Lett.* 579, 1545–1550. doi: 10.1016/j.febslet.2005.01.057

Peck, S., and Mittler, R. (2020). Plant signaling in biotic and abiotic stress. *J. Exper. Bot.* 71, 1649–1651. doi: 10.1093/jxb/eraa051

Peng, Y., Van Wersch, R., and Zhang, Y. (2018). Convergent and divergent signaling in PAMP-triggered immunity and effector-triggered immunity. *Mol. Plant Microb. Interact.* 31, 403–409. doi: 10.1094/MPMI-06-17-0145-CR

Pham, V. N., Kathare, P. K., and Huq, E. (2018). Phytochromes and phytochrome interacting factors. *Plant Physiol.* 176, 1025–1038. doi: 10.1104/pp.17.01384

Pham, V. N., Paik, I., Hoecker, U., and Huq, E. (2020). Genomic evidence reveals SPA-regulated developmental and metabolic pathways in dark-grown *Arabidopsis* seedlings. *Physiol. Plant.* 169, 380–396. doi: 10.1111/ppl.13095

Pichersky, E., and Gershenzon, J. (2002). The formation and function of plant volatiles: perfumes for pollinator attraction and defense. *Curr. Opin. Plant Biol.* 5, 237–243. doi: 10.1016/S1369-5266(02)00251-0

Pieterse, C. M., Pierik, R., and Van Wees, S. C. (2014). Different shades of JAZ during plant growth and defense. *New Phytol.* 204, 261–264. doi: 10.1111/nph.13029

Pittman, J. K. (2011). Vacuolar Ca2+ uptake. *Cell Calc.* 50, 139–146. doi: 10.1016/j.ceca.2011.01.004

Planas-Riverola, A., Gupta, A., Betegón-Putze, I., Bosch, N., Ibañes, M., and Cańo-Delgado, A. I. (2019). Brassinosteroid signaling in plant development and adaptation to stress. *Development* 146:151894. doi: 10.1242/dev.151894

Podolec, R., and Ulm, R. (2018). Photoreceptor-mediated regulation of the COP1/SPA E3 ubiquitin ligase. *Curr. Opin. Plant Biol.* 45, 18–25. doi: 10.1016/j.pbi.2018.04.018

Popescu, S. C., Popescu, G. V., Bachan, S., Zhang, Z., Seay, M., Gerstein, M., et al. (2007). Differential binding of calmodulin-related proteins to their targets revealed through high-density *Arabidopsis* protein microarrays. *Proc. Natl. Acad. Sci. U.S.A.* 104, 4730–4735. doi: 10.1073/pnas.0611615104

Pružinská, A., Tanner, G., Anders, I., Roca, M., and Hörtensteiner, S. (2003). Chlorophyll breakdown: pheophorbide a oxygenase is a Rieske-type iron-sulfur protein, encoded by the accelerated cell death 1 gene. *Proc. Natl. Acad. Sci. U.S.A.* 100, 15259–15264. doi: 10.1073/pnas.2036571100

Ranty, B., Aldon, D., Cotelle, V., Galaud, J.-P., Thuleau, P., and Mazars, C. (2016). Calcium sensors as key hubs in plant responses to biotic and abiotic stresses. *Front. Plant Sci.* 7:327. doi: 10.3389/fpls.2016.00327

Rasool, B., Karpinska, B., Konert, G., Durian, G., Denessiouk, K., Kangasjärvi, S., et al. (2014). Effects of light and the regulatory B-subunit composition of protein phosphatase 2A on the susceptibility of *Arabidopsis thaliana* to aphid (*Myzus persicae*) infestation. *Front. Plant Sci.* 5:405. doi: 10.3389/fpls.2014.00405

Reddy, A. S., Ali, G. S., Celesnik, H., and Day, I. S. (2011). Coping with stresses: roles of calcium-and calcium/calmodulin-regulated gene expression. *Plant Cell* 23, 2010–2032. doi: 10.1105/tpc.111.084988

Rejeb, I. B., Pastor, V., and Mauch-Mani, B. (2014). Plant responses to simultaneous biotic and abiotic stress: molecular mechanisms. *Plants* 3, 458–475. doi: 10.3390/plants3040458

Rizhsky, L., Liang, H., Shuman, J., Shulaev, V., Davletova, S., and Mittler, R. (2004). When defense pathways collide. The response of *Arabidopsis* to a combination of drought and heat stress. *Plant Physiol.* 134, 1683–1696. doi: 10.1104/pp.103.033431

Roberts, M. R., and Paul, N. D. (2006). Seduced by the dark side: integrating molecular and ecological perspectives on the influence of light on plant defence against pests and pathogens. *New Phytol.* 170, 677–699. doi: 10.1111/j.1469-8137.2006.01707.x

Rossel, J. B., Wilson, I. W., and Pogson, B. J. (2002). Global changes in gene expression in response to high light in *Arabidopsis*. *Plant Physiol.* 130, 1109–1120. doi: 10.1104/pp.005595

Rossel, J. B., Wilson, P. B., Hussain, D., Woo, N. S., Gordon, M. J., Mewett, O. P., et al. (2007). Systemic and intracellular responses to photooxidative stress in *Arabidopsis*. *Plant Cell* 19, 4091–4110. doi: 10.1105/tpc.106.045898

Saijo, Y., and Loo, E. P. I. (2020). Plant immunity in signal integration between biotic and abiotic stress responses. *New Phytol.* 225, 87–104. doi: 10.1111/nph.15989

Saiz-Rubio, V., and Rovira-Más, F. (2020). From smart farming towards agriculture 5.0: a review on crop data management. *Agronomy* 10:207. doi: 10.3390/agronomy10020207

Sánchez-Muros, M.-J., Barroso, F. G., and Manzano-Agugliaro, F. (2014). Insect meal as renewable source of food for animal feeding: a review. *J. Clean. Product.* 65, 16–27. doi: 10.1016/j.jclepro.2013.11.068

Santamaria, M. E., Martínez, M., Cambra, I., Grbic, V., and Diaz, I. (2013). Understanding plant defence responses against herbivore attacks: an essential first step towards the development of sustainable resistance against pests. *Transgen. Res.* 22, 697–708. doi: 10.1007/s11248-013-9725-4

Santino, A., Taurino, M., De Domenico, S., Bonsegna, S., Poltronieri, P., Pastor, V., et al. (2013). Jasmonate signaling in plant development and defense response to multiple (a) biotic stresses. *Plant Cell Rep.* 32, 1085–1098. doi: 10.1007/s00299-013-1441-2

Schmale, D. G., and Bergstrom, G. C. (2004). Spore deposition of the ear rot pathogen, *Gibberella zeae*, inside corn canopies. *Can. J. Plant Pathol.* 26, 591–595. doi: 10.1080/07060660409507179

Schmelz, E. A., Engelberth, J., Alborn, H. T., O'donnell, P., Sammons, M., Toshima, H., et al. (2003). Simultaneous analysis of phytohormones, phytotoxins, and volatile organic compounds in plants. *Proc. Natl. Acad. Sci. U.S.A.* 100, 10552–10557. doi: 10.1073/pnas.1633615100

Scholz, S. S., Vadassery, J., Heyer, M., Reichelt, M., Bender, K. W., Snedden, W. A., et al. (2014). Mutation of the *Arabidopsis* calmodulin-like protein CML37 deregulates the jasmonate pathway and enhances susceptibility to herbivory. *Mol. Plant* 7, 1712–1726. doi: 10.1093/mp/ssu102

Schumann, G. L., and D'Arcy, C. J. (2006). *Essential Plant Pathology*. London: APS Press.

Schuurink, R. C., Shartzer, S. F., Fath, A., and Jones, R. L. (1998). Characterization of a calmodulin-binding transporter from the plasma membrane of barley aleurone. *Proc. Natl. Acad. Sci. U.S.A.* 95, 1944–1949. doi: 10.1073/pnas.95.4.1944

Schwechheimer, C., Serino, G., Callis, J., Crosby, W. L., Lyapina, S., Deshaies, R. J., et al. (2001). Interactions of the COP9 signalosome with the E3 ubiquitin ligase SCFTIR1 in mediating auxin response. *Science* 292, 1379–1382. doi: 10.1126/science.1059776

Seo, H. S., Yang, J.-Y., Ishikawa, M., Bolle, C., Ballesteros, M. L., and Chua, N.-H. (2003). LAF1 ubiquitination by COP1 controls photomorphogenesis and is stimulated by SPA1. *Nature* 423, 995–999. doi: 10.1038/nature01696

Serino, G., and Deng, X.-W. (2003). The COP9 signalosome: regulating plant development through the control of proteolysis. *Annu. Rev. Plant Biol.* 54, 165–182. doi: 10.1146/annurev.arplant.54.031902.134847

Sessa, G., Carabelli, M., Possenti, M., Morelli, G., and Ruberti, I. (2018). Multiple pathways in the control of the shade avoidance response. *Plants* 7:102. doi: 10.3390/plants7040102

Seybold, H., Trempel, F., Ranf, S., Scheel, D., Romeis, T., and Lee, J. (2014). Ca2+ signalling in plant immune response: from pattern recognition receptors to Ca2+ decoding mechanisms. *New Phytol.* 204, 782–790. doi: 10.1111/nph.13031

Shafia, A., Sutton, J., Yu, H., and Fletcher, R. (2001). Influence of preinoculation light intensity on development and interactions of *Botrytis cinerea* and *Clonostachys rosea* in tomato leaves. *Can. J. Plant Pathol.* 23, 346–357. doi: 10.1080/07060660109506955

Sharma, M., and Bhatt, D. (2015). The circadian clock and defence signalling in plants. *Mol. Plant Pathol.* 16, 210–218. doi: 10.1111/mpp.12178

Shen, Q., Fu, L., Su, T., Ye, L., Huang, L., Kuang, L., et al. (2020). Calmodulin HvCaM1 negatively regulates salt tolerance via modulation of HvHKT1s and HvCAMTA4. *Plant Physiol.* 183, 1650–1662. doi: 10.1104/pp.20.00196

Shi, H., Wang, X., Mo, X., Tang, C., Zhong, S., and Deng, X. W. (2015). *Arabidopsis* DET1 degrades HFR1 but stabilizes PIF1 to precisely regulate seed germination. *Proc. Natl. Acad. Sci. U.S.A.* 112, 3817–3822. doi: 10.1073/pnas.1502405112

Shigeyama, T., Tominaga, A., Arima, S., Sakai, T., Inada, S., Jikumaru, Y., et al. (2012). Additional cause for reduced JA-Ile in the root of a *Lotus japonicus* phyB mutant. *Plant Signal. Behav.* 7, 746–748. doi: 10.4161/psb.20407

Shin, J., Kim, K., Kang, H., Zulfugarov, I. S., Bae, G., Lee, C.-H., et al. (2009). Phytochromes promote seedling light responses by inhibiting four negatively-acting phytochrome-interacting factors. *Proc. Natl. Acad. Sci. U.S.A.* 106, 7660–7665. doi: 10.1073/pnas.0812219106

Singh, A., Kanwar, P., Yadav, A. K., Mishra, M., Jha, S. K., Baranwal, V., et al. (2014). Genome-wide expressional and functional analysis of calcium transport elements during abiotic stress and development in rice. *FEBS J.* 281, 894–915. doi: 10.1111/febs.12656

Singh, A., Sagar, S., and Biswas, D. K. (2017). Calcium dependent protein kinase, a versatile player in plant stress management and development. *Crit. Rev. Plant Sci.* 36, 336–352. doi: 10.1080/07352689.2018.1428438

Singh, P., and Virdi, A. S. (2013). "Ca 2+, calmodulin and plant-specific calmodulin-binding proteins: implications in abiotic stress adaptation," in *Stress Signaling in Plants: Genomics and Proteomics Perspective*, Vol. 1, eds M. Sarwat, A. Ahmad, and M. Abdin (New York, NY: Springer), 1–23. doi: 10.1007/978-1-4614-6372-6_1

Slattery, R. A., Vanloocke, A., Bernacchi, C. J., Zhu, X.-G., and Ort, D. R. (2017). Photosynthesis, light use efficiency, and yield of reduced-chlorophyll soybean mutants in field conditions. *Front. Plant Sci.* 8:549. doi: 10.3389/fpls.2017.00549

Sobiczewski, P., Iakimova, E., Mikiciński, A., Wêgrzynowicz-Lesiak, E., and Dyki, B. (2017). Necrotrophic behaviour of *Erwinia amylovora* in apple and tobacco leaf tissue. *Plant Pathol.* 66, 842–855. doi: 10.1111/ppa.12631

Soto-Pinto, L., Perfecto, I., and Caballero-Nieto, J. (2002). Shade over coffee: its effects on berry borer, leaf rust and spontaneous herbs in Chiapas, Mexico. *Agroforestry Syst.* 55, 37–45. doi: 10.1023/A:1020266709570

Spalding, E. P., and Harper, J. F. (2011). The ins and outs of cellular Ca2+ transport. *Curr. Opin. Plant Biol.* 14, 715–720. doi: 10.1016/j.pbi.2011.08.001

Spoel, S. H., and Dong, X. (2012). How do plants achieve immunity? Defence without specialized immune cells. *Nat. Rev. Immunol.* 12, 89–100. doi: 10.1038/nri3141

Stamm, P., and Kumar, P. P. (2010). The phytohormone signal network regulating elongation growth during shade avoidance. *J. Exper. Bot.* 61, 2889–2903. doi: 10.1093/jxb/erq147

Stegmann, M., Monaghan, J., Smakowska-Luzan, E., Rovenich, H., Lehner, A., Holton, N., et al. (2017). The receptor kinase FER is a RALF-regulated scaffold controlling plant immune signaling. *Science* 355, 287–289. doi: 10.1126/science.aal2541

Stracke, R., Werber, M., and Weisshaar, B. (2001). The R2R3-MYB gene family in *Arabidopsis thaliana*. *Curr. Opin. Plant Biol.* 4, 447–456. doi: 10.1016/S1369-5266(00)00199-0

Stratmann, J. (2003). Ultraviolet-B radiation co-opts defense signaling pathways. *Trends Plant Sci.* 8, 526–533. doi: 10.1016/j.tplants.2003.09.011

Strong, A. M., Sherry, T. W., and Holmes, R. T. (2000). Bird predation on herbivorous insects: indirect effects on sugar maple saplings. *Oecologia* 125, 370–379. doi: 10.1007/s004420000467

Su, H., Van Bruggen, A., and Subbarao, K. (2000). Spore release of *Bremia lactucae* on lettuce is affected by timing of light initiation and decrease in relative humidity. *Phytopathology* 90, 67–71. doi: 10.1094/PHYTO.2000.90.1.67

Sun, C., Jin, L., Cai, Y., Huang, Y., Zheng, X., and Yu, T. (2019). L-Glutamate treatment enhances disease resistance of tomato fruit by inducing the expression of glutamate receptors and the accumulation of amino acids. *Food Chem.* 293, 263–270. doi: 10.1016/j.foodchem.2019.04.113

Suzuki, A., Suriyagoda, L., Shigeyama, T., Tominaga, A., Sasaki, M., Hiratsuka, Y., et al. (2011). Lotus japonicus nodulation is photomorphogenetically controlled by sensing the red/far red (R/FR) ratio through jasmonic acid (JA) signaling. *Proc. Natl. Acad. Sci. U.S.A.* 108, 16837–16842. doi: 10.1073/pnas.1105892108

Suzuki, N., Rivero, R. M., Shulaev, V., Blumwald, E., and Mittler, R. (2014). Abiotic and biotic stress combinations. *New Phytol.* 203, 32–43. doi: 10.1111/nph.12797

Szechyńska-Hebda, M., Kruk, J., Górecka, M., Karpińska, B., and Karpiński, S. (2010). Evidence for light wavelength-specific photoelectrophysiological signaling and memory of excess light episodes in *Arabidopsis*. *Plant Cell* 22, 2201–2218. doi: 10.1105/tpc.109.069302

Taiz, L., and Zeiger, E. (2006). Secondary metabolites and plant defense. *Plant Physiol.* 4, 315–344.

Takano, M., Inagaki, N., Xie, X., Kiyota, S., Baba-Kasai, A., Tanabata, T., et al. (2009). Phytochromes are the sole photoreceptors for perceiving red/far-red light in rice. *Proc. Natl. Acad. Sci. U.S.A.* 106, 14705–14710. doi: 10.1073/pnas.0907378106

Taneja, M., and Upadhyay, S. K. (2018). Molecular characterization and differential expression suggested diverse functions of P-type II Ca 2+ ATPases in *Triticum aestivum* L. *BMC Genom.* 19:389. doi: 10.1186/s12864-018-4792-9

Tang, R.-J., Wang, C., Li, K., and Luan, S. (2020). The CBL-CIPK calcium signaling network: Unified paradigm from 20 years of discoveries. *Trends Plant Sci.* 25, 604–617. doi: 10.1016/j.tplants.2020.01.009

Tao, Y., Xie, Z., Chen, W., Glazebrook, J., Chang, H.-S., Han, B., et al. (2003). Quantitative nature of *Arabidopsis* responses during compatible and incompatible interactions with the bacterial pathogen *Pseudomonas syringae*. *Plant Cell* 15, 317–330. doi: 10.1105/tpc.007591

Teardo, E., Carraretto, L., Wagner, S., Formentin, E., Behera, S., De Bortoli, S., et al. (2017). Physiological characterization of a plant mitochondrial calcium uniporter in vitro and in vivo. *Plant Physiol.* 173, 1355–1370. doi: 10.1104/pp.16.01359

Thoma, I., Loeffler, C., Sinha, A. K., Gupta, M., Krischke, M., Steffan, B., et al. (2003). Cyclopentenone isoprostanes induced by reactive oxygen species trigger defense gene activation and phytoalexin accumulation in plants. *Plant J.* 34, 363–375. doi: 10.1046/j.1365-313X.2003.01730.x

Thomma, B. P., Eggermont, K., Penninckx, I. A., Mauch-Mani, B., Vogelsang, R., Cammue, B. P., et al. (1998). Separate jasmonate-dependent and salicylate-dependent defense-response pathways in *Arabidopsis* are essential for resistance to distinct microbial pathogens. *Proc. Natl. Acad. Sci. U.S.A.* 95, 15107–15111. doi: 10.1073/pnas.95.25.15107

Thor, K., Jiang, S., Michard, E., George, J., Scherzer, S., Huang, S., et al. (2020). The calcium-permeable channel OSCA1. 3 regulates plant stomatal immunity. *Nature* 585, 569–573. doi: 10.1038/s41586-020-2702-1

Tilbrook, K., Arongaus, A. B., Binkert, M., Heijde, M., Yin, R., and Ulm, R. (2013). The UVR8 UV-B photoreceptor: perception, signaling and response. *Am. Soc. Plant Biol.* 11:e0164. doi: 10.1199/tab.0164

Toledo-Ortiz, G., Johansson, H., Lee, K. P., Bou-Torrent, J., Stewart, K., Steel, G., et al. (2014). The HY5-PIF regulatory module coordinates light and temperature control of photosynthetic gene transcription. *PLoS Genet.* 10:e1004416. doi: 10.1371/journal.pgen.1004416

Torres, M. A. (2010). ROS in biotic interactions. *Physiol. Plant.* 138, 414–429. doi: 10.1111/j.1399-3054.2009.01326.x

Tripathi, S., Hoang, Q. T., Han, Y.-J., and Kim, J.-I. (2019). Regulation of photomorphogenic development by plant phytochromes. *Intern. J. Mol. Sci.* 20:6165. doi: 10.3390/ijms20246165

Trotta, A., Rahikainen, M., Konert, G., Finazzi, G., and Kangasjärvi, S. (2014). Signalling crosstalk in light stress and immune reactions in plants. *Philos. Trans. R. Soc. B Biol. Sci.* 369:20130235. doi: 10.1098/rstb.2013.0235

Turner, J. G., Ellis, C., and Devoto, A. (2002). The jasmonate signal pathway. *Plant Cell* 14, S153–S164. doi: 10.1105/tpc.000679

Vadassery, J., Reichelt, M., Hause, B., Gershenzon, J., Boland, W., and Mithöfer, A. (2012). CML42-mediated calcium signaling coordinates responses to *Spodoptera herbivory* and abiotic stresses in *Arabidopsis*. *Plant Physiol.* 159, 1159–1175. doi: 10.1104/pp.112.198150

Van Bael, S. A., and Brawn, J. D. (2005). The direct and indirect effects of insectivory by birds in two contrasting Neotropical forests. *Oecologia* 143, 106–116. doi: 10.1007/s00442-004-1774-1

van Loon, L. C., Rep, M., and Pieterse, C. M. (2006). Significance of inducible defense-related proteins in infected plants. *Annu. Rev. Phytopathol.* 44, 135–162. doi: 10.1146/annurev.phyto.44.070505.143425

Vandenbussche, F., and Van Der Straeten, D. (2004). Shaping the shoot: a circuitry that integrates multiple signals. *Trends Plant Sci.* 9, 499–506. doi: 10.1016/j.tplants.2004.08.002

VanLaerhoven, S. L., Gillespie, D. R., and Roitberg, B. D. (2003). Diel activity pattern and predation rate of the generalist predator *Dicyphus hesperus*. *Entomol. Exper. Appl.* 107, 149–154. doi: 10.1046/j.1570-7458.2003.00050.x

Verhage, A., Vlaardingerbroek, I., Dicke, M., Van Wees, S., and Pieterse, C. (2012). The transcription factor MYC2 shapes plant defense responses in *Arabidopsis* upon *Pieris rapae* herbivory. *Anim. Behav.* 83, 21–25.

Vincent, T. R., Avramova, M., Canham, J., Higgins, P., Bilkey, N., Mugford, S. T., et al. (2017). Interplay of plasma membrane and vacuolar ion channels, together with BAK1, elicits rapid cytosolic calcium elevations in *Arabidopsis* during aphid feeding. *Plant Cell* 29, 1460–1479. doi: 10.1105/tpc.17.00136

Vollenweider, S., Weber, H., Stolz, S., Chételat, A., and Farmer, E. E. (2000). Fatty acid ketodienes and fatty acid ketotrienes: michael addition acceptors that accumulate in wounded and diseased *Arabidopsis* leaves. *Plant J.* 24, 467–476. doi: 10.1046/j.1365-313x.2000.00897.x

von Arnim, A. G., Osterlund, M. T., Kwok, S. F., and Deng, X.-W. (1997). Genetic and developmental control of nuclear accumulation of COP1, a repressor of photomorphogenesis in *Arabidopsis*. *Plant Physiol.* 114, 779–788. doi: 10.1104/pp.114.3.779

Walker, B. J., Drewry, D. T., Slattery, R. A., Vanloocke, A., Cho, Y. B., and Ort, D. R. (2018). Chlorophyll can be reduced in crop canopies with little penalty to photosynthesis. *Plant Physiol.* 176, 1215–1232. doi: 10.1104/pp.17.01401

Wang, F., Wu, W., Wang, D., Yang, W., Sun, J., Liu, D., et al. (2016). Characterization and genetic analysis of a novel light-dependent lesion mimic mutant, lm3, showing adult-plant resistance to powdery mildew in common wheat. *PLoS One* 11:e0155358. doi: 10.1371/journal.pone.0155358

Wang, G., Zhang, S., Ma, X., Wang, Y., Kong, F., and Meng, Q. (2016). A stress-associated NAC transcription factor (SlNAC35) from tomato plays a positive role in biotic and abiotic stresses. *Physiol. Plant.* 158, 45–64. doi: 10.1111/ppl.12444

Wang, W.-X., Lian, H.-L., Zhang, L.-D., Mao, Z.-L., Li, X.-M., Xu, F., et al. (2016). Transcriptome analyses reveal the involvement of both C and N termini of cryptochrome 1 in its regulation of phytohormone-responsive gene expression in *Arabidopsis*. *Front. Plant Sci.* 7:294. doi: 10.3389/fpls.2016.00294

Wang, P.-H., Lee, C.-E., Lin, Y.-S., Lee, M.-H., Chen, P.-Y., Chang, H.-C., et al. (2019). The glutamate receptor-like protein GLR3. 7 interacts with 14-3-3ω and participates in salt stress response in *Arabidopsis thaliana*. *Front. Plant Sci.* 10:1169. doi: 10.3389/fpls.2019.01169

Wang, Z., Ma, L.-Y., Cao, J., Li, Y.-L., Ding, L.-N., Zhu, K.-M., et al. (2019). Recent advances in mechanisms of plant defense to *Sclerotinia sclerotiorum*. *Front. Plant Sci.* 10:1314. doi: 10.3389/fpls.2019.01314

Wang, Y., Kang, Y., Ma, C., Miao, R., Wu, C., Long, Y., et al. (2017). CNGC2 is a Ca2+ influx channel that prevents accumulation of apoplastic Ca2+ in the leaf. *Plant Physiol.* 173, 1342–1354. doi: 10.1104/pp.16.01222

Woldemariam, M. G., Dinh, S. T., Oh, Y., Gaquerel, E., Baldwin, I. T., and Galis, I. (2013). NaMYC2 transcription factor regulates a subset of plant defense responses in *Nicotiana attenuata*. *BMC Plant Biol.* 13:73. doi: 10.1186/1471-2229-13-73

Xu, D., Jiang, Y., Li, J., Lin, F., Holm, M., and Deng, X. W. (2016a). BBX21, an *Arabidopsis* B-box protein, directly activates HY5 and is targeted by COP1 for 26S proteasome-mediated degradation. *Proc. Natl. Acad. Sci. U.S.A.* 113, 7655–7660. doi: 10.1073/pnas.1607687113

Xu, D., Zhu, D., and Deng, X. W. (2016b). The role of COP1 in repression of photoperiodic flowering. *F1000Research* 5:178. doi: 10.12688/f1000research.7346.1

Xu, D., Lin, F., Jiang, Y., Huang, X., Li, J., Ling, J., et al. (2014). The RING-finger E3 ubiquitin ligase COP1 SUPPRESSOR1 negatively regulates COP1 abundance in maintaining COP1 homeostasis in dark-grown *Arabidopsis* seedlings. *Plant Cell* 26, 1981–1991. doi: 10.1105/tpc.114.124024

Xu, X., Paik, I., Zhu, L., Bu, Q., Huang, X., Deng, X. W., et al. (2014). PHYTOCHROME INTERACTING FACTOR1 enhances the E3 ligase activity of CONSTITUTIVE PHOTOMORPHOGENIC1 to synergistically repress photomorphogenesis in *Arabidopsis*. *Plant Cell* 26, 1992–2006. doi: 10.1105/tpc.114.125591

Xu, H., Martinoia, E., and Szabo, I. (2015a). Organellar channels and transporters. *Cell Calc.* 58, 1–10. doi: 10.1016/j.ceca.2015.02.006

Xu, X., Paik, I., Zhu, L., and Huq, E. (2015b). Illuminating progress in phytochrome-mediated light signaling pathways. *Trends Plant Sci.* 20, 641–650. doi: 10.1016/j.tplants.2015.06.010

Xu, X., Kathare, P. K., Pham, V. N., Bu, Q., Nguyen, A., and Huq, E. (2017). Reciprocal proteasome-mediated degradation of PIFs and HFR1 underlies photomorphogenic development in *Arabidopsis*. *Development* 144, 1831–1840. doi: 10.1242/dev.146936

Yan, C., Fan, M., Yang, M., Zhao, J., Zhang, W., Su, Y., et al. (2018). Injury activates Ca2+/calmodulin-dependent phosphorylation of JAV1-JAZ8-WRKY51 complex for jasmonate biosynthesis. *Mol. Cell* 70, 136–149. doi: 10.1016/j.molcel.2018.03.013

Yang, D., Seaton, D. D., Krahmer, J., and Halliday, K. J. (2016). Photoreceptor effects on plant biomass, resource allocation, and metabolic state. *Proc. Natl. Acad. Sci. U.S.A.* 113, 7667–7672. doi: 10.1073/pnas.1601309113

Yang, D.-L., Shi, Z., Bao, Y., Yan, J., Yang, Z., Yu, H., et al. (2017). Calcium pumps and interacting BON1 protein modulate calcium signature, stomatal closure, and plant immunity. *Plant Physiol.* 175, 424–437. doi: 10.1104/pp.17.00495

Yang, J., Duan, G., Li, C., Liu, L., Han, G., Zhang, Y., et al. (2019). The crosstalks between jasmonic acid and other plant hormone signaling highlight the involvement of jasmonic acid as a core component in plant response to biotic and abiotic stresses. *Front. Plant Sci.* 10:1349. doi: 10.3389/fpls.2019.01349

Yang, J., Lin, R., Sullivan, J., Hoecker, U., Liu, B., Xu, L., et al. (2005). Light regulates COP1-mediated degradation of HFR1, a transcription factor essential for light signaling in *Arabidopsis*. *Plant Cell* 17, 804–821. doi: 10.1105/tpc.104.030205

Yoshioka, K., Kachroo, P., Tsui, F., Sharma, S. B., Shah, J., and Klessig, D. F. (2001). Environmentally sensitive, SA-dependent defense responses in the cpr22 mutant of *Arabidopsis*. *Plant J.* 26, 447–459. doi: 10.1046/j.1365-313X.2001.2641039.x

Yoshioka, K., Moeder, W., Kang, H.-G., Kachroo, P., Masmoudi, K., Berkowitz, G., et al. (2006). The chimeric *Arabidopsis* CYCLIC NUCLEOTIDE-GATED ION CHANNEL11/12 activates multiple pathogen resistance responses. *Plant Cell* 18, 747–763. doi: 10.1105/tpc.105.038786

Yu, J.-W., Rubio, V., Lee, N.-Y., Bai, S., Lee, S.-Y., Kim, S.-S., et al. (2008). COP1 and ELF3 control circadian function and photoperiodic flowering by regulating GI stability. *Mol. Cell* 32, 617–630. doi: 10.1016/j.molcel.2008.09.026

Yu, X., Liu, H., Klejnot, J., and Lin, C. (2010). The cryptochrome blue light receptors. *Am. Soc. Plant Biol.* 8:e0135. doi: 10.1199/tab.0135

Yuan, F., Yang, H., Xue, Y., Kong, D., Ye, R., Li, C., et al. (2014). OSCA1 mediates osmotic-stress-evoked Ca 2+ increases vital for osmosensing in *Arabidopsis*. *Nature* 514, 367–371. doi: 10.1038/nature13593

Zhang, H., Kang, H., Su, C., Qi, Y., Liu, X., and Pu, J. (2018). Genome-wide identification and expression profile analysis of the NAC transcription factor family during abiotic and biotic stress in woodland strawberry. *PLoS One* 13:e0197892. doi: 10.1371/journal.pone.0197892

Zhang, J. X., Dilantha Fernando, W., and Xue, A. G. (2005). Daily and seasonal spore dispersal by *Mycosphaerella pinodes* and development of mycosphaerella blight of field pea. *Can. J. Bot.* 83, 302–310. doi: 10.1139/b05-003

Zhang, M., Liu, Y., He, Q., Chai, M., Huang, Y., Chen, F., et al. (2020). Genome-wide investigation of calcium-dependent protein kinase gene family in pineapple: evolution and expression profiles during development and stress. *BMC Genom.* 21:72. doi: 10.1186/s12864-020-6501-8

Zhang, S., Pan, Y., Tian, W., Dong, M., Zhu, H., Luan, S., et al. (2017). *Arabidopsis* CNGC14 mediates calcium influx required for tip growth in root hairs. *Mol. Plant* 10, 1004–1006. doi: 10.1016/j.molp.2017.02.007

Zhao, Y., Zhou, J., and Xing, D. (2014). Phytochrome B-mediated activation of lipoxygenase modulates an excess red light-induced defence response in *Arabidopsis*. *J. Exper. Bot.* 65, 4907–4918. doi: 10.1093/jxb/eru247

Zhou, L., Lan, W., Jiang, Y., Fang, W., and Luan, S. (2014). A calcium-dependent protein kinase interacts with and activates a calcium channel to regulate pollen tube growth. *Mol. Plant* 7, 369–376. doi: 10.1093/mp/sst125

Zhu, D., Maier, A., Lee, J.-H., Laubinger, S., Saijo, Y., Wang, H., et al. (2008). Biochemical characterization of *Arabidopsis* complexes containing CONSTITUTIVELY PHOTOMORPHOGENIC1 and SUPPRESSOR OF PHYA proteins in light control of plant development. *Plant Cell* 20, 2307–2323. doi: 10.1105/tpc.107.056580

Zhu, L., Bu, Q., Xu, X., Paik, I., Huang, X., Hoecker, U., et al. (2015). CUL4 forms an E3 ligase with COP1 and SPA to promote light-induced degradation of PIF1. *Nat. Commun.* 6, 1–10. doi: 10.1038/ncomms8245

Zipfel, C. (2014). Plant pattern-recognition receptors. *Trends Immunol.* 35, 345–351. doi: 10.1016/j.it.2014.05.004

Conflict of Interest: The authors declare that the research was conducted in the absence of any commercial or financial relationships that could be construed as a potential conflict of interest.

frontiers in Plant Science

ORIGINAL RESEARCH
published: 09 March 2021
doi: 10.3389/fpls.2021.636098

The Sequential Action of MIDA9/PP2C.D1, PP2C.D2, and PP2C.D5 Is Necessary to Form and Maintain the Hook After Germination in the Dark

*Arnau Rovira[1†], Maria Sentandreu[1†], Akira Nagatani[2], Pablo Leivar[1,3] and Elena Monte[1,4]**

[1]Plant Development and Signal Transduction Program, Center for Research in Agricultural Genomics (CRAG) CSIC-IRTA-UAB-UB, Barcelona, Spain, [2]Department of Botany, Graduate School of Science, Kyoto University, Kyoto, Japan, [3]Laboratory of Biochemistry, Institut Químic de Sarrià, Universitat Ramon Llull, Barcelona, Spain, [4]Consejo Superior de Investigaciones Científicas (CSIC), Barcelona, Spain

OPEN ACCESS

Edited by:
Chentao Lin, University of California, Los Angeles, United States

Reviewed by:
Jason Reed, University of North Carolina at Chapel Hill, United States
Jin-Song Zhang, Institute of Genetics and Developmental Biology (CAS), China

***Correspondence:**
Elena Monte
elena.monte@cragenomica.es

[†]These authors share first authorship

Specialty section:
This article was submitted to Plant Physiology, a section of the journal Frontiers in Plant Science

Received: *30 November 2020*
Accepted: *05 February 2021*
Published: *09 March 2021*

Citation:
Rovira A, Sentandreu M, Nagatani A, Leivar P and Monte E (2021) The Sequential Action of MIDA9/PP2C.D1, PP2C.D2, and PP2C.D5 Is Necessary to Form and Maintain the Hook After Germination in the Dark. Front. Plant Sci. 12:636098. doi: 10.3389/fpls.2021.636098

During seedling etiolation after germination in the dark, seedlings have closed cotyledons and form an apical hook to protect the meristem as they break through the soil to reach the surface. Once in contact with light, the hook opens and cotyledons are oriented upward and separate. Hook development in the dark after seedling emergence from the seed follows three distinctly timed and sequential phases: formation, maintenance, and eventual opening. We previously identified *MISREGULATED IN DARK9* (*MIDA9*) as a phytochrome interacting factor (PIF)-repressed gene in the dark necessary for hook development during etiolated growth. *MIDA9* encodes the type 2C phosphatase PP2C.D1, and *pp2c-d1/mida9* mutants exhibit open hooks in the dark. Recent evidence has described that PP2C.D1 and other PP2C.D members negatively regulate SMALL AUXIN UP RNA (SAUR)-mediated cell elongation. However, the fundamental question of the timing of PP2C.D1 action (and possibly other members of the PP2C.D family) during hook development remains to be addressed. Here, we show that PP2C.D1 is required immediately after germination to form the hook. *pp2c.d1/mida9* shows reduced cell expansion in the outer layer of the hook and, therefore, does not establish the differential cell growth necessary for hook formation, indicating that PP2C.D1 is necessary to promote cell elongation during this early stage. Additionally, genetic analyses of single and high order mutants in PP2C.D1, PP2C.D2, and PP2C.D5 demonstrate that the three PP2C.Ds act collectively and sequentially during etiolation: whereas PP2C.D1 dominates hook formation, PP2C.D2 is necessary during the maintenance phase, and PP2C.D5 acts to prevent opening during the third phase together with PP2C.D1 and PP2C.D2. Finally, we uncover a possible connection of PP2C.D1 levels with ethylene physiology, which could help optimize hook formation during post-germinative growth in the dark.

Keywords: skotomorphogenesis, etiolation, hook, MIDA9, PP2C.D phosphatases, phytochrome interacting factor PIF, ethylene

INTRODUCTION

When germination takes place in the dark, young seedlings adopt a developmental strategy called skotomorphogenesis or etiolated growth, which is energetically sustained by seed reserves. This dark-growth strategy is characterized by fast hypocotyl elongation to rapidly reach the soil surface, together with the presence of an apical hook and appressed cotyledons, which protect the apical meristem from damage while pushing through the soil (Wei et al., 1994; Gommers and Monte, 2018).

The apical hook structure is a transient structure that develops after germination as a result of the curvature of the hypocotyl apex just below the cotyledons, and protects the apical meristem during emergence from the soil. Hook development proceeds through three different phases: formation, maintenance, and opening (Vandenbussche et al., 2010; Zádníková et al., 2010). The formation phase starts just after germination when the seedling emerges from the seed coat. This phase lasts about 24–36 h in which the hook reaches 180° when completely formed. The maintenance phase follows, in which the hook remains folded for another 24–48 h. Finally, the opening phase starts and hook progressively unfolds to become completely open (angle 0°). The formation phase is achieved by asymmetrical cell expansion and cell division at the apical part of the hypocotyl. Cell expansion is inhibited in the inner (concave) edge of the hook, while cell division and expansion are promoted in the outer (convex) border (Silk and Erickson, 1979; Raz and Koornneef, 2001; Vandenbussche et al., 2010), which forms an apical hook bending of the hypocotyl apex. This asymmetrical cell expansion is caused by an auxin maximum in the concave part of the apical hook. Mutations in auxin transport genes or auxin-synthesis genes cause defects in hook development (Vandenbussche et al., 2010; Zádníková et al., 2010; Willige et al., 2012). In addition to auxin, other hormones like ethylene (ET) and gibberellins (GAs) are involved in hook formation. Exogenous treatment with the ethylene biosynthesis precursor 1-aminocyclo-propane-1-carboxylic acid (ACC) induces a triple response of the etiolated seedlings characterized by an exaggerated hook, short, and thickened hypocotyl. On the other hand, ethylene biosynthetic mutants, as well as ethylene-insensitive mutants, are hookless (Guzmán and Ecker, 1990; Tsuchisaka et al., 2009). GAs also participate in hook formation, given that inactivation of either GAs synthesis or signaling results in a hookless phenotype (Alabadí et al., 2004; Vriezen et al., 2004). Conversely, treatment with GA or mutations in DELLA genes (transcriptional regulators that negatively regulate the GA signaling pathway) exhibit an exaggerated hook (An et al., 2012). It has been proposed that both GAs and ET modulate asymmetrical auxin distribution depending on the apical hook development (Vandenbussche et al., 2010; Zádníková et al., 2010).

The phytochrome-interacting factors (PIFs) are basic helix-loop-helix (bHLH) transcription factors that function as repressors of photomorphogenesis. The PIF quartet (PIFq) members PIF1, PIF3, PIF4, and PIF5 constitutively promote skotomorphogenesis by repressing the photomorphogenesis state in darkness (Leivar et al., 2008b). Single *Arabidopsis thaliana* *pif1*, *pif3*, *pif4*, and *pif5* mutants show a minor or absent photomorphogenic phenotype in darkness, whereas additive to synergetic effects are observed in higher order mutant combinations. In accordance, *pifq* mutant seedlings display a partial constitutive photomorphogenic phenotype in the dark similar to *cop1* (Leivar et al., 2008b), with short hypocotyl, unfolded hook, and separated cotyledons. Consistent with this observation, the transcriptomic profile of *pifq* mutants in the dark largely resembles that of wild-type (WT) seedlings grown in the light (Leivar et al., 2009; Shin et al., 2009), further illustrating the role of PIFs to maintain the etiolated state. Upon light exposure, PIFs interact with active phytochromes (phy) in their Pfr conformation, and this interaction triggers rapid phosphorylation and proteasome-mediated degradation of PIFs, lifting the repression and allowing photomorphogenesis to initiate (Monte et al., 2004; Al-Sady et al., 2006; Van Buskirk et al., 2012; Leivar and Monte, 2014; Ni et al., 2017). It has been described that cryptochrome (cry) also physically interacts with PIF4 and PIF5 (Pedmale et al., 2016), possibly to repress their transcriptional activity (Ma et al., 2016). Through the action of phys (mainly phyA and phyB) and crys (cry1 and cry2), light rapidly induces complete hook opening, within a few hours (Liscum and Hangarter, 1993; Wu et al., 2010). This hook unfolding occurs due to faster cell elongation at the inner compared to the outer edge (Vandenbussche and Van Der Straeten, 2004; Vriezen et al., 2004). During hook opening, the auxin gradient is greatly reduced (Wu et al., 2010; Willige et al., 2012). Several reports have established direct targets of PIF activity through which PIFs could be contributing to hook development in the dark. PIF5 affects the generation of the auxin gradient by directly regulating *WAG2*, which encodes a protein kinase that regulates auxin transport, and this regulation is modulated by GAs and DELLAs (Willige et al., 2012). PIF5 also directly induce expression of ethylene biosynthesis genes 1-aminocyclopropane-1-carboxulate synthase (ACS) such as ACS5 and ACS8 in a GAs and DELLA-dependent manner (Khanna et al., 2007; Gallego-Bartolomé et al., 2011).

We previously reported a combination of a transcriptomic-based approach with a functional profiling strategy to identify novel regulators of seedling deetiolation downstream of PIF3 (Sentandreu et al., 2011). Four PIF3-regulated genes misexpressed in the dark (*MIDAs*) were defined as novel regulators of seedling deetiolation involved in hypocotyl elongation (*MIDA11*), hook development (*MIDA9* and *MIDA10*), and cotyledon separation (*MIDA1*). Etiolated seedlings deficient in *MIDA9* (*mida9*) showed open hooks after germination and growth in the dark for 4 days (Sentandreu et al., 2011). *MIDA9* encodes the type-2C phosphatase PP2C.D1 belonging to clade D (PP2C.D) of the type-2C phospahatase superfamily in *A. thaliana*. Clade D consists of nine members and is characterized by having a distinct nuclear localization signal and prediction of possible plasma membrane localization (Schweighofer et al., 2004). Recently, MIDA9/PP2C.D1 was reported to modulate the phosphorylation status of the H+-ATPase to regulate cell expansion in the hypocotyl in long day-grown seedlings (Spartz et al., 2014). Interestingly, this activity can be directly inhibited by SMALL AUXIN UP-RNA (SAUR) proteins (Spartz et al., 2014). In addition, expression of *MIDA9/PP2C.D1* has been detected

in hypocotyl and hook (Ren et al., 2018). However, the fundamental question of the timing of PP2C.D1 action (and possibly other members of the PP2C.D family) during post-germinative hook development remains to be addressed.

Here, we show that PP2C.D1 is required immediately after germination for hook formation. *mida9/pp2c.d1* shows reduced cell expansion in the outer layer of the hook and, therefore, does not establish the differential cell growth necessary to form the hook, indicating that PP2C.D1 is necessary to promote cell elongation during this early stage. Additionally, genetic analyses of single and high order mutants in PP2C.D1, D2, and D5 demonstrate that the three PP2C.Ds act collectively and sequentially during etiolation. Finally, we uncover a possible connection of PP2C.D1 levels with ethylene physiology, which could help optimize hook formation during post-germinative growth in the dark.

MATERIALS AND METHODS

Plant Material and Seedling Growth

Arabidopsis thaliana seeds used here include the previously described *mida9-1* mutant (*pp2c.d1/mida9*) in the ecotype Col-0 background (Sentandreu et al., 2011), and the newly characterized *A. thaliana* lines *pp2c.d2*/SALK_203806 and *pp2c.d5*/SALK_049798 from the Salk Institute Genomic Analysis Laboratory database (Alonso et al., 2003). Homozygous T-DNA insertion lines and WT siblings were identified using PCR with T-DNA and gene-specific primers (**Supplementary Table S1**). PP2C.D1-YFP transgenic lines were generated by cloning the 2 kb region upstream of the ATG (*PP2C.D1* promoter) in the pDONR-P4-P1R vector, the *PP2C.D1* coding sequence (CDS) in the pDONR-P2R-P3 vector, and the YFP CDS in the pDONR221 vector. LR recombination reaction using the Gateway cloning system (Invitrogen) was done to generate proPP2C.D1::PP2C.D1:YFP in the pH7m34gw vector. The resulting vector was used to transform *pp2c.d1/mida9* to generate PP2C.D1-YFP.

PP2C.D1-GFP-OX transgenic lines were generated by cloning the *PP2C.D1* CDS under the regulation of the 35S promoter in the pH7WG2 vector using the Gateway cloning system. The resulting 35S::PP2C.D1:GFP was used to transform *pp2c.d1/mida9* to generate MIDA9-GFP-OX lines.

Seeds were sterilized and plated on Murashige and Skoog medium (MS) without sucrose as previously described (Monte et al., 2003). For AgNO3 experiments, seeds were sterilized and plated on MS without sucrose with AgNO3 (50 μM). Seedlings were then stratified for 4 days at 4°C in the dark, followed by 3 h of white light to induce germination. Seedlings were then placed in darkness for the indicated period of time. ACC treatments were done as previously described (Gommers et al., 2020) using a concentration of 2 μM.

Hypocotyl, Hook, and Cell Measurements

For hypocotyl and hook measurements, seedlings grown for 2, 3, and 4 days were arranged horizontally on a plate and photographed using a digital camera (Nikon D80). Measurements were performed using NIH image software (Image J, National Institutes of Health), as described before (Leivar et al., 2008a,b). The angle of a completely closed apical hook was defined as 180°, whereas the angle of a fully opened hook was defined as 0°. Measurements of at least 30 seedlings for each mutant line were tested in R for statically significant differences with the WT sibling controls. Cell size and hook length measurements were visualized at 2-day-old dark-grown seedlings stained with propidium iodine (10 μg/ml; Calbiochem) using a confocal laser microscope Leica SP5 (Emission window: 570–666 nm).

Gene Expression Analysis

RNA was extracted using the Maxwell RSC plant RNA Kit (Promega). One microgram of total RNA was treated with DNase I (Ambion) according to the manufacturer's instructions. First-strand cDNA synthesis was performed using the SuperScript III reverse transcriptase kit (Invitrogen) and oligo dT as a primer in the presence of RNase Out (invitrogen). Two microliter of 1:25 diluted cDNA with water was used for real-time PCR (LightCycler 480 Roche) using SYBR Premix Ex Taq (Takara) and primers at 300 nM concentration. *PP2A (AT1G13320)* was used for normalization. Primers used for gene expression analyses are listed in **Supplementary Table S2**.

Fluorescence Microscopy

PP2C.D1-YFP and PP2C.D1-GFP were visualized in 2-day-old dark-grown PP2C.D1-YFP and PP2C.D1-GFP-OX seedlings, respectively, using a confocal laser scanning microscope Olympus FV1000 (Emission window: 500–600 nm). *pp2c.d1/mida9* was used as a negative control.

Protein Extraction and Immunoblots

Protein extracts were prepared from 2-day-old dark-grown seedlings. Tissue samples were collected and frozen in liquid nitrogen. Samples were manually ground under frozen conditions and resuspended in extraction buffer [100 mM MOPS (pH 7.6), 2% SDS, 10% glycerol, 4 mM EDTA, 50 mM sodium metabisulfite ($Na_2S_2O_5$), 2 μgl^{-1} apoprotein, 3 μgl^{-1} leupeptine, 1 μgl^{-1} pepstatin, and 2 mM PMSF; Al-Sady et al., 2006; Martín et al., 2018].

Total protein was quantified using a Protein DC kit (Bio-Rad), and β-mercaptoethanol was added just before loading. For each sample, 100 μg were treated for 5 min at 95°C and subjected to 12.5% SDS-PAGE gels. Proteins were then transferred to Immobilon-P membrane (Millipore), and immunodetection of PP2C.D1-GFP was performed using an anti-GFP antibody (1:10,000 dilution). Peroxidase-linked anti-rabbit secondary antibody (1:10,000) and SuperSignal West Femto chemiluminescence kit (Pierce) were used for detection of luminescence using a LAS-4000 image imaging system (Fujifilm). The membrane was stained with Ponceau as a loading control.

Statistical Analysis

Levene's test was performed to verify equal variances ($p < 0.05$). When the variances were equal, Student *t*-test ($p < 0.05$) or ANOVA test ($p < 0.05$) followed by a *post-hoc* Tukey-b test were performed. For unequal variances, Kruskal-Wallis test ($p < 0.05$) followed by a *post-hoc* Dunn test was performed.

To quantitatively assess the magnitude of the difference between ACS time courses, we computed pairwise Euclidean distance (EUC), a well-established method in overall clustering as well as in the calculation of similarity between gene expression time courses (Ramoni et al., 2002). For statistical analyses of ACS time courses, we pooled data for each ACS gene and genotype and used ANOVA test to assess whether the differences across genotypes were significant. All analyses were conducted in R.

RESULTS

MIDA9/PP2C.D1 Is Required for Hook Formation During Skotomorphogenic Development

To characterize in detail the role of MIDA9/PP2C.D1 during apical hook development after germination in the dark, we followed the apical hook dynamics in WT (Col-0) and *mida9/d1* mutant seedlings lacking *MIDA9/PP2C.D1* (Sentandreu et al., 2011). The three phases in hook development (formation, maintenance, and aperture) were monitored by measuring the angle of hook curvature at different time points after germination under dark conditions. In Col-0, we observed that under our conditions, hook formation took place after seed emergence during the first 40 h post-germination, reaching a hook closure of 160°. The maintenance phase followed and lasted up to 60 h after germination. Finally, hook opening started (>60 h post-germination) resulting in hook unfolding (about 25°) at 108 h after germination (**Figures 1A**,**B**). Compared to Col-0, *pp2c-d1* mutants emerged from the seed coat at the same time. Interestingly, *pp2c-d1* mutants were not able to fully form the apical hook during the formation phase and reached only about 125° of hook closure (**Figures 1A**,**B**). These differences between Col-0 and *pp2c-d1* were maintained during the maintenance phase. Finally, hook opening started at similar time in both genotypes and eventually resulted in similar hook unfolding in both genotypes (**Figure 1**). Together, these

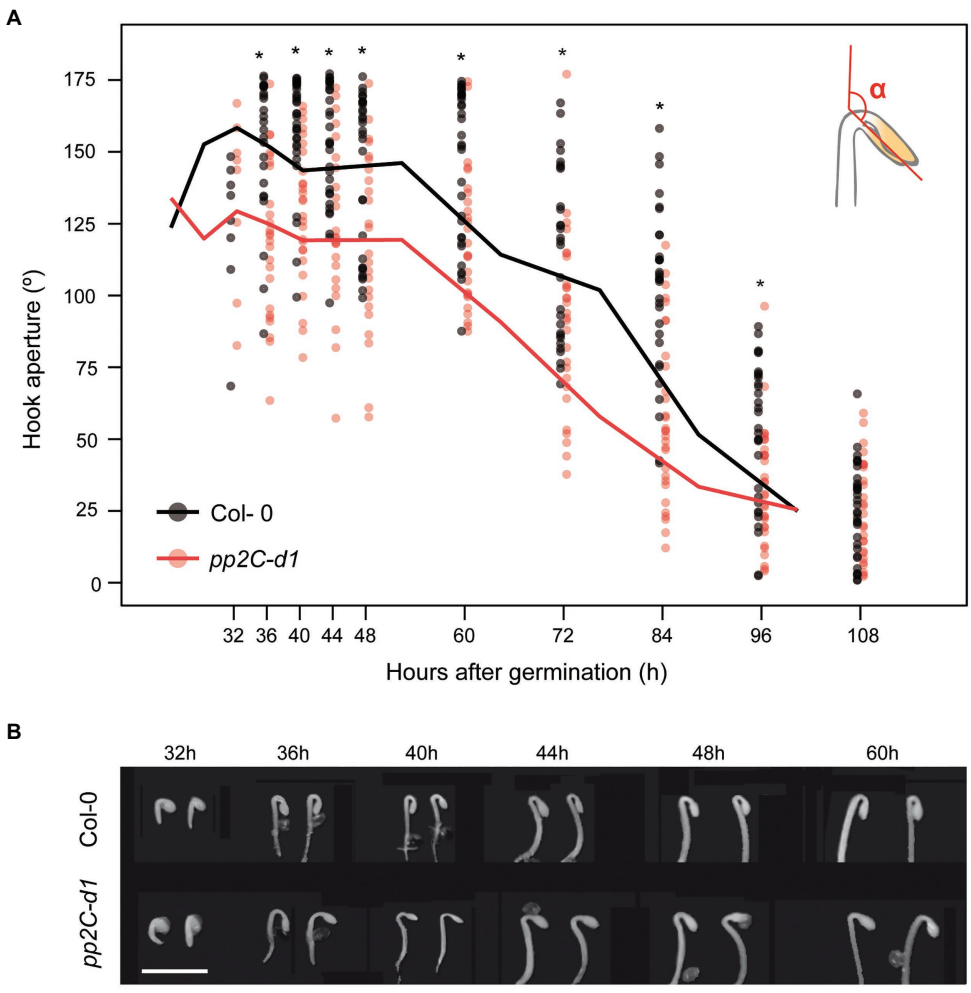

FIGURE 1 | MIDA9/PP2C.D1 is necessary to induce hook formation after germination. **(A)** Time course analysis of apical hook aperture after germination in the dark in Col-0 and *mida9/pp2c-d1*. Lines represent mean values and dots indicate each measurement. Statistical significance relative to Col-0 is indicated by an asterisk (Student *t*-test, $p < 0.05$) $n = 40$. **(B)** Visible phenotypes of seedlings grown in the dark are shown. Bar = 2 mm.

data extend our observation that MIDA9/PP2C.D1 participates in hook development as a positive regulator (Sentandreu et al., 2011), and indicate that this regulation occurs specifically during hook formation when PP2C.D1 activity is required in the first hours of post-germinative growth to form the hook.

MIDA9/PP2C.D1 Is Required to Establish the Asymmetric Growth Necessary for Hook Formation

To understand how PP2C.D1 might regulate hook formation, we combined confocal microscopy and phenotypic measurements to study the early stage of *pp2c.d1* hook development in more detail. To examine hook development under dark-grown conditions, we stained Col-0 and *pp2c.d1* with propidium iodide (PI), which is used to visualize plasma membrane delimiting cells (**Figure 2A**). Because hook formation is achieved mainly as a result of asymmetric elongation of the cells on the outer (convex) edge of the hook compared to the inner edge (concave; Silk and Erickson, 1979; Raz and Koornneef, 2001; illustrated in **Figure 2B**), we hypothesized that *pp2c.d1* seedlings might be affected in establishing this asymmetric growth. The length of the outer and the inner border of the hook was measured in 2-day-old dark-grown seedlings when the hook formation phase is completed. Whereas the inner concave side was similar in Col-0 and *pp2c.d1*, the outer convex side was significantly longer in Col-0 compared to *pp2c.d1* (**Figure 2C** left panel). Cell length of the outer and the inner side of the hook was also measured and compared, and no differences in cell length were found in the inner edge of the apical hook in Col-0 and *pp2c.d1*. However, cells in the outer convex side of the hook were longer in Col-0 compared to *pp2c.d1* [**Figures 2C** (right panel),**E**]. No apparent difference in cell number was observed between both genotypes. As a result, the convex/concave ratio was higher in Col-0 compared to *pp2c.d1* (**Figure 2D**), indicating that asymmetric growth in the hook structure in *pp2c.d1* was less pronounced than that of Col-0. Together, these results suggest that PP2C.D1 induces the elongation of the cells in the outer edge of the hook necessary to establish the

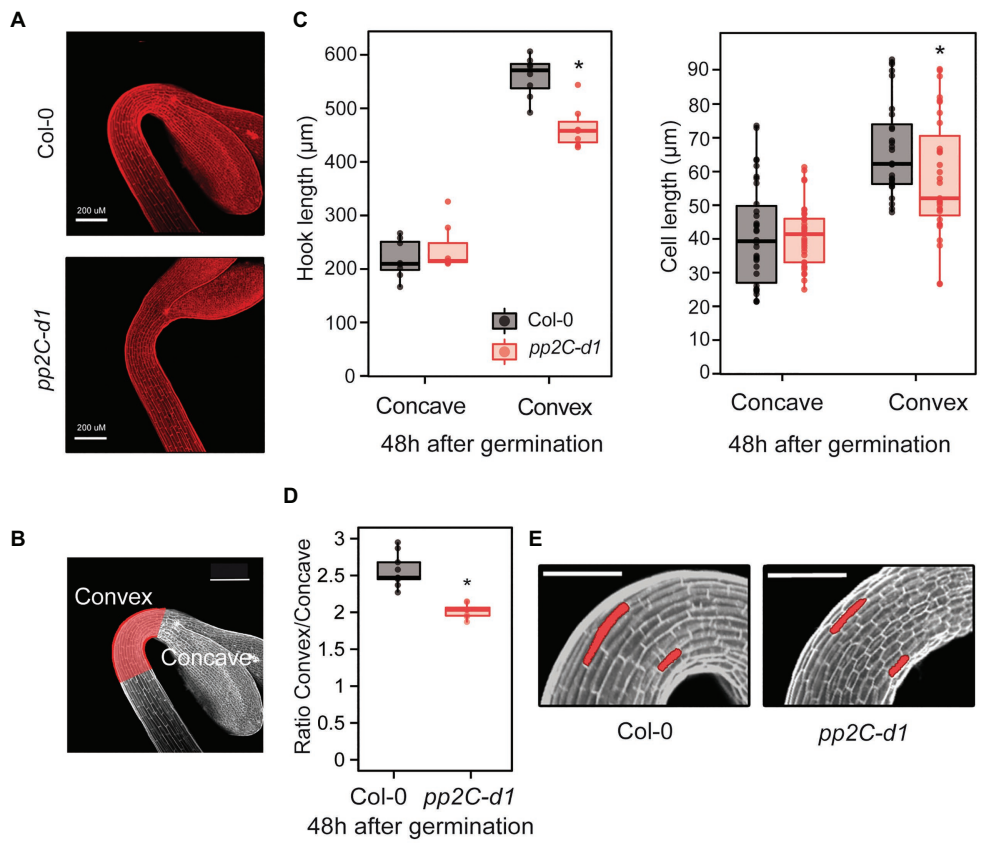

FIGURE 2 | MIDA9/PP2C.D1 induces cell expansion in the outer edge of the apical hook. **(A)** Visual phenotypes of the apical hook in 2-day-old dark-grown Col-0 and *pp2c-d1*. Bar = 200 µm. **(B)** The region of the apical hook is highlighted in red indicating the convex and concave sides. Bar = 200 µm. **(C)** Hook length (left panel) and cell length (right panel) measurements in the concave and convex sides of the apical hook in 2-day-old dark-grown Col-0 and *pp2c-d1*. Dots indicate each measurement. Statistical significance relative to Col-0 is indicated by an asterisk. Right panel (Student *t*-test, $p > 0.05$). Left panel, (Kruskal-Wallis, $p > 0.05$), $n = 15$. **(D)** Apical hook length ratio between convex and concave in Col-0 and *pp2c-d1*. Data are from panel C. Statistical significance relative to Col-0 is indicated by an asterisk (Student *t*-test, $p < 0.05$). **(E)** Visual phenotypes of 2-day-old dark-grown Col-0 and *pp2c-d1*. Cells from concave and convex parts of the hook are highlighted. Bar = 60 µm.

asymmetric growth that results in the hook organ formation after germination in the dark.

MIDA9/PP2C.D1 Localization in the Apical Hook

Transgenic lines were generated expressing fluorescent-tagged fusions under the strong constitutive 35S promoter (PP2C.D1-GFP-OX) or the endogenous PP2C.D1 promoter (PP2C.D1-YFP) in a *pp2c.d1* mutant background (see Materials and Methods section for details). Compared to Col-0, *PP2C.D1* expression levels were about 4-fold higher in PP2C.D1-YFP lines, and 20- and 80-fold higher in in PP2C.D1-GFP-OX #2.2 and PP2C.D1-GFP-OX #1.4, respectively. We did not detect *PP2C.D1* expression in *pp2c.d1*, consistent with previous results (Sentandreu et al., 2011; **Figure 3A**). Western blot analyses confirmed higher accumulation of the fusion protein in the overexpressing PP2C.D1-GFP-OX lines with respect to the PP2C.D1-YFP (**Figure 3B**).

PP2C.D1-YFP transgenic line complemented the hook formation phenotype of *pp2c.d1* (**Figure 3C**), indicating that the expressed fusion protein is active and functional. Visualization of 2-day-old dark-grown PP2C.D1-YFP by confocal microscopy showed subcellular localization of PP2C.D1 to the nucleus (consistent with the predicted nuclear localization signal; Schweighofer et al., 2004) but also in the cytoplasm, in apical hook and hypocotyl cells (**Figure 3D**). A comparable pattern,

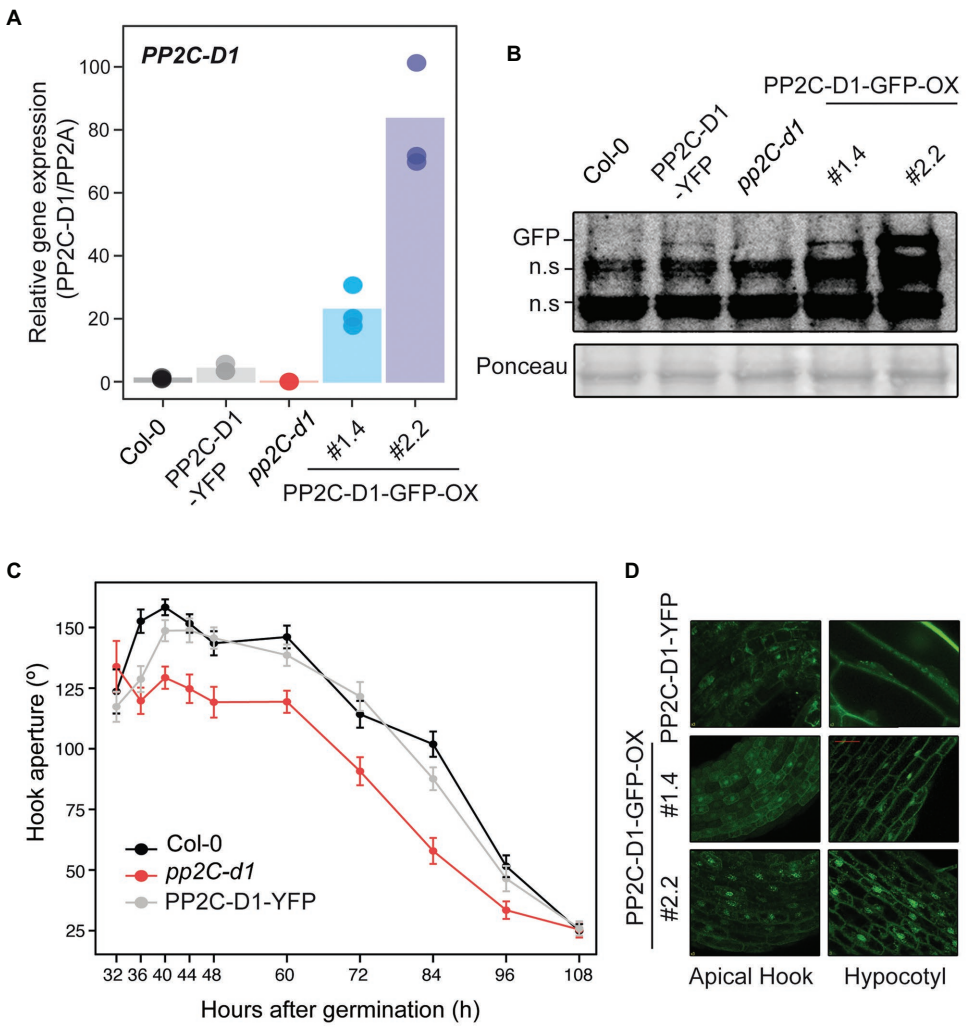

FIGURE 3 | MIDA9/PP2C.D1 is localized to the nucleus and cytoplasm in darkness. **(A)** qRT-PCR analysis of 2-day-old dark-grown Col-0, PP2C.D1-YFP, *pp2c-d1*, PP2C.D1-GFP-OX #1.4, and PP2C.D1-GFP-OX #2.2. *PP2C.D1* expression levels were normalized to *PP2A* and expressed relative to the Col-0 value set at unity. Bars represent mean values and dots indicate each measurement. $n = 3$ biological replicates. **(B)** Immunoblot of protein extracts of 2-day-old dark-grown Col-0, PP2C.D1-YFP, *pp2c-d1*, PP2C.D1-GFP-OX #1.4, and #2.2 seedlings. Protein extracts from Col-0 and *pp2c-d1* were used as negative control. GFP-specific polyclonal antibody was used as a probe. Ponceau staining was used as a loading control. Non-specific cross-reacting bands are marked as n.s. **(C)** Time course analysis of apical hook aperture after germination in the dark of Col-0, *pp2c-d1* and PP2C.D1-YFP. Lines indicate mean values. Error bars indicate s.d. $n = 40$. **(D)** Confocal microscopy images of PP2C.D1-YFP and PP2C.D1-GFP-OX #1.4 and #2.2 in 2-day-old dark-grown seedlings.

although with increased signal, was observed in cells of the PP2C.D1-GFP-OX lines.

Sequential Activity of PP2C.D1, D2, and D5 During Hook Formation and Maintenance

We aimed to assess the role of two other members of the PP2C.D clade during the different phases of hook development after germination in the dark. We used single and higher order mutants of PP2C.D1, PP2C.D2 (*AT3G17090*), and PP2C.D5 (mutated in *AT4G38520*). The *pp2c-d1*, *-d2*, and *-d5* mutant alleles used here differ from previous works (Spartz et al., 2014; Ren et al., 2018). All combinations of *pp2c.d1*, *pp2c.d2*, and *pp2c.d5* double and triple mutants were generated, and the three phases in hook development (formation, maintenance, and aperture) were monitored by measuring the angle of hook curvature over 4 days after germination in the dark.

Single mutant analysis at 2 days during the formation phase showed a prominent open hook in *pp2c.d1* (**Figure 4**), consistent with our previous observations (**Figure 1**). A significant but relatively minor phenotype was observed in *pp2c.d2*, whereas *pp2c.d5* showed no apparent hook phenotype compared to Col-0. Later during the maintenance (3 days) and at the aperture (4 days) phases, *pp2c.d2* mutant displayed a prominent open hook phenotype similar to *pp2c.d1*, and *pp2c.d5* did not show an observable phenotype. Together, these results suggest that (i) PP2C.D1 and PP2C.D2 act together to promote hook formation, with a dominant role of PP2C.D1 and a relatively marginal role of PP2C.D2; (ii) PP2C.D2 promotes hook maintenance together with PP2C.D1; and (iii) PP2C.D5 might have a minor or no contribution in the presence of the other clade D PP2C members.

In order to test for possible redundancy between family members, we next characterized higher order mutants between *PP2C.D1*, *PP2C.D2*, and *PP2C.D5*. No significant additive or synergistic genetic interactions were identified at the hook formation phase at 2 days, as the observed differences were relatively minor in magnitude (**Figure 4**). A similar tendency was observed at the maintenance phase at 3 days, only that the role of PP2C.D2 in maintaining the hook was also evident in the absence of the other two members PP2C.D1 and PP2C.D5 (compare *pp2c.d1d5* with *pp2c.d1d2d5*). Interestingly, additive/synergistic genetic interactions were clearly observed at the opening phase at 4 days. First, relative to the *pp2c.d1* and *pp2c.d2* single mutants, *pp2c.d1d2* showed a significantly more open hook phenotype. Second, in contrast to 2 and 3 days, a clear contribution of *PP2C.D5* was observed in the triple mutant *pp2c.d1d2d5* in the absence of *PP2C.D1* and *PP2C.D2* (compare *pp2c.d1d2* with *pp2c.d1d2d5*).

Together, this genetic analysis unveils a complex scenario where PP2C.D1, PP2C.D2, and PP2C.D5 collectively participate in hook development, but that they do so in a temporal and hierarchical manner. PP2C.D1 has a prevalent role in promoting hook formation, whereas PP2C.D2 plays a relatively marginal role at this phase. In contrast, at the maintenance phase, PP2C.D2 gains quantitative importance. Finally, PP2C.D5, with no apparent role during hook formation or maintenance, acts at the aperture phase to prevent hook opening in combination with PP2C.D1 and PP2C.D2.

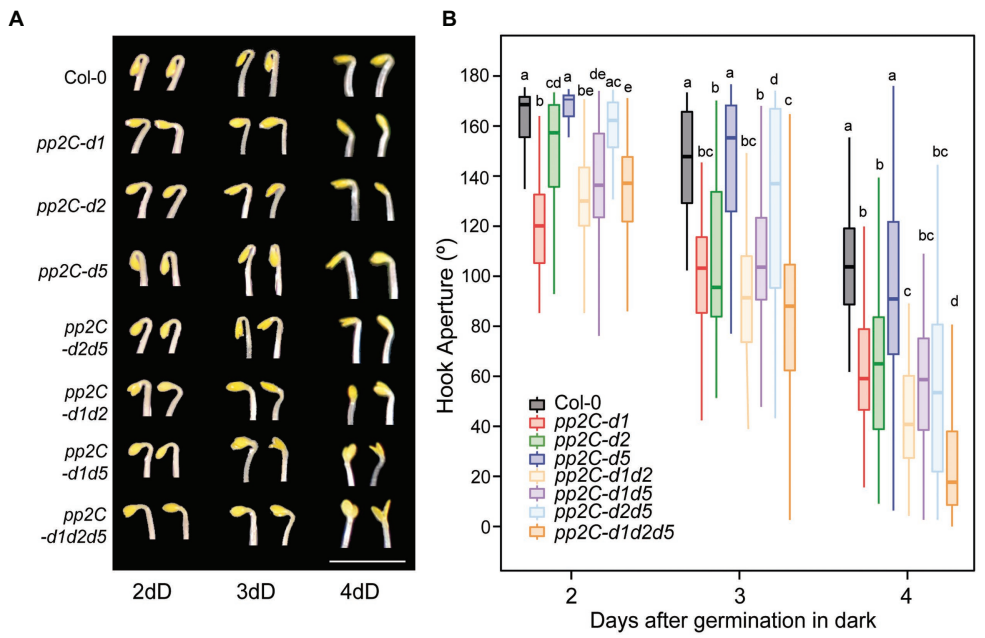

FIGURE 4 | PP2C.D members have distinct temporal functions regulating hook development. **(A)** Visible hook phenotypes of seedlings grown at 2, 3, and 4 days in the dark. Bar = 3 mm. **(B)** Apical hook aperture was measured in 2-, 3-, and 4-day-old dark-grown seedlings in Col-0, *pp2c-d1*, *pp2c-d2*, *pp2c-d5*, *pp2c-d2d5*, *pp2c-d2d1*, *pp2c-d5d1*, and *pp2c-d1d2d5*. Different letters denote statistical differences between means by Kruskal-Wallis test ($p < 0.05$) followed by a *post-hoc* Dunn test. $n = 40$.

Interplay Between MIDA9 and Ethylene Biosynthesis in the Dark

PP2C.D1-GFP-OX seedlings displayed short and thickened hypocotyls under dark-grown conditions compared to Col-0 and *pp2c.d1* seedlings (**Figures 5A**,**B**). This feature has been previously described in mutants with increased ethylene levels (Guzmán and Ecker, 1990), and led us to hypothesize that the observed phenotype of etiolated PP2C.D1-GFP-OX lines may be at least in part related to altered ethylene biosynthesis or response. Treatment with AgNO3 that blocks accessibility to ethylene receptors (Beyer, 1976), resulted in greater hypocotyl elongation responses in PP2C.D1-GFP-OX lines compared to Col-0 in 3-day-old dark-grown seedlings (**Figures 5A**,**B**). Hypocotyl growth differences were calculated by subtracting the hypocotyl length of seedlings grown in MS (mock) from those of seedlings grown in AgNO3, and results showed greater difference in MIDA9-GFP-OX compared to Col-0 (**Figure 5B** lower panel). These results suggest that the short hypocotyl phenotype of MIDA9-GFP-OX lines might be caused by increased ethylene levels, and indicates that the activity of PP2C might impact ethylene biosynthesis or action.

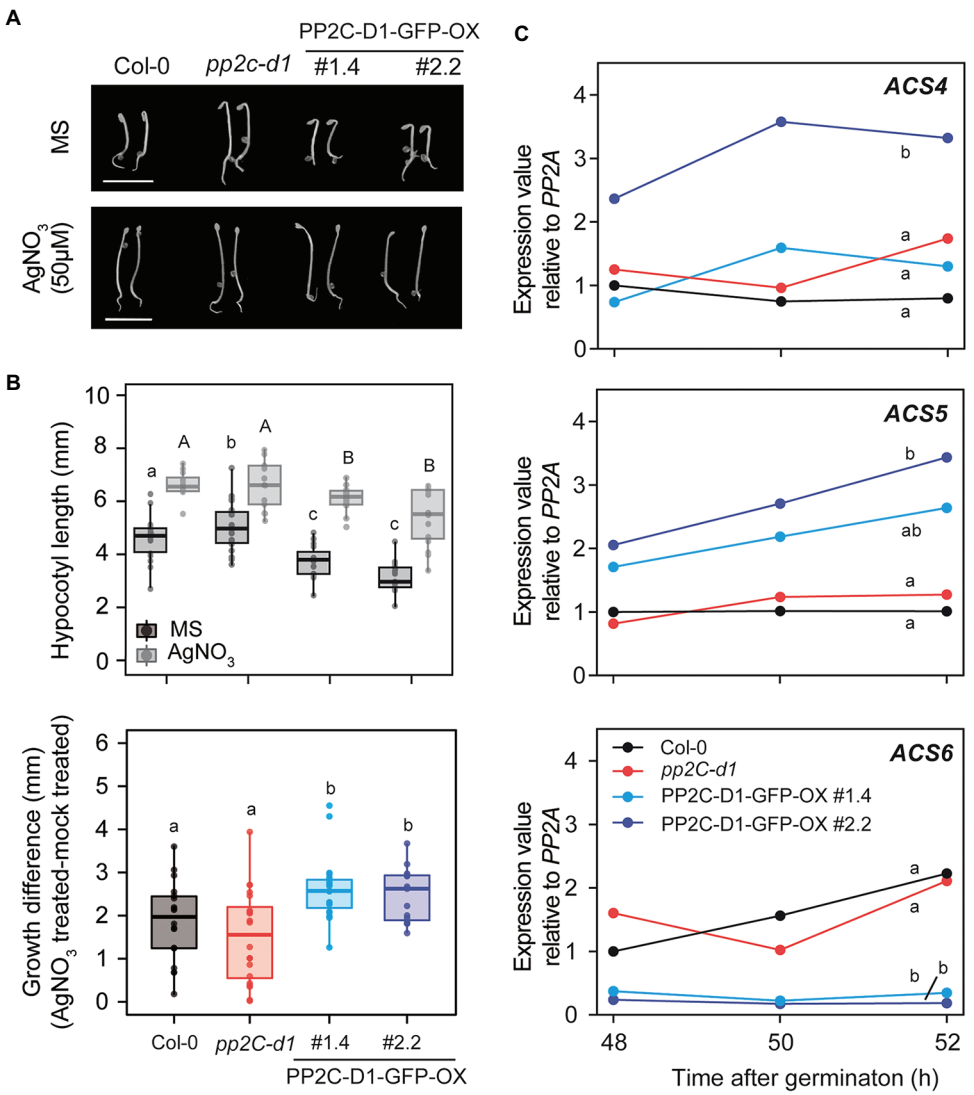

FIGURE 5 | MIDA9/PP2C.D1 participates in ethylene responses modulating 1-aminocyclopropane-1-carboxulate synthase (*ACS*) expression in dark-grown seedlings. **(A)** Visible phenotypes of 2-day-old dark-grown seedlings in MS or MS+ AgNO3 (50 μM) of Col-0, *pp2c-d1*, and PP2C.D1-GFP-OX #1.4 and #2.2. Bar = 5 mm **(B)** Upper panel, hypocotyl length of 2-day-old dark-grown seedlings in MS or MS+ AgNO3 (50 μM) of Col-0, *pp2c-d1*, and PP2C.D1-GFP-OX #1.4 and #2.2. Lower panel, hypocotyl growth differences of AgNO3 (50 μM) treated compared to mock treated plants. **(C)** qRT-PCR time course analysis of Col-0, *pp2c-d1*, and PP2C.D1-GFP-OX #1.4 and #2.2. *ACS* expression levels were normalized to *PP2A* and expressed relative to the Col-0 at 48 h after germination value set at unity. One of two biological replicates with similar results is represented. In panels b and c, different letters denote statistical differences between means by ANOVA ($p < 0.05$) followed by *post-hoc* Tukey-b test.

Stimulation of ethylene production is achieved through upregulation of the transcript levels of enzymes involved in ethylene biosynthesis. Conversion of ACC by ACS is the first committed step in ethylene biosynthesis and is considered to be the rate-limiting step. *ACS* is encoded by a multigene family containing at least eight functional members in *A. thaliana* (Yamagami et al., 2003). We analyzed the levels of *ACS4*, *5*, and *6* at 48, 50, and 52 h after germination in the dark, when the short hypocotyl phenotype is robust (**Figure 5A**). Compared to Col-0, we detected elevated levels of *ACS5* in the PP2C.D1-GFP-OX lines (**Figure 5C**). In contrast, only PP2C.D1-GFP-OX #2.2 line showed elevated *ACS4* expression levels compared to Col-0. The fold-change increase was greater in the PP2C.D1-GFP-OX #2.2 compared to #1.4, in agreement to #2.2 having greater PP2C.D1 levels compared to #1.4 (**Figures 3A**,**B**). In contrast, the *ACS6* expression levels, which are under negative feedback regulation (Chang et al., 2008), were greatly reduced in PP2C.D1-GFP-OX lines compared to Col-0 and *pp2c.d1*. ACS levels were not significantly affected in the *pp2c.d1* mutant. Analysis using a combination of Euclidean distance and ANOVA quantified the differences between time courses and assessed their statistical significance. Col-0 was found to differ the most from PP2C-D1-GFP-OX#2.2 across all three genes in a significant manner (Euclidean distance ACS4: 3.3, ACS5: 2.6, ACS6: 2.6), while Col-0 and *pp2C-d1* were found to be highly similar across all genes (Euclidean distance ACS4: 0.8, ACS5: 0.4, ACS6: 0.8; **Figure 5C**). PP2C-D1-GFP-OX#1.4 was found to be largely different from Col-0 in ACS5 and ACS6 (Euclidean distance 1.7 and 2.4, respectively), but not in ACS4 (Euclidean distance 0.8). These differences were found to be statistically significant for ACS6 but not ACS4, whereas for ACS5, PP2C-D1-GFP-OX#1.4 was found to be undistinguishable to both WT and PP2C-D1-GFP-OX#2.2 (**Figure 5C**). Together, these results suggest that PP2C.D1 levels might impact the regulation of ethylene biosynthesis. Interestingly, ACC treatment induced an exaggerated hook in all PP2C.D mutant lines similar to the control (**Supplementary Figure S1**), suggesting that PP2C.D levels do not affect ethylene signaling mediating hook development.

DISCUSSION

Although much progress has been achieved in the past years, how PIFs impose the different aspects of deetiolation during seedling establishment still remains incomplete. Our laboratory previously identified the PIF3-regulated *MIDA9* encoding the type-2C phosphatase PP2C.D1 as a gene involved in hook development (Sentandreu et al., 2011). Here, we performed a detailed genetic and phenotypic characterization of the role of *MIDA9/PP2C.D1* and two closely related PP2Cs to define their timing of action in the regulation of the different phases of hook development after germination in the dark (hook formation, maintenance, and opening). We found that MIDA9/PP2C.D1 is required for hook formation and that this is achieved by specifically promoting the elongation of the outer part of the apical hook. Furthermore, we identified sequential activity of PP2C.D1, PP2C.D2, and PP2C.D5 in the three phases of hook development, with some redundant roles. Finally, we described a potential connection between MIDA9/PP2C.D1 and ethylene physiology.

MIDA9/PP2C.D1 Is Required for Cell Expansion in the Outer Part of the Apical Hook

Apical hook development is a complex process that takes place in three different phases: formation, maintenance, and opening (Vandenbussche et al., 2010; Zádníková et al., 2010). It is, therefore, important to analyze the temporal stages of the complete dynamic process of hook development to understand how it is achieved, as an unfolded hook in mutated etiolated seedlings could be the result of a deficiency in hook formation, a defective maintenance, or a faster opening phase. Our finding that MIDA9/PP2C.D1 is predominantly involved in the first stage of hook formation (**Figure 1**) suggested that PIF-PP2C.D1 participates in establishing the asymmetric growth that allows bending of the upper part of the hypocotyl to form the hook. Indeed, whereas hook and cell length in the inner part was indistinguishable in WT and *mida9/pp2c.d1* mutants, the mutants did not elongate the cells in the outer convex part of the hook region as much as the WT, resulting in incomplete bending and deficient hook formation (**Figure 2**). These results indicate that PP2C.D1 functions to induce cell expansion in the outer cell layer of the hook to promote hook formation. This was somewhat unexpected because previous reports proposed that PP2C.D1 inhibits cell elongation, although this was based on hypocotyl data (Spartz et al., 2014). Indeed, PP2C.D1 function to induce cell expansion in the hook is in contrast with the role of PP2C.D1 in the hypocotyl: while *mida9/pp2c.d1* mutants were slightly longer than WT, PP2C.D1 overexpressing plants display shorter hypocotyls (**Figure 5**; Spartz et al., 2014). These results suggest that PP2C.D1 inhibits cell elongation in the hypocotyl and are in accordance with previous studies in knockdown amiD2/5/7/8/9 seedlings of five other PP2C.D members (Spartz et al., 2014), and with a triple mutant deficient in PP2C.D2, D5, and D6 (Ren et al., 2018), which showed long hypocotyl phenotype and increased cell expansion compared to WT seedlings. Considering these observations, it was concluded that these PP2C.Ds are negative regulators of hypocotyl cell expansion. A described mechanism involves interaction of PP2C.D1 with plasma membrane H+-ATPases to regulate cell hypocotyl expansion (Spartz et al., 2014; Ren et al., 2018), in a process where the auxin-induced SAURs (Small Auxin-Upregulated RNA) interact with PP2C.Ds proteins to inhibit PP2C activity, and allow activity of the H+-ATPase to promote cell expansion. These data, together with our new findings, indicate that MIDA9/PP2C.D1 might play different roles in different organs which could involve interaction with different partners.

A recent study defined localization patterns of PP2C.D1 in nuclei and cytoplasm similar to our results (Ren et al., 2018).

However, this study reported stronger localization of PP2C.D1 only in the inner side of the hook, in contrast to our findings (**Figure 3D**). Intrigued by this, we compared the PP2C.D1 promoter used in each construct. Significantly, Ren et al. (2018) used 4.4 kb upstream of the transcriptional start site (TSS) of PP2C.D1, whereas here we used a shorter promoter of 2 kb. This suggests that the region between 2 and 4.4 kb upstream of the TSS might contain regulatory elements required for the asymmetric expression in the hook. Interestingly, our results suggest that PP2C.D1 function does not seem to require asymmetric localization, as PP2C.D1-YFP can complement the hook formation phenotype of *pp2c.d1* (**Figure 3C**). A possible alternative explanation is asymmetrical distribution of a necessary partner. Further analyses will be necessary to determine how PP2C.D1 localization is correlated with its function.

A Connection Between MIDA9/PP2C.D1 and Ethylene Physiology in Etiolated Seedlings

It has been described that hook formation takes place by asymmetric growth of the top part of the hypocotyl as a result of inhibition of cell expansion at the inner side of the hook coinciding with a local maxima of the auxin gradient (Silk and Erikson, 1979; Raz and Koornneef, 2001). However, our results showing that *pp2c.d1* has impaired cell elongation in the outer cells of the hook (**Figure 2**) suggest that cell elongation in the outer side is also highly regulated, and that this process requires PP2C.D1. Interestingly, the recent results showing asymmetric accumulation of PP2C.D1 in the hook (Ren et al., 2018) are reminiscent of the asymmetric accumulation of auxin during hook formation, suggesting that PP2C.D1 might be involved in the hormonal regulation of this process. In fact, several PP2Cs have been long-known to be related to hormone responses. The first PP2C in plants was identified as a mutation that gave rise to an ABA-insensitive phenotype of the mutant *abi1* (ABA insensitive 1; Meyer et al., 1994). Moreover, the homologous of ABI1, ABI2 (ABA insensitive 2), was also found to mediate the full range of ABA responses (Rodriguez et al., 1998). These results were the first evidence that PP2C proteins are connected with phytohormones to mediate stress signaling responses. Furthermore, one member of clade F (*PIA1*) also appears to be involved in hormone-mediated responses, by regulating the accumulation of stress hormones such as ethylene and salicylic acid (Widjaja et al., 2010).

Our finding that overexpressing PP2C.D1-GFP lines have altered expression of genes involved in ethylene biosynthesis (*ACS*) in etiolated seedlings suggest that PP2C.D1 might regulate hook formation through affecting ethylene accumulation. Different studies have demonstrated that ethylene is involved in the regulation of hook development, with a role during the formation and maintenance phase of hook development through the induction of auxin biosynthesis and regulating its transport and signaling in the apical hook (Raz and Koornneef, 2001; Mazzella et al., 2014). In fact, dark-grown seedlings treated with the ethylene biosynthesis precursor ACC exhibit an exaggerated apical hook, which is one of the components of the classical triple response together with shortening and thickening of both the hypocotyl and root and a proliferation of root hairs. Interestingly, whereas the levels of overexpression of PP2C.D1 in PP2C.D1-GFP were enough to induce a short hypocotyl, they did not promote exaggerated apical hook, suggesting that necessary partners for PP2C.D1 function in hook formation might be limitant, or that the levels of PP2C.D1 in our overexpressing lines were not enough to elicit a hook phenotype. In favor of these latter possibility, a recent paper by Wang et al. (2020) reports PP2C.D1 overexpressor lines that have a more closed apical hook in the dark. Although our data do not allow us to conclude that PP2C.D1 function in hook formation involves regulation of ethylene biosynthesis, our results suggest a possible connection between PP2C.D1 activity and ethylene physiology that has not been previously recognized. This connection does not seem to involve ethylene signaling, as ACC treatment promoted an exaggerated hook in all our mutant lines. Further experiments should be performed to elucidate the nature of the connection between PP2C.D1 and ethylene.

Hierarchical Role of PP2C.Ds in the Different Stages of Hook Development

Our temporal analysis of single, double, and triple mutants of the PP2C.D family suggest that they participate in a hierarchical and complex manner during hook development. We defined that PP2C.D1 has a predominant role in promoting hook formation and maintenance, while PP2C.D2 showed a negligible role during hook formation but contributes to maintenance similarly to PP2C.D1, and PP2C.D5 acts in the aperture phase to prevent early hook opening in combination with PP2C.D1 and PP2C.D2. Some of these functions became more apparent in high order mutants, suggesting a degree of redundancy among PP2C.D members in the regulation of hook development. Redundancy in hook development has been also shown in the triple mutant *pp2c-d2/d5/d6*, although authors did not explore in the distinct hook development phases (Ren et al., 2018).

The temporal sequential role of PP2C.D1, PP2C.D2, and PP2C.D5 in hook development and the dominant function of PP2C.D1 might be determined by differential abundance, location pattern, and/or activity of these members along the process. It is also possible that the different stages require a different protein accumulation threshold. Ren et al. (2018) examined the expression patterns of *PP2C.D* genes by using *pPP2C.D-GUS* reporter fusions in 3-day-old etiolated seedlings, and found that, whereas PP2C.D1 is almost exclusively expressed in the hook area, PP2C.D2 and PP2C.D5 are distributed more broadly and display high levels in the hypocotyl and low levels in the hook area. This pattern suggests that the dominant function of PP2C.D1 during hook development compared to other PP2C.Ds might be due to its prominent expression in the hook region among the PP2C.D family. Analyses of the accumulation kinetics of PP2C.D1, PP2C.D2, and PP2C.D5 during the different phases of hook development would be necessary to assess whether their temporal accumulation pattern correlate with their sequential function.

DATA AVAILABILITY STATEMENT

The original contributions presented in the study are included in the article/**Supplementary Material**, further inquiries can be directed to the corresponding author.

AUTHOR CONTRIBUTIONS

All authors contributed to design the work. AR and MS acquired and analyzed data. AR, PL, and EM wrote the manuscript. All authors contributed to the article and approved the submitted version.

FUNDING

This work was supported by a "Comissionat per a Universitats i Recerca del Departament d'Innovació, Universitats i Empresa" fellowship of the Generalitat de Catalunya (Beatriu de Pino's program) and Marie Curie IRG PIRG06-GA-2009-256420 grant to PL, by grants from FEDER/Ministerio de Ciencia, Innovación y Universidades – Agencia Estatal de Investigación (project references BIO2009-07675, BIO2015-68460-P, and PGC2018-099987-B-I00) and from the CERCA Programme/ Generalitat de Catalunya (project references 2009-SGR-206 and 2017SGR-718) to EM. MS was recipient of a travel fellowship from the "Comissionat per a Universitats i Recerca del Departament d'Innovacio, Universitats i Empresa" of the Generalitat de Catalunya. We acknowledge financial support from the Spanish Ministry of Economy and Competitiveness, through the "Severo Ochoa Programme for Centres of Excellence in R&D" 2016–2019 (SEV-2015-0533) and support of the publication fee by the CSIC Open Access Publication Support Initiative through its Unit of Information Resources for Research (URICI).

ACKNOWLEDGMENTS

We thank Martí Bernardo-Faura (Molecular Data Analysis Area, CRAG) for his support with the statistical analysis in **Figure 5C**.

SUPPLEMENTARY MATERIAL

The Supplementary Material for this article can be found online at: https://www.frontiersin.org/articles/10.3389/fpls.2021.636098/full#supplementary-material

REFERENCES

Al-Sady, B., Ni, W., Kircher, S., Schäfer, E., and Quail, P. H. (2006). Photoactivated phytochrome induces rapid PIF3 phosphorylation prior to proteasome-mediated degradation. *Mol. Cell* 23, 439–446. doi: 10.1016/j.molcel.2006.06.011

Alabadí, D., Gil, J., Blázquez, M. A., and García-Martínez, J. L. (2004). Gibberellins repress photomorphogenesis in darkness. *Plant Physiol.* 134, 1050–1057. doi: 10.1104/pp.103.035451

Alonso, J. M., Stepanova, A. N., Leisse, T. J., Kim, C. J., Chen, H., Shinn, P., et al. (2003). Genome-wide insertional mutagenesis of *Arabidopsis thaliana*. *Science* 301, 653–657. doi: 10.1126/science.1086391

An, F., Zhang, X., Zhu, Z., Ji, Y., He, W., Jiang, Z., et al. (2012). Coordinated regulation of apical hook development by gibberellins and ethylene in etiolated Arabidopsis seedlings. *Cell Res.* 22, 915–927. doi: 10.1038/cr.2012.29

Beyer, E. M. (1976). A potent inhibitor of ethylene action in plants. *Plant Physiol.* 58, 268–271. doi: 10.1104/pp.58.3.268

Chang, S. -H., Lu, L. -S., Wang, N. N., and Charng, Y. (2008). Negative feedback regulation of system-1 ethylene production by the tomato 1-aminocyclopropane-1-carboxylate synthase 6 gene promoter. *Plant Sci.* 175, 149–160. doi: 10.1016/j.plantsci.2007.11.004

Gallego-Bartolomé, J., Arana, M. V., Vandenbussche, F., Zádníková, P., Minguet, E. G., Guardiola, V., et al. (2011). Hierarchy of hormone action controlling apical hook development in Arabidopsis. *Plant J.* 67, 622–634. doi: 10.1111/j.1365-313X.2011.04621.x

Gommers, C. M. M., and Monte, E. (2018). Seedling establishment: a dimmer switch-regulated process between dark and light Signaling. *Plant Physiol.* 176, 1061–1074. doi: 10.1104/pp.17.01460

Gommers, C. M. M., Ruiz-Sola, M. Á., Ayats, A., Pereira, L., Pujol, M., and Monte, E. (2020). GENOMES UNCOUPLED1-independent retrograde signaling targets the ethylene pathway to repress photomorphogenesis. *Plant Physiol.* kiaa015. doi: 10.1093/plphys/kiaa015

Guzmán, P., and Ecker, J. R. (1990). Exploiting the triple response of Arabidopsis to identify ethylene-related mutants. *Plant Cell* 2, 513–523. doi: 10.1105/tpc.2.6.513

Khanna, R., Shen, Y., Marion, C. M., Tsuchisaka, A., Theologis, A., Schäfer, E., et al. (2007). The basic helix-loop-helix transcription factor PIF5 acts on ethylene biosynthesis and phytochrome signaling by distinct mechanisms. *Plant Cell* 19, 3915–3929. doi: 10.1105/tpc.107.051508

Leivar, P., and Monte, E. (2014). PIFs: systems integrators in plant development. *Plant Cell* 26, 56–78. doi: 10.1105/tpc.113.120857

Leivar, P., Monte, E., Al-Sady, B., Carle, C., Storer, A., Alonso, J. M., et al. (2008a). The Arabidopsis phytochrome-interacting factor PIF7, together with PIF3 and PIF4, regulates responses to prolonged red light by modulating phyB levels. *Plant Cell* 20, 337–352. doi: 10.1105/tpc.107.052142

Leivar, P., Monte, E., Oka, Y., Liu, T., Carle, C., Castillon, A., et al. (2008b). Multiple phytochrome-interacting bHLH transcription factors repress premature seedling photomorphogenesis in darkness. *Curr. Biol.* 18, 1815–1823. doi: 10.1016/j.cub.2008.10.058

Leivar, P., Tepperman, J. M., Monte, E., Calderon, R. H., Liu, T. L., and Quail, P. H. (2009). Definition of early transcriptional circuitry involved in light-induced reversal of PIF-imposed repression of photomorphogenesis in young Arabidopsis seedlings. *Plant Cell* 21, 3535–3553. doi: 10.1105/tpc.109.070672

Liscum, E., and Hangarter, R. P. (1993). Light-stimulated apical hook opening in wild-type *Arabidopsis thaliana* seedlings. *Plant Physiol.* 101, 567–572. doi: 10.1104/pp.101.2.567

Ma, D., Li, X., Guo, Y., Chu, J., Fang, S., Yan, C., et al. (2016). Cryptochrome 1 interacts with PIF4 to regulate high temperature-mediated hypocotyl elongation in response to blue light. *Proc. Natl. Acad. Sci. U. S. A.* 113, 224–229. doi: 10.1073/pnas.1511437113

Martín, G., Rovira, A., Veciana, N., Soy, J., Toledo-Ortiz, G., Gommers, C. M. M., et al. (2018). Circadian waves of transcriptional repression shape PIF-regulated photoperiod-responsive growth in Arabidopsis. *Curr. Biol.* 28, 311–318.e5. doi: 10.1016/j.cub.2017.12.021

Mazzella, M. A., Casal, J. J., Muschietti, J. P., and Fox, A. R. (2014). Hormonal networks involved in apical hook development in darkness and their response to light. *Front. Plant Sci.* 5:52. doi: 10.3389/fpls.2014.00052

Meyer, K., Leube, M. P., and Grill, E. (1994). A protein phosphatase 2C involved in ABA signal transduction in *Arabidopsis thaliana*. *Science* 264, 1452–1455. doi: 10.1126/science.8197457

Monte, E., Alonso, J. M., Ecker, J. R., Zhang, Y., Li, X., Young, J., et al. (2003). Isolation and characterization of phyC mutants in Arabidopsis reveals complex crosstalk between phytochrome signaling pathways. *Plant Cell* 15, 1962–1980. doi: 10.1105/tpc.012971

Monte, E., Tepperman, J. M., Al-Sady, B., Kaczorowski, K. A., Alonso, J. M., Ecker, J. R., et al. (2004). The phytochrome-interacting transcription factor,

PIF3, acts early, selectively, and positively in light-induced chloroplast development. *Proc. Natl. Acad. Sci. U.S.A.* 46, 16091–16098. doi: 10.1073/pnas.0407107101

Ni, W., Xu, S. L., González-Grandío, E., Chalkley, R. J., Huhmer, A. F. R., Burlingame, A. L., et al. (2017). PPKs mediate direct signal transfer from phytochrome photoreceptors to transcription factor PIF3. *Nat. Commun.* 8:15236. doi: 10.1038/ncomms15236

Pedmale, U. V., Huang, S. C., Zander, M., Cole, B. J., Hetzel, J., Ljung, K., et al. (2016). Cryptochromes interact directly with PIFs to control plant growth in limiting blue light. *Cell* 164, 233–245. doi: 10.1016/j.cell.2015.12.018

Ramoni, M. F., Sebastiani, P., and Kohane, I. S. (2002). Cluster analysis of gene expression dynamics. *Proc. Natl. Acad. Sci. U. S. A.* 99, 9121–9126. doi: 10.1073/pnas.132656399

Raz, V., and Koornneef, M. (2001). Cell division activity during apical hook development. *Plant Physiol.* 125, 219–226. doi: 10.1104/pp.125.1.219

Ren, H., Park, M. Y., Spartz, A. K., Wong, J. H., and Gray, W. M. (2018). A subset of plasma membrane-localized PP2C.D phosphatases negatively regulate SAUR-mediated cell expansion in Arabidopsis. *PLoS Genet.* 14:e1007455. doi: 10.1371/journal.pgen.1007455

Rodriguez, P. L., Benning, G., and Grill, E. (1998). ABI2, a second protein phosphatase 2C involved in abscisic acid signal transduction in Arabidopsis. *FEBS Lett.* 421, 185–190. doi: 10.1016/S0014-5793(97)01558-5

Schweighofer, A., Hirt, H., and Meskiene, I. (2004). Plant PP2C phosphatases: emerging functions in stress signaling. *Trends Plant Sci.* 9, 236–243. doi: 10.1016/j.tplants.2004.03.007

Sentandreu, M., Martín, G., González-Schain, N., Leivar, P., Soy, J., Tepperman, J. M., et al. (2011). Functional profiling identifies genes involved in organ-specific branches of the PIF3 regulatory network in Arabidopsis. *Plant Cell* 23, 3974–3991. doi: 10.1105/tpc.111.088161

Shin, J., Kim, K., Kang, H., Zulfugarov, I. S., Bae, G., Lee, C. H., et al. (2009). Phytochromes promote seedling light responses by inhibiting four negatively-acting phytochrome-interacting factors. *Proc. Natl. Acad. Sci. U. S. A.* 106, 7660–7665. doi: 10.1073/pnas.0812219106

Silk, W. K., and Erickson, R. O. (1979). Kinematics of plant growth. *J. Theor. Biol.* 76, 481–501. doi: 10.1016/0022-5193(79)90014-6

Spartz, A. K., Ren, H., Park, M. Y., Grandt, K. N., Lee, S. H., Murphy, A. S., et al. (2014). SAUR inhibition of PP2C-D phosphatases activates plasma membrane H^+-ATPases to promote cell expansion in Arabidopsis. *Plant Cell* 26, 2129–2142. doi: 10.1105/tpc.114.126037

Tsuchisaka, A., Yu, G., Jin, H., Alonso, J. M., Ecker, J. R., Zhang, X., et al. (2009). A combinatorial interplay among the 1-aminocyclopropane-1-carboxylate isoforms regulates ethylene biosynthesis in *Arabidopsis thaliana*. *Genetics* 183, 979–1003. doi: 10.1534/genetics.109.107102

Van Buskirk, E. K., Decker, P. V., and Chen, M. (2012). Photobodies in light signaling. *Plant Physiol.* 158, 52–60. doi: 10.1104/pp.111.186411

Vandenbussche, F., Petrásek, J., Zádníková, P., Hoyerová, K., Pesek, B., Raz, V., et al. (2010). The auxin influx carriers AUX1 and LAX3 are involved in auxin-ethylene interactions during apical hook development in *Arabidopsis thaliana* seedlings. *Development* 137, 597–606. doi: 10.1242/dev.040790

Vandenbussche, F., and Van Der Straeten, D. (2004). Shaping the shoot: a circuitry that integrates multiple signals. *Trends Plant Sci.* 9, 499–506. doi: 10.1016/j.tplants.2004.08.002

Vriezen, W. H., Achard, P., Harberd, N. P., and Van Der Straeten, D. (2004). Ethylene-mediated enhancement of apical hook formation in etiolated *Arabidopsis thaliana* seedlings is gibberellin dependent. *Plant J.* 37, 505–516. doi: 10.1046/j.1365-313X.2003.01975.x

Wang, J., Sun, N., Zhang, F., Yu, R., Chen, H., Deng, X. W., et al. (2020). SAUR17 and SAUR50 differentially regulate PP2C-D1 during apical hook development and cotyledon opening in Arabidopsis. *Plant Cell* 32, 3792–3811. doi: 10.1105/tpc.20.00283

Wei, N., Kwok, S. F., von Arnim, A. G., Lee, A., McNellis, T. W., Piekos, B., et al. (1994). Arabidopsis COP8, COP10, and COP11 genes are involved in repression of photomorphogenic development in darkness. *Plant Cell* 6, 629–643. doi: 10.1105/tpc.6.5.629

Widjaja, I., Lassowskat, I., Bethke, G., Eschen-Lippold, L., Long, H. H., Naumann, K., et al. (2010). A protein phosphatase 2C, responsive to the bacterial effector AvrRpm1 but not to the AvrB effector, regulates defense responses in Arabidopsis. *Plant J.* 61, 249–258. doi: 10.1111/j.1365-313X.2009.04047.x

Willige, B. C., Ogiso-Tanaka, E., Zourelidou, M., and Schwechheimer, C. (2012). WAG2 represses apical hook opening downstream from gibberellin and PHYTOCHROME INTERACTING FACTOR 5. *Development* 139, 4020–4028. doi: 10.1242/dev.081240

Wu, G., Cameron, J. N., Ljung, K., and Spalding, E. P. (2010). A role for ABCB19-mediated polar auxin transport in seedling photomorphogenesis mediated by cryptochrome 1 and phytochrome B. *Plant J.* 62, 179–191. doi: 10.1111/j.1365-313X.2010.04137.x

Yamagami, T., Tsuchisaka, A., Yamada, K., Haddon, W. F., Harden, L. A., and Theologis, A. (2003). Biochemical diversity among the 1-amino-cyclopropane-1-carboxylate synthase isozymes encoded by the Arabidopsis gene family. *J. Biol. Chem.* 278, 49102–49112. doi: 10.1074/jbc.M308297200

Zádníková, P., Petrásek, J., Marhavy, P., Raz, V., Vandenbussche, F., Ding, Z., et al. (2010). Role of PIN-mediated auxin efflux in apical hook development of *Arabidopsis thaliana*. *Development* 137, 607–617. doi: 10.1242/dev.041277

Conflict of Interest: The authors declare that the research was conducted in the absence of any commercial or financial relationships that could be construed as a potential conflict of interest.

frontiers in Plant Science

REVIEW
published: 15 March 2021
doi: 10.3389/fpls.2021.635619

Dark-Induced Barley Leaf Senescence – A Crop System for Studying Senescence and Autophagy Mechanisms

*Ewelina Paluch-Lubawa, Ewelina Stolarska and Ewa Sobieszczuk-Nowicka**

Department of Plant Physiology, Faculty of Biology, Adam Mickiewicz University in Poznań, Poznań, Poland

This review synthesizes knowledge on dark-induced barley, attached, leaf senescence (DILS) as a model and discusses the possibility of using this crop system for studying senescence and autophagy mechanisms. It addresses the recent progress made in our understanding of DILS. The following aspects are discussed: the importance of chloroplasts as early targets of DILS, the role of Rubisco as the largest repository of recoverable nitrogen in leaves senescing in darkness, morphological changes of these leaves other than those described for chloroplasts and metabolic modifications associated with them, DILS versus developmental leaf senescence transcriptomic differences, and finally the observation that in DILS autophagy participates in the circulation of cell components and acts as a quality control mechanism during senescence. Despite the progression of macroautophagy, the symptoms of degradation can be reversed. In the review, the question also arises how plant cells regulate stress-induced senescence via autophagy and how the function of autophagy switches between cell survival and cell death.

Keywords: autophagy, cell death, cell survival, developmental senescence, senescence model, sources and sinks communication, stress-induced senescence

OPEN ACCESS

Edited by:
Péter Poór,
University of Szeged, Hungary

Reviewed by:
Klaus Humbeck,
Martin Luther University of Halle-Wittenberg, Germany
Martina Spundova,
Palacký University, Czechia

****Correspondence:***
Ewa Sobieszczuk-Nowicka
evaanna@amu.edu.pl

Specialty section:
This article was submitted to Plant Physiology, a section of the journal Frontiers in Plant Science

Received: *30 November 2020*
Accepted: *23 February 2021*
Published: *15 March 2021*

Citation:
Paluch-Lubawa E, Stolarska E and Sobieszczuk-Nowicka E (2021) Dark-Induced Barley Leaf Senescence – A Crop System for Studying Senescence and Autophagy Mechanisms. Front. Plant Sci. 12:635619. doi: 10.3389/fpls.2021.635619

INTRODUCTION

In plants, senescence is a highly controlled and active process requiring global metabolic reprogramming, aimed at organized disintegration and remobilization of valuable resources (Himelblau and Amasino, 2001; Maillard et al., 2015). It is a fundamental aspect of plant development, necessary to optimize resource allocation and promote phenotypic plasticity to adapt to the environment under restricted conditions. Being photoautotrophic, plants rely mainly on their leaves to support their growth. Leaves are organs optimized for the use of light energy and the subsequent production of photosynthates while minimizing total anabolic cost. In terms of stress conditions, this can be beneficial to the plant if a leaf which is not photosynthetically productive undergoes senescence, thus making its resources available to other organs. Therefore, the induction of senescence must be strictly controlled to avoid unnecessary activation only under temporarily unfavorable conditions. In congruence with the importance of leaves in photosynthesis, light plays an essential role in regulating leaf senescence. For many species of plants, a lack of light in the form of strong shading or darkening of the leaves leads to rapid senescence, especially when only parts of the plant are affected (reviewed in Liebsch and Keech, 2016).

Dark-induced senescence has been used experimentally as an easy way to study the progress of leaf senescence. However, detailed studies of gene expression patterns have revealed discrepancies between the dark-induced and developmentally controlled process (Becker and Apel, 1993; Lee et al., 2001; Buchanan-Wollaston et al., 2005; van der Graaff et al., 2006; Guo and Gan, 2012; Roberts et al., 2017). The relevance of investigations on dark-induced senescence has often been discussed, but shade is an important scenario for crop yields in dense canopies. Under field conditions, crops are likely to benefit from the lower leaves of the canopy undergoing senescence and thus re-mobilizing nutrients for use in the upper, photosynthetic parts of the plants. Dark-induced leaf senescence (DILS) results in a clear loss of chlorophyll, disassembly of cellular elements and a lack of photosynthetic activity, none of which can be distinguished from the age-dependent natural senescence (Buchanan-Wollaston et al., 2003, 2005). However, the lack of coordinated cell development within a single leaf introduces complexity in the leaf senescence study. Thus, induced senescence, which directs a synchronous process, like dark-induced senescence, has become relevant (Kleber-Janke and Krupinska, 1997; Gepstein et al., 2003; Lin and Wu, 2004; Feller et al., 2008; Christiansen and Gregersen, 2014; Sobieszczuk-Nowicka et al., 2015, 2016; Law et al., 2018). It also eliminates misleading factors that coincide with developmental senescence, such as bolting or flowering (Gregersen et al., 2008). Widely used experimental setups to study dark-induced senescence in barley are (i) detached leaf in darkness (e.g., Becker and Apel, 1993; Legocka and Zajchert, 1999; Chrost and Krupinska, 2000; Rosiak-Figielek and Jackowski, 2000; Chrost et al., 2004; Żelisko and Jackowski, 2004; Conrad et al., 2007; Sobieszczuk-Nowicka et al., 2009, 2015; Kucharewicz et al., 2017; Janečková et al., 2019) (ii) whole plant in darkness (e.g., Kleber-Janke and Krupinska, 1997; Krause et al., 1998; Roulin et al., 2002; Simova-Stoilova et al., 2002; Arnao and Hernández-Ruiz, 2009; Jajić et al., 2014; Avila-Ospina et al., 2015; Zmienko et al., 2015; Sobieszczuk-Nowicka et al., 2016, 2018), and (iii) individually darkened attached leaf, whilst the rest of the plant remained in a normal photoperiod condition (e.g., Rolny et al., 2011; Shi et al., 2012; Christiansen et al., 2016). As the course of the senescence process is related to plant species, plant developmental stage, and plant environmental conditions these treatments cannot be considered the same. However, darkness induces some series of transformations at the cytological, biochemical and molecular levels common within these setups. These features are summarized in **Table 1** and are discussed in the context of the transformations that occur in the DILS program (Sobieszczuk-Nowicka et al., 2018). DILS program setup are barley seedlings grown in growth chamber for 7 days under controlled conditions (day/night 16/8 h, 23°C, light intensity 150 μmol m^{-2} s^{-1}, 60% humidity). Pots with seedlings on seventh day of growth are transferred to dark conditions to initiate senescence.

The genome resources available for *Arabidopsis* have made it a very attractive model of identification and functional analysis of genes regulated by senescence (Buchanan-Wollaston et al., 2003, 2005; Breeze et al., 2011). However, in many plants, such as barley, the removal of developing flowers and pods significantly extends the life of their leaves, while in *Arabidopsis*, male-sterile mutants or plants from which developing bolts have been removed do not extend the life of leaves. Because of these differences, cereal leaves must be used as an equivalent to the *Arabidopsis* model for leaf senescence studies in cereal (*Zea mays* – Smart et al., 1995; *Oryza sativa* – Lee et al., 2001; *Triticum aestivum* – Uauy et al., 2006; and *Hordeum vulgare* – Kleber-Janke and Krupinska, 1997; Jukanti et al., 2008; Christiansen and Gregersen, 2014; Avila-Ospina et al., 2015; Springer et al., 2015; Wehner et al., 2015; Sobieszczuk-Nowicka et al., 2018). Clear differences in the senescence program of *Arabidopsis* compared to monocotyledonous plants were found. The senescence in cereals is generally regulated at the single leaf level. Nutrients from older leaves are remobilized for younger leaves and ultimately for the flag leaf, thus contributing to the nutrients necessary for the development of the grain. Cereal leaves have a meristem base, the leaf tip consists of older cells, and younger ones are concentrated at the base of the leaf. This cell organization makes it easier to differentiate the progression of senescence (Gregersen et al., 2008).

Understanding both dark- and shade-induced senescence is of great economic importance as it can significantly shorten the shelf life after harvest and lead to significant crop losses (Gan and Amasino, 1997; Nam, 1997; Buchanan-Wollaston et al., 2003; Liu et al., 2015; Schippers et al., 2015). Significant progress has been made in our understanding of leaf senescence and its basic regulation at the molecular level over the last decades. Furthermore, a theoretical model (senescence window concept) has emerged which explains how senescence competence is determined during leaf development and how internal and external factors are integrated with age to determine the duration of senescence (Jing et al., 2002). Also, much of the fundamental knowledge about senescence regulation has been tested in cultivated plant species for its potential use to improve productivity. This includes stay-green features (Thomas and Ougham, 2014) and pSAG12:IPT technology (Gan and Amasino, 1995). Further clarification of the senescence window concept and a change that gives plants competence for senescence will allow for more targeted strategies to manipulate senescence by focusing on the different phases of development. Many researchers have discovered that it is extremely difficult to try to separate senescence regulation paths from the stress response because the genetic program underlying senescence is largely in line with the plant defense program. Therefore, changing one senescence parameter can also reduce plant tolerance to stress. Integrative research is needed that not only focuses on the role of single genes in the onset of senescence but also examines the conditions under which manipulation of the senescence process is beneficial for crop yield and nutritional value (a concept reviewed in Schippers et al., 2015).

This review will address the studies that allow showing (i) the survival strategy behind dark-induced senescence in barley plant and (ii) dark-induced barley leaf senescence to be used as a model, referred to in the manuscript also as DILS program, to examine leaf senescence. The idea of a program as applied to living systems has been taken from computer science. The system is built in

TABLE 1 | Overview of the experimental setups of dark-induced barley leaf senescence assays employed through the different studies cited in this review, and comparison of assessed parameters against DILS (Sobieszczuk-Nowicka et al., 2018).

Reference[1]	Experimental setup[2]	Parameters[3]	Assessed parameter in:	
			Reference Paper	DILS[4]
Christiansen et al. (2016)	21-day-old, 2nd leaf, IDL, 3D	Chlorophyll	Decreased relative chlorophyll content	Decreased chlorophyll autofluorescence and chlorophyll content
Kleber-Janke and Krupinska (1997)	9-day-old, 1st leaf, WDP, 2D	Chlorophyll	Decreased chlorophyll content	Decreased chlorophyll autofluorescence and chlorophyll content
		Maximum quantum yield of PSII of the dark-adapted state (Fv/Fm)	Decreased Fv/Fm	Decreased Fv/Fm
		Rubisco	Reduced level of Rubisco large subunit transcript	Reduction in Rubisco large subunit transcript and protein levels
Krause et al. (1998)	9-day-old, 1st leaf, WDP, 2D	Rubisco	Reduced level of Rubisco large subunit transcript	Reduction in Rubisco large subunit transcript and protein levels
Lichtenthaler and Grumbach (1974)	6-day-old, 1st leaf + coleoptile, WDP, 4D	Chlorophyll	Decreased chlorophyll content	Decreased chlorophyll autofluorescence and chlorophyll content
		Thylakoid system	Degradation of thylakoids determined by the destruction of prenyl lipids	Degradation of thylakoids observed in leaf tissue ultrastructure
Peterson and Huffaker (1975)	7-day-old, 1st leaf, DET, 3D	Chlorophyll	Decreased chlorophyll content	Decreased chlorophyll autofluorescence and chlorophyll content
		Rubisco	Reduced level of Rubisco protein	Reduction in Rubisco large subunit transcript and protein levels
Roberts et al. (2017)	15-day-old, 3rd leaf, DET, 6D	Chlorophyll	Decreased relative chlorophyll content	Decreased chlorophyll autofluorescence and chlorophyll content
		Subtilases	Increased level of subtilases transcript	Decreased level of subtilases transcript
Rolny et al. (2011)	13-day-old, 1st leaf, DET, IDL, 8D	Chlorophyll	Decreased relative chlorophyll content	Decreased chlorophyll autofluorescence and chlorophyll content
Scharrenberg et al. (2003)	9-day-old, 1st leaf, WDP, 6D	Chlorophyll	Decreased relative chlorophyll content	Decreased chlorophyll autofluorescence and chlorophyll content
		Maximum quantum yield of PSII of the dark-adapted state (Fv/Fm)	Decreased Fv/Fm	Decreased Fv/Fm
		Level of cysteine protease transcript	Increased level of cysteine protease transcript	Increased level of cysteine protease transcript
Scheumann et al. (1999)	7-day-old, 1st leaf, DET, 8D	Chlorophyll	Decreased chlorophyll content	Decreased chlorophyll autofluoresence and chlorophyll content
Simova-Stoilova et al. (2002)	10-day-old, 1st leaf, WDP, 5D	Rubisco	Decreased level of Rubisco protein	Reduction in Rubisco large subunit transcript and protein levels
Spundova et al. (2003)	Plants in growth phase 1.2 according to Feekes (1941), 1st leaf, DET, 5D	Chlorophyll	Decreased chlorophyll content	Decreased chlorophyll autofluorescence and chlorophyll content
		Effective quantum yield of PSII electron transport (ΦPSII)	Decreased ΦPSII	Decreased ΦPSII
		Thylakoid system	Degradation of thylakoids observed in leaf tissue ultrastructure	Degradation of thylakoids observed in leaf tissue ultrastructure
		Number of plastoglobuli	Increased number of plastoglobules observed in leaf tissue ultrastructure	Increased number of plastoglobules observed in leaf tissue ultrastructure

(Continued)

TABLE 1 | Continued

Reference[1]	Experimental setup[2]	Parameters[3]	Assessed parameter in:	
Wood et al. (1998)	7-day-old, 2nd leaf, WDP, 5D	Single strand nucleases (SSN)	Increased SSN enzyme activity	Increased level of SSN transcript

[1] *Literature references to dark-induced barley leaf senescence as given in the main text.*
[2] *Experimental setups used in different studies of senescence analysis: age at which the leaf was investigated, type of dark induction (DET, detached leaf in darkness; EDP, whole plant in darkness; IDL, individually darkened attached leaf), the number of days in darkness (D) and days of light re-exposure (L).*
[3] *The parameters that were used in the study of DILS models (Sobieszczuk-Nowicka et al., 2018).*
[4] *Barley (Hordeum vulgare) seedlings were grown in growth chamber for 7 days under controlled conditions (day/night 16/8 h, 23°C, light intensity 150 μmol m^{-2} s^{-1}, 60% humidity). Thereafter plants in growth phase 11 according to BBCH scale (Lancashire et al., 1991), were transferred to darkness for 3/7/10D. For experiments that determined the optimal day(s) of darkness when the physiological recovery from senescence becomes irreversible, plants grew in sequence: 3D+2/5/7L, 7D+2/5/7L, and 10D+2/5/7L.*

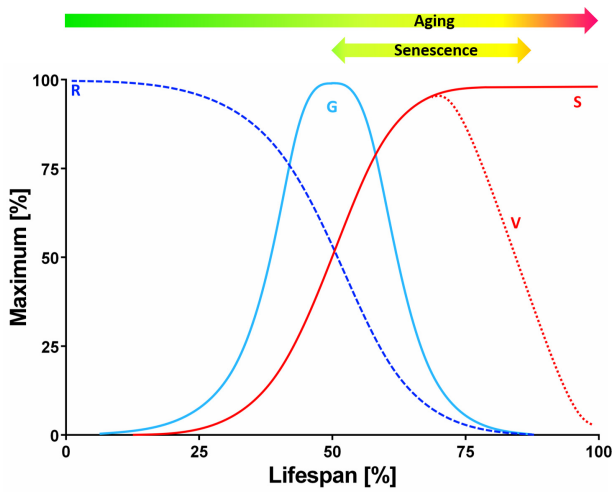

FIGURE 1 | Theoretical curves of plant growth and viability. The pattern of cell mass, tissue, organ, whole plant or population growth in size (S) follows a typical sigmoidal curve. The instantaneous growth rate (G) is maximal at the point of breakdown of the S curve, whereas the relative growth rate (R = G/S) slopes down systematically over time. The viability of the plant (V) starts to decline gradually after the peak of G. The decreasing V is antagonistic to senescence. It should be noted that aging refers, in this context, to transition in time (not deterioration) and it comprises the period of senescence and the final phase of declining V (but it is not limited or defined by these) (modified from Thomas, 2013).

a particular way, and so, always starts and fails in more or less the same manner.

We present transcriptomic, cytological, and physiological data that reveal events in barley DILS program, differences from developmental senescence, the time limit for dark-to-light transition for reversal of the senescence process, and progression of senescence through autophagy into the PCD phase.

Senescence, aging, and death are topics that notoriously attract semantic disputes. The review, will begin with a brief discussion about the terminology used here. Growth in size (S) of a cell mass, tissue, organ, whole plant or population follows a typical sigmoid pattern (**Figure 1**). The instantaneous growth rate (G) is maximal at the point of breakdown of the S curve. The relative growth rate (R = G/S) decreases gradually over time. The declining life span (V) is antagonistic to senescence. Aging refers to changes (not deterioration) over time and includes, but is not limited to or defined by, the senescence period and the final phase of V decline. Senescence thus generally refers to the process or condition of growing old (from the Latin *senescere*, to grow old). Senescence, according to the current physiological understanding, is the developmental phase that: (i) constitutes an episode of transient differentiation at the termination of growth; (ii) may or may not be succeeded by death; and (iii) is completely dependent on cell viability and specific gene expression (Thomas, 2013).

PROCESSES IN CHLOROPLASTS ARE EARLY TARGETS OF DARK-INDUCED BARLEY LEAF SENESCENCE

The first symptoms of leaf senescence are chloroplast degeneration (Dodge, 1970; Gepstein et al., 2003; Lim et al., 2007) and the decline in photosynthesis associated with it (Krieger-Liszkay et al., 2019). The earliest effects of DILS are visible in the chloroplast ultrastructure within the first 72 h of the plant's stay in the dark. During DILS program leaf yellowing is observed, and is further identified as a result of chlorophyll (Chl) degradation, which is associated with a decrease in its autofluorescence (Sobieszczuk-Nowicka et al., 2018). Also the works of, Lichtenthaler and Grumbach (1974), Peterson and Huffaker (1975), Rolny et al. (2011), Kleber-Janke and Krupinska (1997), Scheumann et al. (1999), Scharrenberg et al. (2003), Spundova et al. (2003), and Roberts et al. (2017) on barley showed a significant decrease in chlorophyll in the early stages of dark-induced barley leaf senescence. The loss of Chl indicates the remobilization of nitrogen compounds and is accompanied by an increase in flavonoids (Flv). Most likely, this is due to the fact that, in the absence of nitrogen, excess carbon is used to synthesize polyphenols, which include Flv (Cartelat et al., 2005). Cytological studies on barley chloroplasts senescing in dark show a gradual degradation of the thylakoid system, an increase in the size and number of plastoglobuli, and, as a result, the breakdown of chloroplasts (Lichtenthaler and Grumbach, 1974; Spundova et al., 2003; Sobieszczuk-Nowicka et al., 2018). In parallel, in dark-induced senescing leaves of barley, changes in parameters determining photosynthetic quantum conversion are observed. The parameter of chlorophyll fluorescence decrease ratio (Rfd) called the vitality index ratio is dynamically falling in

the early stage of DILS model in barley, which is why it is considered a significant marker parameter for stress caused by darkness. The effective quantum yield of PSII electron transport (ΦPSII) is characterized by lesser sensitivity, decreasing less intensely than Rfd (Sobieszczuk-Nowicka et al., 2018). Both Rfd and ΦPSII are referred to as net CO_2 assimilation rates (Fracheboud and Leipner, 2003; Baker and Oxborough, 2004; Lichtenthaler et al., 2005; Wong et al., 2014). The remaining parameters slightly decreased during DILS model: maximum quantum yield of PSII of the dark-adapted state (Fv/Fm), maximum quantum yield of PSII in the light-adapted state (Fv′/Fm′), and photochemical quenching of Chl fluorescence (qP). All parameters of the values listed above showed a decrease only in the advanced stage of DILS (Sobieszczuk-Nowicka et al., 2018). A decrease in the Fv/Fm and ΦPSII parameters during senescence was also demonstrated in other studies on dark induced leaf senescence of barley (Kleber-Janke and Krupinska, 1997; Scharrenberg et al., 2003; Spundova et al., 2003).

van Doorn and Yoshimoto (2010) stated that the terminal, senescing stage of a plant cell may be reversed if the functions of the chloroplasts can be restored. To assess the limits of the ability of senescence reversal for the DILS model, it was measured the photosynthetic quantum conversion parameters and nitrogen status in barley leaves subjected to light re-exposure after various periods of dark incubation. During this process of re-exposure to light, it was observed that the parameters such as Fv/Fm, Fv′/Fm′, qP, Chl. Flv and NBI that had gradually decreased during DILS program began to recover. The Rfd and ΦPSII parameters were also restored, although with a delay. This reversal occurred in samples exposed to darkness until, but not beyond, day 7, with dark incubation lasting longer than day 7, causing an irreversible decline in all the measured parameters (Sobieszczuk-Nowicka et al., 2018). Also for each analyzed indicator, a 2-day period of light re-exposure does not suffice to return the level to that of the light control. This suggests that, in spite of the high potential of chloroplasts to restore the photochemical efficacy of solar energy conversion, the energy conversion of excitation and/or the use of potential energy, coupled with the transport of electrons, may be restricted by some unidentified factor whose reversibility is compromised.

RUBISCO IS THE LARGEST REPOSITORY OF RECOVERABLE NITROGEN IN BARLEY LEAF SENESCING IN DARKNESS

Mature leaves are the place of carbon (C) assimilation in the process of photosynthesis. The leaves are the sources, which means that the metabolism precursors are exported from them where they are needed: to the sinks, such as developing seeds (Lim et al., 2007; Thomas, 2013; Law et al., 2018). Sources and sinks communicate using the vascular system. At the beginning, young, expanding leaves are developing as sinks, but when they fully develop, they become sources. Leaves mainly export C obtained from photosynthesis, but when the leaves begin to grow old and cease to photosynthesize, they become sources of nitrogen (N) derived from the decomposition of leaf tissue proteins. The beginning of leaf senescence can be considered the moment of transition: from the assimilation of nutrients, to their remobilization. In other words, it is the point where leaves cease to be the sources of C, and become the sources of N (Masclaux et al., 2000; Thomas, 2013; Law et al., 2018). Therefore, leaves are, on the one hand, the location of C assimilation, and on the other, the N storage place. Behind this leaf bifunctionality is the main chloroplast protein, ribulose-1,5-bisphosphate carboxylase/oxygenase – Rubisco (Thomas, 2013). Rubisco is a photosynthetic enzyme that binds C from CO_2 and is also a reserve of mobilizable N as Rubisco proteins contain up to 35% of total leaf nitrogen and up to 70% of chloroplasts' nitrogen (Hörtensteiner and Feller, 2002; Krieger-Liszkay et al., 2019). Storage proteins, including Rubisco, are characterized by either a very low level, or no simultaneous protein synthesis and decomposition. When the leaves are young and growing, there is a very high level of Rubisco synthesis, and only once the synthesis stops does the protein breakdown begin (Thomas, 2013). In general, Rubisco degrades rapidly during any type of senescence (Hörtensteiner and Feller, 2002; Lan and Miao, 2019). In dark-induced senescence of barely leaves, this was confirmed by Peterson and Huffaker (1975), Simova-Stoilova et al. (2002), and Roberts et al. (2017). The level of Rubisco protein, drop significantly throughout DILS model (Sobieszczuk-Nowicka et al., 2018). This decrease was correlated with the level of expression of Rubisco large subunit gene, which decreased significantly during early phase of the process (Sobieszczuk-Nowicka et al., 2018). Also Krause et al. (1998) and Kleber-Janke and Krupinska (1997) has reported that the transcript levels of small and large subunits of Rubisco were significantly decreased during the dark-induced senescence of the barley leaves.

In contrast, the second marker protein for chloroplasts' biochemistry – PSII reaction center D1 protein photosystems (Mattoo et al., 1989) – is quite stable and only slightly decreases in the late phase of DILS (Sobieszczuk-Nowicka et al., 2018). It might be due to the fact that the system complexes are active up to point of no return. Interestingly, the level of *PSBA* genes encoding D1 protein dropped in the early phase of DILS program. The difference between the decline in D1 protein and its transcript seems to stem from the fact that the D1 protein is under posttranscriptional control (Sobieszczuk-Nowicka et al., 2018). These differences in the degradation rate of the two chloroplast marker proteins, Rubisco and D1, in the early stage of DILS could be part of the stress adaptation strategy, as a result of which the degradation of the highly important ATP synthesis machinery in dark-induced senescence is delayed (Krupinska et al., 2012). This sequence of events is supported by the remaining microarray results of barley DILS program, which show a high level of ATP-dependent metabolism of amino acids, fatty acids, hormones and pigments, and active complexes of photosystems up to the time when

senescing in darkness leaves entering the point of no return (Sobieszczuk-Nowicka et al., 2018).

MORPHOLOGICAL CHANGES OF BARLEY LEAVES SENESCING IN DARKNESS OTHER THAN THOSE DESCRIBED FOR CHLOROPLASTS AND METABOLIC MODIFICATIONS ASSOCIATED WITH THEM

In plant cells during dark-induced senescence chromatin condensation and nuclear fragmentation occur. At the beginning of senescence, the ultrastructure of the nucleus does not differ significantly from mature leaves. The condensation of chromatin typically starts at the periphery of the nucleus and moves inward (Sakamoto and Takami, 2014; Liu et al., 2017). During the early stages of DILS, the ultrastructure of the nucleus of barley does not differ from mature leaves. However, with the progression of senescence the shape and structure of the nucleus becomes more irregular. These changes are accompanied by DNA fragmentation (Sobieszczuk-Nowicka et al., 2018). Similar results were also reported for *Phaseolus vulgaris* (Lambert et al., 2017) and *Petroselinum crispum* (Canetti et al., 2002). The nuclear breakdown is accompanied by the release of nucleases and proteases, acidification of the cytoplasm, and rapid degradation of nucleic acids and proteins (Obara et al., 2001; Kuriyama and Fukuda, 2002), which can be a source of carbon and nitrogen. The Bnuc1 gene that encodes a BNUC1 endonuclease is generally associated with senescence (Sakamoto and Takami, 2014) and is a marker of DNA degradation of DILS. DILS program is associated with very high induction of Bnuc1 gene expression (Sobieszczuk-Nowicka et al., 2018). Wood et al. (1998) demonstrated in dark incubated barley an increase in activity of single strand preferring nuclease (SSN), which also is overexpressed in later stage of DILS.

In addition to changes in nucleus organization, changes in the tonoplast's topology occur during dark-induced senescence. At the start of senescence, invagination of the tonoplast and cytoplasmic fragments near the vacuole can be observed. Together with these, shrinking of the protoplast is notable. With the progression of DILS in barley leaf cells, gaps in the cell membrane appear and eventually the tonoplast ruptures (Sobieszczuk-Nowicka et al., 2018). This consequently leads to the release of lytic enzymes and degradation of the nucleus and mitochondria. Usually, the rupture of the tonoplast is the final step of senescence ending in PCD (Rogers, 2015).

Since chloroplasts are one of the first to be degraded, the senescing cells must rely on mitochondria to obtain energy (Keech et al., 2007). Keech et al. (2007) reported that the morphology and abundance of these organelles change during dark-induced senescence in leaves of *Arabidopsis thaliana*. Mitochondria then are less abundant and rounder or even almost spherical. The decrease in the number of mitochondria can also be observed in different ways in different parts of the leaf, i.e., mesophyll compared to epidermal cells. Interestingly, mitochondrial numbers in stomata are not affected by dark-induced senescence (Keech et al., 2007), which takes place in developmental senescence, as was shown for *Vitis vinifera* (Ruberti et al., 2014). Also, during the final stages of the process, Keech et al. (2007) reported a cellular distribution of the organelle changes. Mitochondria clump together in loose aggregates in comparison to the relatively homogeneous distribution in control *Arabidopsis* plants (Keech et al., 2007). When the source of sugars is depleted in leaves kept in the dark, amino acids become a source of nutrients to sustain mitochondria respiration. Ammonium released in this way is assimilated by cytosolic glutamine synthetase 1 (GS1) isoforms and remobilized (Masclaux et al., 2000, 2001). The mitochondrial glutamate dehydrogenase that is known to catabolize glutamate to provide 2-oxoglutarate (2-OG) to the mitochondria is one of the catabolic enzymes releasing ammonium and 2-OG during DILS (Masclaux-Daubresse et al., 2006; Araujo et al., 2010; Kleessen et al., 2012). During DILS in barley one can also observe up-regulation of other enzymes responsible for remobilization of degraded nitrogen compounds such as cysteine and aspartyl proteases, ubiquitination enzymes, Hsp70, cytosolic Gln synthetase (Gln-1-3 isoform of low affinity to ammonia), and Orn cycle enzymes (P5C dehydrogenase, arginase, acetyl-Orn transaminase) (Sobieszczuk-Nowicka et al., 2018). Also during this specific time, lipid catabolism increases, which suggests that lipid degradation may participate in the production of energy, which in turn involves succinate synthesis within glyoxysomes and export thereafter to mitochondria (Sobieszczuk-Nowicka et al., 2018). Mitochondrial metabolism during DILS in barley is demonstrated to be important in relocation of recycled carbon and nitrogen substrates which come from proteins, lipids and other cellular components, since after crossing the point of no return the deterioration processes coupled with respiration intensify, which is observed by e.g., overexpression of genes involved in vesicle recycling (signalosome complex, SNARE complex or vesicle-fusing ATPase) (Sobieszczuk-Nowicka et al., 2018). Increased expression of key genes of gluconeogenesis and glycolysis along with upregulation of glyoxysomal enzymes are also supportive of recycling of substrates (Hollmann et al., 2014).

AUTOPHAGY AND SENESCENCE OCCUR SYNCHRONOUSLY IN DARK-INDUCED BARLEY LEAF SENESCENCE

During plant growth and development, damaged or aging cells' components undergo degrading processes inside vacuoles in a process called autophagy. Autophagy does not occur at a very high level under physiological conditions, and it is a housekeeping process during normal conditions, allowing the organism to adapt to changing environmental conditions and allowing its survival and prolonging its life span (Avila-Ospina et al., 2014; Borek et al., 2017; Stefaniak et al., 2020). The process of autophagy is phylogenetically conserved, involving intracellular degradation where cytoplasmic compounds are

broken down in the vacuole to supply basic components and energy to maintain essential functions. During autophagy also damaged cells and toxic compounds are utilized (van Doorn and Woltering, 2005; Janawad et al., 2012). As DILS is a process of transition from nutrient assimilation to nutrient remobilization (Buchanan-Wollaston et al., 2005), autophagy plays a key role in it. In plants, several types of autophagy can be distinguished, mainly microautophagy and macroautophagy (Bassham et al., 2006) as well as a third, plant-specific pathway, called megaautophagy (Floyd et al., 2015). Microautophagy consists of tonoplast invagination which results in engulfment of tonoplast and cytoplasmic components by intravacuolar vesicles and their uptake into the vacuole (Bassham et al., 2006; Sienko et al., 2020). Megaautophagy also leads to disintegration of cell contents using vacuolar enzymes, but the material is not taken up inside the vacuole. Instead, vacuolar hydrolases are released to the cytoplasm after permeabilization and disruption of the tonoplast (Hara-Nishimura et al., 2005; Bollhöner et al., 2012). In turn, macroautophagy begins with the appearance in the cytoplasm of an elongated vesicle (phagophore) composed of a single, bilayer lipid-protein membrane, which elongates and engulfs a fragment of the cytoplasm with cell organelles and/or protein complexes. The resultant autophagosome is then transported to the vacuole, where the cargo is hydrolyzed (Borek et al., 2015). Macroautophagy is responsible for maintaining standard function of the cell (Lamb et al., 2013). Hence, organized development of DILS requires effective recycling machinery which allows the correct development of a plant to be maintained. During dark-induced senescence, the increased degradation of macromolecules such as nucleic acids, proteins, and sugars, provides components for regulated recycling and reuse by other parts of the plant (Jing et al., 2003).

It was reported that Rubisco and its degradation products can be transported into vacuoles via Rubisco-containing bodies (RCBs) after darkness treatment (Chiba et al., 2003). Ishida et al. (2008) found that RCB targeting to the vacuole are autophagy-dependent. They also observed, using plants expressing both the GFP–ATG8 fusion marker specific for autophagosomes and autophagic bodies, and stroma-targeted RFP, co-localization of the two fluorescent markers within the vacuole (Ishida and Yoshimoto, 2008; Ishida et al., 2008).

In leaves senescing in darkness autophagy is apparent as small autophagic bodies in vacuoles, presence of autophagosomes in protoplasts and in the process of tonoplast rupturing. Also, a number of autophagy-related genes (ATGs) have been identified during dark-induced senescence, which are highly expressed during the progress of the process (Chung et al., 2009; Xia et al., 2012; Avila-Ospina et al., 2016; Sobieszczuk-Nowicka et al., 2018). In barley Sobieszczuk-Nowicka et al. (2018) showed that at the onset of DILS program the tonoplast membrane invaginates, small cytoplasmic fragments are near the vacuole and the cytoplasm shrinks, which indicates the involvement of microautophagy in the early stages of senescence. When DILS proceeds, leaf cells demonstrate cell membrane discontinuity, which indicates the processes of macroautophagy. However, even at this stage, the effects of DILS degradation processes have been shown to be reversible. In the final stages of DILS these processes are followed by megaautophagy, which is a rupture of the tonoplast and release of hydrolases. In consequence, organelles undergo progressive degradation and are localized in the center of the cell, and the intracellular compartmentation is lost due to the plasma membrane loosening. When megaautophagy occurs, the cell enters the "point of no return" after which degradation of the cell nucleus and mitochondria take place, and the cell proceeds into PCD, Sobieszczuk-Nowicka et al. (2018). **Figure 2** summarizes the described stages of senescence occurring in barley cells during darkness, taking into account the characteristic autophagy types: micro-, macro-, and mega-autophagy. Despite the progression of macroautophagy, the symptoms of degradation can be reversed, until megaautophagy occurs, showing a clear point of no return. Together with these changes a number of *ATGs* are upregulated as well as genes encoding vacuolar-processing enzymes (i.e., α*VPE* and *VPE2c*), whose expression increases with the progression of senescence. *VPE* genes are involved in ATG-independent alternative cell degradation pathways via senescence-associated vacuole formation. During dark-induced senescence a vital role is played by these 0.5–0.8 μm vacuoles (SAVs). SAVs have been identified in the senescent leaves of several plants, including soybean, *Arabidopsis*, and tobacco, but are absent in non-senescing leaves (Martinez et al., 2008a,b). There are soluble proteins (such as Rubisco) and resident proteases (such as senescence-specific *SAG12*) in the acid lumen of these vacuoles (Pascual et al., 1994; Otegui et al., 2005; Martinez et al., 2008a,b). In DILS relative to the expression of α*VPE* and *VPE2c*, that of the known senescence-activated marker gene Cys protease (*SAG12*) was minimally induced (Sobieszczuk-Nowicka et al., 2018).

Turnover of macromolecules via selective autophagy may contribute to cell homeostasis, nutrient recycling, and clearance of damaged structures during DILS. The fact that autophagy might be important in N mobilization in the course of developmental leaf senescence of barley has been proposed before (Hollmann et al., 2014). We do not know the mechanisms that condition the metabolic reprogramming that directs to or leads out leaf cells senescing in darkness from the PCD pathway, switching cells between survival and death. However, we know that cell death occurs by suppressing macroautophagy and triggering megaautophagy. It is possible that VPEs are mediators of the crosstalk between senescence-dependent autophagy and PCD (Patel et al., 2006; Floyd et al., 2015; Wang et al., 2018). Supporting the hypothesis that autophagy works to keep cells healthy, controlling the cell component turnover during dark-induced senescence, is the fact that plants with low autophagic activity, i.e., *Arabidopsis* mutants, are more susceptible to stress and exhibit premature senescence symptoms and cell death (Phillips et al., 2008). The efficiency of regulation of autophagic processes is a symptom of the vitality of senescing cells, which at each stage must hold the ability to maintain homeostasis. Thus, we suggest that a critical step that determines the point of no return in DILS model is macroautophagy control.

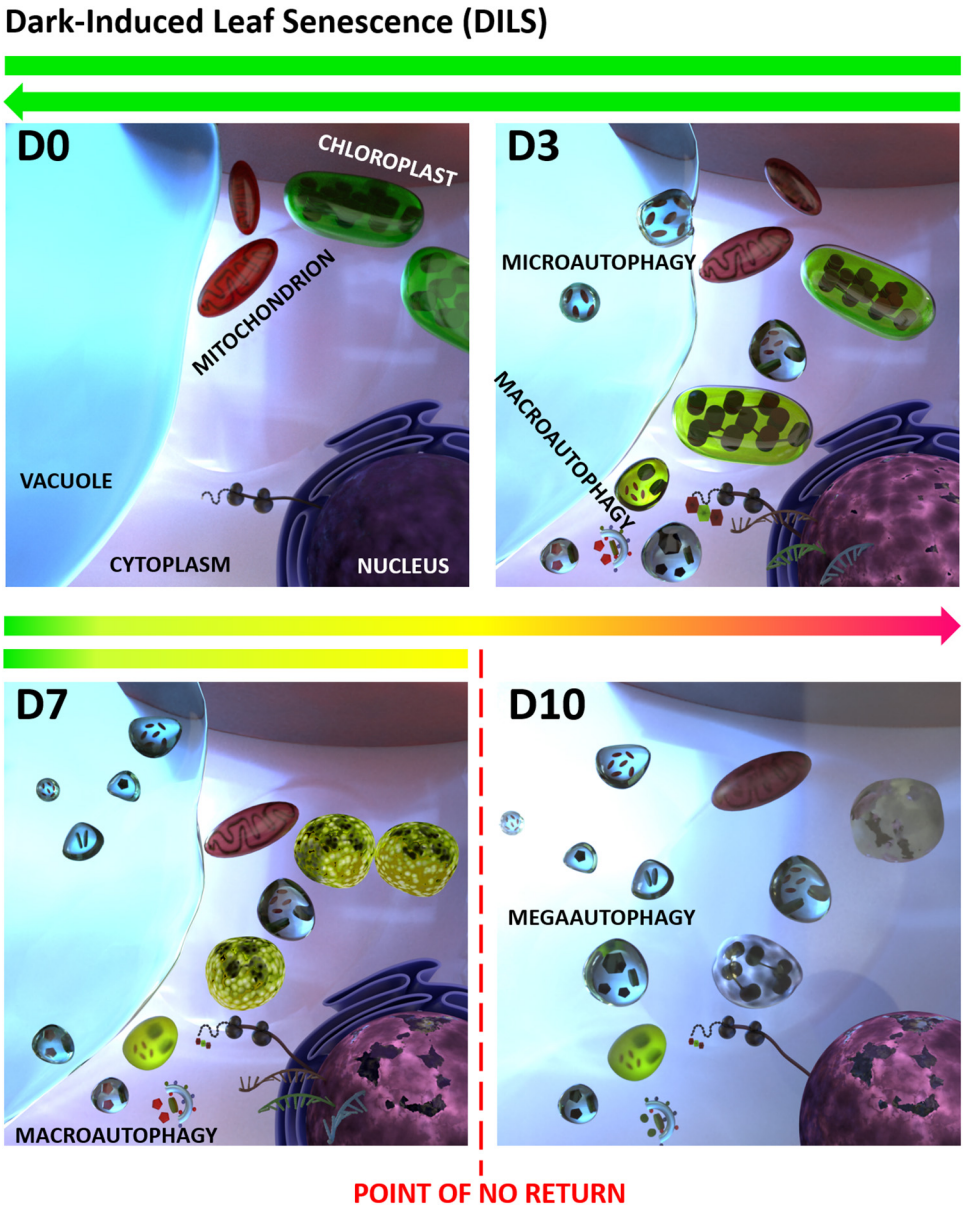

FIGURE 2 | Dark-induced leaf senescence (DILS) model vs. autophagy. D0 stands for control, D3 to D10 stand for days of senescence. A critical time limit was identified when it is possible to reverse the leaf senescence and prevent cell death. It was found that in DILS autophagy participates in the circulation of cell components and acts as a quality control mechanism during senescence. DILS is also a good model for studying the pathways of autophagy and programmed cell death. At each stage, DILS is accompanied by different types of autophagy: micro-, macro-, and mega-autophagy. Despite the progression of macroautophagy, the symptoms of degradation can be reversed. How the function of autophagy switches between cell survival and cell death is not known (modified from Sobieszczuk-Nowicka et al., 2018).

DARK-INDUCED BARLEY LEAF SENESCENCE VERSUS DEVELOPMENTAL BARLEY LEAF SENESCENCE; TRANSCRIPTOMIC STUDY

Large scale data analysis of barley DILS program using microarrays and re-analyzed data of Christiansen and Gregersen (2014) and Hollmann et al. (2014) of developmental leaf senescence showed that genes expressed during DILS and developmental senescence show quite some similarities (Sobieszczuk-Nowicka et al., 2018). Genes encoding glyoxysomal citrate synthase (Hollmann et al., 2014) and mitochondrial succinate dehydrogenase (Christiansen and Gregersen, 2014) are common for both types of senescence and are upregulated during that time (Christiansen and Gregersen, 2014; Sobieszczuk-Nowicka et al., 2018). The regulation of

these processes that allow for the organelles to gain energy seems to be necessary for the cell to replace the lack of ATP synthesis in chloroplasts for both dark-induced senescence and developmental senescence as the chloroplasts are dismantled at early stages of senescence, whereas mitochondria prevail until cell death (Peterson and Huffaker, 1975; Matile, 1992; Chrobok et al., 2016). Another resemblance is the downregulation of malate dehydrogenase, which is correlated with inhibition of glyceraldehyde-3-phosphate dehydrogenase in chloroplasts (Sobieszczuk-Nowicka et al., 2018). This enzyme functions as a fragment of the starch-degradation pathway that supports malate for other organelles in unstressed cells (Foyer et al., 2011). In both senescence models, low-affinity ammonia remobilization (by a cytosolic isoform of Gln synthetase 1 and Glu dehydrogenase) and Orn cycle transamination are also found to be activated (Sobieszczuk-Nowicka et al., 2018). Another similarity between DILS and developmental senescence of barley is common expression of some cysteine proteases (CPs). They are the most abundant enzymes associated with leaf senescence (Bhalerao et al., 2003; Parrott et al., 2010). Scharrenberg et al. (2003) have also reported that transcripts of CP *HvSF42* (HvPap-1) increase in both senescence scenarios in barley. What is more, these authors demonstrated, that in both dark-induced and developmental senescence an *NAC* transcription factor (HvSF6/HvNAC008) is up-regulated (Scharrenberg et al., 2003). *HvSF6* was observed to be induced by the cross talk of jasmonic acid and ethylene in senescing barley in both developmental and dark-induced senescence (Scharrenberg et al., 2003). This observation was later confirmed by Christiansen et al. (2011), who identified 48 NACs in barley. This suggests the participation of *NAC* transcription factors as regulators of a range of processes in plant development and stress responses, senescence being one of them.

On the other hand, the most notable differences in gene medleys between DILS and developmental senescence were observed for signaling pathways which are activated by plant hormones, lipid catabolism, low-affinity ammonia remobilization, carbohydrate metabolism and DNA and RNA methylation. The differences between DILS and developmental senescence in the activity of carbohydrate and lipid metabolism enzymes were proven by recording the increase in expression of glycolytic glyceraldehyde-3-phosphate dehydrogenase and enolase in the first process but not in the other, whereas during DLS β-amylase and trehalose-6-phosphate synthase are up-regulated (Sobieszczuk-Nowicka et al., 2018). Similar results were obtained in *Arabidopsis*, in which lipid catabolism genes are considerably more upregulated during dark-induced senescence than in developmental (Buchanan-Wollaston et al., 2005). This causes an increase in beta-oxidation due to depletion of carbohydrates. In barley DILS there was noted upregulation of gluconeogenesis, to which the by-product of this pathway, phosphoenolpyruvate, can be directed. The pivotal enzyme of this process, pyruvate phosphate dikinase, is downregulated during developmental senescence. This is consistent with an increase in expression of Suc synthase in DILS, which was decreased during developmental senescence (Sobieszczuk-Nowicka et al., 2018). A number of other crucial differences have also been revealed between these two processes. In DILS downregulation of C- and D-type phospholipase genes can be observed. Phospholipases are well-established enzymes taking part in both lipid catabolism and signaling pathways dependent on GTP, where they constrain the α-subunit of G-protein coupled receptors (Fukami, 2002; Jenkins and Frohman, 2005). Another process differing between DILS and developmental senescence is the gibberellin synthesis pathway, which is upregulated in the former but not in the latter. But then, signaling through jasmonic acid and auxin seems to be crucial for developmental senescence as the overexpression of 3-ketoacyl-CoA thiolase and auxin response factor 19 is observed during this process. On the other hand, in *A. thaliana* during dark-induced senescence, three cytosolic glutamine synthetase genes are not expressed, in contrast to developmental senescence (Buchanan-Wollaston et al., 2005). The mentioned enzymes have a pivotal role in N mobilization, which may imply that different pathways may operate during differentially triggered senescence. The upregulated genes also observed only in DILS in barley are ones encoding aminotransferases (Sobieszczuk-Nowicka et al., 2018). The release of branched-chain amino acids confirms this upregulation during dark incubation of *Arabidopsis* leaves, which counteracts the toxicity of free ammonia from amino acids with a high N:C ratio (Law et al., 2018). Interestingly, genes responsible for proteolysis are differentially expressed in DILS and developmental senescence. During DILS in barley, for example, ubiquitin-conjugated enzyme is down-regulated while during development this enzyme is overexpressed. Similarly, an opposite expression profile can be observed for a vacuolar-processing enzyme precursor (changes in *VPE* are discussed in more detail in the section on autophagy), which is overexpressed during DILS whereas in developmental senescence it is down-regulated (Sobieszczuk-Nowicka et al., 2018). Also some members of subtilases – a family of serine-rich proteases (SPs) – can be differentially expressed in barley depending on the type of senescence. Subtilases in DILS, denoted *HvSBT45*, compared to developmental senescence were down-regulated during late stages of DILS, while in developmental senescence their expression level rises (Christiansen and Gregersen, 2014; Sobieszczuk-Nowicka et al., 2018). Roberts et al. (2017) tested gene expression of eleven subtilases in barley plants subjected to developmental and dark-induced senescence. They demonstrated that two out of all tested enzymes (*HvSBT3* and *HvSBT6*) are up-regulated in both senescence conditions, while one differentiated developmental and dark-induced senescence. *HvSBT2* is only up-regulated during dark-induced senescence (Roberts et al., 2017). This shows that different subgroups of proteases take part in proteolysis, depending on the type of factor inducing senescence. Lastly, the RNA methylation index is higher in DILS than in developmental senescence, showing an increase in gene expression of for example RNA 2-O-methyltransferase fibrillarin two during DILS and inhibition during developmental senescence (Sobieszczuk-Nowicka et al., 2018; Ostrowska-Mazurek et al., 2020).

THE DARK-INDUCED LEAF SENESCENCE CROP MODEL AND ITS POINT OF NO RETURN – A SUMMARY

There has been developed a crop model that demonstrates and explains early and late events of DILS and identifies the time limit for dark to light transition for reversal of the induced-senescence process within a leaf – DILS. DILS in barley occurs in two phases. The first phase is more strongly emphasized by cessation of photosynthesis, loss of chlorophyll, and disintegration of chloroplasts. Disintegration of chloroplasts correlated with the degradation of Rubisco and PsbA-D1 proteins. Despite the advanced state of macroautophagy in this phase, the processes of degradation turned out to be reversible. The reversal of DILS program involves regaining photosynthesis and increase of chlorophyll content, and it takes place irrespectively of the activation of ATG genes. The second, terminal phase, occurring beyond day 7 of darkness, is characterized by irreversibility of senescence and its progression into PCD, exemplified by the involvement of both autophagy and PCD pathways, and involves disruption of the nucleus, mitochondria, chromatin condensation accompanied with nDNA fragmentation, shrinking of the protoplast, tonoplast interruption, and disintegration of the cell membrane.

Non-invasive methods for quantifying photosynthetic efficiency and barley leaf nitrogen status established the time frame during which DILS enters the irreversible phase. Rfd is determined there as the earliest parameter that correlated well with the cessation of photosynthesis, together with the appearance of micro-autophagy symptoms. DILS program is also found to be characterized by the upregulation of processes that enable the recycling of degraded metabolites in darkness, including increased NH_4^+ remobilization, gluconeogenesis, glycolysis, and partial upregulation of glyoxylate and tricarboxylate acid cycles.

AUTHOR CONTRIBUTIONS

ES-N conceived the topic of the manuscript. EP-L, ES, and ES-N wrote the manuscript. EP-L prepared the figures. ES was responsible for the layout of the manuscript and prepared the table. ES-N coordinated writing of the manuscript. All authors listed have made a substantial, direct and intellectual contribution to the work, and approved it for publication.

FUNDING

The publication was co-financed within the National Science Centre, Poland (Project Numbers 2018/29/B/NZ9/00734 and 2018/30/E/NZ9/00827 to ES-N and 2017/27/N/NZ9/02135 to EP-L).

ACKNOWLEDGMENTS

We thank Richard Ashcroft (bioscience editor) for the professional language editing of the manuscript. We thank Krzysztof Polcyn for preparing the graphics for **Figure 2**.

REFERENCES

Araujo, W. L., Ishizaki, K., Nunes-Nesi, A., Larson, T. R., Tohge, T., Krahnert, I., et al. (2010). Identification of the 2-hydroxyglutarate and isovaleryl-CoA dehydrogenases as alternative electron donors linking lysine catabolism to the electron transport chain of *Arabidopsis mitochondria*. *Plant Cell* 22, 1549–1563. doi: 10.1105/tpc.110.075630

Arnao, M. B., and Hernández-Ruiz, J. (2009). Protective effect of melatonin against chlorophyll degradation during the senescence of barley leaves. *J. Pineal Res.* 46, 58–63.

Avila-Ospina, L., Marmagne, A., Soulay, F., and Masclaux-Daubresse, C. (2016). Identification of barley (*Hordeum vulgare* L.) autophagy genes and their expression levels during leaf senescence, chronic nitrogen limitation and in response to dark exposure. *Agronomy* 6:15.

Avila-Ospina, L., Marmagne, A., Talbotec, J., Krupinska, K., and Masclaux-Daubresse, C. (2015). The identification of new cytosolic glutamine synthetase and asparagine synthetase genes in barley (*Hordeum vulgare* L.), and their expression during leaf senescence. *J. Exp. Bot.* 66, 2013–2026. doi: 10.1093/jxb/erv003

Avila-Ospina, L., Moison, M., Yoshimoto, K., and Masclaux-Daubresse, C. (2014). Autophagy, plant senescence, and nutrient recycling. *J. Exp. Bot.* 65, 3799–3811. doi: 10.1093/jxb/eru039

Baker, N. R., and Oxborough, K. (2004). "Chlorophyll fluorescence as a probe of photosynthetic productivity," in *Chlorophyll a Fluorescence: A Signature of Photosynthesis*, eds G. C. Papageorgiou and K. Govindjee (Dordrecht: Springer), 65–82.

Bassham, D. C., Laporte, M., Marty, F., Moriyasu, Y., Ohsumi, Y., Olsen, L. J., et al. (2006). Autophagy in development and stress responses of plants. *Autophagy* 2, 2–11. doi: 10.4161/auto.2092

Becker, W., and Apel, K. (1993). Differences in gene expression between natural and artificially induced leaf senescence. *Planta* 189, 74–79.

Bhalerao, R., Keskitalo, J., Sterky, F., Erlandsson, R., Bjorkbacka, H., Birve, S. J., et al. (2003). Gene expression in autumn leaves. *Plant Physiol.* 131, 430–442. doi: 10.1104/pp.012732

Bollhöner, B., Prestele, J., and Tuominen, H. (2012). Xylem cell death: emerging understanding of regulation and function. *J. Exp. Bot.* 63, 1081–1094. doi: 10.1093/jxb/err438

Borek, S., Paluch-Lubawa, E., Pukacka, S., Pietrowska-Borek, M., and Ratajczak, L. (2017). Asparagine slows down the breakdown of storage lipid and degradation of autophagic bodies in sugar-starved embryo axes of germinating lupin seeds. *J. Plant Physiol.* 209, 51–67. doi: 10.1016/j.jplph.2016.10.016

Borek, S., Ruta-Piosik, M., Paluch, E., and Pietrowska-Borek, M. (2015). Selective kinds of autophagy. *Postepy Biol. Komorki* 42, 505–538.

Breeze, E., Harrison, E., McHattie, S., Hughes, L., Hickman, R., Hill, C., et al. (2011). High-resolution temporal profiling of transcripts during *Arabidopsis* leaf senescence reveals a distinct chronology of processes and regulation. *Plant Cell* 23, 873–894. doi: 10.1105/tpc.111.083345

Buchanan-Wollaston, V., Earl, S., Harrison, E., Mathas, E., Navabpour, S., Page, T., et al. (2003). The molecular analysis of leaf senescence — a genomics approach. *Plant Biotechnol. J.* 1, 3–22. doi: 10.1046/j.1467-7652.2003.00004.x

Buchanan-Wollaston, V., Page, T., Harrison, E., Breeze, E., Lim, P. O., Nam, H. G., et al. (2005). Comparative transcriptome analysis reveals significant differences in gene expression and signalling pathways between developmental and dark/starvation-induced senescence in *Arabidopsis*. *Plant J.* 42, 567–585. doi: 10.1111/j.1365-313X.2005.02399.x

Canetti, L., Lomaniec, E., Elkind, Y., and Lers, A. (2002). Nuclease activities associated with dark-induced and natural leaf senescence in parsley. *Plant Sci.* 163, 873–880. doi: 10.1016/S0168-9452(02)00242-X

Cartelat, A., Cerovic, Z. G., Goulas, Y., Meyer, S., Lelarge, C., Prioul, J. L., et al. (2005). Optically assessed contents of leaf polyphenolics and chlorophyll as indicators of nitrogen deficiency in wheat (*Triticum aestivum* L.). *Field Crops Res.* 91, 35–49. doi: 10.1016/j.fcr.2004.05.002

Chiba, A., Ishida, H., Nishizawa, N. K., Makino, A., and Mae, T. (2003). Exclusion of ribulose-1,5-bisphosphate carboxylase/oxygenase from chloroplasts by specific bodies in naturally senescing leaves of wheat. *Plant Cell Physiol.* 44, 914–921. doi: 10.1093/pcp/pcg118

Christiansen, M. W., and Gregersen, P. L. (2014). Members of the barley NAC transcription factor gene family show differential co-regulation with senescence-associated genes during senescence of flag leaves. *J. Exp. Bot.* 65, 4009–4022. doi: 10.1093/jxb/eru046

Christiansen, M. W., Holm, P. B., and Gregersen, P. L. (2011). Characterization of barley (*Hordeum vulgare* L.) NAC transcription factors suggests conserved functions compared to both monocots and dicots. *BMC Res. Notes* 4:302. doi: 10.1186/1756-0500-4-302

Christiansen, M. W., Matthewman, C., Podzimska-Sroka, D., O'Shea, C., Lindemose, S., Møllegaard, N. E., et al. (2016). Barley plants over-expressing the NAC transcription factor gene HvNAC005 show stunting and delay in development combined with early senescence. *J. Exper. Bot.* 67, 5259–5273. doi: 10.1093/jxb/erw286

Chrobok, D., Law, S. R., Brouwer, B., Linden, P., Ziolkowska, A., Liebsch, D., et al. (2016). Dissecting the metabolic role of mitochondria during developmental leaf senescence. *Plant Physiol.* 172, 2132–2153. doi: 10.1104/pp.16.01463

Chrost, B., Daniel, A., and Krupinska, K. (2004). Regulation of α-galactosidase gene expression in primary foliage leaves of barley (*Hordeum vulgare* L.) during dark-induced senescence. *Planta* 218, 886–889.

Chrost, B., and Krupinska, K. (2000). Genes with homologies to known α-galactosidases are expressed during senescence of barley leaves. *Physiol. Plant.* 110, 111–119.

Chung, T., Suttangkakul, A., and Vierstra, R. D. (2009). The ATG autophagic conjugation system in maize: ATG transcripts and abundance of the ATG8-lipid adduct are regulated by development and nutrient availability. *Plant Physiol.* 149, 220–234. doi: 10.1104/pp.108.126714

Conrad, K., Motyka, V., and Schlüter, T. (2007). Increase in activity, glycosylation and expression of cytokinin oxidase/dehydrogenase during the senescence of barley leaf segments in the dark. *Physiol. Plant.* 130, 572–579.

Dodge, J. D. (1970). Changes in chloroplast fine structure during the autumnal senescence of betula leaves. *Ann. Bot.* 34, 817–824. doi: 10.1093/oxfordjournals.aob.a084412

Feekes, W. (1941). *De Tarwe en Haar Milieu*. Groningen: Hoitsema.

Feller, U., Anders, I., and Mae, T. (2008). Rubiscolytics: fate of Rubisco after its enzymatic function in a cell is terminated. *J. Exp. Bot.* 59, 1615–1624. doi: 10.1093/jxb/erm242

Floyd, B. E., Pu, Y., Soto-Burgos, J., and Bassham, D. C. (2015). "To Live or Die: autophagy in plants," in *Plant Programmed Cell Death*, eds A. N. Gunawardena and P. F. McCabe (Cham: Springer International Publishing), 269–300.

Foyer, C. H., Noctor, G., and Hodges, M. (2011). Respiration and nitrogen assimilation: targeting mitochondria-associated metabolism as a means to enhance nitrogen use efficiency. *J. Exp. Bot.* 62, 1467–1482. doi: 10.1093/jxb/erq453

Fracheboud, Y., and Leipner, J. (2003). "The application of chlorophyll fluorescence to study light, temperature, and drought stress," in *Practical Applications of Chlorophyll Fluorescence in Plant Biology*, eds J. R. DeEll and P. M. A. Toivonen (Boston, MA: Springer), 125–150.

Fukami, K. (2002). Structure, regulation, and function of phospholipase C isozymes. *J. Biochem.* 131, 293–299. doi: 10.1093/oxfordjournals.jbchem.a003102

Gan, S., and Amasino, R. M. (1995). Inhibition of leaf senescence by autoregulated production of cytokinin. *Science* 270, 1986–1988. doi: 10.1126/science.270.5244.1986

Gan, S., and Amasino, R. M. (1997). Making sense of senescence (molecular genetic regulation and manipulation of leaf senescence). *Plant Physiol.* 113, 313–319. doi: 10.1104/pp.113.2.313

Gepstein, S., Sabehi, G., Carp, M. J., Hajouj, T., Nesher, M. F., Yariv, I., et al. (2003). Large-scale identification of leaf senescence-associated genes. *Plant J.* 36, 629–642. doi: 10.1046/j.1365-313x.2003.01908.x

Gregersen, P. L., Holm, P. B., and Krupinska, K. (2008). Leaf senescence and nutrient remobilisation in barley and wheat. *Plant Biol.* 10(Suppl. 1), 37–49. doi: 10.1111/j.1438-8677.2008.00114.x

Guo, Y., and Gan, S. S. (2012). Convergence and divergence in gene expression profiles induced by leaf senescence and 27 senescence-promoting hormonal, pathological and environmental stress treatments. *Plant Cell Environ.* 35, 644–655. doi: 10.1111/j.1365-3040.2011.02442.x

Hara-Nishimura, I., Hatsugai, N., Nakaune, S., Kuroyanagi, M., and Nishimura, M. (2005). Vacuolar processing enzyme: an executor of plant cell death. *Curr. Opin. Plant Biol.* 8, 404–408. doi: 10.1016/j.pbi.2005.05.016

Himelblau, E., and Amasino, R. M. (2001). Nutrients mobilized from leaves of *Arabidopsis thaliana* during leaf senescence. *J. Plant Physiol.* 158, 1317–1323. doi: 10.1078/0176-1617-00608

Hollmann, J., Gregersen, P. L., and Krupinska, K. (2014). Identification of predominant genes involved in regulation and execution of senescence-associated nitrogen remobilization in flag leaves of field grown barley. *J. Exp. Bot.* 65, 3963–3973. doi: 10.1093/jxb/eru094

Hörtensteiner, S., and Feller, U. (2002). Nitrogen metabolism and remobilization during senescence. *J. Exp. Bot.* 53, 927–937. doi: 10.1093/jexbot/53.370.927

Ishida, H., and Yoshimoto, K. (2008). Chloroplasts are partially mobilized to the vacuole by autophagy. *Autophagy* 4, 961–962. doi: 10.4161/auto.6804

Ishida, H., Yoshimoto, K., Izumi, M., Reisen, D., Yano, Y., Makino, A., et al. (2008). Mobilization of rubisco and stroma-localized fluorescent proteins of chloroplasts to the vacuole by an ATG gene-dependent autophagic process. *Plant Physiol.* 148, 142–155. doi: 10.1104/pp.108.122770

Jajić, I., Wiśniewska-Becker, A., Sarna, T., Jemioła-Rzemińska, M., and Strzałka, K. (2014). EPR spin labeling measurements of thylakoid membrane fluidity during barley leaf senescence. *J. Plant Physiol.* 171, 1046–1053.

Janawad, C. S., Jyothi, G., Manu, T., and Murali, R. (2012). Autophagy is the emerging role in plant defense against pathogen attack. *Glob. J. Biol. Agric. Health Sci.* 1, 33–39.

Janečková, H., Husičková, A., Lazár, D., Ferretti, U., Pospíšil, P., and Špundová, M. (2019). Exogenous application of cytokinin during dark senescence eliminates the acceleration of photosystem II impairment caused by chlorophyll b deficiency in barley. *Plant Physiol. Biochem.* 136, 43–51.

Jenkins, G. M., and Frohman, M. A. (2005). Phospholipase D: a lipid centric review. *Cell Mol. Life Sci.* 62, 2305–2316. doi: 10.1007/s00018-005-5195-z

Jing, H. C., Hille, J., and Dijkwel, P. P. (2003). Ageing in plants: conserved strategies and novel pathways. *Plant Biol.* 5, 455–464. doi: 10.1055/s-2003-44779

Jing, H. C., Sturre, M. J., Hille, J., and Dijkwel, P. P. (2002). *Arabidopsis* onset of leaf death mutants identify a regulatory pathway controlling leaf senescence. *Plant J.* 32, 51–63. doi: 10.1046/j.1365-313x.2002.01400.x

Jukanti, A. K., Heidlebaugh, N. M., Parrott, D. L., Fischer, I. A., McInnerney, K., and Fischer, A. M. (2008). Comparative transcriptome profiling of near-isogenic barley (*Hordeum vulgare*) lines differing in the allelic state of a major grain protein content locus identifies genes with possible roles in leaf senescence and nitrogen reallocation. *New Phytol.* 177, 333–349. doi: 10.1111/j.1469-8137.2007.02270.x

Keech, O., Pesquet, E., Ahad, A., Askne, A., Nordvall, D., Vodnala, S. M., et al. (2007). The different fates of mitochondria and chloroplasts during dark-induced senescence in *Arabidopsis* leaves. *Plant Cell Environ.* 30, 1523–1534. doi: 10.1111/j.1365-3040.2007.01724.x

Kleber-Janke, T., and Krupinska, K. (1997). Isolation of cDNA clones for genes showing enhanced expression in barley leaves during dark-induced senescence as well as during senescence under field conditions. *Planta* 203, 332–340. doi: 10.1007/s004250050199

Kleessen, S., Araujo, W. L., Fernie, A. R., and Nikoloski, Z. (2012). Model-based confirmation of alternative substrates of mitochondrial electron transport chain. *J. Biol. Chem.* 287, 11122–11131. doi: 10.1074/jbc.M111.310383

Krause, K., Falk, J., Humbeck, K., and Krupinska, K. (1998). Responses of the transcriptional apparatus of barley chloroplasts to a prolonged dark period and to subsequent reillumination. *Physiol. Plant.* 104, 143–152.

Krieger-Liszkay, A., Krupinska, K., and Shimakawa, G. (2019). The impact of photosynthesis on initiation of leaf senescence. *Physiol. Plant* 166, 148–164. doi: 10.1111/ppl.12921

Krupinska, K., Mulisch, M., Hollmann, J., Tokarz, K., Zschiesche, W., Kage, H., et al. (2012). An alternative strategy of dismantling of the chloroplasts during

leaf senescence observed in a high-yield variety of barley. *Physiol. Plant* 144, 189–200. doi: 10.1111/j.1399-3054.2011.01545.x

Kucharewicz, W., Distelfeld, A., Bilger, W., Müller, M., Munné-Bosch, S., Hensel, G., et al. (2017). Acceleration of leaf senescence is slowed down in transgenic barley plants deficient in the DNA/RNA-binding protein WHIRLY1. *J. Exper. Bot.* 68, 983–996.

Kuriyama, H., and Fukuda, H. (2002). Developmental programmed cell death in plants. *Curr. Opin. Plant Biol.* 5, 568–573. doi: 10.1016/s1369-5266(02)00305-9

Lamb, C. A., Yoshimori, T., and Tooze, S. A. (2013). The autophagosome: origins unknown, biogenesis complex. *Nat. Rev. Mol. Cell Biol.* 14, 759–774. doi: 10.1038/nrm3696

Lambert, R., Quiles, F. A., Galvez-Valdivieso, G., and Piedras, P. (2017). Nucleases activities during French bean leaf aging and dark-induced senescence. *J. Plant Physiol.* 218, 235–242. doi: 10.1016/j.jplph.2017.08.013

Lan, W., and Miao, Y. (2019). "Chapter 15 - Autophagy and senescence," in *Senescence Signalling and Control in Plants*, eds M. Sarwat and N. Tuteja (New York, NY: Academic Press), 239–253.

Lancashire, P. D., Bleiholder, H., Boom, T. V. D., Langelüddeke, P., Stauss, R., Weber, E., et al. (1991). A uniform decimal code for growth stages of crops and weeds. *Ann. Appl. Biol.* 119, 561–601.

Law, S. R., Chrobok, D., Juvany, M., Delhomme, N., Linden, P., Brouwer, B., et al. (2018). Darkened leaves use different metabolic strategies for senescence and survival. *Plant Physiol.* 177, 132–150. doi: 10.1104/pp.18.00062

Lee, R. H., Wang, C. H., Huang, L. T., and Chen, S. C. (2001). Leaf senescence in rice plants: cloning and characterization of senescence up-regulated genes. *J. Exp. Bot.* 52, 1117–1121. doi: 10.1093/jexbot/52.358.1117

Legocka, J., and Zajchert, I. (1999). Role of spermidine in the stabilization of the apoprotein of the light-harvesting chlorophyll a/b-protein complex of photosystem II during leaf senescence process. *Acta Physiol. Plant.* 21, 127–132.

Lichtenthaler, H., Langsdorf, G., Lenk, S., and Buschmann, C. (2005). Chlorophyll fluorescence imaging of photosynthetic activity with the flash-lamp fluorescence imaging system. *Photosynthetica* 43, 355–369. doi: 10.1007/s11099-005-0060-8

Lichtenthaler, H. K., and Grumbach, K. H. (1974). Kinetic of lipoquinone and pigment synthesis in green Hordeum seedlings during an artificial day-night rhythm with a prolonged dark phase. *Zeitschrift Naturforschung C* 29, 532–540.

Liebsch, D., and Keech, O. (2016). Dark-induced leaf senescence: new insights into a complex light-dependent regulatory pathway. *New Phytol.* 212, 563–570. doi: 10.1111/nph.14217

Lim, P. O., Kim, H. J., and Nam, H. G. (2007). Leaf senescence. *Annu. Rev. Plant Biol.* 58, 115–136. doi: 10.1146/annurev.arplant.57.032905.105316

Lin, J. F., and Wu, S. H. (2004). Molecular events in senescing *Arabidopsis* leaves. *Plant J.* 39, 612–628. doi: 10.1111/j.1365-313X.2004.02160.x

Liu, J. D., Goodspeed, D., Sheng, Z., Li, B., Yang, Y., Kliebenstein, D. J., et al. (2015). Keeping the rhythm: light/dark cycles during postharvest storage preserve the tissue integrity and nutritional content of leafy plants. *BMC Plant Biol.* 15:92. doi: 10.1186/s12870-015-0474-9

Liu, Y., Zhang, W., Zhang, K., You, Q., Yan, H., Jiao, Y., et al. (2017). Genome-wide mapping of DNase I hypersensitive sites reveals chromatin accessibility changes in *Arabidopsis* euchromatin and heterochromatin regions under extended darkness. *Sci. Rep.* 7:4093. doi: 10.1038/s41598-017-04524-9

Maillard, A., Diquelou, S., Billard, V., Laine, P., Garnica, M., Prudent, M., et al. (2015). Leaf mineral nutrient remobilization during leaf senescence and modulation by nutrient deficiency. *Front. Plant Sci.* 6:317. doi: 10.3389/fpls.2015.00317

Martinez, D. E., Costa, M. L., Gomez, F. M., Otegui, M. S., and Guiamet, J. J. (2008a). 'Senescence-associated vacuoles' are involved in the degradation of chloroplast proteins in tobacco leaves. *Plant J.* 56, 196–206. doi: 10.1111/j.1365-313X.2008.03585.x

Martinez, D. E., Costa, M. L., and Guiamet, J. J. (2008b). Senescence-associated degradation of chloroplast proteins inside and outside the organelle. *Plant Biol.* 10(Suppl. 1), 15–22. doi: 10.1111/j.1438-8677.2008.00089.x

Masclaux, C., Quillere, I., Gallais, A., and Hirel, B. (2001). The challenge of remobilisation in plant nitrogen economy. A survey of physio-agronomic and molecular approaches. *Ann. Appl. Biol.* 138, 69–81. doi: 10.1111/j.1744-7348.2001.tb00086.x

Masclaux, C., Valadier, M. H., Brugiere, N., Morot-Gaudry, J. F., and Hirel, B. (2000). Characterization of the sink/source transition in tobacco (*Nicotiana tabacum* L.) shoots in relation to nitrogen management and leaf senescence. *Planta* 211, 510–518. doi: 10.1007/s004250000310

Masclaux-Daubresse, C., Reisdorf-Cren, M., Pageau, K., Lelandais, M., Grandjean, O., Kronenberger, J., et al. (2006). Glutamine synthetase-glutamate synthase pathway and glutamate dehydrogenase play distinct roles in the sink-source nitrogen cycle in tobacco. *Plant Physiol.* 140, 444–456. doi: 10.1104/pp.105.071910

Matile, P. (1992). "Chloroplast senescence," in *Crop Photosynthesis: Spatial and Temporal Determinants*, eds N. R. Baker and N. Thomas (Amsterdam: Elsevier), 413–440.

Mattoo, A. K., Marder, J. B., and Edelman, M. (1989). Dynamics of the photosystem II reaction center. *Cell* 56, 241–246. doi: 10.1016/0092-8674(89)90897-0

Nam, H. G. (1997). The molecular genetic analysis of leaf senescence. *Curr. Opin. Biotechnol.* 8, 200–207. doi: 10.1016/S0958-1669(97)80103-6

Obara, K., Kuriyama, H., and Fukuda, H. (2001). Direct evidence of active and rapid nuclear degradation triggered by vacuole rupture during programmed cell death in zinnia. *Plant Physiol.* 125, 615–626. doi: 10.1104/pp.125.2.615

Ostrowska-Mazurek, A., Kasprzak, P., Kubala, S., Zaborowska, M., and Sobieszczuk-Nowicka, E. (2020). Epigenetic landmarks of leaf senescence and crop improvement. *Int. J. Mol. Sci.* 21:125. doi: 10.3390/ijms21145125

Otegui, M. S., Noh, Y. S., Martinez, D. E., Vila Petroff, M. G., Staehelin, L. A., Amasino, R. M., et al. (2005). Senescence-associated vacuoles with intense proteolytic activity develop in leaves of *Arabidopsis* and soybean. *Plant J.* 41, 831–844. doi: 10.1111/j.1365-313X.2005.02346.x

Parrott, D. L., Martin, J. M., and Fischer, A. M. (2010). Analysis of barley (*Hordeum vulgare*) leaf senescence and protease gene expression: a family C1A cysteine protease is specifically induced under conditions characterized by high carbohydrate, but low to moderate nitrogen levels. *New Phytol.* 187, 313–331. doi: 10.1111/j.1469-8137.2010.03278.x

Pascual, V., Cha, S., Gershwin, M. E., Capra, J. D., and Leung, P. S. (1994). Nucleotide sequence analysis of natural and combinatorial anti-PDC-E2 antibodies in patients with primary biliary cirrhosis. Recapitulating immune selection with molecular biology. *J. Immunol.* 152, 2577–2585.

Patel, S., Caplan, J., and Dinesh-Kumar, S. P. (2006). Autophagy in the control of programmed cell death. *Curr. Opin. Plant Biol.* 9, 391–396. doi: 10.1016/j.pbi.2006.05.007

Peterson, L. W., and Huffaker, R. C. (1975). Loss of ribulose 1,5-Diphosphate carboxylase and increase in proteolytic activity during senescence of detached primary barley leaves. *Plant Physiol.* 55, 1009–1015. doi: 10.1104/pp.55.6.1009

Phillips, A. R., Suttangkakul, A., and Vierstra, R. D. (2008). The ATG12-conjugating enzyme ATG10 is essential for autophagic vesicle formation in *Arabidopsis thaliana*. *Genetics* 178, 1339–1353. doi: 10.1534/genetics.107.086199

Roberts, I. N., Veliz, C. G., Criado, M. V., Signorini, A., Simonetti, E., and Caputo, C. (2017). Identification and expression analysis of 11 subtilase genes during natural and induced senescence of barley plants. *J. Plant Physiol.* 211, 70–80. doi: 10.1016/j.jplph.2017.01.005

Rogers, H. J. (2015). "Senescence-associated programmed cell death," in *Plant Programmed Cell Death*, eds A. N. Gunawardena and P. F. McCabe (Cham: Springer International Publishing), 203–233.

Rolny, N., Costa, L., Carrion, C., and Guiamet, J. J. (2011). Is the electrolyte leakage assay an unequivocal test of membrane deterioration during leaf senescence? *Plant Physiol. Biochem.* 49, 1220–1227. doi: 10.1016/j.plaphy.2011.06.010

Rosiak-Figielek, B., and Jackowski, G. (2000). The disappearance kinetics of Lhcb polypeptides during dark-induced senescence of leaves. *Funct. Plant Biol.* 27, 245–251.

Roulin, S., Buchala, A. J., and Fincher, G. B. (2002). Induction of (1→ 3, 1→ 4)-ß-D-glucan hydrolases in leaves of dark-incubated barley seedlings. *Planta* 215, 51–59.

Ruberti, C., Barizza, E., Bodner, M., La Rocca, N., De Michele, R., Carimi, F., et al. (2014). Mitochondria change dynamics and morphology during grapevine leaf senescence. *PLoS One* 9:e102012. doi: 10.1371/journal.pone.0102012

Sakamoto, W., and Takami, T. (2014). Nucleases in higher plants and their possible involvement in DNA degradation during leaf senescence. *J. Exper. Bot.* 65, 3835–3843. doi: 10.1093/jxb/eru091

Scharrenberg, C., Falk, J., Quast, S., Haussühl, K., Humbeck, K., and Krupinska, K. (2003). Isolation of senescence-related cDNAs from flag leaves of field grown barley plants. *Physiol. Plant.* 118, 278–288.

Scheumann, V., Schoch, S., and Rüdiger, W. (1999). Chlorophyll b reduction during senescence of barley seedlings. *Planta* 209, 364–370.

Schippers, J. H., Schmidt, R., Wagstaff, C., and Jing, H. C. (2015). Living to die and dying to live: the survival strategy behind leaf senescence. *Plant Physiol.* 169, 914–930. doi: 10.1104/pp.15.00498

Shi, R., Weber, G., Köster, J., Reza-Hajirezaei, M., Zou, C., Zhang, F., et al. (2012). Senescence-induced iron mobilization in source leaves of barley (*Hordeum vulgare*) plants. *New Phytol.* 195, 372–383.

Sienko, K., Poormassalehgoo, A., Yamada, K., and Goto-Yamada, S. (2020). Microautophagy in plants: consideration of its molecular mechanism. *Cells* 9:887. doi: 10.3390/cells9040887

Simova-Stoilova, L., Demirevska-Kepova, K., and Stoyanova, Z. (2002). Ribulose-1, 5-bisphosphate carboxylase/oxygenase specific proteolysis in barley chloroplasts during dark induced senescence. *Photosynthetica* 40, 561–566.

Smart, C. M., Hosken, S. E., Thomas, H., Greaves, J. A., Blair, B. G., and Schuch, W. (1995). The timing of maize leaf senescence and characterisation of senescence-related cDNAs. *Physiol. Plant.* 93, 673–682.

Sobieszczuk-Nowicka, E., Kubala, S., Zmienko, A., Malecka, A., and Legocka, J. (2015). From accumulation to degradation: reprogramming polyamine metabolism facilitates dark-induced senescence in barley leaf cells. *Front. Plant Sci.* 6:1198.

Sobieszczuk-Nowicka, E., Kubala, S., Zmienko, A., Małecka, A., and Legocka, J. (2016). From accumulation to degradation: reprogramming polyamine metabolism facilitates dark-induced senescence in barley leaf cells. *Front. Plant Sci.* 6:1198. doi: 10.3389/fpls.2015.01198

Sobieszczuk-Nowicka, E., Wieczorek, P., and Legocka, J. (2009). Kinetin affects the level of chloroplast polyamines and transglutaminase activity during senescence of barley leaves. *Acta Biochim. Polon.* 56, 255–259.

Sobieszczuk-Nowicka, E., Wrzesinski, T., Bagniewska-Zadworna, A., Kubala, S., Rucinska-Sobkowiak, R., Polcyn, W., et al. (2018). Physio-genetic dissection of dark-induced leaf senescence and timing its reversal in barley. *Plant Physiol.* 178, 654–671. doi: 10.1104/pp.18.00516

Springer, A., Acker, G., Bartsch, S., Bauerschmitt, H., Reinbothe, S., and Reinbothe, C. (2015). Differences in gene expression between natural and artificially induced leaf senescence in barley. *J. Plant Physiol.* 176, 180–191. doi: 10.1016/j.jplph.2015.01.004

Spundova, M., Popelkova, H., Ilik, P., Skotnica, J., Novotny, R., and Naus, J. (2003). Ultra-structural and functional changes in the chloroplasts of detached barley leaves senescing under dark and light conditions. *J. Plant Physiol.* 160, 1051–1058. doi: 10.1078/0176-1617-00902

Stefaniak, S., Wojtyla, L., Pietrowska-Borek, M., and Borek, S. (2020). Completing autophagy: formation and degradation of the autophagic body and metabolite salvage in plants. *Int. J. Mol. Sci.* 21:2205. doi: 10.3390/ijms21062205

Thomas, H. (2013). Senescence, ageing and death of the whole plant. *New Phytol.* 197, 696–711. doi: 10.1111/nph.12047

Thomas, H., and Ougham, H. (2014). The stay-green trait. *J. Exp. Bot.* 65, 3889–3900. doi: 10.1093/jxb/eru037

Uauy, C., Distelfeld, A., Fahima, T., Blechl, A., and Dubcovsky, J. (2006). A NAC gene regulating senescence improves grain protein, zinc, and iron content in wheat. *Science* 314, 1298–1301.

van der Graaff, E., Schwacke, R., Schneider, A., Desimone, M., Flugge, U. I., and Kunze, R. (2006). Transcription analysis of *arabidopsis* membrane transporters and hormone pathways during developmental and induced leaf senescence. *Plant Physiol.* 141, 776–792. doi: 10.1104/pp.106.079293

van Doorn, W. G., and Woltering, E. J. (2005). Many ways to exit? Cell death categories in plants. *Trends Plant Sci.* 10, 117–122. doi: 10.1016/j.tplants.2005.01.006

van Doorn, W. G., and Yoshimoto, K. (2010). Role of chloroplasts and other plastids in ageing and death of plants and animals: a tale of Vishnu and Shiva. *Age. Res. Rev.* 9, 117–130. doi: 10.1016/j.arr.2009.08.003

Wang, P., Mugume, Y., and Bassham, D. C. (2018). New advances in autophagy in plants: regulation, selectivity and function. *Semin. Cell Dev. Biol.* 80, 113–122. doi: 10.1016/j.semcdb.2017.07.018

Wehner, G. G., Balko, C. C., Enders, M. M., Humbeck, K. K., and Ordon, F. F. (2015). Identification of genomic regions involved in tolerance to drought stress and drought stress induced leaf senescence in juvenile barley. *BMC Plant Biol.* 15:125. doi: 10.1186/s12870-015-0524-3

Wong, S.-L., Chen, C.-W., Huang, M.-Y., and Weng, J.-H. (2014). Relationship between photosynthetic CO_2 uptake rate and electron transport rate in two C 4 perennial grasses under different nitrogen fertilization, light and temperature conditions. *Acta Physiol. Plant.* 36, 849–857. doi: 10.1007/s11738-013-1463-y

Wood, M., Power, J. B., Davey, M. R., Lowe, K. C., and Mulligan, B. J. (1998). Factors affecting single strand-preferring nuclease activity during leaf aging and dark-induced senescence in barley (*Hordeum vulgare* L.). *Plant Sci.* 131, 149–159. doi: 10.1016/S0168-9452(97)00253-7

Xia, T., Xiao, D., Liu, D., Chai, W., Gong, Q., and Wang, N. N. (2012). Heterologous expression of *ATG8c* from soybean confers tolerance to nitrogen deficiency and increases yield in *Arabidopsis*. *PLoS One* 7:e37217. doi: 10.1371/journal.pone.0037217

Żelisko, A., and Jackowski, G. (2004). Senescence-dependent degradation of Lhcb3 is mediated by a thylakoid membrane-bound protease. *J. Plant Physiol.* 161, 1157–1170.

Zmienko, A., Samelak-Czajka, A., Goralski, M., Sobieszczuk-Nowicka, E., Kozlowski, P., and Figlerowicz, M. (2015). Selection of reference genes for qPCR-and ddPCR-based analyses of gene expression in senescing barley leaves. *PLoS One* 10:e0118226. doi: 10.1371/journal.pone.00118226

Conflict of Interest: The authors declare that the research was conducted in the absence of any commercial or financial relationships that could be construed as a potential conflict of interest.

Advantages of publishing in Frontiers

OPEN ACCESS
Articles are free to read for greatest visibility and readership

FAST PUBLICATION
Around 90 days from submission to decision

HIGH QUALITY PEER-REVIEW
Rigorous, collaborative, and constructive peer-review

TRANSPARENT PEER-REVIEW
Editors and reviewers acknowledged by name on published articles

Frontiers
Avenue du Tribunal-Fédéral 34
1005 Lausanne | Switzerland

Visit us: www.frontiersin.org
Contact us: frontiersin.org/about/contact

REPRODUCIBILITY OF RESEARCH
Support open data and methods to enhance research reproducibility

DIGITAL PUBLISHING
Articles designed for optimal readership across devices

FOLLOW US
@frontiersin

IMPACT METRICS
Advanced article metrics track visibility across digital media

EXTENSIVE PROMOTION
Marketing and promotion of impactful research

LOOP RESEARCH NETWORK
Our network increases your article's readership